frontiers | Research Topics

Endocrine regulation and physiological adaptation of stress response in aquatic organisms, volume II

Edited by
Yiming Li, Marco António Campinho, Yi-Feng Li and Juan Fuentes

Published in
Frontiers in Marine Science
Frontiers in Physiology

ISSN 1664-8714
ISBN 978-2-8325-5883-6
DOI 10.3389/978-2-8325-5883-6

About Frontiers

Frontiers is more than just an open access publisher of scholarly articles: it is a pioneering approach to the world of academia, radically improving the way scholarly research is managed. The grand vision of Frontiers is a world where all people have an equal opportunity to seek, share and generate knowledge. Frontiers provides immediate and permanent online open access to all its publications, but this alone is not enough to realize our grand goals.

Frontiers journal series

The Frontiers journal series is a multi-tier and interdisciplinary set of open-access, online journals, promising a paradigm shift from the current review, selection and dissemination processes in academic publishing. All Frontiers journals are driven by researchers for researchers; therefore, they constitute a service to the scholarly community. At the same time, the *Frontiers journal series* operates on a revolutionary invention, the tiered publishing system, initially addressing specific communities of scholars, and gradually climbing up to broader public understanding, thus serving the interests of the lay society, too.

Dedication to quality

Each Frontiers article is a landmark of the highest quality, thanks to genuinely collaborative interactions between authors and review editors, who include some of the world's best academicians. Research must be certified by peers before entering a stream of knowledge that may eventually reach the public - and shape society; therefore, Frontiers only applies the most rigorous and unbiased reviews. Frontiers revolutionizes research publishing by freely delivering the most outstanding research, evaluated with no bias from both the academic and social point of view. By applying the most advanced information technologies, Frontiers is catapulting scholarly publishing into a new generation.

What are Frontiers Research Topics?

Frontiers Research Topics are very popular trademarks of the *Frontiers journals series*: they are collections of at least ten articles, all centered on a particular subject. With their unique mix of varied contributions from Original Research to Review Articles, Frontiers Research Topics unify the most influential researchers, the latest key findings and historical advances in a hot research area.

Find out more on how to host your own Frontiers Research Topic or contribute to one as an author by contacting the Frontiers editorial office: frontiersin.org/about/contact

Endocrine regulation and physiological adaptation of stress response in aquatic organisms, volume II

Topic editors

Yiming Li — Fishery Machinery and Instrument Research Institute, China

Marco António Campinho — University of Algarve, Portugal

Yi-Feng Li — Shanghai Ocean University, China

Juan Fuentes — Institute of Marine Sciences of Andalusia, Spanish National Research Council (CSIC), Spain

Citation

Li, Y., Campinho, M. A., Li, Y.-F., Fuentes, J., eds. (2025). *Endocrine regulation and physiological adaptation of stress response in aquatic organisms, volume II*. Lausanne: Frontiers Media SA. doi: 10.3389/978-2-8325-5883-6

Table of contents

frontiers | Frontiers in Marine Science

TYPE Editorial
PUBLISHED 19 December 2024
DOI 10.3389/fmars.2024.1536027

OPEN ACCESS

EDITED AND REVIEWED BY
Pung Pung Hwang,
Academia Sinica, Taiwan

*CORRESPONDENCE
Yi-Feng Li
yifengli@shou.edu.cn
Yiming Li
liyiming183@163.com

RECEIVED 28 November 2024
ACCEPTED 06 December 2024
PUBLISHED 19 December 2024

CITATION
Li Y-F, Li Y, Campinho MA and Fuentes J (2024) Editorial: Endocrine regulation and physiological adaptation of stress response in aquatic organisms, volume II.
Front. Mar. Sci. 11:1536027.
doi: 10.3389/fmars.2024.1536027

Editorial: Endocrine regulation and physiological adaptation of stress response in aquatic organisms, volume II

Yi-Feng Li[1,2]*, Yiming Li[3]*, Marco António Campinho[4,5] and Juan Fuentes[6]

[1]International Research Centre for Marine Biosciences, Ministry of Science and Technology, Shanghai Ocean University, Shanghai, China, [2]Key Laboratory of Exploration and Utilization of Aquatic Genetic Resources, Ministry of Education, Shanghai Ocean University, Shanghai, China, [3]East China Sea Fisheries Research Institute, Chinese Academy of Fishery Sciences, Shanghai, China, [4]Algarve Biomedical Centre-Research Institute, Faro, Portugal, [5]Faculty of Medicine and Biomedical Sciences, University of the Algarve, Faro, Portugal, [6]Instituto de Ciencias Marinas de Andalucíía (ICMAN), Consejo Superior de Investigaciones Cientiíficas (CSIC), Puerto Real, Spain

KEYWORDS

aquatic organisms, endocrine regulation, stress response, physiological adaptation, homeostasis

Editorial on the Research Topic
Endocrine regulation and physiological adaptation of stress response in aquatic organisms, volume II

At the individual level, organisms develop many complex morphological and physiological adaptations to maintain homeostasis, of which endocrine regulation is the key. By adjusting physiological mechanisms, organisms adapt their response to the external environment, enabling the acquisition of new homeostatic equilibrium that allows survival.

The physiological adaptative mechanism plays an important role in maintaining homeostasis and adapting to changes in the external environment. Well-known environmental factors such as ambient temperature, pH, ammonia nitrogen, salinity, and exposure to new pollutants can disrupt homeostasis, resulting in growth and physiological and endocrine disorders. Thus, in a rapidly changing climate, it is important to explore the biological adaptive regulation mechanism and endocrine regulation strategy under stress, which has an important impact on the protection of aquatic ecology. The main purpose of the Research Topic is to explore and discuss these potential physiological and molecular mechanisms to provide new insights for developing new green ecological activities.

Lopes et al. explored the impact of chronic stress on the physiological and immune responses of lumpfish (*Cyclopterus lumpus*), revealing that increased stress exposure led to significant alterations in immunity and elevated nutritional demands, particularly for branched-chain amino acids and lysine. Notably, while initial stress exposure enhanced immune parameters, such as plasma nitric oxide and peroxidase levels, these effects diminished by the end of the experiment, coinciding with the worst health conditions observed in the most frequently stressed group. The findings emphasize the complex

relationship between stress, immunity, and nutrition, suggesting a need for tailored dietary strategies and improved rearing practices.

Duan et al. elucidated the detrimental effects of acute heat stress on the intestinal health of a cold water schizothoracine fish *Gymnocypris eckloni*, revealing significant morphological damage, increased oxidative stress, and elevated inflammatory markers, indicating compromised intestinal barrier function. Transcriptomic analyses highlighted the HIF-1 signaling pathway's critical role under heat stress, with downregulation of adaptive immunity-related genes suggesting impaired immune function. Additionally, notable shifts in the intestinal microbiota composition were observed, correlating with stress-related gene expression changes, enhancing our understanding of the adaptive mechanisms in response to high temperatures and informing future aquaculture practices for cold-water fish.

Mao et al. demonstrated that moderate high-temperature stress (32°C–34°C) significantly improves growth performance and enhances immune responses in the rice field eel *Monopterus albus*, as indicated by improved feed conversion ratio, body weight gain, and increased expression of immune-related genes. However, elevated temperatures (36°C and 38°C) negatively impacted liver cell integrity and digestive enzyme activities. Additionally, the study found that the α diversity of intestinal microbiota peaked at 34°C, highlighting the beneficial effects of appropriate thermal conditions on the adaptability and health of *M. albus* in aquaculture settings.

Sun et al. utilized an integrated multi-omics approach to elucidate the physiological responses of the razor clam (*Sinonovacula constricta*) to ammonia nitrogen exposure, revealing significant increases in free amino acids, immune-related enzyme activities, and antioxidant enzyme levels only after long-term exposure. Additionally, transcriptomic and metabolomic analyses indicated alterations in metabolic pathways, particularly in amino acid, lipid, and carbohydrate metabolism, alongside significant changes in gene expression related to detoxification and ammonia excretion. These findings suggest that mechanisms such as the conversion of endogenous ammonia to alanine and urea synthesis may serve as adaptive strategies to ammonia stress in benthic mollusks.

Liu et al. characterized the cytochrome P450 enzyme CYP26B1 gene in the black-spotted frog (*Pelophylax nigromaculatus*). Chronic exposure to the antibiotic sulfamethoxazole (SMX) significantly upregulated CYP26B1 expression in liver tissues at 1 and 10 μg/L concentrations, with SMX displaying an affinity of −7.6 kcal/mol for the enzyme. These results highlight the role of CYP enzymes in detoxification and the potential ecological impacts of antibiotic exposure on amphibian species.

Li et al. assessed the effects of ammonia and heat stress on the growth performance, antioxidant activity, and immunity of wild and breeding strains of the juvenile rice field eels (*Monopterus albus*). Results indicated that both strains experienced significant growth inhibition, with breeding strains exhibiting superior growth and survival rates attributed to enhanced growth-related gene expression (*gh*). Furthermore, breeding strains showed increased enzyme activity and immune gene expression in response to oxidative stress. However, evidence of oxidative damage and inflammatory responses was observed in both strains, highlighting their differing adaptability to environmental stressors.

Li et al. conducted a transcriptomic analysis of pearl oysters (*Pinctada fucata martensii*) exposed to titanium dioxide nanoparticles (TiO_2-NPs) for 14 days, identifying 911 differentially expressed genes related to oxidative stress, apoptosis and disrupted protein homeostasis. Gene ontology and KEGG pathway analyses revealed enrichments in pathways associated with hydrolase activity, immune response, and metabolic processes, indicating significant negative impacts on biomineralization and cellular metabolism. Despite a brief recovery period of 7 days, the oysters continued to exhibit adverse effects from TiO_2-NP exposure, highlighting the complexity of their stress responses.

Zhou et al. characterized the fad6 gene in yellow catfish (*Pelteobagrus fulvidraco*), revealing its conserved sequence and significant expression in the heart and liver. Transcription levels are influenced by dietary composition and nutritional status, suggesting a regulatory role of Fad6 in HUFA biosynthesis.

Lin et al. identified three carnitine palmitoyltransferase isoforms (*cpt-1a*, *cpt-1b*, and *cpt-2*) in the mud crab *Scylla paramamosain*. The expression of all isoforms was markedly upregulated in response to fasting and low salinity stress, particularly *cpt-1a* in the hepatopancreas, highlighting their crucial roles in energy metabolism under these conditions. These findings contribute to understanding CPT phylogenetic evolution and the metabolic adaptations of crustaceans.

Li et al. investigated the effects of flowing water stimulation on hormonal regulation during the artificial reproduction of the conger eel (*Conger myriaster*). Results indicated that flowing water significantly enhanced follicle-stimulating hormone (FSH) synthesis in early ovarian development and luteinizing hormone (LH) synthesis in late stages while reducing estradiol levels. The findings provide insights into optimizing artificial reproduction techniques for this economically important species.

Shu et al. examined the effects of water velocity stimulation on ovarian maturation and antioxidant capacity in adult grass carp (*Ctenopharyngodon idellus*). While water velocity did not significantly alter ovarian development, it elevated concentrations of key hormones (estradiol, testosterone, progesterone, 17a,20b-DHP, and vitellogenin) and enhanced gene expression in the hypothalamus-pituitary-gonad (HPG) axis. This study indicates that appropriate water velocity improved antioxidant enzyme activities in the ovary and liver, supporting the physiological health of the fish.

Zhu et al. revealed that ocean warming significantly alters the microbiome of hard-shelled mussel (*Mytilus coruscus*) larvae, with a notable decrease in the abundance of beneficial genera such as *Delftia* and *Neptunomonas* under prolonged temperature exposure. At the same time, *Tenacibaculum*, an opportunistic pathogen, increased. Although overall microbiota diversity remained stable, species abundance rose at elevated temperatures. This suggests that climate-induced marine heat waves may impair the larvae's ability to degrade environmental toxins and enhance disease risk. These findings highlight the potential negative impacts of climate change on mussel larval health and survival. This study explores the physiological response mechanism of aquatic organisms under different environmental stimuli based on different technical means and analytical methods. Molecular and comparative biology methods have been applied to provide a new

understanding of growth, metabolism, and endocrine adaptation regulation in shellfish, fish, and other aquatic organisms. The results provide a theoretical basis for analyzing the complex interaction between species, environment, and physiology.

Understanding the molecular response and regulatory mechanism of endocrine regulation and physiological adaptation under environmental stimulation is important for developing early warning and protection systems related to aquatic organisms. Further research should focus on mechanisms, target analysis, and developing environmental early warning and monitoring systems to improve our understanding of how aquatic organisms respond to different environmental changes. By systematically revealing the adaptation mechanism of aquatic organisms to the environment, it can provide information for the subsequent development of sustainable aquaculture and environmental and ecological protection strategies.

Author contributions

YL: Conceptualization, Data curation, Methodology, Writing – original draft. Y-FL: Conceptualization, Methodology, Resources, Writing – original draft. MC: Investigation, Methodology, Writing – original draft. JF: Investigation, Methodology, Writing – original draft.

Conflict of interest

The authors declare that the research was conducted without any commercial or financial relationships that could potentially create a conflict of interest.

The author(s) declared that they were an editorial board member of Frontiers, at the time of submission. This had no impact on the peer review process and the final decision.

Publisher's note

frontiers | Frontiers in Marine Science

TYPE Original Research
PUBLISHED 22 March 2024
DOI 10.3389/fmars.2024.1381263

OPEN ACCESS

EDITED BY
Yiming Li,
Fishery Machinery and Instrument Research Institute, China

REVIEWED BY
Yewei Dong,
Zhongkai University of Agriculture and Engineering, China
Xueshan Li,
Jimei University, China

*CORRESPONDENCE
Kunhuang Han
hankunhuang@Foxmail.com
Weiqing Huang
07huangweiqing163.com

RECEIVED 03 February 2024
ACCEPTED 22 February 2024
PUBLISHED 22 March 2024

CITATION
Lin Z, Huang C, Zhuo Z, Xie J, Lan H, Hu B, Zhang C, Han K and Huang W (2024) Molecular cloning and characterization of three carnitine palmitoyltransferase (*cpt*) isoforms from mud crab (*Scylla paramamosain*) and their roles in respond to fasting and ambient salinity stress. *Front. Mar. Sci.* 11:1381263. doi: 10.3389/fmars.2024.1381263

Molecular cloning and characterization of three carnitine palmitoyltransferase (*cpt*) isoforms from mud crab (*Scylla paramamosain*) and their roles in respond to fasting and ambient salinity stress

Zhideng Lin[1,2], Chaoyang Huang[1], Zhengrui Zhuo[1], Jun Xie[1], Hongliang Lan[1], Bixing Hu[1], Chengkang Zhang[3], Kunhuang Han[1,2]* and Weiqing Huang[1,2]*

[1]College of Marine Science, Ningde Normal University, Ningde, China, [2]Engineering Research Center of Mindong Aquatic Product Deep-Processing, Ningde Normal University, Ningde, China, [3]College of Biological Sciences and Engineering, Ningde Normal University, Ningde, China

As rate-limiting enzymes of β-oxidation of fatty acids in mitochondria, the carnitine palmitoyltransferase (CPT) played an important role in regulating energy homeostasis of aquatic animals. However, there was very little research on β-oxidation of fatty acids in crustaceans. In the present study, the full-length cDNA sequences of *cpt-1a*, *cpt-1b* and *cpt-2* were isolated from the hepatopancreas of *Scylla paramamosain*, and contained 4206, 5303 and 3486 bp respectively. Sequence analysis showed that the CPT-1A, CPT-1B and CPT-2 encoded proteins with 777, 775 and 672 amino acids respectively, and only the CPT-1A possessed a transmembrane region. In addition, both the CPT-1B and CPT-2 contained conservative functional domains like N-terminal domain and acyltransferases choActase 2, while the CPT-1A lacked. The results of phylogenetic tree indicated that the CPT-1A, CPT-1B and CPT-2 of *S. paramamosain* gathered together with their corresponding orthologues from crustaceans. The tissue distribution exhibited that the *cpt-1a* was highly expressed in hepatopancreas, followed by muscle, eyestalk and cranial ganglia, and the muscle, eyestalk and heart were main expressed tissues of *cpt-1b*. Furthermore, the high expression levels of *cpt-2* were mainly detected in hepatopancreas, muscle and heart. The transcriptional levels of *cpt-1a*, *cpt-1b* and *cpt-2* were significantly up-regulated under chronic low salinity stress. Besides, at the acute low salinity stress condition, the expression levels of *cpt-1a*, *cpt-1b* and *cpt-2* in hepatopancreas were dramatically increased in 14‰ and 4‰ salinity groups at the 6h and 48h, while the transcriptional levels of *cpt-1a*, *cpt-1b* and *cpt-2* in muscle were signally up-regulated in 14‰ and 4‰ salinity groups at the 12h and 24h, showing an alternate response pattern. Similarly, the present study found that fasting could markedly increase the expression levels of *cpt-1a*, *cpt-1b* and *cpt-2* in hepatopancreas and muscle, especially *cpt-1a* in hepatopancreas as well as *cpt-1a* and *cpt-1b* in muscle. The results above

indicated that the *cpt-1a*, *cpt-1b* and *cpt-2* played a crucial part in providing energy for coping with fasting and salinity stress. These results would contribute to enhancing the knowledge of *cpt* phylogenetic evolution and their roles in energy metabolism of crustaceans.

KEYWORDS

β-oxidation of fatty acids, carnitine palmitoyltransferase, fasting, salinity stress, *Scylla paramamosain*

1 Introduction

Carnitine palmitoyltransferase (CPT) is a rate-limiting enzyme for β-oxidation of long-chain fatty acids in mitochondria including two subtypes CPT-1 and CPT-2, which plays an important role in maintaining energy balance of body (Bartlett and Eaton, 2004). The enzymes involved in β-oxidation of fatty acids are existed in the mitochondrial matrix, while the activated long-chain acyl-coenzyme A (CoA) in cytoplasm cannot pass freely through the mitochondrial inner membrane (Xu et al., 2017; Wang et al., 2021). The CPT-1 and CPT-2 are located in the inner and outer membrane of mitochondria respectively, and mutual collaboration participate in transport of long-chain fatty acids in mitochondria (Kerner and Hoppel, 2000). The CPT-1 can catalyze acyl groups of long-chain acyl-CoA and carnitine to form acyl carnitine, and the complex above further passed, and then the complex above passes through the inner membrane into the matrix via the carnitine-acylcarnitine translocase (De Paula et al., 2023). Ultimately, the acyl groups are separated from the hydroxyl group of carnitine to become long-chain acyl-CoA and carnitine under the catalysis of CPT-2 (Akieda et al., 2024). After entering the mitochondrial matrix, acyl CoA becomes the substrate of β-oxidation.

Currently, the study of *cpt* paid more attention to the *cpt-1*, and studies have confirmed that there were three subtypes of *cpt-1* in mammals including *cpt-1a* (Liver type), *cpt-1b* (Muscle type) and *cpt-1c* (Brain type) (Price et al., 2002; Lopes-Marques et al., 2015). There were significant differences in the expression of these three genes in different tissues. The *cpt-1a* was mainly distributed in liver, kidney and colon, the *cpt-1b* was highly expressed in skeletal muscle, heart, and testicles (McGarry and Brown et al., 1997), while the *cpt-1c* was only observed in neurons (Price et al., 2002). By contrast, *cpt-1* in teleosts only existed two subtypes, named *cpt-1a* and *cpt-1b*, which were found in *Monopterus albus* (Chao et al., 2024), *Takifugu obscurus* (Liu Q. et al., 2020), *Pelteobagrus fulvidraco* (Zheng et al., 2013), *Larimichthys crocea* (Wang et al., 2019), *Ctenopharyngodon idellus* (Shi et al., 2017), *Oreochromis niloticus* (Bayır et al., 2020), *Sparus aurata* (Boukouvala et al., 2010) and *Oncorhynchus mykiss* (Gutières et al., 2003). Besides, studies in *C. idellus* (Shi et al., 2017), *O. niloticus* (Bayır et al., 2020) and *P. fulvidraco* (Zheng et al., 2013) observed that their *cpt-1a* subtypes possessed multiple isoforms, which may be the results of the multiplication of fish genomes. The *cpt-1* of most fish was primarily high expression in tissues with high-energy requirements like liver, heart and muscle (Zheng et al., 2013; Shi et al., 2017; Wang et al., 2019; Bayır et al., 2020; Chao et al., 2024). Compared with the *cpt-1*, the *cpt-2* did not observe the presence of subtypes and there are few studies on *cpt-2* in teleosts, which was merely covered in *C. idellus* (Shi et al., 2017) and *M. albus* (Chao et al., 2024). In addition, the structure and function of *cpt-1* and *cpt-2* were still poorly understood in crustaceans and only reported in *Eriocheir sinensis* (Liu et al., 2018).

β-oxidation of fatty acids is one of the most important lipolysis reactions in animals, which is precisely regulated. The currently known regulatory mechanisms about β-oxidation of fatty acids in teleosts were mainly involved in hormone, nuclear receptor and microRNA (Dreyer et al., 1992; Esau et al., 2006; Wu et al., 2016; Ning et al., 2019). The hormone regulation primarily included insulin and glucagon, the insulin was negatively correlated with β-oxidation of fatty acids, but glucagon showed positive correlation. Peroxisome proliferation-activated receptor (PPARs) is one of the main nuclear receptors controlling lipid catabolism. Studies have found that PPARs existed three subtypes named PPARα, the PPARβ and PPARγ, and the PPARα and PPARβ subtypes played a regulatory role in promoting β-oxidation of fatty acids, while the PPARγ focused on regulating the process in β-oxidation of fatty acids (Dreyer et al., 1992; Berger and Moller, 2002). In addition, the β-oxidation of fatty acids in fish was affected by many factors including physiology (growth stage and nutriture), environment (water temperature, salinity and pollutants) and diets (lipid sources, lipid levels, carnitine, choline, betaine and vitamins) (Ning et al., 2019). In comparison, influence factors and regulatory mechanisms about β-oxidation of fatty acids in crustaceans were still unclear.

The mud crab (*Scylla paramamosain*) is an economically important crustacean. Due to large size, fast growth and special flavor, the mud crab has been widely cultured in southern China and many Indo-Pacific countries, and the production of mud crab in China was reported as 154,661 tons in 2022 (China Fishery Statistical Yearbook, 2023). Improving the energy supply of lipid decomposition can help to exert the "protein-saving effect" of lipid as well as alleviate the problems of growth inhibition, decline in stress resistance and impaired food quality caused by abnormal accumulation of lipid, thus the study of lipid catabolism in aquatic

animals has gradually become a hot spot in the current research of aquatic animal physiology. The β-oxidation of fatty acids was considered as the most important pathway of lipid catabolism in animals. However, the studies of β-oxidation of fatty acids in crustaceans were still in infancy. Therefore, in the present study, we investigated the molecular characterization of three rate-limiting enzymes of fatty acids β-oxidation (*cpt-1a*, *cpt-1b* and *cpt-2*) in mud crab and their roles in respond to fasting and ambient salinity stress. These results will contribute to providing new insights into *cpt* phylogenetic evolution and increasing the knowledge of *cpt* roles in lipid catabolism of crustaceans.

2 Materials and methods

2.1 Salinity and starvation stress experiments

The acute low salinity stress experiment was performed in the farming system of Ningde Normal University. Healthy mud crabs procured from a local crab farm in Sandu bay (Ningde, Fujian, China), were temporarily cultured for acclimatization before processing. Three salinity levels were set in the present study containing one control group (24‰ salinity) and two groups (14‰ and 4‰ salinity). Seventy-two vibrant mud crabs (average weight: 68.66 ± 1.38 g) were selected and randomly allocated into twelve polypropylene buckets (Zhongkehai, Qingdao, China). There were three treatments, each with four replicates, and each replicate with six crabs. During the experiment, the mud crabs were fed with a local bivalve mollusk (*Sinonovacula constrzcta*), and seawater was exchanged twice daily. The hepatopancreas, muscle and gill were obtained at 0, 6, 12, 24, 48 and 96 h after the salinity stress treatment, and the samples were immediately frozen in liquid nitrogen and kept in −80°C for further RNA extraction. In addition, the chronic low salinity stress experiment contained four experimental groups (22‰, 17‰, 12‰ and 7‰ salinity) and one control group (27‰ salinity), and the starvation stress experiment included starvation group (experimental group) and feeding group (control group). The crab size, design, experimental condition, and sampling of the chronic low salinity stress and starvation stress experiments have been presented in our previous study (Lin et al., 2023).

2.2 Gene cloning

As the center of lipid metabolism, the fresh hepatopancreas of mud crab was applied for isolating the total RNA by using TRNzol Universal Reagent (Tiangen, Beijing, China). After assessing integrity and purity of the total RNA, the high quality samples were reverse transcribed into first-strand cDNA by using SMART RACE cDNA Amplification kit (Clontech, USA) according to manufacturer's protocol. The obtained cDNA was stored at -20°C for further processing. Partial *cpt-1a*, *cpt-1b* and *cpt-2* cDNA sequences of mud crab were obtained from transcriptome data. Based on the partial sequences above, primers were designed for obtaining 5' and 3' untranslated region (UTR) sequence information of the *cpt-1a*, *cpt-1b* and *cpt-2* cDNA. The primes used for cloning have been shown in Table 1. Combining the touch-down PCR (first round PCR) and nested PCR (second round PCR) strategies, 5' and 3' UTR of *cpt-1a*, *cpt-1b* and *cpt-2* cDNA were obtained by 5' and 3' rapid amplification of cDNA ends (RACE) methods respectively. The amplification program and reaction system of touch-down PCR and nested PCR have been given in our previous study (Lin et al., 2023). The target fragments were separated with 1% agarose gel and purified with a TIANgel MIDI Purification Kit (Tiangen, China). The purified target fragments were further connected to pMD19-T vector (Takara, China) and sequenced by a commercial company (Tsingke, China).

2.3 Sequence and phylogenetic analysis

The identity and similarity of sequences were analyzed by using BLAST at the National Center for Biotechnology Information (http://www.ncbi.nlm.nih.gov/). The open reading frame position was predicted by using ORF Finder (https://www.ncbi.nlm.nih.gov/orffinder/). Transmembrane structure was forecasted by making use of TMHMM 2.0 (https://services.healthtech.dtu.dk/services/TMHMM-2.0/). ExPASy ProtParam tool (https://web.expasy.org/protparam/) was applied to calculate the proteic molecular mass and isoelectric point. Proteic secondary structure and structural domain were analyzed by using NPS Server (https://npsa-prabi.ibcp.fr/cgi-bin/npsa_automat.pl?page=/NPSA/npsa_sopma.html) and InterPro (https://www.ebi.ac.uk/interpro/), respectively. SignalP5.0 Server (https://services.healthtech.dtu.dk/services/SignalP-5.0/) was chosen to predict signal peptide. SWISS-MODEL (https://swissmodel.expasy.org/) was used to

TABLE 1 Names and sequences of primers used in the present study.

Primer	Sequence (5'-3')	Objective
Oligo-	AAGCAGTGGTATCAACGCAGAGTACXXXXX	First-Strand cDNA Synthesis
UPM (long)	CTAATACGACTCACTATAGGGCA AGCAGTGGTATCAACGCAGAGT	RACE-PCR
UPM (short)	CTAATACGACTCACTATAGGGC	RACE-PCR
NUP	AAGCAGTGGTATCAACGCAGAGT	RACE-PCR
β-actin F	GCCCTTCCTCACGCTATCCT	qRT-PCR
β-actin R	GCGGCAGTGGTCATCTCCT	qRT-PCR
18S rRNA F	TACCGATTGAATGATTTAGTGAGG	qRT-PCR
18S rRNA R	CTACGGAAACCTTGTTACGACTT	qRT-PCR
M13F	CGCCAGGGTTTTCCCAGTCACGAC	PCR screening
M13R	AGCGGATAACAATTTCACACAGGA	PCR screening

(Continued)

TABLE 1 Continued

Primer	Sequence (5′-3′)	Objective
For *cpt-1a* clone and qRT-PCR		
cpt-1a 3-1	GGCCGGTGTCTGATGAGGGATACG	3'RACE
cpt-1a 3-2	GTCCCAAGCCTGTGCTAGTTCCCG	3'RACE
cpt-1a 5-1	GCTTGAAGGACTTGGGTGGAGGCA	5'RACE
cpt-1a 5-2	CGCTGGCAGGAGTACAGGGAAGGCT	5'RACE
Q-cpt-1a F	CCAGGCAGGTATCAAGAGCAGC	qRT-PCR
Q-cpt-1a R	GAACTCGCACAGTGGAGAAGAGG	qRT-PCR
For *cpt-1b* clone and qRT-PCR		
cpt-1b 3-1	TGATCCATTACCATGTGGCAGGAAGGC	3'RACE
cpt-1b 3-2	GGAAGCCAGCTTGTGAAGAGAACCATG	3'RACE
cpt-1b 5-1	CAGTTGCGTGGGATCATCAGGGCTAT	5'RACE
cpt-1b 5-2	CATGTGTCACATTGGCTGCCCGAG	5'RACE
Q-cpt-1b F	AATGTGCAATGCGGTCTGTTTC	qRT-PCR
Q-cpt-1b R	ACACTTTGGGCTGGTTCCTCTAA	qRT-PCR
For *cpt-2* clone and qRT-PCR		
cpt-2 3-1	TGGCCAGCTTGATGTCACACCTGTG	3'RACE
cpt-2 3-2	AGATGGTCATGGGGGAGCAGTGTGA	3'RACE
cpt-2 5-1	GAACTCCAGCCTGCGGACAAGTTTTG	5'RACE
cpt-2 5-2	GCTTTGGGATGCGAGTGGAGTTGAA	5'RACE
Q-cpt-2 F	ACAAGGCAAATAAACACACCAGC	qRT-PCR
Q-cpt-2 R	ATGAACCTCAGAGACGACACCAA	qRT-PCR

X, undisclosed base in the proprietary SMARTer oligo sequence.

evaluate tertiary protein structure. Multiple alignments were performed using DNAMAN software. The phylogenetic tree construction was built using the software MEGA version 7.0 with confidence in the resulting phylogenetic tree branch topology measured by bootstrapping through 10000 iterations.

2.4 Quantitative real-time PCR

For tissue distribution analysis, six mud crabs (body weight: 49.50 ± 1.18 g) were purchased from a local crab farm in Sandu bay (Ningde, Fujian, China). After being anesthetized with ice, the crabs above were dissected for obtaining tissues of hepatopancreas, cranial ganglia, thoracic ganglia, eyestalk, gill, intestine, muscle and heart. Quantitative real-time PCR was applied to determine the expression levels of *cpt-1a*, *cpt-1b* and *cpt-2* in different tissues above as well as expression levels in respond to salinity and starvation stress. The TRNzol Universal Reagent (Tiangen, China) was used to extract the total RNA of samples. Then, 1 μg high-quality total RNA of each sample was applied to synthesize cDNA template with PrimeScript® RT reagent Kit with gDNA Eraser (Takara, Dalian, China), and further diluted into working fluid by adding 4 times ultra-pure water. The quantitative real-time PCR was performed in QuantStudio 3 (Thermo Fisher, USA). The procedure of quantitative real-time PCR contained a hold stage (95°C for 30 s), PCR stage (40 cycles of 95°C for 10 s and 60°C for 30 s) and melt curve stage (95°C for 15 s, 60°C for 60 s and 95°C for 15 s). The reaction system of quantitative real-time PCR executed in a total volume of 20 μL including 10 μL 2 × ChamQ Universal SYBR qPCR Master Mix (Q711-02/03, Vazyme Biotech Co., Ltd., Nanjing, China), 1.0 μL of the diluted cDNA template, 0.4 μL of each primer (10μM) and 8.2 μL of sterile distilled H_2O. The *18S rRNA* and *β-actin* were selected as reference genes. The amplification efficiency of primers was investigated by five different thinned cDNA samples and counted with formula $E = 10^{(-1/Slope)} - 1$. The amplification efficiency of primers used in the presented study was between 90% and 110%. The relative mRNA levels of target genes were calculated by $2^{-\Delta\Delta Ct}$ method (Livak and Schmittgen, 2001). The primes involved in quantitative real-time PCR have been presented in Table 1.

2.5 Statistical analysis

SPSS 20.0 software was applied to perform all statistical analysis in the present study, and *P* values less than 0.05 was deemed to be statistically significant. The results were given as means ± standard error. Independent-sample T-test was used to determine the significant differences between the feeding group and starvation group. Besides, one-way analysis of variance (ANOVA) followed by Duncan's multiple comparison test was chosen to identify the significant differences of acute and chronic salinity stress experiments as well as tissue distribution after determining the normality and homogeneity.

3 Results

3.1 Sequence analysis

The full-length cDNA sequences of *cpt-1a* (GenBank accession number PP259098), *cpt-1b* (GenBank accession number PP259102) and *cpt-2* (GenBank accession number PP259103) are 4206, 5303 and 3486 bp, respectively. Concretely, the *cpt-1a* consists of a 196 bp of 5'- UTR, 1676 bp of 3'-UTR with a poly (A) tail and 2334 bp open reading frame encoded a protein with 777 amino acids (Supplementary Figure 1). The *cpt-1b* is composed of a 117 bp of 5'-UTR, 2858 bp of 3'-UTR with a poly (A) tail and 2328 bp open

reading frame encoded a protein with 775 amino acids (Supplementary Figure 2). In addition, the *cpt-2* includes a 252 bp of 5'-UTR, 1215 bp of 3'-UTR with a poly (A) tail and 2019 bp open reading frame encoded a protein with 672 amino acids (Supplementary Figure 3). The molecular weights of CPT-1A, CPT-1B and CPT-2 proteins are 89.36, 88.16 and 75.37 kDa, respectively. The theoretical isoelectric point of CPT-1A protein is 8.86, the CPT-1B is 8.75 and the CPT-2 is 8.24.

The NPS Server prediction showed that α-helix, extended chain, random curl and β-corner together constitute the secondary structures of CPT-1A, CPT-1B and CPT-2 proteins, in which α-helix structure accounts for the largest proportion, 49.42% (CPT-1A), 48.90% (CPT-1B) and 46.28% (CPT-2), respectively. The predicted three-dimensional structures of CPT-1A, CPT-1B and CPT-2 proteins have been given in Figure 1. The SignalP 5.0 analysis showed that there are no signal peptides among the CPT-1A, CPT-1B and CPT-2. The TMHMM 2.0 predicted that the CPT-1A protein only contains a transmembrane structure (WLANLVGSVGLSFVFFVILM, 99~118 region) (Supplementary Figure 1), while the CPT-1B and CPT-2 have no transmembrane structures. In addition, the function domain prediction displayed that both the CPT-1B and CPT-2 possess typical characteristics of CPT proteins including the N-terminal domain (CPT-1B, 1~46 region; CPT-2, 48~149 region) and acyltransferases choActase 2 (CPT-1B, 455~482 region; CPT-2, 368~395 region), while the CPT-1A has no the structures of N-terminal domain and acyltransferases choActase (Figure 2).

3.2 Phylogenetic analysis

The results of phylogenetic tree exhibited that the CPT-1A and CPT-1B of *S. paramamosain* gathered together with their corresponding orthologues from crustaceans and separated from mollusks and vertebrates (mammals, birds, reptiles, amphibians and fish) (Figure 3). Concretely, the *S. paramamosain* CPT-1A first grouped into a branch with *Portunus trituberculatus* CPT-1A, and then gathered with *E. sinensis* CPT-1A into a bigger branch. Subsequently, the CPT-1A from *S. paramamosain*, *P. trituberculatus* and *E. sinensis* further clustered together with other crustaceans including *Cherax quadricarinatus*, *Procambarus clarkii*, *Penaeus japonicas*, *Penaeus monodon* and *Penaeus vannamei*. Similarly, the *S. paramamosain* CPT-1B first gathered with *P. trituberculatus* CPT-1B, and then grouped with *E. sinensis* CPT-1B. The branch above was further clustered with *Homarus americanus* CPT-1, and finally grouped with mollusks (like *Crassostrea gigas*, *Crassostrea virginica*, *Mytilus galloprovincialis* and *Pecten maximus*) into a bigger branch. In addition, the *S. paramamosain* CPT-2 gathered with the CPT-2 from crustacean group and isolated from mammals, birds, reptiles, amphibians, fish and mollusks (Figure 4). Specifically, the *S. paramamosain* CPT-2 clustered most closely with *P. trituberculatus* CPT-2, and then further gathered together with CPT-2 of *E. sinensis* and *Chionoecetes opilio*, forming a bigger branch, finally grouped with other CPT-2 from other crustaceans.

3.3 Tissue distribution

The relative expression levels of *cpt-1a*, *cpt-1b* and *cpt-2* in different tissues have been given in the Figure 5. The highest expression levels of *cpt-1a* and *cpt-2* were the hepatopancreas among all the tissues ($P < 0.05$). The muscle, eyestalk and cranial ganglia exhibited markedly higher *cpt-1a* mRNA levels than the thoracic ganglia, intestine, heart and gill ($P < 0.05$). In addition, except for hepatopancreas, the *cpt-2* was also highly expressed in the muscle when compared with the eyestalk, thoracic ganglia, intestine and gill ($P < 0.05$). By contrast, the muscle, eyestalk and heart were main sites of *cpt-1b* expression, and the muscle showed markedly higher the *cpt-1b* mRNA levels than the cranial ganglia, thoracic ganglia, intestine and gill ($P < 0.05$).

3.4 Transcriptional levels of *cpt-1a*, *cpt-1b* and *cpt-2* in response to chronic low salinity stress

The relative expression levels of *cpt-1a*, *cpt-1b* and *cpt-2* in response to chronic low salinity stress have been presented in the Figure 6. The results showed that the *cpt-1a* transcriptional level in hepatopancreas was markedly increased in the 7‰ salinity group when compared with the 27‰, 22‰, 17‰ and 12‰ salinity groups

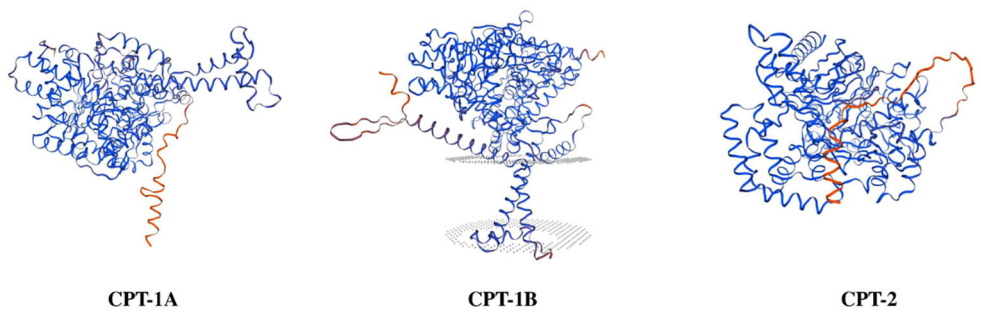

FIGURE 1
Three-dimensional structure prediction of carnitine palmitoyltransferase proteins in *Scylla paramamosain*.

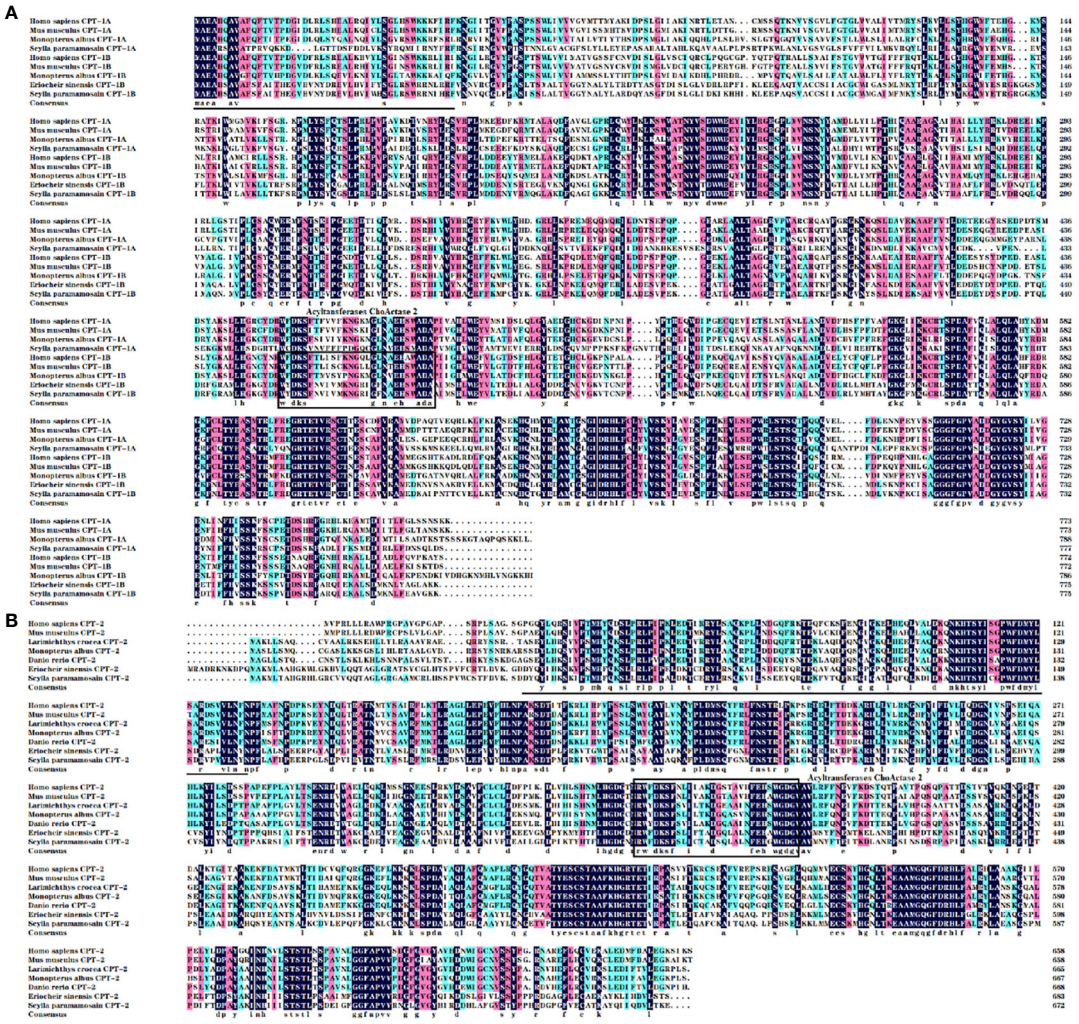

FIGURE 2
Multiple alignments of the carnitine palmitoyltransferase 1 [CPT-1; **(A)**] and CPT-2 **(B)** amino acid sequences from *Scylla paramamosain* with other species. The threshold for similarity shading was set at 50%. Identical residues are shaded black. The similarity of amino acid residues more than 75% and 50% are shaded in pink and cyan, respectively. The conserved acyltransferases ChoActase domain is marked with boxes, and the predicted N-terminal region is underlined. The sequences used for comparison are as follows: *Homo sapiens* CPT-1A (EAW74722), *Mus musculus* CPT-1A (EDL32931), *Monopterus albus* CPT-1A (WHB10902), *H. sapiens* CPT-1B (BAD96894), *M. musculus* CPT-1B (EDL04340), *M. albus* CPT-1B (WHB10903), *Eriocheir sinensis* CPT-1B (AXY87731), *H. sapiens* CPT-2 (EAX06753), *M. musculus* CPT-2 (EDL30761), *Danio rerio* CPT-2 (NP_001007448), *Larimichthys crocea* CPT-2 (TMS20131), *M. albus* CPT-2 (WHB10904), *E. sinensis* CPT-2 (AXY87732).

($P < 0.05$), and the 7‰ salinity group exhibited higher mRNA levels of *cpt-2* in hepatopancreas than the 27‰ and 22‰ salinity groups ($P < 0.05$). There were no significant differences in *cpt-1b* expression of hepatopancreas among all groups, although the 7‰, 12‰ and 17‰ salinity groups showed higher levels than the 27‰ and 22‰ salinity groups ($P > 0.05$). In addition, no significant differences were observed in *cpt-1a* transcriptional levels of muscle among all salinity groups ($P > 0.05$). Compared with the 27‰ group, the *cpt-1b* mRNA level in muscle was significantly up-regulated in the 7‰ salinity group ($P < 0.05$), and the 7‰ salinity group showed markedly higher *cpt-2* expression level than the 27‰, 22‰, 17‰ salinity groups ($P < 0.05$). Besides, the *cpt-1a* transcriptional levels in gill were markedly increased in the 7‰ and 12‰ salinity groups when compared with the 17‰ 22‰ and 27‰ salinity groups ($P < 0.05$), and 17‰ and 22‰ salinity groups also showed higher value than the 27‰ salinity group ($P < 0.05$). There were no significant differences in *cpt-1b* expression of gill among all groups ($P > 0.05$). The 7‰ salinity group had higher *cpt-2* expression levels than the 27‰, 22‰, 17‰ and 12‰ salinity groups ($P < 0.05$).

3.5 Transcriptional levels of *cpt-1a*, *cpt-1b* and *cpt-2* in response to acute low salinity stress

To investigate the transcriptional levels of *cpt-1a, cpt-1b and cpt-2* in response to acute low salinity stress, the total RNA were isolated from the hepatopancreas and muscle at different time points. The relative expression levels of *cpt-1a*, *cpt-1b* and *cpt-2* of hepatopancreas in response to acute low salinity stress have been presented in the Figure 7. Compared with the 24‰ salinity group (control group), the transcriptional levels of *cpt-1a* and *cpt-2* in

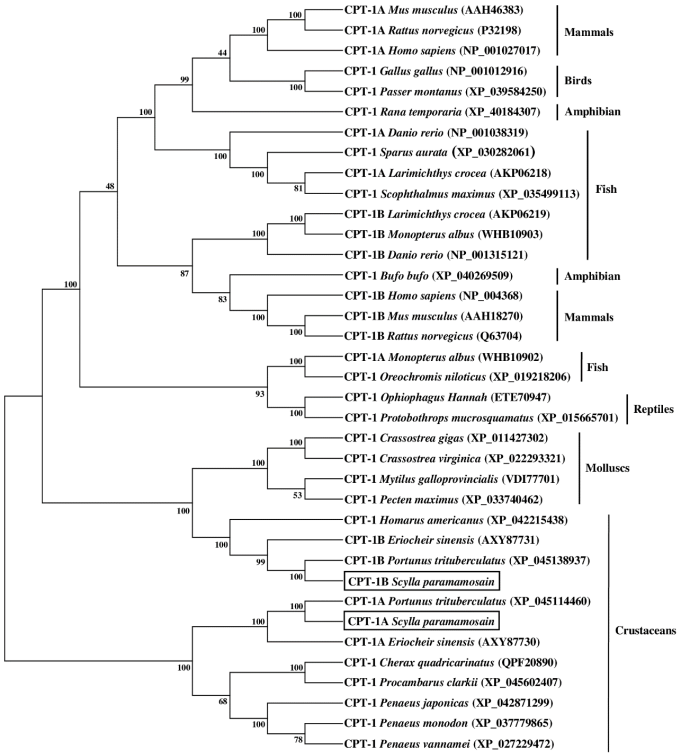

FIGURE 3
Neighbor-joining phylogenetic tree of representative vertebrate and invertebrate carnitine palmitoyltransferase 1 (CPT-1) amino acid sequences. The tree was constructed using the neighbor joining method with MEGA 7.0. The horizontal branch length is proportional to amino acid substitution rate per site. Numbers represent the frequencies with which the tree topology presented was replicated after 1000 bootstrap iterations.

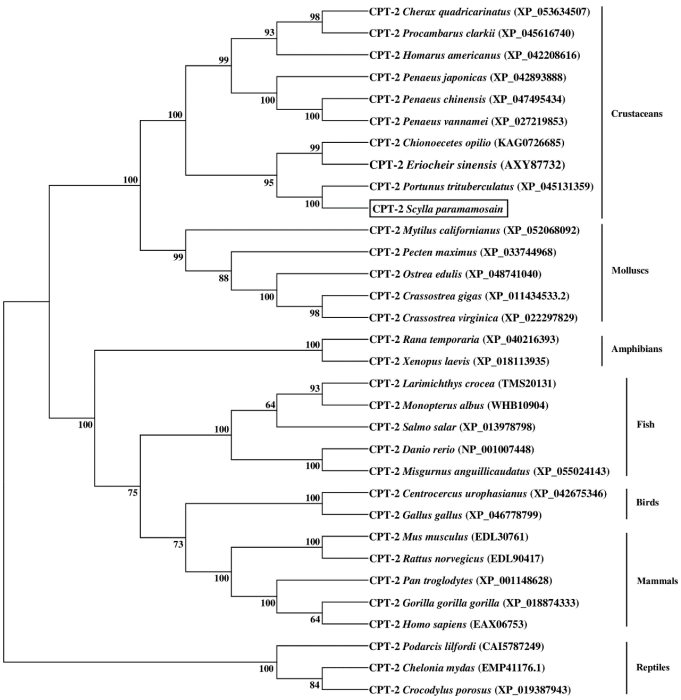

FIGURE 4
Neighbor-joining phylogenetic tree of representative vertebrate and invertebrate carnitine palmitoyltransferase 2 (CPT-2) amino acid sequences. The tree was constructed using the neighbor joining method with MEGA 7.0. The horizontal branch length is proportional to amino acid substitution rate per site. Numbers represent the frequencies with which the tree topology presented was replicated after 1000 bootstrap iterations.

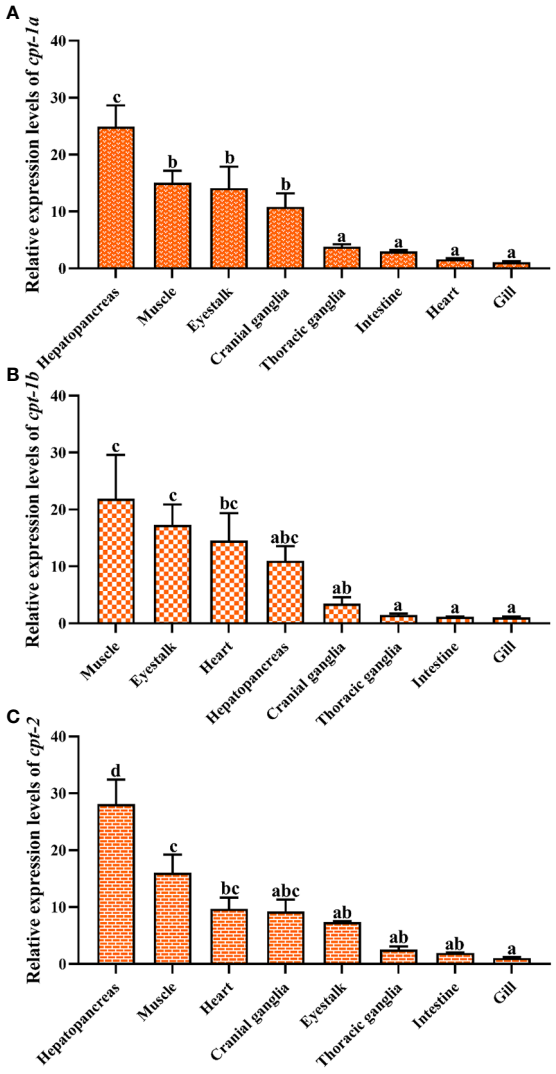

FIGURE 5
Relative expression levels of carnitine palmitoyltransferase (*cpt*) in different tissues of *Scylla paramamosain*. **(A)**: tissue distribution of *cpt-1a*; **(B)**: tissue distribution of *cpt-1b*; **(C)**: tissue distribution of *cpt-2*. Vertical bars represented mean ± standard error of the mean (n = 6) for each tissue. Letters show significant differences ($P < 0.05$) among tissues as determined by one-way ANOVA followed by Duncan's multiple comparison test.

hepatopancreas were up-regulated in the 14‰ and 4‰ salinity groups at 6 h and 48 h, and the 4‰ salinity group showed markedly higher mRNA levels than the 24‰ salinity group ($P < 0.05$). There were no significant differences in *cpt-1a* and *cpt-2* expression of hepatopancreas among the 24‰, 14‰ and 4‰ salinity groups at the other time points ($P > 0.05$). Similarly, the 14‰ and 4‰ salinity groups also exhibited higher mRNA levels of *cpt-1b* in hepatopancreas than the 24‰ salinity group at 48 h, while only the 4‰ and 24‰ salinity groups showed significant differences ($P < 0.05$). In addition, there were no significant differences in *cpt-1b* expression of hepatopancreas among the 24‰, 14‰ and 4‰ salinity groups at the other time points ($P > 0.05$), although the mRNA levels of *cpt-1b* in 24‰ salinity group was lower than the 14‰ and 4‰ salinity groups at 6 h.

The relative expression levels of *cpt-1a*, *cpt-1b* and *cpt-2* of muscle in response to acute low salinity stress have been presented in the Figure 8. Compared with the 24‰ salinity group, the transcriptional levels of *cpt-1a* and *cpt-2* in muscle were up-regulated in the 14‰ and 4‰ salinity groups at 12 h and 24 h, while only the expression levels of *cpt-2* in 4‰ salinity group showed significant differences with the 24‰ salinity group at 12 h ($P < 0.05$). Likewise, the *cpt-1b* expression levels of muscle in 24‰ salinity group were also lower than the 14‰ and 4‰ salinity groups at the 12 h and 24 h, and the 4‰ salinity group showed markedly higher mRNA levels than the 24‰ salinity group ($P < 0.05$).

3.6 Transcriptional levels of *cpt-1a*, *cpt-1b* and *cpt-2* in response to starvation stress

The relative expression levels of *cpt-1a*, *cpt-1b* and *cpt-2* of hepatopancreas and muscle in response to starvation stress have been shown in the Figure 9. Compared with the feeding group, the transcriptional levels of *cpt-1a*, *cpt-1b* and *cpt-2* in hepatopancreas were markedly up-regulated in the starvation group ($P < 0.05$), especially *cpt-1a* showing an extremely significant difference ($P < 0.01$). In addition, the expression levels of *cpt-1a*, *cpt-1b* and *cpt-2* in muscle of starvation group were also significantly higher than those in the feeding group ($P < 0.05$), and the *cpt-1a* and *cpt-1b* exhibited a highly significant difference ($P < 0.01$).

4 Discussion

With the rapid intensive development of aquaculture industry, increasing lipid utilization for saving dietary protein and reducing the negative effects of abnormal lipid deposition have become the needs for the healthy development of the industry (Bu et al., 2023). Therefore, the study of lipid metabolism in aquatic animals, especially lipid catabolism, is a research hotspot of nutritional physiology at present. The lipid catabolism is mainly achieved through the β-oxidation of fatty acids in peroxisome and mitochondria. Currently, the studies about β-oxidation of fatty acids in aquatic animals were more focused on fish, while few were reported in crustaceans (Lavarías et al., 2009; Liu et al., 2018).

The CPT, as rate-limiting enzymes, included CPT-1 and CPT-2 subtypes, which played critical roles in the β-oxidation of fatty acids in mitochondria (Kerner and Hoppel, 2000; Bayır et al., 2020). In the present study, the full-length cDNA sequences of three *cpt* isoforms were successfully cloned from the hepatopancreas of mud crab. Sequence analysis showed that the three genes were *cpt-1a*, *cpt-1b* and *cpt-2* subtypes respectively. Previous studies have indicated that the *cpt-1a* existed the phenomenon of genome replication such as *P. fulvidraco* (Zheng et al., 2013), *O. niloticus* (Bayır et al., 2020), *C. idellus* (Shi et al., 2017) and *Synechogobius hasta* (Wu et al., 2016), while this phenomenon was not found in the present study, meanwhile, *cpt-1c* was also not observed. These results were in lined with the studies of *E. sinensis* (Liu et al., 2018) and *M. albus* (Chao et al., 2024), which only found three *cpt* isoforms named *cpt-1a*, *cpt-1b* and *cpt-2*. The *cpt-1a*, *cpt-1b* and *cpt-2* subtypes of mud

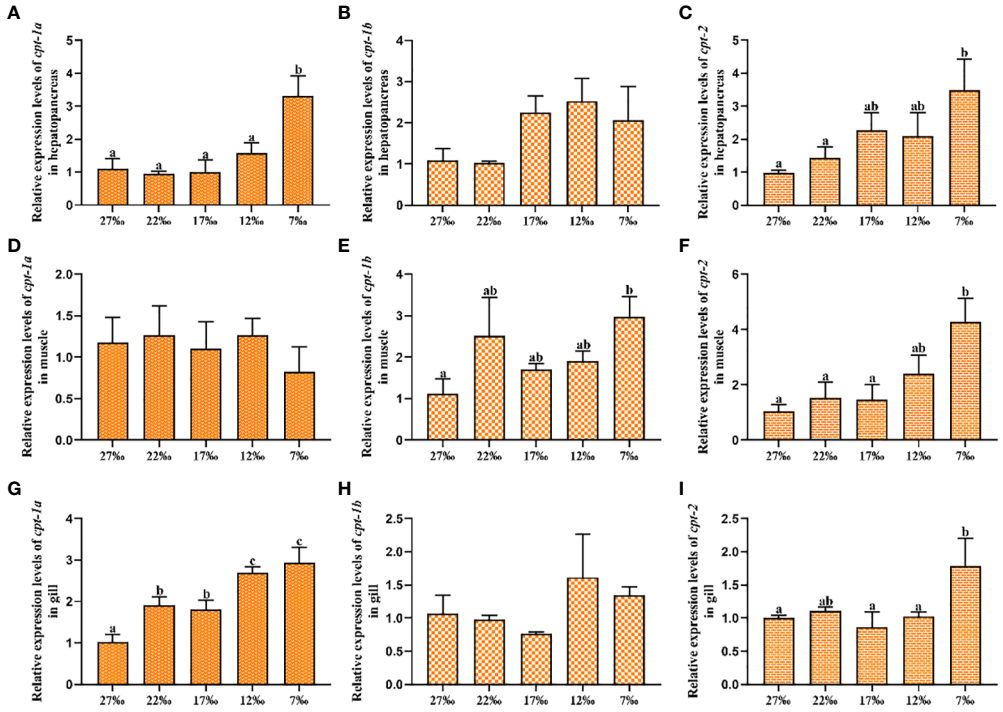

FIGURE 6
Relative expression levels of carnitine palmitoyltransferase (*cpt*) in hepatopancreas, muscle and gill of *Scylla paramamosain* in response to chronic salinity stress. **(A–C)**: *cpt-1a*, *cpt-1b* and *cpt-2* expression in hepatopancreas; **(D–F)**: *cpt-1a*, *cpt-1b* and *cpt-2* expression in muscle; **(G–I)**: *cpt-1a*, *cpt-1b* and *cpt-2* expression in gill. Bars with different superscripts are significantly different ($P < 0.05$, one-way ANOVA and Duncan's multiple comparison test). Numerical values refer to seawater salinity.

crab encoded 777, 775 and 672 amino acids respectively and these sequences of amino acids showed high similarity with mammals, fish and crustaceans, which indicated that CPT-1A, CPT-1B and CPT-2 were conserved among different species. Studies in mammals observed that the CPT-1 possessed two transmembrane structures (Bonnefont et al., 2004; Jogl et al., 2004). Similarly, Liu et al. (2018) reported that both the CPT-1A and CPT-1B of *E. sinensis* contained two transmembrane regions. However, the present study found that the CPT-1A of mud crab only possessed a transmembrane region and CPT-1B had no transmembrane structure, and the reason may be related to the mutation of key amino acids in genome replication. In addition, the CPT-2 of mud crab did not contain transmembrane structures possibly because it primarily played a catalytic role within the membrane. Similar results were also found in *E. sinensis* (Liu et al., 2018) and *M. albus* (Chao et al., 2024).

Studies in mammals and teleosts have indicated that the CPT-1 existed a N-terminal domain (residues 1~150), which played important roles in regulating catalytic activity and malonyl-CoA sensitivity (Cohen et al., 1998; Bonnefont et al., 2004; Jogl et al., 2004; Zheng et al., 2013; Chao et al., 2024). The present study showed that the CPT-1B of mud crab also possessed the conserved N-terminal domain, while the CPT-1A lacked the structure. Consistently, Liu et al. (2018) found that the CPT-1A of *E. sinensis* contained the N-terminal domain and the CPT-1B was absent. In addition, previous studies observed that the *E. sinensis* (Liu et al., 2018), *C. idellus* (Shi et al., 2017) and *M. albus* (Chao et al., 2024) have no N-terminal domain in CPT-2. Intriguingly, we found the CPT-2 of mud crab included a N-terminal domain in the present study, suggesting that the CPT-2 structure of mud crab was different from other species. As transporting sites of medium-chain acyl-CoA, both the CPT-1B and CPT-2 of mud crab contained an acyltransferases choActase 2 domain, while the CPT-1A was not observed. These results were consistent with the study of Liu et al. (2018), who found that both the CPT-1B and CPT-2 of *E. sinensis* possessed acyltransferases choActase domain, and the CPT-1A lacked. Besides, Chao et al. (2024) showed that all the CPT-1A, CPT-1B and CPT-2 of *M. albus* contained the acyltransferases choActase domain, and except in CPT-1B, CPT-1 peptides of *C. idellus* included acyltransferases choActase domain (Shi et al., 2017). The CPT-1A of mud crab above did not possess the structures of N-terminal domain and acyltransferases choActase, indicating that the CPT-1A may be not necessary for uptake of fatty acids in mitochondria of mud crab. The results of phylogenetic tree exhibited that the CPT-1A, CPT-1B and CPT-2 gathered together with their corresponding crustacean orthologues, which further supported the genes isolated in the present study belonged to the *cpt* family.

To determine the tissue distribution, it was of great significance for investigating physiological functions of genes. In mammals, there were three subtypes of *cpt-1* including *cpt-1a*, *cpt-1b* and *cpt-1c*, and their expression in tissues showed tissue specificity (Price et al., 2002; Lopes-Marques et al., 2015). The *cpt-1a* was highly expressed in liver and kidney, the *cpt-1b* was mainly distributed in skeletal muscle and heart, and the *cpt-1c* was only detected in neurons (McGarry and Brown, 1997; Price et al., 2002). Compared with the mammals, the *cpt-1* of teleosts merely possessed two

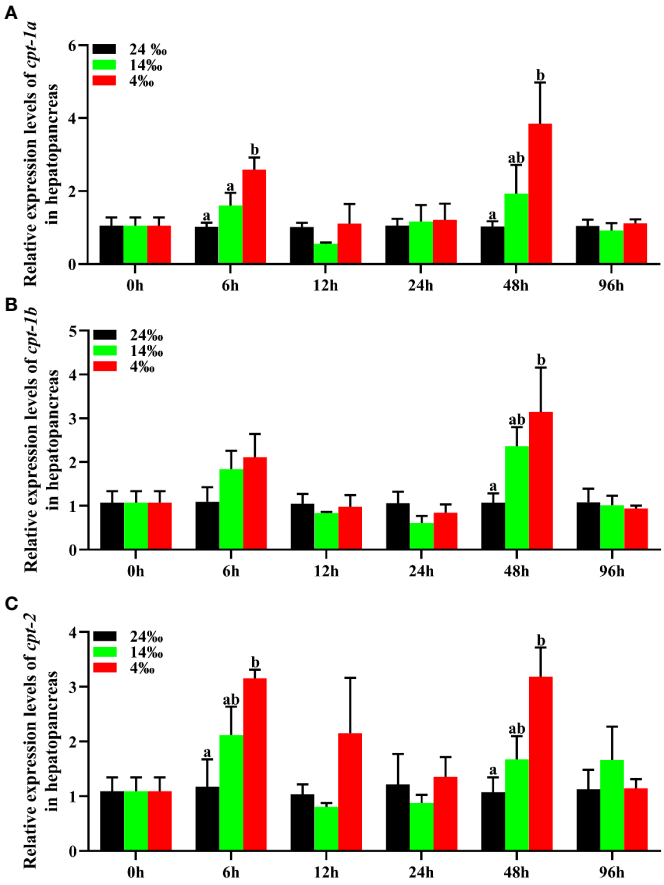

FIGURE 7
Relative expression levels of carnitine palmitoyltransferase (*cpt*) in hepatopancreas of *Scylla paramamosain* in response to acute salinity stress. **(A)**: *cpt-1a* expression in hepatopancreas; **(B)**: *cpt-1b* expression in hepatopancreas; **(C)**: *cpt-2* expression in hepatopancreas. Total RNA was extracted from hepatopancreas of *S. paramamosain* at different time points after 24‰, 14‰ and 4‰ salinity stress, respectively. Samples challenged with 24‰ salinity were adopted as control. Significance was compared between the experimental groups and the control group at the same time point. Bars with different superscripts are significantly different ($P < 0.05$, one-way ANOVA and Duncan's multiple comparison test).

subtypes named *cpt-1a* and *cpt-1b*. In addition, the *cpt-1a* of fish existed multiple isoforms, and different fish exhibited different expression profiles. Studies indicated that the *cpt-1a* of fish was mainly expressed in liver, muscle and heart (Zheng et al., 2013; Wu et al., 2016), and the *cpt-1b* was primarily distributed in white muscle, heart and adipose tissues (Shi et al., 2017; Chao et al., 2024). In the present study, the hepatopancreas showed markedly higher expression levels of *cpt-1a* than other tissues. This result was in accordance with the study of Liu et al. (2018), who reported that the *cpt-1a* of male and female *E. sinensis* was chiefly distributed in hepatopancreas compared with other tissues. The hepatopancreas of crustaceans has been regarded as center of lipid metabolism, which was akin to fat body in insects and liver in vertebrates (Wen et al., 2001). The present results may suggest that the *cpt-1a* play an important role in lipolysis of hepatopancreas in mud crab. Besides, the present study found that the muscle, eyestalk and heart were main sites of *cpt-1b* expression, which may indicate that the *cpt-1b* involved in β-oxidation of fatty acids in these tissues. Consistently, study in *E. sinensis* indicated that the *cpt-1b* was mainly expressed in muscle and heart (Liu et al., 2018). Similar results were also observed in *M. albus* (Chao et al., 2024), *P. fulvidraco* (Zheng et al., 2013), *S. aurata* (Boukouvala et al., 2010) and *C. idellus* (Shi et al., 2017). The results above suggested that the *cpt-1a* and *cpt-1b* of mud crab may belonged to liver and muscle isoforms, respectively. There were relatively few studies about *cpt-2*. The present study showed that the highest expression level of *cpt-2* was the hepatopancreas among all the tissues, which was similar to *cpt-1a*. This result was in in agreement with the studies of *E. sinensis* (Liu et al., 2018), while Chao et al. (2024) and Shi et al. (2017) reported that the *cpt-2* of *C. idellus* and *M. albus* was highly expressed in heart and stomach, respectively. The high expression of *cpt-2* in hepatopancreas further supported that the *cpt* played a vital role in β-oxidation of fatty acids in hepatopancreas of mud crab.

Based on the important functions of β-oxidation of fatty acids in energy homeostasis, numerous studies have been performed to determine the regulatory mechanisms and influence factors of the β-oxidation of fatty acids in teleost (Gutières et al., 2003; Boukouvala et al., 2010; Zheng et al., 2013; Bayır et al., 2020; Li et al., 2020; Liu Q. et al., 2020; Liu Y. et al., 2020). The findings showed that the regulatory mechanisms primarily involved in the malonyl-CoA, hormone, nuclear receptor and microRNA, and the influence factors mainly included physiology, environment and diets (Bonnefont et al., 2004;

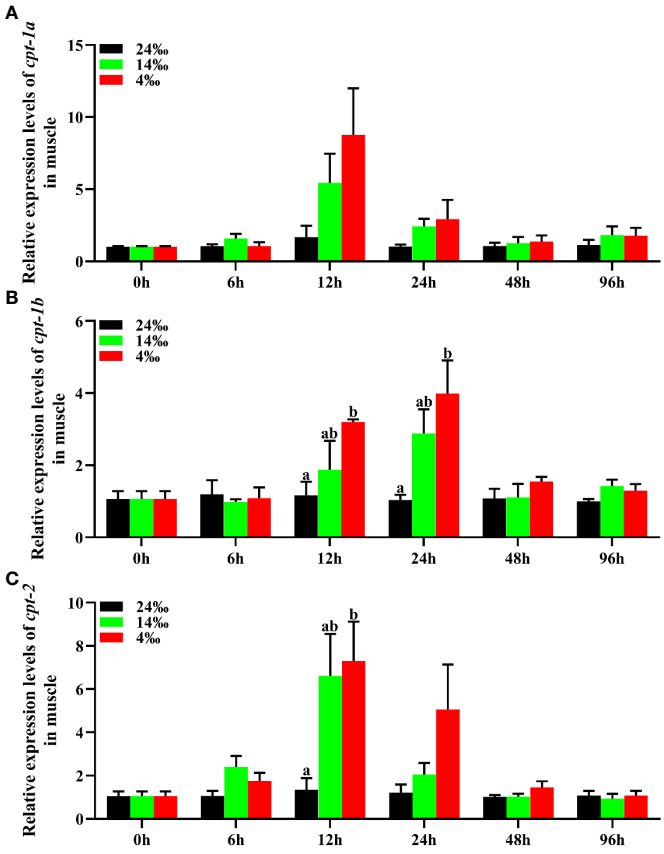

FIGURE 8
Relative expression levels of carnitine palmitoyltransferase (*cpt*) in muscle of *Scylla paramamosain* in response to acute salinity stress. **(A)**: *cpt-1a* expression in muscle; **(B)**: *cpt-1b* expression in muscle; **(C)**: *cpt-2* expression in muscle. Total RNA was extracted from muscle of *S. paramamosain* at different time points after 24‰, 14‰ and 4‰ salinity stress, respectively. Samples challenged with 24‰ salinity were adopted as control. Significance was compared between the experimental groups and the control group at the same time point. Bars with different superscripts are significantly different ($P < 0.05$, one-way ANOVA and Duncan's multiple comparison test).

Morash and McClelland, 2011; Ning et al., 2019; Li et al., 2020). By contrast, the studies about oxidation of fatty acids in crustaceans were still in infancy, which was only reported in *E. sinensis*, and the results found that the blend vegetable oil (soybean oil: rapeseed oil, 1: 1) instead of fish oil could markedly up-regulated the expression levels of *cpt-1a*, *cpt-1b* and *cpt-2* in hepatopancreas of *E. sinensis* (Liu et al., 2018). Salinity stress and food shortages are two important factors that aquatic animals often need to confront, and this process is closely related to energy metabolism. Therefore, in the present study, we investigated the roles of *cpt-1a*, *cpt-1b* and *cpt-2* in coping with

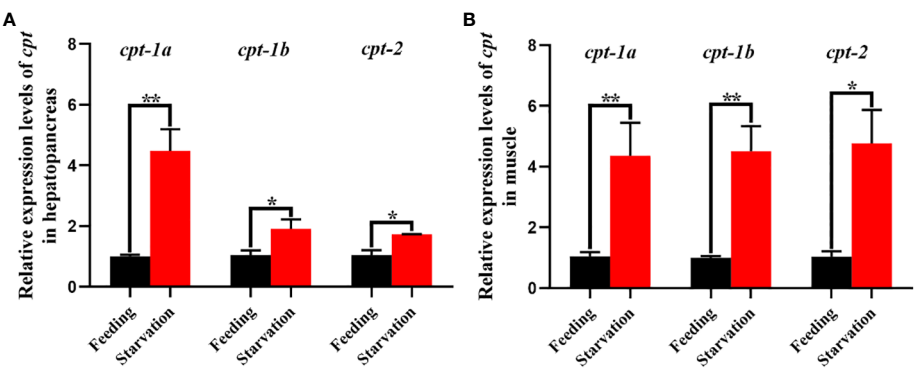

FIGURE 9
Relative expression levels of carnitine palmitoyltransferase (*cpt*) in hepatopancreas and muscle of *Scylla paramamosain* in response to starvation stress. **(A)**: *cpt-1a, cpt-1b* and *cpt-2* expression in hepatopancreas; **(B)**: *cpt-1a, cpt-1b* and *cpt-2* expression in muscle. Asterisks indicated significant differences between feeding group and starvation group (*$P < 0.05$ and **$P < 0.01$).

starvation and ambient salinity stress. The results of acute low salinity stress showed that the transcriptional levels of *cpt-1a*, *cpt-1b* and *cpt-2* in hepatopancreas were markedly increased in 14‰ and 4‰ groups at the 6 h and 48 h, while the mRNA levels of these three genes in muscle were markedly up-regulated in 14‰ and 4‰ groups at the 12 h and 24 h. These results indicated that the *cpt-1a*, *cpt-1b* and *cpt-2* of hepatopancreas in mud crab responded to acute salinity stress earlier than muscle, and hepatopancreas and muscle showed an alternate response pattern. Similar results were also observed in the findings of Hong et al. (2019) and Zeng et al. (2004), who found that the expression of *cpt* was significantly increased under the condition of acute salinity stress. Consistently, the *cpt-1a*, *cpt-1b* and *cpt-2* of mud crab were also significantly increased under chronic salinity conditions. The results above suggested that the *cpt-1a*, *cpt-1b* and *cpt-2* of mud crab played an important role in providing energy for coping with salinity stress. As for most animals in the starvation period, especially the long-term starvation period, fatty acids are the main source of energy, and the animals meet the energy demand through regulating β-oxidation of fatty acids. Studies found that the *cpt-1a* expression levels of *L. crocea* and *S. hasta* were extremely up-regulated after fasting (Wang et al., 2019; Zhou et al., 2021), and Arslan et al. (2020) reported that starvation could markedly increase the transcriptional level of *cpt-1b* in *Salmo trutta*. In addition, fasting gave rise to a significant increase of CPT-1 enzymatic activity in liver of *O. mykiss* (Morash and McClelland, 2011). Similarly, the present study exhibited that the expression levels of *cpt-1a*, *cpt-1b* and *cpt-2* in hepatopancreas and muscle were significantly up-regulated after fasting. In addition, the expression levels of *cpt-1a* in hepatopancreas as well as *cpt-1a* and *cpt-1b* in muscle showed more significant differences, indicating their important roles in β-oxidation of fatty acids in hepatopancreas and muscle during fasting, which also further supported the results of tissue distribution.

5 Conclusion

The full-length cDNA sequences of *cpt-1a*, *cpt-1b* and *cpt-2* were isolated from the hepatopancreas of mud crab using the RACE technology in the present study, and this was first time to obtain complete sequences in crustaceans. Subsequently, we identified the homology, structural characteristics and phylogenetic tree of CPT-1A, CPT-1B and CPT-2, and compared the expression discrepancy of *cpt-1a*, *cpt-1b* and *cpt-2* in different tissues. Finally, based on their functions in regulating energy homeostasis, the present study further systematically investigated the roles of *cpt-1a*, *cpt-1b* and *cpt-2* in response to fasting and salinity stress. These results were conducive to increasing the knowledge of *cpt* phylogenetic evolution as well as their roles in energy metabolism of crustaceans.

Data availability statement

The original contributions presented in the study are included in the article/Supplementary Material. Further inquiries can be directed to the corresponding authors.

Ethics statement

The animal study was approved by The Committee on the Ethics of Animal Experiments of Ningde Normal University (NDNU-LL-202308). The study was conducted in accordance with the local legislation and institutional requirements.

Author contributions

ZL: Writing – review and editing, Writing – original draft, Formal analysis, Data curation. CH: Writing – original draft, Methodology, Investigation, Formal analysis. ZZ: Writing – original draft, Methodology, Investigation, Formal analysis. JX: Writing – original draft, Methodology, Investigation, Formal analysis. HL: Writing – original draft, Methodology, Investigation, Formal analysis. BH: Writing – original draft, Methodology, Investigation, Formal analysis. CZ: Writing – original draft, Methodology. KH: Writing – original draft, Funding acquisition, Data curation, Conceptualization. WH: Writing – original draft, Funding acquisition, Data curation, Conceptualization.

Funding

The author(s) declare financial support was received for the research, authorship, and/or publication of this article. This study was supported by the Natural Science Foundation of Fujian Province, China (Grant number 2022J05273), Scientific Research Foundation of Ningde Normal University (Grant number 2022Y04, 2023ZX505), the United Front Special project of Good Strategies for the Construction of New Fujian (Grant number JAT22118) and the Innovation and Entrepreneurship Training Program for Undergraduate of Ningde Normal University (Grant number X202310398004).

Conflict of interest

The authors declare that the research was conducted in the absence of any commercial or financial relationships that could be construed as a potential conflict of interest.

Publisher's note

Supplementary material

The Supplementary Material for this article can be found online at: https://www.frontiersin.org/articles/10.3389/fmars.2024.1381263/full#supplementary-material

References

Akieda, K., Takegawa, K., Ito, T., Nagayama, G., Yamazaki, N., Nagasaki, Y., et al. (2024). Unique behavior of bacterially expressed rat carnitine palmitoyltransferase 2 and its catalytic activity. *Biol. Pharm. Bull.* 47, 23–27. doi: 10.1248/bpb.b23-00612

Arslan, G., Bayır, M., Yağanoğlu, A. M., and Bayır, A. (2020). Changes in fatty acids, blood biochemistry and mRNA expressions of genes involved in polyunsaturated fatty acid metabolism in brown trout (*Salmo trutta*) during starvation and refeeding. *Aquac. Res.* 52, 494–504. doi: 10.1111/are.14908

Bartlett, K., and Eaton, S. (2004). Mitochondrial β-oxidation. *Eur. J. Biochem.* 271, 462–469. doi: 10.1046/j.1432-1033.2003.03947.x

Bayır, M., Arslan, G., and Bayır, A. (2020). Identification and characterization of carnitine palmitoyltransferase 1 (*cpt 1*) genes in nile tilapia, *oreochromis niloticus*. Evol. *Bioinform.* 16, 1–7. doi: 10.1177/117693432091325

Berger, J., and Moller, D. E. (2002). The mechanisms of action of PPARs. *Annu. Rev. Med.* 53, 409–435. doi: 10.1146/annurev.med.53.082901.104018

Bonnefont, J., Djouadi, F., Prip-Buus, C., Gobin, S., Munnich, A., and Bastin, J. (2004). Carnitine palmitoyltransferases 1 and 2: biochemical, molecular and medical aspects. *Mol. Aspects Med.* 25, 495–520. doi: 10.1016/j.mam.2004.06.004

Boukouvala, E., Leaver, M. J., Favre-Krey, L., Theodoridou, M., and Krey, G. (2010). Molecular characterization of a gilthead sea bream (*Sparus aurata*) muscle tissue cDNA for carnitine palmitoyltransferase 1B (CPT1B). *Comp. Biochem. Phys. B.* 157, 189–197. doi: 10.1016/j.cbpb.2010.06.004

Bu, X., Li, Y., Lai, W., Yao, C., Liu, Y., Wang, Z., et al. (2023). Innovation and development of the aquaculture nutrition research and feed industry in China. *Rev. Aquacult*, 1–16. doi: 10.1111/raq.12865

Chao, B., Chen, X., Huang, S., Zhou, Q., Xiong, L., and Zhang, Y. (2024). Cloning and tissue distribution analysis of swamp eel (*Monopterus albus*) carnitine palmyltransferase gene. *Genomics Appl. Biol.*, 1–16.

China Fishery Statistical Yearbook (2023). *China fishery statistical yearbook* (Beijing, China: China Agriculture Press), 28.

Cohen, I., Kohl, C., McGarry, J. D., Girard, J., and Prip-Buus, C. (1998). The N-terminal domain of rat liver carnitine palmitoyltransferase 1 mediates import into the outer mitochondrial membrane and is essential for activity and malonyl-CoA sensitivity. *J. Biol. Chem.* 273, 29896–29904. doi: 10.1074/jbc.273.45.29896

De Paula, I. F., Santos-Araujo, S., Majerowicz, D., Ramos, I., and Gondim, K. C. (2023). Knockdown of carnitine palmitoyltransferase I (CPT1) reduces fat body lipid mobilization and resistance to starvation in the insect vector *Rhodnius prolixus*. Front. *Physiol.* 14. doi: 10.3389/fphys.2023.1201670

Dreyer, C., Krey, G., Keller, H., Givel, F., Helftenbein, G., and Wahli, W. (1992). Control of the peroxisomal β-oxidation pathway by a novel family of nuclear hormone receptors. *Cell.* 68, 879–887. doi: 10.1016/0092-8674(92)90031-7

Esau, C., Davis, S., Murray, S. F., Yu, X. X., Pandey, S. K., Pear, M., et al. (2006). miR-122 regulation of lipid metabolism revealed by *in vivo* antisense targeting. *Cell Metab.* 3, 87–98. doi: 10.1016/j.cmet.2006.01.005

Gutières, S., Damon, M., Panserat, S., Kaushik, S., and Médale, F. (2003). Cloning and tissue distribution of a carnitine palmitoyltransferase I gene in rainbow trout (*Oncorhynchus mykiss*). *Comp. Biochem. Phys. B.* 135, 139–151. doi: 10.1016/S1096-4959(03)00074-5

Hong, M., Li, N., Li, J., Li, W., Liang, L., Li, Q., et al. (2019). Adenosine monophosphate-activated protein kinase signaling regulates lipid metabolism in response to salinity stress in the red-eared slider turtle *Trachemys scripta elegans*. *Front. Physiol.* 10. doi: 10.3389/fphys.2019.00962

Jogl, G., Hsiao, Y. S., and Tong, L. (2004). Structure and function of carnitine acyltransferases. *Ann. New York Acad. Sci.* 1033, 17–29. doi: 10.1196/annals.1320.002

Kerner, J., and Hoppel, C. (2000). Fatty acid import into mitochondria. *BBA-Mol. Cell Biol. L.* 1486, 1–17. doi: 10.1016/S1388-1981(00)00044-5

Lavarías, S., Pasquevich, M. Y., Dreon, M. S., and Heras, H. (2009). Partial characterization of a malonyl-CoA-sensitive carnitine O-palmitoyltransferase I from *Macrobrachium borellii* (Crustacea: Palaemonidae). *Comp. Biochem. Phys. B.* 152, 364–369. doi: 10.1016/j.cbpb.2009.01.004

Li, L., Li, J., Ning, L., Lu, D., Luo, Y., Ma, Q., et al. (2020). Mitochondrial fatty acid β-Oxidation inhibition promotes glucose utilization and protein deposition through energy homeostasis remodeling in fish. *J. Nutr.* 150, 2322–2335. doi: 10.1093/jn/nxaa187

Lin, Z., Wu, Z., Huang, C., Lin, H., Zhang, M., Chen, M., et al. (2023). Cloning and expression characterization of elongation of very long-chain fatty acids protein 6 (*elovl6*) with dietary fatty acids, ambient salinity and starvation stress in *Scylla paramamosain*. Front. *Physiol.* 14. doi: 10.3389/fphys.2023.1221205

Liu, Y., Han, S., Luo, Y., Li, L., Chen, L., Zhang, M., et al. (2020). Impaired peroxisomal fat oxidation induces hepatic lipid accumulation and oxidative damage in Nile tilapia. *Fish Physiol. Biochem.* 46, 1229–1242. doi: 10.1007/s10695-020-00785-w

Liu, Q., Liao, Y., Wu, Y., Xu, M., Sun, Z., and Ye, C. (2020). Cloning and characterization of carnitine palmitoyltransferase Iα (*CPT1α*) from obscure puffer (*Takifugu obscurus*), and its gene expression in response to different lipid sources. *Aquacult. Rep.* 18, 100424. doi: 10.1016/j.aqrep.2020.100424

Liu, L., Long, X., Deng, D., Cheng, Y., and Wu, X. (2018). Molecular characterization and tissue distribution of carnitine palmitoyltransferases in Chinese mitten crab *Eriocheir sinensis* and the effect of dietary fish oil replacement on their expression in the hepatopancreas. *PloS One* 13, e0201324. doi: 10.1371/journal.pone.0201324

Livak, K. J., and Schmittgen, T. D. (2001). Analysis of relative gene expression data using real-time quantitative PCR and the $2^{-\Delta\Delta CT}$ Method. *Methods.* 25, 402–408. doi: 10.1006/meth.2001.1262

Lopes-Marques, M., Delgado, I. L. S., Ruivo, R., Torres, Y., Sainath, S. B., Rocha, E., et al. (2015). The origin and diversity of *Cpt1* genes in vertebrate species. *PloS One* 10, e0138447. doi: 10.1371/journal.pone.0138447

McGarry, J. D., and Brown, N. F. (1997). The mitochondrial carnitine palmitoyltransferase system-Fom concept to molecular analysis. *Eur. J. Biochem.* 244, 1–14. doi: 10.1111/j.1432-1033.1997.00001.x

Morash, A. J., and McClelland, G. B. (2011). Regulation of carnitine palmitoyltransferase (CPT) I during fasting in rainbow trout (*Oncorhynchus mykiss*) promotes increased mitochondrial fatty acid oxidation. *Physiol. Biochem. Zool.* 84, 625–633. doi: 10.1086/662552

Ning, L., Li, J., Sun, S., and Du, Z. (2019). Fatty acid β-oxidation in fish: a review. *J. Fisheries China.* 43, 128–142. doi: 10.11964/jfc.20181211589

Price, N. T., van der Leij, F. R., Jackson, V. N., Corstorphine, C. G., Thomson, R., Sorensen, A., et al. (2002). A novel brain-expressed protein related to carnitine palmitoyltransferase I. *Genomics.* 80, 433–442. doi: 10.1006/geno.2002.6845

Shi, X., Sun, J., Yang, Z., Li, X., Ji, H., Li, Y., et al. (2017). Molecular characterization and nutritional regulation of carnitine palmitoyltransferase (CPT) family in grass carp (*Ctenopharyngodon idellus*). *Comp. Biochem. Phys. B.* 203, 11–19. doi: 10.1016/j.cbpb.2016.08.006

Wang, C., Si, L., Li, W., and Zheng, J. (2019). A functional gene encoding carnitine palmitoyltransferase 1 and its transcriptional and kinetic regulation during fasting in large yellow croaker. *Comp. Biochem. Phys. B.* 231, 26–33. doi: 10.1016/j.cbpb.2019.01.015

Wang, M., Wang, K., Liao, X., Hu, H., Chen, L., Meng, L., et al. (2021). Carnitine palmitoyltransferase system: a new target for anti-inflammatory and anticancer therapy? *Front. Pharmacol.* 12. doi: 10.3389/fphar.2021.760581

Wen, X., Chen, L., Ai, C., Zhou, Z., and Jiang, H. (2001). Variation in lipid composition of Chinese mitten-handed crab, *Eriocheir sinensis* during ovarian maturation. *Comp. Biochem. Phys. B.* 130, 95–104. doi: 10.1016/S1096-4959(01)00411-0

Wu, K., Zheng, J.-L., Luo, Z., Chen, Q.-L., Zhu, Q.-L., and Wei, H. (2016). Carnitine palmitoyltransferase I gene in *Synechogobius hasta*: Cloning, mRNA expression and transcriptional regulation by insulin *in vitro*. *Gene.* 576, 429–440. doi: 10.1016/j.gene.2015.10.055

Xu, Y., Luo, Z., Wu, K., Fan, Y., You, W., and Zhang, L. (2017). Structure and functional analysis of promoters from two liver isoforms of CPT I in grass carp *Ctenopharyngodon idella*. Int. *J. Mol. Sci.* 18, 2405. doi: 10.3390/ijms18112405

Zeng, L., Xiong, Y., Song, W., Xie, Z., and Wang, Y. (2004). The effect and mechanism of salinity stress on energy metabolism and mitochondrial autophagy in large yellow croaker. *Acta Hydrobiologica Sinica.*, 1–10.

Zheng, J., Luo, Z., Zhu, Q., Chen, Q., and Gong, Y. (2013). Molecular characterization, tissue distribution and kinetic analysis of carnitine palmitoyltransferase I in juvenile yellow catfish *Pelteobagrus fulvidraco*. *Genomics.* 101, 195–203. doi: 10.1016/j.ygeno.2012.12.002

Zhou, R., Wu, G., Qu, L., Zhong, X., Gao, Y., Ding, Z., et al. (2021). Effect of starvation on intestinal morphology, digestive enzyme activity and expression of lipid metabolism-related genes in javelin goby (*Synechogobius hasta*). *Aquac. Res.* 53, 87–97. doi: 10.1111/are.15555

frontiers | Frontiers in Marine Science

TYPE Original Research
PUBLISHED 08 April 2024
DOI 10.3389/fmars.2024.1367608

OPEN ACCESS

EDITED BY
Yafei Duan,
South China Sea Fisheries Research Institute, China

REVIEWED BY
Houguo Xu,
Chinese Academy of Fishery Sciences (CAFS), China
Lijun Ning,
South China Agricultural University, China

*CORRESPONDENCE
Yi-Feng Li
yifengli@shou.edu.cn
Jin-Long Yang
jlyang@shou.edu.cn

†These authors have contributed equally to this work and shared the first authorship

RECEIVED 09 January 2024
ACCEPTED 12 March 2024
PUBLISHED 08 April 2024

CITATION
Zhu Y-T, Liang X, Liu T-T, Power DM, Li Y-F and Yang J-L (2024) The mussel larvae microbiome changes in response to a temperature rise.
Front. Mar. Sci. 11:1367608.
doi: 10.3389/fmars.2024.1367608

The mussel larvae microbiome changes in response to a temperature rise

You-Ting Zhu[1,2†], Xiao Liang[1,2†], Tian-Tian Liu[1,2†], Deborah M. Power[1,3], Yi-Feng Li[1,2*] and Jin-Long Yang[1,2*]

[1]International Research Center for Marine Biosciences, Ministry of Science and Technology, Shanghai Ocean University, Shanghai, China, [2]China-Portugal Belt and Road Joint Laboratory on Space & Sea Technology Advanced Research, Shanghai, China, [3]Centro de Ciências do Mar (CCMAR), Comparative Endocrinology and Integrative Biology, Universidade do Algarve, Faro, Portugal

Ocean warming caused by global climate change influences the function, diversity, and community dynamics of commensal microorganisms, including the hemolymph and the gut microbiota in mussels. However, the microbiota in hard-shelled mussel (*Mytilus coruscus*) larvae and the effect of temperature on the microbial community structure have yet to be studied. Herein, we investigated the core microbiota of *M. coruscus* larvae and the impact of acute (4 h) and gradual (4 days) exposure to a rise in seawater temperature from 21 to 25 °C. Eleven core genera were identified in *M. coruscus* larvae by 16S rDNA gene sequencing: *Alteromonas*, *Brevundimonas*, *Delftia*, *Microbacterium*, *Neptuniibacter*, *Neptunomonas*, *Pseudoalteromonas*, *Rhodococcus*, *Stenotrophomonas*, *Tenacibaculum*, and *Thalassotalea*. The microbiota of larvae in the short exposure treatment was similar to the control. However, the abundance of *Delftia*, *Neptunomonas*, *Pseudoalteromonadaceae*, *Rhodococcus*, and *Stenotrophomonas* decreased significantly in the long-exposure larvae. In contrast, at the genus level, the abundance of *Tenacibaculum* increased significantly. Diversity and multivariate analyses confirmed that the microbiota patterns were linked to seawater warming over the long term. Microbiota diversity did not change significantly, regardless of whether the seawater temperature increased quickly or slowly; however, we observed a significant increase in the microbiota species abundance at higher temperatures. Among the altered bacterial genera, *Delftia*, *Neptunomonas*, and *Rhodococcus* function in the degradation of organic compounds; *Pseudoalteromonas* is closely associated with mussel attachment and metamorphosis, and *Tenacibaculum* is an opportunistic pathogen that can cause marine mollusk death. The results suggest that marine heat waves caused by climate change may reduce the ability of symbiotic bacteria to degrade environmental toxins, will affect mussel larvae metamorphosis, and increase the abundance of opportunistic pathogens, thereby increasing the risk of disease and death of mussel larvae.

KEYWORDS

microbe-environment interaction, seawater temperature, larval microbiota, Mytilus coruscus, toxin degradation, opportunistic pathogens

1 Introduction

Multicellular life originated in a microorganism-dominated environment, and interactions between animals and their microbiomes have markedly influenced animal evolution (Nyholm and Graf, 2012). The most studied microbial community, the animal gut microbiome, performs various vital functions, including immune response stimulation, defense against pathogen colonization, essential nutrient provision, and digestive support (Nyholm and Graf, 2012; McFall-Ngai et al., 2013). Research has shown that the composition of host-microbial communities is dictated chiefly by the phylogeny of the host and their environment. Within an individual host, microbes might be unevenly distributed (Cárdenas et al., 2014; Pantos et al., 2015; Brooks et al., 2016; Carrier and Reitzel, 2018). Moreover, environmental factors can change the microbiota composition, significantly affecting the host's development, homeostasis, survival, and metabolism (Tremaroli and Bäckhed, 2012; McFall-Ngai et al., 2013).

Recent advances in sequencing technology have enabled the investigation of microbiota from marine invertebrates, such as mollusks, corals, sponges, tunicates, echinoderms, polychaetes, and crustaceans (Gobet et al., 2018; Dubé et al., 2019). Such research has revealed that marine invertebrates are hosts to varied core microbial communities that are phylogenetically different from the microbes in the surrounding aquatic environment, and such microbial associations are often host-specific, irrespective of geography (Moitinho-Silva et al., 2014; Reveillaud et al., 2014; Lokmer et al., 2016a; Zhang et al., 2016; Brener-Raffalli et al., 2018). Several biological factors, such as host physiology and genetics (Jaenike, 2012; Wegner et al., 2013; Amato et al., 2019), host health (Cárdenas et al., 2012; Sweet and Bulling, 2017), diet (Carrier et al., 2018), life stage (Trabal et al., 2012; Lema et al., 2014), host-tissue differentiation (Meisterhans et al., 2016; Høj et al., 2018; Dubé et al., 2019), stressors (e.g., antibiotic stress, infection, temperature, starvation, and translocation) (Green and Barnes, 2010; Wegner et al., 2013; Lokmer and Wegner, 2015; Lokmer et al., 2016a, b), and season (Pierce et al., 2016; Gobet et al., 2018) can also contribute to specific variation in microbial communities or shift the microbiome.

In marine ecosystems, microbial community dynamics, function, and diversity are affected by global climate change (Webster et al., 2007), causing shifts in host-microbe interactions which could result in a shift toward pathogen-dominated microbes rather than beneficial bacteria (Lafferty et al., 2004). Temperature changes can influence the composition of hemolymph and gut microbiomes of many invertebrates (Olafsen et al., 1993; Lokmer and Wegner, 2015; Li et al., 2018), and exceeding a species' thermal tolerance limit is likely to have specific adverse effects on bivalves (Xiao et al., 2005; Li et al., 2018; Li et al., 2019a, b). For example, adult mussels (*M. coruscus* and *Mytilus galloprovincialis*) microbiomes and susceptibility to bacterial infections were modified in response to increased water temperature (Li et al., 2018).

In bivalves, the larval microbiota comprises mainly bacteria acquired from the surrounding seawater, with the prevalence of certain groups of bacteria, such as Vibrionaceae, which are presumed to multiply within the gut (Prieur, 1976), and the larval microbiota might be more susceptible to changes in the environment. However, adult mollusks can retain their core microbial communities by selective digestion and multiplication of the bacteria from surrounding seawater (Kueh and Chan, 1985).

The hard-shelled mussel (*M. coruscus*) is a commercially important species in the Eastern China Sea, and its range covers the coastal waters of the East Asia temperate zones. Our previous study showed that high water temperatures promoted the growth of opportunistic bacteria, such as Arcobacter and Bacteroides, in the gut of *M. coruscus*, which suggests increased host susceptibility to pathogens at higher temperatures (Li et al., 2018). In addition, increased temperatures reduced the *M. coruscus* hemolymph microbiome diversity, which could reduce the bacterial elimination function against *Vibrio* infection in the hemolymph (Li et al., 2019a). However, the life cycle of *M. coruscus* comprises planktonic larval and benthic adult phases, and the effects of temperature on the larval microbial community are little understood.

The present study investigated the effect of increasing seawater temperature from the perspective of a short-term increase typical of marine heat waves (Field et al., 2014) on the *M. coruscus* larval microbiota structure and diversity. 16S rRNA gene sequencing was used to provide insight into the likely effects of global warming on the survival of marine bivalve larvae.

2 Materials and methods

2.1 Biological material

Adult *M. coruscus* were acquired from Gouqi Island, China (30° 72'N, 122°77'E) and transported to the laboratory on the same day. The mussels were cleaned and placed in a 10 L polycarbonate tank filled with seawater filtered through a 1.2 µm pore size acetate-fiber membrane (FSW). The water temperature was maintained at 21°C to reflect the collection site's average winter temperature. The mussels received a daily mixed diet comprising *Isochrysis zhanjiangensis* and *Platymonas helgolandica*.

Mussel spawning was induced using a previously described method (Yang et al., 2008) with modifications. In brief, after overnight storage on ice, mussels were placed in 10 L polycarbonate tanks at 21°C until spawning began, when they were transferred immediately to 2 L beakers containing FSW. Egg and sperm FSW suspensions were collected and mixed gently to achieve fertilization, followed by incubation for 20 min. Excess sperm was washed off with FSW using a 20 µm mesh size nylon plankton net, and the fertilized eggs were incubated in a 2 L beaker with FSW at 18°C. Two days later, the swimming larvae were fed daily with 5×10^4 cells/mL of *I. zhanjiangensis* and *P. helgolandica* and cultured at 21°C.

2.2 Experimental setup and sampling collection

The Institutional Animal Care and Use Committee (IACUC) of Shanghai Ocean University approved the animal handling procedures and experimentation.

Pediveliger larvae (35 days post fertilization, larva at this stage can metamorphose into a juvenile) were randomly and evenly distributed in three randomized triplicate groups. The groups were subjected to three temperature treatments terminating at the same time: the larvae were placed directly in seawater at 25°C for 4 hours group Mc25.S); 4 days at 25°C (group Mc25.L), by raising the water one degree a day; and 21°C as control (group Mc21). Four degrees of warming represents the differential temperature rise predicted for 2100. The global mean temperature will have increased by 3.2–4.6 °C (Rogelj et al., 2016), and the increase in seawater temperature over a short time during marine heat waves (Field et al., 2014).

During the trial, the larvae were fed microalgae as usual. At the end of the experiment, 50 μg of larva were combined into a sample (every treatment group has three replicates), frozen, and stored at −80 °C for microbiome analysis.

2.3 Extraction of DNA and PCR amplification

According to the manufacturer's instructions, a FastDNATM Spin Kit for Soil (MP Biomedicals, Santa Anna, CA, USA) was used to extract genomic DNA from the larval samples. The purity and concentration of the DNA were measured on a Nanodrop One instrument (Thermo Fisher Scientific, Waltham, MA, USA). Sterile, filtered (0.2 μm) water was added to standardize the DNA concentration to 5 ng/μl for all samples.

The universal bacterial primers, 338F (5'-ACTCCTACG GGAGGCAGCAG-3') and 806R (5'-GGACTACHVG GGTWTCTAAT-3') with a 12 bp barcode (synthesized by Invitrogen, Carlsbad, CA, USA) were used to amplify the bacterial 16S rRNA gene V3-V4 region. The 50 μl PCR reactions comprised 25 μl of 2× Premix Taq (Takara Biotechnology, Dalian, China), one μl of each primer (10 M), three μl of DNA (20 ng/μl) template, and 20 μl of distilled water. The reactions were run on a BioRadS1000 instrument (Bio-Rad, Hercules, CA, USA) with the following thermocycling conditions: initialization for 5 min at 94°C; 30 cycles of 30 s of denaturation at 94°C, 30 s of annealing at 52°C, and 30 s extension at 72°C; followed by a 10 min final elongation at 72°C.

2.4 Illumina HiSeq sequencing

Gel electrophoresis in 1% agarose was used to detect the PCR amplicons. GeneTools (version 4.03.05.0, SynGene, New Delhi, India) was used to assess the density of the PCR bands. The amplicons showing bright leading bands were mixed at equidensity ratios. An EZNA Gel Extraction Kit (Omega Bio-tek, Norcross, GA, USA) was used to purify mixed PCR products. A NEBNext® Ultra™ DNA Library Prep Kit for Illumina® (New England Biolabs, Ipswich, MA, USA) was used to generate the sequencing libraries with index codes according to the manufacturer's protocol. A Qubit@ 2.0 Fluorometer (Thermo Fisher Scientific) and an Agilent Bioanalyzer 2100 system (Agilent Technologies, Waldbron, Germany) were used to assess the quality of the libraries. The Illumina Hiseq 2500 platform (Illumina Inc., San Diego, CA, USA) was used to sequence the libraries, generating 250 bp paired-end reads. The sequencing was carried out by Guangdong Magigene Biotechnology Co. Ltd (Guangzhou, China).

2.5 Bioinformatics and statistics

The Trimmomatic V0.33 (Bolger et al., 2014) was used to filter the raw paired-end reads to generate high-quality, clean reads. FLASH V1.2.11 (Magoč and Salzberg, 2011) was used to merge the clean reads dependent on the overlap between the paired-end reads. Mothur V1.35.1 (Kozich et al., 2013) used the unique barcodes and primers to assign the sequences to the samples, then, the barcodes and primers were removed to obtain effective clean tags. USEARCH V10 (Edgar, 2010) was used for sequence analysis. Sequences sharing greater than or equal to 97% similarity were assigned to the same operational taxonomic unit (OTU). Each OTU was represented by the most frequently occurring sequence, which was screened and annotated. We used the SILVA (Quast et al., 2013) database to annotate the taxonomic information for each representative sequence (using the default confidence threshold ≥ 0.5). After removing contaminating OTUs, we determined the total number of OTU sequences and the OTU types, respectively. A normalized (subsampled) OTU table was obtained based on the sample with the fewest sequences. Using the OTU table, we calculated the annotation ratio for each classification level to determine the sequence composition of each sample at each classification level. The OTU table was also used to construct a Venn graph, histogram, and heat map displayed using R software (v2.15.3).

The complexity of species diversity in the samples was represented by the Chao1 richness index and Simpson's and Shannon diversity indices, calculated using QIIME software (v1.9.1) (Bolyen et al., 2019) and displayed using the R software (v2.15.3). The vegan package of R software was used to carry out non-metric multidimensional scaling (NMDS) based on the weighted and unweighted distance matrix. Linear discriminant analysis Effect Size (LEfSe) was used to find the biomarker of each group. The obtained raw sequences were submitted to the NCBI database and received the accession number PRJNA1029461.

GraphPad Prism 9.0 (GraphPad Software, Boston, MA, USA) and one-way ANOVA tests were used to analyze the larval microbiota's relative abundance and taxonomical composition at the different levels and Alpha Diversity.

2.6 Ethics statement

The Animal Ethics Committee at Shanghai Ocean University approved all the protocols for mussel acclimation and experimentation in the present study (registration number SHOU-DW-2020-032).

3 Results

3.1 Composition of *M. coruscus* microbiota under different temperature treatments

The 16S rDNA gene sequencing yielded 1,233,013 sequences clustered into 6,830 distinct OTUs (Supplementary Table S1). The larvae hosted 29 unique phyla, 72 classes, and 198 orders of bacteria. The most abundant phylum in the Mc21 group was Proteobacteria (73.1%), followed by Actinobacteria (21.2%), Bacteroidetes (4.5%), and many other unclassified bacteria (1.2%). The most abundant phyla in the Mc25.S group were Proteobacteria (71.0%), Actinobacteria (23.0%), Bacteroidetes (4.6%), and many other unclassified bacteria (1.4%). The most abundant phyla in the Mc25.L group were Proteobacteria (35.7%), Actinobacteria (3.8%), and Bacteroidetes (59.2%), and many other unclassified bacteria (1.2%) (Supplementary Table S2, Supplementary Figure S1).

3.2 *M. coruscus* larvae microbiota at family's level

We identified 18 different families with an abundance > 1%, and 235 families with an abundance < 1% were classified as "others" (Figure 1A). Most reads (16.60–31.53% of the OTUs) were obtained from the Mc21 and Mc25.S groups and were assigned to Burkholderiaceae, Nocardiaceae, and Xanthomonadaceae. In contrast, most reads (5.00–54.55% of total OTUs) obtained from the Mc25.L group were assigned to Burkholderiaceae, Flavobacteriaceae, and Rhodobacteraceae (Figure 1A; Supplementary Table S3). The analysis of the relative abundance showed that at the family level, the microbial community structure between the Mc21 and Mc25.S groups was similar but different from the Mc25.L group. The relative abundance of Burkholderiaceae, Nitrincolaceae, Nocardiaceae, and Xanthomonadaceae decreased significantly, and that of Flavobacteriaceae and Rhodobacteraceae increased significantly in the Mc25.L group compared with those in the Mc21 and Mc25.S ($P < 0.05$) (Figures 1B, C; Supplementary Table S3). Notably, the abundance of Pseudoalteromonadaceae decreased significantly irrespective of whether the larvae were in warmer seawater for 4 hours or 4 days. ($P < 0.05$) (Figures 1B, C; Supplementary Table S3).

3.3 *M. coruscus* larvae microbiota at genera's level

At the genus level, 21 genera were identified with an abundance > 1%, and 443 genera with an abundance < 1% were classified as "others" (Figure 2A). In the Mc21 and Mc25.S groups, the dominant genera were *Alteromonas*, *Brevundimonas*, *Delftia*, *Microbacterium*, *Neptuniibacter*, *Neptunomonas*, *Pseudoalteromonas*, *Rhodococcus*, *Stenotrophomonas*, *Tenacibaculum*, and *Thalassotalea* (average reads per group 1.04–31.40% of the total OTUs) (Figure 2A; Supplementary Table S4). *Delftia*, *Lewinella*, *Neptuniibacter*, *Pseudoalteromonas*,

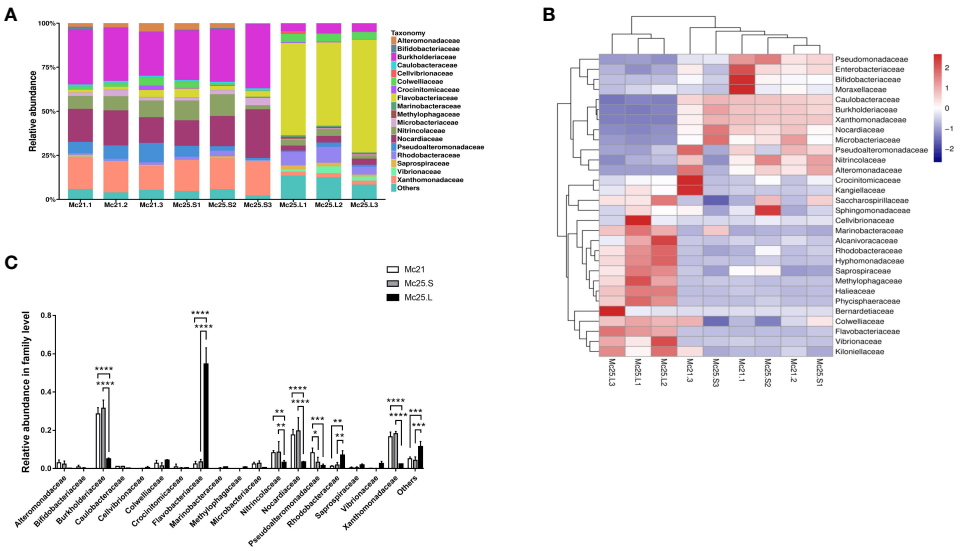

FIGURE 1
Relative abundance and taxonomical composition of the larval microbiota at family level. The suffix number in the group names indicate individual replicates. **(A)** Each bar represents the larval bacterial community associated with individual samples. **(B)** Heatmap showing the top 30 bacterial families (%). Red signifies higher abundance, and blue signifies lower abundance. **(C)** Comparison of the relative abundance of the 18 main microbial families between the three groups of larvae. *P*-values mark significant differences in community diversity between the different treatment groups (one-way ANOVA). *$p < 0.05$, **$p < 0.01$, ***$p < 0.001$, ****$p < 0.0001$.

10.3389/fmars.2024.1367608

Rhodococcus, *Ruegeria*, *Stenotrophomonas*, *Tenacibaculum*, *Thalassotalea*, and *Vibrio* were the dominant genera in the Mc25.L group (average reads per group 1.09–52.65% of the total OTUs) (Figure 2A; Supplementary Table S4). By comparing the abundance in the different experimental groups, the results showed the similarity of the microbiota between the Mc21 and Mc25.S groups, except for *Pseudoalteromonas* ($P < 0.05$) (Figure 2C; Supplementary Table S4). In the Mc25.L group, the larval microbiota had more differences. The abundance of *Delftia*, *Neptunomonas*, *Pseudoalteromonadaceae*, *Rhodococcus*, and *Stenotrophomonas* decreased significantly, and *Tenacibaculum* increased considerably compared with that in the Mc21 and Mc25 groups ($P < 0.05$) (Figures 2B, C; Supplementary Table S4). These results indicated that rapid warming in a short time does not impact the *M. coruscus* larval microbial community structure. Conversely, a gradual increase in temperature over four days can change the population levels of certain bacterial species and possibly alter the microbial community composition.

3.4 Composition and temperature-driven fluctuations of the core digestive microbiota

Based on the Venn diagrams, the core microbial communities, i.e., occurring in all treatment groups, included 145 families and 216 genera, representing 57.31% of the total families and 47.68% of the entire genera (Figure 3). Eighteen families and 21 genera with an abundance > 1% belonged to these core families and genera bacterial communities (Supplementary Tables S3, S4). In contrast, unique bacterial communities had an abundance of < 1% in each treatment group (Supplementary Tables S3, S4).

3.5 Diversity patterns of the microbial community

The microbiota richness and evenness were investigated between the control and the temperature treatment groups. There were no significant differences among the treatment groups in the Shannon and Simpson diversity indices ($P > 0.05$, Figures 4A, B). However, the Chao1 index of the Mc25.L group was significantly higher than that of the Mc25.S and Mc21 ($P < 0.05$, Figure 4C), indicating that the gradual increase in temperature caused a significant increment in the microbiota species abundance.

The NMDS analysis was employed as a proxy for temporal stability. It showed that the samples were homogenous in the Mc25.L group, and the larvae microbiota in this group changed compared with the other two groups, which showed some overlap (Figure 5).

Linear discriminant analysis effect size (LEfSe) analysis was performed to reveal the significant ranking of abundant modules. The linear discriminant analysis (LDA) score and the cladogram showed differences between Mc25.S, Mc25.L, and Mc21 (Figure 6). At the phylum or order level, the biomarkers demonstrating significant differences between the three groups were Caulobacterales in Mc25.S; PB19, Cellvibrionales (genus *Halioglobus*), Rhodobacterales (genus *Litoreibacter* and *Kiloniella*), Caulobacterales (family Hyphomonadaceae), Oceanospirillales (family Alcanivoracaceae), Micavibrionales (family Micavibrionaceae) in Mc25.L; and

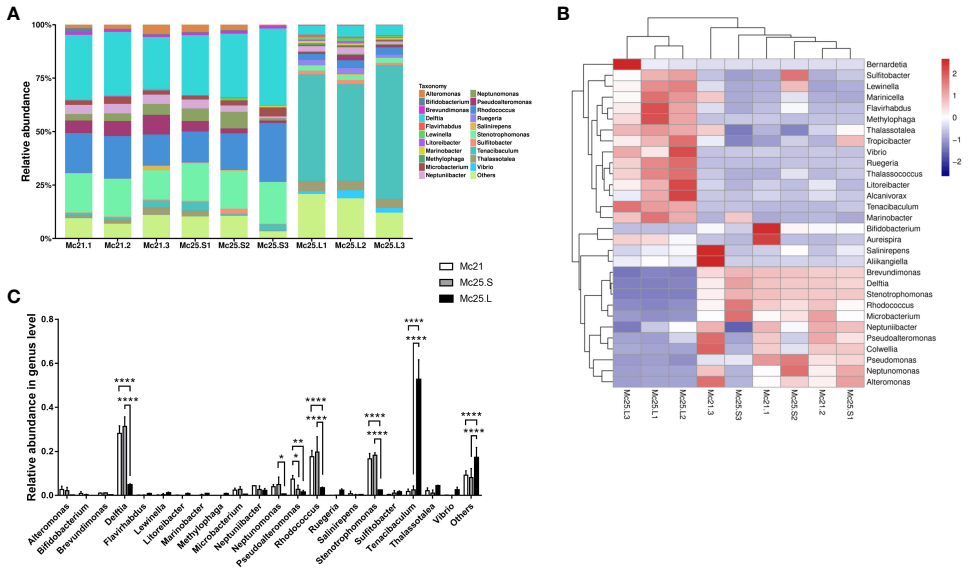

FIGURE 2
Relative abundance and taxonomical composition of the larval microbiota at the genus level. The suffix number in the group names indicate individual replicates. **(A)** Each bar represents the larval bacterial community associated with individual samples. **(B)** Heatmap showing the top 30 bacterial (%). Red signifies higher abundance, and blue signifies lower abundance. **(C)** Comparison of relative abundance of 21 main microbial genus between the three groups of larvae. *P*-values mark significant differences in community diversity between different treatment groups (tested using one-way ANOVA). *$p < 0.05$, **$p < 0.01$, ****$p < 0.0001$.

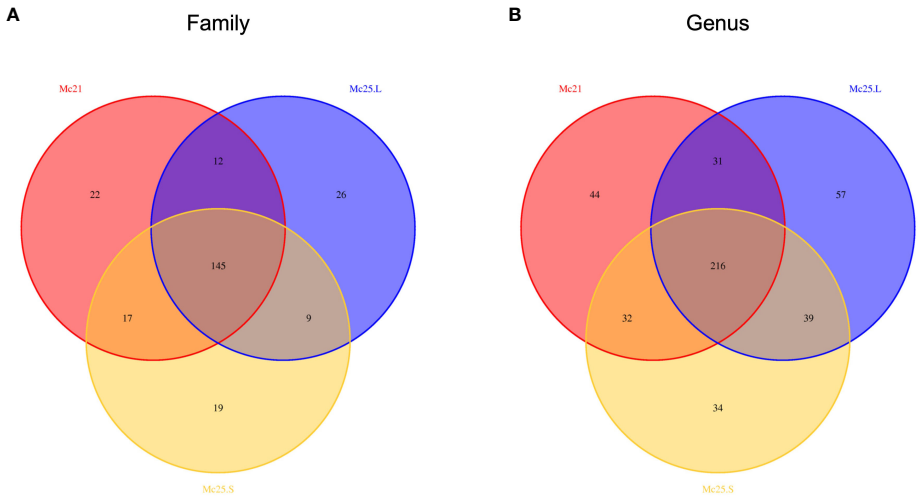

FIGURE 3
Venn diagrams showing the numbers of microbial OTU composition associated with the three temperature treatment groups in family **(A)** and genus **(B)** level. Comparisons are described by numbers of shared or unique OTUs in Mc25.S, Mc25.L, and Mc21 groups.

Alteromonadales (family Pseudoalteromonadaceae and genus *Colwellia*), Firmicutes (phylum Firmicutes and order Lactobacillales) in Mc21 (Figure 6; Supplementary Table S5).

4 Discussion

Marine invertebrates host diverse core microbial communities, and we show that this is also the case with the hard-shell mussel larva. However, the microbiome is sensitive to a rise in temperature from 21 to 25°C over 4 days, although it is little affected if the rise is only over 4 hours. In the gradual warming group, temperature impacts some Phyla's abundance and the community's richness (Chao1 index). Still, it does not affect the diversity richness and evenness (Shannon and Simpson indices). The little impact over 4 hours may reflect that bacterial growth rates may not be sufficient to make a difference in the number of bacteria in the population.

Marine invertebrates generally have complex life cycles with larval stages, and each of these developmental stages owns different microbiotas, although they also share core microbes (Trabal et al., 2012). The microbiome of the *M. coruscus* pediveliger in the present study was dominated by Proteobacteria, Actinobacteria, and Bacteroidetes. Adult *M. coruscus* had fewer than 14 dominant phyla (abundance > 1%), while there were 9 dominant phyla in adult *M. galloprovincialis* (abundance > 1%), suggesting that the microbiota diversity increases with age (Li et al., 2019a, b). This could be because adult mussels are exposed to environmental microbes over a longer time, and that their more complex bodies offer more niches than larvae for bacteria to colonize. However, there were few dominant phyla in adults of yesso scallop (*Patinopecten yessoensis*) from Northern China (four phyla) (Lu et al., 2017), sponges *Stylissa carteri* and *Xestospongia testudinaria* from the Red Sea (three phyla) (Moitinho-Silva et al., 2014), and Chinese mitten crab (*Eriocheir sinensis*) from East China (four phyla) (Zhang et al., 2016), which could be indicative of a possible role of the genotype (Wegner et al., 2013), condition (Lokmer and Wegner, 2015), and of neutral processes (Nemergut et al., 2013) in shaping the host microbiome. In addition, at lower taxonomic levels, the untreated pediveliger larvae contained eleven main microbial genera, including *Alteromonas*, *Brevundimonas*, *Delftia*, *Microbacterium*, *Neptuniibacter*, *Neptunomonas*, *Pseudoalteromonas*, *Rhodococcus*, *Stenotrophomonas*, *Tenacibaculum*, and *Thalassotalea*. *Pseudoalteromonas* and *Tenacibaculum* were the dominant genera in adult *M. coruscus*, suggesting that these are core bacterial genera throughout this mussel's life cycle.

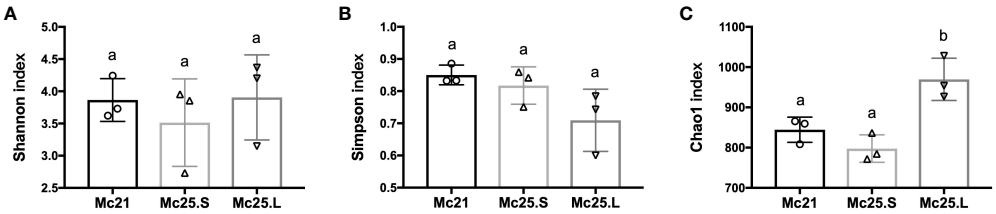

FIGURE 4
Analysis of microbial diversity. The results of Shannon **(A)**, Simpson **(B)**, and Chao1 **(C)** indices analysis. Data are presented as the mean ± SE (n = 3). Different low case letters represent significant differences ($p < 0.05$, one-way ANOVA).

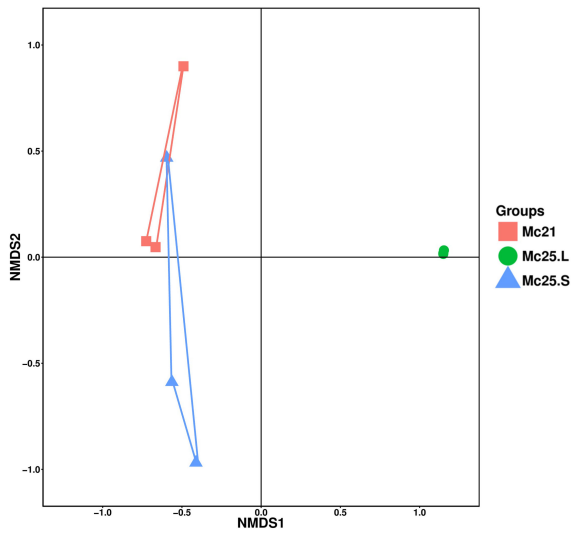

FIGURE 5
Non-metric multidimensional scaling (NMDS) analysis of the larval bacterial community composition at the OTU-level. Treatment groups are indicated using different colors (Mc21 = red, Mc25.L = green, Mc25.S = blue).

In marine poikilotherms, it was proposed that temperature is an important factor that shapes microbial communities by affecting the host and their symbiotic bacteria. Higher temperatures promote the growth of better-adapted microbes and compromise the host defense, leading to a rapid increase in opportunistic pathogens (Malham et al., 2009; Lokmer and Wegner, 2015). In oysters, warmer temperatures led to a higher mortality rate when infected with *Vibrio* sp., and among the dominant microbiota, the genus *Arcobacter*, a hemolymph-specific symbiont, decreased in abundance (Lokmer and Wegner, 2015). In contrast, infected oysters harbored more pathogen-containing genera, e.g., *Photobacterium* and *Shewanella* (Lokmer and Wegner, 2015). Our previous studies on adult *M. coruscus* revealed a decreasing abundance of hemolymph *Arcobacter* when reared in warmer water. In contrast, the abundance of gut *Bacteroides*, an opportunistic pathogen, increased (Li et al., 2007; Patrick et al., 2009; Li et al., 2018; Li et al., 2019a). The present study is consistent with those observations as indicated by an increase in species richness with higher temperature exposure and a simultaneous decrease in the abundance of the dominant bacteria *Delftia*, *Neptunomonas*, *Pseudoalteromonadaceae*, *Rhodococcus*, and *Stenotrophomonas*. The abundance of *Tenacibaculum* also increased significantly, suggesting that warmer temperatures changed the microbiome's stability towards more pathogen-dominated communities (Erwin et al., 2012; Lokmer and Wegner, 2015).

Several studies have shown that a healthy bacterial community can help stabilize the microbiome, a requirement for animal health (Green and Barnes, 2010; Lozupone et al., 2012; Lokmer and Wegner, 2015; King et al., 2018; Li et al., 2019a). Among the bacteria that decreased in abundance, *Delftia* spp. often forms biofilms associated with wastewater treatment and river wetlands (Barrionuevo and Vullo, 2012; Wu et al., 2015) and breaks down or transforms a variety of pollutants, such as acetaminophen (De Gusseme et al., 2011), polycyclic aromatic hydrocarbon (PAH) (Wu et al., 2016), chloroaniline (Zhang et al., 2010), and herbicides (Leibeling et al., 2010). *Delftia*, *Neptunomonas*, and *Rhodococcus* are also in seawater and can degrade PAHs and other organic compounds (Hedlund et al., 1999; Larkin et al., 2005). Interestingly, *Neptunomonas* has been found in dead clams, although there is no evidence that it is a pathogen (Lee et al., 2012). Members of *Pseudoalteromonas* have versatile metabolic capacities and can be found in multiple marine habitats where they have vital ecological functions (Ivanova et al., 2014). Moreover, some free species in this genus are associated with mussel metamorphosis and attachment, and it was unclear whether the decline in the genus *Pseudoalteromonas* would affect larval metamorphosis (Yang et al., 2013; Peng et al., 2020, 2020). *Tenacibaculum* (family Flavobacteriaceae) is a motile genus and an opportunistic pathogen in fish, which causes an ulcerative disease known as tenacibaculosis (Avendaño-Herrera et al., 2006). *Tenacibaculum* also causes mortality in mollusk species, including adult Pacific oysters (Burioli et al., 2018). The abundance of

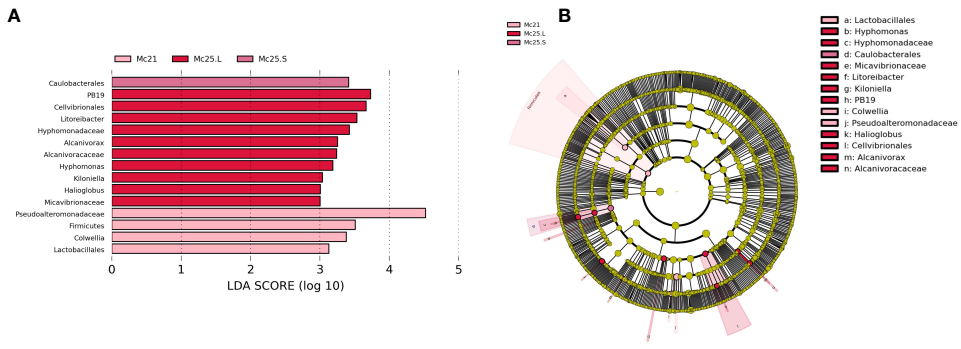

FIGURE 6
Unique biomarker community composition in larvae. **(A)** A bar chart of the log-transformed LDA scores for bacterial taxa identified using LEfSe analysis. The threshold used to identify significant taxa was as log-transformed LDA score of 2. LEfSe analysis identified 15 taxa (shown). **(B)** The phylogenetic relationships for the 15 LEfSe-identified bacterial taxa shown in a cladogram.

Tenacibaculum increased significantly with temperature, supporting the idea that warmer waters could affect mussel larvae by accelerating the proliferation of opportunistic pathogens.

5 Conclusion

In summary, the most striking finding of this study is that the symbiotic bacteria seem to have already been established during the larval stage of the mussel life cycle and that increased seawater temperatures alter the proportion of the symbiotic microbiota. This could reduce the ability of symbiotic bacteria to degrade environmental toxins, regulate metamorphosis in mussel larvae, and increase the abundance of opportunistic pathogens, which together are likely to increase the risk of larval death and reduced larval recruitment in the face of a warmer environment.

Data availability statement

The original contributions presented in the study are publicly available. This data can be found here: https://www.ncbi.nlm.nih.gov/, BioProject: PRJNA1029461.

Ethics statement

The animal study was approved by the Animal Ethics Committee of Shanghai Ocean University (SHOW-DW-2020-032). The study was conducted in accordance with the local legislation and institutional requirements.

Author contributions

YZ: Conceptualization, Data curation, Formal analysis, Funding acquisition, Investigation, Methodology, Software, Visualization, Writing – original draft. XL: Data curation, Investigation, Writing – original draft, Methodology. T-TL: Data curation, Formal analysis, Investigation, Writing – original draft. DP: Writing – review & editing, Validation. Y-FL: Project administration, Resources, Supervision, Writing – review & editing. J-LY: Conceptualization, Funding acquisition, Project administration, Resources, Supervision, Writing – review & editing.

Funding

The author(s) declare that financial support was received for the research, authorship, and/or publication of this article. This work was supported by the National Key R&D Program of China (No.2022YFE0204600, 2023YFE0115500, 2022YFD2401700), and the National Science Foundation of China (No.32002410, 32172992).

Acknowledgments

This short text acknowledges the contributions of specific colleagues, institutions, or agencies that aided the authors' efforts.

Conflict of interest

The authors declare that the research was conducted in the absence of any commercial or financial relationships that could be construed as a potential conflict of interest.

Publisher's note

Supplementary material

The Supplementary Material for this article can be found online at: https://www.frontiersin.org/articles/10.3389/fmars.2024.1367608/full#supplementary-material

References

Amato, K. R., Sanders, J. G., Song, S. J., Nute, M., Metcalf, J. L., Thompson, L. R., et al. (2019). Evolutionary trends in host physiology outweigh dietary niche in structuring primate gut microbiomes. *ISME J.* 13, 576–587. doi: 10.1038/s41396-018-0175-0

Avendaño-Herrera, R., Toranzo, A. E., and Magariños, B. (2006). Tenacibaculosis infection in marine fish caused by Tenacibaculum maritimum: a review. *Dis. Aquat Organ* 71, 255–266. doi: 10.3354/dao071255

Barrionuevo, M. R., and Vullo, D. L. (2012). Bacterial swimming, swarming and chemotactic response to heavy metal presence: which could be the influence on wastewater biotreatment efficiency? *World J. Microbiol. Biotechnol.* 28, 2813–2825. doi: 10.1007/s11274-012-1091-5

Bolger, A. M., Lohse, M., and Usadel, B. (2014). Trimmomatic: a flexible trimmer for Illumina sequence data. *Bioinformatics* 30, 2114–2120. doi: 10.1093/bioinformatics/btu170

Bolyen, E., Rideout, J. R., Dillon, M. R., Bokulich, N. A., Abnet, C. C., Al-Ghalith, G. A., et al. (2019). Reproducible, interactive, scalable and extensible microbiome data science using QIIME 2. *Nat. Biotechnol.* 37, 852–857. doi: 10.1038/s41587-019-0209-9

Brener-Raffalli, K., Clerissi, C., Vidal-Dupiol, J., Adjeroud, M., Bonhomme, F., Pratlong, M., et al. (2018). Thermal regime and host clade, rather than geography, drive *Symbiodinium* and bacterial assemblages in the scleractinian coral *Pocillopora damicornis sensu lato*. *Microbiome* 6, 39. doi: 10.1186/s40168-018-0423-6

Brooks, A. W., Kohl, K. D., Brucker, R. M., Opstal, E. J., and Bordenstein, S. R. (2016). Phylosymbiosis: Relationships and functional effects of microbial communities across host evolutionary history. *PloS Biol.* 14, e2000225. doi: 10.1371/journal.pbio.2000225

Burioli, E. A. V., Varello, K., Trancart, S., Bozzetta, E., Gorla, A., Prearo, M., et al. (2018). First description of a mortality event in adult Pacific oysters in Italy associated with infection by a *Tenacibaculum soleae strain*. *J. Fish Dis.* 41, 215–221. doi: 10.1111/jfd.12698

Cárdenas, A., Rodriguez-R, L. M., Pizarro, V., Cadavid, L. F., and Arévalo-Ferro, C. (2012). Shifts in bacterial communities of two caribbean reef-building coral species affected by white plague disease. *ISME J.* 6, 502–512. doi: 10.1038/ismej.2011.123

Cárdenas, C. A., Bell, J. J., Davy, S. K., Hoggard, M., and Taylor, M. W. (2014). Influence of environmental variation on symbiotic bacterial communities of two temperate sponges. *FEMS Microbiol. Ecol.* 88, 516–527. doi: 10.1111/fem.2014.88.issue-3

Carrier, T. J., and Reitzel, A. M. (2018). Convergent shifts in host-associated microbial communities across environmentally elicited phenotypes. *Nat. Commun.* 9, 952. doi: 10.1038/s41467-018-03383-w

Carrier, T. J., Wolfe, K., Lopez, K., Gall, M., Janies, D. A., Byrne, M., et al. (2018). Diet-induced shifts in the crown-of-thorns (*Acanthaster* sp.) larval microbiome. *Mar. Biol.* 165, 157. doi: 10.1007/s00227-018-3416-x

De Gusseme, B., Vanhaecke, L., Verstraete, W., and Boon, N. (2011). Degradation of acetaminophen by Delftia tsuruhatensis and Pseudomonas aeruginosa in a membrane bioreactor. *Water Res.* 45, 1829–1837. doi: 10.1016/j.watres.2010.11.040

Dubé, C. E., Ky, C. L., and Planes, S. (2019). Microbiome of the black-lipped pearl oyster Pinctada margaritifera, a multi-tissue description with functional profiling. *Front. Microbiol.* 10. doi: 10.3389/fmicb.2019.01548

Edgar, R. C. (2010). Search and clustering orders of magnitude faster than BLAST. *Bioinformatics* 26, 2460–2461. doi: 10.1093/bioinformatics/btq461

Erwin, P. M., Pita, L., López-Legentil, S., and Turon, X. (2012). Stability of sponge-associated bacteria over large seasonal shifts in temperature and irradiance. *Appl. Environ. Microbiol.* 78, 7358–7368. doi: 10.1128/AEM.02035-12

Field, C. B., Barros, V. R., Dokken, D. J., Mach, K. J., Mastrandrea, M. D., Bilir, T. E., et al. (2014). "IPCC 2014: Climate Change 2014: Impacts, adaptation, and vulnerability. Part A: Global and sectoral aspects," in *Contribution of working group II to the fifth assessment report of the intergovernmental panel on climate change* (Cambridge University Press, Cambridge, United Kingdom and New York, NY, USA), 1132.

Gobet, A., Mest, L., Perennou, M., Dittami, S. M., Caralp, C., Coulombet, C., et al. (2018). Seasonal and algal diet-driven patterns of the digestive microbiota of the European abalone *Haliotis tuberculata*, a generalist marine herbivore. *Microbiome* 6, 60. doi: 10.1186/s40168-018-0430-7

Green, T. J., and Barnes, A. C. (2010). Bacterial diversity of the digestive gland of Sydney rock oysters, Saccostrea glomerata infected with the paramyxean parasite, Marteilia sydneyi. *J. Appl. Microbiol.* 109, 613–622. doi: 10.1111/j.1365-2672.2010.04687.x

Hedlund, B. P., Geiselbrecht, A. D., Bair, T. J., and Staley, J. T. (1999). Polycyclic aromatic hydrocarbon degradation by a new marine bacterium, Neptunomonas naphthovorans gen. nov., sp. Nov. *Appl. Environ. Microbiol.* 65, 251–259. doi: 10.1128/AEM.65.1.251-259.1999

Høj, L., Levy, N., Baillie, B. K., Clode, P. L., Strohmaier, R. C., Siboni, N., et al. (2018). Crown-of-thorns sea star *Acanthaster* cf. *solaris* has tissue-characteristic microbiomes with potential roles in health and reproduction. *Appl. Environ. Microbiol.* 84, e00181–e00118. doi: 10.1128/AEM.00181-18

Ivanova, E. P., Ng, H. J., and Webb, H. K. (2014). "The Family Pseudoalteromonadaceae," in *The Prokaryotes* (Springer, Berlin, Heidelberg). doi: 10.1007/978-3-642-38922-1_229

Jaenike, J. (2012). Population genetics of beneficial heritable symbionts. *Trends Ecol. Evol.* 27, 226–232. doi: 10.1016/j.tree.2011.10.005

King, W. L., Jenkins, C., Seymour, J. R., and Labbate, M. (2018). Oyster disease in a changing environment: Decrypting the link between pathogen, microbiome and environment. *Mar. Environ. Res.* 143, 124–140. doi: 10.1016/j.marenvres.2018.11.007

Kozich, J. J., Westcott, S. L., Baxter, N. T., Highlander, S. K., and Schloss, P. D. (2013). Development of a dual-index sequencing strategy and curation pipeline for analyzing amplicon sequence data on the MiSeq Illumina sequencing platform. *Appl. Environ. Microbiol.* 79, 5112–5120. doi: 10.1128/AEM.01043-13

Kueh, C. S., and Chan, K. Y. (1985). Bacteria in bivalve shellfish with special reference to the oyster. *J. Appl. Bacteriol.* 59, 41–47. doi: 10.1111/j.1365-2672.1985.tb01773.x

Lafferty, K. D., Porter, J. W., and Ford, S. E. (2004). Are diseases increasing in the ocean? *Annu. Rev. Ecol. Evol. Syst.* 35, 31–54. doi: 10.1146/annurev.ecolsys.35.021103.105704

Larkin, M. J., Kulakov, L. A., and Allen, C. C. (2005). Biodegradation and Rhodococcus – masters of catabolic versatility. *Curr. Opin. Biotechnol.* 16, 282–290. doi: 10.1016/j.copbio.2005.04.007

Lee, H. W., Shin, N. R., Lee, J., Roh, S. W., Whon, T. W., and Bae, J. W. (2012). *Neptunomonas concharum* sp. nov., isolated from a dead ark clam, and emended description of the genus *Neptunomonas*. *Int. J. Syst. Evol. Microbiol.* 62, 2657–2661. doi: 10.1099/ijs.0.037473-0

Leibeling, S., Schmidt, F., Jehmlich, N., von Bergen, M., Müller, R. H., and Harms, H. (2010). Declining capacity of starving *Delftia acidovorans* MC1 to degrade phenoxypropionate herbicides correlates with oxidative modification of the initial enzyme. *Environ. Sci. Technol.* 44, 3793–3799. doi: 10.1021/es903619j

Lema, K. A., Bourne, D. G., and Willis, B. L. (2014). Onset and establishment of diazotrophs and other bacterial associates in the early life history stages of the coral *Acropora millepora*. *Mol. Ecol.* 23, 4682–4695. doi: 10.1111/mec.12899

Li, Y. F., Chen, Y. W., Xu, J. K., Ding, W. Y., Shao, A. Q., Zhu, Y. T., et al. (2019a). Temperature elevation and *Vibrio cyclitrophicus* infection reduce the diversity of haemolymph microbiome of the mussel Mytilus coruscus. *Sci. Rep.* 9, 16391. doi: 10.1038/s41598-019-52752-y

Li, K., Guan, W., Wei, G., Liu, B., Xu, J., Zhao, L., et al. (2007). Phylogenetic analysis of intestinal bacteria in the Chinese mitten crab (*Eriocheir sinensis*). *J. Appl. Microbiol.* 103, 675–682. doi: 10.1111/j.1365-2672.2007.03295.x

Li, Y. F., Xu, J. K., Chen, Y. W., Ding, W. Y., Shao, A. Q., Liang, X., et al. (2019b). Characterization of gut microbiome in the mussel *Mytilus galloprovincialis* in response to thermal stress. *Front. Physiol.* 10. doi: 10.3389/fphys.2019.01086

Li, Y. F., Yang, N., Liang, X., Yoshida, A., Osatomi, K., Power, D., et al. (2018). Elevated seawater temperatures decrease microbial diversity in the gut of *mytilus coruscus*. *Front. Physiol.* 9. doi: 10.3389/fphys.2018.00839

Lokmer, A., Goedknegt, M. A., Thieltges, D. W., Fiorentino, D., Kuenzel, S., Baines, J. F., et al. (2016a). Spatial and temporal dynamics of pacific oyster hemolymph microbiota across multiple scales. *Front. Microbiol.* 7. doi: 10.3389/fmicb.2016.01367

Lokmer, A., Kuenzel, S., Baines, J. F., and Wegner, K. M. (2016b). The role of tissue-specific microbiota in initial establishment success of Pacific oysters. *Environ. Microbiol.* 18, 970–987. doi: 10.1111/1462-2920.13163

Lokmer, A., and Wegner, K. M. (2015). Hemolymph microbiome of Pacific oysters in response to temperature, temperature stress and infection. *ISME J.* 9, 670–682. doi: 10.1038/ismej.2014.160

Lozupone, C. A., Stombaugh, J. I., Gordon, J. I., Jansson, J. K., and Knight, R. (2012). Diversity, stability and resilience of the human gut microbiota. *Nature* 489, 220–230. doi: 10.1038/nature11550

Lu, G., Wang, F., Yu, Z., Lu, M., Wang, Y., Liu, C., et al. (2017). Bacterial communities in gills and intestines of yesso scallop (*Patinopecten yessoensis*) and its habitat waters in Changhai (Dalian, China). *Invertebr Surviv J.* 14, 340–351. doi: 10.25431/1824-307x/isj.v14i.340-351

Magoč, T., and Salzberg, S. L. (2011). FLASH: fast length adjustment of short reads to improve genome assemblies. *Bioinformatics* 27, 2957–2963. doi: 10.1093/bioinformatics/btr507

Malham, S. K., Cotter, E., O'Keeffe, S., Lynch, S., Culloty, S. C., King, J. W., et al. (2009). Summer mortality of the Pacific oyster, *Crassostrea gigas*, in the Irish Sea: The influence of temperature and nutrients on health and survival. *Aquaculture* 287, 128–138. doi: 10.1016/j.aquaculture.2008.10.006

McFall-Ngai, M., Hadfield, M. G., Bosch, T. C. G., Carey, H. V., Domazet-Lošo, T., Douglas, A. E., et al. (2013). Animals in a bacterial world, a new imperative for the life sciences. *Proc. Natl. Acad. Sci. U S A* 110, 3229–3236. doi: 10.1073/pnas.1218525110

Meisterhans, G., Raymond, N., Girault, E., Lambert, C., Bourrasseau, L., de Montaudouin, X., et al. (2016). Structure of Manila clam (Ruditapes philippinarum) microbiota at the organ scale in contrasting sets of individuals. *Microb. Ecol.* 71, 194–206. doi: 10.1007/s00248-015-0662-z

Moitinho-Silva, L., Bayer, K., Cannistraci, C. V., Giles, E. C., Ryu, T., Seridi, L., et al. (2014). Specificity and transcriptional activity of microbiota associated with low and high microbial abundance sponges from the Red Sea. *Mol. Ecol.* 23, 1348–1363. doi: 10.1111/mec.12365

Nemergut, D. R., Schmidt, S. K., Fukami, T., Neill, S. P., Bilinski, T. M., Stanish, L. F., et al. (2013). Patterns and processes of microbial community assembly. *Microbiol. Mol. Biol. Rev.* 77, 342. doi: 10.1128/MMBR.00051-12

Nyholm, S. V., and Graf, J. (2012). Knowing your friends: invertebrate innate immunity fosters beneficial bacterial symbioses. *Nat. Rev. Microbiol.* 10, 815–827. doi: 10.1038/nrmicro2894

Olafsen, J. A., Mikkelsen, H. V., Giaever, H. M., and Høvik Hansen, G. (1993). Indigenous bacteria in hemolymph and tissues of marine bivalves at low temperatures. *Appl. Environ. Microbiol.* 59, 1848–1854. doi: 10.1128/aem.59.6.1848-1854.1993

Pantos, O., Bongaerts, P., Dennis, P. G., Tyson, G. W., and Hoegh-Guldberg, O. (2015). Habitat-specific environmental conditions primarily control the microbiomes of the coral *Seriatopora hystrix*. *ISME J.* 9, 1916–1927. doi: 10.1038/ismej.2015.3

Patrick, S., Houston, S., Thacker, Z., and Blakely, G. W. (2009). Mutational analysis of genes implicated in LPS and capsular polysaccharide biosynthesis in the opportunistic pathogen Bacteroides fragilis. *Microbiology* 155, 1039–1049. doi: 10.1099/mic.0.025361-0

Peng, L. H., Liang, X., Xu, J. K., Dobretsov, S., and Yang, J. L. (2020). Monospecific biofilms of Pseudoalteromonas promote larval settlement and metamorphosis of *Mytilus coruscus*. *Sci. Rep.* 10, 2577. doi: 10.1038/s41598-020-59506-1

Pierce, M. L., Ward, J. E., Holohan, B. A., Zhao, X., and Hicks, R. E. (2016). The influence of site and season on the gut and pallial fluid microbial communities of the eastern oyster, *Crassostrea virginica* (Bivalvia, Ostreidae): community-level physiological profiling and genetic structure. *Hydrobiologia* 765, 97–113. doi: 10.1007/s10750-015-2405-z

Quast, K., Pruesse, E., Yilmaz, P., Gerken, J., Schweer, T., Yarza, P., et al. (2013). The SILVA ribosomal RNA gene database project: improved data processing and web-based tools. *Nucleic Acids Res.* 41, 590–596. doi: 10.1093/nar/gks1219

Reveillaud, J., Maignien, L., Eren, A. M., Huber, J. A., Apprill, A., Sogin, M. L., et al. (2014). Host-specificity among abundant and rare taxa in the sponge microbiome. *ISME J.* 8, 1198–1209. doi: 10.1038/ismej.2013.227

Rogelj, J., den Elzen, M., Höhne, N., Fransen, T., Fekete, H., Winkler, H., et al. (2016). Paris Agreement climate proposals need a boost to keep warming well below 2 °C. *Nature* 534, 631–639. doi: 10.1038/nature18307

Sweet, M. J., and Bulling, M. T. (2017). On the importance of the microbiome and pathobiome in coral health and disease. *Front. Mar. Sci.* 4. doi: 10.3389/fmars.2017.00009

Trabal, N., Mazón-Suástegui, J. M., Vázquez-Juárez, R., Asencio-Valle, F., Morales-Bojórquez, E., and Romero, J. (2012). Molecular analysis of bacterial microbiota associated with oysters (*Crassostrea gigas* and *Crassostrea corteziensis*) in different growth phases at two cultivation sites. *Microb. Ecol.* 64, 555–569. doi: 10.1007/s00248-012-0039-5

Tremaroli, V., and Bäckhed, F. (2012). Functional interactions between the gut microbiota and host metabolism. *Nature* 489, 242–249. doi: 10.1038/nature11552

Webster, N., Hill, R.Great Barrier Reef Marine Park Authority. (2007). "Vulnerability of marine microbes on the Great Barrier Reef to climate change," in *Climate Change and the Great Barrier Reef: A Vulnerability Assessment*, 97–120. Townsville: The Great Barrier Reef Marine Park Authority Available at: http://hdl.handle.net/11017/538.

Wegner, K. M., Volkenborn, N., Peter, H., and Eiler, A. (2013). Disturbance induced decoupling between host genetics and composition of the associated microbiome. *BMC Microbiol.* 13, 252. doi: 10.1186/1471-2180-13-252

Wu, W., Huang, H., Ling, Z., Yu, Z., Jiang, Y., Liu, P., et al. (2016). Genome sequencing reveals mechanisms for heavy metal resistance and polycyclic aromatic hydrocarbon degradation in *Delftia lacustris* strain LZ-C. *Ecotoxicology* 25, 234–247. doi: 10.1007/s10646-015-1583-9

Wu, Y., Shukal, S., Mukherjee, M., and Cao, B. (2015). Involvement in denitrification is beneficial to the biofilm lifestyle of *Comamonas testosteroni*: a mechanistic study and its environmental implications. *Environ. Sci. Technol.* 49, 11551–11559. doi: 10.1021/acs.est.5b03381

Xiao, J., Ford, S. E., Yang, H., Zhang, G., Zhang, F., and Guo, X. (2005). Studies on mass summer mortality of cultured zhikong scallops (*Chlamys farreri* Jones et Preston) in China. *Aquaculture* 250, 602–615. doi: 10.1016/j.aquaculture.2005.05.002

Yang, J. L., Satuito, C. G., Bao, W. Y., and Kitamura, H. (2008). Induction of metamorphosis of pediveliger larvae of the mussel *Mytilus galloprovincialis* Lamarck 1819 using neuroactive compounds, KCl, NH4Cl and organic solvents. *Biofouling* 24, 461–470. doi: 10.1080/08927010802340309

Yang, J. L., Shen, P. J., Liang, X., Li, Y. F., Bao, W. Y., and Li, J. L. (2013). Larval settlement and metamorphosis of the mussel *Mytilus coruscus* in response to monospecific bacterial biofilms. *Biofouling* 29, 247–259. doi: 10.1080/08927014.2013.764412

Zhang, L. L., He, D., Chen, J. M., and Liu, Y. (2010). Biodegradation of 2-chloroaniline, 3-chloroaniline, and 4-chloroaniline by a novel strain *Delftia tsuruhatensis* H1. *J. Hazard Mater.* 179, 875–882. doi: 10.1016/j.jhazmat.2010.03.086

Zhang, M., Sun, Y., Chen, L., Cai, C., Qiao, F., Du, Z., et al. (2016). Symbiotic bacteria in gills and guts of Chinese mitten crab (*Eriocheir sinensis*) differ from the free-living bacteria in water. *PloS One* 11, e0148135. doi: 10.1371/journal.pone.0148135

frontiers | Frontiers in Physiology

TYPE Original Research
PUBLISHED 24 April 2024
DOI 10.3389/fphys.2024.1397818

OPEN ACCESS

EDITED BY
Yiming Li,
Fishery Machinery and Instrument Research Institute, China

REVIEWED BY
Lanmei Wang,
Freshwater Fisheries Research Center (CAFS), China
Zhiquan Liu,
Hangzhou Normal University, China

*CORRESPONDENCE
Wenzong Zhou,
zhouwz001@163.com
Mingyou Li,
myli@shou.edu.cn

†These authors have contributed equally to this work and share first authorship

RECEIVED 08 March 2024
ACCEPTED 04 April 2024
PUBLISHED 24 April 2024

CITATION
Mao Y, Lv W, Huang W, Yuan Q, Yang H, Zhou W and Li M (2024), Effects on growth performance and immunity of *Monopterus albus* after high temperature stress.
Front. Physiol. 15:1397818.
doi: 10.3389/fphys.2024.1397818

Effects on growth performance and immunity of *Monopterus albus* after high temperature stress

Yifan Mao[1†], Weiwei Lv[2†], Weiwei Huang[2], Quan Yuan[2], Hang Yang[2], Wenzong Zhou[2*] and Mingyou Li[1*]

[1]Key Laboratory of Integrated Rice-Fish Farming, Ministry of Agriculture and Rural Affairs, Shanghai Ocean University, Shanghai, China, [2]Eco-Environmental Protection Research Institute, Shanghai Academy of Agricultural Sciences, Shanghai, China

To investigate the impact of the effect of high temperature stimulation on *Monopterus albus* larvae after a certain period of time, five experimental groups were established at different temperatures. Then, the *M. albus* under high temperature stress was fed at 30°C for 70 days. After that, the growth index of the *M. albus* was counted and analyzed. In terms of growth index, high temperature stress had significant effects on FCR, FBW, WGR, and SGR of *M. albus* ($p < 0.05$). The SR increased after being stimulated by temperature ($p < 0.1$). The study revealed that liver cells of *M. albus* were harmed by elevated temperatures of 36°C and 38°C. In the experimental group, the activities of digestive enzymes changed in the same trend, reaching the highest point in the 32°C group and then decreasing, and the AMS activity in the 38°C group was significantly different from that in the 30°C group ($p < 0.05$). The activities of antioxidase in liver reached the highest at 34°C, which was significantly different from those at 30°C ($p < 0.05$). In addition, the expression levels of *TLR1*, *C3*, *TNF-α*, and other genes increased in the experimental group, reaching the highest point at 34°C, and the expression level of the *IL-1β* gene reached the highest point at 32°C, which was significantly different from that at 30°C ($p < 0.05$). However, the expression level of the *IRAK3* gene decreased in the experimental group and reached its lowest point at 34°C ($p < 0.05$). The expression level of the *HSP90α* gene increased with the highest temperature stimulus and reached its highest point at 38°C ($p < 0.05$). In the α diversity index of intestinal microorganisms in the experimental group, the observed species, Shannon, and Chao1 indexes in the 34°C group were the highest ($p < 0.05$), and β diversity analysis revealed that the intestinal microbial community in the experimental group was separated after high temperature stimulation. At the phylum level, the three dominant flora are *Proteus*, *Firmicutes*, and *Bacteroides*. *Bacteroides* and *Macrococcus* abundance increased at the genus level, but *Vibrio* and *Aeromonas* abundance decreased. To sum up, appropriate high-temperature stress can enhance the immunity and adaptability of *M. albus*. These results show that the high temperature stimulation of 32°C–34°C is beneficial to the industrial culture of *M. albus*.

KEYWORDS

***Monopterus albus*, high temperature stress, immunity, liver, intestinal microorganisms**

1 Introduction

In recent years, with climate warming and global temperatures rising, the impact of high temperature stress on aquatic organisms has become increasingly prominent. A fish is a vertebrate whose immune system lags behind that of mammals, and its immune function is affected by environmental factors to some extent, among which temperature is one of the main factors. Extreme weather and precipitation alter temperature, salinity, and dissolved oxygen levels, creating stressors that impact the physiological wellbeing of aquatic species. These changes subsequently influence the health of cultured fish through hosts and/or infectious sources (Reid et al., 2019; Mugwanya et al., 2022).

Researchers found that moderate temperature rise enhances the immune defense ability of salmon by promoting the expression of immune-related genes (Gruli Barbosa et al., 2020). Proper temperature control can influence how the transcriptome responds to a virus and highlight the significant function of temperature in regulating the fish immune response (Hori et al., 2012). Further research shows that high temperature stimulation can promote heat shock response, apoptosis, and the expression of immune defense-related genes (Jeyachandran et al., 2023) which is especially obvious in the classical activation of the complement system (Beemelmanns et al., 2021). As a key part of teleosts' natural defenses, the classical complement system can kill pathogens that get inside through LZM (Bai et al., 2022). In addition, stimulation at high temperatures can also trigger the inflammatory reaction of animals at variable temperatures, which is a key mechanism to deal with virus infection (Sanhueza et al., 2021). Dixon et al. (2016)'s research found that the survival rate of infectious hematopoietic necrosis virus (IHNV) in rainbow trout tissues was inversely proportional to temperature, emphasizing the influence of temperature on the interaction between pathogen survival and host immune response.

Environmental temperature significantly influences the microbial makeup and function of vertebrates that experience fluctuating temperatures (Fontaine et al., 2018), which is especially remarkable in fish because their immune response can be changed through the regulation of intestinal microbial flora (Sun et al., 2021). Compared with land animals, fish are more susceptible to continuous change in the environment, which may interfere with the stability of microbial communities (Butt and Volkoff, 2019). High temperature stress can result in damage to intestinal and accumulation of fat, reduced development rate, and decreased antioxidant capacity. The gut bacteria may contribute to these effects (He et al., 2019).

However, the stress process at too high a temperature may also have some side effects. For example, it has been found that the development of young pomfret ovata will be seriously affected in a high-temperature environment, leading to skeletal deformity (Yang et al., 2016). Under extreme temperature events, fish will use more energy to restore internal balance. Specifically, Fish might have to reallocate energy previously devoted to facilitating growth, maturation, immune functions, and reproductive activities towards repairing cells in injured tissues. This shift in energy usage could ultimately result in reduced growth efficiency and weakened immune responses (Islam et al., 2022). In addition, too high a temperature may also impair the immune system of fish, inhibit its immune function, and increase its risk of infection with pathogens.

When temperatures surpass the fish's ideal living conditions, enzymatic activities tend to decelerate owing to the denaturation of enzymes (Strzelczak et al., 2021), especially the activities of various energy metabolism-related enzymes (such as alanine aminotransferase) and digestive enzymes (such as AMS) (Mazumder et al., 2018), and the decline of their activities will directly affect the digestion and absorption capacity of fish. In addition, high temperatures will also alter the pH value and ion concentration of the intestine, further inhibiting the activity of enzymes (Solovyev and Izvekova, 2016).

Moderate environmental pressure can promote the adaptability of fish. Temperature stress can activate and enhance the immune system of fish, improve its ability to adapt to environmental changes, and resist pathogen invasion, especially for *Monopterus albus* (*M. albus*), a wide-temperature fish. This mechanism promotes the functional regulation and promotion of the fish immune system through moderate stimulation and then enhances its defense ability against pathogens. For example, studies on *Paralichthys olivaceus* and *Oncorhynchus mykiss* show that Fish that are pre-exposed to elevated temperatures can enhance their immune response and boost their resistance to high temperatures, provided that these temperatures are marginally below their critical threshold (Golovanova et al., 2013; Li et al., 2024). Precisely controlling temperature stress can significantly improve the immune defense capability of fish.

M. albus is a common benthic fish in lakes, rivers, ditches, and rice fields. *M. albus* can be found in subtropical and tropical monsoon climate areas, from Java Island to the Liaohe River Basin, and can tolerate temperatures from 0°C to 40°C. Environmental temperature closely influences its growth and immune status. In 2022, the total output of *M. albus* in China was 334,251 tons, of which the output of Hubei Province accounted for 46% ("2022 China Fishery Statistics Yearbook," 2023), and the output of *M. albus* in 2020 also has 313,790 tons, and the proportion of Hubei Province remained unchanged. Compared with 386,137 tons in 2017, the total output of *M. albus* decreased but remained at the same order of magnitude. Since China exceeded 300,000 tons in output in 2012, the culture technology of *M. albus* has not advanced, leaving the culture industry of *M. albus* in a bottleneck state.

Artificial propagation, opening, and high mortality of *M. albus* are three major problems faced by *M. albus* culture, which seriously restrict the development of the *M. albus* industry. The artificial propagation technology of *M. albus* has some defects, such as affecting the survival rate of parents, a low fertilization rate, a low hatching rate, and a low fry survival rate. At present, the main fry of the *M. albus* industry comes from capture in the wild, but in the wild environment, *M. albus* seedlings may carry some germs or viruses (Ou et al., 2013; Xia et al., 2019), which will explode rapidly in high-density artificial culture of *M. albus*, resulting in a large number of fish deaths. As a result, in the process of raising *M. albus*, farmers will choose the method of high temperature stimulation to reduce fry mortality. This study aims to examine the physiological and biochemical reactions of *M. albus* following acute high temperature stress at various temperatures during seedling development. It also seeks to assess

the impact of different levels of high temperature stress on the immunity and growth of *M. albus*.

2 Materials and methods

2.1 Ethical statement

Animal experiments were carried out following the protocols described in the "Guide to Experimental Animals" issued by the Ministry of Science and Technology in China.

2.2 Experimental materials

The samples used in this study are from the Shanghai Academy of Agricultural Sciences. Prior to formal breeding trials, in order to ensure that the *M. albus* is able to adapt to the specific environment and conditions required for the experiment, all *M. albus* are fed in a 1.0 × 1.0 × 1.0 m cement pond. We used the natural ingredients that *M. albus* likes, namely, earthworms. The earthworm slurry was used as an attractant to make *M. albus* seedlings adapt to artificial feeding. A mixture of fish meal and water with a ratio of 3:7 was used as the main nutrient source. In the first week, they were mixed together in a ratio of 1: 1 to make a paste-like open mixture, which was easily accepted by *M. albus* to initially stimulate the eating behavior of *M. albus*. In the next week, the proportion of earthworm slurry in the mixture gradually decreased to prevent the sudden change of feed from causing discomfort to *M. albus*. Until the feed used in the experiment was completely replaced by fish meal, this ensured that all the related *M. albus* smoothly transitioned to the standardized fish feed used in the experiment. At the end of the domestication phase, we randomly chose 150 healthy *M. albus* from the group as a whole. These *M. albus* were close together and had an average weight of 12.5 ± 0.7 g. They were then put into five trial groups and did so three times in each group. In order to maintain water quality conditions suitable for the growth of *M. albus*, exposure measures are used to replace new water daily, at about one-third of the total amount of water per replacement (NH^{4+}-N < 0.5 mg/L, soluble oxygen ≥55.8 mg/L, and PH 7.3 ± 0.2). *M. albus* is bred using commodity feed (Hubei Hui Biotechnology Co., Ltd.). Artificial feeding at 16:00 every day is controlled in proportion to 4 to 5 percent of the weight of the fish. The temperature of the domestication phase is controlled at 30°C ± 1°C, and changes are made after the start of the experiment.

The experiment is divided into 5 groups according to the temperature stimulation: 30°C, 32°C, 34°C, 36°C and 38°C. Each barrel contains 12 fish. The 30°C group kept the temperature unchanged as the 30°C as a control group; the rest controlled the temperature rise at a speed of 0.5°C/h (the error is within ±0.1°C); the stimulus total duration is controlled at 8 days; and the arrival time at the same speed controls the temperature drop to 30°C. Continue feeding for 10 weeks at 30°C after the end of the high-temperature stimulation experiment.

2.3 Sample collection and analysis

At the end of the high-temperature experiment, a 24-h fasting process was carried out, with a total of 45 fish randomly selected from the three nets of each experimental group, 3 fish selected for sampling in each net cage. The batch was rapidly anesthetized with MS-222 solution at a concentration of 100 mg/L (Shanghai Experimental Reactor Co., Ltd., Shanghai, China), and tissue samples were obtained.

TABLE 1 Primer sequence for qPCR.

Genes	Primers (5′–3′)	Accession No
IL-1β	F: 5′ AGCACTGAAGCCAGACCA 3′	XM_020585780.1
	R: 5′ GAACAGAAATCGCACCATA 3′	
TLR1	F: 5′AACCGGGCTGCTTTTATGGA3′	XM_020624433.1
	R: 5′TGGGCTTCATTGTCTGCCTTT3′	
irak3	F: 5′ GACCAAGCATGGAGAAGGTACT 3′	XM_020601231.1
	R: 5′ GTATGGACAACAGGGGGCTC 3′	
C3	F: 5’ GACTGTTGTTTGGACGGCAT 3′	XM_020587458.1
	R: 5′ GTCATCTTCCTCACTCCGACC 3′	
TNF-α	F: 5′ TGACAAACCCGCAGAAGA 3′	XM_020621700.1
	R: 5′ CGTAAACCTCCAGGTAATCG 3′	
HSP90α	F: 5′ GTAGGCTGGGCTTTCTCGAAT 3′	XM_020603713.1
	R: 5′ GTGTGCTTCAGGCATCTCTATC 3′	
β-actin	F: 5′ GCGTGACATCAAGGAGAAGC 3′	XM_020621264.1
	R: 5′ CTCTGGGCAACGGAACCTCT 3′	

At the end of the feeding experiment, three fish were selected again from each net box using the same method, and the fish were rapidly anesthetized, precisely measuring the weight and length of each fish.

Three fish are selected from each net box, and their intestinal tissues are harvested. They are first cleaned with a cold phosphate buffer solution (PBS) and then cut into small pieces of intestinal tissue. The remainder is ground in cold saline water (at a ratio of 1: 10 w/v) for further treatment. After 10 min of centrifugation at a speed of 4,000 rpm at 4°C, the supernate is collected, which is then used to measure the activity of digestive enzymes (including AMS, LPS and TRY), and the measurement is done through the commercial reagent box provided by the Nanjing Institute of Health and Biotechnology. Their liver tissue is collected according to the same processing method and is divided into three parts. First, use cold phosphate buffer solution (PBS) cleaning; the first part retains a 2–3 cm length; a more complete-shaped part of the tissue is fixed in polymorphic formaldehyde for 24 h; the tissues were embedded in paraffin, and the wax blocks are cut into 3 μm thick; Hematoxylin-Eosin dye (H&E dyeing); and finally, dehydration and sealing are performed. The vertical Ni-E microscope of the Nikon Ds-Ri2 camera (Nikon, Tokyo, Japan) was used for microscopic examination, and the slice images were collected. Half of the second part of the liver tissue is used to measure the activity of oxidative stress-related enzymes (including SOD, peroxide, and hydroxide) and LZM using the same method as the intestine using physiological salt water grinding, centrifugation, and collecting supernate using commercial reagent boxes (provided by the Nanjing Institute of Biotechnology). The third part is ground

TABLE 2 Effect of high temperature stimulation on growth performance of *M. albus* after 10 weeks.

Parameters	Temperature level					*p*-value
	30°C	32°C	34°C	36°C	38°C	ANOVA
IBW[a]	12.73 ± 0.81	12.62 ± 0.55	12.44 ± 0.63	12.2 ± 0.57	12.69 ± 0.48	0.366
FBW[b]	36.04 ± 0.47[b]	36.07 ± 1.23[b]	38.08 ± 1.73[a]	34.54 ± 1.13[b]	31.45 ± 1.12[c]	< 0.001
SR[c]	0.78 ± 0.05	0.81 ± 0.1	0.83 ± 0.08	0.72 ± 0.17	0.58 ± 0.09	0.097
WGR[d]	184.09 ± 16.57[b]	186.38 ± 18.88[ab]	206.48 ± 16.72[a]	183.69 ± 16.83[b]	148.19 ± 12.56[c]	< 0.001
SGR[e]	1.49 ± 0.08[a]	1.5 ± 0.09[a]	1.6 ± 0.08[a]	1.49 ± 0.09[a]	1.3 ± 0.07[b]	< 0.001
FCR[f]	2.25 ± 0.06[b]	2.25 ± 0.14[b]	2.06 ± 0.14[c]	2.36 ± 0.15[b]	2.81 ± 0.17[a]	0.039
CF[g]	7.89 ± 1.19	7.82 ± 1.05	7.52 ± 1.64	6.31 ± 1.33	6.77 ± 0.88	0.069
HSI[h]	1.46 ± 0.59	2.36 ± 0.89	1.76 ± 0.41	1.81 ± 0.78	2.37 ± 1.08	0.181
VSI[i]	5.95 ± 1.13	7.81 ± 1.99	6.2 ± 2.89	5.51 ± 1.39	6.36 ± 2.20	0.157

Note: Value are presented as means ± SD (standard deviation). Different lowercase letters indicate significance difference among the groups ($p < 0.05$).
[a]IBW, initial body weight (g).
[b]FBW, final body weight (g).
[c]SR, survival rate (%) = 100 × final number of fish/initial number of fish.
[d]WGR, weight gain rate (%) = 100 × (final body weight—initial body weight)/initial body eight.
[e]SGR, specific growth rate (%/d) = 100 × (ln FBW—ln IBW)/70 days.
[f]FCR, feed conversion rate = feed intake/(final body weight—initial body weight).
[g]CF, condition factor (%) = 100 × (body weight)/(body length)^c.
[h]HSI, hepatopancreas index (%) = 100% × (liver weight)/(final body weight).
[i]VSI, viscerosomatic index (%) = 100% × (viscera weight)/(final body weight).

with liquid nitrogen freezing, and the total RNA is obtained through Trizol reagent (Ambion, Texas, United States) from lysed tissue cells. The Agilent 2100 bioanalyzers (Agilent Technologies, Santa Clara, CA, United States) and NanoDrop 2000 (Thermo Scientific, Wilmington, DE, United States) are used to evaluate RNA integrity and quality. Following the detailed steps in the instructions that come with the cDNA synthesis reagent box (Ambion, Texas, United States), a reverse transcriptase reaction is carried out on total RNA. The gene sequence came from the GenBank database, and Biobio Engineering Co., Ltd. (Shanghai, China) synthesized the qPCR derivatives needed for the experiments (Table 1). The SYBR Green PCR Master Mix reagent box (TaKaRa, Kusatsu, Japan) is used for real-time PCR (qPCR) with the ROCHE Light Cycler 96 real-time system (Roche, Switzerland). The amplification conditions included preheating at 95°C for 120 s and 45 PCR cycles (94°C for 10 s; 62°C 30 s; 72°C 10 s). Each reaction system contains 5.2 μL of SYBR mixture, 2.8 μL of ultrapure water, 0.5 μL of forward primer, 0.5 μL of reverse primer, and 1 μL of cDNA as templates. In this experimental step, β-actin is used as an internal reference gene gene to calibrate the expression data of the target gene, ensuring the accuracy and reliability of the analysis results. The relative abundance of target gene mRNA was calculated by $R = 2^{-\Delta\Delta CT}$, and each liver sample was repeated three times to ensure the stability of the experimental results.

For intestinal microbiome analysis, DNA from the sample was extracted from the DNeasyPowerSoil reagent box (QIAGEN, Hilden, Germany), and the DNA concentration was detected by NanoDrop 2000 (Thermo Fisher Scientific, Waltham, MA, United States). The 16S rRNA gene sequencing was completed on the NovaSeq 6000 platform of Ilumina (Santiago Illumina, California, United States; Shanghai OE Biotechnology, China).

2.4 Statistical analysis

The data is computed using Microsoft Excel, evaluated with SPSS 22.0 program (IBM Company, NY, United States) for statistical analysis, and GraphPad Prism version 9.5 is utilized for graphing. Significant differences in groups were assessed using single-factor differential analysis (ANOVA) and graphical testing. All information is displayed as the average standard deviation (SD), where $p < 0.05$ is considered statistically significant.

3 Results

3.1 Basic growth parameters

Table 2 displays the impact of high temperature stimulation on the growth rate of *M. albus*. CF, HSI, and VSI did not exhibit a statistically significant difference ($p > 0.05$). The FCR, FBW, WGR, and SGR of *M. albus* larvae at 38°C differed substantially from the other four groups ($p < 0.05$). Compared with the 30°C group, the survival rate of other groups tends to increase ($p < 0.1$). When the high temperature stimulation reached 34°C, the growth performance of *M. albus* reached the highest level. When the high temperature stimulation reached 36°C, the growth performance of *M. albus* were inhibited.

3.2 Intestinal digestive enzyme activity

The levels of digestive enzyme activity are measured in order to conduct an in-depth analysis of the effects that high-temperature

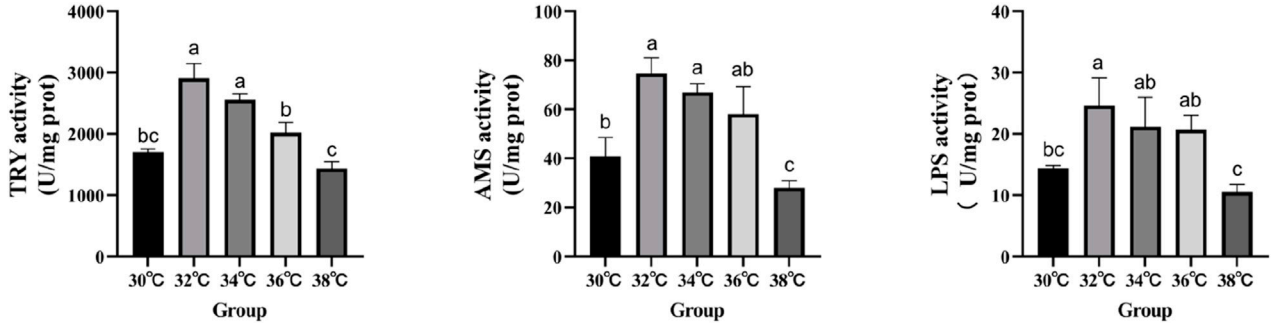

FIGURE 1
Effect of high temperature stimulation on digestive enzyme activity in the intestine of *M. albus*.

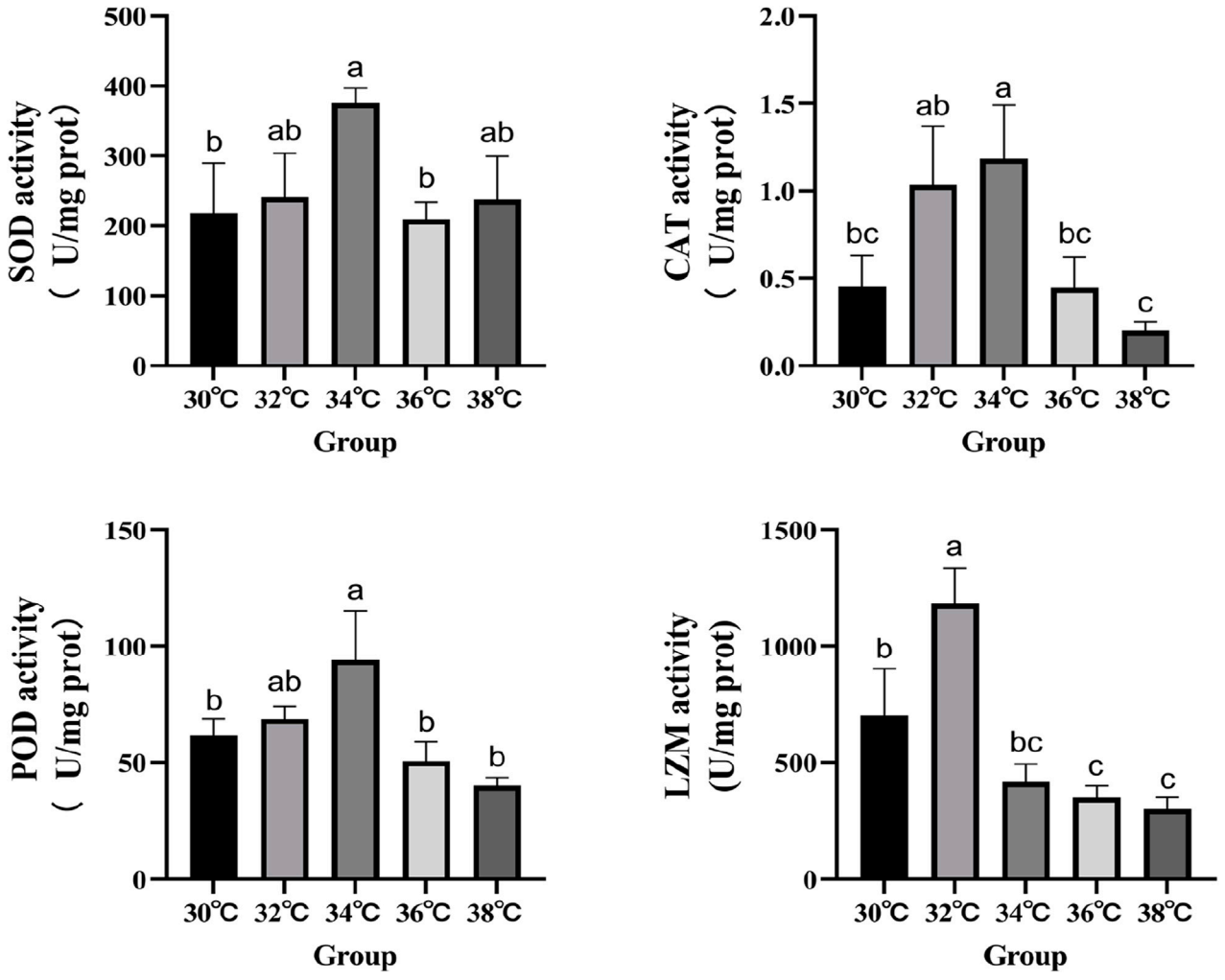

FIGURE 2
Effects of high temperature stimulation on activities of antioxidant enzymes and lysozyme in the liver of *M. albus*.

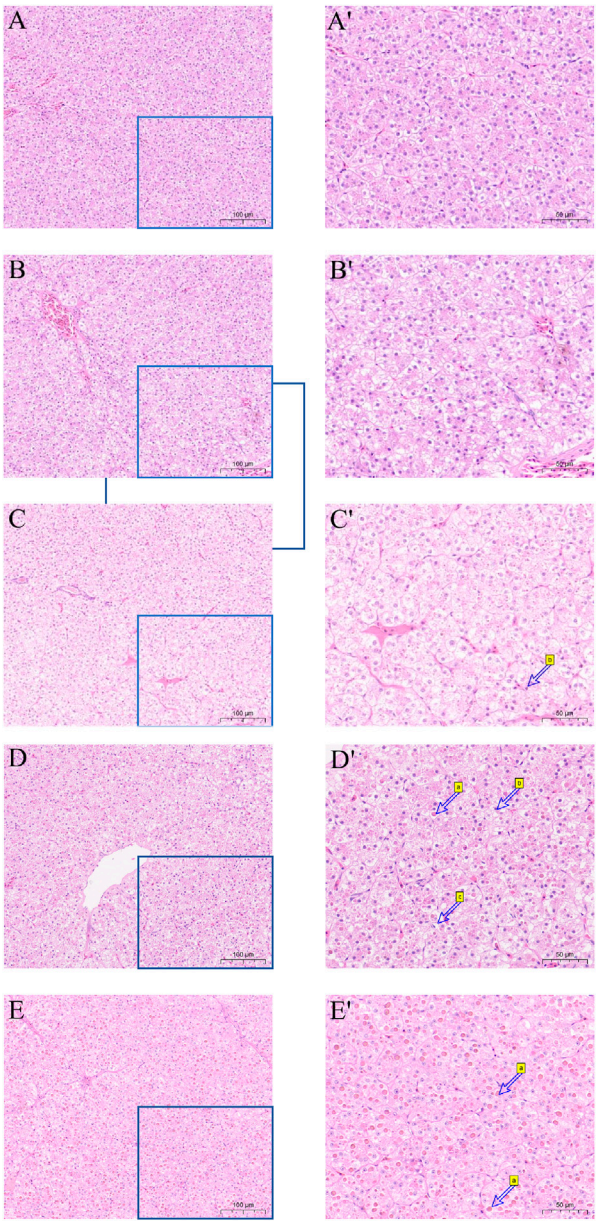

FIGURE 3
Effect of high temperature stress on liver morphology (× 100 and × 200) of *M. albus*. **(A,A')** 30°C **(B,B')** 32°C **(C,C')** 34°C **(D,D')** 36°C **(E,E')** 38°C, a cell necrosis, b nucleus condensation and c vacuole.

stimulation has on the levels of nutritional absorption in the intestinal tract (Figure 1). When the stimulation temperature reaches 34°C, the activity of AMS, LPS and TRY is at its peak.

3.3 Liver antioxidant and antibacterial enzymes activity

The levels of antioxidant activity were measured in order to investigate the effects of high-temperature stimulation on oxidative stress and immunity (Figure 2). The study demonstrated that the levels of SOD, CAT, and POD activity in the experimental group reached their highest point ($p < 0.05$) when exposed to high-temperature stimulation of 34°C. LZM's performance significantly increased at 32°C compared to the 30°C group, reaching statistical significance ($p < 0.05$).

3.4 Liver morphology

Hematoxylin and eosin (H&E) were utilized to stain the liver tissue sections, and the outcome is displayed in Figure 3. The liver cell shape of the 30°C group is normal, the arrangement is smooth, the boundaries are clear, and the cell mass is uniform. When the temperature stimulus reaches 36°C, the liver cells are markedly damaged, including foam deformation, cell death, cell shape blurred, and nucleic solidificaion. As the degree of thermal suppression increases, tissue damage becomes more noticeable.

3.5 Expression of genes associated to the hepatic immune system

Figure 4 displays the variations in the expression of *IRAK3*, *C3*, *TNF-α*, *IL-β*, *Hsp90*, and *TLR1* in the liver of *M. albus* larvae under various temperature conditions. The gene expression of *Hsp90* significantly increased when the temperature stimulus changed in comparison to the 30°C group. Genes including *C3*, *TNF-α*, *IL-β*, and *TLR1* show a similar pattern of expression following exposure to high temperatures, initially increasing and then reducing before peaking at 34°C. In contrast, the *IRAK3* gene exhibits an opposite trend, initially decreasing in expression before increasing ($p < 0.05$).

3.6 Intestinal microbial diversity index calculated on the basis of 16S rDNA gene sequence

The α diversity index reflects the abundance and diversity of intestinal microbial populations, as shown in Table 3. All groups had 100% goods coverage of commodities, suggesting that the sequencing depth adequately represented all species in the sample. Compared with the 30°C group, the indexes of observed species, Shannon and Chao1 in the 34°C group increased significantly ($p < 0.05$), and were also better than those in other treatment groups, and the change trend of these diversity indexes was the same. The main coordinate analysis of all groups (PCoA) divides samples into groups on the coordinate chart, showing how high temperatures change the make-up of microbes in the gut. PCoA showed that the intestinal microflora of the other group was separated from that of the 30°C group. The results showed that the intestinal microflora showed significant differences in β diversity after being stimulated by high temperature (Figure 5A). The abundance of the intestinal microbial communities of the *M. albus* samples surveyed is shown in Figure 5B, with *Proteus*, *Firmicutes*, *Bacteroides* and *Actinomycetes* as the main phylums. The abundance of *Proteobacteria* initially declined and then increased compared to the 30°C group, whereas the abundance of *Bacteroides* increased. *Firmicutes* initially developed and

10.3389/fphys.2024.1397818

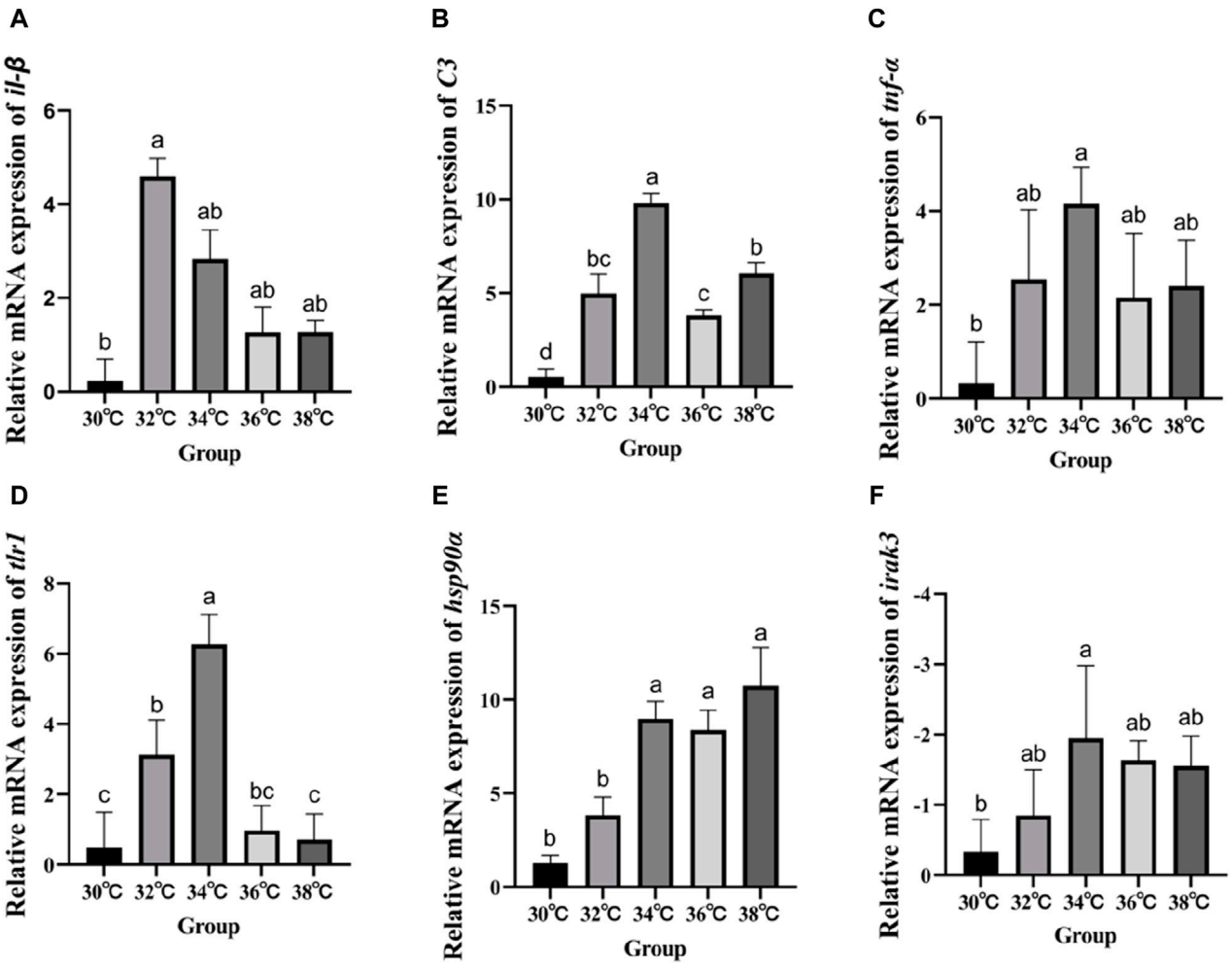

FIGURE 4
Effect of high temperature stimulation on mRNA expression level in liver of *M. albus*. **(A)** *IL-1β*: Interleukin 1β, **(B)** *C3*: complement component 3, **(C)** *TNF-α*: tumor necrosis factor α, **(D)** *tlr1*:Toll-like receptor 1, **(E)** *hsp90α*: heat shock protein 90α, and **(F)** *irak3*: IL-1 receptor-associated kinase 3.

TABLE 3 Effect of temperature stimulation level on α diversity of intestinal microorganisms in *M. albus*.

Parameters	Temperature level					*p*-value
	30°C	32°C	34°C	36°C	38°C	ANOVA
Goods coverage	1.00 ± 0.00	1.00 ± 0.00	1.00 ± 0.00	1.00 ± 0.00	1.00 ± 0.00	—
Shannon	3.31 ± 0.64^{b}	4.03 ± 0.74^{ab}	5.28 ± 1.57^{a}	3.48 ± 0.32^{b}	4.36 ± 0.25^{ab}	0.011
Observed species	82.14 ± 18.65^{ab}	78.04 ± 15.19^{ab}	162.32 ± 77.20^{a}	75.48 ± 11.36^{b}	71.22 ± 30.01^{b}	0.022
Simpson	0.87 ± 0.07	0.88 ± 0.05	0.94 ± 0.03	0.83 ± 0.04	0.86 ± 0.08	0.083
Chao1	84.47 ± 20.47^{ab}	97.2 ± 24.37^{ab}	153.03 ± 87.74^{a}	73.85 ± 10.79^{b}	65.22 ± 21.02^{b}	0.033

Note: Value are presented as means ± SD (standard deviation). Different lowercase letters indicate significance difference among the groups ($p < 0.05$).

subsequently declined. To further study the specific differences in microbiomes, Figure 5C shows the abundance of microbiomes in the first 15 genus. In the other group, *Bacteroides* and *Muribaculaceae* was increasing compared to the 30°C group, while the *Vibrio*, *Aeromonas* were decreasing.

4 Discussions

Generally, there is an optimum temperature for the growth of fish. If the temperature is too high, it will reduce growth performance and even lead to death (Islam et al., 2022). The

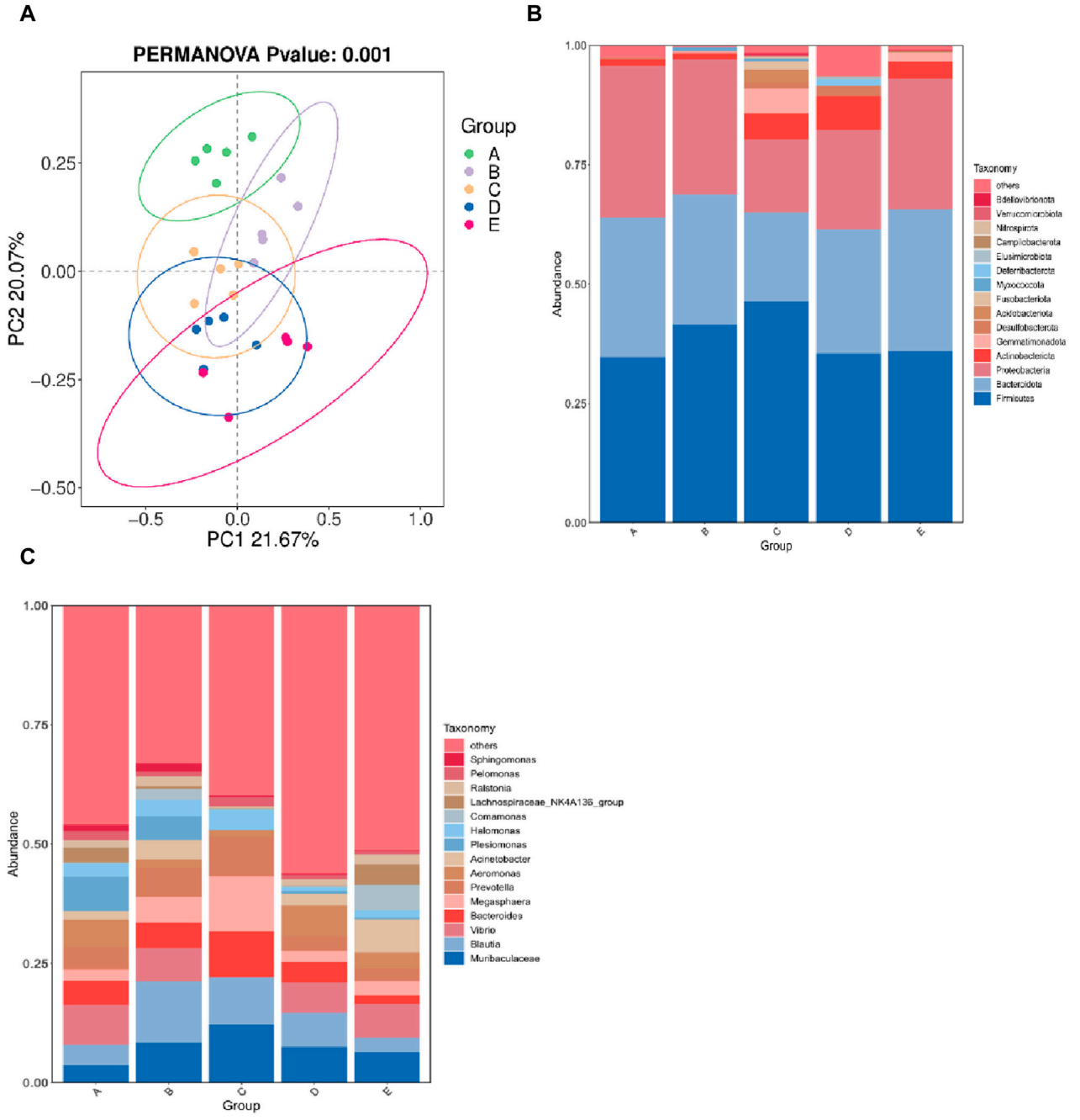

FIGURE 5
Effect of high temperature stimulation on intestinal flora of *M. albus*. Group A: 30°C group; Group B: 32°C group; Group C: 34°C group; Group D: 36°C group; Group E: 38°C group. **(A)** Principal Coordinate Analysis (PCoA) of the effect of high temperature stimulation on the diversity index of *M. albus* microbial community. **(B)** Effect of high temperature stimulation on phylum of microbiota diversity index in *M. albus*. **(C)** Effect of high temperature stimulation on genus of microbiota diversity index in *M. albus*.

findings of this study demonstrated that, after acute temperature stress, *M. albus*'s FBW, WGR, SGR, and FCR exhibited a significant tendency of first increasing and then dropping with temperature as compared to the 30°C group. Similar to studies on other fish, this demonstrates that suitable temperature stress can enhance *M. albus* growth performance and is a driving factor in regulating its growth performance (Pang et al., 2016; Ashaf-Ud-Doulah et al., 2020; Huss et al., 2021; Zhang et al., 2021). It is worth noting that, similar to this study, these results are aimed at the young fish of the research object. In fish with variable temperatures, the environmental temperature will affect the growth performance by affecting the fish's food intake, digestion, absorption, and metabolic activities (Fu et al., 2018; Volkoff and Rønnestad, 2020), and an appropriate temperature increase will improve these performances (Takasuka and Aoki, 2006; Sotoyama et al., 2018; Li et al., 2023). The growth performance in this experiment indicated that 32°C–34°C was the

ideal temperature for *M. albus* under high temperature stress, which was in line with our earlier hypothesis. In the long-term feeding procedure that followed, *M. albus* under this temperature stress exhibited good activity and food intake. The growth performance of *M. albus* in the follow-up feeding procedure was, however, inhibited to various degrees in the two groups of 36°C and 38°C due to the increase in stress temperature. It is speculated that more energy should be allocated and the cell structure damage caused by temperature stress should be repaired, which showed lower activity and food intake compared with the 32°C and 34°C groups in the follow-up feeding process. It's interesting that the development of gonads got a lot better in the 32°C and 34°C groups compared to the 30°C group. This suggests that the right amount of temperature stress may help *M. albus* reproduce, but more research is needed to be sure.

As is well knowledge, fish growth and development performance are directly correlated with the activity of their digestive enzymes. AMS, TRY, and LPS are three common digestive enzymes that can hydrolyze carbohydrates, proteins, and lipids, respectively, so as to obtain the energy needed for maintaining life activities, growth, and reproduction. Our findings indicate that following high temperature stress, the 34°C group's various enzymes activity were significantly higher than those of the 30°C group. They also did better than other treatment groups. This more intuitively explains why the growth performance of *M. albus* in the 34°C group was significantly improved, and similar conclusion were obtained in other fish (Qiang et al., 2017; Liu et al., 2023).

As the most vital organ in *M. albus*, the liver is directly communicates with the heart, intestine and gallbladder, related to growth and development, substance metabolism, detoxification, and hematopoiesis and can also reflect the physiological, pathological, and nutritional status of *M. albus*. Excessive temperature can also cause structural damage to fish, especially the liver, which has been confirmed in many species (Dettleff et al., 2022; E. Liu et al., 2022; Zhao et al., 2022). Excessive temperature will also stimulate the production of endogenous reactive oxygen species (ROS) (Wiens et al., 2017). The stability of the liver's structure is directly linked to its function as a site for the production of detoxified reactive oxygen species; yet, an excess of ROS can impact the liver's structure by changing the condition of the hepatocytes (Qin et al., 2023). The results from the 36°C and 38°C groups support the conclusion that high temperature stress will cause irreversible damage to the liver of *M. albus*, leading to significant impacts on its growth performance. High temperature has been proven to damage the livers of fish, especially cold-water fish (Ma et al., 2023).

The health of the liver is also very important for the normal operation of the immune system of *M. albus*, but the damage to the liver structure will have a serious impact on the immunological system of fish (Peng et al., 2022). SOD and CAT are considered the important first lines of defense against ROS because they can transform ROS into harmless metabolites, thus effectively preventing the accumulation of ROS (Yang et al., 2023). LZM is a crucial defensive molecule of the fish natural immune system that can take part in the immunological response to bacterial attack and heat stress (Saurabh and Sahoo, 2008; C. Zhang et al., 2018). Our research shows that, compared with the 30°C group, the activity of these antioxidant enzymes can be significantly improved at 34°C after high temperature stress, and it is more stable, but it tends to decrease at higher temperatures. This shows that individuals can eliminate the damage of peroxides and superoxide radicals by enhancing the activity of antioxidant enzymes in the culture of *M. albus* under a high temperature stress of 34°C, so as to improve the health status and growth and metabolic performance of the liver. The opposite effect will occur at too high a temperature. The expression of complement and heat shock proteins is beneficial to the improvement of immunity. *C3* complement is one of the key proteins for fish to adapt to temperature change, and it is expressed in immune-related tissues such as the gills, blood, and liver (Qi et al., 2011; Xu et al., 2018). High temperature stress will strengthen the expression of the *C3* complement gene in fish, thus affecting its immunity (Najafpour et al., 2020), which is proved by the research findings of carp (Dietrich et al., 2018). Heat shock proteins, including *HSP90α*, also participate in the immune response of fish (Wan et al., 2020). In some studies, the transcription level of HSP mRNA is regarded as a molecular biomarker of liver histological disorder caused by high temperature stress (Li et al., 2019). Fish immune systems can sense heat shock proteins and interact with pattern recognition receptors to activate antigens (Baharloei et al., 2021), thus regulating the immunological system to enhance the ability of fish to resist bacterial and viral infections (Jeyachandran et al., 2023). Therefore, the expression of the *HSP90α* gene in response to temperature changes may affect immune ability by regulating protein deposition and participating in innate and adaptive cellular immunity (Hoter et al., 2018). The toll-like receptor (*TLR1*) signal system plays a crucial role in the natural immunity of *M. albus TLR1* is a significant contributor to the natural immune response (Arancibia et al., 2007), and *TLR1*s are the fastest natural immune receptors to respond to fish infection (Li et al., 2017). Fish-specific *TLR1* acts a key role in the natural immune response of teleost (Nie et al., 2018; Shan et al., 2021). The *TLR1*-mediated signal transduction pathway is complex, involving a variety of proteins, including *IL-1β*, *TNF-α*, and *IRAK* (Fitzgerald and Kagan, 2020). High temperatures can stimulate the transcription of *IL-1β* and *TNF-α*, thus affecting the Toll-like receptor-mediated immunity in fish (Basu et al., 2012; Zou and Secombes, 2016). *IL-1β* may induce other cells to produce pro-inflammatory molecules. *TNF-α* triggers apoptosis and activates endothelium cells, hence enhancing the immunological response of fish against bacterial and viral infections (Roca et al., 2008) and has a function in the immune response against bacterial and viral pathogens. *IRAK*, which includes *IRAK3*, is responsible for facilitating the connection of various *IL-1* signaling pathways and increasing the release of cytokines that promote inflammation (Zheng and He, 2022). These cytokines can stop *TLR1* signals from activating (Rebl and Goldammer, 2018), lowering the immune response. The decrease in *IRAK3* gene expression and the increase in *TNF-α*, *IL-β*, and *TLR1* gene expression indicate that high temperature stress activates this signaling pathway. Fish benefit from even a temporary boost in immunity as it helps them adjust to their new immunological environment, even though the effects of high temperature stimulation eventually diminish (Wang et al., 2023).

An increasing amount of studies indicates that fish growth and development, as well as intestinal health, are influenced by the makeup of intestinal bacteria (El-Saadony et al., 2021; Y. Liu et al., 2022; López Nadal et al., 2020). The predominant bacterial species in the gut of *M. albus* were discovered to be Firmicutes, Bacteroidota, and

Proteobacteria. This finding is in line with studies on the intestinal flora composition of numerous other aquatic creatures. Following a period of high temperature stress, Firmicute abundance first declined and subsequently increased as temperature rose. Firmicutes are thought to contribute to intestinal health because of their capacity to interact with intestinal mucosa and ferment dietary fiber (Sun et al., 2023). Furthermore, research indicates that animal obesity and fat accumulation may be associated with the ratio of Firmicutes to Bacteroidota (Ley et al., 2006; Mariat et al., 2009; Sun et al., 2023). The findings of our investigation are comparable. Following a stress of high temperature, 34°C Group is able to demonstrate greater growth performance when compared to the control group. Muribaculaceae perform a number of crucial functions at the genus level in the breakdown of complex polysaccharides. Numerous multifunctional carbohydrate active enzymes, found in humans, mice, and other animals, are present in the studied genome (Ormerod et al., 2016). These enzymes are similar to the trend of improvement in perch's digestive function (Lin et al., 2023). Muribaculaceae contributes to the breakdown of complex carbohydrates, which can result in the production of acetic and propionic acids, and is positively correlated with the intestinal mucus layer's barrier function (Lagkouvardos et al., 2019). It's interesting to note that our findings indicate that 34°C Group has a substantially higher Megasphaera abundance than the other groups. The presence of Megasphaera in the body is associated with increased levels of immune genes in the gut and blood nutritional indicators (Brown et al., 2019), suggesting that it may be a probiotic. It is a bacteria that can convert many kinds of short-chain fatty acids (SCFA) from lactic acid, including acetate, propionate, butyrate, and valerate (J. Zhang et al., 2018). Since they are the host's energy source, these SCFA are crucial for intestinal health. As probiotics, Megasphaera has been shown to benefit pig and rodent digestive systems (Hashizume et al., 2003; Xie et al., 2017). Thus, we hypothesize that *M. albus*'s intestinal microorganisms can be reshaped and that the quantity of some bacteria can be markedly increased following the temperature stress of 34°C. The beneficial effects of these bacteria on intestinal health and obesity in animals have been demonstrated by science. This demonstrates that *M. albus* growth performance can be enhanced following appropriate temperature stress.

5 Conclusion

The high temperature stress of 34°C can stimulate the growth rate of *M. albus* larvae and when the temperature exceeds 36°C, it has a negative effect on the body, cause cell damage in the liver of *M. albus* and stimulate the immune system. The activities of digestive enzymes such as AMS, LPS and TRY in the intestine increased. The activities of SOD, POD and LZM will increase after high temperature stress, and the expression of *HSP90α*, *C3* and other immune-related protein synthesis genes will be enhanced. The expression of *TLR1*, *IL-1β*, *TNF-α* and other genes increased under high temperature stress, while the expression of *IRAK3* gene decreased, and the *TLR1* signaling pathway was activated. High temperature stimulation will also change the diversity of intestinal microorganisms and affect the nutritional absorption of the intestine. The changes in the physiological status and gene expression of *M. albus* after being stimulated by high temperatures below 36°C, will generally have beneficial effects on immunity and growth rate. Generally speaking, when the temperature rises to 34°C, it is beneficial to the growth and immunity of the cultured objects. When it exceeds this limit, the body of *M. albus* is damaged, but there is no significant difference in its mortality.

Data availability statement

The raw data supporting the conclusions of this article will be made available by the authors, without undue reservation.

Ethics statement

The animal study was approved by the Ministry of Science and Technology in China. The study was conducted in accordance with the local legislation and institutional requirements.

Author contributions

YM: Conceptualization, Data curation, Formal Analysis, Investigation, Writing–original draft. WL: Conceptualization, Data curation, Investigation, Writing–original draft, Writing–review and editing. WH: Conceptualization, Investigation, Writing–review and editing. QY: Conceptualization, Investigation, Writing–review and editing. HY: Conceptualization, Data curation, Investigation, Writing–review and editing. WZ: Conceptualization, Funding acquisition, Investigation, Writing–review and editing. ML: Conceptualization, Funding acquisition, Investigation, Supervision, Writing–review and editing.

Funding

The author(s) declare that financial support was received for the research, authorship, and/or publication of this article. This work was supported by the National Key R&D Program of China (2022YFD2400102).

Conflict of interest

The authors declare that the research was conducted in the absence of any commercial or financial relationships that could be construed as a potential conflict of interest.

Publisher's note

References

Arancibia, S. A., Beltrán, C. J., Aguirre, I. M., Silva, P., Peralta, A. L., Malinarich, F., et al. (2007). Toll-like receptors are key participants in innate immune responses. *Biol. Res.* 40 (2), 97–112. doi:10.4067/s0716-97602007000200001

Ashaf-Ud-Doulah, M., Mamun, A. A., Rahman, M. L., Islam, S. M. M., Jannat, R., Hossain, M. A. R., et al. (2020). High temperature acclimation alters upper thermal limits and growth performance of Indian major carp, rohu, *Labeo rohita* (Hamilton, 1822). *J. Therm. Biol.* 93, 102738. doi:10.1016/j.jtherbio.2020.102738

Baharloei, M., Heidari, B., Zamani, H., Ghafouri, H., and Hadavi, M. (2021). Effects of heat shock protein inducer on Hsp70 gene expression and immune parameters during Streptococcus iniae infection in a Persian sturgeon fry. *Vet. Res. Forum* 12 (4), 473–479. doi:10.30466/vrf.2019.115181.2740

Bai, H., Mu, L., Qiu, L., Chen, N., Li, J., Zeng, Q., et al. (2022). Complement C3 regulates inflammatory response and monocyte/macrophage phagocytosis of Streptococcus agalactiae in a teleost fish. *Int. J. Mol. Sci.* 23, 15586. doi:10.3390/ijms232415586

Basu, M., Swain, B., Maiti, N. K., Routray, P., and Samanta, M. (2012). Inductive expression of toll-like receptor 5 (*TLR5*) and associated downstream signaling molecules following ligand exposure and bacterial infection in the Indian major carp, mrigal (*Cirrhinus mrigala*). *Fish Shellfish Immunol.* 32 (1), 121–131. doi:10.1016/j.fsi.2011.10.031

Beemelmanns, A., Zanuzzo, F. S., Sandrelli, R. M., Rise, M. L., and Gamperl, A. K. (2021). The Atlantic salmon's stress- and immune-related transcriptional responses to moderate hypoxia, an incremental temperature increase, and these challenges combined. *G3 (Bethesda)* 11 (7), jkab102. doi:10.1093/g3journal/jkab102

Brown, E. M., Ke, X., Hitchcock, D., Jeanfavre, S., Avila-Pacheco, J., Nakata, T., et al. (2019). Bacteroides-derived sphingolipids are critical for maintaining intestinal homeostasis and symbiosis. *Cell Host Microbe* 25 (5), 668–680. doi:10.1016/j.chom.2019.04.002

Butt, R. L., and Volkoff, H. (2019). Gut microbiota and energy homeostasis in fish. *Front. Endocrinol.* 10, 9. doi:10.3389/fendo.2019.00009

China Fishery 2022 Statistics Yearbook, 2023 2022 China Fishery Statistics Yearbook (2023). *World agriculture(03)*.

Dettleff, P., Zuloaga, R., Fuentes, M., Gonzalez, P., Aedo, J., Estrada, J. M., et al. (2022). High-temperature stress effect on the red cusk-eel (*Geypterus chilensis*) liver: transcriptional modulation and oxidative stress damage. *Biology* 11 (7), 990. doi:10.3390/biology11070990

Dietrich, M. A., Hliwa, P., Adamek, M., Steinhagen, D., Karol, H., and Ciereszko, A. (2018). Acclimation to cold and warm temperatures is associated with differential expression of male carp blood proteins involved in acute phase and stress responses, and lipid metabolism. *Fish Shellfish Immunol.* 76, 305–315. doi:10.1016/j.fsi.2018.03.018

Dixon, P., Paley, R., Alegria-Moran, R., and Oidtmann, B. (2016). Epidemiological characteristics of infectious hematopoietic necrosis virus (IHNV): a review. *Veterinary Res.* 47 (1), 63. doi:10.1186/s13567-016-0341-1

El-Saadony, M. T., Alagawany, M., Patra, A. K., Kar, I., Tiwari, R., Dawood, M. A. O., et al. (2021). The functionality of probiotics in aquaculture: an overview. *Fish. Shellfish Immunol.* 117, 36–52. doi:10.1016/j.fsi.2021.07.007

Fitzgerald, K. A., and Kagan, J. C. (2020). Toll-like receptors and the control of immunity. *Cell* 180 (6), 1044–1066. doi:10.1016/j.cell.2020.02.041

Fontaine, S. S., Novarro, A. J., and Kohl, K. D. (2018). Environmental temperature alters the digestive performance and gut microbiota of a terrestrial amphibian. *J. Exp. Biol.* 221 (Pt 20), jeb187559. doi:10.1242/jeb.187559

Fu, K.-K., Fu, C., Qin, Y.-L., Bai, Y., and Fu, S.-J. (2018). The thermal acclimation rate varied among physiological functions and temperature regimes in a common cyprinid fish. *Aquaculture* 495, 393–401. doi:10.1016/j.aquaculture.2018.06.015

Golovanova, I., Golovanov, V. K., Smirnov, A. K., and Pavlov, D. D. (2013). Effect of ambient temperature increase on intestinal mucosa amylolytic activity in freshwater fish. *Fish Physiology Biochem.* 39, 1497–1504. doi:10.1007/s10695-013-9803-9

Gruli Barbosa, L. M., Moraes, G., de Freitas Anibal, F., and Marzocchi-Machado, C. M. (2020). Effect of environmental thermal fluctuations on innate immune responses in pacu Piaractus mesopotamicus juveniles. *Aquac. Rep.* 17, 100303. doi:10.1016/j.aqrep.2020.100303

Hashizume, K., Tsukahara, T., Yamada, K., Koyama, H., and Ushida, K. (2003). Megasphaera elsdenii JCM1772T normalizes hyperlactate production in the large intestine of fructooligosaccharide-fed rats by stimulating butyrate production. *J. Nutr.* 133 (10), 3187–3190. doi:10.1093/jn/133.10.3187

He, J., He, Y., Pan, D., Cao, J., Sun, Y., and Zeng, X. (2019). Associations of gut microbiota with heat stress-induced changes of growth, fat deposition, intestinal morphology, and antioxidant capacity in ducks. *Front. Microbiol.* 10, 903. doi:10.3389/fmicb.2019.00903

Hori, T. S. F., Gamperl, A. K., Booman, M., Nash, G. W., and Rise, M. L. (2012). A moderate increase in ambient temperature modulates the Atlantic cod (*Gadus morhua*) spleen transcriptome response to intraperitoneal viral mimic injection. *BMC Genomics* 13, 431. doi:10.1186/1471-2164-13-431

Hoter, A., El-Sabban, M. E., and Naim, H. Y. (2018). The HSP90 family: structure, regulation, function, and implications in health and disease. *Int. J. Mol. Sci.* 19 (9), 2560. doi:10.3390/ijms19092560

Huss, M., van Dorst, R. M., and Gårdmark, A. (2021). Larval fish body growth responses to simultaneous browning and warming. *Ecol. Evol.* 11 (21), 15132–15140. doi:10.1002/ece3.8194

Islam, M. J., Kunzmann, A., and Slater, M. J. (2022). Responses of aquaculture fish to climate change-induced extreme temperatures: a review. *J. World Aquac. Soc.* 53 (2), 314–366. doi:10.1111/jwas.12853

Jeyachandran, S., Chellapandian, H., Park, K., and Kwak, I.-S. (2023). A review on the involvement of heat shock proteins (extrinsic chaperones) in response to stress conditions in aquatic organisms. *Antioxidants* 12 (7), 1444. doi:10.3390/antiox12071444

Lagkouvardos, I., Lesker, T. R., Hitch, T. C. A., Gálvez, E. J. C., Smit, N., Neuhaus, K., et al. (2019). Sequence and cultivation study of Muribaculaceae reveals novel species, host preference, and functional potential of this yet undescribed family. *Microbiome* 7 (1), 28. doi:10.1186/s40168-019-0637-2

Ley, R. E., Turnbaugh, P. J., Klein, S., and Gordon, J. I. (2006). Microbial ecology: human gut microbes associated with obesity. *Nature* 444 (7122), 1022–1023. doi:10.1038/4441022a

Li, B., Sun, S., Zhu, J., Yanli, S., Wuxiao, Z., and Ge, X. (2019). Transcriptome profiling and histology changes in juvenile blunt snout bream (*Megalobrama amblycephala*) liver tissue in response to acute thermal stress. *Genomics* 111 (3), 242–250. doi:10.1016/j.ygeno.2018.11.011

Li, H., Yu, H., Zhang, X., Huang, W., Zhang, C., Wang, C., et al. (2024). Temperature acclimation improves high temperature tolerance of rainbow trout (*Oncorhynchus mykiss*) by improving mitochondrial quality and inhibiting apoptosis in liver. *Sci. Total Environ.* 912, 169452. doi:10.1016/j.scitotenv.2023.169452

Li, X., Wu, X., Li, X., Zhu, T., Zhu, Y., Chen, Y., et al. (2023). Effects of water temperature on growth performance, digestive enzymes activities, and serum indices of juvenile Coreius guichenoti. *J. Therm. Biol.* 115, 103595. doi:10.1016/j.jtherbio.2023.103595

Li, Y., Li, Y., Cao, X., Jin, X., and Jin, T. (2017). Pattern recognition receptors in zebrafish provide functional and evolutionary insight into innate immune signaling pathways. *Cell. Mol. Immunol.* 14 (1), 80–89. doi:10.1038/cmi.2016.50

Lin, H., Zhou, S., Huang, Z., Ma, J., Kong, L., Lin, Y., et al. (2023). The effects of porphyra yezoensis polysaccharides on intestinal health of spotted sea bass, lateolabrax maculatus. *Fishes* 8, 419. doi:10.3390/fishes8080419

Liu, E., Zhao, X., Li, C., Wang, Y., Li, L., Zhu, H., et al. (2022). Effects of acute heat stress on liver damage, apoptosis and inflammation of pikeperch (*Sander lucioperca*). *J. Therm. Biol.* 106, 103251. doi:10.1016/j.jtherbio.2022.103251

Liu, H., Yang, R., Fu, Z., Yu, G., Li, M., Dai, S., et al. (2023). Acute thermal stress increased enzyme activity and muscle energy distribution of yellowfin tuna. *PLoS One* 18 (10), e0289606. doi:10.1371/journal.pone.0289606

Liu, Y., Zhou, H., Fan, J., Huang, H., Deng, J., and Tan, B. (2022). Assessing effects of guar gum viscosity on the growth, intestinal flora, and intestinal health of *Micropterus salmoides*. *Int. J. Biol. Macromol.* 222 (Pt A), 1037–1047. doi:10.1016/j.ijbiomac.2022.09.220

López Nadal, A., Ikeda-Ohtsubo, W., Sipkema, D., Peggs, D., McGurk, C., Forlenza, M., et al. (2020). Feed, microbiota, and gut immunity: using the zebrafish model to understand fish health. *Front. Immunol.* 11, 114. doi:10.3389/fimmu.2020.00114

Ma, F., Zhao, L., Ma, R., Wang, J., and Du, L. (2023). FoxO signaling and mitochondria-related apoptosis pathways mediate tsinling lenok trout (*Brachymystax lenok tsinlingensis*) liver injury under high temperature stress. *Int. J. Biol. Macromol.* 251, 126404. doi:10.1016/j.ijbiomac.2023.126404

Mariat, D., Firmesse, O., Levenez, F., Guimarães, V., Sokol, H., Doré, J., et al. (2009). The Firmicutes/Bacteroidetes ratio of the human microbiota changes with age. *BMC Microbiol.* 9, 123. doi:10.1186/1471-2180-9-123

Mazumder, S. K., Das, S. K., Rahim, S. M., and Abd Ghaffar, M. (2018). Temperature and diet effect on the pepsin enzyme activities, digestive somatic index and relative gut length of Malabar blood snapper (*Lutjanus malabaricus* Bloch & Schneider, 1801). *Aquac. Rep.* 9, 1–9. doi:10.1016/j.aqrep.2017.11.003

Mugwanya, M., Dawood, M. A. O., Kimera, F., and Sewilam, H. (2022). Anthropogenic temperature fluctuations and their effect on aquaculture: a comprehensive review. *Aquac. Fish.* 7 (3), 223–243. doi:10.1016/j.aaf.2021.12.005

Najafpour, B., Cardoso, J. C. R., Canário, A. V. M., and Power, D. M. (2020). Specific evolution and gene family expansion of complement 3 and regulatory factor H in fish. *Front. Immunol.* 11, 568631. doi:10.3389/fimmu.2020.568631

Nie, L., Cai, S. Y., Shao, J. Z., and Chen, J. (2018). Toll-like receptors, associated biological roles, and signaling networks in non-mammals. *Front. Immunol.* 9, 1523. doi:10.3389/fimmu.2018.01523

Ormerod, K. L., Wood, D. L. A., Lachner, N., Gellatly, S. L., Daly, J. N., Parsons, J. D., et al. (2016). Genomic characterization of the uncultured Bacteroidales family S24-7

inhabiting the guts of homeothermic animals. *Microbiome* 4 (1), 36. doi:10.1186/s40168-016-0181-2

Ou, T., Zhu, R. L., Chen, Z. Y., and Zhang, Q. Y. (2013). Isolation and identification of a lethal rhabdovirus from farmed rice field eels *Monopterus albus*. *Dis. Aquat. Organ* 106 (3), 197–206. doi:10.3354/dao02660

Pang, X., Fu, S. J., and Zhang, Y. G. (2016). Acclimation temperature alters the relationship between growth and swimming performance among juvenile common carp (*Cyprinus carpio*). *Comp. Biochem. Physiol. A Mol. Integr. Physiol.* 199, 111–119. doi:10.1016/j.cbpa.2016.06.011

Peng, K., Chen, B., Zhao, H., Wang, Y., and Huang, W. (2022). Condensed tannins improve glycolipid metabolism but induce liver injury of Chinese seabass (*Lateolabrax maculatus*). *Front. Mar. Sci.* 9. [Original Research]. doi:10.3389/fmars.2022.902633

Qi, Z.-H., Liu, Y.-F., Wang, W.-N., Wu, X., Xin, Y., Lu, Y.-F., et al. (2011). Molecular characterization and functional analysis of a complement C3 molecule in the orange-spotted grouper (*Epinephelus coioides*). *Fish Shellfish Immunol.* 31 (6), 1284–1290. doi:10.1016/j.fsi.2011.09.018

Qiang, J., Tao, Y.-F., He, J., Bao, J.-W., Li, H.-X., Shi, W.-b., et al. (2017). Influences of dietary lipid and temperature on growth, fat deposition and lipoprotein lipase expression in darkbarbel catfish (*Pelteobagrus vachellii*). *J. Therm. Biol.* 69, 191–198. doi:10.1016/j.jtherbio.2017.07.014

Qin, H., Long, Z., Huang, Z., Ma, J., Kong, L., Lin, Y., et al. (2023). A comparison of the physiological responses to heat stress of two sizes of juvenile spotted seabass (lateolabrax maculatus). *Fishes* 8 (7), 340. doi:10.3390/fishes8070340

Rebl, A., and Goldammer, T. (2018). Under control: the innate immunity of fish from the inhibitors' perspective. *Fish Shellfish Immunol.* 77, 328–349. doi:10.1016/j.fsi.2018.04.016

Reid, G. H., Gurney-Smith, H., Marcogliese, D. J., Knowler, D., Benfey, T. J., Garber, A., et al. (2019). Climate change and aquaculture: considering biological response and resources. *Aquac. Environ. Interact.* 11, 569–602. doi:10.3354/aei00332

Roca, F. J., Mulero, I., López-Muñoz, A., Sepulcre, M. P., Renshaw, S. A., Meseguer, J., et al. (2008). Evolution of the inflammatory response in vertebrates: fish *TNF-alpha* is a powerful activator of endothelial cells but hardly activates phagocytes. *J. Immunol.* 181 (7), 5071–5081. doi:10.4049/jimmunol.181.7.5071

Sanhueza, N., Fuentes, R., Aguilar, A., Carnicero, B., Vega, K., Muñoz, D., et al. (2021). Behavioural fever promotes an inflammatory reflex circuit in ectotherms. *Int. J. Mol. Sci.* 22, 8860. doi:10.3390/ijms22168860

Saurabh, S., and Sahoo, P. K. (2008). Lysozyme: an important defence molecule of fish innate immune system. *Aquac. Res.* 39 (3), 223–239. doi:10.1111/j.1365-2109.2007.01883.x

Shan, S., Liu, R., Feng, H., Meng, F., Aizaz, M., and Yang, G. (2021). Identification and functional characterization of a fish-specific tlr19 in common carp (*Cyprinus carpio L.*) that recruits TRIF as an adaptor and induces ifn expression during the immune response. *Veterinary Res.* 52 (1), 88. doi:10.1186/s13567-021-00957-3

Solovyev, M., and Izvekova, G. (2016). Seasonal changes in pH values in the intestine of fish from Lake Chany (West Siberia). *Inland Water Biol.* 9, 400–404. doi:10.1134/s1995082916040131

Sotoyama, Y., Yokoyama, S., Ishikawa, M., Koshio, S., Hashimoto, H., Oku, H., et al. (2018). Effects of a superoptimal temperature on aquacultured yellowtail *Seriola quinqueradiata*. *Fish. Sci.* 84 (6), 1063–1071. doi:10.1007/s12562-018-1247-9

Strzelczak, A., Balejko, J., Szymczak, M., and Witczak, A. (2021). Effect of protein denaturation temperature on rheological properties of baltic herring (*Clupea harengus membras*) muscle tissue. *Foods* 10 (4), 829. doi:10.3390/foods10040829

Sun, B.-Y., Yang, H.-X., He, W., Tian, D.-Y., Kou, H.-Y., Wu, K., et al. (2021). A grass carp model with an antibiotic-disrupted intestinal microbiota. *Aquaculture* 541, 736790. doi:10.1016/j.aquaculture.2021.736790

Sun, Y., Zhang, S., Nie, Q., He, H., Tan, H., Geng, F., et al. (2023). Gut firmicutes: relationship with dietary fiber and role in host homeostasis. *Crit. Rev. Food Sci. Nutr.* 63 (33), 12073–12088. doi:10.1080/10408398.2022.2098249

Takasuka, A., and Aoki, I. (2006). Environmental determinants of growth rates for larval Japanese anchovy *Engraulis japonicus* in different waters. *Fish. Oceanogr.* 15 (2), 139–149. doi:10.1111/j.1365-2419.2005.00385.x

Volkoff, H., and Rønnestad, I. (2020). Effects of temperature on feeding and digestive processes in fish. *Temp. (Austin)* 7 (4), 307–320. doi:10.1080/23328940.2020.1765950

Wan, Q., Song, D., Li, H., and He, M.-l. (2020). Stress proteins: the biological functions in virus infection, present and challenges for target-based antiviral drug development. *Signal Transduct. Target. Ther.* 5 (1), 125. doi:10.1038/s41392-020-00233-4

Wang, B., Thompson, K. D., Wangkahart, E., Yamkasem, J., Bondad-Reantaso, M. G., Tattiyapong, P., et al. (2023). Strategies to enhance tilapia immunity to improve their health in aquaculture. *Rev. Aquac.* 15 (S1), 41–56. doi:10.1111/raq.12731

Wiens, L., Banh, S., Sotiri, E., Jastroch, M., Block, B. A., Brand, M. D., et al. (2017). Comparison of mitochondrial reactive oxygen species production of ectothermic and endothermic fish muscle. *Front. Physiol.* 8, 704. doi:10.3389/fphys.2017.00704

Xia, L., Han, P., Cheng, X., Li, Y., Xu, Q., Yuan, H., et al. (2019). Aeromonas veronii caused disease and pathological changes in Asian swamp eel *Monopterus albus*. *Aquac. Res.* 50 (7), 2978–2985. doi:10.1111/are.14253

Xie, M., Chen, G., Wan, P., Dai, Z., Hu, B., Chen, L., et al. (2017). Modulating effects of dicaffeoylquinic acids from Ilex kudingcha on intestinal microecology *in vitro*. *J. Agric. food Chem.* 65 (47), 10185–10196. doi:10.1021/acs.jafc.7b03992

Xu, Y., Yu, Y., Zhang, X., Huang, Z., Li, H., Dong, S., et al. (2018). Molecular characterization and expression analysis of complement component 3 in dojo loach (*Misgurnus anguillicaudatus*). *Fish Shellfish Immunol.* 72, 484–493. doi:10.1016/j.fsi.2017.11.022

Yang, Q., Ma, Z., Zheng, P., Jiang, S., Qin, J. G., and Zhang, Q. (2016). Effect of temperature on growth, survival and occurrence of skeletal deformity in the golden pompano Trachinotus ovatus larvae. *Indian J. Fish.* 63 (1), 74–82. doi:10.21077/ijf.2016.63.1.51490-10

Yang, Y., Xu, W., Du, X., Ye, Y., Tian, J., Li, Y., et al. (2023). Effects of dietary melatonin on growth performance, antioxidant capacity, and nonspecific immunity in crayfish, *Cherax destructor*. *Fish Shellfish Immunol.* 138, 108846. doi:10.1016/j.fsi.2023.108846

Zhang, C., Zhang, J., Liu, M., and Huang, M. (2018). Molecular cloning, expression and antibacterial activity of goose-type lysozyme gene in Microptenus salmoides. *Fish Shellfish Immunol.* 82, 9–16. doi:10.1016/j.fsi.2018.07.058

Zhang, J., Chen, X., Liu, P., Zhao, J., Sun, J., Guan, W., et al. (2018). Dietary Clostridium butyricum induces a phased shift in fecal microbiota structure and increases the acetic acid-producing bacteria in a weaned piglet model. *J. Agric. food Chem.* 66 (20), 5157–5166. doi:10.1021/acs.jafc.8b01253

Zhang, Z., Zhou, C., Fan, K., Zhang, L., Liu, Y., and Liu, P. F. (2021). Metabolomics analysis of the effects of temperature on the growth and development of juvenile European seabass (*Dicentrarchus labrax*). *Sci. Total Environ.* 769, 145155. doi:10.1016/j.scitotenv.2021.145155

Zhao, X., Li, L., Li, C., Liu, E., Zhu, H., and Ling, Q. (2022). Heat stress-induced endoplasmic reticulum stress promotes liver apoptosis in largemouth bass (*Micropterus salmoides*). *Aquaculture* 546, 737401. doi:10.1016/j.aquaculture.2021.737401

Zheng, Y., and He, J.-Q. (2022). Interleukin receptor associated kinase 1 signaling and its association with cardiovascular diseases. *RCM* 23 (3), 97. doi:10.31083/j.rcm2303097

Zou, J., and Secombes, C. J. (2016). The function of fish cytokines. *Biology* 5 (2), 23. doi:10.3390/biology5020023

frontiers | Frontiers in Physiology

TYPE Original Research
PUBLISHED 02 May 2024
DOI 10.3389/fphys.2024.1404834

OPEN ACCESS

EDITED BY
Yiming Li,
Fishery Machinery and Instrument Research Institute, China

REVIEWED BY
Zhijian Huang,
Sun Yat-sen University, China
Ermeng Yu,
Chinese Academy of Fishery Sciences, China

*CORRESPONDENCE
Kang Li,
kli@shou.edu.cn
Liping Liu,
lp-liu@shou.edu.cn

†These authors have contributed equally to this work

RECEIVED 21 March 2024
ACCEPTED 11 April 2024
PUBLISHED 02 May 2024

CITATION
Li Z, Liu R, Liu J, Jiang Z, Ba X, Li K and Liu L (2024), Effects of flowing water stimulation on hormone regulation during the maturation process of *Conger myriaster* ovaries. *Front. Physiol.* 15:1404834. doi: 10.3389/fphys.2024.1404834

Effects of flowing water stimulation on hormone regulation during the maturation process of *Conger myriaster* ovaries

Zhengcheng Li[1,2†], Rucong Liu[1,2†], Jingwei Liu[1,2,3], Zhixin Jiang[1,2], Xubing Ba[1,2], Kang Li[1,2,3*] and Liping Liu[1,2,3*]

[1]China-ASEAN Belt and Road Joint Laboratory on Mariculture Technology (Shanghai), Shanghai Ocean University, Shanghai, China, [2]Center for Ecological Aquaculture (CEA), Shanghai Ocean University, Shanghai, China, [3]Shanghai Engineering Research Center of Aquaculture, Shanghai Ocean University, Shanghai, China

Conger eel (*Conger myriaster*) is an economically important species in China. Due to the complex life history of the conger eel, achieving artificial reproduction has remained elusive. This study aimed to explore the effect of water stimulation on hormonal regulation during the artificial reproduction of conger eel. The experiment was divided into four groups: A1 (no hormone injection, still water), A2 (no hormone injection, flowing water), B1 (hormone injection, still water), and B2 (hormone injection, flowing water). The flowing water group maintained a flow velocity of 0.4 ± 0.05 m/s for 12 h daily throughout the 60-day period. Steroid hormone levels in the serum and ovaries of conger eels were analyzed using UPLC-MS/MS and ELISA on the 30th and 60th days of the experiment. The relative expression levels of follicle-stimulating hormone (*FSHβ*) and luteinizing hormone (*LHβ*) in the pituitary were determined by quantitative PCR. The results showed a significantly lower gonadosomatic index (GSI) in B2 compared to B1 ($p < 0.05$) on the 30th day. FSH was found to act only in the early stages of ovarian development, with water stimulation significantly enhancing FSH synthesis ($p < 0.05$), while *FSHβ* gene was not expressed after hormone injection. Conversely, LH was highly expressed in late ovarian development, with flowing water stimulation significantly promoting LH synthesis ($p < 0.05$). Serum cortisol (COR) levels were significantly higher in the flowing water group than in the still water group ($p < 0.05$). Furthermore, estradiol (E2) content of B2 was significantly lower than that of B1 on the 30th and 60th day. Overall, flowing water stimulation enhanced the synthesis of FSH in early ovarian development and LH in late ovarian development, while reducing E2 accumulation in the ovaries. In this study, the effect of flowing water stimulation on hormone regulation during the artificial reproduction of conger eel was initially investigated to provide a theoretical basis for optimizing artificial reproduction techniques.

KEYWORDS

conger eel, artificial reproduction, swimming, ovarian development, hormone regulation

1 Introduction

Conger eel (*Conger myriaster*) is a highly economically valuable demersal fish found in the Pacific Northwest (Ma et al., 2018).They are often referred to as sand eels due to their predominant habitat in coastal mud, sand, and gravel substrates (Ma et al., 2018). Currently, artificial propagation of eels remains challenging, with eel culture industries relying solely on wild-caught larvae resources (Horie et al., 2010). Previous studies have successfully obtained and hatched fertilized eel eggs through exogenous hormone-induced maturation. However, challenges persist, including high larval mortality rates and poor quality of fertilized eggs (Utoh et al., 2010b; Horie et al., 2010). Therefore, optimizing the artificial breeding techniques is of great importance for both research and industrial practice in eels.

The conger eel is a deep-sea migratory fish (Hao et al., 2020). The ovaries of the conger eel gradually mature during migration and lay eggs near the spawning grounds (Okamura et al., 2000; Li et al., 2018; Xiaolong et al., 2021). Under captive breeding condition, the ovarian development of female broodstock stops at the secondary yolk globule stage (Utoh et al., 2010a; Chiba et al., 2010). The development of ovaries in eels only occurs when exogenous hormones are injected (Utoh et al., 2010a; Chiba et al., 2010). Swimming behavior is the main way to realize the physiological activity of migratory fish, which is important for individual survival and population reproduction (Liu et al., 2015). Swimming can promote gonadal maturation in male eels, and promote lipid accumulation in female eels' oocytes (Couillard et al., 1997; Palstra et al., 2007; Palstra et al., 2009; Palstra et al., 2010b). The development of the gonads in teleost is controlled by the hypothalamic-pituitary-gonadal (HPG) axis (Kr et al., 2020). Inhibition of gonadal development in eels is caused by dopamine suppression and gonadotropin-releasing hormone deficiency, which in turn inhibits the synthesis of follicle-stimulating hormone (FSH) and luteinizing hormone (LH) (Palstra et al., 2009; Wang et al., 2015). FSH primarily promotes the biosynthesis of testosterone T) and estradiol (E2), which are essential for spermatogenesis and oogenesis (Yaron et al., 2003). LH induces final gonadal maturation and ovulation more effectively by stimulating the secretion of mature steroid hormones (Yaron et al., 2003).

Therefore, artificial breeding in an indoor environment may affect the development of ovaries by blocking migration behavior. Previous studies have shown that water stimulation can significantly reduce mortality in conger eels during ovarian maturation (Meng, 2020). Studying the regulatory effect of swimming on the ovarian development of conger eel is necessary for optimizing artificial breeding techniques of conger eels. In this study, conger eels were induced to swim for 30 or 60 days through water stimulation with hormone injection and no-hormone injection. To explore the effects of flowing water stimulation on hormone regulation during the artificial reproduction of conger eel, we analyzed the relative expression levels of *FSHβ* and *LHβ* genes in the pituitary gland, as well as the changes in steroid hormones in the ovary and serum. The present study may provide a theoretical basis for the optimization of artificial reproduction technology of conger eel and other fish.

2 Materials and methods

2.1 Ethics statement

All fish samples were handled by the Animal Ethics Committee of Shanghai Ocean University (2016 NO.4) and the Regulations for the Administration of Affairs Concerning Experimental Animals approved and authorized by the State Council of the People's Republic of China.

2.2 Experimental eels

The female conger eel (n = 86, 303.64 ± 10.02 g) with oocytes at the oil droplet stage and primary yolk globule stage were obtained from Shenghang Aquatic Technology Co. Ltd. (Weihai, China). The developmental stages of the female eels were determined by observing the histological sections of ovaries. Oocytes in the oil droplet stage contain numerous vacuolar small lipid droplets, while oocytes in the primary yolk globule stage exhibit light purple yolk protein granules at the cell periphery. The experiment begun in May 2021 at the company's fish farm. The eels were acclimated in a cement tank (30.0 ± 0.5 psu, 18°C ± 0.5°C) for 2 weeks before the experiment.

A cylindrical glass fiber tank (radius = 0.75 m, height = 1.5 m, aquaculture water body = 1000 L) with a built-in pump was designed to provide circulating water flow for fish swimming (Liu et al., 2022). According to a previous study on flow velocity (0.4 ± 0.05 m/s) and the findings of the eel migration route, the swimming duration was set at 12 h per day (Hammer, 1995; Miller et al., 2011; Meng, 2020).

2.3 Experiment design and sampling

Eels were selected and randomly distributed into four cylindrical glass fiber tanks (n = 20, 30.0 ± 0.5 psu, 18°C ± 0.5°C), and the criteria for selecting healthy eels include appropriate size, good vitality, absence of injuries or illnesses, and a silver-white abdomen. Six acclimated eels were sampled and measured as a control group on the first day. Circulating water flow and hormone injection regime were two factors set in the following trials: A1 (no hormone injection, still water), A2 (no hormone injection, flowing water), B1 (hormone injection, still water), and B2 (hormone injection, flowing water). All experimental groups were placed in a dark environment.

A mixture of carp pituitary extract (CPE, 20 mg/kg) and human chorionic gonadotropin (HCG, 100 IU/kg) was intraperitoneally injected weekly to induce eel development of the hormone injection groups (B1 and B2), while the no hormone injection groups (A1 and A2) were injected with an equal amount of physiological saline solution until the end of the experiment. On the 30th and 60th days of the trial, six eels in each group were anesthetized using MS-222 (0.05 g/L). The weight of each eel was measured. Blood samples were collected from the bulbous arteriosus using a syringe and centrifuged at 3000 rpm for 15 min at 4°C. The Serum was frozen at −80°C. The pituitary and ovary were weighed and stored in a RNase-free tube at −80°C for Quantitative real-time PCR analysis.

TABLE 1 Primers' sequences of Target Genes in qPCR from Conger eel.

Primer	Sequence of primer	Target gene
β-actin-F	5′- CAGGTCATCACCATCGGCAA -3′	*β-actin*
β-actin-R	5′- TCCTTCTGCATTCTGTCGGC -3′	
FSHβ-F	5′- GTTGATGCTGGCTCCTGCTCTG -3′	*FSHβ*
FSHβ-R	5′- ACACAGGGTCCTGGGTGAAGC -3′	
LHβ-F	5′- GACAGTCCGTCTGCCAGATTGC -3′	*LHβ*
LHβ-R	5′- GCACAGGTTACAGTCACAGCTCAG -3′	

2.4 Quantitative real-time PCR

The distinct functions of FSH and LH are determined by their respective β subunits, encoded by the *FSHβ* and *LHβ* genes. After obtaining the gene sequences of *FSHβ* (GenBank accession no. AB045157.1) and *LHβ* (GenBank accession no. AB045158.1) of conger eel on NCBI, specific primers were designed by primer software and used for quantitative real-time PCR to analyze gene expression. The *β-actin* gene served as an internal control. Before the experiment, the specificity and amplification efficiency of *β-actin* primers were verified (Table 1).

Total RNA was extracted from the liver using a kit (Tiangen Biotech Co., Ltd.) according to the manufacturer's instructions. About 1 μg of total RNA was reverse transcribed with Hifair® II first Strand cDNA Synthesis SuperMix for qPCR (gDNA digester plus) (CAT:11123 ES). Diluted cDNA (1:10) was used in all qPCR reactions. The qRT-PCR experiments were carried out in triplicate on CFX96 Touch Real-time PCR Detection System (Applied Biosystems®, BIO-RAD, America) using 1 μL of diluted cDNA as a template for each reaction with SYBR Green PCR Master Mix (Bio-Rad). Thermal cycling conditions included an initial heat denaturation step at 95°C for 30 s, 40 cycles at 95°C for 5 s, 60°C for 30 s, and at 95°C for 15 s. Melting curves of the PCR products were determined from 60°C to 95°C to ascertain the specificity of the amplification. Relative gene expression was calculated using the $2^{-\Delta\Delta Ct}$ method.

2.5 Ultra-high-performance liquid chromatography–tandem mass spectrometry (UPLC-MS/MS)

The extraction of steroid hormones in serum followed the method described by Dang (Dang, 2020). Specifically, 10 μL serum was homogenized with methyl tert-butyl ether (MTBE) and condensed to dry. Subsequently, 50 μL methanol (chromatographic grade) was added to dissolve the residue. After thorough shaking and mixing, the mixture was filtered through a microporous filter membrane (0.22 μm, Shanghai Amp Biotechnology Co., LTD.) into a 1.5 mL sample bottle for machine detection.

The extraction of steroid hormones from ovaries was conducted based on the protocol outlined by Ma (Ma et al., 2016). Pre-cooled methanol (chromatographic grade) was added to the ovarian tissue and thoroughly homogenized. The homogenate was then subjected to centrifugation (4°C, 10000r/min, 10min), and the supernatant was collected. Following this, the crude extract underwent solid-phase extraction using an HLB solid-phase extraction column (Shanghai Amp Biotechnology Co., LTD.). The resulting extract was evaporated nearly to dryness using a nitrogen blower at 40°C, and the volume was adjusted to 500 μL with methanol. After shaking and mixing, the extract was filtered through a microporous filter membrane (0.22 μm) into a 1.5 mL sample bottle, which was to be tested by the machine.

Calibration stock solutions of E2, cortisol (COR), 17α-hydroxyprogesterone (17α-OHP), T, and 11-Ketoltestosterone (11-KT) were prepared from Shanghai Amp Biotechnology Co., LTD. The concentration of the standard curve was 1, 5, 25, 50, 100, and 200 ng/mL.

2.6 Enzyme–linked immunosorbent assay (ELISA)

The E2 content in the ovarian and FSH, LH content in the serum was determined using an enzyme-linked immunosorbent assay kit (Shanghai Enzyme-linked Biotechnology Co., Ltd., China) by the instructions of the kit.

2.7 Statistical analysis

The UPLC-MS/MS and ELISA data were processed and imported into EXCEL for analysis using Mass Lynx V4.1 and ELISA Calc software respectively. All statistical tests were performed in SPSS 22.0 software, and graphical representations were generated using GraphPad Prism 9.0. Two-way analysis of variance (ANOVA) was used for multi-group statistical analysis. Results were expressed as Mean ± standard deviation (Mean ± SD). $p < 0.05$ was considered statistically significant.

3 Results

3.1 Ovarian development

In the two groups without injection (A1 and A2), there was no significant difference in gonadosomatic index (GSI, Figure 1A). The GSI of eels in groups B1 and B2 increased gradually during the experiment (Figure 1B). On the 30th day, the GSI of B1 was 17.62% ± 0.42%, which was significantly higher than that of B2 11.41% ± 4.37%. However, by the 60th day, there was no significant difference between the two groups with GSI of 26.36% ± 17.09% and 23.748% ± 12.21% respectively.

3.2 Changes of hormone content in ovary and serum

The concentrations of COR, 17α-OHP, T, 11-KT and E2 in serum and ovary were detected by UPLC-MS/MS, and they were well separated on XBridge C18 column. The correlation coefficients of the above standard curves were all above 0.9,

10.3389/fphys.2024.1404834

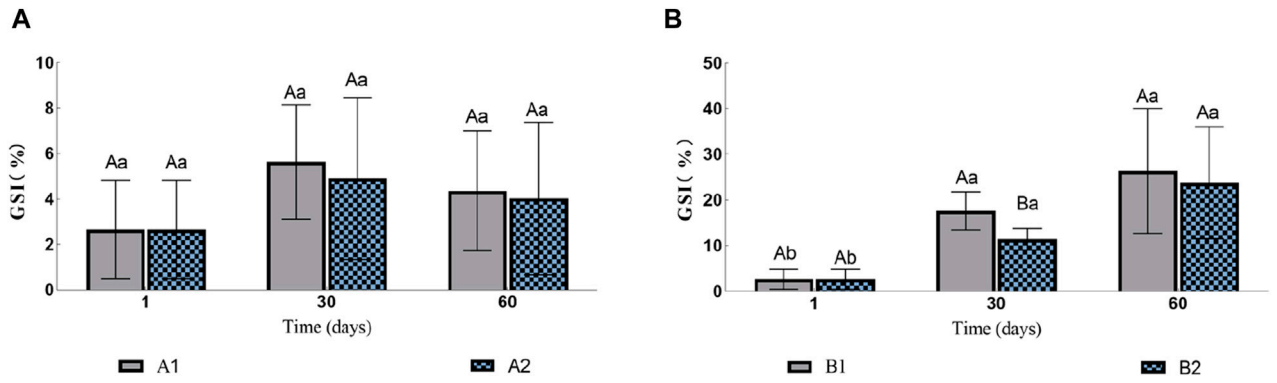

FIGURE 1
Effects of water stimulation and hormone injection on GSI of conger eel. **(A)** GSI in the no hormone group and **(B)** GSI in the hormone group. The capital letters marked in the chart indicate significant differences between the swimming group and the resting group at the same sampling time ($p < 0.05$). Lowercase letters indicate differences within the same group at different sampling periods ($p < 0.05$). A1, no hormone still water group; A2, no hormone flowing water group; B1, hormone still water group; B2, hormone flowing water group. GSI, gonadosomatic index.

indicating that there was a good linear relationship between the four hormones detected by this method and the results were reliable. The Transition one values of COR, 17α-OHP, T and 11-kT were 407.5 > 331.4, 331.4 > 96.9, 298.4 > 97.1, 303.1 > 109.1. The detection limits were 0.1, 0.04, 0.01, 0.25 ng/mL. The recoveries were 78%–98%. Therefore, this method can accurately detect five hormones of conger eel.

3.2.1 COR, 17α-OHP, T, 11-KT and E2 in ovary

The contents of E2 and T in the ovary of the groups A1 and A2 had no significant changes (Figures 2A, C). The content of 17α-OHP in A2 gradually decreased, while the content of 17α-OHP in A1 was significantly higher than that in A2 on the 60th day (1.10 ± 0.15 ng/mL vs. 0.55 ± 0.03 ng/mL; Figure 2E). The content of COR in A1 decreased initially and then increased, but there was no significant difference between A1 and A2 (Figure 2G). The content of 11-kT was lower than the detection limit.

The contents of E2 in both B1 and B2 increased initially and then decreased, but the group B1 was always significantly higher than B2 (Figure 2B). The contents of T and COR in B1 and B2 increased gradually; the contents of these two hormones in B1 were significantly higher than that in B2 on the 30th day (T: 14.36 ± 2.12 ng/mL vs. 9.23 ± 1.69 ng/mL; COR: 13.51 ± 3.22 ng/mL vs. 6.88 ± 2.34 ng/mL; Figures 2D,H), but no significant difference was observed on the 60th day (T: 15.71 ± 1.95 ng/mL vs. 9.75 ± 4.28 ng/mL; COR: 17.52 ± 5.25 ng/mL vs. 15.81 ± 1.42 ng/mL; Figures 2D,H). The contents of 17α-OHP decreased on the 60th day, but there was no significant difference between B1 and B2 (0.6901 ± 0.2315 ng/mL vs. 0.7047 ± 0.1995 ng/mL; Figure 2F). The contents of 11-KT in B2 were 0.97 ± 0.31 ng/mL on 30th day and there was no significant difference between the two groups on 60th day (1.10 ± 0.41 ng/mL vs. 1.05 ± 0.36 ng/mL).

3.2.2 COR, 11-KT and E2 levels in serum

The contents of 17α-OHP and T in the serum of the four experimental groups were lower than the detection limit, while E2 and 11-KT had no significant change (Table 2). In all four experimental groups, COR levels were consistently significantly higher in the flowing water group than in the still water group (Table 2).

3.3 *FSHβ* and *LHβ* gene expression and content changes

The expression levels of *FSHβ* in A1 and A2 increased continuously compared to those in the control group, with A2 significantly higher than A1 on the 60th day (Figure 3A). However, with hormone injection, the expression levels of *FSHβ* of B1 and B2 decreased rapidly. Similarly, B2 was significantly higher than B1 on the 60th day (Figure 3B). The expression levels of *LHβ* in all four groups increased significantly. On the 60th day, the expression levels of *LHβ* in A1 and B1 were significantly higher than A2 and B2 (Figures 3C, D), respectively.

The contents of FSH in A1 first decreased and then increased, while in A2 they first increased and then decreased. Additionally, the contents of FSH in A2 were consistently significantly higher than in A1 (the 30th day: 35.85 ± 2.81 U/L vs. 51.15 ± 1.46 U/L; the 60th day: 44.00 ± 2.61 U/L vs. 49.69 ± 3.25 U/L; Figure 3E). The contents of FSH in B1 were decreased significantly on the 60th day, while in B2 they first increased and then decreased. In addition, the contents of FSH in B2 were significantly higher than in B1 on the 30th day, and B1 was significantly higher than B2 on the 60th day (the 30th day: 43.46 ± 3.02 U/L vs. 48.91 ± 3.30 U/L; the 60th day: 38.56 ± 2.39 U/L vs. 31.72 ± 2.61 U/L; Figure 3F). The changes in the LH contents and the FSH contents in A1 and A2 were consistent. The contents of LH in A2 were significantly higher than in A1 on the 30th day, and A1 were significantly higher than A2 on the 60th day (the 30th day: 33.41 ± 2.43 pg/L vs. 47.98 ± 2.39 pg/L; the 60th day: 42.32 ± 2.31 pg/L vs. 36.39 ± 3.38 pg/L; Figure 3G). The contents of LH in B1 decreased significantly on the 60th day, while in B2 they first decreased and then increased. The contents of LH in B1 were significantly higher than in B2 on the 30th day, and B2 was significantly higher than B1 on the 60th day (the 30th day: 42.56 ± 2.18 pg/L vs. 39.62 ± 1.24 pg/L; the 60th day: 34.72 ± 3.46 pg/L vs. 48.36 ± 1.53 pg/L; Figure 3H).

10.3389/fphys.2024.1404834

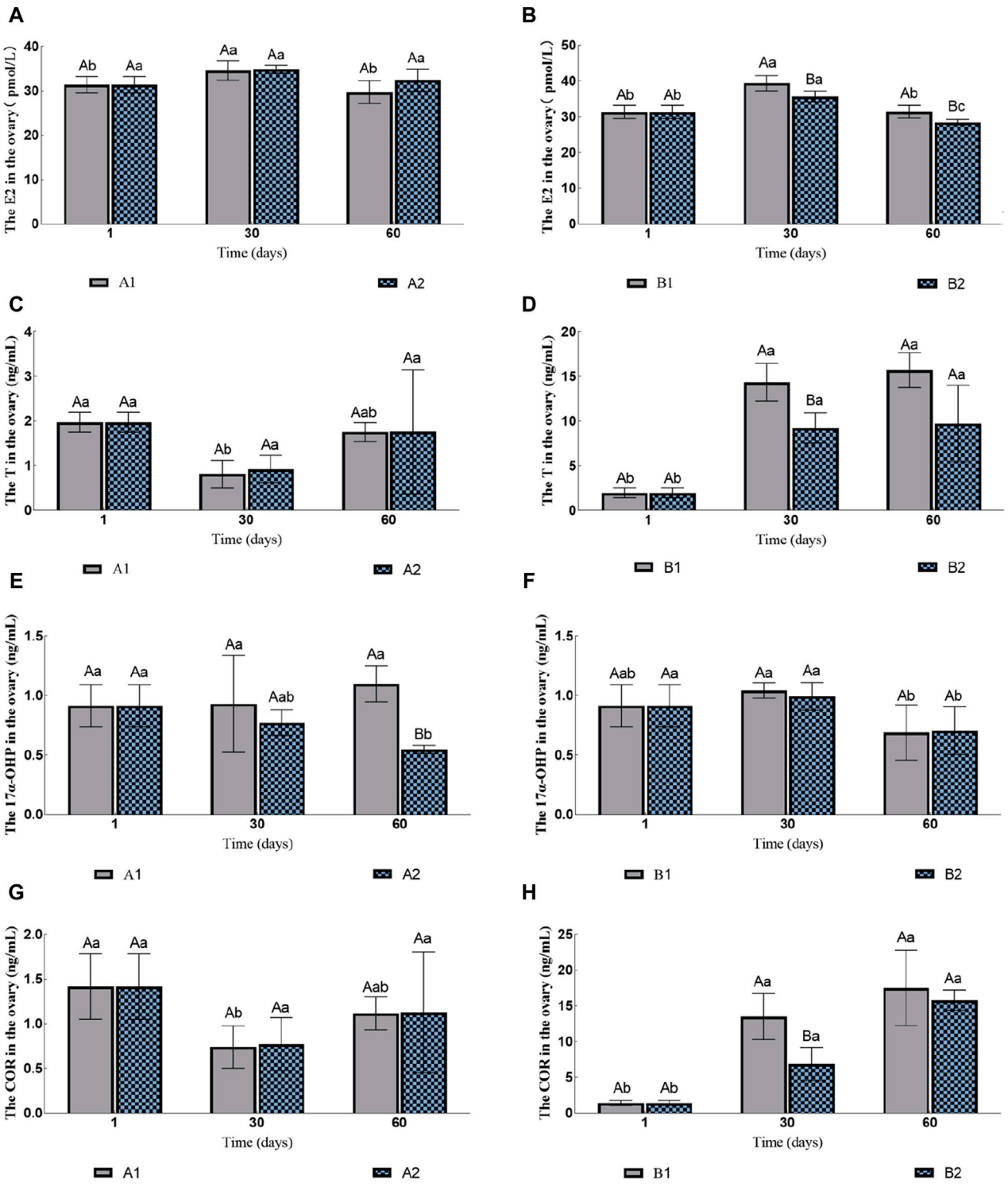

FIGURE 2
Effects of water stimulation and hormone injection on the contents of COR, 17α-OHP, T and E2 in the gonads of conger eel. **(A)** The content of E2 in ovary of no hormone group, **(B)** The content of E2 in ovary of hormone group, **(C)** The content of T in ovary of no hormone group, **(D)** The content of T in ovary of hormone group, **(E)** The content of 17α-OHP in ovary of no hormone group, **(F)** The content of 17α-OHP in ovary of hormone group, **(G)** The content of COR in ovary of no hormone group, **(H)** The content of COR in ovary of hormone group. The capital letters marked in the chart indicate significant differences between the swimming group and the resting group at the same sampling time ($p < 0.05$). Lowercase letters indicate differences within the same group at different sampling periods ($p < 0.05$). A1, no hormone still water group; A2, no hormone flowing water group; B1, hormone still water group; B2, hormone flowing water group. E2, estradiol; T, testosterone; 17α-OHP, 17α-hydroxyprogesterone; COR, cortisol.

10.3389/fphys.2024.1404834

TABLE 2 Effects of water stimulation and hormone injection on the levels of COR, 11-KT and E2 in serum of Conger eel.

	The first day (control group)	The 30th day	The 60th day	The 30th day	The 60th day
		A1		A2	
11-KT (ng/mL)	1.31 ± 0.39^{a}	1.09 ± 0.11^{Aa}	1.04 ± 0.28^{Aa}	1.01 ± 0.12^{Aa}	1.01 ± 0.19^{Aa}
E2 (ng/mL)	6.24 ± 0.69^{a}	4.12 ± 1.62^{Aa}	6.50 ± 2.37^{Aa}	3.96 ± 1.04^{Aa}	4.39 ± 1.35^{Aa}
COR (ng/mL)	-	5.09 ± 2.07^{B}	7.24 ± 5.88^{B}	14.25 ± 6.97^{A}	22.16 ± 11.36^{A}
		B1		B2	
11-KT (ng/mL)	1.31 ± 0.39^{a}	0.96 ± 0.18^{Aa}	1.07 ± 0.38^{Aa}	1.09 ± 0.32^{Aa}	1.09 ± 0.25^{Aa}
E2 (ng/mL)	6.24 ± 0.69^{a}	7.42 ± 3.18^{Aa}	4.92 ± 2.40^{Aa}	5.46 ± 2.21^{Aa}	5.28 ± 1.68^{Aa}
COR (ng/mL)	-	7.30 ± 5.00^{B}	7.24 ± 4.92^{B}	22.04 ± 9.77^{A}	19.11 ± 6.38^{A}

Note: The capital letters marked in the chart indicate significant differences between the swimming group and the resting group at the same sampling time ($p < 0.05$). Lowercase letters indicate differences within the same group at different sampling periods ($p < 0.05$). "-" indicates that the hormone content is lower than the detection limit. A1, no hormone still water group; A2, no hormone flowing water group; B1, hormone still water group; B2, hormone flowing water group. 11-KT, 11-Ketoltestosterone; E2, estradiol; COR, cortisol.

4 Discussion

Water stimulation is crucial for some fish species, as it can stimulate ovarian development, spawning and fertilization (Li et al., 2020; Chen et al., 2021; Shu et al., 2023). This study found that water stimulation slowed down the development of ovary. Prolonged swimming can also delay ovulation in rainbow trout (*Oncorhynchus mykiss*) (Contreras, 1998). However the inhibition of vitellogenin (VTG) synthesis by water stimulation may be the main reason for the slow growth of ovary (Liu et al., 2022). Swimming can inhibit the synthesis of VTG from conger eel, a similar phenomenon also found in European eel (Palstra et al., 2010b). In the process of ovarian development, the synthesis of VTG will lead to the shedding of calcium, phosphorus, and other elements from the bone, which are then transported to the ovary. This process is extremely detrimental to long-term migration (Gao, 2011). In addition, swimming exercise suppresses oocyte development by inhibiting VTG uptake in rainbow trout, and it downregulates protein biosynthesis and energy supply functions in the ovary to conserve energy (Palstra et al., 2010a; Palstra and Planas, 2011). Therefore, water stimulation can inhibit ovarian development in migrating conger eels, conserving energy to meet their energy demands during reproduction and increasing reproductive efficiency.

FSHβ gene is highly expressed in the early stage of ovarian development, while *LHβ* gene is highly expressed in the late ovarian development in conger eels. The increase in hormone levels may be the cause of this phenomenon. A similar pattern was found in Japanese eel, with higher mRNA levels of *FSHβ* were found in immature fish and higher mRNA levels of *LHβ* were found in adult female and male fish treated with exogenous hormones (Yoshiura et al., 1999). In this experiment, the increase of gonad steroid content was also observed during the development of conger eel, but no change in ovarian steroid content was observed in the two groups without hormone treatment. The non-expression of *FSHβ* in the later stage of hormone injection may be due to the regulatory effect of increased steroid hormone content in the pituitary gland. Increased levels of T and E2 have been shown to significantly reduced the level of *FSHβ* mRNA in Japanese eels and European eels (Schmitz et al., 2005; Jeng et al., 2007). In the study, increased levels of hormones such as T and COR in the gonads were found in both hormone groups. These increased hormone levels may be responsible for the inhibition of FSH gene expression.

Water stimulation can promote the synthesis of FSH and LH at different stages of ovarian development in conger eels. Swimming was also observed to increase serum COR levels in this experiment. After long-term swimming, the levels of FSH and LH in conger eel significantly increased during gonadal development, which may be due to the regulation of COR on the HPG axis. When changes in the external environment put stress on the fish organisms, teleost fish adapt to the changes by promoting the synthesis of hormones such as COR through the hypothalamic-pituitary-adrenal axis (HPA) (Kr et al., 2020). COR can significantly elevate the *LHβ* mRNA content in European eels, and stimulate *FSHβ* gene expression in Atlantic cod as well (Huang et al., 1999; Krogh et al., 2019). The widespread presence of glucocorticoid receptors in both the brain and gonads of fish underscores the pivotal role of COR and other glucocorticoids in the reproductive process of fish (Teitsma, 1999; Maruska and Fernald, 2011; Ogawa and Ishwar, 2014). However, COR exerts species-specific regulatory effects on organisms, and its mechanism needs further exploration (Mommsen et al., 1999). Studies have shown that during the silver plating period of Japanese eels and European eels, the expression of *FSHβ* and *LHβ* significantly increased and effectively reduced the expression of dopamine receptors (Jeng et al., 2014). After swimming for 60 days the expression level of *FSHβ* significantly increased in fish without hormone injection, suggesting that swimming can help with the early development of fish. In zebrafish, both males and females lacking the FSH gene were able to reproduce normally, but the gonad development rate was slow, and females lacking the LH gene were unable to lay eggs (Zhang et al., 2015). When the gonads of Japanese eels mature, it is necessary to inject the hormones DHP or OHP to induce spawning in captivity (Jiang, 2012). Therefore, the observed inability of eels to ovulate naturally in our study could potentially be attributed to inadequate LH synthesis. Stimulating LH synthesis through water

10.3389/fphys.2024.1404834

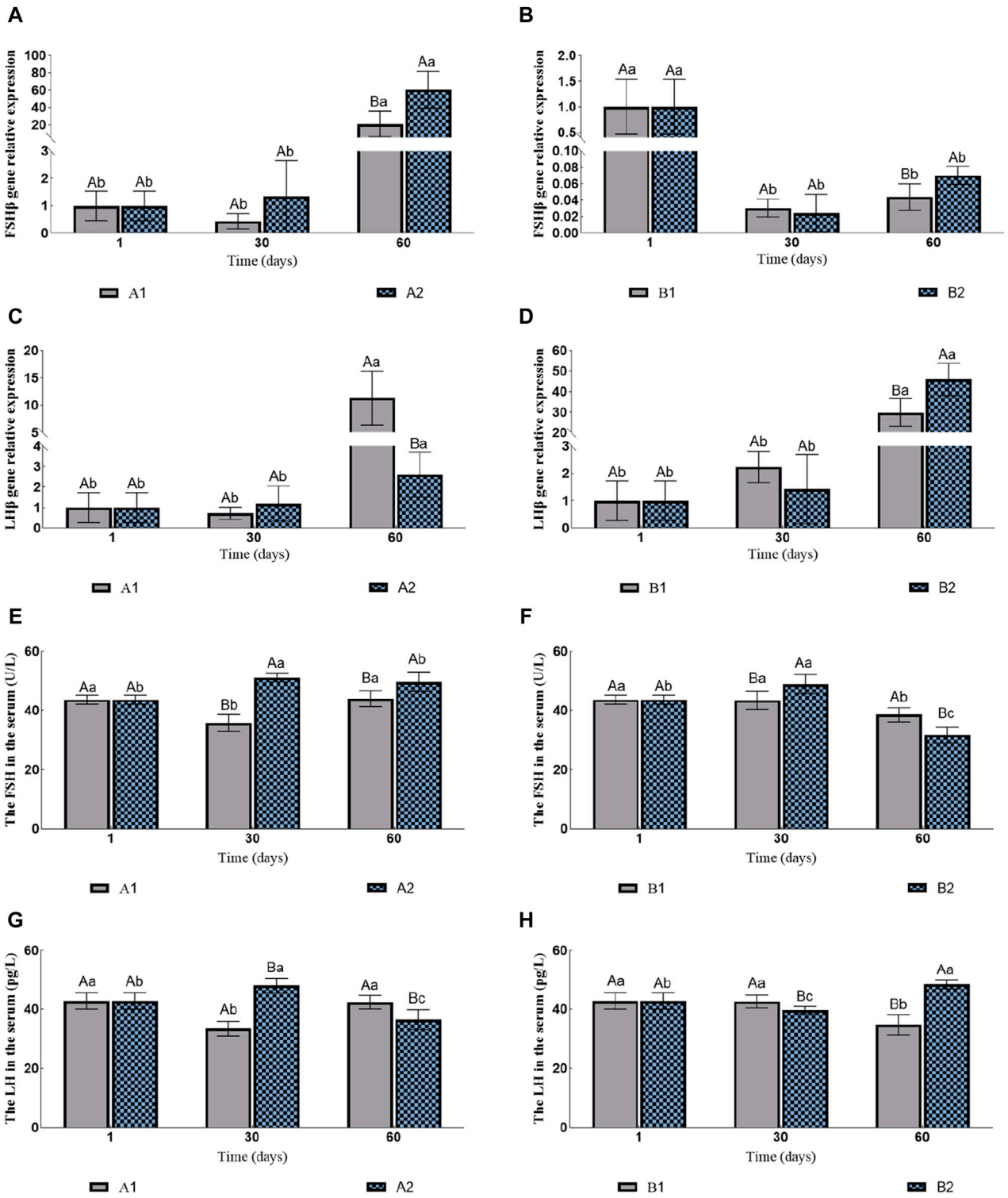

FIGURE 3
Effects of fluid stimulation and hormone injection on the expression of Follicle stimulating hormone (*FSHβ*) and luteinizing hormone (*LHβ*) genes in the pituitary, and follicle stimulating hormone (FSH) and Luteinizing hormone (LH) in the serum of conger eel. **(A)** The relative expression of *FSHβ* in the no hormone group, **(B)** The relative expression of *FSHβ* in the hormone group, **(C)** The relative expression of *LHβ* in the no hormone group, **(D)** The relative expression of *LHβ* in the hormone group, **(E)** The content of FSH in the hormone group, **(F)** The content of FSH in the hormone group, **(G)** The content of LH in the hormone group, **(H)** The content of LH in the hormone group. The capital letters marked in the chart indicate significant differences between the swimming group and the resting group at the same sampling time ($p < 0.05$). Lowercase letters indicate differences within the same group at different sampling periods ($p < 0.05$). A1, no hormone still water group; A2, no hormone flowing water group; B1, hormone still water group; B2, hormone flowing water group. *FSHβ*, Follicle-stimulating hormone beta subunit; *LHβ*, Luteinizing hormone beta subunit. FSH, Follicle-stimulating hormone; LH, Luteinizing hormone.

stimulation might prove beneficial for facilitating the final maturation and ovulation of the gonads.

Water stimulation increased the level of 11-KT in B2 ovaries on the 30th day, and reduced E2 levels in the ovaries. 11-KT is known to promote the absorption of lipid substances by oocytes (Endo et al., 2008). Similarly, swimming in European eel has also been found to increase the level of 11-KT in serum and promote the accumulation of lipid droplets in oocytes (Ginneken et al., 2007). E2 binds to estrogen receptors in the liver and promotes vitellogenin synthesis (Williams et al., 2013; Hara et al., 2016). Therefore, the decrease in E2 may lead to a decrease in vitellogenin synthesis. Palstra et al. found that swimming inhibited the expression of two VTG genes in European eel (Palstra et al., 2010b). In oviparous vertebrates, maternally derived miRNAs and hormones enter the oocytes during vitellogenesis and participate in seedling embryonic development (Groothuis and Schwabl, 2008; Tokarz et al., 2015). The contents of E2 and DHP in oocytes of European eel are negatively correlated with the quality of oocytes (Kottmann et al., 2021). Changes in serum hormone levels with no discernible pattern were observed, and were consistent with previous studies (Li, 2019). Furthermore, there are notable differences between conger eel and other eels, necessitating further study into specific regulatory mechanisms. Therefore, we should not blindly pursue the increase of hormone content related to reproduction in future reproduction work.

5 Conclusion

In this study, we employed qPCR to detect the relative expression levels of *FSHβ* and *LHβ* in the pituitary of the Conger eel. Additionally, we utilized ELISA and UPLC-MS/MS to assess hormone content in the serum and ovaries. FSH hormone in Conger eel only functions in the early stage of ovarian development, with water flow stimulation can significantly promote the synthesis of FSH. After hormone injection, the mRNA level of *FSHβ* gene was below detection. *LHβ* gene in Conger eel exhibits high expressions in the later stage of ovarian development, with water flow stimulation significantly promoting the synthesis of LH in the late stage of ovarian development. Water flow stimulation notably reduces the content of hormones such as COR, E2, and T in the ovaries of Conger eel while promoting COR content in the serum. This study contributes to our understanding of the impact of water flow stimulation on hormone regulation in Conger eel. Moreover, further investigation is warranted to determine whether the inhibitory effect of water stimulation on hormone content in the ovary of the Conger eel can improve the hatching rate of fertilized eggs and the survival rate of seedlings.

Data availability statement

The original contributions presented in the study are included in the article/supplementary material. The gene sequences of FSHβ and LHβ of conger eel were obtained from NCBI, and their accession numbers are AB045157.1 (https://www.ncbi.nlm.nih.gov/nuccore/AB045157.1) and AB045158.1 (https://www.ncbi.nlm.nih.gov/nuccore/AB045158.1) respectively. Further inquiries can be directed to the corresponding authors.

Ethics statement

The animal study was approved by the Animal Ethics Committee of Shanghai Ocean University (2016 No. 4) and the Regulations for the Administration of Affairs Concerning Experimental Animals approved and authorized by the State Council of the People's Republic of China. The study was conducted in accordance with the local legislation and institutional requirements.

Author contributions

ZL: Conceptualization, Data curation, Formal Analysis, Investigation, Methodology, Project administration, Software, Supervision, Validation, Visualization, Writing–original draft, Writing–review and editing. RL: Conceptualization, Data curation, Formal Analysis, Investigation, Methodology, Project administration, Software, Supervision, Validation, Visualization, Writing–original draft. JL: Conceptualization, Data curation, Funding acquisition, Methodology, Project administration, Resources, Supervision, Writing–review and editing. ZJ: Methodology, Investigation, Writing–original draft. XB: Methodology, Investigation, Writing–original draft. KL: Conceptualization, Data curation, Funding acquisition, Methodology, Project administration, Resources, Supervision, Writing–review and editing. LL: Conceptualization, Data curation, Funding acquisition, Methodology, Project administration, Resources, Supervision, Writing–review and editing.

Funding

The author(s) declare that financial support was received for the research, authorship, and/or publication of this article. National Natural Science Foundation of China (32072994).

Conflict of interest

The authors declare that the research was conducted in the absence of any commercial or financial relationships that could be construed as a potential conflict of interest.

The author(s) declared that they were an editorial board member of Frontiers, at the time of submission. This had no impact on the peer review process and the final decision.

Publisher's note

References

Chen, Q., Zhang, J., Chen, Y., Mo, K., Wang, J., Tang, L., et al. (2021). Inducing flow velocities to manage fish reproduction in regulated rivers. *Engineering* 7 (2), 178–186. doi:10.1016/j.eng.2020.06.013

Chiba, H., Ijiri, S., Iwata, M., Nakamura, M., Adachi, S., and Yamauchi, K. (2010). Changes in serum steroid hormones during ovarian development in the captive common Japanese Conger *Conger myriaster* (brevoort). *Aquac. ence* 53, 189–198. doi:10.11233/aquaculturesci1953.53.189

Contreras, W. M., Schreck, C. B., Fitzpatrick, M. S., and Pereira, C. B. (1998). Effects of stress on the reproductive performance of rainbow trout (*Oncorhynchus mykiss*). *Biol. Reproduction* 58 (2), 439–447. doi:10.1095/biolreprod58.2.439

Couillard, C. M., Hodson, P. V., and Castonguay, M. (1997). Correlations between pathological changes and chemical contamination in American eels, *Anguilla rostrata*, from the St. Lawrence River. *Can. J. Fish. Aquatic Sci.* 54 (8), 1916–1927. doi:10.1139/f97-097

Dang, V. D. (2020). Simultaneous measurement of sex steroid hormones in largemouth bass (*Micropterus salmoides*) plasma by application of liquid chromatography–tandem Mass spectrometry. *J. Chromatogr. Sci.* 59, 7–14. doi:10.1093/chromsci/bmaa048

Endo, T., Todo, T., Lokman, P. M., Ijiri, S., and Yamauchi, K. (2008). *In vitro* induction of oil droplet accumulation into previtellogenic oocytes of Japanese eel, *Anguilla japonica*. *Cybium Int. J. Ichthyology* 32 (2), 239–240.

Gao, X. (2011). *The preliminary study on artificial propagation and biochemical component transfer of Japanese eel*. Shanghai Ocean University.

Ginneken, V., Dufour, S., Sbaihi, M., Balm, P., Noorlander, K., de Bakker, M., et al. (2007). Does a 5500-km swim trial stimulate early sexual maturation in the European eel (*Anguilla anguilla L.*)? *Comp. Biochem. Physiol. A Mol. Integr. Physiol.* 147 (4), 1095–1103. doi:10.1016/j.cbpa.2007.03.021

Groothuis, T. G. G., and Schwabl, H. (2008). Hormone-mediated maternal effects in birds: mechanisms matter but what do we know of them? *Philos. Trans. R. Soc. Lond B Biol.* 363 (1497), 1647–1661. doi:10.1098/rstb.2007.0007

Hammer, C. (1995). Fatigue and exercise tests with fish. *Comp. Biochem. Physiology Part A Physiology* 112 (1), 1–20. doi:10.1016/0300-9629(95)00060-k

Hao, Y., Bao, S., Hua xin, N., Dai qiang, Z., and Jing, L. (2020). Advances and future prospects in *Conger myriaster* research. *Mar. Sci.* 44 (06), 154–160.

Hara, A., Hiramatsu, N., and Fujita, T. (2016). Vitellogenesis and choriogenesis in fishes. *Fish. Sci.* 82 (2), 187–202. doi:10.1007/s12562-015-0957-5

Horie, N., Utoh, T., Yama Da, Y., Okamura, A., Zhang, H., Mikawa, N., et al. (2010). Development of embryos and larvae in the common Japanese conger *Conger myriaster*. *Fish. ence* 68 (5), 972–983. doi:10.1046/j.1444-2906.2002.00521.x

Huang, Y., Karine, R., Miskal, S., Nadine, L. B., Monika, S., and Sylvie, D. (1999). Cortisol selectively stimulates pituitary gonadotropin β-subunit in a primitive teleost, *Anguilla anguilla*. *Endocrinology* 140, 1228–1235. doi:10.1210/endo.140.3.6598

Jeng, S. R., Yueh, W. S., Chen, G. R., Lee, Y. H., Dufour, S., and Chang, C. F. (2007). Differential expression and regulation of gonadotropins and their receptors in the Japanese eel, *Anguilla japonica*. *General and Comp. Endocrinol.* 154 (1-3), 161–173. doi:10.1016/j.ygcen.2007.05.026

Jeng, S. R., Yueh, W. S., Pen, Y. T., Lee, Y. H., Chen, G. R., Dufour, S., et al. (2014). Neuroendocrine gene expression reveals a decrease in dopamine D2B receptor with no changes in GnRH system during prepubertal metamorphosis of silvering in wild Japanese eel. *General and Comp. Endocrinol.* 206, 8–15. doi:10.1016/j.ygcen.2014.08.001

Jiang, T. (2012). *Artificially reproductive technologies optimization of Japanese eel (Anguilla japonica) and changes of female ovarian histologic with some physiological and biochemical factors*. Shanghai Ocean University.

Kottmann, J. S., Tveiten, H., Miest, J. J., and Tomkiewicz, J. (2021). Sex steroid dynamics and mRNA transcript profiles of growth- and development-related genes during embryogenesis following induced follicular maturation in European eel. *Gen. Comp. Endocrinol.* 311, 113854. doi:10.1016/j.ygcen.2021.113854

Kr, A., Pp, B., and Sd, A. (2020). Special features of neuroendocrine interactions between stress and reproduction in teleosts. *General Comp. Endocrinol.* 300, 113634. doi:10.1016/j.ygcen.2020.113634

Krogh, K. V., Bjrndal, G. T., Nourizadeh-Lillabadi, R., Ropstad, E., and Weltzien, F. A. (2019). Cortisol differentially affects cell viability and reproduction-related gene expression in Atlantic cod pituitary cultures dependent on stage of sexual maturation. *Comp. Biochem. Physiology Part A Mol. Integr. Physiology* 236, 110517. doi:10.1016/j.cbpa.2019.06.017

Li, F.-F., Wei, J.-H., Qiu, J., and Jiang, H. (2020). Determining the most effective flow rising process to stimulate fish spawning via reservoir operation. *J. hydrology* 582, 124490. doi:10.1016/j.jhydrol.2019.124490

Li, M., Zhang, C., Li, M., Mu, X., and Ren, Y. (2018). Relationship between the spatiotemporal distribution of *Conger myriaster* and environmental factors in the southern waters off the Shan dong Peninsula during autumn and winter. *J. Fish. Sci. China* 25 (05), 1115–1122. doi:10.3724/sp.j.1118.2018.17426

Li, X. (2019). *Comparative analysis of the effects of acclimation and different hormone combinations on the sexual maturation of common Japanese conger* Conger Myriaster. Shanghai Ocean University.

Liu, H., Cao, Z., and Fu, S. (2015). Effect of flow stimulation on the swimming performance and metabolism in Juvenile *Zacco platypus*. *Animal Sci.* 32 (1), 6.

Liu, R., Li, K., Wang, G., Jiang, Z., Ba, X., and Liu, L. (2022). Effect of swimming on the induction of vitellogenin in Conger eel (*Conger myriaster*). *Front. Mar. Sci.* 9, 887074. doi:10.3389/fmars.2022.887074

Ma, Q., Mu, X., Ren, Y., and Sun, Y. (2018). The growth, mortality and yield per recruitment of white-spotted conger (*Conger myriaster*) in the Yellow Sea and the East China Sea. *J. Fish.* 42 (6), 8. doi:10.11964/jfc.20171111040

Ma, Y., Gui, W., Cheng, J., and Zhu, G. (2016). Analysis of steroid hormones in ovaries of zebrafish (*Danio rerio*) by ultra performance liquid chromatography - tandem Mass spectrometry. *J. Instrum. Analysis* 35 (4), 6.

Maruska, K. P., and Fernald, R. D. (2011). Plasticity of the reproductive axis caused by social status change in an african cichlid fish: II. testicular gene expression and spermatogenesis. *Endocrinology* 152 (1), 291–302. doi:10.1210/en.2010-0876

Meng, W. (2020). *The impact of flowing water and starvation on gonad development during artificial ripening of the conger eel* (Conger myriaster). Shanghai: Shanghai Ocean University. dissertation/master's thesis.

Miller, M. J., Yoshinaga, T., Aoyama, J., Otake, T., Mochioka, N., Kurogi, H., et al. (2011). Offshore spawning of *Conger myriaster* in the western North Pacific: evidence for convergent migration strategies of anguilliform eels in the Atlantic and Pacific. *Naturwissenschaften* 98, 537–543. doi:10.1007/s00114-011-0787-y

Mommsen, T. P., Vijayan, M. M., and Moon, T. W. (1999). Cortisol in teleosts: dynamics, mechanism of action, and metabolic regulation. *Rev. Fish Biol. Fish.* 9 (3), 211–268. doi:10.1023/a:1008924418720

Ogawa, S., and Parhar, I. S. (2014). Structural and functional divergence of gonadotropininhibitory hormone from jawless fish to mammals. *Front. Endocrinol.* 5, 177. doi:10.3389/fendo.2014.00177

Okamura, A., Utoh, T., Zhang, H., Yamada, Y., Horie, N., Mikawa, N., et al. (2000). Seasonal changes in maturity in the conger eel *Conger myriaster* at the Pacific coast of Atsumi Peninsula, central Japan. *Nihon-suisan-gakkai-shi* 66 (3), 412–416. doi:10.2331/suisan.66.412

Palstra, A., Curiel, D., Fekkes, M., Bakker, M., Székely, C., Ginneken, V. V., et al. (2007). Swimming stimulates oocyte development in European eel. *Aquaculture* 270 (1-4), 321–332. doi:10.1016/j.aquaculture.2007.04.015

Palstra, A., Ginneken, V. V., and Thillart, G. (2009). *Effects of swimming on silvering and maturation of the European eel,* Anguilla anguilla L. spawning migration of the european eel, 229–251.

Palstra, A. P., Crespo, D., van den Thillart, G. E., and Planas, J. V. (2010a). Saving energy to fuel exercise: swimming suppresses oocyte development and downregulates ovarian transcriptomic response of rainbow trout *Oncorhynchus mykiss*. *Am. J. Physiology-Regulatory, Integr. andjournals.physiology* 299 (2), R486–R499. doi:10.1152/ajpregu.00109.2010

Palstra, A. P., and Planas, J. V. (2011). Fish under exercise. *Fish. Physiol. Biochem.* 37 (2), 259–272. doi:10.1007/s10695-011-9505-0

Palstra, A. P., Schnabel, D., Nieveen, M. C., Spaink, H. P., and Thillart, G. (2010b). Swimming suppresses hepatic vitellogenesis in European female silver eels as shown by expression of the estrogen receptor 1, vitellogenin1 and vitellogenin2 in the liver. *Reproductive Biol. Endocrinol.* 8 (1), 27. doi:10.1186/1477-7827-8-27

Schmitz, M., Aroua, S., Vidal, B., Belle, N. L., Elie, P., and Dufour, S. (2005). Differential regulation of luteinizing hormone and follicle-stimulating hormone expression during ovarian development and under sexual steroid feedback in the European eel. *Neuroendocrinology* 81 (2), 107–119. doi:10.1159/000086404

Shu, T., Chen, Y., Xiao, K., Huang, H., Jia, J., Yu, Z., et al. (2023). Effects of short-term water velocity stimulation on the biochemical and transcriptional responses of grass carp (*Ctenopharyngodon idellus*). *Front. Physiology* 14, 1248999. doi:10.3389/fphys.2023.1248999

Teitsma, C. A., Anglade, I., Lethimonier, C., Le Dréan, G., Saligaut, D., Ducouret, B., et al. (1999). Glucocorticoid receptor immunoreactivity in neurons and pituitary cells implicated in reproductive functions in rainbow trout: a double immunohistochemical study. *Biol. Reproduction* 60 (3), 642–650. doi:10.1095/biolreprod60.3.642

Tokarz, J., Möller, G., deAngelis, M. H., and Adamski, J. (2015). Steroids in teleost fishes: a functional point of view. *Steroids* 103, 123–144. doi:10.1016/j.steroids.2015.06.011

Utoh, T., Horie, N., Mikawa, N., Okamura, A., Yamada, Y., Akazawa, A., et al. (2010a). Annual changes in ovarian development and plasma estradiol-17β level in reared female common Japanese conger, *Conger myriaster*. *Fish. Sci.* 71 (1), 38–47. doi:10.1111/j.1444-2906.2005.00928.x

Utoh, T., Horie, N., Okamura, A., Yamada, Y., Tanaka, S., Mikawa, N., et al. (2010b). Oogenesis in the common Japanese conger *Conger myriaster*. *Fish. Sci.* 69 (1), 181–188. doi:10.1046/j.1444-2906.2003.00604.x

Wang, L., Li, X., Liu, F., and Liu, L. (2015). Impact of injection of different hormones on gonadosomatic index and expression of gonadotropin genes(GtHα, FSHβ, LHβ) in female marbled eel(*Anguilla marmorata*). *J. Fish.* 39 (5), 9. doi:10.11964/jfc.20141109559

Williams, V. N., Reading, B. J., Hiramatsu, N., Amano, H., Sullivan, C. V., et al. (2013). Multiple vitellogenins and product yolk proteins in striped bass, *Morone saxatilis*: molecular characterization and processing during oocyte growth and maturation. *Fish Physiology Biochem.* 40 (2), 395–415. doi:10.1007/s10695-013-9852-0

Xiaolong, L., Kang, L., Gaomeng, R. U., Xinglong, J., and Liping, L. (2021). Comparative analysis of the effects of HCG and CPE combinations on the sexual maturation of common Japanese conger *Conger myriaster*. *J. Shanghai Ocean Univ.* 30 (01), 29–38. doi:10.12024/jsou.20190502657

Yaron, Z., Gur, G., Melamed, P., Rosenfeld, H., and Levavi-Sivan, B. (2003). Regulation of fish gonadotropins. *Int. Rev. Cytol.* 225 (4), 131–185. doi:10.1016/s0074-7696(05)25004-0

Yoshiura, Y., Suetake, H., and Aida, K. (1999). Duality of gonadotropin in a primitive teleost, Japanese eel (*Anguilla japonica*). *Gen. Comp. Endocrinol.* 114 (1), 121–131. doi:10.1006/gcen.1998.7242

Zhang, Z., Zhu, B., and Ge, W. (2015). Genetic analysis of zebrafish gonadotropin (FSH and LH) functions by TALEN-mediated gene disruption. *Mol. Endocrinol.* 29 (1), 76–98. doi:10.1210/me.2014-1256

frontiers | Frontiers in Physiology

TYPE Original Research
PUBLISHED 09 May 2024
DOI 10.3389/fphys.2024.1412943

OPEN ACCESS

EDITED BY
Yi-Feng Li,
Shanghai Ocean University, China

REVIEWED BY
Lin Cheng,
Chinese Academy of Sciences (CAS), China
Kaibo Huang,
Hainan University, China

*CORRESPONDENCE
Zhiquan Liu,
liuzhiquan1024@163.com

†These authors have contributed equally to this work

RECEIVED 06 April 2024
ACCEPTED 22 April 2024
PUBLISHED 09 May 2024

CITATION
Liu Z, Shi C, Wang B, Zhang X, Ding J, Gao P, Yuan X, Liu Z and Zhang H (2024), Cytochrome P450 enzymes in the black-spotted frog (*Pelophylax nigromaculatus*): molecular characterization and upregulation of expression by sulfamethoxazole.
Front. Physiol. 15:1412943.
doi: 10.3389/fphys.2024.1412943

Cytochrome P450 enzymes in the black-spotted frog (*Pelophylax nigromaculatus*): molecular characterization and upregulation of expression by sulfamethoxazole

Zhiqun Liu[1†], Chaoli Shi[1†], Bingyi Wang[1], Xiaofang Zhang[1], Jiafeng Ding[1,2], Panpan Gao[1,2], Xia Yuan[1,2], Zhiquan Liu[1,2,3]* and Hangjun Zhang[1,2]

[1]Hangzhou Normal University, Hangzhou, China, [2]Zhejiang Provincial Key Laboratory of Urban Wetlands and Regional Change, Hangzhou, China, [3]State Environmental Protection Key Laboratory of Environmental Health Impact Assessment of Emerging Contaminants, Shanghai Academy of Environment Sciences, Shanghai, China

Cytochrome P450 (CYP) enzymes are crucial for the detoxification of xenobiotics, cellular metabolism, and homeostasis. This study investigated the molecular characterization of CYP enzymes in the black-spotted frog, *Pelophylax nigromaculatus*, and examined the regulation of CYP expression in response to chronic exposure to the antibiotic sulfamethoxazole (SMX) at various environmental concentrations (0, 1, 10, and 100 μg/L). The full-length cDNA of Pn-CYP26B1 was identified. The sequence included open reading frames of 1,536 bp, encoding proteins comprising 511 amino acids. The signature motif, FxxGxxxCxG, was highly conserved when compared with a number of selected animal species. SMX significantly upregulated the expression of the protein CYP26B1 in frog livers at concentrations of 1 and 10 μg/L. SMX showed an affinity for CYP26B1 of −7.6 kcal/mol, indicating a potential mechanism for SMX detoxification or adaptation of the frog. These findings contributed to our understanding of the environmental impact of antibiotics on amphibian species and underscored the importance of CYP enzymes in maintaining biochemical homeostasis under exposure to xenobiotic stress.

KEYWORDS

***Pelophylax nigromaculatus*, sulfamethoxazole, cytochrome P450, expression analysis, molecular docking**

1 Introduction

Antibiotics have emerged as a new category of pollutant, eliciting widespread public concern due to their potential ecological and biological health threats (Kümmerer, 2009). Antibiotics, including β-lactams, macrolides, quinolones, tetracyclines, sulfonamides, aminoglycosides, and chloramphenicol, are crucial in the treatment of infectious diseases in aquaculture and livestock (Shao et al., 2021). Antibiotics are now widely distributed pollutants in aquatic environments, including all types of surface water. Rivers, lakes, and coastal zones now constitute a principal reservoir and conduit for antibiotic accumulation and spread (Liu et al., 2018). One of most commonly used antibiotics, sulfamethoxazole (SMX) has been frequently detected

10.3389/fphys.2024.1412943

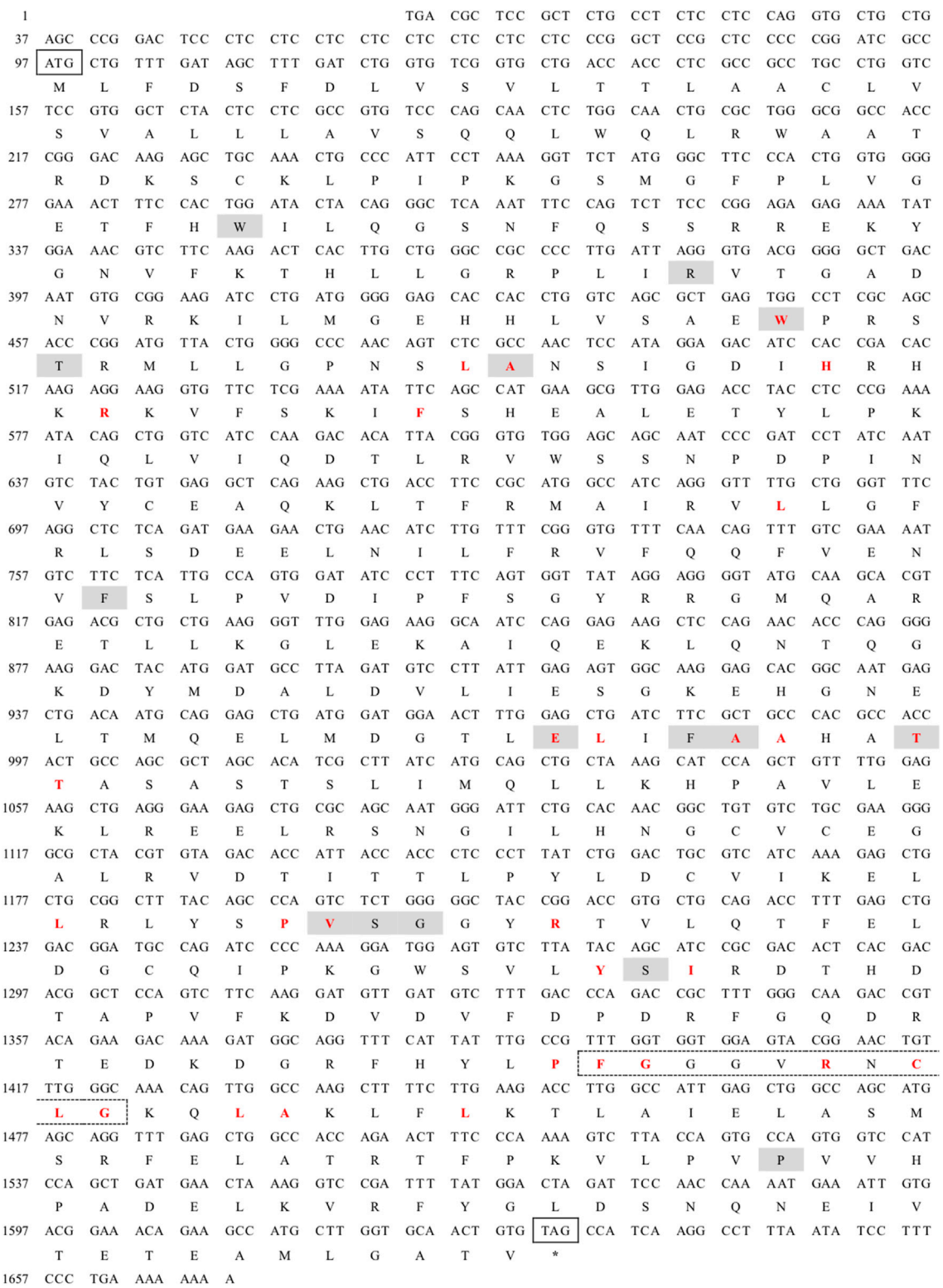

FIGURE 1
Nucleotide sequence and deduced amino acid sequences of *Pelophylax nigromaculatus* CYP26B1. The start (ATG) and stop (TAG) codons are indicated by solid boxes, and the stop codon is marked with an asterisk. The heme binding site is highlighted in red, while the chemical substrate binding pockets are shaded. The heme-iron ligand signature sequence (FXXGXRXCXG) is identified by a dashed box.

TABLE 1 Details of the full-length cDNA sequences of GSTα and CYP26B1 in the frog, *Pelophylax nigromaculatus*.

	Pn-CYP26B1
Full Length (bp)	1,669
5′-UTR (bp)	96
3′-UTR (bp)	37
ORF (bp)	1,536
Number of amino acids	511
Protein isoelectric point	7.65
Molecular weight	57,637.72

in various aquatic environments, including drinking water, groundwater, surface water, and wastewater treatment plant effluents, in concentrations varying from 2.9 to 216 ng/L (Huang et al., 2020; Zainab et al., 2020; Cui et al., 2021). In particular, SMX concentrations in wastewater effluents range from 200 to 2,000 ng/L (Christou et al., 2017). The bioaccumulation of SMX through the food chain may adversely affect aquatic life (Yang et al., 2024). As it becomes more broadly disseminated and bacterial antibiotic resistance becomes more widespread, SMX constitutes a burgeoning environmental pollution issue that poses risks to ecosystems and human health.

Amphibians, many species of which primarily inhabit agricultural areas, serve as indicators for environmental and ecological health and have experienced significant declines in population size and species diversity in recent decades (Jiang et al., 2016). Their vulnerability to antibiotics, such as SMX, stems from their lack of a protective eggshell, highly permeable skin, and the aquatic environments in which their embryos and larvae develop (Alford et al., 2001). Studies have shown that SMX can induce hepatocellular damage in amphibians, adversely affecting their growth, development, and behavior (Rutkoski et al., 2022). The black-spotted frog, *Pelophylax nigromaculatus* is characterized by its highly permeable skin and sensitivity to environmental pollutants, and has suffered a reduction in its global distribution (Lin et al., 2022). Increasing evidence suggests that environmental pollutants are contributing to declining frog population worldwide, prompting the selection of this species for this study of SMX toxicity (Wang et al., 2019).

The cytochrome P450 (CYP) enzymes are a group of membrane-bound hemoproteins found in nearly all living organisms, and play a vital role in synthesizing various endogenous compounds (Baune et al., 1999; Pikuleva and Cartier, 2021; Pang et al., 2022). As major phase I metabolizing enzymes, CYP enzymes biotransform xenobiotics, such as antibiotics, within the body (Ha-Duong et al., 2001; Lim et al., 2024). While some studies indicate that antibiotics can influence CYP enzyme activity in aquatic organisms, there is little comprehensive research on the transcriptional profiles of specific classes of CYP (Samrani et al., 2023). In contrast, the influence of other pollutants, such as polycyclic aromatic hydrocarbons, crude oil and nanoplastics, on the gene expression patterns of CYP enzymes has been studied more, suggesting a need for a more focused examination of the molecular mechanisms of antibiotics (Han et al., 2015; Lie et al., 2019; Wu et al., 2019). The cytochrome P450 family 26 (CYP26) enzymes are crucial for retinoic acid (RA) metabolism and homeostasis in humans, mammals, and other chordates, efficiently metabolizing all-trans-retinoic acid and its isomers, as well as primary metabolites (White et al., 2000; Maden, 2002). The CYP26 enzyme is regulated by both inflammatory cytokines and endogenous processes, exhibiting tissue and cell-type-specific expression patterns in animal models (Lampen et al., 2001; Rydeen and Waxman, 2014). Notably, the loss of CYP26B1 in mice causes alveolar inflation failure and alveolar type 1 cell reduction (Daniel et al., 2020). In zebrafish, tight control of CYP26B1 activity and RA levels is critical for skeletogenesis (Spoorendonk et al., 2008). However, data linking emerging pollutants to altered CYP expression or activity is scarce, and the impact of environmental pollutants, particularly antibiotics, on CYP activity is not yet fully understood.

To address this gap, we identified the full-length cDNA of the CYP26B1 in *P. nigromaculatus*, and examined its transcriptional response to various environmental concentrations of SMX to elucidate the regulation of CYP26B1 under SMX stress. This study aimed to determine whether chronic exposure to SMX could activate the phase I detoxification system in *P. nigromaculatus*. This study enhanced our understanding of the biochemistry of CYP in frogs, especially *P. nigromaculatus*, and the gene expression patterns in response to environmental contaminants, especially antibiotics. It should enable further investigation into the molecular mechanisms of the effects of antibiotic pollution on amphibians.

2 Materials and methods

2.1 Chemicals

Sigma-Aldrich (Shanghai, China) and Yeasen Biotechnology (Shanghai, China) provided analytical standard SMX (CAS No. 763-46–6, Product Number: 31,737, purity ≥98.0%) and dimethyl sulfoxide (DMSO) (CAS No. 67-68–5, purity >99.9%), respectively. All of the other reagents used were of chromatographic or analytical grade.

2.2 Culture of frogs

Healthy *P. nigromaculatus* for our study were obtained from the ChangXing Agriculture Development Co., Ltd (Huzhou, China). To ensure their wellbeing and acclimatization, the frogs were housed in laboratory conditions with a natural light-dark cycle in distilled water tanks at a temperature of 20°C ± 1°C. The water quality parameters were carefully monitored, with dissolved oxygen content maintained at 7 ± 1 mg/L and pH at 6.5 ± 0.5. During a 2-week acclimatization period, the water in the tanks was completely refreshed every 24 h to ensure optimal dissolved oxygen levels.

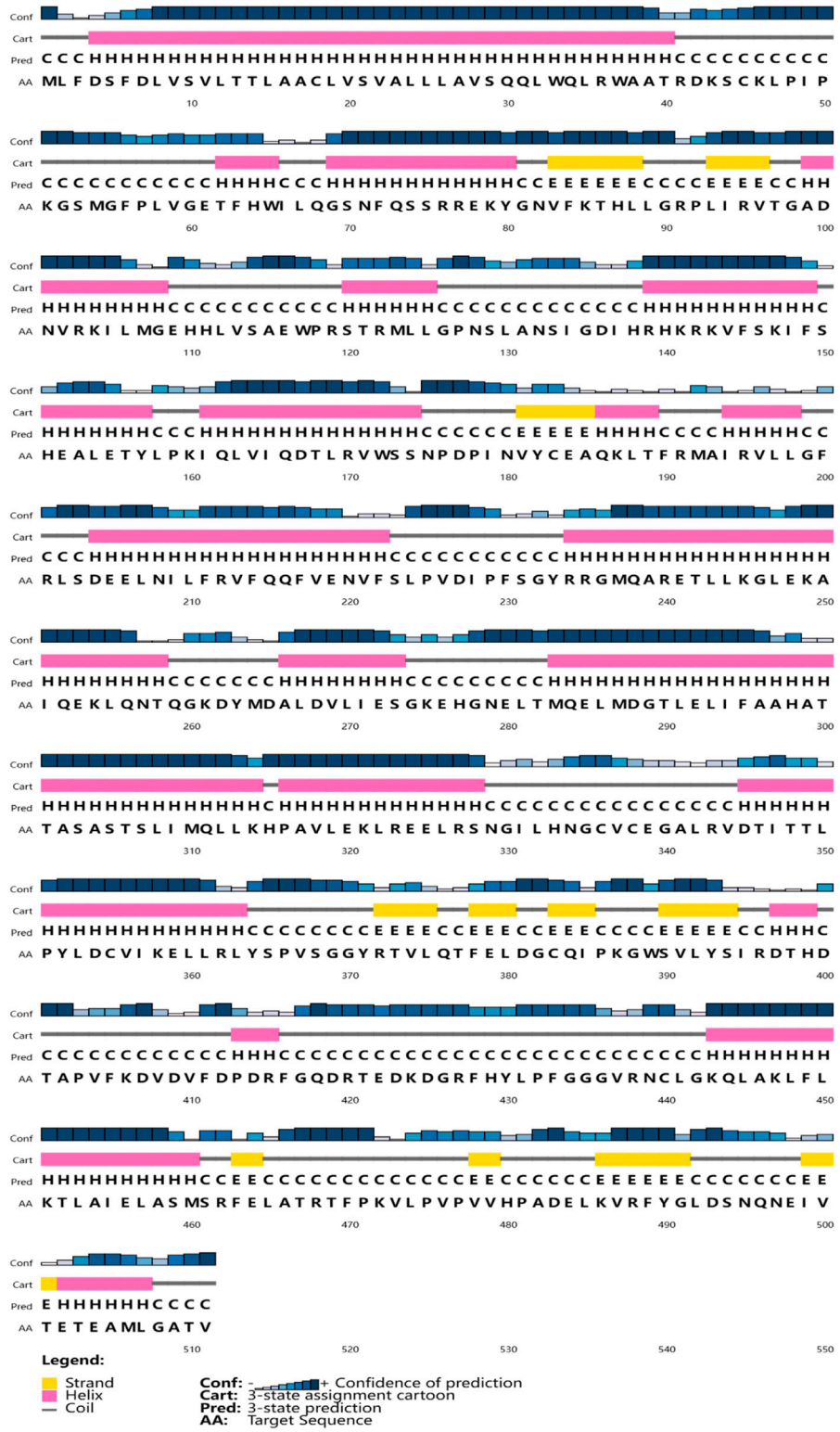

FIGURE 2
The secondary structures of Pn-CYP26B1. Strands and helixes are indicated by yellow and pink boxes, respectively.

2.3 Experimental design

After the acclimatization period, healthy male frogs, weighing approximately 30 g, were used for the exposure experiment. Males were selected based on the field observation that wild males may have higher levels of pollutants in their bodies than females (Cui et al., 2018). Considering the known range of environmental SMX concentrations and drawing on previous studies into the mechanism

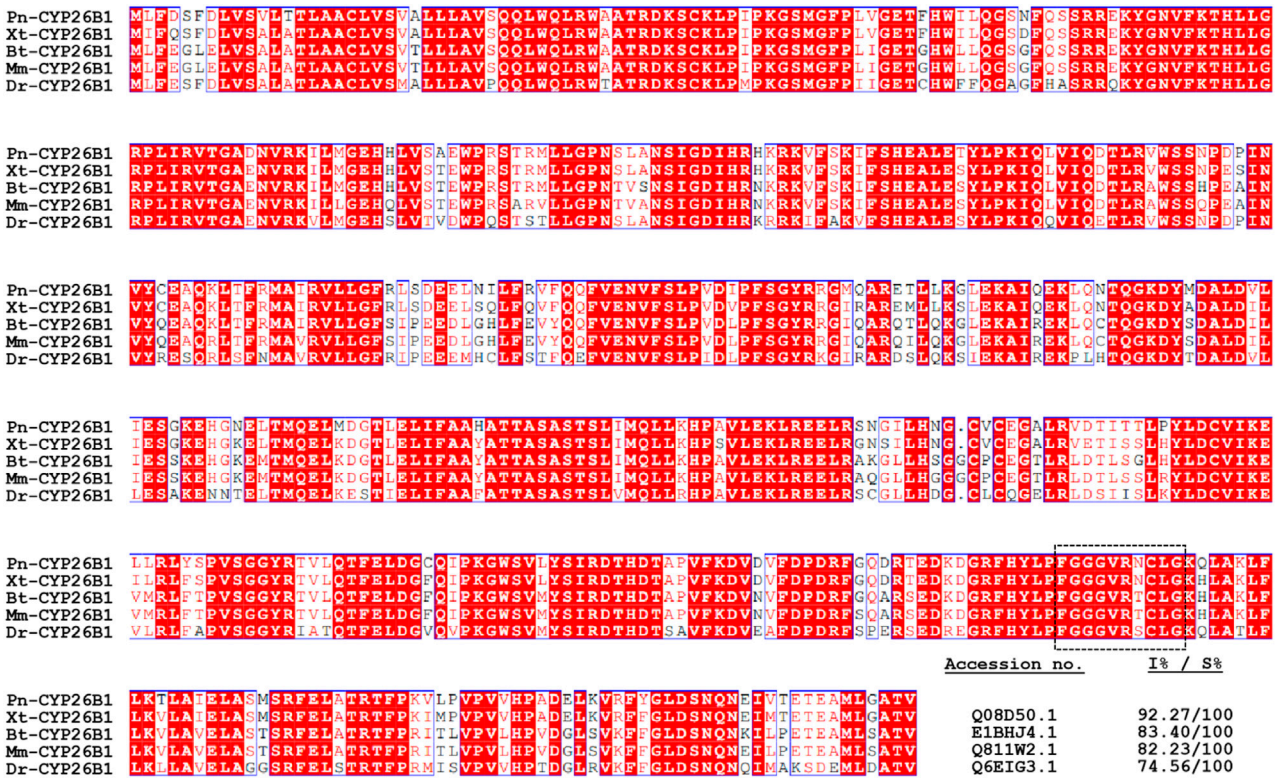

FIGURE 3
Multiple amino acid sequence alignment of *Pelophylax nigromaculatus* CYP26B1 with known homologs from other species. Completely (100%) conserved residues are shown in white text against a red background. Residues shown in red signify strong conservation. The heme-binding motif, FXXGXRXCXG, is outlined using dashed lines. The GenBank accession numbers and percentages of identity (I%) and similarity (S%) for the aligned sequences are provided in the lower right-hand section of the figure.

of SMX toxicity (Bielen et al., 2017; Xiong et al., 2019), the frogs were exposed to several SMX concentrations for a period of 21 days. Each experimental group consisted of three replicate aquaria, each measuring 30 cm × 30 cm × 60 cm. Twenty frogs were placed into each aquarium and exposed to either a test SMX solution or a 0.01% DMSO solution, which served as the control. The exposure solutions and control solutions were carefully prepared to maintain a constant temperature of 20°C ± 1°C, pH of 6.5 ± 0.5, and dissolved oxygen content of 7 ± 1 mg/L. The groups comprised a control group treated with 0.01% DMSO and three experimental groups exposed to concentrations of 1, 10, and 100 μg/L of SMX. After 21 days exposure, the frogs were humanely euthanized and their bodies were carefully dissected. Liver samples were collected from the dissected frogs and stored at −80°C for further analysis. All of the procedures strictly adhered to the guidelines established by the Association of Laboratory Animal Sciences, to ensure the ethical treatment of the frogs throughout the study.

2.4 PCR RNA isolation and cDNA synthesis

A rigorous methodology was employed to isolate total RNA from the liver samples (n = 3 replicates), using TRIzol reagent (Beijing ComWin Biotech Co., Ltd., Beijing, China). The completeness and purity of the isolated RNA was tested using electrophoresis on a 1.2% agarose gel in a Nanodrop spectrophotometer (Thermo Fisher Scientific, Waltham, MA, United States). Contaminated genomic DNA was eliminated and Hifair® III 1st Strand cDNA Synthesis SuperMix for qPCR (gDNA digester plus) kits (Yeasen Biotechnology Co., Ltd., Shanghai, China) were used for the reverse transcription of RNA.

2.5 Bioinformatics sequence analysis

Amino acid sequences and open reading frames (ORFs) were predicted using ORFFinder (https://www.ncbi.nlm.nih.gov/orffinder/). Sequence homology was analyzed using BLASTP (https://blast.ncbi.nlm.nih.gov/). The prediction of signal peptides and amino acid functional domains was conducted using SignalP v.6.0 (https://services.healthtech.dtu.dk/services/SignalP-6.0/) and ExPASy-PROSITE (http://prosite.expasy.org/), respectively. Secondary structure analysis of proteins was performed using PSIPRED Workbench (http://bioinf.cs.ucl.ac.uk/psipred/). Protein transmembrane helical structures were predicted using TMHMM (https://services.healthtech.dtu.dk/services/TMHMM-2.0/). Pairwise and multiple sequence alignments were performed using ClustalX and ESPript (http://espript.ibcp.fr/ESPript/ESPript/). Phylogenetic analysis was conducted by constructing a neighbor-joining tree based on the alignments using the MEGA 11.0 software (https://www.megasoftware.net/).

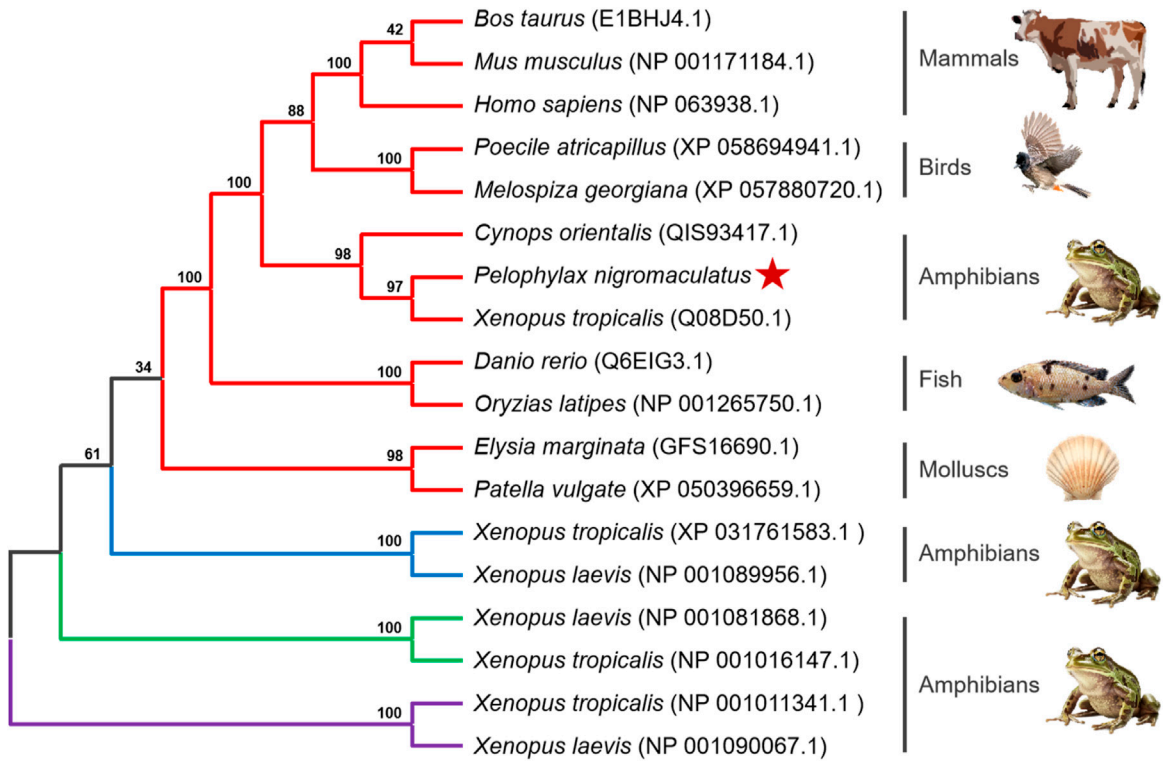

FIGURE 4
Un-rooted phylogenetic tree portraying the relationship between *Pelophylax nigromaculatus* CYP26 with *CYP* genes from other organisms. Each color represents a different class of *CYP* genes: red for CYP26B1; blue for CYP26C1; green for CYP26A1; and purple for CYP27C1. This tree, derived from the alignment of full-length amino acid sequences, was generated using the Neighbor-Joining (NJ) method in ClustalW and MEGA 11, and was bootstrapped 1,000 times.

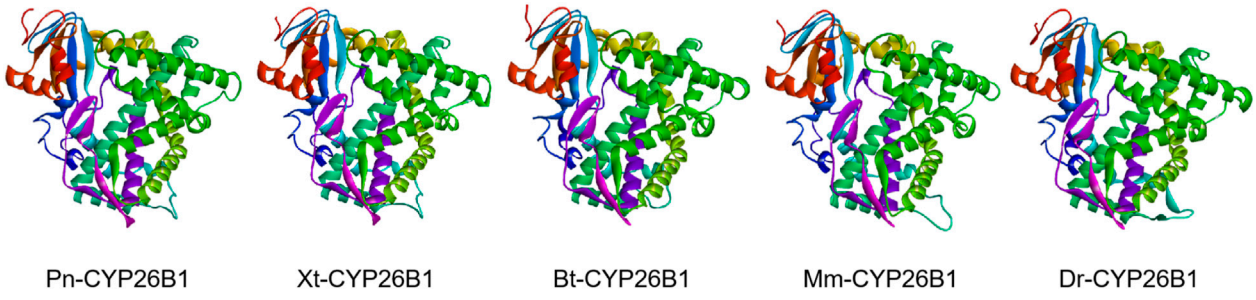

FIGURE 5
The predicted spatial structures of Pn-CYP26B1, Xt-CYP26B1, Bt-CYP26B1, Mm-CYP26B1, and Dr-CYP26B1. These structures were predicted using the SWISS-MODEL program, based on the crystal structure of *Synechocystis* sp. *PCC 6803* CYP (PDB entry 2VE3) as a reference for CYP26B1. Pn: *Pelophylax nigromaculatus*. Xt: *Xenopus tropicalis*. Bt: *Bos taurus*. Mm: *Mus musculus*. Dr: *Danio rerio*.

2.6 Quantitative real-time polymerase chain reaction (qRT-PCR) analyses

QRT-PCR analysis of the CYP in *P. nigromaculatus* was performed after 21 days of exposure to three different SMX concentrations (1, 10, 100 μg/L) and a DMSO control (Supplementary Figure S1). RNA extraction and cDNA synthesis were performed as described in Section 2.4. QRT-PCR was conducted using Hieff® qPCR SYBR® Green Master Mix (No Rox) kits (Yeasen Biotechnology Co., Ltd., Shanghai, China) on a CFX 96 Touch Real-Time PCR Detection System (Bio-Rad, Feldkirchen, Germany), following the protocol: initial denaturation at 95°C for 5 min; followed by 40 cycles at 95°C for 10 s, 60°C for 20 s, and 72°C for 20 s. Specific primers for target genes were designed using the Primer Premier v.6.0 software (https://primer-premier.software.informer.com/6.0/). The primer sequences used for the qRT-PCR are described in Supplementary Table S1. All primer pairs produced a single dissociation peak in every reaction, confirming specificity, and no amplification was observed in template-absent reactions. Due to its stable expression across all

TABLE 2 Sequence identity, GMQE, and QMEAN for GSTα and CYP26B1 in different organisms.

(B)	Gene name (B)	Seq identity (%)	GMQE	Qmean
CYP261	Pn-CYP261	35.01	0.69	−1.44
	Xt-CYP261	36.49	0.69	−1.38
	Bt-CYP261	34.87	0.68	−1.53
	Mm-CYP261	35.42	0.68	−1.35
	Dr-CYP261	37.04	0.68	−1.64

Pn, *Pelophylax nigromaculatus*; Xt, *Xenopus tropicalis*; Bt, *Bos taurus*; Mm, *Mus musculus*; Dr, *Danio rerio*.

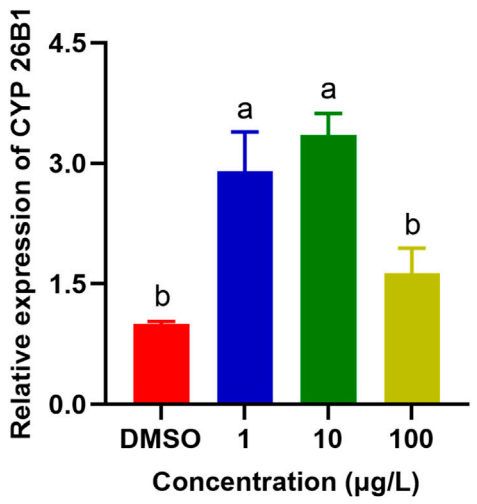

FIGURE 6
Effects of SMX exposure at different concentrations on the expression of CYP26B1 in the livers of *Pelophylax nigromaculatus*. Values are given as mean ± SE (n = 3). Significant differences are denoted by differing letters ($p < 0.05$).

exposure groups, actin was selected as the reference gene for the transcriptional assay. The relative mRNA levels of the target genes were determined using the $2^{-\Delta\Delta CT}$ method (Livak and Schmittgen, 2001).

2.7 Molecular docking

ORFFinder was used to translate the gene sequence into amino acid sequences for protein encoding, followed by alignment using BLAST search (BLASTP). The 3D structures were constructed using a homology modeling approach using the CYP26B1 template (PDB entry 2VE3) in the Alignment Mode of SWISS-MODEL (https://swissmodel.expasy.org/). The 3-D structures of SMX were acquired from ZINC (http://zinc.docking.org/) using CAS numbers. Prior to molecular docking, PlayMolecule (https://www.playmolecule.com/) was used to predict ligand binding pockets, and AutoDock (https://autodock.scripps.edu/) Tools v.1.5.7 to prepare the ligands and receptors. Protein modeling involved removing water molecules and extraneous ligands, adding hydrogen atoms, and applying Kollman charges. The grid box, central to the core site (43.61, −1.36, 10.59) of CYP26B1, was established with a coverage of 60 × 60 × 60 Å^3. AutoDock Vina was used to conduct the molecular docking, with 10 independent runs per docking and the binding mode selected for the lowest energy for analysis. The results displaying the lowest docked energy were examined visually using the Discovery Studio Visualizer 2021 Client (San Diego, CA, United States).

2.8 Data analysis

Data were presented as means ± standard error. Statistical variances between the control and treatment groups were determined using one-way analysis of variance (ANOVA) followed by Tukey's test, with significance set at $p < 0.05$. Normality and homogeneity of the data were validated before the ANOVA analysis using the Shapiro-Wilk's test and Levene's test. For skewed data distributions, the significant Kruskal–Wallis test was employed, followed by the Dunn-Bonferroni *post hoc* method. All statistical analyses were conducted using SPSS Statistics v.27.0 (IBM Corporation, Somers, NY, United States).

3 Results and discussion

3.1 Molecular characterization

The full-length cDNA of CYP26B1 from *P. nigromaculatus* was shown to be 1,669 bp in length, using our prior transcriptome sequencing data (Figure 1). To the best of our knowledge, this is the first reported instance of a full-length CPY gene cDNA in *P. nigromaculatus*. The sequence included ORFs of 1,536 bp, encoding proteins comprising 511 amino acids. Pn-CYP26B1 possessed a 96 bp UTR at the 5′-end and a 37 bp UTR at the 3′-end. The molecular mass and theoretical isoelectric point of Pn-CYP26B1 were determined as 57.64 kDa and 7.65, respectively (Table 1). Pn-CYP26B1 showed several characteristics common to the P450 superfamily, including function-critical sequence motifs that are highly conserved throughout evolution and pivotal for heme binding within the CYP26B1 sequences (Zhang et al., 2016). Following protein functional domain analysis, we identified a transmembrane helix region spanning positions 7–29 (Supplementary Figure S2), a conserved functional domain for CPY spanning 50–465 (PFAM00067), and a putative cysteine heme-iron ligand signature spanning 433–442 (FGLGKRSCIG) (PS00086). The estimated percentages of coil, helix, and strand structures were 41.49%, 50.10%, and 8.41%, respectively (Figure 2).

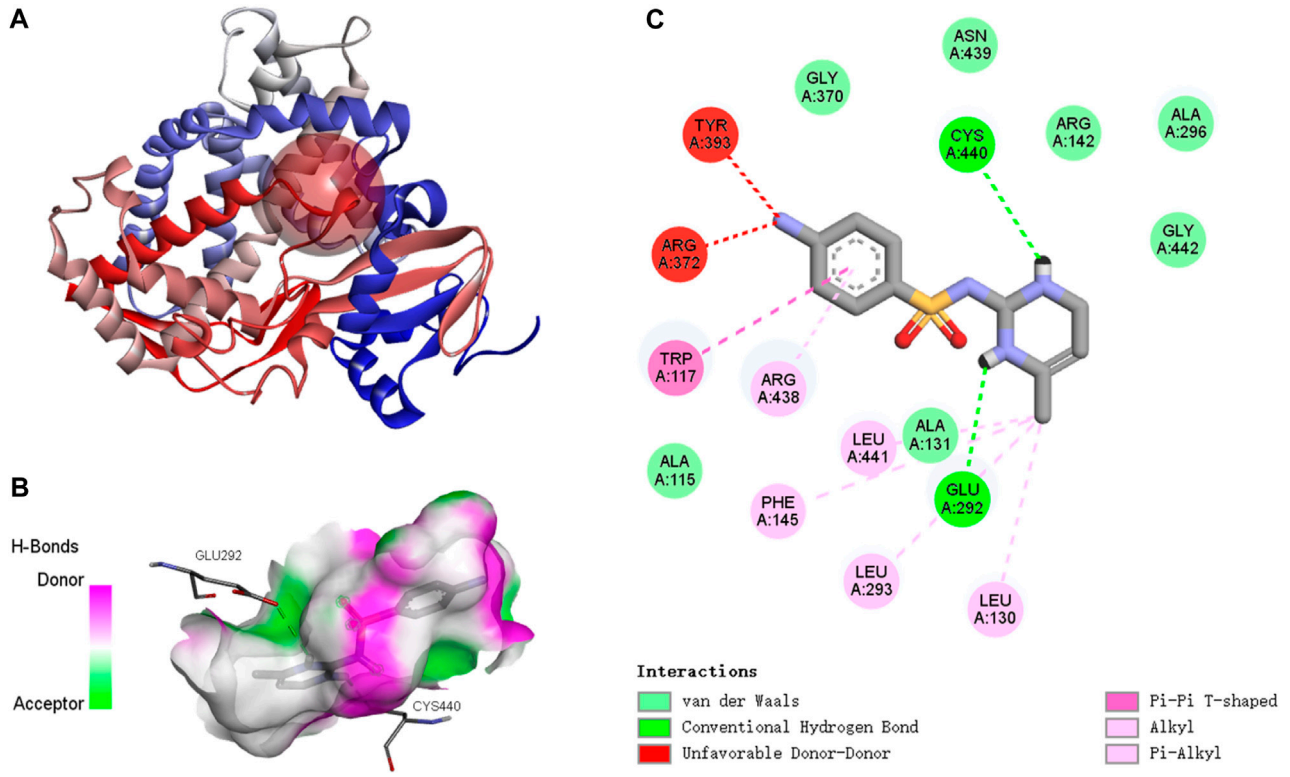

FIGURE 7
Molecular docking results of SMX with *Pelophylax nigromaculatus* CYP26B1. **(A)** The active binding sites. **(B)** The docking mode. **(C)** The hydrogen bond interactions.

3.2 Multiple sequence alignment

A multiple alignment analysis comparing Pn-CYP26B1 with the CYPs of other species revealed a high degree of homology. Pn-CYP26B1 exhibited 100% identity with sequences from *Bos taurus*, *Danio rerio*, *Mus musculus*, and *Xenopus tropicalis*. Among these animal species, the signature motif, FxxGxxxCxG, was highly conserved (Figure 3). A crucial feature of CYP enzymes is their heme-centered active site, featuring a Cys axial ligand. This identifies them as heme-thiolate proteins, primarily active as monooxygenases despite their conventional classification as cytochromes (Dermauw et al., 2020). Based on the systematic organization of the Cytochrome P450 Nomenclature Committee, the deduced amino acid sequence of Pn-CYP26B1 belonged to the CYP family 26, subfamily B, polypeptide 1.

3.3 Phylogenetic characterization

To determine the evolutionary position of Pn-CYP26B1, the Neighbor-Joining method (Saitou and Nei, 1987) was used to construct an unrooted phylogenetic tree. Our analysis included the CPY450 family members from both invertebrate and vertebrate species. The resulting phylogenetic tree not only clearly distinguished between invertebrate and vertebrate CYPs but also revealed four distinct groups, the classes CYP26B1, CYP26A1, CYP26C1, and CYP27C1, which were clearly separated (Figure 4). Three CPY26 enzymes, namely, CYP26A1, CYP26B1, and CYP26C1, have been previously identified in vertebrates (White et al., 1996; Nelson, 1999; Gu et al., 2005). CYP26 and CYP27 were classified into distinct CYP450 families, consistent with the branching results of our phylogenetic tree. CYPs belonging to the same class formed tight clusters, demonstrating their close evolutionary relationships. The protein encoded by Pn-CYP26B1 grouped first, with its ortholog in *X. tropicalis*, and subsequently clustered with other vertebrates. Although molluscs and vertebrates having the same CYP26B1 were grouped together, their evolutionary affinity was low. CYP26B1 did not cluster with the amphibian proteins encoded by CYP26C1, CYP26A1, and CYP27C1, highlighting its distinct evolutionary trajectory.

3.4 Tertiary structure

Based on the template of the crystal structure of *Synechocystis* sp. PCC 6803 CYP (PDB entry 2VE3), the potential tertiary structures of CYP26B1 from *B. taurus*, *D. rerio*, *M. musculus*, *P. nigromaculatus*, and *X. tropicalis* were established using the SWISS-MODEL prediction algorithm (Figure 5). The similarity between the template and the Pn-CYP26B1, Xt-CYP26B1, Bt-CYP26B1, Mm-CYP26B1, and Dr-CYP26B1 sequences ranged from 34.87% to 37.04%. The Global Model Quality Estimations were >0.68 (Table 2), indicating the high quality of these results, and the Qualitative Model Energy Analyses were > −1.64 (Table 2).

3.5 Binding and activation characteristics of SMX with CYP26B1

3.5.1 Aberrant expressions of the CYP26B1 proteins

CYP enzymes are predominantly found in the microsomal fraction of livers, where they play a vital role in bile acid biosynthesis and the metabolism of xenobiotics (Zanger and Schwab, 2013; Manikandan and Nagini, 2018). In addition, they contribute significantly to the homeostasis of steroid hormones, being located in the inner mitochondrial membrane within the steroidogenic tissues (Estabrook et al., 1963). They are also crucial in the metabolism of vitamins, unsaturated fatty acids, and cholesterol (Lane et al., 1999; Omura, 1999). SMX caused significant upregulation of the expression of CYP26B1 in *P. nigromaculatus* livers at concentrations of 1 and 10 μg/L ($p < 0.05$) (Figure 6), but no significant upregulation at 100 μg/L, compared with the control ($p > 0.05$). They are pivotal in xenobiotic metabolism within hepatocytes and central to biotransformation processes. Beyond hydroxylation, CYP enzymes facilitate diverse biotransformation reactions, e.g., dehalogenation, dehydrogenation, oxygenation, epoxidation, and dealkylation. Phase I metabolism also involves non-CYP mediated pathways through flavin-containing monooxygenases, amine oxidases, alcohol dehydrogenases, esterases, and peroxidases (Esteves et al., 2021). As with our findings, previously observed expression patterns of the four *CYP* genes in *Daphnia pulex* all exhibited elevation at low nanoplastic treatment doses, and reduction at higher doses without significant differences compared to the control (Wu et al., 2019). Elevated concentrations of SMX probably induced increased toxicity and a shift in metabolic homeostasis, potentially leading to the downregulation of numerous metabolism-related genes (Zhang et al., 2020; Huang et al., 2021).

3.5.2 Binding of SMX to the CYP26B1 proteins

The active binding sites of SMX to the *P. nigromaculatus* CYP26B1 proteins are shown in Figure 7A. The docking modes of SMX onto the CYP26B1 proteins are shown in Figure 7B and the hydrogen bond interactions are shown in Figure 7C. SMX showed an affinity of −7.6 kcal/mol for CYP26B1. Hydrogen bonding plays a major role in ligand binding to target receptors. The affinity of a ligand for the CYP26B1 protein can influence its activity and mediate its effects. In this study, a strong affinity between SMX and the CYP26B1 proteins was observed. CYP26 enzymes are essential for maintaining RA homeostasis by regulating its availability for receptor binding and signaling (Roberts, 2020). RA signaling plays a vital role in a myriad of biological functions across organisms, including modulation of immune responses (Oliveira et al., 2018). It also contributes to the metabolism of lipids and fatty acids, energy metabolism, adipocyte differentiation and remodeling, and the regulation of postnatal skeletal growth and homeostasis (Williams et al., 2009). The primary role of CYP26 is to degrade endogenous all-trans RA, which is found in high concentrations in tissues (Perlmann, 2002). This acid efficiently binds to retinoic acid receptors (RARs) and represents the primary biologically active retinoid *in vivo* (Horton and Maden, 1995). Retinoids, which are crucial in cell signaling, bind to two classes of retinoid receptors, RARs and retinoid X receptors. These ligand-regulated transcription factors are essential for development and physiology (Carvalho et al., 2017). The importance of retinoids is well-documented, with significant developmental abnormalities arising from either retinoid deficiency or excess (Emoto et al., 2005). Embryos from CYP26-deficient mice display defects akin to those resulting from all-trans-retinoic acid-induced teratogenicity (Uehara et al., 2009). It is hypothesised that activation of CYP26, which functions in retinoic acid hydroxylation, increases the metabolism and excretion rate of all-trans retinoic acid. This, in turn, raises the demand for all-trans retinoic acid precursors such as retinol and retinal, resulting in the depletion of retinoid stores, as observed in Atlantic salmon (*Salmo salar*) following exposure to benzo(a)pyrene (Beníšek et al., 2011; Berntssen et al., 2016). Abnormal expression of CYP26B1, induced by SMX, may disrupt RA homeostasis, potentially causing harm to organisms.

4 Conclusion

Our research provided novel insights into the molecular and functional dynamics of CYP26B1, a critical enzyme in the detoxification pathway, in *P. nigromaculatus* exposed to SMX. The study confirmed that SMX exposure significantly upregulated the expression of CYP26B1, suggesting its involvement in mitigating antibiotic-induced toxicity. This adaptive response underscored the role of CYP enzymes in the environmental resilience and health of amphibians, offering a molecular basis for further investigations into the impacts of emerging pollutants on aquatic wildlife. Furthermore, our findings emphasized the need for environmentally sustainable practices in antibiotic usage to mitigate its pervasive effects on non-target organisms and ecosystems.

Data availability statement

The datasets presented in this study can be found in online repositories. The names of the repository/repositories and accession number(s) can be found in the article/Supplementary Material.

Ethics statement

The animal study was approved by the Hangzhou Normal University ethics committee. The study was conducted in accordance with the local legislation and institutional requirements.

Author contributions

ZL: Conceptualization, Methodology, Writing–review and editing, Data curation, Formal Analysis, Investigation, Resources, Visualization, Writing–original draft. CS: Conceptualization, Data curation, Formal Analysis, Investigation, Methodology, Resources, Visualization, Writing–original draft, Writing–review and editing.

BW: Conceptualization, Methodology, Resources, Writing–review and editing. XZ: Conceptualization, Methodology, Resources, Writing–review and editing. JD: Conceptualization, Methodology, Resources, Writing–review and editing. PG: Conceptualization, Methodology, Resources, Writing–review and editing. XY: Conceptualization, Methodology, Resources, Writing–review and editing. ZL: Conceptualization, Methodology, Writing–review and editing, Funding acquisition, Project administration, Supervision. HZ: Conceptualization, Methodology, Resources, Writing–review and editing.

Funding

The author(s) declare that financial support was received for the research, authorship, and/or publication of this article. This work was supported by the Natural Science Foundation of Zhejiang Province of China (LQ22C030003), the National Natural Science Foundation of China (42207323), and the special fund of the State Environmental Protection Key Laboratory of Environmental Health Impact Assessment of Emerging Contaminants (SEPKL-EHIAEC-202201).

Conflict of interest

The authors declare that the research was conducted in the absence of any commercial or financial relationships that could be construed as a potential conflict of interest.

Publisher's note

All claims expressed in this article are solely those of the authors and do not necessarily represent those of their affiliated organizations, or those of the publisher, the editors and the reviewers. Any product that may be evaluated in this article, or claim that may be made by its manufacturer, is not guaranteed or endorsed by the publisher.

Supplementary material

The Supplementary Material for this article can be found online at: https://www.frontiersin.org/articles/10.3389/fphys.2024.1412943/full#supplementary-material

References

Alford, R. A., Dixon, P. M., and Pechmann, J. H. K. (2001). Ecology. Global amphibian population declines. *Nature* 412 (6846), 499–500. doi:10.1038/35087658

Baune, B., Flinois, J. P., Furlan, V., Gimenez, F., Taburet, A. M., Becquemont, L., et al. (1999). Halofantrine metabolism in microsomes in man: major role of CYP 3A4 and CYP 3A5. *J. Pharm. Pharmacol.* 51 (4), 419–426. doi:10.1211/0022357991772628

Beníšek, M., Kubincová, P., Bláha, L., and Hilscherová, K. (2011). The effects of PAHs and N-PAHs on retinoid signaling and Oct-4 expression *in vitro*. *Toxicol. Lett.* 200 (3), 169–175. doi:10.1016/j.toxlet.2010.11.011

Berntssen, M. H., Ørnsrud, R., Rasinger, J., Søfteland, L., Lock, E. J., Kolås, K., et al. (2016). Dietary vitamin A supplementation ameliorates the effects of poly-aromatic hydrocarbons in Atlantic salmon (*Salmo salar*). *Aquat. Toxicol.* 175, 171–183. doi:10.1016/j.aquatox.2016.03.016

Bielen, A., Šimatović, A., Kosić-Vukšić, J., Senta, I., Ahel, M., Babić, S., et al. (2017). Negative environmental impacts of antibiotic-contaminated effluents from pharmaceutical industries. *Water Res.* 126, 79–87. doi:10.1016/j.watres.2017.09.019

Carvalho, J., Lahaye, F., Croce, J., and Schubert, M. (2017). CYP26 function is required for the tissue-specific modulation of retinoic acid signaling during amphioxus development. *Int. J. Dev. Biol.* 61 (10-11-12), 733–747. doi:10.1387/ijdb.170227ms

Christou, A., Karaolia, P., Hapeshi, E., Michael, C., and Fatta-Kassinos, D. (2017). Long-term wastewater irrigation of vegetables in real agricultural systems: concentration of pharmaceuticals in soil, uptake and bioaccumulation in tomato fruits and human health risk assessment. *Water Res.* 109, 24–34. doi:10.1016/j.watres.2016.11.033

Cui, H., Chang, H., Zheng, H., and Wan, Y. (2021). Determination and occurrence of sulfonamide transformation products in surface waters. *Sci. Total Environ.* 779, 146562. doi:10.1016/j.scitotenv.2021.146562

Cui, Q., Pan, Y., Zhang, H., Sheng, N., Wang, J., Guo, Y., et al. (2018). Occurrence and tissue distribution of novel perfluoroether carboxylic and sulfonic acids and legacy per/polyfluoroalkyl substances in black-spotted frog (Pelophylax nigromaculatus). *Environ. Sci. Technol.* 52 (3), 982–990. doi:10.1021/acs.est.7b03662

Daniel, E., Barlow, H. R., Sutton, G. I., Gu, X., Htike, Y., Cowdin, M. A., et al. (2020). Cyp26b1 is an essential regulator of distal airway epithelial differentiation during lung development. *Development* 147 (4), dev181560. doi:10.1242/dev.181560

Dermauw, W., Van Leeuwen, T., and Feyereisen, R. (2020). Diversity and evolution of the P450 family in arthropods. *Insect Biochem. Mol. Biol.* 127, 103490. doi:10.1016/j.ibmb.2020.103490

Emoto, Y., Wada, H., Okamoto, H., Kudo, A., and Imai, Y. (2005). Retinoic acid-metabolizing enzyme Cyp26a1 is essential for determining territories of hindbrain and spinal cord in zebrafish. *Dev. Biol.* 278 (2), 415–427. doi:10.1016/j.ydbio.2004.11.023

Estabrook, R. W., Cooper, D. Y., and Rosenthal, O. (1963). The light reversible carbon monoxide inhibition of the steroid C21-hydroxylase system of the adrenal cortex. *Biochem. Z* 338, 741–755.

Esteves, F., Rueff, J., and Kranendonk, M. (2021). The central role of cytochrome P450 in xenobiotic metabolism—a brief review on a fascinating enzyme family. *J. Xenobiot.* 11, 94–114. doi:10.3390/jox11030007

Gu, X., Xu, F., Wang, X., Gao, X., and Zhao, Q. (2005). Molecular cloning and expression of a novel CYP26 gene (cyp26d1) during zebrafish early development. *Gene Expr. Patterns* 5 (6), 733–739. doi:10.1016/j.modgep.2005.04.005

Ha-Duong, N. T., Marques-Soares, C., Dijols, S., Sari, M. A., Dansette, P. M., and Mansuy, D. (2001). Interaction of new sulfaphenazole derivatives with human liver cytochrome p450 2Cs: structural determinants required for selective recognition by CYP 2C9 and for inhibition of human CYP 2Cs. *Arch. Biochem. Biophys.* 394 (2), 189–200. doi:10.1006/abbi.2001.2511

Han, J., Won, E.-J., Kim, H.-S., Nelson, D. R., Lee, S.-J., Park, H. G., et al. (2015). Identification of the full 46 cytochrome P450 (CYP) complement and modulation of CYP expression in response to water-accommodated fractions of crude oil in the cyclopoid copepod paracyclopina nana. *Environ. Sci. Technol.* 49 (11), 6982–6992. doi:10.1021/acs.est.5b01244

Horton, C., and Maden, M. (1995). Endogenous distribution of retinoids during normal development and teratogenesis in the mouse embryo. *Dev. Dyn.* 202 (3), 312–323. doi:10.1002/aja.1002020310

Huang, F., An, Z., Moran, M. J., and Liu, F. (2020). Recognition of typical antibiotic residues in environmental media related to groundwater in China (2009–2019). *J. Hazard Mater* 399, 122813. doi:10.1016/j.jhazmat.2020.122813

Huang, Y., Ding, J., Zhang, G., Liu, S., Zou, H., Wang, Z., et al. (2021). Interactive effects of microplastics and selected pharmaceuticals on red tilapia: role of microplastic aging. *Sci. Total Environ.* 752, 142256. doi:10.1016/j.scitotenv.2020.142256

Jiang, J., Xie, F., Zang, C., Cai, L., Li, C., Wang, B., et al. (2016). Assessing the threat status of amphibians in China. *Biodivers. Sci.* 24, 588–597. doi:10.17520/biods.2015348

Kümmerer, K. (2009). Antibiotics in the aquatic environment – a review – Part I. *Chemosphere* 75 (4), 417–434. doi:10.1016/j.chemosphere.2008.11.086

Lampen, A., Meyer, S., and Nau, H. (2001). Effects of receptor-selective retinoids on CYP26 gene expression and metabolism of all-trans-retinoic acid in intestinal cells. *Drug metabolism Dispos. Biol. fate Chem.* 29 (5), 742–747.

Lane, M. A., Chen, A. C., Roman, S. D., Derguini, F., and Gudas, L. J. (1999). Removal of LIF (leukemia inhibitory factor) results in increased vitamin A (retinol) metabolism to 4-oxoretinol in embryonic stem cells. *Proc. Natl. Acad. Sci. U. S. A.* 96 (23), 13524–13529. doi:10.1073/pnas.96.23.13524

Lie, K. K., Meier, S., Sørhus, E., Edvardsen, R. B., Karlsen, Ø., and Olsvik, P. A. (2019). Offshore crude oil disrupts retinoid signaling and eye development in larval atlantic haddock. *Front. Mar. Sci.* 6. doi:10.3389/fmars.2019.00368

Lim, S. Y. M., Pan, Y., Alshagga, M., Lim, W., Cin, K., Alshehade, S. A., et al. (2024). CYP14 family in *Caenorhabditis elegans*: mitochondrial function, detoxification, and lifespan. *J. Appl. Toxicol.* doi:10.1002/jat.4597

Lin, H., Liu, Z., Yang, H., Lu, L., Chen, R., Zhang, X., et al. (2022). Per- and polyfluoroalkyl substances (PFASs) impair lipid metabolism in *Rana nigromaculata*: a field investigation and laboratory study. *Environ. Sci. Technol.* 56 (18), 13222–13232. doi:10.1021/acs.est.2c03452

Liu, X., Lu, S., Guo, W., Xi, B., and Wang, W. (2018). Antibiotics in the aquatic environments: a review of lakes, China. *Sci. Total Environ.* 627, 1195–1208. doi:10.1016/j.scitotenv.2018.01.271

Livak, K. J., and Schmittgen, T. D. (2001). Analysis of relative gene expression data using real-time quantitative PCR and the 2(-Delta Delta C(T)) Method. *Methods* 25 (4), 402–408. doi:10.1006/meth.2001.1262

Maden, M. (2002). Retinoid signalling in the development of the central nervous system. *Nat. Rev. Neurosci.* 3 (11), 843–853. doi:10.1038/nrn963

Manikandan, P., and Nagini, S. (2018). Cytochrome P450 structure, function and clinical significance: a review. *Curr. Drug Targets* 19 (1), 38–54. doi:10.2174/1389450118666170125144557

Nelson, D. R. (1999). A second CYP26 P450 in humans and zebrafish: CYP26B1. *Arch. Biochem. Biophys.* 371 (2), 345–347. doi:10.1006/abbi.1999.1438

Oliveira, L. M., Teixeira, F. M. E., and Sato, M. N. (2018). Impact of retinoic acid on immune cells and inflammatory diseases. *Mediat. Inflamm.* 2018, 3067126. doi:10.1155/2018/3067126

Omura, T. (1999). Forty years of cytochrome P450. *Biochem. Biophys. Res. Commun.* 266 (3), 690–698. doi:10.1006/bbrc.1999.1887

Pang, L., Shao, J., Wen, X., Liu, D., Zhang, Z., and Shuang, W. (2022). Effect of the neuropathic pain receptor P2X3 on bladder function induced by intraperitoneal injection of cyclophosphamide (CYP) in interstitial cystitis rats. *Transl. Androl.* 11 (3), 304–312. doi:10.21037/tau-22-23

Perlmann, T. (2002). Retinoid metabolism: a balancing act. *Nat. Genet.* 31 (1), 7–8. doi:10.1038/ng877

Pikuleva, I. A., and Cartier, N. (2021). Cholesterol hydroxylating cytochrome P450 46A1: from mechanisms of action to clinical applications. *Front. Aging Neurosci.* 13, 696778. doi:10.3389/fnagi.2021.696778

Roberts, C. (2020). Regulating retinoic acid availability during development and regeneration: the role of the CYP26 enzymes. *Int. J. Dev. Biol.* 8, 6. doi:10.3390/jdb8010006

Rutkoski, C. F., Grott, S. C., Israel, N. G., Carneiro, F. E., de Campos Guerreiro, F., Santos, S., et al. (2022). Hepatic and blood alterations in Lithobates catesbeianus tadpoles exposed to sulfamethoxazole and oxytetracycline. *Chemosphere* 307, 136215. doi:10.1016/j.chemosphere.2022.136215

Rydeen, A. B., and Waxman, J. S. (2014). Cyp26 enzymes are required to balance the cardiac and vascular lineages within the anterior lateral plate mesoderm. *Development* 141 (8), 1638–1648. doi:10.1242/dev.105874

Saitou, N., and Nei, M. (1987). The neighbor-joining method: a new method for reconstructing phylogenetic trees. *Mol. Biol. Evol.* 4 (4), 406–425. doi:10.1093/oxfordjournals.molbev.a040454

Samrani, L. M. M., Dumont, F., Hallmark, N., Bars, R., Tinwell, H., Pallardy, M., et al. (2023). Nervous system development related gene expression regulation in the zebrafish embryo after exposure to valproic acid and retinoic acid: a genome wide approach. *Toxicol. Lett.* 384, 96–104. doi:10.1016/j.toxlet.2023.07.005

Shao, Y., Wang, Y., Yuan, Y., and Xie, Y. (2021). A systematic review on antibiotics misuse in livestock and aquaculture and regulation implications in China. *Sci. Total Environ.* 798, 149205. doi:10.1016/j.scitotenv.2021.149205

Spoorendonk, K. M., Peterson-Maduro, J., Renn, J. r., Trowe, T., Kranenbarg, S., Winkler, C., et al. (2008). Retinoic acid and Cyp26b1 are critical regulators of osteogenesis in the axial skeleton. *Development* 135 (22), 3765–3774. doi:10.1242/dev.024034

Uehara, M., Yashiro, K., Takaoka, K., Yamamoto, M., and Hamada, H. (2009). Removal of maternal retinoic acid by embryonic CYP26 is required for correct *Nodal* expression during early embryonic patterning. *Gene Dev.* 23 (14), 1689–1698. doi:10.1101/gad.1776209

Wang, X., Zheng, R., Yao, Q., Liang, Z., Wu, M., and Wang, H. (2019). Effects of fluoride on the histology, lipid metabolism, and bile acid secretion in liver of *Bufo gargarizans* larvae. *Environ. Pollut.* 254 (Pt B), 113052. doi:10.1016/j.envpol.2019.113052

White, J. A., Guo, Y. D., Baetz, K., Beckett-Jones, B., Bonasoro, J., Hsu, K. E., et al. (1996). Identification of the retinoic acid-inducible all-trans-retinoic acid 4-hydroxylase. *J. Biol. Chem.* 271 (47), 29922–29927. doi:10.1074/jbc.271.47.29922

White, J. A., Ramshaw, H., Taimi, M., Stangle, W., Zhang, A., Everingham, S., et al. (2000). Identification of the human cytochrome P450, P450RAI-2, which is predominantly expressed in the adult cerebellum and is responsible for all-trans-retinoic acid metabolism. *Proc. Natl. Acad. Sci.* 97 (12), 6403–6408. doi:10.1073/pnas.120161397

Williams, J. A., Kondo, N., Okabe, T., Takeshita, N., Pilchak, D. M., Koyama, E., et al. (2009). Retinoic acid receptors are required for skeletal growth, matrix homeostasis and growth plate function in postnatal mouse. *Dev. Biol.* 328 (2), 315–327. doi:10.1016/j.ydbio.2009.01.031

Wu, D., Liu, Z., Cai, M., Jiao, Y., Li, Y., Chen, Q., et al. (2019). Molecular characterisation of cytochrome P450 enzymes in waterflea (*Daphnia pulex*) and their expression regulation by polystyrene nanoplastics. *Aquat. Toxicol.* 217, 105350. doi:10.1016/j.aquatox.2019.105350

Xiong, J.-Q., Kim, S.-J., Kurade, M. B., Govindwar, S., Abou-Shanab, R. A. I., Kim, J.-R., et al. (2019). Combined effects of sulfamethazine and sulfamethoxazole on a freshwater microalga, Scenedesmus obliquus: toxicity, biodegradation, and metabolic fate. *J. Hazard Mater* 370, 138–146. doi:10.1016/j.jhazmat.2018.07.049

Yang, J. H., Park, J. W., Kim, H. S., Lee, S., Yerke, A. M., Jaiswal, Y. S., et al. (2024). Effects of antibiotic residues on fish gut microbiome dysbiosis and mucosal barrier-related pathogen susceptibility in zebrafish experimental model. *Antibiot. Basel* 13 (1), 82. doi:10.3390/antibiotics13010082

Zainab, S. M., Junaid, M., Xu, N., and Malik, R. N. (2020). Antibiotics and antibiotic resistant genes (ARGs) in groundwater: a global review on dissemination, sources, interactions, environmental and human health risks. *Water Res.* 187, 116455. doi:10.1016/j.watres.2020.116455

Zanger, U. M., and Schwab, M. (2013). Cytochrome P450 enzymes in drug metabolism: regulation of gene expression, enzyme activities, and impact of genetic variation. *Pharmacol. Ther.* 138 (1), 103–141. doi:10.1016/j.pharmthera.2012.12.007

Zhang, D.-D., Wang, X.-Y., Chen, J.-Y., Kong, Z.-Q., Gui, Y.-J., Li, N.-Y., et al. (2016). Identification and characterization of a pathogenicity-related gene VdCYP1 from Verticillium dahliae. *Sci. Rep.* 6 (1), 27979. doi:10.1038/srep27979

Zhang, W., Liu, Z., Tang, S., Li, D., Jiang, Q., and Zhang, T. (2020). Transcriptional response provides insights into the effect of chronic polystyrene nanoplastic exposure on *Daphnia pulex*. *Chemosphere* 238, 124563. doi:10.1016/j.chemosphere.2019.124563

frontiers | Frontiers in Marine Science

TYPE Original Research
PUBLISHED 28 June 2024
DOI 10.3389/fmars.2024.1444210

OPEN ACCESS

EDITED BY
Yiming Li,
Fishery Machinery and Instrument Research Institute, China

REVIEWED BY
Lanmei Wang,
Freshwater Fisheries Research Center (CAFS), China
Donglei Wu,
East China Normal University, China
Qing Wang,
Nanjing Fisheries Research Institute, China
Guizhen Feng,
East China Jiaotong University, China

*CORRESPONDENCE
Weiwei Lv
wwlv1986@sina.com
Wenzong Zhou
wzzhou505@sina.com

†These authors have contributed equally to this work

RECEIVED 05 June 2024
ACCEPTED 17 June 2024
PUBLISHED 28 June 2024

CITATION
Li M, Huang W, Zhao Y, Yuan Q, Yang H, Lv W and Zhou W (2024) Effects of long-term ammonia and heat stress on growth performance, antioxidant and immunity of wild and breeding juvenile rice field eel (*Monopterus albus*). *Front. Mar. Sci.* 11:1444210. doi: 10.3389/fmars.2024.1444210

Effects of long-term ammonia and heat stress on growth performance, antioxidant and immunity of wild and breeding juvenile rice field eel (*Monopterus albus*)

Muyan Li[1,2†], Weiwei Huang[1,3†], Yifan Zhao[1,2], Quan Yuan[1,3], Hang Yang[1,3], Weiwei Lv[1,3*] and Wenzong Zhou[1,3*]

[1]Eco-environmental Protection Research Institute, Shanghai Academy of Agricultural Sciences, Shanghai, China, [2]Key Laboratory of Integrated Rice-Fish Farming, Ministry of Agriculture and Rural Affairs, Shanghai Ocean University, Shanghai, China, [3]Key Laboratory of Integrated Rice-Fish Farming, Ministry of Agriculture and Rural Affairs, Shanghai Academy of Agricultural Sciences, Shanghai, China

This study aimed to evaluate the impacts of wild and breeding juvenile rice field eel under conditions of ammonia and heat stress. The growth performance (FBW, WGR, SGR, and FCR) of 360 wild (24.22 ± 0.30 g) and 360 breeding (24.16 ± 0.27 g) strains was significantly hindered by ammonia and heat stress. The inhibitory effects were more obvious when the two stresses were combined. The growth performance and survival rates of the breeding strains outperformed that of the wild strains under identical stress conditions, this was explained by the expression of the growth-related gene (*gh*). They have increased the enzyme activity (CAT and GSH-Px) and expression of immune-related genes (*cat*, *gpx3*, and *hsp90α*) in response to oxidative stress. However, the results of certain indicator enzymes indicate the presence of oxidative damage in their tissues. The presence of an inflammatory response in the tissues was suggested by the up-regulation of genes associated with pro-inflammatory cytokines (*il-1β* and *il-8*) and the down-regulation of genes related to anti-inflammatory cytokines (*il-10*). Additionally, the presence of tissue damage was shown by the up-regulation of genes connected to apoptosis (*cas2*, *cas8*, and *cas9*) and the down-regulation of genes connected to tight junctions (*zo-1*). Nevertheless, it is noteworthy that breeding strains exhibited superior adaptability to ammonia and heat stress in comparison to wild strains.

KEYWORDS

***Monopterus albus*, ammonia stress, heat stress, growth, antioxidant, immunity**

1 Introduction

Rice field eel (*Monopterus albus*) is a common freshwater fish in Asian countries that taxonomically belongs to Osteichthyes, Synbranchiformes, and Synbranchidae. Due to its delicious taste, rich nutrition, and officinal value, eel is considered to be one of the most economically valuable fish in China, with a yield up to 334,215 tons in 2022. However, this yield is far from meeting consumer demands. One of the important reasons to restrict this yield is the scarcity of breeding fry and the abuse of wild fry. Meanwhile, the efficiency of breeding and wild fry has been the focus of debate in the industry.

In China, the traditional net-cage farming mode has been adopted by more than 95% of eel farmers. Due to their open farming environment, the eels are highly vulnerable to extreme climate changes, such as high temperatures and typhoons. Moreover, with the increase in rearing density, ammonia in water will become one of the main threats to eel rearing, may exhibit toxic effects on fish, and can result in widespread fatalities (Ip and Chew, 2010; Bucking, 2017). In order to break the restrictions of natural conditions, a novel method of recycled water rearing was proposed. However, since few studies have focused on the physiological effects of environmental factors on *M. albus* larvae, the popularization of this technology may be subject to certain resistance.

Water temperature is one of the important environmental factors affecting the growth of aquatic animals (Rebl et al., 2013; Reid et al., 2019; Wu et al., 2021). A latest study demonstrated that the breeding strains of eel larvae showed the best growth performance under a temperature of 34°C (Mao et al., 2024). Nevertheless, the wild strains do not encounter such elevated water temperatures in their natural habitat. Excessively high-water temperatures can have devastating consequences for aquatic organisms, leading to reduced growth and increased mortality in fish (Dominguez et al., 2004; Zhang et al., 2014). Moreover, high water temperatures may also cause other environmental problems, such as the occurrence of ammonia, nitrogen, and nitrite, because part of the beneficial bacteria will be inactivated at high temperatures, making it harder for residual erbium and feces to be degraded (Li et al., 2022). When exposed to a certain concentration of nitrite, aquatic animals often show significant oxidative stress and even exhibit inflammatory responses (Li et al., 2020). In addition, prior research has demonstrated that elevated concentrations of ammonia in the water column hinder the development and immune response of aquatic species (Kim et al., 2015; Cui et al., 2022; Ou et al., 2022). However, no studies have focused on the effects of nitrite on eel larvae. In aquaculture, high temperatures are often accompanied by multiple negative environmental factors. In this study, a comparative study was conducted to detect the differences in growth performance, antioxidant, immune, and apoptosis indices between wild and breeding strains of eel larvae under the combined exposure of heat and ammonia. These results will provide a reference for the factory farming of swamp eels.

2 Materials and methods

2.1 Experimental fish

Wild strains of juvenile eels (WS) obtained from nearby rice farms or ponds in their natural habitat were transported to be temporarily reared under laboratory conditions for one week to continuously check the fish's health status. During this period, aeration of the water was maintained constantly, and one-third of the water volume was replaced on a daily basis. Over the next two weeks, WS were adapted to the feeding experiment until commercial feed (Hubei Zhaoliang Biotechnology Co., Ltd., Hubei, China) could be consumed. After two weeks of acclimatization, a total of 360 healthy fish with a similar weight (24.22 ± 0.30 g) were selected for the experiment. The fish were placed in a random and equal manner throughout 12 cylindrical tanks (r = 0.5 m, h = 0.3 m), with 30 fish per tank.

Breeding strains of juvenile eels (BS) were obtained from the Zhuanghang Comprehensive Experiment Station of the Shanghai Academy of Agricultural Sciences, and acclimation was completed according to the same method. Similarly, a total of 360 healthy fish with a similar weight (24.16 ± 0.27 g) were selected for distribution in 12 cylindrical tanks.

2.2 Experimental design and sample

The test site was a greenhouse at the Zhuanghang Comprehensive Experiment Station of the Shanghai Academy of Agricultural Sciences, which had a thermostatic heating system. The initial temperature of the experimental group was 26°C, which corresponds to room temperature, and this was used as a constant water temperature for the control and unheated groups. The heat stress (HS) groups were set at 34°C and warmed at 1°C/h (the error is within ± 0.1°C). Ammonium chloride (NH_4Cl) is a compound used as a source of ammonia to attain the appropriate concentration of ammonia in a solution. The actual concentration of nitrite-N in test solutions is measured using spectrophotometry. The ammonia concentration in the ammonia stress (AS) groups was maintained at 12.0 ± 0.5 mg/L. Eels in 12 tanks from WS were divided into four experimental groups (WS-CT, WS-HS, WS-AS, and WS-HS+AS), and each group consisted of three replicates. Eels from BS follow this method as (BS-CT, BS-HS, BS-AS, and BS-HS+AS).

For the WS and BS feeding experiments, growth performance was accomplished over an eight-week period, where the temperature was maintained at the same stress temperature (the error is within ± 0.3°C). The fish were manually fed at 16:00 each day with an amount of food equal to 4-5% of their body weight. Any food that was not eaten was collected within 30 min of feeding. It was then dried until it achieved a constant weight and finally weighed to determine the amount of food consumed. During the feeding trial, the aeration of the water was maintained constantly, and the rest of the water conditions were kept constant (dissolved O_2 ≥ 5.8 mg/L, pH 7.2 ± 0.2). The tank's water quality is regularly assessed six times a day using a portable water

quality analyzer (model HQ40D, HACH, Colorado, USA) to measure water temperature, pH levels, and dissolved oxygen. After feeding was completed, the concentration of nitrite-N in the water was measured spectrophotometrically and adjusted to the same concentration as the preset concentration within two hours.

After fasting for 24 h, the survival rate of each tank was counted, and the weight and length of each fish were measured accurately. Then, a total of 144 fish were randomly selected (six fish per tank), after being anesthetized with 100 mg/L of MS-222 (Shanghai Reagent Corp., Shanghai, China), the liver and viscera were accurately weighed. A total of 72 fish were randomly selected (three fish per tank), the muscle, intestine, and liver tissues were stored at -80°C after being snap-frozen in liquid nitrogen.

2.3 Growth performance

The growth performance indices in this experiment were calculated using the following formula:

IBW : Initial body weight (g).

FBW : Final body weight (g).

SR : Survival rate(%)

$= 100 \times$ final number of fish/initial number of fish.

WGR : Weight gain rate(%) $= 100 \times (\text{FBW} - \text{IBW})/\text{IBW}$.

SGR : Specific growth rate(% /d) $= 100 \times (\ln \text{FBW} - \ln \text{IBW})/56$ d.

FCR : Feed conversion rate = feed intake/(FBW − IBW)

CF : Condition factor(%)

$= 100\,\% \times 100 \times$ (body weight)/(body length)3.

HSI : Hepatopancreas index(%) $= 100\,\% \times$liver weight/FBW.

VSI : Viscerosomatic index(%) $= 100\,\% \times$viscera weight/FBW.

2.4 Biochemical analysis

Intestine and liver tissues from three fish in each tank were rinsed with ice-cold phosphate buffered saline (PBS) and then sliced into minute fragments. Tissue homogenates were obtained by utilizing a freshly made ice-cold saline solution (1:10 w/v). Afterwards, the homogenate was centrifuged at a speed of 4,000 rpm for 10 min at a temperature of 4°C. The liquid portion that settled at the top, known as the supernatant, was collected and stored for further measurement.

Commercially available kits (Nanjing Jiancheng Biotechnic Institute, Nanjing, China) were utilized to quantify the biochemical indicators of antioxidant enzyme (superoxide dismutase, catalase, and glutathione peroxidase) and biochemical indicators of body injury (alkaline phosphatase, acid phosphatase, and malondialdehyde) in the liver and intestine. Digestive enzymes (amylase, trypsin, and lipase) in the intestine were determined in the same way.

2.5 RNA extraction and quantitative polymerase chain reaction

Total RNA was extracted from intestine and liver tissues from three fish in each tank by Trizol reagent (Sigma, Burlington, USA). The reverse transcription was performed following the instructions provided by the cDNA synthesis kit (TaKaRa, Kusatsu, Japan). The gene sequence was acquired from GenBank, and qPCR primers (Table 1) were produced by Sangon Biotech Co., Ltd. (Shanghai, China).

The Roche LightCycler®480 II Real-Time System (Roche, Basel, Switzerland) was used to perform qPCR, and the SYBR Green PCR Master Mix Kit (TaKaRa, Kusatsu, Japan) was utilized for this purpose. Each reaction system consisted of 10 μl of SYBR mix, 6.4 μl of ddH_2O, 0.8 μl of forward primer, 0.8 μl of reverse primer, and 2 μl

TABLE 1 Primer sequence for qPCR.

Genes	Primers (5′ - 3′)	Accession No.
hsp90α	F: 5′ GTAGGCTGGGCTTTCTCGAAT 3’ R: 5’ GTGTGCTTCAGGCATCTCTATC 3’	XM_020603713.1
il-1β	F: 5′ AGCACTGAAGCCAGACCA 3′ R: 5′ GAACAGAAATCGCACCATA 3′	XM_020585780.1
il-8	F: 5′ CGCTACTGGTTCTGCTTAC 3′ R: 5′ CAGGATTCACCTCCACATT 3′	XM_020597092.1
il-10	F: 5′ CTGTCCATCCTGGTTCTCC 3′ R: 5′ CGCCGTGTCTAGGTCATT 3′	XM_020593115.1
zo-1	F: 5′ TGGCAGTCAAAGAAGTCG 3′ R: 5′ GTCCAGGCTGAGCATACA 3′	XM_020621576.1
gpx3	F: 5’ TACAAATACCAGGCAAAGA 3’ R: 5’ AATCCAAGAACGGTGAGT 3’	XM_020593355.1
cat	F: 5’ CCTACCCAGACACCCAT 3’ R: 5’ TTATCAAATACGCACATCG 3’	XM_020624985.1
sod1	F: 5’ AGATCATGTTGCCAAGATAG 3’ R: 5’ ACTCCACAAGCCAGACG 3’	XM_020598412.1
gh1	F: 5’ TCCTGCTATCAGTCCTATCT 3’ R: 5’ AGTTGACGCTGCTCCTC 3’	XM_020621687.1
cas2	F: 5’ GAAGAGCGAGGGTCAGT 3’ R: 5’ TCCTGGGTTGGAAATGG 3’	XM_020610781.1
cas8	F: 5’ GAGGGTTTGGGAGCATA 3’ R: 5’ CAATCTTTATCAGTCGCAGT 3’	XM_020596453.1
cas9	F: 5’ AAGTCACAACCGCTTCC 3’ R: 5’ CTCTTTCACCTCCTCCAC 3’	XM_020612566.1
β-actin	F: 5′ GCGTGACATCAAGGAGAAGC 3′ R: 5′ CTCTGGGCAACGGAACCTCT 3′	XM_020621264.1

hsp90α, heat shock protein 90-α; il-1β, interleukin-1 β; il-8, interleukin-8; il-10, interleukin-10; zo-1, tight junction protein-1; gpx3, glutathione peroxidase 3; cat, catalase; sod1, superoxide dismutase 1; gh1, growth hormone 1; cas2, caspase 2; cas8, caspase 8; cas9, caspase 9.

of cDNA as the template. A two-step PCR reaction procedure was used: pre-denaturation at 95°C for 30 s, 40 cycles of denaturation at 95°C for 5 s, and annealing at 60°C for 20 s. Following each qPCR experiment, a melting curve analysis was conducted on the products to verify their specificity. The relative abundance of target gene mRNA was calculated by $R=2^{-\Delta\Delta Ct}$, *β-actin* was utilized as a calibration standard to standardize the expression of the target genes, each sample was replicated three times.

2.6 Statistical analysis

The data were calculated using Microsoft Excel and analyzed using SPSS 22.0 software. Differences in the same strain under different stress conditions were assessed by one-way analysis of variance (ANOVA) followed by Tukey's test. Validation of differences between wild and breeding strains under the same stress conditions using independent-sample *t*-tests. The results were reported as means ± SD (standard deviation), and statistical significance was assessed using a *P*-value< 0.05.

3 Results

3.1 Survival rates and growth performance

Table 2 displays the growth performance of each group of eels in WS and BS under varying stress conditions. Under the same strain, the survival rate was lowest under the combined stress condition, followed by the ammonia stress condition, and highest under the heat stress condition. Under identical stress conditions, the survival rate of BS was higher than that of WS.

Between WS and BS, the effects of stress conditions on growth performance were in ascending order: HS, AS, and HS+AS. But BS showed better growth performance in FBW, SR, WGR, SGR, and FCR compared to WS under the same stress conditions. HSI under combined stress showed a significant decrease ($P< 0.05$) compared to single-factor stress.

3.2 Antioxidant enzyme activity

The hepatic SOD activity exhibited a decreasing trend in response to stress (Figure 1A), while the activities of CAT and GSH had an increasing trend, with both significantly elevated ($P< 0.05$) under combined stress (Figure 1B, C). There was no significant change ($P > 0.05$) in the activity of SOD in the intestine (Figure 1D), but the activities of CAT and GSH exhibited an overall increasing trend, and both increased significantly ($P< 0.05$) under combined stress (Figure 1E, F).

3.3 Injury-indicating enzyme activity

The liver and intestine activities of AKP and ACP showed different trends of decrease, with the lowest levels observed under combined stress in the WS and ammonia stress in the BS (Figure 2A, B, D, E). The levels of MDA showed an increase in both the liver and the intestine, and in general, the BS exhibited lower activity compared to the WS (Figure 2C, F).

3.4 Growth-related gene expression

The mRNA expression of *gh* in muscle exhibited a significant decrease ($P< 0.05$) in both WS and BS, with both reaching a minimal level under combined stress (Figure 3).

3.5 Immune-related gene expression

The levels of mRNA expression of genes (*il-1β*, *il-8*, *il-10*) associated with immunity in the liver and intestine were measured to investigate intestinal health under varying stress conditions. Across all stress conditions, the expression of *il-1β* and *il-8* was markedly elevated under the same strain. However, the increase in BS expression was not as pronounced as the increase in WS expression under the same stress conditions (Figure 4A, B, D, E).

TABLE 2 Effects of varying stress conditions on the growth performance of *M. albus* after 8 weeks.

Item	WS-CT	WS-HS	WS-AS	WS-HS+AS	BS-CT	BS-HS	BS-AS	BS-HS+AS
IBW	24.22 ± 0.30	24.22 ± 0.30	24.22 ± 0.30	24.22 ± 0.30	24.16 ± 0.27	24.16 ± 0.27	24.16 ± 0.27	24.16 ± 0.27
FBW	60.25 ± 1.99^{bA}	54.27 ± 1.52^{bB}	51.98 ± 1.78^{bC}	44.50 ± 1.57^{bD}	64.01 ± 1.54^{aA}	58.12 ± 1.34^{aB}	55.01 ± 1.37^{aC}	49.39 ± 1.72^{aD}
SR	91.11 ± 1.92^{aA}	85.56 ± 1.92^{aAB}	83.33 ± 3.33^{aB}	75.56 ± 1.92^{bC}	94.44 ± 1.92^{aA}	87.78 ± 3.85^{aB}	86.67 ± 3.33^{aB}	81.11 ± 1.92^{aB}
WGR	148.76 ± 8.21^{bA}	124.07 ± 6.27^{bB}	114.63 ± 7.35^{bC}	83.75 ± 6.48^{bD}	164.95 ± 6.39^{aA}	140.57 ± 5.54^{aB}	127.71 ± 5.66^{aC}	104.44 ± 7.12^{aD}
SGR	1.63 ± 0.06^{bA}	1.44 ± 0.05^{bB}	1.36 ± 0.06^{bC}	1.09 ± 0.06^{bD}	1.74 ± 0.04^{aA}	1.57 ± 0.04^{aB}	1.47 ± 0.05^{aC}	1.28 ± 0.06^{aD}
FCR	1.79 ± 0.10^{aC}	1.95 ± 0.11^{aC}	2.27 ± 0.14^{aB}	2.61 ± 0.19^{aA}	1.70 ± 0.07^{bD}	1.85 ± 0.08^{bC}	2.03 ± 0.10^{bB}	2.49 ± 0.18^{aA}
CF	11.49 ± 0.79^{aA}	10.34 ± 0.49^{aB}	9.84 ± 0.38^{aBC}	9.07 ± 0.98^{aC}	11.87 ± 0.98^{aA}	10.70 ± 0.90^{aB}	9.58 ± 0.75^{aC}	9.14 ± 0.77^{aC}
HSI	7.76 ± 0.65^{aA}	6.44 ± 0.82^{bB}	6.15 ± 0.88^{aB}	4.36 ± 0.63^{bC}	7.53 ± 0.67^{aA}	7.24 ± 0.47^{aA}	7.48 ± 0.47^{aA}	5.50 ± 0.57^{aB}
VSI	16.68 ± 1.35^{aAB}	17.12 ± 1.40^{aA}	16.28 ± 1.43^{aAB}	15.18 ± 1.57^{aB}	17.60 ± 1.16^{aAB}	18.32 ± 1.13^{aA}	16.61 ± 1.48^{aB}	16.46 ± 1.29^{aB}

Value are presented as means ± SD (standard deviation). Different letters indicate significant differences ($P< 0.05$), while the same letters indicate no significant differences ($P > 0.05$). Lowercase letters indicate differences between wild and breeding strains under the same stress conditions, uppercase letters indicate differences between stress conditions under the same strain.

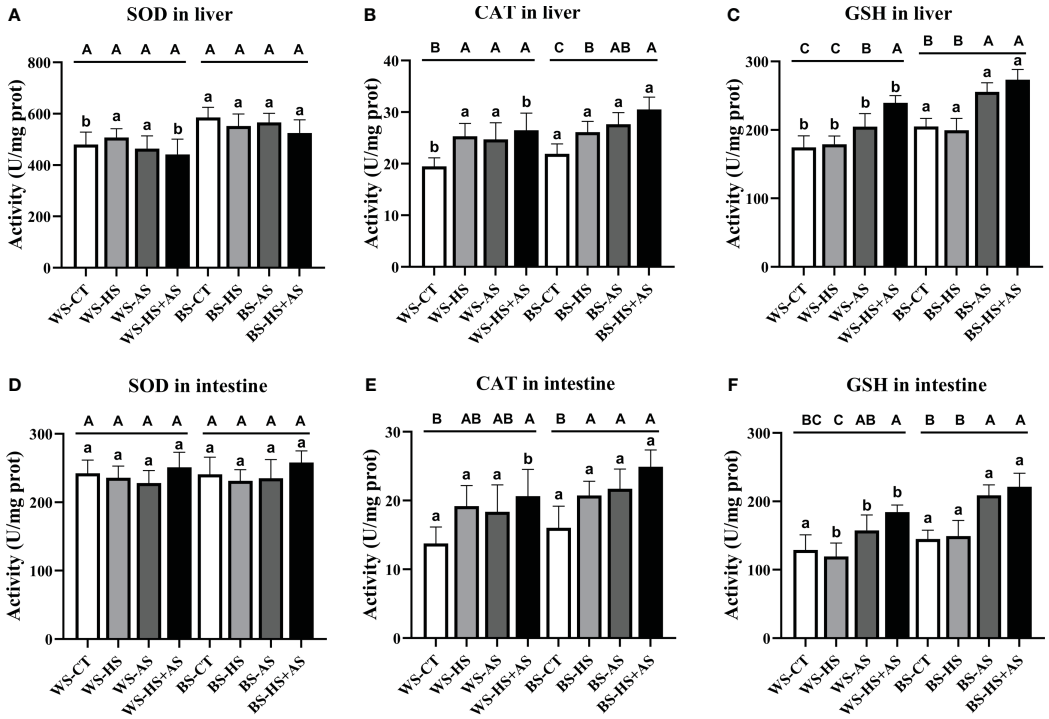

FIGURE 1
Effect of varying stress conditions on the antioxidant enzyme activity of *M. albus* after 8 weeks. Superoxide dismutase (SOD), catalase (CAT), and glutathione peroxidase (GSH). **(A-C)** SOD, CAT, and GSH activity in the liver, **(D-F)** SOD, CAT, and GSH activity in the intestine. Different letters indicate significant differences ($P < 0.05$), while the same letters indicate no significant differences ($P > 0.05$). Lowercase letters indicate differences between wild and breeding strains under the same stress conditions, uppercase letters indicate differences between stress conditions under the same strain.

Conversely, the levels of *il-10* expression exhibited a declining pattern; furthermore, when subjected to identical stress circumstances, the decline in BS expression was less pronounced compared to WS (Figure 4C, F).

3.6 Antioxidant-related gene expression

The analysis of antioxidant-related gene expression revealed that, with the exception of *cat* in the liver and *sod1* in the liver and intestine, all genes (*hsp90α* and *gpx3*) exhibited elevated expression to varying extents, with the maximum expression observed under combined stress (Figure 5).

3.7 Apoptosis-related gene expression

Under each stress condition, the expression of *cas2*, *cas8*, and *cas9* in the liver and intestine was up-regulated. In contrast, *zo-1* showed a down-regulated expression pattern (Figure 6). In general, the patterns of expression between WS and BS were similar, with no notable discrepancies.

4 Discussion

Aquatic organisms might experience growth inhibition or death when exposed to ammonia and elevated temperatures for an extended period (Paust et al., 2011; Chen et al., 2019; Dettleff et al., 2022). Hence, it is crucial to investigate the growth performance of fish under such stress conditions and elucidate the underlying factors contributing to it.

The current study shows that after eight weeks of feeding experiments, the FBW, WGR, and SGR of eels experienced a substantial decrease when subjected to either HS or AS stress individually. Furthermore, this suppression was further intensified when the eels were exposed to combined stress (HS+AS) together. This was verified by its impact on survival, as both WS and AS exhibited elevated death rates when exposed to the combined exposure. This phenomenon could be attributed to the reduction in the rate of food intake experienced by the fish when subjected to stressful circumstances, a finding that has been corroborated in other fish species, including yellow catfish (*Pelteobagrus fulvidraco*) (Wang et al., 2024), tra catfish (*Pangasianodon hypophthalmus*) (Lee et al., 2023), and largemouth bass (*Micropterus salmoides*) (Du et al., 2024). This phenomenon can be more intuitively explained by the significant decrease in the expression of growth-related genes in muscle.

Tissue damage has been identified as the cause of impaired one of growth performance in aquatic species exposed to heat stress and ammonia stress in the water column. Aquatic species experienced altered metabolic, immunological, and oxidative processes, leading to decreased growth and elevated rates of death and morbidity (Kolarevic et al., 2013; Zhang et al., 2019; Esam et al., 2022). Oxidative stress in fish is a reaction to external environmental

10.3389/fmars.2024.1444210

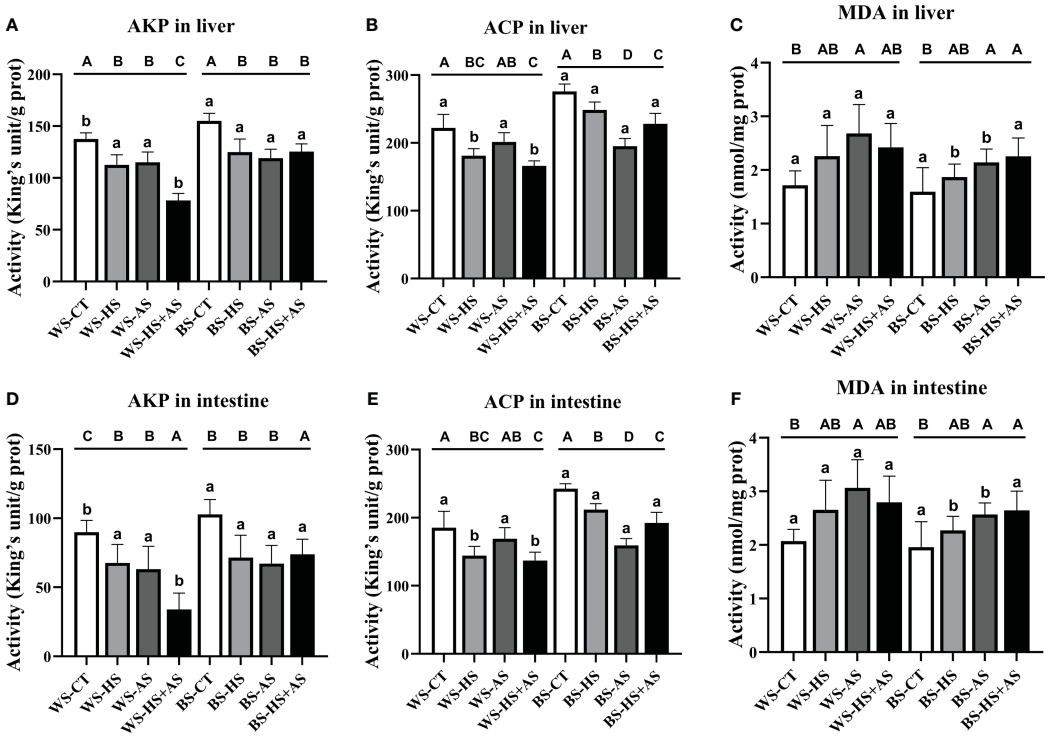

FIGURE 2
Effect of varying stress conditions on the injury-indicating enzyme activity of *M. albus* after 8 weeks. Alkaline phosphatase (AKP), acid phosphatase (ACP), and malondialdehyde (MDA). **(A-C)** AKP, ACP, and MDA activity in the liver, **(D-F)** AKP, ACP, and MDA activity in the intestine. Different letters indicate significant differences ($P < 0.05$), while the same letters indicate no significant differences ($P > 0.05$). Lowercase letters indicate differences between wild and breeding strains under the same stress conditions, uppercase letters indicate differences between stress conditions under the same strain.

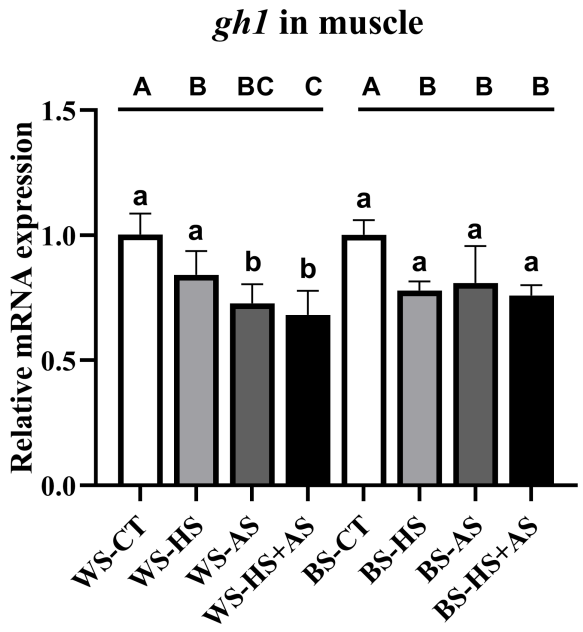

FIGURE 3
Effect of varying stress conditions on the growth-related gene expression of *M. albus* after 8 weeks. Different letters indicate significant differences ($P < 0.05$), while the same letters indicate no significant differences ($P > 0.05$). Lowercase letters indicate differences between wild and breeding strains under the same stress conditions, uppercase letters indicate differences between stress conditions under the same strain.

conditions, including temperature, low oxygen levels, salinity, ammonia concentration, and other stressors. It serves as a crucial detoxification mechanism for aquatic species in response to environmental stresses (Birnie-Gauvin et al., 2017; Zhang et al., 2020). Reactive oxygen species (ROS) are products produced under physiological or pathological conditions, and the balance of ROS is thought to be relevant in apoptosis, control of signaling, and maintaining homeostasis *in vivo* (Ye et al., 2023). In typical circumstances, oxygen-free radicals are normal products of tissue metabolism, but oxidative stress arises when the formation of ROS surpasses the cellular antioxidant capability, resulting in structural harm caused by ROS (Horssen et al., 2008).

SOD, CAT, and GSH-Px play a crucial role in combating ROS by transforming them into harmless metabolites, thereby efficiently avoiding the buildup of ROS (Rahimnejad et al., 2020; Zhu et al., 2023). Our investigation revealed that the activities of CAT and GSH in the liver and intestine were elevated in response to oxidative stress induced by various stressors, but there was no significant change in SOD. The explanation was elucidated through studies on the expression of related antioxidant genes. The organism up-regulated the expression of *cat* and *gpx4* in response to long-term environmental stress. The decrease in *sod* expression was likely caused by the inhibitory effects of ammonia and heat stress, which were especially noticeable under combined stress. Heat shock proteins are biomarkers of a stress response that carry out distinct protective roles in all living species (Wan et al., 2020). *hsp90α*, as a member of the heat shock

10.3389/fmars.2024.1444210

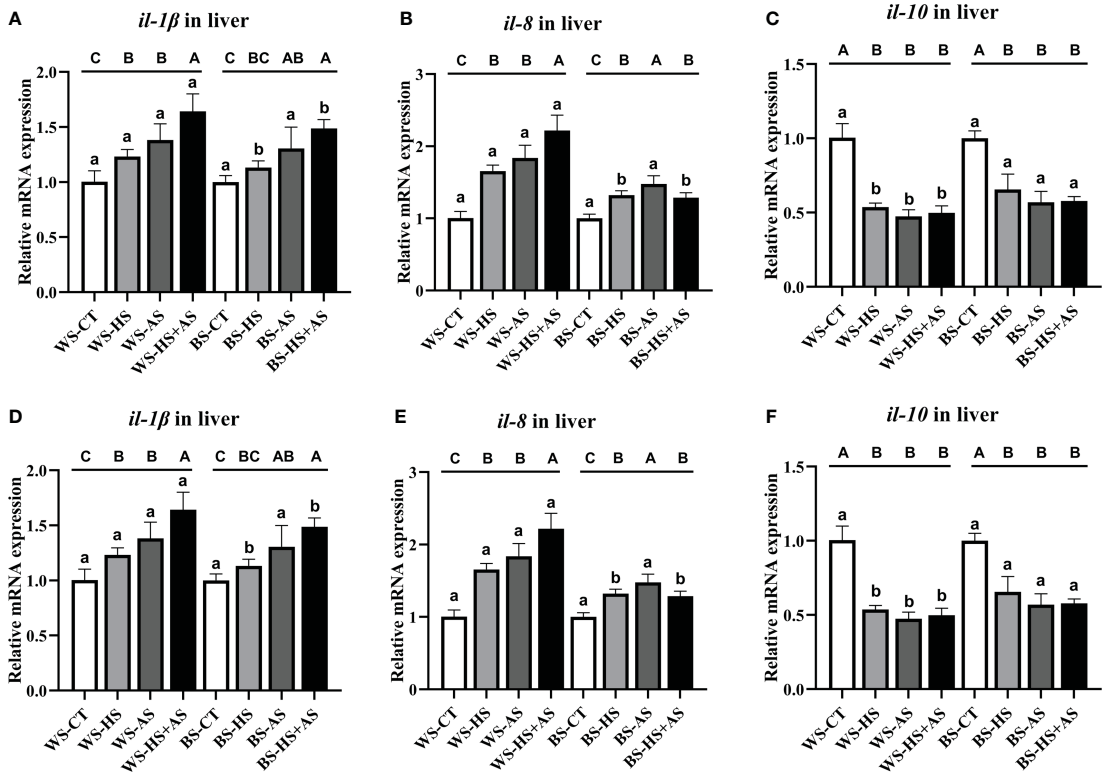

FIGURE 4
Effect of varying stress conditions on the immune-related gene expression of *M. albus* after 8 weeks. Interleukin-1 β (*il-1β*), interleukin-8 (*il-8*), and interleukin-10 (*il-10*). **(A-C)** Relative mRNA expression of *il-1β, il-8*, and *il-10* in the liver, **(D-F)** Relative mRNA expression of *il-1β, il-8,* and *il-10* in the intestine. Different letters indicate significant differences ($P < 0.05$), while the same letters indicate no significant differences ($P > 0.05$). Lowercase letters indicate differences between wild and breeding strains under the same stress conditions, uppercase letters indicate differences between stress conditions under the same strain.

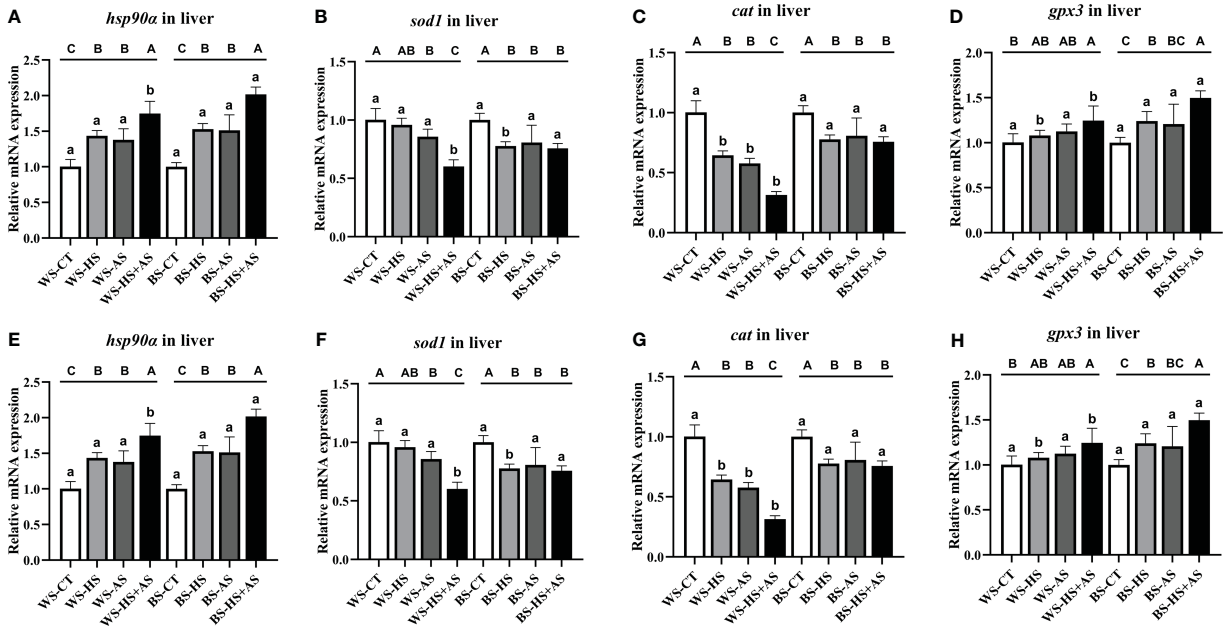

FIGURE 5
Effect of varying stress conditions on the antioxidant-related gene expression of *M. albus* after 8 weeks. Heat shock protein 90-α (*hsp90α*), superoxide dismutase 1 (*sod1*), catalase (*cat*), and glutathione peroxidase 3 (*gpx3*). **(A–D)** Relative mRNA expression of *hsp90α, sod1, cat,* and *gpx3* in the liver, **(E–H)** Relative mRNA expression of *hsp90α, sod1, cat,* and *gpx3* in the intestine. Different letters indicate significant differences ($P < 0.05$), while the same letters indicate no significant differences ($P > 0.05$). Lowercase letters indicate differences between wild and breeding strains under the same stress conditions, uppercase letters indicate differences between stress conditions under the same strain.

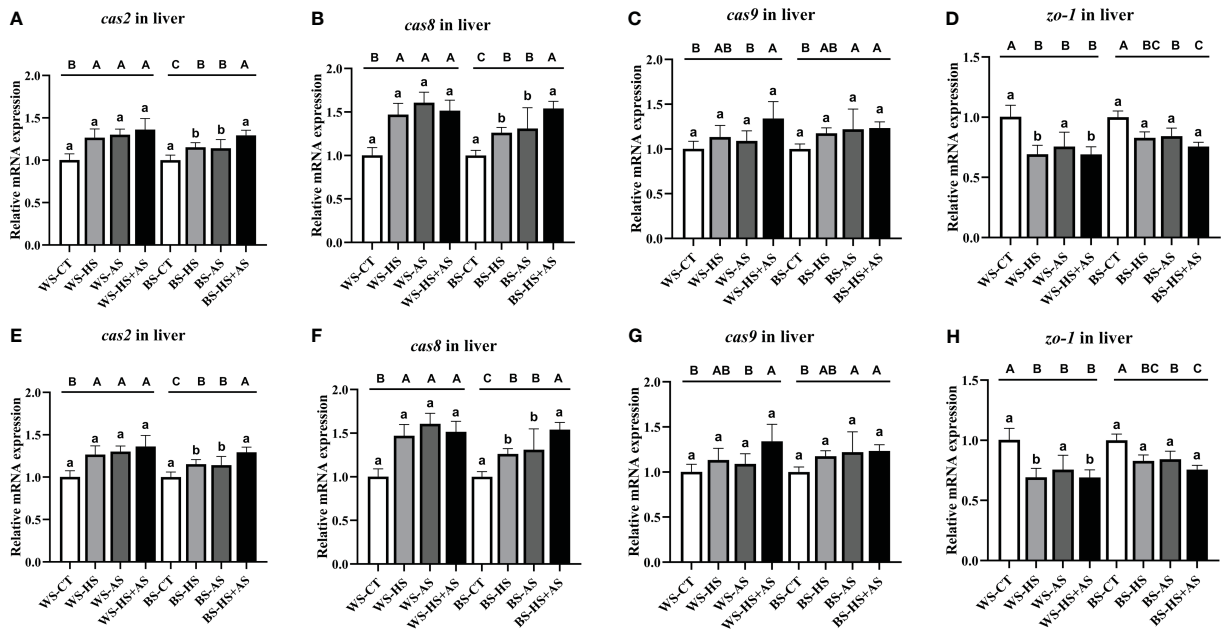

FIGURE 6
Effect of varying stress conditions on the apoptosis-related gene expression of *M. albus* after 8 weeks. Caspase 2 (*cas2*), caspase 8 (*cas8*), caspase 9 (*cas9*), and tight junction protein-1 (*zo-1*). **(A–D)** Relative mRNA expression of *cas2, cas8, cas9,* and *zo-1* in the liver, **(E-H)** Relative mRNA expression of *cas2, cas8, cas9,* and *zo-1* in the intestine. Different letters indicate significant differences ($P < 0.05$), while the same letters indicate no significant differences ($P > 0.05$). Lowercase letters indicate differences between wild and breeding strains under the same stress conditions, uppercase letters indicate differences between stress conditions under the same strain.

protein family, can enhance immunological and antioxidant abilities in reaction to environmental stress by activating both innate and adaptive cellular immunity (Hoter et al., 2018). This gene's expression is also increased in the liver and intestines, indicating its role in the body's antioxidant response. AKP and ACP, functioning as biomarker enzymes, are crucial components of lysosomal enzymes. They are widely present in tissues and play a significant role as hydrolytic enzymes in immune defense, and their activity levels reflect the strength of tissue immunity (Song et al., 2006; Elabd et al., 2016). MDA also functions as a biomarker enzyme, and its concentration can indirectly indicate the antioxidant capability of lipids (Kanner and Lapidot, 2001). The findings of our study demonstrated that the levels of AKP and ACP were decreased to different extents in both the liver and intestine, whereas MDA was dramatically elevated, indicating the occurrence of oxidative stress in the tissues. Remarkably, BS outperformed WS in its ability to counteract oxidative damage under the same stress conditions.

The expression of mRNAs associated with intestinal and liver immunity in eels further revealed that environmental stress can modify immune responses. Activation of inflammatory cytokines induces a range of pro-inflammatory cytokines (*il-1β* and *il-8*) (Luissint et al., 2016). In innate immunity, these cytokines are recruited by macrophages, neutrophils, and lymphocytes to infected tissues and ultimately trigger inflammation as a response to pathogen infection (Yusuf et al., 2020). *il-1β* is primarily released by activated macrophages and activates diverse pro-inflammatory transcription factors in various target cells, leading to the release of other inflammatory molecules (Zhu et al., 2013). *il-8*, a chemokine, primarily stimulates the movement of neutrophils towards the gastrointestinal mucosa as a result of inflammation, damage, and infection (Lemme-Dumit et al., 2022). *il-10* has demonstrated efficacy in suppressing the production of pro-inflammatory chemicals, hence safeguarding the integrity of the intestinal mucosal barrier, known as an anti-inflammatory cytokine (Zhao et al., 2020). The results of our study showed a large increase in the expression of *il-1β* and *il-8* in both the liver and intestine under various stress conditions; conversely, the expression of *il-10* showed a considerable decrease. This indicates that the tissue experiences an inflammatory response when exposed to the environment. *zo-1* is a tight junction protein, plays a vital role in preserving the structural integrity and optimal functioning of intact epithelial cells (Turner, 2009). Caspase activity serves as a reliable indication of apoptosis in fish cells (Zhang et al., 2023). *cas2*, *cas8*, and *cas9* have significant functions in the processes of apoptosis and immune response (Fu et al., 2020; Cui et al., 2023). The current work demonstrates that the expression of *cas2*, *cas8*, and *cas9* was increased in response to ammonia and heat stress, whereas the expression of zo-1 was decreased. This suggests a potential association between apoptotic pathways that rely on caspase activity and these two types of stress.

5 Conclusion

In summary, the presence of ammonia and heat stress seemed to inhibit the growth performance of both wild and breeding eels; these inhibitory effects were more noticeable when combined with stress. In response to oxidative stress, they have upregulated the activity and gene expression of immune-related enzymes, while the results of some indicator enzymes suggest the occurrence of

oxidative damage in their tissues. The presence of an inflammatory response in the tissues was suggested by the up-regulation of genes associated with pro-inflammatory cytokines and the down-regulation of genes related to anti-inflammatory cytokines. Furthermore, the up-regulation of genes connected to apoptosis revealed tissue damage. Nevertheless, it is worth noting that breeding strains exhibited superior adaptability to ammonia and heat stress in comparison to wild strains.

Data availability statement

The original contributions presented in the study are included in the article/supplementary material. Further inquiries can be directed to the corresponding author/s.

Ethics statement

The animal study was approved by Statute of Experimental Animal Ethics Committee of Shanghai Academy of Agricultural Sciences with Approval Number SAASPZ0520016. The study was conducted in accordance with the local legislation and institutional requirements.

Author contributions

ML: Writing – original draft, Visualization, Investigation, Formal Analysis, Data curation, Conceptualization. WH: Validation, Investigation, Data curation, Conceptualization, Writing – review & editing. YZ: Writing – original draft, Formal Analysis, Data curation. QY: Writing – review & editing, Investigation, Conceptualization. HY: Writing – review & editing, Investigation, Conceptualization. WL: Writing – review & editing, Project administration, Investigation, Funding acquisition, Conceptualization. WZ: Writing – review & editing, Supervision, Resources, Investigation, Conceptualization.

Funding

The author(s) declare financial support was received for the research, authorship, and/or publication of this article. This work was supported by the Shanghai Municipal Agricultural Commission (grant number 2022-02-08-00-12-F01187); and the China Agriculture Research System of MOF and MARA (grant number CARS-46).

Conflict of interest

The authors declare that the research was conducted in the absence of any commercial or financial relationships that could be construed as a potential conflict of interest.

Publisher's note

References

Birnie-Gauvin, K., Costantini, D., Cooke, S. J., and Willmore, W. G. (2017). A comparative and evolutionary approach to oxidative stress in fish: A review. *Fish Fish* 18, 928–942. doi: 10.1111/faf.12215

Bucking, C. (2017). A broader look at ammonia production, excretion, and transport in fish: a review of impacts of feeding and the environment. *J. Comp. Physiol. B* 187, 1–18. doi: 10.1007/s00360-016-1026-9

Chen, K., Tang, T., Song, Q., Wang, Z., He, K., Liu, X., et al. (2019). Transcription analysis of the stress and immune response genes to temperature stress in *ostrinia furnacalis*. *Front. Physiol.* 10. doi: 10.3389/fphys.2019.01289

Cui, T., Liu, P., Chen, X., Liu, Z., Wang, B., Gao, C., et al. (2023). Identification and functional characterization of caspases in turbot (*Scophthalmus maximus*) in response to bacterial infection. *Fish Shellfish Immun.* 137, 108757. doi: 10.1016/j.fsi.2023.108757

Cui, Y., Zhao, N., Wang, C., Long, J., Chen, Y., Deng, Z., et al. (2022). Acute ammonia stress-induced oxidative and heat shock responses modulated by transcription factors in *Litopenaeus vannamei*. *Fish Shellfish Immun.* 128, 181–187. doi: 10.1016/j.fsi.2022.07.060

Dettleff, P., Zuloaga, R., Fuentes, M., Gonzalez, P., Aedo, J., Manuel Estrada, J., et al. (2022). High-temperature stress effect on the red cusk-eel (*Geypterus Chilensis*) liver: transcriptional modulation and oxidative stress damage. *Biology-Basel* 11, 990. doi: 10.3390/biology11070990

Dominguez, M., Takemura, A., Tsuchiya, M., and Nakamura, S. (2004). Impact of different environmental factors on the circulating immunoglobulin levels in the Nile tilapia. *Oreochromis niloticus*. *Aquacult.* 241, 491–500. doi: 10.1016/j.aquaculture.2004.06.027

Du, J., Xie, Y., Li, M., Zhu, T., Lei, C., Song, H., et al. (2024). Effects of chronic heat stress on growth performance, liver histology, digestive enzyme activities, and expressions of HSP genes in different populations of Largemouth bass (*Micropterus salmoides*). *Aquacult. Rep.* 35, 101972. doi: 10.1016/j.aqrep.2024.101972

Elabd, H., Wang, H.-P., Shaheen, A., Yao, H., and Abbass, A. (2016). Feeding *Glycyrrhiza glabra* (liquorice) and *Astragalus membranaceus* (AM) alters innate immune and physiological responses in yellow perch (*Perca flavescens*). *Fish Shellfish Immun.* 54, 374–384. doi: 10.1016/j.fsi.2016.04.024

Esam, F., Khalafalla, M. M., Gewaily, M. S., Abdo, S., Hassan, A. M., and Dawood, M. A. O. (2022). Acute ammonia exposure combined with heat stress impaired the histological features of gills and liver tissues and the expression responses of immune and antioxidative related genes in Nile tilapia. *Ecotox Environ. Safe* 231, 113187. doi: 10.1016/j.ecoenv.2022.113187

Fu, S., Ding, M., Wang, J., Yin, X., Zhou, E., Kong, L., et al. (2020). Identification and functional characterization of three caspases in *Takifugu obscurus* in response to bacterial infection. *Fish Shellfish Immun.* 106, 252–262. doi: 10.1016/j.fsi.2020.07.047

Horssen, J., Schreibelt, G., Drexhage, J., Hazes, T., Dijkstra, C. D., van der Valk, P., et al. (2008). Severe oxidative damage in multiple sclerosis lesions coincides with enhanced antioxidant enzyme expression. *Free Radical Bio Med.* 45, 1729–1737. doi: 10.1016/j.freeradbiomed.2008.09.023

Hoter, A., El-Sabban, M. E., and Naim, H. Y. (2018). The HSP90 family: structure, regulation, function, and implications in health and disease. *Int. J. Mol. Sci.* 19, 2560. doi: 10.3390/ijms19092560

Ip, Y. K., and Chew, S. F. (2010). Ammonia production, excretion, toxicity, and defense in fish: a review. *Front. Physiol.* 1. doi: 10.3389/fphys.2010.00134

Kanner, J., and Lapidot, T. (2001). The stomach as a bioreactor: Dietary lipid peroxidation in the gastric fluid and the effects of plant-derived antioxidants. *Free Radical Bio Med.* 31, 1388–1395. doi: 10.1016/S0891-5849(01)00718-3

Kim, S.-H., Kim, J.-H., Park, M.-A., Hwang, S. D., and Kang, J.-C. (2015). The toxic effects of ammonia exposure on antioxidant and immune responses in Rockfish, *Sebastes schlegelii* during thermal stress. *Environ. Toxicol. Phar.* 40, 954–959. doi: 10.1016/j.etap.2015.10.006

Kolarevic, J., Selset, R., Felip, O., Good, C., Snekvik, K., Takle, H., et al. (2013). Influence of long term ammonia exposure on Atlantic salmon (*Salmo salar* L.) parr growth and welfare. *Aquac. Res.* 44, 1649–1664. doi: 10.1111/j.1365-2109.2012.03170.x

Lee, Y.-C., Huang, Y.-T., Chang, C.-C., and Lin, Y.-H. (2023). Physiological responses to hypothermal stress of Tra catfish (*Pangasianodon hypophthalmus*) subjected to different feeding rates. *Aquacult. Rep.* 33, 101809. doi: 10.1016/j.aqrep.2023.101809

Lemme-Dumit, J. M., Doucet, M., Zachos, N. C., and Pasetti, M. F. (2022). Epithelial and neutrophil interactions and coordinated response to *shigella* in a human intestinal enteroid-neutrophil coculture model. *Mbio* 13, 00944–00922. doi: 10.1128/mbio.00944-22

Li, Y., Liu, Z., Li, M., Jiang, Q., Wu, D., Huang, Y., et al. (2020). Effects of nanoplastics on antioxidant and immune enzyme activities and related gene expression in juvenile *Macrobrachium nipponense*. *J. Hazard Mater.* 398, 122990. doi: 10.1016/j.jhazmat.2020.122990

Li, Y., Xiang, Y., Jiang, Q., Yang, Y., Huang, Y., Fan, W., et al. (2022). Comparison of immune defense and antioxidant capacity between broodstock and hybrid offspring of juvenile shrimp (*Macrobrachium nipponense*): Response to acute ammonia stress. *Anim. Genet.* 53, 380–392. doi: 10.1111/age.13182

Luissint, A.-C., Parkos, C. A., and Nusrat, A. (2016). Inflammation and the intestinal barrier: leukocyte-epithelial cell interactions, cell junction remodeling, and mucosal repair. *Gastroenterology* 151, 616–632. doi: 10.1053/j.gastro.2016.07.008

Mao, Y., Lv, W., Huang, W., Yuan, Q., Yang, H., Zhou, W., et al. (2024). Effects on growth performance and immunity of *Monopterus albus* after high temperature stress. *Front. Physiol.* 15. doi: 10.3389/fphys.2024.1397818

Ou, H., Liang, J., and Liu, J. (2022). Effects of acute ammonia exposure on oxidative stress, endoplasmic reticulum stress and apoptosis in the kuruma shrimp (*Marsupenaeus japonicus*). *Aquacult. Rep.* 27, 101383. doi: 10.1016/j.aqrep.2022.101383

Paust, L. O., Foss, A., and Imsland, A. K. (2011). Effects of chronic and periodic exposure to ammonia on growth, food conversion efficiency and blood physiology in juvenile Atlantic halibut (*Hippoglossus hippoglossus* L.). *Aquaculture* 315, 400–406. doi: 10.1016/j.aquaculture.2011.03.008

Rahimnejad, S., Yuan, X.-Y., Liu, W.-B., Jiang, G.-Z., Cao, X.-F., Dai, Y.-J., et al. (2020). Evaluation of antioxidant capacity and immunomodulatory effects of yeast hydrolysates for hepatocytes of blunt snout bream (*Megalobrama amblycephala*). *Fish Shellfish Immun.* 106, 142–148. doi: 10.1016/j.fsi.2020.06.019

Rebl, A., Verleih, M., Koebis, J. M., Kuehn, C., Wimmers, K., Koellner, B., et al. (2013). Transcriptome profiling of gill tissue in regionally bred and globally farmed rainbow trout strains reveals different strategies for coping with thermal stress. *Mar. Biotechnol.* 15, 445–460. doi: 10.1007/s10126-013-9501-8

Reid, G. K., Gurney-Smith, H. J., Marcogliese, D. J., Knowler, D., Benfey, T., Garber, A. F., et al. (2019). Climate change and aquaculture: considering biological response and resources. *Aquacult. Env. Interac.* 11, 569–602. doi: 10.3354/aei00332

Song, Z.-f., Wu, T.-x., Cai, L.-s., Zhang, L.-j., and Zheng, X.-d. (2006). Effects of dietary supplementation with clostridium butyricum on the growth performance and humoral immune response in Miichthys miiuy. *J. Zhejiang Univ-Sc B* 7, 596–602. doi: 10.1631/jzus.2006.B0596

Turner, J. R. (2009). Intestinal mucosal barrier function in health and disease. *Nat. Rev. Immunol.* 9, 799–809. doi: 10.1038/nri2653

Wan, Q., Song, D., Li, H., and He, M.-l. (2020). Stress proteins: the biological functions in virus infection, present and challenges for target-based antiviral drug development. *Signal Transduct Tar* 5, 125. doi: 10.1038/s41392-020-00233-4

Wang, S., Li, X., Zhang, M., and Li, M. (2024). Effects of dietary sodium acetate on growth, intestinal microbiota composition, and ammonia tolerance of juvenile yellow catfish *Pelteobagrus fulvidraco*. *Aquaculture* 581, 740480. doi: 10.1016/j.aquaculture.2023.740480

Wu, Y., Zhou, Z., Pan, Y., Zhao, J., Bai, H., Chen, B., et al. (2021). GWAS identified candidate variants and genes associated with acute heat tolerance of large yellow croaker. *Aquaculture* 540, 736696. doi: 10.1016/j.aquaculture.2021.736696

Ye, Y., Zhu, B., Yun, J., Yang, Y., Tian, J., Xu, W., et al. (2023). Comparison of antioxidant capacity and immune response between low salinity tolerant hybrid and normal variety of Pacific white shrimp (*Litopenaeus vannamei*). *Aquacult. Int.* 32, 1879–1894. doi: 10.1007/s10499-023-01248-8

Yusuf, A., Huang, X., Chen, N., Apraku, A., Wang, W., Cornel, A., et al. (2020). Impact of dietary vitamin c on plasma metabolites, antioxidant capacity and innate immunocompetence in juvenile largemouth bass, *Micropterus salmoides*. *Aquacult. Rep.* 17, 100383. doi: 10.1016/j.aqrep.2020.100383

Zhang, C., Hu, Q.-Y., Feng, L., Wu, P., Liu, Y., Kuang, S.-Y., et al. (2023). Isalo scorpion Cytotoxic peptide (IsCT) improved the physical barrier of the intestine on on-growing grass carp (*Ctenopharyngodon idella*). *Aquaculture* 577, 739895. doi: 10.1016/j.aquaculture.2023.739895

Zhang, C.-N., Tian, H.-Y., Li, X.-F., Zhu, J., Cai, D.-S., Xu, C., et al. (2014). The effects of fructooligosaccharide on the immune response, antioxidant capability and HSP70 and HSP90 expressions in blunt snout bream (*Megalobrama amblycephala* Yih) under high heat stress. *Aquaculture* 433, 458–466. doi: 10.1016/j.aquaculture.2014.07.007

Zhang, T., Yan, Z., Zheng, X., Wang, S., Fan, J., and Liu, Z. (2020). Effects of acute ammonia toxicity on oxidative stress, DNA damage and apoptosis in digestive gland and gill of Asian clam (*Corbicula fluminea*). *Fish Shellfish Immun.* 99, 514–525. doi: 10.1016/j.fsi.2020.02.046

Zhang, W., Xia, S., Zhu, J., Miao, L., Ren, M., Lin, Y., et al. (2019). Growth performance, physiological response and histology changes of juvenile blunt snout bream, *Megalobrama amblycephala* exposed to chronic ammonia. *Aquaculture* 506, 424–436. doi: 10.1016/j.aquaculture.2019.03.072

Zhao, J., Wang, H., Yang, H., Zhou, Y., and Tang, L. (2020). Autophagy induction by rapamycin ameliorates experimental colitis and improves intestinal epithelial barrier function in IL-10 knockout mice. *Int. Immunopharmacol.* 81, 105977. doi: 10.1016/j.intimp.2019.105977

Zhu, L.-y., Nie, L., Zhu, G., Xiang, L.-x., and Shao, J.-z. (2013). Advances in research of fish immune-relevant genes: A comparative overview of innate and adaptive immunity in teleosts. *Dev. Comp. Immunol.* 39, 39–62. doi: 10.1016/j.dci.2012.04.001

Zhu, C., Zhou, W., Han, M., Yang, Y., Li, Y., Jiang, Q., et al. (2023). Dietary polystyrene nanoplastics exposure alters hepatic glycolipid metabolism, triggering inflammatory responses and apoptosis in *Monopterus albus*. *Sci. Total Environ.* 891, 164460. doi: 10.1016/j.scitotenv.2023.164460

frontiers | Frontiers in Marine Science

TYPE Original Research
PUBLISHED 11 July 2024
DOI 10.3389/fmars.2024.1441426

OPEN ACCESS

EDITED BY
Yi-Feng Li,
Shanghai Ocean University, China

REVIEWED BY
Sofia Priyadarsani Das,
National Taiwan Ocean University, Taiwan
Mi Ou,
Chinese Academy of Fishery Sciences, China
Ji Cheng,
Soochow University Medical College, China

*CORRESPONDENCE
Tingting Shu
18778004858@163.com
Wei Jiang
jiang_wei6@ctg.com.cn

RECEIVED 31 May 2024
ACCEPTED 20 June 2024
PUBLISHED 11 July 2024

CITATION
Shu T, Yang J, Yu Z, Xiao K, Huang H, Dai L, Yin Z and Jiang W (2024) Influences of water velocity on ovarian maturation and antioxidant capacity in adult grass carp (*Ctenopharyngodon idellus*). *Front. Mar. Sci.* 11:1441426. doi: 10.3389/fmars.2024.1441426

Influences of water velocity on ovarian maturation and antioxidant capacity in adult grass carp (*Ctenopharyngodon idellus*)

Tingting Shu[1,2]*, Jing Yang[1,2], Zhaoxi Yu[1,2], Kan Xiao[1,2], Hongtao Huang[1,2], Lingquan Dai[1,2], Zhan Yin[3] and Wei Jiang[1,2]*

[1]Chinese Sturgeon Research Institute, China Three Gorges Corporation, Yichang, Hubei, China, [2]Hubei Key Laboratory of Three Gorges Project for Conservation of Fishes, Yichang, Hubei, China, [3]Institute of Hydrobiology, Chinese Academy of Sciences, Wuhan, Hubei, China

Ecological operation of hydraulic engineering is essential for the conservation of fishery resources. Water velocity is known to affect the spawning of fishes delivering drifting eggs. This study aims to explore the effects of water velocity stimulation on the ovarian maturation and antioxidant capacity of adult grass carp (*Ctenopharyngodon idellus*) through laboratory experiments in order to understand the physiological mechanism underlying the response of natural reproduction to ecological flows. We examined the histology, sex hormones and vitellogenin (VTG) concentrations of ovary, and the transcripts of key genes in the hypothalamus-pituitary-gonad (HPG) axis, as well as the antioxidant activities of ovary and liver in grass carp. The results showed that although there was no discernible difference on the ovarian development characteristics of grass carp under water velocity stimulation, estradiol, testosterone, progesterone, 17α,20β-dihydroxy-4-pregnen-3-one (17α,20β-DHP), and VTG concentrations were elevated, which was related to the transcriptional regulation of the HPG axis genes. The gene expression levels (*gnrh2*, *fshβ*, *lhβ*, *cgα*, *hsd20b*, *hsd17b3*, and *vtg*) in the HPG axis were significantly elevated under water velocity stimulation, while those of *hsd3b1*, *cyp17a1*, *cyp19a1a*, *hsd17b1*, *star*, and *igf3* were suppressed. In addition, appropriate water velocity stimulation could enhance body health status by increasing the activities of antioxidant enzymes in the ovary and liver. The results of this study provide the fundamental knowledge and data support for ecological operation of hydropower projects and river ecological restoration.

KEYWORDS

water velocity, ovarian maturation, sex hormones, oxidative stress, grass carp

Introduction

The Three Gorges Dam (TGD), located in the middle stretch of the Yangtze River, is the world's largest hydropower project and plays a crucial role in harnessing and exploiting the river's power (Tang et al., 2016). However, the operation of the TGD not only significantly alters the hydrological processes of rivers but also threatens aquatic habitats both upstream and downstream of the dam site, thereby contributing to the degradation of riverine ecosystems (Zhang et al., 2021). In detail, the regulation of reservoirs homogenizes the flow processes of rivers and weakens or eliminates the natural flood peaks, thus leading to a decrease in fish eggs (She et al., 2023).

Fish spawning activity is likely influenced by a variety of environmental factors, including water velocity, water temperature, and dissolved oxygen. By influencing hormone synthesis and secretion, these environmental factors affect the gonadal development of fish (Liu et al., 2021). In particular, water velocity has been recognized to affect the spawning of fishes delivering drifting eggs in rivers (Chen et al., 2021a). In order to mitigate the adverse effects of dam operations on fish spawning, it is necessary to establish specific eco-hydrological processes to stimulate fish spawning (Wang et al., 2020).

The four major Chinese carps (FMCC), including black carp (*Mylopharyngodon piceus*), grass carp (*Ctenopharyngodon idellus*), silver carp (*Hypophthalmichthys molitrix*), and bighead carp (*Hypophthalmichthys nobilis*), which are highly sensitive to hydrological processes, represent the most economically important fishes in China. The FMCC population would migrate to the spawning sites and start spawning in response to high-flow pulses from March to June, while the construction and operation of TGD alter the natural hydrological rhythm and hinder fish migration (Zhang et al., 2023). Therefore, incorporating ecological flow into the operation scheme of TGD would be a mitigation measure to protect the spawning of FMCC. It has been demonstrated that implementing controlled man-made floods as part of the TGD operation enhances the reproductive success of FMCC in downstream regions (Xiao et al., 2022). Since 2011, several attempts have been organized to promote the spawning behavior of FMCC in order to mitigate the decline in FMCC from the Yangtze River. It was found that the water velocity that induces FMCC spawning ranged from 1.11 to 1.49 m/s (Cao et al., 2022), with an optimal flow velocity of 1.31 m/s was identified for the spawning of FMCC in rivers (Chen et al., 2021a). Although water velocity plays a crucial role in the reproduction of FMCC, there is a notable scarcity of research on the physiological mechanism underlying the response of natural reproduction to ecological flows.

In this study, we took adult grass carp as target species to assess the effects of water velocity stimulation on the ovarian maturation and antioxidant capacity through laboratory experiments. Histology, sex hormones and vitellogenin (VTG) concentrations of ovary, and the transcripts of key genes in the hypothalamus-pituitary-gonad (HPG) axis, as well as antioxidant activities of ovary and liver in grass carp were measured. The findings of this study will provide a theoretical basis for ecological operation.

Materials and methods

Experimental fish and hormones

In the present study, five-year-old sexually mature grass carp were purchased from Tengda Ecological Agriculture Development Co., Ltd. in Zhijiang City, Hubei Province, China. The average weight of female grass carp was 4.66 ± 0.75 kg (n = 60) while male grass carp was 4.50 ± 0.82 kg (n = 60). Before the experiment, all fish were acclimatized in the laboratory facility for one week. Next, a total of 120 healthy grass carp were allocated into five groups randomly with three replicates per group (fifteen 20,000 L PVC circular tanks in total, 4 females and 4 males in each tank). During the acclimatized and experimental period, the fish were fed in excess duckweed twice daily at 9:00 and 16:00. Water temperature, pH, and dissolved oxygen was maintained at 23 ± 1°C, 7.0–7.5, and 6.0 –6.5 mg/L, respectively, and the light conditions followed a natural light/dark cycle (approximately 12/12 h).

Two hormones or agents were used in this study: luteinizing hormone-releasing hormone analogue (LHRH-A2) and domperidone (DOM), purchased from Ningbo Second Hormone Factory (Ningbo, China), and dissolved in physiological saline.

Experimental design

Research showed that an optimal water velocity of 1.3 m/s was identified for the spawning of FMCC in rivers, and no spawning activity was observed in flume at a velocity of 0.8 m/s (Chen et al., 2021a). Therefore, we set water velocities ranging from 0.8 to 1.3 m/s to explore the influence of water velocity on the gonad development in fish. Two submerged pumps (SHIMGE, China) were installed to accelerate the flow of water in a PVC circular tank with an inner diameter of 4.5 m and a water depth of 0.9 m (Figure 1A). Since the water velocity at the center of the tank was quite different from that at other locations, an isolation net with a diameter of 1.0 m was placed at the center to limit the swimming area of the grass carp. Twelve measuring points were arranged around the tank, and the velocity at a depth of 0.45 m was measured using a portable current meter (LS300-A, China) (Figure 1B). In artificial propagation, LHRH-A2 and DOM, which efficiently induce ovulation in females, have been utilized as oxytocic drugs in Cyprinid fishes (Hu et al., 2020; Zhong et al., 2021). Thus, hormone injection was chosen as the positive control. In detail, the experiment consisted of five groups: a control group with no water velocity (negative control), a low water velocity group at 0.8 m/s, a graded water velocity group with velocities increasing from 0.8 to 1.3 m/s gradually, a high water velocity group at 1.3 m/s, and a hormone injection group where females were injected with 2 mg/kg DOM and 2.5 μg/kg LHRH-A2 at the base of the pectoral fin, with a half dose for males (positive control), labeled NS, DS, ZS, GS, and JS, respectively (Figure 2). Flow stimulation was carried out from 8:00 to 11:00 and 15:00 to 18:00 every day for five days. The experiment was conducted at Hubei Key Laboratory of Three Gorges Project for Conservation of Fishes.

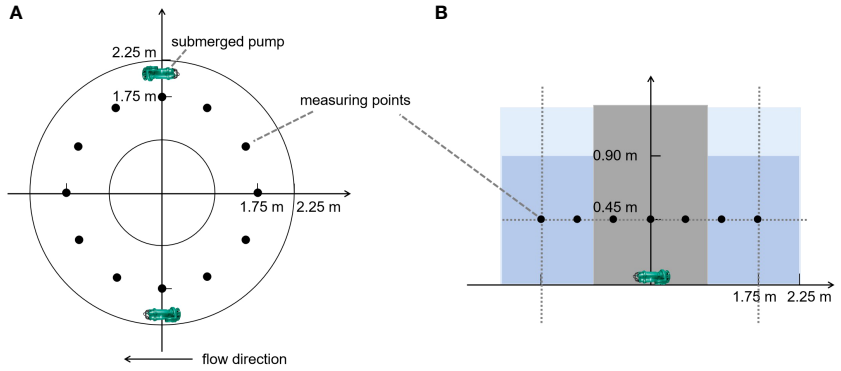

FIGURE 1
Schematic diagram of the experiment system for water velocity stimulation. **(A)** Vertical view of circular tank. **(B)** Front view of circular tank.

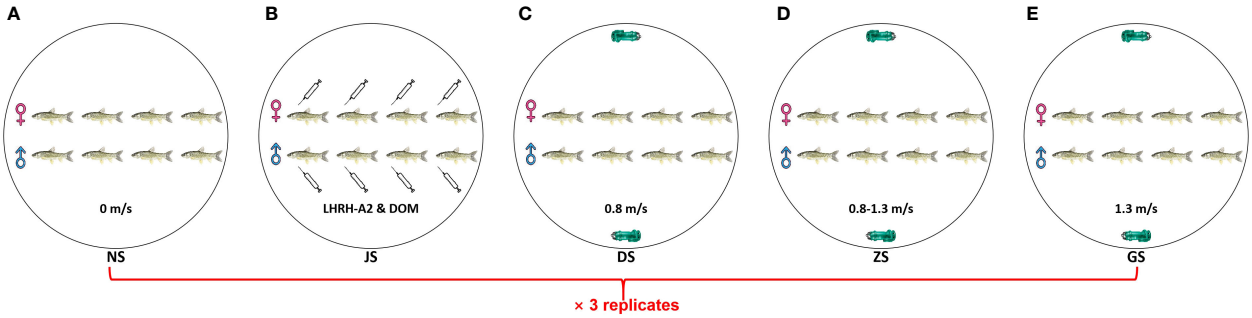

FIGURE 2
Schematic diagram of five experiment groups. **(A)** NS group. **(B)** JS group. **(C)** DS group. **(D)** ZS group. **(E)** GS group.

Sample collection

At the end of the experiment, females were anesthetized by immersion in a benzocaine solution at a concentration of 200 mg/L according to the previous procedure (Shu et al., 2023). The fish were then slaughtered, and their hypothalami, pituitaries, ovaries, and livers were promptly dissected. One part of each ovary was put into Bouin's solution for subsequent histological analysis, while the hypothalami, pituitaries, livers, and the remaining ovary tissue were frozen immediately in liquid nitrogen, then transferred and stored at −80°C for the subsequent determination of various parameters.

Histological examination

The ovary slides were performed following the methods described previously (Lau et al., 2016). Briefly, ovary tissues of grass carp were put into Bouin's solution for 24 h, then dehydrated through graded ethanol solutions, infiltrated with xylene, embedded in paraffin, and subsequently sliced into 5 μm thick sections for hematoxylin-eosin (H&E) staining. These sections were examined using a Nikon Eclipse Ni-U microscope (Nikon, Japan) for histopathological analysis. Scale bars are provided in the lower left corner of each image.

Antioxidant index analysis

Superoxide enzyme (SOD), glutathione peroxidase (GSH-Px), catalase (CAT), total antioxidant capacity (T-AOC), and peroxidase (POD) activities, as well as malondialdehyde (MDA) concentration in the ovaries and livers of grass carp were determined according to the kit instructions (Nanjing Jiancheng, China) via spectrophotometric analysis with a microplate reader. The serial numbers of SOD, GSH-Px, CAT, T-AOC, and POD enzyme activity kits, as well as MDA concentration kit were A001–3-2, A005–1-2, A007–1-1, A015–2-1, A084–1-1, and A003–1-2, respectively. The 0.1 g ovary or liver samples were isolated and homogenized in 900 μL of 0.9% sodium chloride solution (1:9 w/v) in a TGrinder H24R Tissue Homogenizer (TIANGEN, China) at 4°C, and then centrifuged at 2,000 rpm for 10 min. The supernatants were collected and allocated for antioxidant index analysis.

Sex hormones and VTG analysis

The concentrations of sex hormones [estradiol, testosterone, progesterone, and 17α,20β-dihydroxy-4-pregnen-3-one (17α,20β-DHP)] and VTG in ovaries were determined using commercial ELISA kits (Shanghai mlbio, China). The serial numbers of estradiol, testosterone, progesterone, 17α,20β-DHP, and VTG

ELISA kits were ml003452, ml025781, ml003449, ml625990, and ml103464, respectively. The 0.1 g ovary samples were isolated and then mixed with 1 mL PBS before homogenization at 4°C. Following homogenization, the sex hormones and VTG were extracted with an organic solvent four times according to the manufacturer's protocols. The layers were separated by vortexing and centrifugation, and then the organic phase was immediately transferred into a new tube and evaporated at 30°C under a gentle stream of nitrogen. Finally, the extracts were dissolved in 200 μL ELISA buffer, and the sex hormone and VTG concentrations were determined according to the manufacturer's protocols.

Gene expression analysis

Total RNA extraction, reverse transcription, and quantitative real-time PCR (qRT-PCR) were carried out according to our recent study (Shu et al., 2023). Briefly, total RNA was extracted from hypothalamus, pituitary, ovary samples by TRIzol reagent (Ambion, America). The integrity and quality of extracted RNA were assessed by agarose gel electrophoresis, meanwhile, the concentration was measured using NanoDrop One (Thermo Scientific, America). Then, EasyScript® One-Step gDNA Removal and cDNA Synthesis SuperMix kit (TransGen, China) was used to reverse transcribe 1.5 μg RNA to synthesize cDNA. qRT-PCR was conducted using the TransStart® Tip Green qPCR SuperMix (TransGen, China) and StepOnePlus™ real-time system (ABI, America).

Partial sequences of gonadotropin-releasing hormone 2 (*gnrh2*), gonadotropin-releasing hormone 3 (*gnrh3*), follicle stimulating hormone beta polypeptide (*fshβ*), luteinizing hormone beta polypeptide (*lhβ*), glycoprotein hormones alpha polypeptide (*cgα*), cytochrome P450-mediated side-chain cleavage enzyme (*cyp11a1*), 3-beta-hydroxysteroid dehydrogenase 1 (*hsd3b1*), cytochrome P450c17 (*cyp17a1*), ovarian cytochrome P450 aromatase (*cyp19a1a*), 20-beta-hydroxysteroid dehydrogenase (*hsd20b*), 17-beta-hydroxysteroid dehydrogenase 1 (*hsd17b1*), 17-beta-hydroxysteroid dehydrogenase 3 (*hsd17b3*), steroidogenic acute regulatory protein (*star*), vitellogenin (*vtg*), and insulin-like growth factor 3 (*igf3*) were obtained from the previous transcriptome of grass carp (Shu et al., 2023). Based on our previous study on the assessment of internal control genes (Shu et al., 2023), *β-actin* was used as a reference gene. All specific primers used for qRT-PCR were either designed by Primer-BLAST in National Center for Biotechnology Information (NCBI) or obtained from previous studies and synthesized commercially, and were confirmed approximately 100% effective. The sequences of the primers are listed in Table 1. Each sample was run in triplicate and the relative gene expression was normalized *to β-actin* compared to the control group and calculated using the $2^{-\Delta\Delta CT}$ method (Schmittgen and Livak, 2008).

Statistical analysis

Statistical analysis was analyzed in GraphPad Prism 8.0 software (GraphPad software, America). All results are presented as mean ± standard deviation (SD) for each experimental group. Differences were assessed using one-way ANOVA followed by Fisher's least significant difference (LSD) test for multiple comparisons. For all statistical comparisons, $P < 0.05$ was identified as statistically significant.

Results

Ovarian histology analysis

To evaluate the effect of water velocity on the ovarian development characteristics of grass carp, we performed dissections and histological analysis of females to observe the ovarian morphology and the development of each oocyte types by H&E staining. Histological examination revealed that the oocyte type at different developmental stages existed in ovaries of all sampled female grass carp, including primary growth oocytes (PGs), pre-vitellogenic oocytes (PVs), and full-grown oocytes (FGs), primarily composed of full-grown oocytes (Figure 3). After the hormone injection and 5-day water velocity stimulation, respectively, the ovarian development characteristics were similar to those of the control group. To be specific, during this stage, the nuclear membrane vanished, and the nucleoplasm and cytoplasm started to integrate, accompanied by the yolk protein granules of a large size filling the entire oocyte, and zona radiata proteins form the inner layer of the envelope surrounding the oocyte, indicating the fulfillment of vitellogenesis. In maturing and growing oocytes, the zona radiata is overlaid with follicle cells (granulosa and theca cells) (Arukwe and Goksoyr, 2003; von Schalburg et al., 2023). The cortical alveoli were mainly present in the cytoplasm (Lubzens et al., 2017; Zhang et al., 2017). No discernible difference was observed in the histological sections among the five groups.

Sex hormones and VTG concentrations in ovary tissue

A total of four sex hormones, including estradiol, testosterone, progesterone, and 17α,20β-DHP, as well as VTG concentrations, were detected in the ovary tissue. The estradiol concentration in the NS group was observed as 0.3649 ± 0.0146 pmol/g, which significantly increased to 0.5318 ± 0.0195 pmol/g and 0.5016 ± 0.0415 pmol/g in the JS and ZS groups, respectively. The estradiol concentrations in the DS and GS groups were slightly increased, although they were not statistically significant. Besides, the distribution of ovary estradiol concentration was significantly higher in the JS group than the distribution in the DS group (Figure 4A). The testosterone concentrations in the JS, DS, ZS, and GS groups ranged from 2,444 to 2,781 pg/g, which was significantly higher than that in the NS group (1905 ± 88.15 pg/g). However, no significant differences in testosterone concentrations were detected between the hormone injection and water velocity stimulation groups (Figure 4B). The progesterone concentrations in the NS, JS, DS, ZS, and GS groups were 71.43 ± 6.13, 87.13 ± 4.68, 84.22 ± 3.23, 130.2 ± 3.17, 105.1 ± 2.39 ng/g, respectively. Although progesterone concentrations were higher in the JS, DS, ZS, and GS groups

TABLE 1 Primer sequences used for qRT-PCR analysis.

Gene	Direction[a]	Primer Sequences (5′ to 3′)	Primer Length (bp[b])	Amplicon Length (bp)
gnrh2	F	TGTGTCTAGGTGCCCAGTTTG	21	187
	R	GCATCCAGCAGTATTGTCTTCA	22	
gnrh3	F	ACTGGTCATACGGTTGGCTTC	21	202
	R	CCTCGTCTGTTGGGAAATCTCT	22	
lhβ	F	ACATCCTCCTTCTCTTATTCTG	22	251
	R	CAAGCGGACCGTCTCATAG	19	
fshβ	F	TTCGTTGTTATGGTGATGCT	20	282
	R	CGTGAAAACCGAGTCAGTCC	20	
cgα	F	GATATGACTAACTTTGGATGTG	22	263
	R	TAGTAACAGGTGCTACAGTGG	21	
cyp19a1a	F	CATCATACTGAATGTGGGTC	20	113
	R	CGAACGGCTGAAAGAA	16	
igf3	F	CTCGTGGGAAAGGGATC	17	165
	R	TCTGGTATTGCCTCAGAAAC	20	
cyp17a1	F	TGAGGAACACAAGGTGACCTACAG	24	109
	R	GACATCACGAGTGCTGCTG	19	
hsd17b1	F	GGCACCATCCGCACCA	16	111
	R	CTCGTTGAATGGCAAACCCT	20	
star	F	CTGGACCTGGACCTAGTGCT	20	176
	R	CTCAGTTTGCCAGCCATCCT	20	
hsd17b3	F	TTATCTTGACCGGGACTTGCAC	22	212
	R	GCTGATGACGATCACGCTCA	20	
hsd3b1	F	AGCTTGCTGAGATCAGATTG	20	208
	R	AATTCACTGTATTCAACTGCTCC	23	
cyp11a1	F	CACCTCACCCATGCTGTACCTA	22	107
	R	GGTCAGCCTGGTTAAAGATGC	21	
hsd20b	F	TGGAGAACAGGCTGAGGTGAC	21	81
	R	CGTAGTATCGGCAGAAGAGCAT	22	
vtg	F	GTGATGCACCTGCCCAGATTG	21	159
	R	CCTTGAACTGAGACCAGATAGCCTC	25	
β-actin	F	TGGACTCTGGTGATGGTGTGAC	22	247
	R	GAGGAAGAAGAGGCAGCGGTTC	22	

[a]F, Forward; R, Reverse.
[b]base pairs.

compared to the NS group, significant differences were detected only in the ZS and GS groups. Moreover, the ZS and GS groups showed significantly higher progesterone concentrations than the JS group (Figure 4C). The 17α,20β-DHP concentrations in the JS and GS groups were 135.6 ± 6.396, 134.1 ± 7.626 ng/g, respectively, which showed obviously higher levels than that in the NS group (100.2 ± 8.276 ng/g), wherein no significant differences in 17α,20β-DHP concentrations were observed among the NS, DS, and ZS groups. And hormone injection and water velocity stimulation groups display no significant differences in 17α,20β-DHP concentrations (Figure 4D). The VTG concentration reached 3152 ± 47.04 ng/g in the NS group and was highest at 4267 ± 112.3 ng/g in the ZS group. The distribution of ovary VTG concentration was significantly higher in the ZS group than the distribution in the NS and JS groups. No

10.3389/fmars.2024.1441426

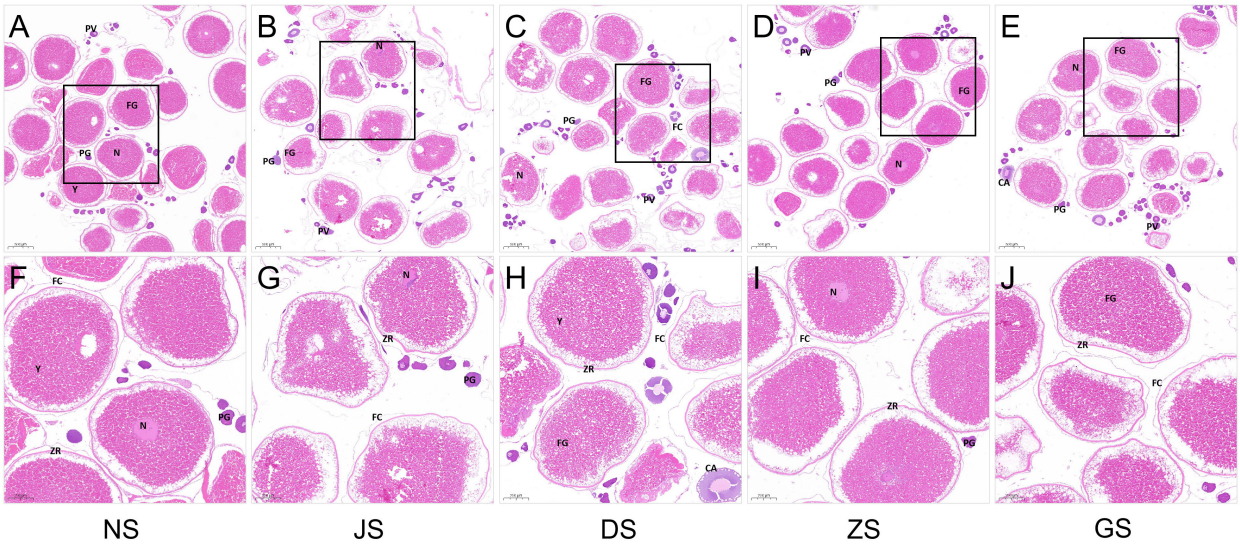

FIGURE 3
Histological sections of the ovarian status of grass carp (n = 6 for each group). **(A, F)** NS group. **(B, G)** JS group. **(C, H)** DS group. **(D, I)** ZS group. **(E, J)** GS group. PG, primary growth follicle; PV, previtellogenic follicle; FG, full-grown follicle; N, nucleus; Y, yolks; FC, follicle cells; ZR, zona radiata; CA, cortical alveoli. Scale bars: **(A–E)**: 500 μm; **(F–J)**: 200 μm.

significant differences were observed among the NS, JS, DS, and GS groups (Figure 4E).

Gene expressions along the HPG axis

The relative mRNA expression levels of key genes along the HPG axis were systematically examined using qRT-PCR. Hormone injection and water velocity stimulation significantly upregulated the transcript levels of *gnrh2* in the hypothalamus (Figure 5A), accompanied by elevated expressions of *fshβ*, *lhβ*, and *cgα* in the pituitary, compared with those in the NS group (Figures 5C–E). Moreover, the transcription of *hsd20b* in the ovary was markedly upregulated in response to hormone injection and water velocity stimulation when compared to the control group (Figure 5J). Specifically, the transcriptions of *gnrh2*, *fshβ*, *lhβ*, *cgα*, and *hsd20b* in the JS group increased by 14.4-, 457.5-, 3.1-, 4.6-, and 1.4-fold, respectively, while in fish stimulated by water velocity, the levels were elevated up to 2.0-, 1854.0-, 4.2-, 10.8-, and 1.5-fold, respectively (Figures 5A, C–E, J). Accordingly, apart from hypothalamus *gnrh2* and ovary *hsd20b* (Figures 5A, J), water velocity stimulation caused significantly greater levels of mRNA for pituitary *fshβ*, *lhβ*, and *cgα* than hormone injection (Figures 5C–E). However, there were no significant differences in gene expression of *gnrh3* in the hypothalamus (Figure 5B), as well as *cyp11a1* in the ovary of female grass carp among the five groups (Figure 5F). The expressions of *hsd3b1*, *cyp17a1*, *cyp19a1a*, *hsd17b1*, and *igf3* in the ovary were significantly downregulated following hormone injection and water velocity stimulation in comparison with the control group (Figures 5G–I, K, O). Additionally, no significant differences were observed for ovary *hsd3b1*, *hsd17b1*, and *igf3* between the hormone injection and water velocity stimulation groups (Figures 5G, K, O), while the transcriptions of *cyp17a1* and *cyp19a1a* were significantly higher in the DS, ZS, and GS groups compared to the JS group (Figures 5H, I). Although the gene expression levels of *hsd17b3*, *star*, and *vtg* in the ovary of female grass carp did not show significant differences between the JS and NS groups (Figures 5L–N), water velocity stimulation led to a notable increase in *hsd17b3* transcript levels in the DS group and elevated *vtg* levels in the ZS and GS groups (Figures 5L, N), while reducing the expression of *star* mRNA at all velocities (Figure 5M).

Antioxidant enzyme activities in ovary and liver tissues

We examined the antioxidant enzyme capacities in the ovary of female grass carp. Compared with the NS group, ovary SOD and CAT activities were significantly higher in the JS, ZS, and GS groups. However, ovary SOD and CAT activities in the DS group were not different from those in the NS group (Figures 6A, B). Ovary POD activity in the NS group was obviously lower than that in the treated groups (Figure 6C). Additionally, no significant differences in ovary SOD and POD activities were observed between the hormone injection and water velocity stimulation groups (Figures 6A, C). A significant increase in ovary CAT activity was detected in the ZS group compared to the other experimental groups (Figure 6B). No significant differences in ovary GSH-Px activity were found among the five groups (Figure 6D). The ZS group had the highest ovary T-AOC activity, but there was a non-significant increase compared to the NS group. Overall, various types of water velocity stimulation had no effect on ovary T-AOC activity compared to the control group, but ovary T-AOC activity significantly increased in the ZS group compared to the JS group (Figure 6E). Ovary MDA concentration in the GS group was significantly lower than that in the NS and JS groups, while there were no significant differences in ovary MDA concentration among the NS, JS, DS, and ZS groups (Figure 6F).

10.3389/fmars.2024.1441426

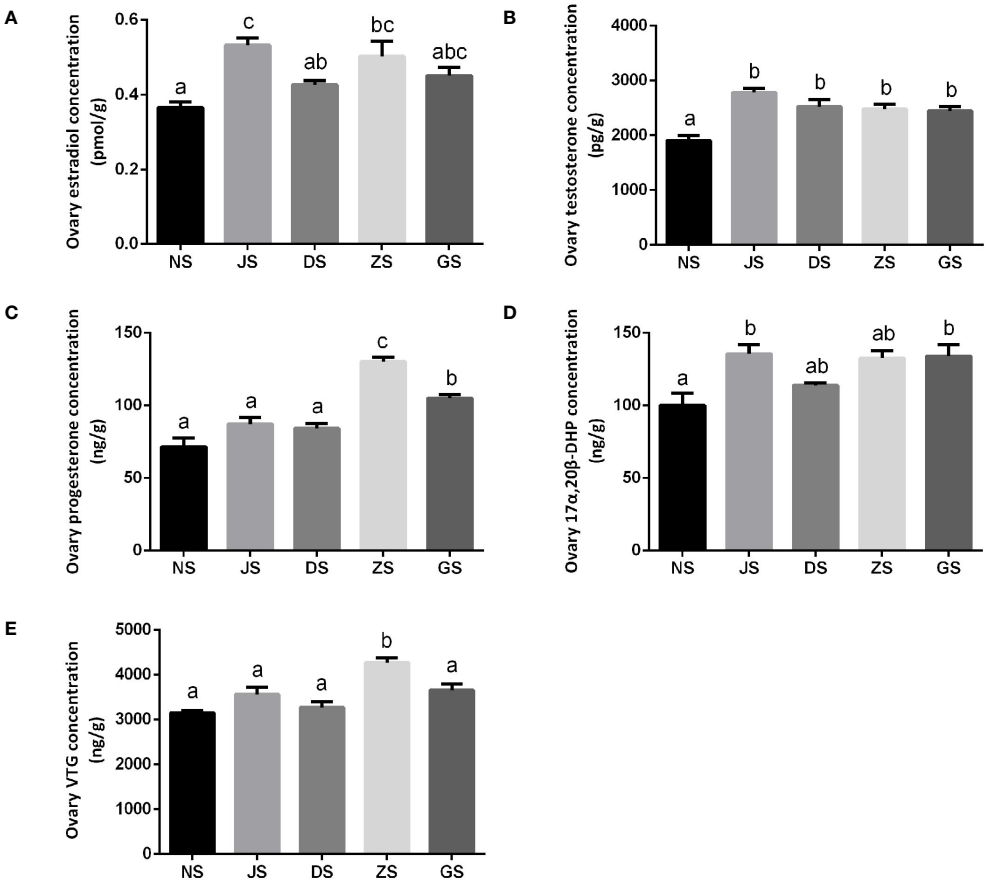

FIGURE 4
The sex hormones and VTG measurements (n = 6 for each group). Ovary concentrations of estradiol **(A)**, testosterone **(B)**, progesterone **(C)**, 17α,20β-DHP **(D)**, and VTG **(E)** in the NS, JS, DS, ZS, and GS groups. The letters in the bar charts represent significant differences.

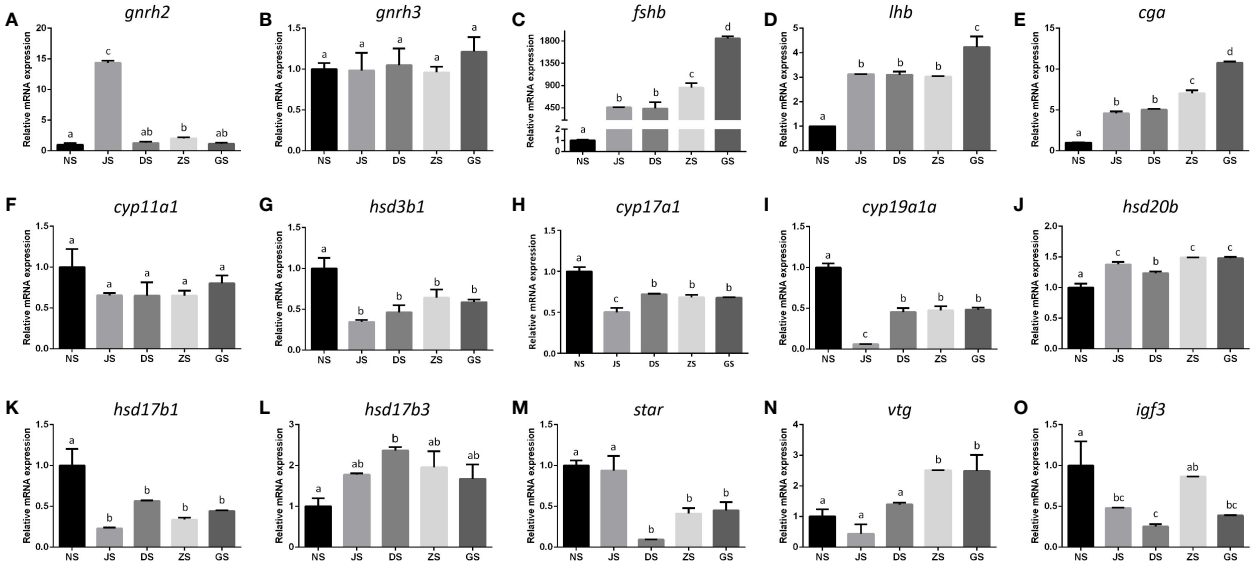

FIGURE 5
The mRNA expression levels of reproductive hormone genes in the HPG axis. All mRNA levels were calculated as the fold expression relative to *β-actin* (n = 6 for each group). *gnrh2* **(A)** and *gnrh3* **(B)** gene expression in the hypothalamus. *fshβ* **(C)**, *lhβ* **(D)**, and *cgα* **(E)** gene expression in the pituitary. *cyp11a1* **(F)**, *hsd3b1* **(G)**, *cyp17a1* **(H)**, *cyp19a1a* **(I)**, *hsd20b* **(J)**, *hsd17b1* **(K)**, *hsd17b3* **(L)**, *star* **(M)**, *vtg* **(N)**, and *igf3* **(O)** gene expression in the ovary. The letters in the bar charts represent significant differences.

Meanwhile, hepatic antioxidant enzyme capacities were also measured in female grass carp. Hepatic SOD activity in the ZS and GS groups increased significantly when compared to the NS group, while the values did not show significant differences among the NS, JS, and DS groups (Figure 7A). There were few changes in hepatic CAT activity among all treatments compared to the NS group, except for the ZS group (Figure 7B). Changes in hepatic POD activity in the JS and ZS groups were also not obvious when compared to the NS group. However, hepatic POD activity in the DS and GS groups increased significantly (Figure 7C). No significant changes in hepatic SOD, CAT, and POD activities were detected between the hormone injection and water velocity stimulation groups (Figures 7A–C). Hepatic GSH-Px activity was significantly higher in the JS and ZS groups than in the NS group, while no significant differences were found among the NS, DS, and GS groups. Moreover, the JS group showed significantly higher hepatic GSH-Px activity than the DS group (Figure 7D). Hepatic T-AOC activity was significantly higher in all treatments relative to the NS group, but no significant differences were observed between the hormone injection and water velocity stimulation groups for hepatic T-AOC activity (Figure 7E). However, hepatic MDA concentration was not significantly affected by hormone injection and water velocity stimulation (Figure 7F).

Discussion

We explored the effects of water velocity stimulation on the ovarian maturation and antioxidant capacity of adult grass carp through laboratory experiments. Our research provided evidence that a certain water velocity is necessary for the ovarian maturation of grass carp. Regrettably, no spawning activity was observed. In the natural spawning sites of Yangtze River, there are complicated hydrological conditions and habitat characteristics. It has been well known that environmental conditions, such as warm temperatures, long photoperiod, and rising discharge, are considered to be crucial factors in controlling the reproductive cycles in teleost. In particular, a rising discharge serves as the primary cue for the spawning of FMCC (Chen et al., 2021a). Apparently, more research is needed to fully understand how environmental conditions influence grass carp spawning.

Estradiol, testosterone, progesterone, and 17α,20β-DHP, along with VTG concentrations, are commonly utilized as important biomarkers to assess gonad development and maturation of fish in various studies (Gadekar, 2014; Tucker et al., 2020). VTG, a large-molecular-weight glycolipoprotein synthesized in the liver and transported to egg cells, has a significant effect on the development of oocytes (Liu et al., 2022). Estradiol can stimulate VTG synthesis and secretion from the liver to developing oocytes via the bloodstream (Ghiasi et al., 2023). Testosterone, serving as the androgenic precursor, is converted to estradiol under the action of aromatase, inducing maturation processes of post-vitellogenic oocytes (Golmoradizadeh et al., 2021; Wang et al., 2023). Progesterone, a precursor of 17α,20β-DHP in the steroidogenic pathway, has been demonstrated to trigger final oocyte maturation and ovulation in fish species (Jéhannet et al., 2023). 17α,20β-DHP, recognized as the main maturation inducing hormone (MIH), plays a crucial role in the final maturation of oocytes and the induction of spawning in fish (Barcellos et al., 2001). Our study showed that a suitable water velocity stimulation (ZS group) could significantly enhance the concentrations of estradiol, testosterone, progesterone, and 17α,20β-DHP, as well as VTG in the ovaries of grass carp compared to the control group, indicating that water velocity stimulation could promote gonadal development and maturation. This agreed well with previous study, which showed that flow stimulation had a positive effect on the hormone rate of change for estradiol and testosterone (Liu et al., 2021). Furthermore, it has been proven that during ovarian development in the European eel (*Anguilla anguilla*), the estrogen receptor in the liver binds with estradiol and facilitates VTG synthesis (Morini et al., 2020). In female grass carp, water velocity may accelerate the accumulation of yolk by promoting VTG expression.

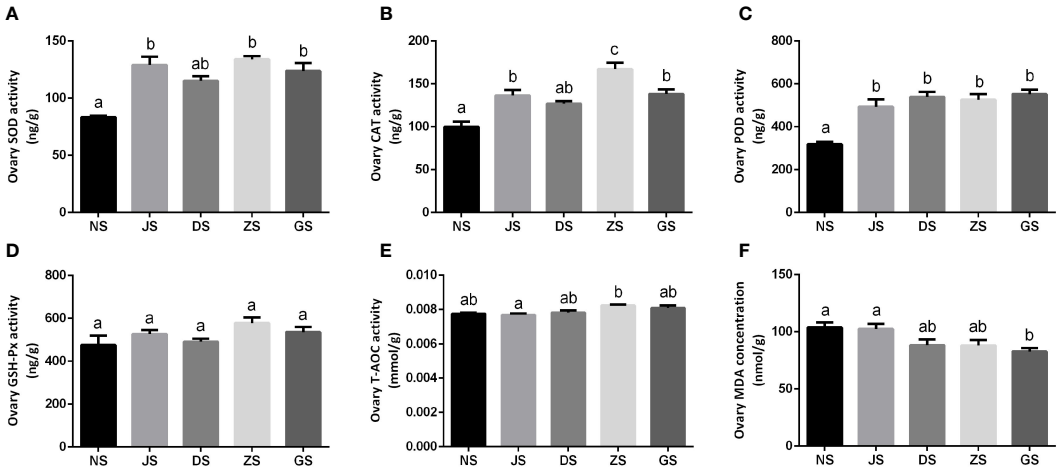

FIGURE 6
The ovary antioxidant enzyme activities measurements (n = 6 for each group). Ovary activities of SOD **(A)**, CAT **(B)**, POD **(C)**, GSH-Px **(D)**, T-AOC **(E)**, and MDA **(F)** in the NS, JS, DS, ZS, and GS groups. The letters in the bar charts represent significant differences.

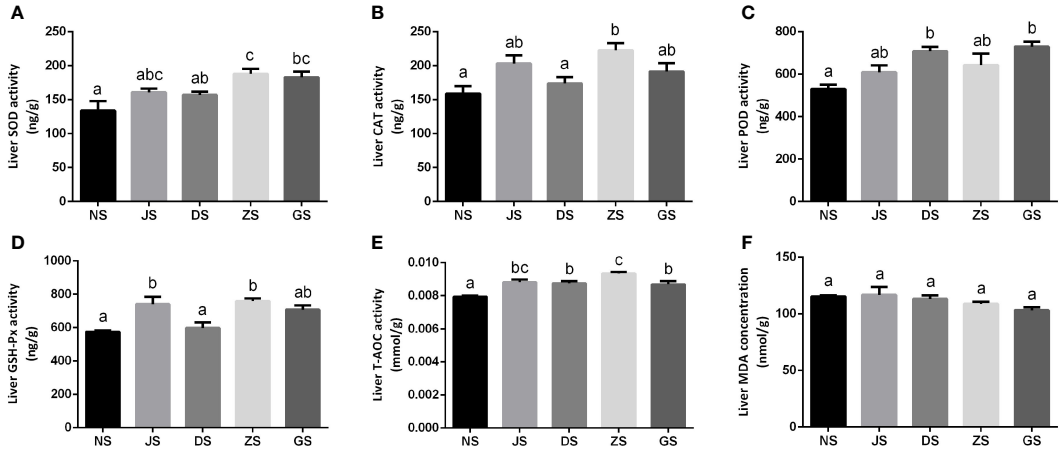

FIGURE 7
The hepatic antioxidant enzyme activities measurements (n = 6 for each group). Hepatic activities of SOD **(A)**, CAT **(B)**, POD **(C)**, GSH-Px **(D)**, T-AOC **(E)**, and MDA **(F)** in the NS, JS, DS, ZS, and GS groups. The letters in the bar charts represent significant differences.

We utilized qRT-PCR to investigate the transcriptional changes of major genes associated with the HPG axis pathway, specifically concerning gonadotropin-releasing hormone (GnRH), gonadotropins (GTHs), and sex hormones. GnRH, an essential neuropeptide produced in the hypothalamus, plays a crucial role in regulating the levels of pituitary GTHs, referring to follicle-stimulating hormone (FSH) and luteinizing hormone (LH) in vertebrates. Several studies have reported that two GnRH variants, known as GnRH2 and GnRH3, could stimulate pituitary FSH and LH secretion in teleost (Li et al., 2022). In the present study, although the transcript level of *gnrh3* showed little difference, hormone injection and graded water velocity stimulation could significantly induce hypothalamus *gnrh2* mRNA expression in female grass carp. In goldfish (*carassius auratus*), GnRH2 elicited a stronger LH secretion compared to GnRH3 in sexually mature, pre-spawning fish (Khakoo et al., 1994; Murthy and Peter, 1994). Similarly, recent studies in grass carp pituitary cells, GnRH2 was found to significantly induce *fshβ* and *lhβ* mRNA expression (Li et al., 2022). Moreover, the *gnrh2* deficiency leads to decreased oocyte quality in female zebrafish (*Danio rerio*) (Marvel et al., 2019). These results indicated that GnRH2 may play an important role in ensuring the integrity of reproduction.

Gonadotropins are complex heterodimers consisting of a common α-glycoprotein subunit (CGα) and a hormone-specific β subunit (FSHβ or LHβ), which are bound together by non-covalent interactions. We found that both hormone injection and water velocity stimulation could significantly induce pituitary-releasing hormones gene (*fshβ*, *lhβ*, and *cgα*) mRNA expression. In Red Seabream (*Pagrus major*), the *cgα* mRNA expression was high during vitellogenesis and at the spawning phase but sharply declined in the regressed phase (Gen et al., 2000). Besides, the mRNA expression levels of *fshβ* and *lhβ* showed a significant increase in the pituitary gland of mature tiger puffer (*Takifugu rubripes*) (Zahangir et al., 2021). In grass puffer (*Takifugu niphobles*), there was a sharp increase in the transcription of *fshβ* during the mature stage, while the transcription of *lhβ* peaked during the spawning period (Yamanoue et al., 2009). Studies haves shown that the development of both ovary and testis in *fshβ*-deficient zebrafish was significantly retarded, and *lhβ*-deficient females failed to spawn, rendering them infertile (Zhang, 2015). Therefore, we speculate that water velocity stimulation might play an important role in stimulating GTHs secretion and sexual maturation in female grass carp.

Vertebrate reproduction is controlled by sex hormones. Upon stimulation of GTHs, biologically active sex hormones such as estradiol, testosterone, progesterone, and 17α,20β-DHP are abundantly produced in gonads, primarily derived from cholesterol (Tenugu et al., 2021). Moreover, sex hormones can regulate the transcription of gonadotropin subunit genes, either by acting on the GnRH-releasing hypothalamus or directly through the pituitary gonadotrope cells. Genes such as *cyp11a1*, *hsd3b1*, *cyp17a1*, *cyp19a1a*, *hsd20b*, *hsd17b1*, *hsd17b3*, and *star* are involved in the steroidogenesis pathway and play crucial roles during gonadal development. In this study, our data showed that *hsd20b* and *hsd17b3* mRNA expressions were significantly upregulated in response to water velocity stimulation. In Nile tilapia (*Oreochromis niloticus*), elevated expression of *hsd20b* in post-vitellogenic immature follicles during final oocyte maturation strongly suggests its crucial role in mediating the final gamete maturation (Senthilkumaran et al., 2002). High expression of *hsd17b3* at vitellogenesis was observed in zebrafish during ovarian follicular development (Ings and van der Kraak, 2006). However, *cyp17a1*, *cyp19a1a*, and *hsd17b1* mRNA expressions were significantly downregulated in the ovary under water velocity stimulation in this study and our previous study (Shu et al., 2023). Similar patterns were found in half-smooth tongue sole (*Cynoglossus semilaevis*), with reduced mRNA levels of *cyp17a1*, *cyp19a1a*, and *hsd17b1* during oocyte maturation (Dong et al., 2021). Studies also have reported that the transcription of *cyp19a1a* was found to be high during the vitellogenic phase, while a significant decline was observed during the final oocyte maturation in Nile tilapia (Yoshiura et al., 2003). In addition,

significant downregulation of *hsd3b1* and *star* were observed following water velocity stimulation. In zebrafish, the expressions of *star*, *hsd3b1*, *cyp17a1*, *hsd17b1*, and *cyp19a1a* were decreased in mature follicles (Ings and van der Kraak, 2006). Taken together, our data demonstrated that water velocity stimulation promoted the synthesis of sex hormones, which in turn activated the HPG axis pathway to ensure ovarian development and maturation in grass carp. However, the molecular mechanisms need to be further determined.

For oxidative stress regulation, it has been reported that reactive oxygen species (ROS) refer to highly oxidizing compounds, ions, and free radicals (Ma et al., 2023). Under normal physiological conditions, ROS maintain a dynamic balance between constantly being generated and removed to alleviate oxidative stress by antioxidant defense system in organisms, which helps maintain long-term health (Liao et al., 2023). SOD, CAT, POD, and GSH-Px are typical enzymes in the biological antioxidant defense system that play a crucial part in scavenging ROS within the body, thereby providing protection for cell membranes and nucleic acids from oxidative damage (Tse et al., 2004; Li et al., 2023). T-AOC reflects the body's ability to compensate for external stimuli and indicates the status of free radical metabolism (Tan et al., 2016; Kong et al., 2021). In our study, water velocity stimulation significantly enhanced the activities of hepatic SOD, CAT, POD, GSH-Px, and T-AOC, as well as ovary SOD, CAT, and POD in female grass carp. This phenomenon is consistent with the results obtained from a previous study on exercise training in juvenile qingbo (*Spinibarbus sinensis*) (Yu et al., 2014). The study by Liu et al. also shows similarities to this result (Liu et al., 2023). Furthermore, MDA is one of the most important decomposition products of membrane lipid peroxidation, and the MDA concentration can serve as a reliable bioindicator of the degree of cellular damage (Zhou et al., 2016). In this study, it was found that high water velocity stimulation significantly reduced the MDA concentration in the ovary, indicating that fish in the GS group possessed stronger antioxidant capacity. Similar to the results of the present experiment, previous work in juvenile largemouth bass (*Micropterus salmoides*) also reported that the MDA content of the high flow group was significantly lower than that of the middle flow and low flow groups (Chen et al., 2021b). This could be attributed to the fact that with the increase in water velocity, the fish's energy consumption increases and its metabolism is accelerated, thereby metabolizing oxygen-free radicals more quickly. These findings revealed that water velocity stimulation can significantly increase antioxidant enzyme activity in female grass carp, decrease the level of MDA, inhibit lipid peroxidation, and protect against damage caused by oxidative stress.

In summary, our comprehensive study demonstrates that a suitable water velocity stimulation (ZS group) can promote ovarian development and maturation by elevating sex hormones and VTG concentrations, as well as regulating the expression of HPG axis genes. It also can enhance the antioxidant activity in the ovary and liver of grass carp. We recommend graded water velocity (0.8–1.3 m/s, water velocity increased from 0.8 m/s to 1.3 m/s gradually) as an appropriate water velocity, which is suitable for gonadal development. This study provides important evidence for understanding the response of fish's natural reproduction to ecological flows.

Data availability statement

The original contributions presented in the study are included in the article/supplementary material. Further inquiries can be directed to the corresponding authors.

Ethics statement

The animal study was approved by Animal Ethics Committee of Institute of Hydrobiology, Chinese Academy of Sciences (Approval ID: IHBLL2017035; Approval Date: January 11, 2017). The study was conducted in accordance with the local legislation and institutional requirements.

Author contributions

TS: Conceptualization, Data curation, Formal analysis, Funding acquisition, Investigation, Methodology, Project administration, Resources, Software, Validation, Visualization, Writing – original draft, Writing – review & editing. JY: Conceptualization, Project administration, Writing – review & editing. ZXY: Data curation, Formal analysis, Investigation, Methodology, Software, Visualization, Writing – original draft, Writing – review & editing. KX: Investigation, Methodology, Resources, Validation, Writing – review & editing. HH: Investigation, Methodology, Writing – review & editing. LD: Funding acquisition, Writing – review & editing. ZY: Supervision, Writing – review & editing. WJ: Funding acquisition, Supervision, Writing – review & editing.

Funding

The author(s) declare financial support was received for the research, authorship, and/or publication of this article. This research was funded by National Key Research and Development Program of China (Grant No. 2022YFC3204200), Hubei Provincial Natural Science Foundation of China (Grant Nos. 2022CFB738 and 2024AFA036), Hubei Provincial Chenguang Project for Young Scientific and Technological Talents (Grant No. 202350), and Key Laboratory of Breeding Biotechnology and Sustainable Aquaculture, Chinese Academy of Sciences (Grant No. 2023FB01).

Acknowledgments

We would like to thank Dezhi Zhang, Yang Li, Binzhong Wang, Zixuan Hu, Pei Chen, and Wei Wang from Chinese Sturgeon Research Institute, China Three Gorges Corporation for the support of the culture system in this research work.

Conflict of interest

Authors TS, JY, ZXY, KX, HH, LD, and WJ are employed by China Three Gorges Corporation.

The remaining author declares that the research was conducted in the absence of any commercial or financial relationships that could be construed as a potential conflict of interest.

Publisher's note

References

Arukwe, A., and Goksoyr, A. (2003). Eggshell and egg yolk proteins in fish: hepatic proteins for the next generation: oogenetic, population, and evolutionary implications of endocrine disruption. *Comp. Hepatol.* 2, 4. doi: 10.1186/1476-5926-2-4

Barcellos, L. J. G., Wassermann, G. F., Scott, A. P., Woehl, V. M., Quevedo, R. M., Ittzés, I., et al. (2001). Steroid profiles in cultured female jundia, the siluridae Rhamdia quelen (Quoy and Gaimard, Pisces Teleostei), during the first reproductive cycle. *Gen. Comp. Endocrinol.* 121, 325–332. doi: 10.1006/gcen.2001.7603

Cao, Y., Wang, C., and Qian, D. (2022). Influence of cascaded hydropower development on high and low flows in the spawning grounds of the four major Chinese carps. *J. Hydroecology* 43, 18–26. doi: 10.15928/j.1674–3075.202011130323

Chen, Q., Zhang, J., Chen, Y., Mo, K., Wang, J., Tang, L., et al. (2021a). Inducing flow velocities to manage fish reproduction in regulated rivers. *Engineering* 7, 178–186. doi: 10.1016/j.eng.2020.06.013

Chen, Z. L., Ye, Z. Y., Ji, M. D., Zhou, F., Ding, X. Y., Zhu, S. M., et al. (2021b). Effects of flow velocity on growth and physiology of juvenile largemouth bass (Micropterus salmoides) in recirculating aquaculture systems. *Aquaculture Res.* 52, 3093–3100. doi: 10.1111/are.15153

Dong, Y., Lyu, L., Zhang, D., Li, J., Wen, H., and Shi, B. (2021). Integrated lncRNA and mRNA Transcriptome Analyses in the Ovary of Cynoglossus semilaevis Reveal Genes and Pathways Potentially Involved in Reproduction. *Front. Genet.* 12. doi: 10.3389/fgene.2021.671729

Gadekar, G. P. (2014). Studies on the seasonal histomorphological changes in the ovary of Indian major carp, Labeo Rohita (HAM.). *Bioscan* 9, 1037–1042.

Gen, K., Okuzawa, K., Senthilkumaran, B., Tanaka, H., Moriyama, S., and Kagawa, H. (2000). Unique expression of gonadotropin-I and -II subunit genes in male and female red seabream (Pagrus major) during sexual maturation. *Biol. Reprod.* 63, 308–319. doi: 10.1095/biolreprod63.1.308

Ghiasi, S., Falahatkar, B., and Sajjadi, M. (2023). Effect of dietary flaxseed meal on growth, blood biochemistry, reproductive hormones and oocyte development in previtellogenic Siberian sturgeon (Acipenser baerii Brandt 1869). *Anim. Feed Sci. Technol.* 295. doi: 10.1016/j.anifeedsci.2022.115546

Golmoradizadeh, A., Noori, A., and Amiri, B. M. (2021). Physiological effects of the lunar cycle on the spawning of a coral reef fish, Abudefduf Vaigiensis: in *vivo* and in *vitro* trait. *Coral Reefs* 40, 1757–1767. doi: 10.1007/s00338-021-02183-x

Hu, W. H., Huang, P. P., Xiong, Y., Guo, W. J., Wang, Y. H., Fan, Q. X., et al. (2020). Synergistic combination of exogenous hormones to improve the spawning and post-spawning survival of female yellow catfish. *Front. Genet.* 11. doi: 10.3389/fgene.2020.00961

Ings, J. S., and van der Kraak, G. J. (2006). Characterization of the mRNA expression of StAR and steroidogenic enzymes in zebrafish ovarian follicles. *Mol. Reprod. Dev.* 73, 943–954. doi: 10.1002/mrd.20490

Jéhannet, P., Palstra, A. P., Meijerhof, M., Schipper, H., Giménez, I. N., Dirks, R. P., et al. (2023). The induction of oocyte maturation and ovulation in the European eel (Anguilla Anguilla): in *vitro* and in *vivo* comparison of progesterone with 17α,20β-dihydroxy-4-pregnen-3-one. *Front. Physiol.* 14. doi: 10.3389/fphys.2023.1207542

Khakoo, Z., Bhatia, A., Gedamu, L., and Habibi, H. R. (1994). Functional specificity for salmon gonadotropin-releasing hormone (GnRH) and chicken GnRH-II coupled to the gonadotropin release and subunit messenger ribonucleic acid level in the goldfish pituitary. *Endocrinology* 134, 838–847. doi: 10.1210/en.134.2.838

Kong, Y. D., Li, M., Chu, G. S., Liu, H. J., Shan, X. F., Wang, G. Q., et al. (2021). The positive effects of single or conjoint administration of lactic acid bacteria on Channa argus: Digestive enzyme activity, antioxidant capacity, intestinal microbiota and morphology. *Aquaculture* 531. doi: 10.1016/j.aquaculture.2020.735852

Lau, E. S.-W., Zhang, Z., Qin, M., and Ge, W. (2016). Knockout of Zebrafish ovarian aromatase gene (cyp19a1a) by TALEN and CRISPR/Cas9 leads to all-male offspring due to failed ovarian differentiation. *Sci. Rep.* 6. doi: 10.1038/srep37357

Li, P. J., Chen, X. Y., Hou, D. Q., Chen, B., Peng, K., Huang, W., et al. (2023). Positive effects of dietary Clostridium butyricum supplementation on growth performance, antioxidant capacity, immaunity and viability against hypoxic stress in largemouth bass. *Front. Immunol.* 14. doi: 10.3389/fimmu.2023.1190592

Li, W., Du, R. X., Xia, C. H., Zhang, H. Y., Xie, Y. Y., Gao, X. W., et al. (2022). Novel pituitary actions of GnRH in teleost: The link between reproduction and feeding regulation. *Front. Endocrinol.* 13. doi: 10.3389/fendo.2022.982297

Liao, Z. H., Liu, Y. T., Wei, H. L., He, X. S., Wang, Z. Q., Zhuang, Z. X., et al. (2023). Effects of dietary supplementation of Bacillus subtilis DSM 32315 on growth, immune response and acute ammonia stress tolerance of Nile tilapia (Oreochromis niloticus) fed with high or low protein diets. *Anim. Nutr.* 15, 375–385. doi: 10.1016/j.aninu.2023.05.016

Liu, R. C., Li, K., Wang, G. X., Jiang, Z. X., Ba, X. B., and Liu, L. P. (2022). Effect of swimming on the induction of vitellogenin in conger eel (Conger myriaster). *Front. Mar. Sci.* 9. doi: 10.3389/fmars.2022.887074

Liu, H., Yin, X. A., Qiu, X., Qin, J., Yang, W., and Zhang, J. (2021). Coupled influence of flow velocity and water temperature on grass carp swimming behaviour and gonad development. *Hydrological Processes* 35. doi: 10.1002/hyp.14052

Liu, M., Yuan, J., Lian, Q., Ni, M., and Gu, Z. (2023). Different water flow rates on the growth performance, antioxidant capacity, energy metabolism and tissue structure of Micropterus salmoides under an in-pond recirculating aquaculture system. *Acta Hydrobiologica Sin.* 47, 25–36. doi: 10.7541/2022.2021.0167

Lubzens, E., Bobe, J., Young, G., and Sullivan, C. V. (2017). Maternal investment in fish oocytes and eggs: The molecular cargo and its contributions to fertility and early development. *Aquaculture* 472, 107–143. doi: 10.1016/j.aquaculture.2016.10.029

Ma, F., Ma, B. H., Zhang, B. X., He, Y. D., and Wang, Y. (2023). Disturbance of oxidation/antioxidant status and histopathological damage in tsinling lenok trout under acute thermal stress. *Trop. Anim. Health Production* 55. doi: 10.1007/s11250-023-03705-1

Marvel, M. M., Spicer, O. S., Wong, T. T., Zmora, N., and Zohar, Y. (2019). Knockout of Gnrh2 in zebrafish (Danio rerio) reveals its roles in regulating feeding behavior and oocyte quality. *Gen. Comp. Endocrinol.* 280, 15–23. doi: 10.1016/j.ygcen.2019.04.002

Morini, M., Lafont, A. G., Maugars, G., Baloche, S., Dufour, S., Asturiano, J. F., et al. (2020). Identification and stable expression of vitellogenin receptor through vitellogenesis in the European eel. *Animal* 14, 1213–1222. doi: 10.1017/S1751731119003355

Murthy, C. K., and Peter, R. E. (1994). Functional evidence regarding receptor subtypes mediating the actions of native gonadotropin-releasing hormones (GnRH) in goldfish, carassius auratus. *Gen. Comp. Endocrinol.* 94, 78–91. doi: 10.1006/gcen.1994.1062

Schmittgen, T. D., and Livak, K. J. (2008). Analyzing real-time PCR data by the comparative CT method. *Nat. Protoc.* 3, 1101–1108. doi: 10.1038/nprot.2008.73

Senthilkumaran, B., Sudhakumari, C. C., Chang, X. T., Kobayashi, T., Oba, Y., Guan, G. J., et al. (2002). Ovarian carbonyl reductase-like 20β-hydroxysteroid dehydrogenase shows distinct surge in messenger RNA expression during natural and gonadotropin-induced meiotic maturation in Nile tilapia. *Biol. Reprod.* 67, 1080–1086. doi: 10.1095/biolreprod67.4.1080

She, Z. Y., Tang, Y. M., Chen, L. H., Nong, X. Z., and Li, X. F. (2023). Determination of suitable ecological flow regimes for spawning of four major Chinese carps: A case study of the Hongshui River, China. *Ecol. Inf.* 76. doi: 10.1016/j.ecoinf.2023.102061

Shu, T. T., Chen, Y., Xiao, K., Huang, H. T., Jia, J. Y., Yu, Z. X., et al. (2023). Effects of short-term water velocity stimulation on the biochemical and transcriptional responses of grass carp (*Ctenopharyngodon idellus*). *Front. Physiol.* 14. doi: 10.3389/fphys.2023.1248999

Tan, X. H., Lin, H. Z., Huang, Z., Zhou, C. P., Wang, A. L., Qi, C. L., et al. (2016). Effects of dietary leucine on growth performance, feed utilization, non-specific immune responses and gut morphology of juvenile golden pompano (*Trachinotus ovatus*). *Aquaculture* 465, 100–107. doi: 10.1016/j.aquaculture.2016.08.034

Tang, Q., Bao, Y. H., He, X. B., Fu, B. J., Collins, A. L., and Zhang, X. B. (2016). Flow regulation manipulates contemporary seasonal sedimentary dynamics in the reservoir fluctuation zone of the Three Gorges Reservoir, China. *Sci. Total Environ.* 548, 410–420. doi: 10.1016/j.scitotenv.2015.12.158

Tenugu, S., Pranoty, A., Mamta, S.-K., and Senthilkumaran, B. (2021). Development and organisation of gonadal steroidogenesis in bony fishes - A review. *Aquaculture Fisheries* 6, 223–246. doi: 10.1016/j.aaf.2020.09.004

Tse, H. M., Milton, M. J., and Piganelli, J. D. (2004). Mechanistic analysis of the immunomodulatory effects of a catalytic antioxidant on antigen-presenting cells: Implication for their use in targeting oxidation-reduction reactions in innate immunity. *Free Radical Biol. Med.* 36, 233–247. doi: 10.1016/j.freeradbiomed.2003.10.029

Tucker, E. K., Zurliene, M. E., Suski, C. D., and Nowak, R. A. (2020). Gonad development and reproductive hormones of invasive silver carp (Hypophthalmichthys molitrix) in the Illinois River. *Biol. Reprod.* 102, 647–659. doi: 10.1093/biolre/ioz207

von Schalburg, K. R., Gowen, B. E., Christensen, K. A., Ignatz, E. H., Hall, J. R., and Rise, M. L. (2023). The late-evolving salmon and trout join the GnRH1 club. *Histochem. Cell Biol.* 160, 517–539. doi: 10.1007/s00418-023-02227-z

Wang, L., Chen, Q. W., Zhang, J. Y., Xia, J., Mo, K. L., and Wang, J. (2020). Incorporating fish habitat requirements of the complete life cycle into ecological flow regime estimation of rivers. *Ecohydrology* 13. doi: 10.1002/eco.2204

Wang, X. B., Li, Y. Y., Hu, J. B., Zhang, Y. Y., Zhang, M., Wang, G. L., et al. (2023). Effects of different photoperiods on growth and ovarian development and maturation of silver pomfret Pampus argenteus. *J. Fish Biol.* 103, 59–72. doi: 10.1111/jfb.15413

Xiao, Y., Deng, J. H., Yang, S. F., Hu, J., Wang, L., and Li, W. J. (2022). Study on the spawning habitat suitability of four major Chinese carps in the fluctuating backwater area of the Three Gorges Reservoir. *Ecol. Indic.* 143. doi: 10.1016/j.ecolind.2022.109314

Yamanoue, Y., Miya, M., Matsuura, K., Miyazawa, S., Tsukamoto, N., Doi, H., et al. (2009). Explosive speciation of Takifugu: another use of fugu as a model system for evolutionary biology. *Mol. Biol. Evol.* 26, 623–629. doi: 10.1093/molbev/msn283

Yoshiura, Y., Senthilkumaran, B., Watanabe, M., Oba, Y., Kobayashi, T., and Nagahama, Y. (2003). Synergistic expression of Ad4BP/SF-1 and cytochrome P-450 aromatase (ovarian type) in the ovary of Nile tilapia, Oreochromis niloticus, during vitellogenesis suggests transcriptional interaction. *Biol. Reprod.* 68, 1545–1553. doi: 10.1095/biolreprod.102.010843

Yu, L., Li, X., Yi, J., Huang, Z., Chen, D., and Wang, Z. (2014). Effects of different water velocities on the free radical metabolism of juvenile Spinibarbus sinensis. *J. Fishery Sci. China* 21, 101–107. doi: 10.3724/SP.J.1118.2014.00101

Zahangir, M. M., Matsubara, H., Ogiso, S., Suzuki, N., Ueda, H., and Ando, H. (2021). Expression dynamics of the genes for the hypothalamo-pituitary-gonadal axis in tiger puffer (Takifugu rubripes) at different reproductive stages. *Gen. Comp. Endocrinol.* 301. doi: 10.1016/j.ygcen.2020.113660

Zhang, Z. (2015). *Genetic Analysis of Gonadotropins and Their Receptors in the Zebrafish*. Hongkong, China: The Chinese University of Hongkong.

Zhang, W. W., Jia, Y. F., Wang, F., Du, Q. Y., and Chang, Z. J. (2017). Identification of differentially-expressed genes in early developmental ovary of Yellow River carp (Cyprinus carpio var) using Suppression Subtractive Hybridization. *Theriogenology* 97, 9–16. doi: 10.1016/j.theriogenology.2017.04.017

Zhang, P., Qiao, Y., Grenouillet, G., Lek, S., Cai, L., and Chang, J. B. (2021). Responses of spawning thermal suitability to climate change and hydropower operation for typical fishes below the Three Gorges Dam. *Ecol. Indic.* 121. doi: 10.1016/j.ecolind.2020.107186

Zhang, Y., Zhang, J., Zhang, L. C., Hu, K. L., Wang, Y., and Ji, Y. (2023). Balancing economic and ecological benefits for hydro-junction operation based on the ecological flow from the four major Chinese carps: a case study from Xinjiang River, China. *Environ. Res. Commun.* 5. doi: 10.1088/2515-7620/acd912

Zhong, H., Hu, J., and Zhou, Y. (2021). Transcriptomic evidence of luteinizing hormone-releasing hormone agonist (LHRH-A) regulation on lipid metabolism in grass carp (Ctenopharyngodon idella). *Genomics* 113, 1265–1271. doi: 10.1016/j.ygeno.2020.09.043

Zhou, D. X., Ning, Y. C., Liu, J. B., Deng, J., Rong, G. H., Bilige, S., et al. (2016). Effects of oxidative stress reaction for the Eisenia fetida with exposure in Cd2+. *Environ. Sci. Pollut. Res.* 23, 21883–21893. doi: 10.1007/s11356-016-7422-6

frontiers | Frontiers in Marine Science

TYPE Original Research
PUBLISHED 18 July 2024
DOI 10.3389/fmars.2024.1448313

OPEN ACCESS

EDITED BY
Yi-Feng Li,
Shanghai Ocean University, China

REVIEWED BY
Basanta Kumar Das,
Central Inland Fisheries Research Institute (ICAR), India
Zheng-Yong Wen,
Neijiang Normal University, China
Liqin Ji,
Chinese Academy of Fishery Sciences, China

*CORRESPONDENCE
Luo Lei
leiluo12311@163.com
Chaowei Zhou
zcwlzq666@163.com

†These authors have contributed equally to this work and share first authorship

RECEIVED 13 June 2024
ACCEPTED 04 July 2024
PUBLISHED 18 July 2024

CITATION
Duan Y, Li H, Li J, Bai S, Fu S, Zhou Y, Liu S, Li R, Liu H, Zhou C and Lei L (2024) Integrated transcriptome and 16S rDNA analyses reveal that acute heat stress induces intestinal damage in *Gymnocypris eckloni*. *Front. Mar. Sci.* 11:1448313. doi: 10.3389/fmars.2024.1448313

Integrated transcriptome and 16S rDNA analyses reveal that acute heat stress induces intestinal damage in *Gymnocypris eckloni*

Yuting Duan[1,2†], Hejiao Li[1,2†], Junting Li[1,2], Shuhao Bai[1], Suxing Fu[1,2], Yinhua Zhou[1,2], Shidong Liu[1], Rundong Li[1], Haiping Liu[2], Chaowei Zhou[1,2*] and Luo Lei[1,2*]

[1]College of Fisheries, Southwest University, Chongqing, China, [2]Integrative Science Center of Germplasm Creation in Western China (CHONGQING) Science City, Southwest University, Chongqing, China

Gymnocypris eckloni (*G. eckloni*), a cold-water economic fish, is widely cultivated in southwestern China. The increase in extreme summer weather conditions owing to global warming can significantly affect their survival and health. The fish intestine and its microbiota are closely associated with fish feeding and growth, nutritional metabolism, and immune defense. However, the mechanisms underlying the changes in the *G. eckloni* intestine and its microbiota under acute heat stress remain unknown. In this study, we investigated the effects of acute heat stress on the *G. eckloni* intestine employing histology, plasma biochemical indices, transcriptomics, and 16S rDNA sequencing. Histological analysis showed that acute heat stress induced significant morphological damage to the intestine, with microvilli detachment and mitochondrial abnormalities in the ultrastructure. Biochemical indicators associated with stress (reactive oxygen species and catalase), inflammation (interleukin-1β and tumor necrosis factor-α), and intestinal permeability (diamine oxidase and lipopolysaccharide) were significantly elevated after acute heat stress, indicating an intestinal inflammatory response and disruption of barrier function. Many DEGs were mined by transcriptomic analysis, with *tfrc, pfkp, egln1* enriched in the HIF-1 signaling pathway, *hsp70, hsp90aa1* and *hspa4* enriched in the Antigen processing and presentation pathway, *pmm1*, *pfkfb3* and *hk1* enriched in the Fructose and mannose metabolism patyway. The HIF-1 signaling pathway is a crucial regulatory pathway during acute heat stress in the *G. eckloni* intestine, while significant downregulation of genes associated with adaptive immunity (*mica*, *hla-dpa1*, *hla-dpb1*, and *hla-dqb2*) suggested impaired immune function. Additionally, the composition of the intestinal microbiota was dominated by *Aeromonas*, *Citrobacter*, and *Acinetobacter* in the control group; but there was a significant decrease in the abundance of *Citrobacter* and *Acinetobacter*, and a significantly increased in *Shewanella* and *Hafnia-Obesumbacterium* after acute heat stress. Correlation analyses revealed that changes in the abundance of *Hafnia-Obesumbacterium*, *Buttiauxella*, and

Pseudomonas were closely associated with changes in gene expression associated with stress, inflammation, and immunity. These results comprehensively demonstrate the adaptive mechanisms of the *G. eckloni* intestine in response to acutely high temperatures and provide a theoretical basis for the future advancement of artificial culture of cold-water fish.

KEYWORDS

***Gymnocypris eckloni*, acute heat stress, intestine, transcriptome, 16S rDNA**

1 Introduction

Temperature is a crucial environmental factor that influences the survival and growth of animals, significantly impacting their metabolism, physiology, and behavior (Polsky and von Keyserlingk, 2017; Farag and Alagawany, 2018; Ern et al., 2023). In recent years, rising temperatures have become an increasing threat to freshwater ecosystems, exposing aquatic organisms to more frequent climate extremes (Barbarossa et al., 2021). Fish, which cannot maintain a constant body temperature, are more vulnerable to these temperature fluctuations (GusChina and Harwood, 2006). High temperatures can induce heat stress in fish, with acute heat stress from short-term temperature spikes causing significant disruptions to their physiological homeostasis, thereby threatening their health and survival (Stewart et al., 2019; Alfonso et al., 2021). To predict the adaptive capacity of fish in response to climate change, understanding the mechanisms through which acute temperature changes affect their physiology and adaptation is essential.

The intestine is an extremely complex ecosystem composed of the gastrointestinal epithelium, a mucus layer, immune cells, and resident microbiota (Cornick et al., 2015). It is a critical digestive and absorptive organ for fish and also influences their immunity, endocrinology, and defense mechanisms (Zhu et al., 2013). The intestine is sensitive to various stressors, including heat stress, hypoxia, and transport (Sundh et al., 2010; Cao et al., 2021; Zheng et al., 2022; Liu et al., 2024). Stress can alter intestinal function by affecting the brain-intestine axis, potentially leading to inflammation or intestinal disease (Zhou et al., 2022). Numerous studies have shown that heat stress not only affects feeding and growth processes in fish (Wade et al., 2019; Chen et al., 2022), but also influences intestinal barrier function, alters the intestinal microbiota, and disrupts homeostasis (Sundh et al., 2010; Huyben et al., 2019; Sepulveda and Moeller, 2020). Intestinal microbiota are crucial for teleost fish in terms of nutrient supply, disease resistance, and immune maintenance (Nayak, 2010; Llewellyn et al., 2014; Wang et al., 2018). Research on the effects of temperature on intestinal microbiology have been conducted in various fish species, such as sturgeons (Yang et al., 2022b), *Seriola lalandi* (Soriano et al., 2018), and rainbow trout (Zhou et al., 2022), demonstrating that high temperatures severely affect intestinal microbiota. Intestinal microbiota play an essential role in stress response and help the host adapt to temperature changes (Sekirov et al., 2010; Kokou et al., 2018). However, previous studies have primarily focused on observations of intestinal histology or changes in intestinal function due to heat stress (Olsen et al., 2005; Golovanova et al., 2013; Huyben et al., 2019), or preliminary analyses of the intestinal microbiome (Yang et al., 2022b). Few studies have been conducted on the interaction between heat stress, fish intestinal microbiota, and transcriptional profiles. Integrating intestinal transcriptomics and microbiome analyses can better explore regulatory mechanisms in fish under adverse environmental conditions (Czech et al., 2022; Yang et al., 2022c).

Gymnocypris eckloni, a schizothoracine fish endemic to the Qinghai-Tibetan Plateau, is a significant aquatic biological resource. It is widely distributed in the Golmud River, isolated lakes, and the upper reaches of the Yellow River. *G. eckloni* serves as a crucial aquatic wildlife germplasm resource in Qinghai Province and a component of biodiversity in the upper waters of the Yellow River, playing an important role in the freshwater ecosystem of the plateau (Wu and Wu, 1992; Wang et al., 2022a). In addition, it has a high economic exploitation value due to its delicious taste and rich nutrition, and has been cultured on a large scale in Southwest China (Yang et al., 2017). Artificial breeding studies have shown that *G. eckloni* exhibits strong sensitivity to high temperatures, with optimal growth rates at water temperatures between 16°C and 18°C, with growth rates decreasing above 20°C (Jian et al., 2020). Consequently, the species is susceptible to acute heat stress caused by increased climatic extremes of high temperature. Current research on *G. eckloni* has focused on genome assembly (Wang et al., 2022a), phylogeny (Wanghe et al., 2022), biological characteristics (Yang et al., 2017), and artificial breeding (Dong et al., 2016), but studies on the effects of high temperatures remain relatively scarce (Li et al., 2024b). Thus, in this study, we integrated histology, biochemical indicators, transcriptomics, and 16S rDNA analysis to examine the effects of acute heat stress on the *G. eckloni* intestine. This comprehensive approach provided a better understanding of how temperature affects fish intestinal physiology and microbiota, providing a theoretical basis for future advancements in the artificial culture of cold-water fish.

2 Materials and methods

2.1 Fish and experimental design

A total of 90 healthy *G. eckloni* (body weight 262 ± 19.8 g) were acquired from Chuanze Fisheries Co. Ltd. (Sichuan, China), and transported to the indoor laboratory at the Aquaculture Base of Southwest University in November 2023 for subsequent experiment. They were equally distributed among six glass tanks (15 fish per tank), and the size of each tank was approximately 0.18 m^3 (110 cm×40 cm ×40 cm) with ~ 0.15 m^3 water, and equipped with electric heaters and thermometers. After two weeks of acclimatization, the six tanks were divided into two groups: the control (CO) group and the acute heat stress (AH) group. During the experiment, the CO group was maintained at a water temperature of 16 ± 0.5°C, while the water temperature of the AH group was increased from 16°C to 28°C at a rate of 2°C/h and maintained for 12 h (Pérez-Casanova et al., 2008). The fish were fed with commercial feed (Rongchuan Feed Co. Ltd., Sichuan, China) twice daily at 9:00 and 18:00 during the experiment. Water quality parameters were measured using the water Quality tester AZ86031 (AZ Instrument Corp., Guangdong, China). They were as follows: pH 7.6-8.5, dissolved oxygen > 6.0 mg/L, ammonia nitrogen and nitrite concentration ≤ 0. 5 mg/L. The study protocol was approved by the Institutional Animal Care of the Southwest University, Chongqing, China, and was performed in compliance with the guidelines for the care and use of laboratory animals.

2.2 Sample collection

Nine fish (three per tank) were randomly selected from each experimental group and anesthetized with 40 mg/L MS-222 (Sigma, Shanghai, China) to collect blood and intestinal samples. Blood samples were collected using disposable syringes containing ethylenediaminetetraacetic acid (EDTA), centrifuged at 5,000 rpm for 15 min, and the supernatant was preserved as plasma for the detection of biochemical indicators. Based on the study of the digestive tract of *G. eckloni* (Yang et al., 2017), the intact intestine was removed after dissection and divided into the three sections (foregut, midgut, and hindgut). Since foregut has more microvilli and mitochondria and is more suitable for histological observations, two small segments of foregut were collected from each fish and preserved separately in 4% paraformaldehyde and 2.5% glutaraldehyde for histological and ultrastructural observations. Following the collection methods of previous studies (Zhu et al., 2022; Zhou et al., 2024), the midgut of nine fish from each experimental group was collected, divided into three replicates, and preserved in liquid nitrogen for transcriptome sequencing. The hindgut contents of the nine fish were carefully squeezed into centrifuge tubes, thoroughly mixed, divided into six replicate samples, and stored in liquid nitrogen for subsequent microbial DNA extraction.

2.3 Histological analysis

The obtained foregut was fixed in 4% paraformaldehyde for 24 h. The samples were dehydrated in a series of ethanol solutions (70%, 80%, 90% and 100%), embedded in paraffin, and sectioned to a thickness of 5 μm. These sections were stained with hematoxylin and eosin (H&E) according to the procedures outlined in previous studies (Novelli et al., 2015). Observation and photography were then conducted using a microscope (Olympus, Tokyo, Japan) equipped with a microscope imager (Leica, Wetzlar, Germany). Additionally, a total of 10 microscopic fields at 40 × magnification were randomly selected to determine the morphological index, including villus length, villus width, and muscle thickness, using ImageJ software (National Institutes of Health, Bethesda, USA).

Tissue sections for transmission electron microscopy (TEM) were prepared as previously described (He and Woods, 2004; Wu et al., 2008). Foregut samples were fixed in 2.5% glutaraldehyde for 4 h and in 4% osmium tetroxide for 1 h. They were then washed in PBS and dehydrated using a series of alcohol concentrations. The tissue was embedded in resin, and ultrathin sections were obtained using an ultrathin sectioning machine. These sections were stained with uranyl acetate and lead citrate and subsequently observed using a Hitachi H7650 TEM.

2.4 Detection and analysis of plasma biochemical indicators

The collected plasma samples were used to detect biochemical indicators of various reactions. The levels of the stress indicator cortisol, the intestinal permeability indicators diamine oxidase (DAO) and lipopolysaccharide (LPS), as well as the inflammatory factors interleukin 1β (IL-1β) and tumor necrosis factor-α (TNF-α), were measured using an enzyme labeling analyzer (Rayto RT-6100) and enzyme-linked immunosorbent assay (ELISA) kits (Jiancheng Bioengineering Institute, Nanjing, China).

Oxidative stress indicators, including superoxide dismutase (SOD), catalase (CAT), and glutathione peroxidase (GSH-Px), as well as metabolic indicators such as glucose (GLU), triacylglycerol (TG), and cholesterol (CHO), were detected using kits procured from ZCIBIO Technology Co., Ltd., China (A001-1, A007-1, A005, S03039, A110–1, and A111–1-1). Reactive oxygen species (ROS) were identified using fluorescent probe assay kits (ZC-A4108, ZCIBIO, Shanghai, China). All biochemical indicators were measured strictly in accordance with the operating instructions.

2.5 Transcriptome data and analysis

Total RNA was extracted from three replicate samples of the CO and AH groups using TRIzol reagent, following the instructions. The integrity, purity, and quality of the RNA were assessed using agarose gel electrophoresis, a Nanodrop microspectrophotometer assay (NanoDrop Technologies, Wilmington, USA), and an Agilent 2100 assay (Agilent Technologies, CA, USA). Six cDNA libraries were constructed using the Hieff NGS® Ultima Dual-mode mRNA Library Prep Kit (12309ES, Yeasen, Shanghai, China), and the library quality was evaluated with the DNA 1000 Assay Kit (5067-1504, Agilent

Technologies, Beijing, China). The cDNA libraries were sequenced using the Illumina NovaSeq 6000 by Gene Denovo Biotechnology Co. (Guangzhou, China). After sequencing, the raw reads were quality controlled using Fastp (version 0.18.0) to filter low-quality data and obtain clean reads. The paired-end sequences were aligned to the reference genome (GenBank accession: JAMHKY000000000, https://www.ncbi.nlm.nih.gov/datasets/taxonomy/334712/) using HISAT 2 (Wang et al., 2022a). The expression level of each transcript was calculated using the reads per kilobase of exon per million mapped reads (RPKM) method using RSEM software. Differentially expressed genes (DEGs) were identified with a false discovery rate (FDR) < 0.05 and an absolute fold change ≥ 2 using DESeq2 software. In addition, functional enrichment analysis (GO and KEGG analysis) of the DEGs was performed, and terms or pathways with a corrected P value < 0.05 were considered significantly enriched. Pathway diagram is drawn by Figdraw.

To verify the reliability of the transcriptome data, we randomly selected seven DEGs—the *heat shock protein 90 alpha family class A member 1* (*hsp90aa1*), the *heat shock protein 70* (*hsp70*), the *phosphoenolpyruvate carboxykinase 1* (*pck1*), the *cold shock domain-containing protein C2-like* (csdc2), the *GTPase IMAP Family Member 7* (*gimap7*), the *jumonji and AT-rich interaction domain containing 2* (*jarid*), and the *(glutamate-ammonia ligase) glul*—for quantitative reverse-transcription polymerase chain reaction (qRT-PCR) to obtain their expression profiles. The total RNA used was consistent with that used for RNA sequencing. cDNA synthesis and qRT-PCR were performed following the manufacturer's protocols, utilizing the HiScript III All-in-one RT SuperMix Perfect Kit for qPCR and ChamQ Universal SYBR qPCR Master Mix (Vazyme, Nanjing, China). All reactions were performed in three biological replicates and three technical replicates, with *β-actin* serving as the reference gene. Primer sequences for the seven DEGs and the reference gene are detailed in Supplementary Table 1. Relative expression in the qPCR results was calculated using the $2^{-\Delta\Delta Ct}$ method, and statistical significance was determined by one-way analysis of variance (ANOVA) (Livak and Schmittgen, 2001).

2.6 Intestinal microbiological data and analysis

Six content samples (n = 6) were collected from each experimental group, and DNA was extracted using HiPure Stool DNA Kits (Magen, Guangzhou, China). The purity and integrity of nucleic acids were verified using a NanoDrop microspectrophotometer (Thermo, Massachusetts, USA) and agarose gel electrophoresis (Liuyi Biotechnology Co. Ltd., Beijing, China). The V3 to V4 regions of the 16S rDNA gene were amplified, purified, and sequenced on the NovaSeq 6000 platform after quality assessment. The primers used were 341F (5′-CCTAYGGGRBGCASCAG-3′) and 806R (3′-GACTACNNGGGGTATCTAAT-5′). Raw data underwent quality control and chimera filtering, and operational taxonomic units (OTUs) were obtained using UPARSE (version 9.2.64) clustering. The representative OTU sequences were classified into organisms using a naive Bayesian model, and the species composition was analyzed at the phylum and genus levels. A Venn diagram was used to identify unique and shared OTUs between the CO and AH groups. Alpha diversity analyses were performed using QIIME2 software (version 1.9.1) to calculate Chao1, ACE, Shannon, and Simpson indices. Based on OTUs and species abundance tables, the Bray–Curtis algorithm was used to evaluate the beta diversity of all samples, including principal component analysis (PCA) based on out, unweighted Unifrac Distance-based Principal Coordinate analysis (PCoA), and Binary-Jaccard-based non-metric multidimensional scaling (NMDS) analysis. Functional prediction of OTUs and KEGG pathway analysis were performed using Tax4Fun (version 1.0). Biomarker features in each group were identified using LEfSe software (version 1.0).

2.7 Integrated analysis of the microbiome and transcriptome

Pearson correlation analyses were performed to examine the relationship between the intestinal microbiota and DEGs. On the basis of the transcriptome results, we focused on the major DEGs in the hypoxia-inducible factor-1 (HIF-1) signaling pathway, as well as immune-related DEGs. Heat maps and correlation network diagrams were generated using the Omicsmart platform (http://www.omicsmart.com).

2.8 Statistical analysis

All data are presented as mean ± SD. Data were processed and plotted using SPSS 26.0 (SPSS Inc., Chicago, USA) and GraphPad Prism 9.5 (GraphPad Software Inc., CA, USA). Differences between the CO and AH groups were determined using a t-test. A significance level of $P < 0.05$ was considered statistically significant, $P < 0.01$ was considered highly significant, and $P < 0.001$ was considered extremely significant.

3 Results

3.1 Effects of acute heat stress on intestinal organization and structure

The histology and ultrastructure of the foregut demonstrated changes in intestinal organization and structure following acute heat stress. In the CO group, the intestinal histology of *G. eckloni* appeared normal, with an intact mucosal layer and goblet cells (Figure 1A). After acute heat stress (Figure 1B), some obvious pathological symptoms indicative of intestinal damage were observed, including numerous swollen goblet cells, vacuoles in the lamina propria, localized necrosis of the mucosal layer, and detached cells in the intestinal cavity. Measurements of the midgut's morphological indices revealed a significant decrease in villus length and width, along with a significant increase in muscle

10.3389/fmars.2024.1448313

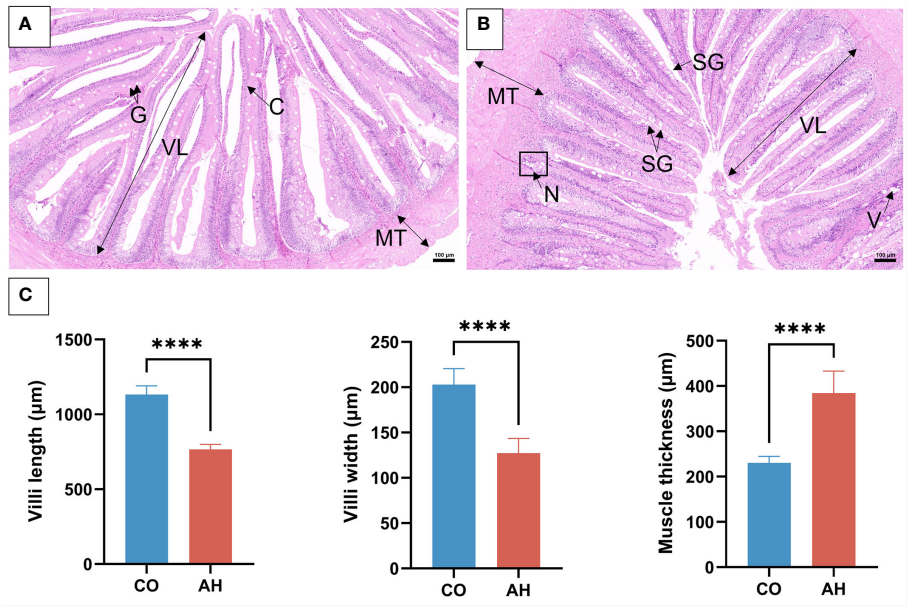

FIGURE 1
Histological changes in the intestine after acute heat stress. **(A)**: CO group. **(B)**: AH group. **(C)**: The intestine morphological index measurement. G, goblet cell; C, columnar cells; N, necrosis; V, vacuolization; SG, swollen goblet cell; lV, villi length; MT, muscle thickness. Scale bar: 100 μm. "****" represents $P<0.0001$.

thickness in the AH group (Figure 1C). The ultrastructure of the intestine in the CO group showed well-arranged microvilli and clearly visible, structurally intact mitochondria (Figures 2A, B). However, in the AH group (Figures 2C, D), the microvilli structure was ruptured, leading to breakage and detachment. Moreover, the mitochondria exhibited notable swelling, cristae dissolution, and even vacuolization, resulting in mitochondrial abnormalities. Therefore, both histological and ultrastructure analyses indicated that the intestinal organization and structure of *G. eckloni* were damaged following acute heat stress.

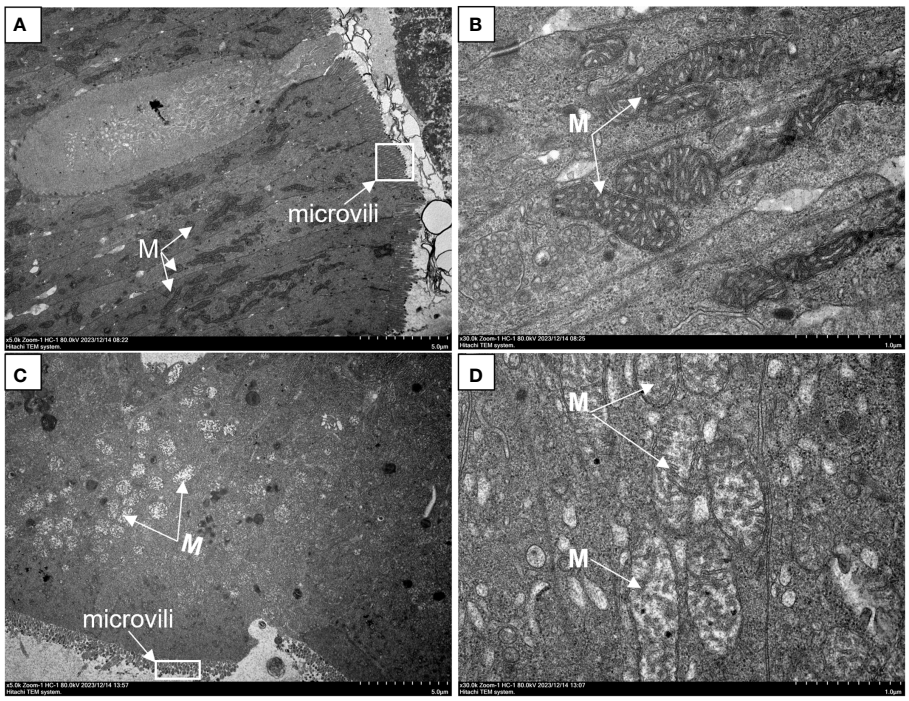

FIGURE 2
Changes in the intestinal ultrastructure of *G eckloni* in the CO group compared to the AH group. **(A, B)**: CO group. **(C, D)**: AH group. M: mitochondria.

3.2 Effects of acute heat stress on plasma biochemical indicators

The effect of acute heat stress on the plasma biochemical indices of *G. eckloni* is illustrated in Figure 3. The levels of ROS, a marker of oxidative damage, were significantly higher after heat stress compared to the CO group ($P < 0.05$). Among the several antioxidant enzymes studied, a highly significant increase was observed in the activity of SOD ($P < 0.01$), a highly significant decrease in the activity of CAT ($P < 0.01$), and no significant change in the activity of GSH-Px.

Compared with those in the CO group, plasma DAO and LPS levels were markedly increased ($P < 0.001$), indicating heightened intestinal permeability following acute heat stress. The levels of pro-inflammatory factors (IL-1β and TNF-α) and the stress indicator cortisol were also significantly elevated ($P < 0.05$), suggesting an inflammatory response in the intestine of *G. eckloni* owing to increased stress under acute heat stress. In terms of energy metabolism, a highly significant increase was observed in plasma glucose levels ($P < 0.01$), as well as a significant increase in cholesterol ($P < 0.05$), while triglyceride levels showed no significant change.

3.3 Transcriptome data and analysis

The CO and AH groups assembled six transcriptome libraries and obtained a total of 24,250,5574 raw reads. Following low-quality filtering, a total of 24,111,06070 clean reads were obtained, ranging from 4,780,859,426–8,961,080,914. The Q20 and Q30 values were above 97.00% and 94.00%, respectively, indicating the viability of the sequencing data (Supplementary Table 2). Differential expression analysis revealed a total of 786 DEGs after acute heat stress compared to controls, with 535 DEGs upregulated and 251 DEGs downregulated (Figures 4A, B).

The detailed GO terms and the top 10 significantly enriched GO terms are shown in Supplementary Figure 1; Figure 4C. A total of 41 GO terms were enriched in the comparison between the CO and AH groups. Within the molecular function category, most DEGs were enriched for binding and catalytic activity. Regarding biological processes, cellular processes and metabolic processes were the most represented. The top 10 significantly enriched terms were associated with metabolic processes, including cofactor metabolic processes, carbohydrate catabolic processes, glycolytic processes, nucleoside diphosphate phosphorylation, nucleotide phosphorylation, and purine nucleoside diphosphate metabolic processes.

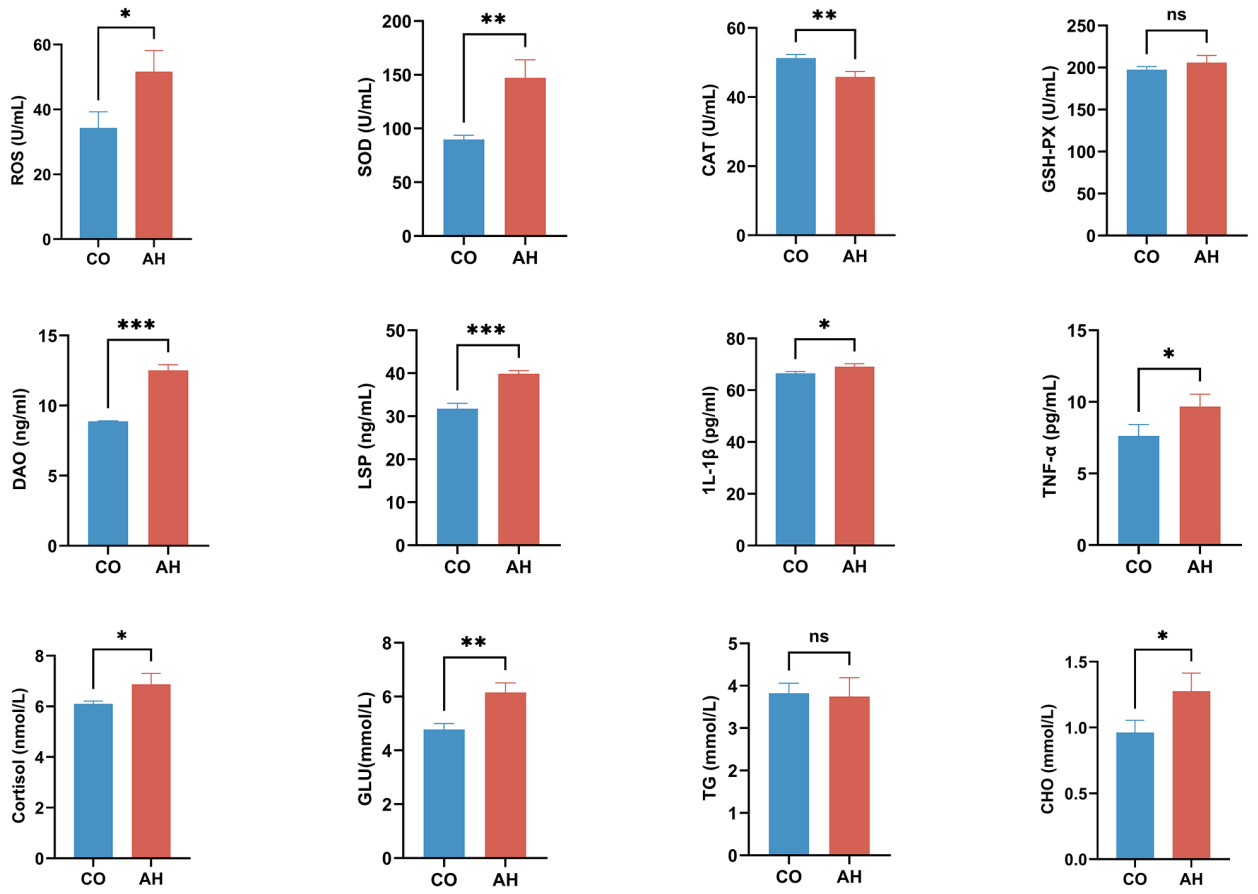

FIGURE 3
Effect of acute heat stress on plasma biochemical indicators. Statistical significance was defined as *$P < 0.05$, **$P < 0.01$, and ***$P < 0.001$. "ns", not significant.

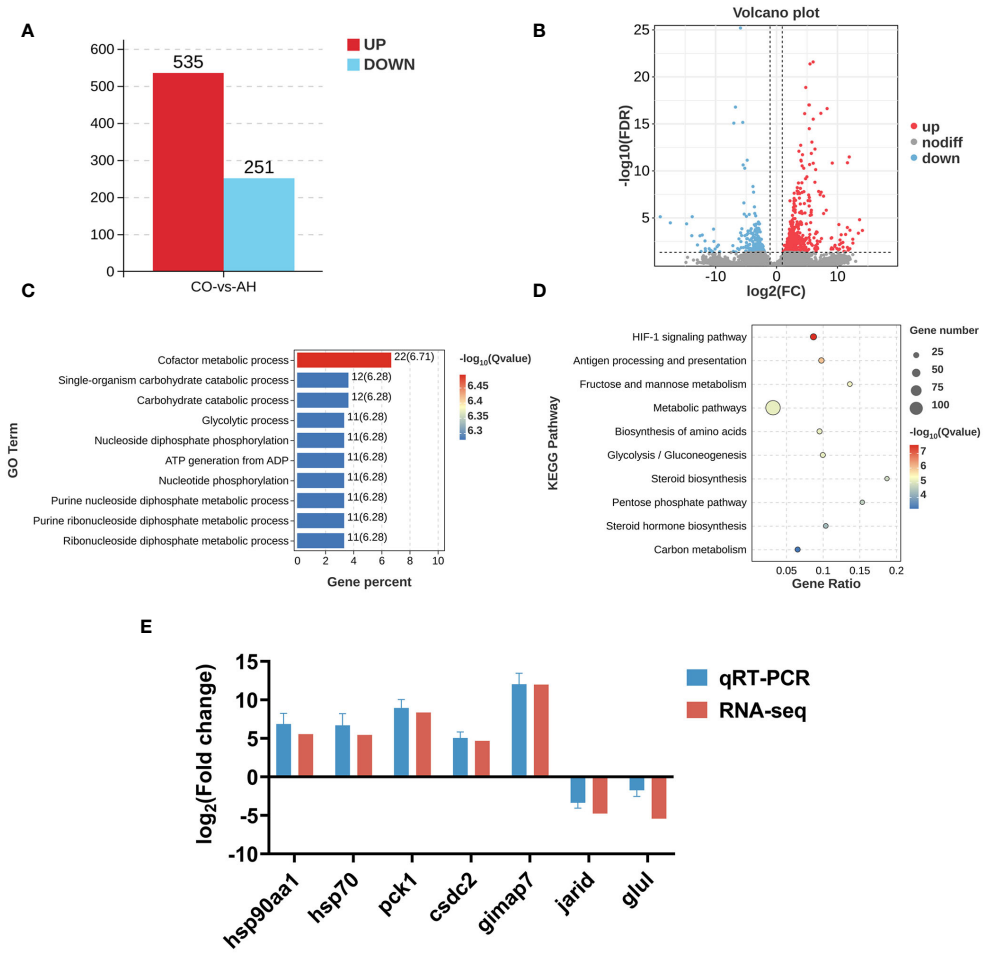

FIGURE 4
Effect of acute heat stress on the transcriptome. **(A)**: The numbers of DEGs between the CO and AH groups. **(B)**: A volcano map. **(C)**: A bar chart of the top 10 significantly enriched GO terms. **(D)**: A bubble diagram of the top 10 significantly enriched KEGG pathways. **(E)**: Validation of qPCR.

KEGG enrichment analysis revealed that DEGs in the "CG vs. CH" comparison were significantly enriched in 25 pathways ($q < 0.05$). The top 10 pathways included the HIF-1 signaling pathway, antigen processing and presentation, fructose and mannose metabolism, metabolic pathways, biosynthesis of amino acids, glycolysis/gluconeogenesis, steroid biosynthesis, pentose phosphate pathway, steroid hormone biosynthesis, and carbon metabolism (Figure 4D). Changes of DEGs in the HIF-1 signaling pathway were shown in Figure 5.

Furthermore, to validate the accuracy of the transcriptome data, we randomly selected seven genes for qPCR, including *hsp90aa1*, *hsp70*, *pck1*, *csdc2*, *gimap7*, *jarid*, and *glul*. The qPCR data exhibited a high degree of consistency with the transcriptomic profiles (Figure 4E), indicating that the transcriptome results are reliable and credible.

3.4 Intestinal microbiological data and analysis

A total of 850,182 high-quality clean reads were obtained from 16S rDNA amplicon gene sequencing in all intestinal content samples, with a mean number of clean reads per sample of 70,849. Venn diagram analysis elucidated a total of 1,690 OTUs in the CO and AH groups, of which 601 were CO group-specific OTUs and 824 were AH group-specific OTUs (Figure 6C). Species composition analysis showed that the major bacterial phylum in all groups was *Proteobacteria*, followed by *Fusobacteriota* and *Firmicutes* (Figure 6A). At the genus level, *Aeromonas*, *Shewanella*, *Citrobacter*, *Acinetobacter*, and *Hafnia-Obesumbacterium* were the dominant species in the intestinal contents of *G. eckloni* (Figure 6B). Following acute heat stress, the percentage of *Aeromonas* increased from 45.69% to 46.86%, *Shewanella* increased from 1.31% to 17.16%, *Citrobacter* decreased from 23.43% to 1.73%, *Acinetobacter* decreased from 16.99% to 4.79%, and *Hafnia-Obesumbacterium* increased from 0.52% to 10.08%.

The alpha diversity analysis (Figures 6D-G) revealed that the differences in diversity indices, including Chao1, Shannon, Simpson, and ACE, between the CO and AH groups were not statistically significant, indicating that acute heat stress had a minimal effect on the diversity of the intestinal microbiota in *G. eckloni*. In contrast, the beta diversity analysis (Figures 6H-J) showed clear separation between the CO and AH groups on the

10.3389/fmars.2024.1448313

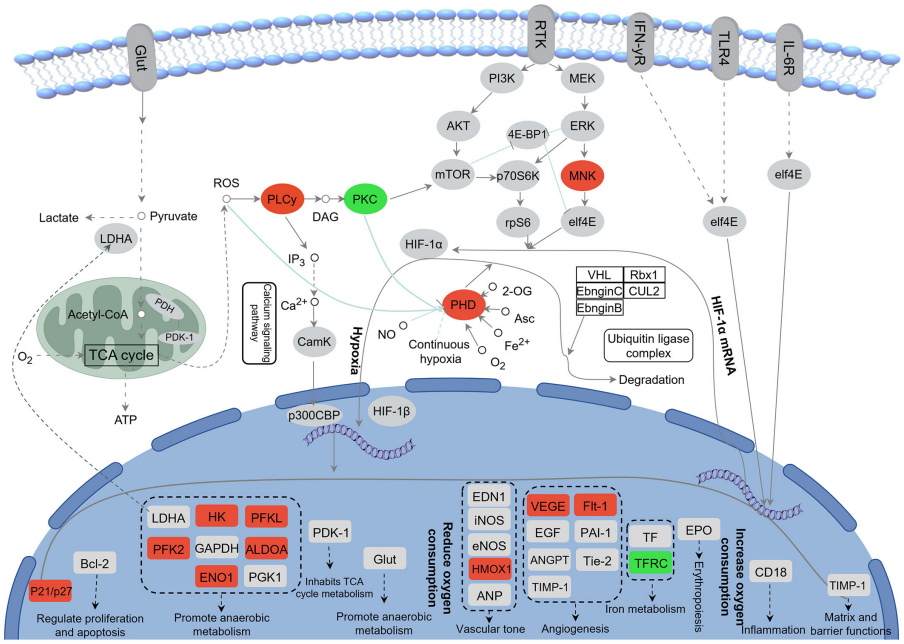

FIGURE 5
Changes of DEGs in HIF-1 signaling pathway after acute heat stress. Red color represents up-regulation of gene expression and green color represents down-regulation of gene expression.

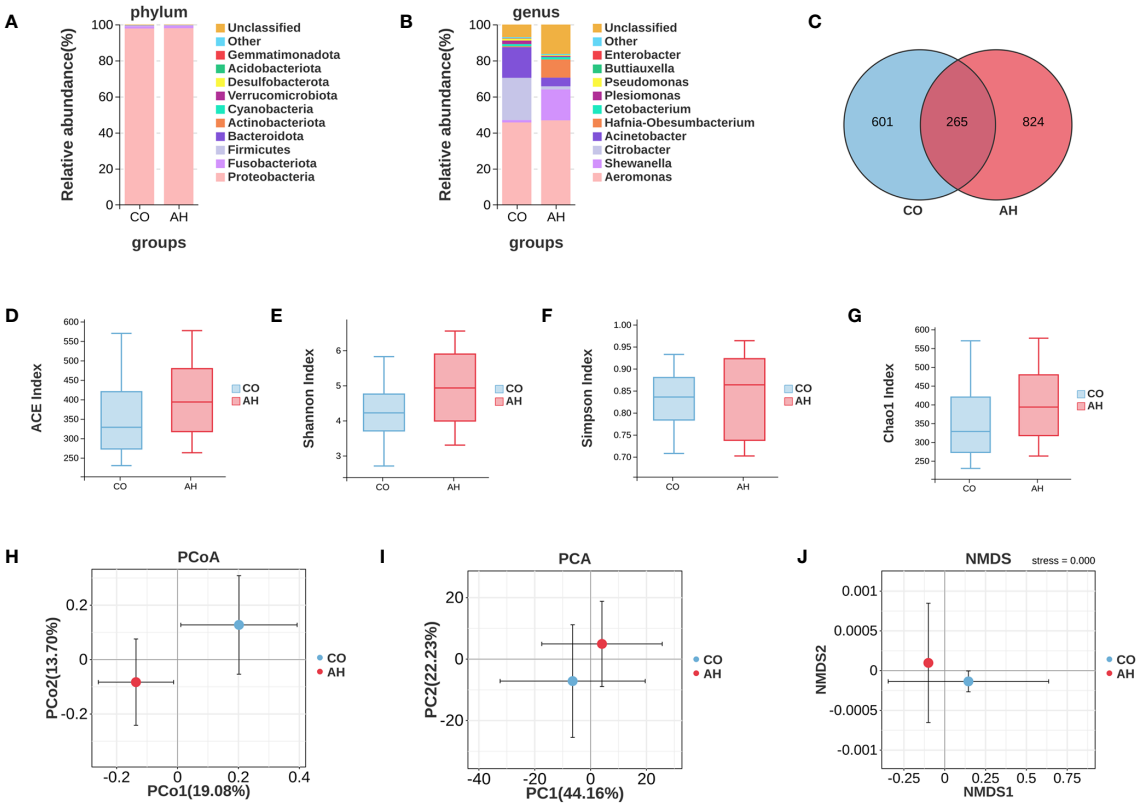

FIGURE 6
Effects of acute heat stress on the composition and diversity of the intestinal microbiota. **(A)**: A Venn diagram depicting OTUs. **(B, C)**: The average relative abundances of intestinal microbiota at phylum and genus levels. **(D–G)**: Analysis of alpha diversity of the intestinal microbiota. **(H-J)**: Analysis of beta diversity of the intestinal microbiota.

two-dimensional coordinate plots of PCoA, PCA, and NMDS, suggesting that acute heat stress significantly affected the composition of the intestinal microbiota in *G. eckloni*.

Tax4Fun was employed for predictive analysis of the intestinal microbiota's function (Figure 7A). The results indicated that the functions of the intestinal microbiota of *G. eckloni* were primarily focused on carbohydrate metabolism, membrane transport, amino acid metabolism, and signal transduction. LEfSe analysis elucidated biomarkers with significant differences between the two groups (Figures 7B, C). In total, 11 strains of differential microflora were identified in the CO and AH groups, with *Shewanella* sp., *Lachnospira multipara*, and *Peptostreptococcaceae* serving as biomarkers in the AH group.

3.5 Integrated analysis of the microbiome and transcriptome

The potential relationship between the intestinal microbiota and DEGs was analyzed using the Pearson correlation method. On the basis of the transcriptome results, we focused on the major DEGs in the HIF-1 signaling pathway and immune-related DEGs. The heatmaps and network diagrams depicting the correlation between gene expression and the intestinal microbiota are presented in Figure 8. The results indicated that the heat shock protein family (*hsp70*, *hsp90aa1*, and *hspa4*) showed a strong positive correlation with the abundance of *Hafnia-Obesumbacterium*, *Buttiauxella*, and *Cetobacterium*. In the HIF-1 signaling pathway, the expression of the *transferrin receptor* (*trfc*) and the *protein kinase C, beta b* (*prkcbb*) was positively correlated with *Pseudomonas* abundance, while the expression of the *phosphofructokinase, platelet* (*pfkp*) was negatively correlated. In the antigen presentation and processing pathway of the immune system, changes in the expression of the *major histocompatibility complex, class II, DP alpha 1* (*hla_dpa1*), the *major histocompatibility complex, class II, DP beta 1* (*hla_dpb1*), the *major histocompatibility complex, class II, DQ beta 2* (*hla_dqb2*), and *mica* were positively correlated with the abundance of *Pseudomonas*, *Streptococcus*, or *Plesiomonas*. Conversely, the expression of *IL1β* was negatively correlated with *Pseudomonas* abundance.

4 Discussion

4.1 Effects of acute heat stress on intestinal organization and structure of *G. eckloni*

The intestine is the central organ for digestion and absorption, and it plays a crucial barrier function against the environment (Vancamelbeke and Vermeire, 2017). Previous studies have found significant structural changes in the intestine under stressful conditions, particularly in the villi and goblet cells, in species such as *Oncorhynchus mykiss* (Li et al., 2023a), *Crassostrea gigas* (Zhao et al., 2023), and *Nile tilapia* (Ran et al., 2016). Villus length influences the body's ability to absorb nutrients by increasing the surface area of the villi (Wei et al., 2024). Goblet cells secrete mucus for lubrication, protect the intestine, and resist bacteria (Johansson

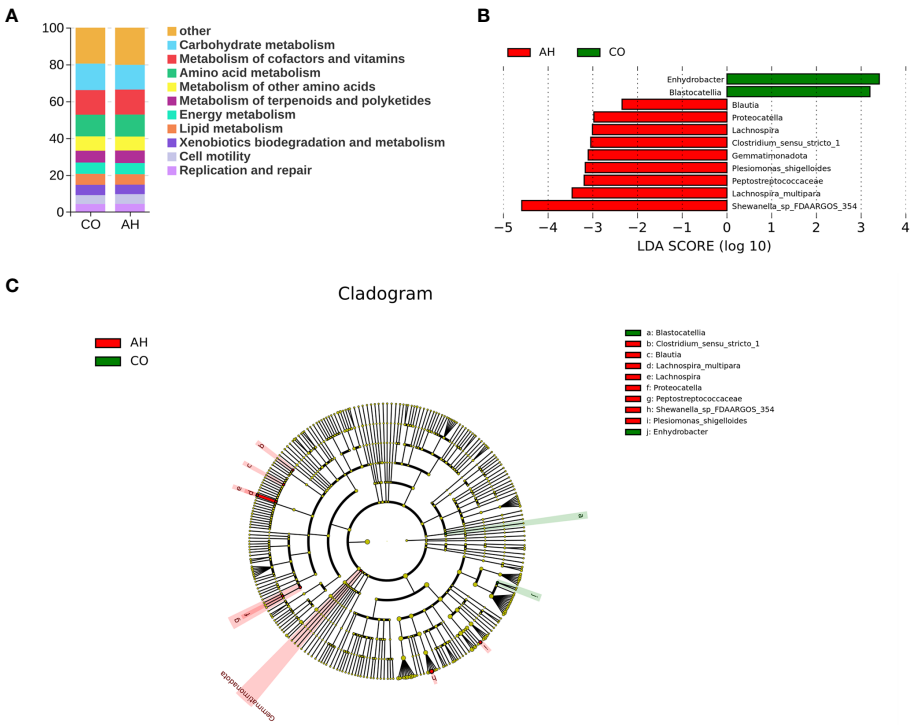

FIGURE 7
Intergroup variation in the relative abundance of the intestinal microbial communities. **(A)**: Function prediction analysis of the intestinal microbiota using PICRUSt2. **(B)**: LDA score at the genus level from Lefse-PICRUSt. **(C)**: Cladogram from Lefse.

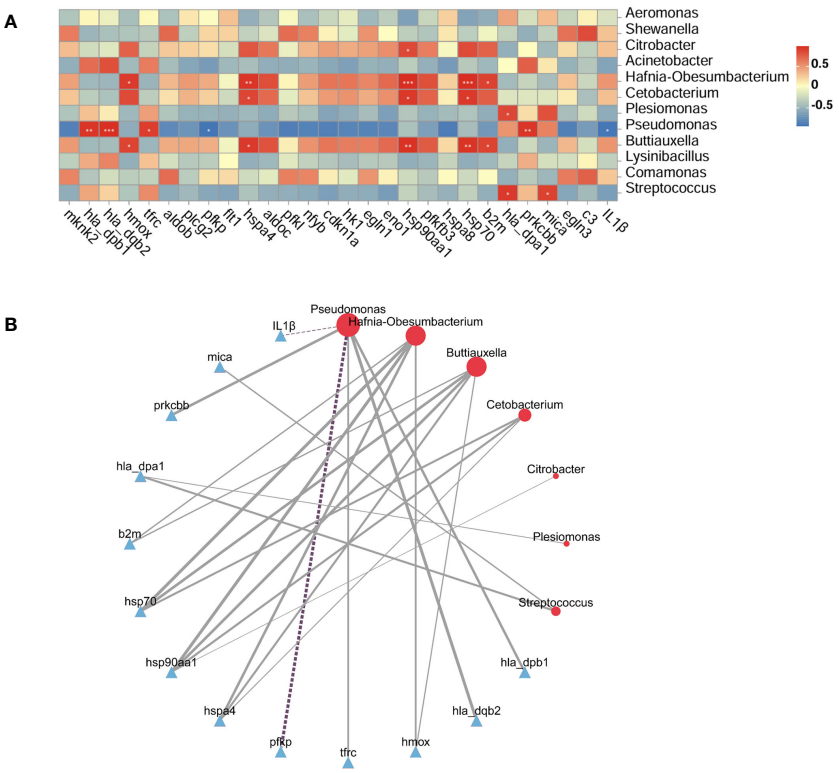

FIGURE 8
Correlation between the intestinal microbiota and DEGs. **(A)**: Correlation heatmap. The X-axis represents the selected DEGs, the Y-axis represents the microbiota, and the color indicates the strength of the correlation. Statistical significance was defined as $*P < 0.05$, $**P < 0.01$, and $***P < 0.001$. **(B)**: Network diagram: Full lines denote positive correlations and dotted lines denote negative correlations. Line thickness represents the strength of the correlation.

and Hansson, 2016). In addition, muscular thickness is an important indicator of intestinal health, with increased thickness promoting intestinal motility (Sanders et al., 2012). In our study, we observed shortening of villus length, swelling of goblet cells, and increased thickness of the muscularis propria in the intestinal histology of *G. eckloni* after heat stress, indicating that acute heat stress impaired the intestinal health of *G. eckloni* and caused barrier damage, similar to the observations in *Oxygymnocypris stewarti* (Zhu et al., 2022). Following heat stress, the intestinal ultrastructure of *G. eckloni* exhibited notable damage, including microvilli detachment and mitochondrial structural abnormalities. Microvilli are the final site for digestion and absorption of nutrients, and defects in microvilli can affect intestinal function and cause diseases (Pavelka and Roth, 2010; Orbach and Su, 2020). Following high-temperature stress in oysters, the shortening and shedding of microvilli impede intestinal nutrient absorption (Zhao et al., 2023). Mitochondria, as the main organelles providing energy, are also the primary site of oxidative stress (Munro and Treberg, 2017). We observed significant swelling, cristae lysis, and even vacuolization of mitochondria, suggesting that intestinal damage in *G. eckloni* is closely associated with oxidative stress and that mitochondrial damage may result from a lack of adequate energy supply (Zhou et al., 2023). Thus, acute heat stress can cause damage to the intestinal morphology and structure of *G. eckloni*, subsequently affecting its digestion and absorption abilities.

4.2 Effects of acute heat stress on the physiological responses of *G. eckloni*

Generally, high temperatures induce oxidative stress in body tissues (Blier, 2014). To avoid oxidative damage caused by excess ROS generated by oxidative stress, the activation of antioxidant enzymes in the antioxidant defense system plays a dominant role (Cheng et al., 2018). In this study, following acute heat stress, a significant increase in the plasma level of ROS was observed in *G. eckloni*, potentially inducing changes in antioxidant enzymes. We examined the changes in several antioxidant enzymes, including CAT, SOD, and GSH-Px, and found that only the level of SOD increased significantly. This indicates that under acute heat stress, *G. eckloni* mitigates the harmful effects of ROS and alleviates oxidative damage by increasing the activity of SOD, similar to *Labeo rohita* (Kumar et al., 2011) and *Litopenaeus vannamei* (Al-Masqari et al., 2022). The level of CAT was significantly reduced, which may be associated with excess ROS exceeding the threshold of antioxidant enzymes, leading to enzyme degradation or inactivation (Zhang et al., 2008; Chen et al., 2021). No significant changes in GSH-Px were observed, which we speculated was due to the low sensitivity of GSH-Px to oxidative damage (Li et al., 2022). Previous studies have provided a rationale for these phenomena, noting that the duration of heat stress, fish species, or compensatory mechanisms can all lead to differences in the activation of

antioxidant enzyme systems (Wu et al., 2021). In addition, with disruption in the balance between the oxidative-antioxidant system and inflammatory cytokines, oxidative damage may further affect fish immunity, leading to an inflammatory response (Slimen et al., 2014; Dang et al., 2022). This study showed that the pro-inflammatory cytokines IL-1β and TNF-α were significantly increased, indicating that there may be inflammation in the intestine of *G. eckloni* after acute heat stress, and that the changes in inflammatory cytokines are associated with intestinal mucosal injury (Konturek et al., 2011). Intestinal inflammation is often accompanied by permeability dysfunction (Lambert, 2009). Plasma LPS and DAO levels were extremely significantly elevated in the AH group, suggesting that intestinal permeability increases after acute heat stress, making it easier for harmful substances to infiltrate and cause systemic inflammation (Chelakkot et al., 2018). Therefore, this study suggests that acute heat stress affects intestinal homeostasis and barrier function in *G. eckloni*.

The metabolic demands of fish increase in response to stress (Przepiura et al., 2019). Stress activates the hypothalamic-pituitary-adrenal axis, leading to an increase in cortisol, an indicator of the stress response, which is accompanied by an increase in energy expenditure (Montero et al., 1999; Faheem et al., 2022). In *Wuchang bream* (Ming et al., 2012), *Lateolabrax maculatus* (Qin et al., 2023), and *Epinephelus akaara* (Cho et al., 2021), elevated cortisol levels enhance gluconeogenesis and glycogenolysis to meet the heightened energy demand due to heat stress. In this study, plasma cortisol and glucose levels were significantly increased in *G. eckloni* following acute heat stress, suggesting that gluconeogenesis accelerates in response to the increased metabolic demand to resist heat stress. In addition, CHO content was significantly increased in the AH group, suggesting the promotion of lipid metabolism to fulfill the energy demand following heat stress in *G. eckloni*, similar to the response observed in rainbow trout (Lu et al., 2022).

4.3 Effects of acute heat stress on the intestinal transcriptome of *G. eckloni*

Transcriptome sequencing revealed that regulatory pathways and key genes are affected by acute heat stress. In this study, DEGs were predominantly and significantly enriched in the HIF-1 signaling pathway in the comparison between the CO and AH groups. The HIF signaling pathway is a crucial metabolic regulatory pathway for maintaining organismal stability under hypoxic conditions. This pathway is involved in vascular development, the transcription of genes associated with vascular development, glucose metabolism, immune function, and cell growth and survival (He et al., 2019; Lin et al., 2021). Previous studies have found that the activation of the HIF-1 pathway may be associated with oxidative stress (Zhang et al., 2023), and it has been validated to play a vital role in the heat adaptation mechanism (Treinin et al., 2003). In addition, compared with other organs, the oxygen concentration in the intestine is lower. The increase in oxygen consumption and blood redistribution after heat stress reduces the energy and oxygen supply to intestinal epithelial cells, which may lead to pathological hypoxia in the intestine (Albenberg et al., 2014; Taylor and Colgan, 2017; Li et al., 2024a). The HIF-1 pathway determines the stability of HIFs during hypoxia by influencing the activity of proline hydroxylase (Egln) through various factors and can regulate downstream genes to help cells adapt to hypoxia (Luo et al., 2022; Strocchi et al., 2022). Meanwhile, excess ROS production induces phospholipase Cγ (PLCγ), leading to inflammation (Tsai et al., 2022). Protein kinase C (PKC) is recognized as a potential mediator of gene expression induced by inflammatory stimulation. The inhibition of PKC may play a role in HS-induced myocardial protection and the prevention of intestinal epithelial dysfunction (Wu et al., 2003; Arnaud et al., 2004; Yang et al., 2007). In our experiments, the expression of *egln*, *plcg1*, and *plcg2* was significantly upregulated, while the expression of PKC-encoded genes (*prkac*, *prkcb*, and *prkcg*) was significantly downregulated. We hypothesize that hypoxia occurs in the intestine of *G. eckloni*, inducing inflammation after heat stress, and that the HIF-1 pathway is activated to protect the intestine. Activation of the HIF-1 pathway also regulates its downstream target genes, affecting oxygen delivery (by regulating angiogenesis and remodeling) and oxygen utilization (by regulating glucose metabolism and oxidation-reduction) (Baptista et al., 2016). Following acute heat stress, the expression of glycolysis-related genes (*hk*, *pfka*, *aldo*, *eno*, and *pfkfb3*) is upregulated in the intestine of *G. eckloni*, increasing the rate of glycolysis to sustain energy production and reducing hypoxia-induced ROS production (Deng et al., 2022). Additionally, the upregulation of vascular endothelial growth factor A (*vegfa*) and its receptor *flt1* induces angiogenesis, enhancing oxygen transport (Kim et al., 2021). Haem oxygenase 1 (*hmox1*) is considered an antioxidant with many anti-inflammatory properties (Campbell et al., 2021), and its expression is also upregulated in response to oxidative stress and inflammation. Thus, the HIF-1 signaling pathway is an important regulatory mechanism during acute heat stress in the intestine of *G. eckloni*.

Additionally, we found that many genes were significantly enriched in immune system pathways, including antigen processing and presentation, the IL-17 signaling pathway, complement and coagulation cascades, and the hematopoietic cell lineage. The immune system is mainly divided into innate and adaptive immunity (Furuta and Eguchi, 2021).The primary role of heat shock proteins (HSPs) under heat stress conditions is to prevent protein misfolding and accumulation. This function contributes to both peptide-specific (adaptive) and non-specific (innate) components, which can trigger the activation of the immune system and stimulate immune responses (Srivastava, 2002; Park et al., 2021). In our experiments, the expression of *hsp90aa1* and *hsp70* was significantly upregulated in antigen presentation and processing, suggesting that these proteins may induce adaptive immunity through antigen presentation (Xu et al., 2018). Two major classes of glycoproteins responsible for antigen presentation, MHC I and MHC II, are essential for T cell-mediated adaptive immunity (Cruz-Tapias et al., 2013). However, we found that the expression of genes encoded by MHC I and MHC II (*mica*, *hla-dpa1*, *hla-dpb1*, and *hla-dqb2*) was downregulated after acute heat stress. This downregulation may be due to suppression by inflammation, similar to findings in the study of *Micropterus salmoides* (Yang et al., 2022a). This finding is also supported by

the upregulation of proinflammatory cytokine expression, including IL-1B, and the increased enzymatic activity of IL-1β and TNF-α. The complement system is the primary line of defense in innate immunity and serves as a crucial barrier against pathogens (Parra-Medina et al., 2013). C3 is central to multiple complement pathways and is known as an evolutionarily conserved building block of immunology, coordinating immune responses through the detection and elimination of hazards (Ricklin et al., 2016). C3 expression following inflammation in zebrafish has been found to regulate the quality and magnitude of innate immune responses to various inflammatory stimuli (Dodds and Matsushita, 2007). In this study, the expression of *c3* in the intestine of *G. eckloni* was upregulated, indicating that *G. eckloni* can respond to heat stress by upregulating *c3*. Thus, we found that acute heat stress significantly induces intestinal inflammation and affects immune function in *G. eckloni*.

4.4 Changes in the intestinal microbiota of *G. eckloni* under acute heat stress

The intestinal microbiota plays a crucial role in maintaining host health and regulating various physiological functions, particularly nutrient metabolism and immune defense (Jin et al., 2017). A healthy and stable intestinal microbiota produces beneficial components that help the host resist pathogen infections and maintain the structural integrity of the intestinal barrier (Song et al., 2024). However, under deleterious conditions, disturbances in the intestinal microbiota can lead to intestinal diseases and reduced immune function (Zhang et al., 2020). Intestinal microbiota may also serve as biomarkers of stress response (Llewellyn et al., 2014). Previous studies have shown that heat stress can significantly affect the composition and abundance of microflora, disrupting intestinal homeostasis and immune barriers in aquatic animals such as *Eriocheir sinensis* (Li et al., 2023c), *Penaeus vannamei* (Song et al., 2024), *Micropterus salmoides* (Yu et al., 2023), and *Crassostrea gigas* (Li et al., 2023b). The intestinal microbiota of *G. eckloni* changed significantly at the genus level after acute heat stress. In *Proteobacteria*, the abundance of *Shewanella*, *Hafnia-Obesumbacterium*, and *Buttiauxella* increased after acute heat stress, whereas the abundance of *Citrobacter*, *Acinetobacter*, *Plesiomonas*, *Pseudomonas*, and *Enterobacter* decreased. In *Oncorhynchus mykiss* (Zhou et al., 2022), a decrease in the abundance of multiple microbiota under acute heat stress can affect the diversity of intestinal microbes and even disrupt homeostasis. *Shewanella*, which is composed of Gram-negative *Proteobacteria*, increases significantly as a pathogen under harmful conditions, causing intestinal infection or disease in fish or crustaceans (Lemaire et al., 2020; Yu et al., 2022), such as *Cyprinus rubrofuscus*, *Procambarus clarkii* and Nile tilapia (Ruan et al., 2022; Reda et al., 2024; Rich and Naguib, 2024). Meanwhile, *Hafnia-Obesumbacterium* plays an important role in enteritis and intestinal infections (Janda and Abbott, 2006). *Citrobacter* assists in the clearance of intestinal pathogens and stimulates host immune defense (Sonnenburg et al., 2006; Buffie and Pamer, 2013; Guo et al., 2021). In this study, acute heat stress significantly altered the intestinal microbiota of *G. eckloni*, with a significant increase in the abundance of *Shewanella* and *Hafnia-Obesumbacterium* and a decrease in the abundance of *Citrobacter*. This is similar to a recent study in which chronic heat stress in *G. eckloni* resulted in a severe dysbiosis of the intestinal flora, characterized by an increase in *Aeromonas* and a decrease in *Citrobacter* (Zhou et al., 2024). Based on these findings, it is reasonable to hypothesize that acute heat stress leads to ecological imbalance of intestinal microbiota and intestinal inflammation in *G. eckloni*. We also observed an increasing trend in the abundance of *Cetobacterium* in *Fusobacteriota*. This increase can promote inflammatory pathways and is associated with immunosuppression (Huang et al., 2022). Therefore, acute heat stress may induce inflammation in the intestine of *G. eckloni* by altering the intestinal microbiota, adversely affecting immune function.

A robust interdependence exists between the intestinal microbiota and DEGs, with gene expression possibly mediating the link between microbial communities and host functions (Wang et al., 2022b; Liu et al., 2023). To further elucidate the host-microbiota relationship, we focused on the HIF-1 signaling pathway and immune-related DEGs in relation to the intestinal microbiota, using Pearson correlation analysis based on transcriptome results. We found that *Hafnia-Obesumbacterium*, *Buttiauxella*, and *Cetobacterium* exhibited robust positive correlations with heat shock proteins (*hsp90aa1*, *hsp70*, and *hspa4*). Additionally, *Pseudomonas* was associated with downstream target genes (*prkcbb*, *tfrc*, *hmox*, and *pfkp*) in the HIF-1 signaling pathway. These findings reveal significant interactions between the intestinal transcriptome and microbiota and suggest that the HIF-1 signaling pathway is an important regulatory pathway in the intestine of *G. eckloni* under acute heat stress. *Pseudomonas*, as a beneficial bacterium, helps balance the intestinal microbiota and immune system (Ruan et al., 2022). Significant correlations between *Pseudomonas* and immune DEGs (*IL1β*, *hla_dqb2*, and *hla_dqb1*) suggest that changes in *Pseudomonas* abundance significantly impact intestinal immune function in *G. eckloni* after acute heat stress. In this study, both *Pseudomonas* abundance and adaptive immunity-related genes (*hla_dqb2* and *hla_dqb1*) were reduced, leading us to hypothesize that acute heat stress affects adaptive immunity in the intestines of *G. eckloni* and reduces immune function.

5 Conclusion

In this study, we evaluated the effects of acute heat stress on the intestine of *G. eckloni* using histological analysis, plasma biochemical indicators, transcriptomics, and 16S rDNA methods. The results indicated that acute heat stress induces damage to the intestinal morphology and structure of *G. eckloni*. Furthermore, biochemical indicators indicated that acute heat stress induced significant oxidative stress and inflammatory responses, affecting intestinal permeability and barrier function. Transcriptome analysis revealed that the HIF-1 signaling pathway is a crucial regulatory pathway during acute heat stress in the intestine of *G. eckloni*, while

the expression of adaptive immunity genes (*mica*, *hla-dpa1*, *hla-dpb1*, and *hla-dqb2*) was significantly downregulated. This further suggests that acute heat stress causes intestinal inflammation and affects immune defense function. Furthermore, the composition of the intestinal microbiota was significantly altered at the genus level, affecting intestinal homeostasis. Changes in the abundance of the intestinal microbiota were strongly associated with changes in gene expression in response to stress, inflammation, and immunity. These findings provide novel avenues for ameliorating high-temperature stress in the artificial culture of *G. eckloni*.

Data availability statement

The datasets presented in this study can be found in online repositories. The names of the repository/repositories and accession number(s) can be found below: https://www.ncbi.nlm.nih.gov/genbank/, PRJNA1121983.

Ethics statement

The animal study was approved by Institutional Animal Care of the Southwest University, Chongqing, China. The study was conducted in accordance with the local legislation and institutional requirements.

Author contributions

YD: Conceptualization, Data curation, Writing – original draft. HeL: Conceptualization, Software, Writing – original draft. JL: Conceptualization, Writing – review & editing. SB: Investigation, Writing – original draft. SF: Resources, Writing – original draft. YZ: Resources, Writing – original draft. SL: Software, Validation, Writing – original draft. RL: Software, Validation, Writing – original draft. HaL: Resources, Writing – review & editing. CZ: Conceptualization, Funding acquisition, Supervision, Writing – review & editing. LL: Conceptualization, Funding acquisition, Supervision, Writing – review & editing.

Funding

The author(s) declare financial support was received for the research, authorship, and/or publication of this article. This research was supported by the National Natural Science Foundation of China (32160864); the Natural Science Foundation of Chongqing Province of China (CSTB2022NSCQ-MSX0566); the "Special Fund for Youth team of the Southwest University" (SWU-XJPY202302); the Fundamental Research Funds for the Central Universities (SWU-KQ24008); and the "National Talent Research Grant for 2023" (5330500953).

Conflict of interest

The authors declare that the research was conducted in the absence of any commercial or financial relationships that could be construed as a potential conflict of interest.

Publisher's note

Supplementary material

The Supplementary Material for this article can be found online at: https://www.frontiersin.org/articles/10.3389/fmars.2024.1448313/full#supplementary-material

References

Albenberg, L., Esipova, T. V., Judge, C. P., Bittinger, K., Chen, J., Laughlin, A., et al. (2014). Correlation between intraluminal oxygen gradient and radial partitioning of intestinal microbiota. *Gastroenterology* 147, 1055–1063.e8. doi: 10.1053/j.gastro.2014.07.020

Alfonso, S., Gesto, M., and Sadoul, B. (2021). Temperature increase and its effects on fish stress physiology in the context of global warming. *J. Fish Biol.* 98, 1496–1508. doi: 10.1111/jfb.14599

Al-Masqari, Z. A., Guo, H., Wang, R., Yan, H., Dong, P., Wang, G., et al. (2022). Effects of high temperature on water quality, growth performance, enzyme activity and the gut bacterial community of shrimp (*Litopenaeus vannamei*). *Aquacult. Res.* 53, 3283–3296. doi: 10.1111/are.15836

Arnaud, C., Joyeux-Faure, M., Bottari, S., Godin-Ribuot, D., and Ribuot, C. (2004). New insight into the signalling pathways of heat stress-induced myocardial preconditioning: protein kinase C-ε translocation and heat shock protein 27 phosphorylation. *Clin. Exp. Pharmacol. Physiol.* 31, 129–133. doi: 10.1111/j.1440-1681.2004.03966.x

Baptista, R. B., Souza-Castro, N., and Almeida-Val, V. M. F. (2016). Acute hypoxia up-regulates HIF-1α and VEGF mRNA levels in Amazon hypoxia-tolerant Oscar (*Astronotus ocellatus*). *Fish Physiol. Biochem.* 42, 1307–1318. doi: 10.1007/s10695-016-0219-1

Barbarossa, V., Bosmans, J., Wanders, N., King, H., Bierkens, M. F. P., Huijbregts, M. A. J., et al. (2021). Threats of global warming to the world's freshwater fishes. *Nat. Commun.* 12, 1701. doi: 10.1038/s41467-021-21655-w

Blier, P. (2014). Fish health: an oxidative stress perspective. *Fish. Aquacult. J.* 05, e105. doi: 10.4172/2150-3508.1000e105

Buffie, C. G., and Pamer, E. G. (2013). Microbiota-mediated colonization resistance against intestinal pathogens. *Nat. Rev. Immunol.* 13, 790–801. doi: 10.1038/nri3535

Campbell, N. K., Fitzgerald, H. K., and Dunne, A. (2021). Regulation of inflammation by the antioxidant haem oxygenase 1. *Nat. Rev. Immunol.* 21, 411–425. doi: 10.1038/s41577-020-00491-x

Cao, C., Chowdhury, V. S., Cline, M. A., and Gilbert, E. R. (2021). The microbiota-gut-brain axis during heat stress in chickens: A review. *Front. Physiol.* 12. doi: 10.3389/fphys.2021.752265

Chelakkot, C., Ghim, J., and Ryu, S. H. (2018). Mechanisms regulating intestinal barrier integrity and its pathological implications. *Exp. Mol. Med.* 50, 1–9. doi: 10.1038/s12276-018-0126-x

Chen, C.-Z., Li, P., Wang, W.-B., and Li, Z.-H. (2022). Response of growth performance, serum biochemical parameters, antioxidant capacity, and digestive enzyme activity to different feeding strategies in common carp (*Cyprinus carpio*) under high-temperature stress. *Aquaculture* 548, 737636. doi: 10.1016/j.aquaculture.2021.737636

Chen, Y., Liu, E., Li, C., Pan, C., Zhao, X., Wang, Y., et al. (2021). Effects of heat stress on histopathology, antioxidant enzymes, and transcriptomic profiles in gills of pikeperch *Sander lucioperca*. *Aquaculture* 534, 736277. doi: 10.1016/j.aquaculture.2020.736277

Cheng, C.-H., Guo, Z.-X., Luo, S.-W., and Wang, A.-L. (2018). Effects of high temperature on biochemical parameters, oxidative stress, DNA damage and apoptosis of pufferfish (*Takifugu obscurus*). *Ecotoxicol. Environ. Saf.* 150, 190–198. doi: 10.1016/j.ecoenv.2017.12.045

Cho, Y. S., Jeong, T. H., Choi, M.-J., Kim, J.-M., and Lim, H. K. (2021). Heat shock protein 70 gene expression and stress response of red-spotted (*Epinephelus akaara*) and hybrid (*E. akaara* female × *E. lanceolatus* male) groupers to heat and cold shock exposure. *Fish Physiol. Biochem.* 47, 2067–2080. doi: 10.1007/s10695-021-00966-1

Cornick, S., Tawiah, A., and Chadee, K. (2015). Roles and regulation of the mucus barrier in the gut. *Tissue Barriers* 3, e982426. doi: 10.4161/21688370.2014.982426

Cruz-Tapias, P., Castiblanco, J., and Anaya, J.-M. (2013).Major histocompatibility complex: Antigen processing and presentation. In: *Autoimmunity: From Bench to Bedside* (El Rosario University Press). Available online at: https://www.ncbi.nlm.nih.gov/books/NBK459467/ (Accessed May 12, 2024).

Czech, B., Wang, Y., Wang, K., Luo, H., Hu, L., and Szyda, J. (2022). Host transcriptome and microbiome interactions in Holstein cattle under heat stress condition. *Front. Microbiol.* 13. doi: 10.3389/fmicb.2022.998093

Dang, Y., Sun, Y., Zhou, Y., Men, X., Wang, B., Li, B., et al. (2022). Effects of probiotics on growth, the toll-like receptor mediated immune response and susceptibility to *Aeromonas salmonicida* infection in rainbow trout *Oncorhynchus mykiss*. *Aquaculture* 561, 738668. doi: 10.1016/j.aquaculture.2022.738668

Deng, C.-C., Zhang, J.-P., Huo, Y.-N., Xue, H.-Y., Wang, W., Zhang, J.-J., et al. (2022). Melatonin alleviates the heat stress-induced impairment of Sertoli cells by reprogramming glucose metabolism. *J. Pineal Res.* 73, e12819. doi: 10.1111/jpi.12819

Dodds, A. W., and Matsushita, M. (2007). The phylogeny of the complement system and the origins of the classical pathway. *Immunobiology* 212, 233–243. doi: 10.1016/j.imbio.2006.11.009

Dong, Y., Deng, S., and Xiao, W. (2016). Artificial propagation of *Gymnocypris eckloni Herzenstein*. *Anim. Husbandry Feed Sci.* 37, 8–10. doi: 10.16003/j.cnki.issn1672-5190.2016.z1.003

Ern, R., Andreassen, A. H., and Jutfelt, F. (2023). Physiological mechanisms of acute upper thermal tolerance in fish. *Physiol. (Bethesda)* 38, 141–158. doi: 10.1152/physiol.00027.2022

Faheem, M., Khaliq, S., Abbas, R. Z., and Mansour, A. T. (2022). Moringa oleifera alleviated oxidative stress, physiological and molecular disruption induced by acute thermal stress in grass carp, *Ctenopharyngodon idella*. *Fish Physiol. Biochem.* 48, 1463–1473. doi: 10.1007/s10695-022-01147-4

Farag, M. R., and Alagawany, M. (2018). Physiological alterations of poultry to the high environmental temperature. *J. Therm Biol.* 76, 101–106. doi: 10.1016/j.jtherbio.2018.07.012

Furuta, K., and Eguchi, T. (2021). "Roles of HSP on antigen presentation," in *Heat Shock Proteins in Human Diseases*. Eds. A. A. A. Asea and P. Kaur (Springer International Publishing, Cham), 275–280. doi: 10.1007/7515_2020_5

Golovanova, I. L., Golovanov, V. K., Smirnov, A. K., and Pavlov, D. D. (2013). Effect of ambient temperature increase on intestinal mucosa amylolytic activity in freshwater fish. *Fish Physiol. Biochem.* 39, 1497–1504. doi: 10.1007/s10695-013-9803-9

Guo, K., Zhao, Z., Luo, L., Wang, S., Zhang, R., Xu, W., et al. (2021). Immune and intestinal microbiota responses to aerial exposure stress in Chinese mitten crab (*Eriocheir sinensis*). *Aquaculture* 541, 736833. doi: 10.1016/j.aquaculture.2021.736833

GusChina, I. A., and Harwood, J. L. (2006). Mechanisms of temperature adaptation in poikilotherms. *FEBS Lett.* 580, 5477–5483. doi: 10.1016/j.febslet.2006.06.066

He, S., and Woods, L. C. (2004). Changes in motility, ultrastructure, and fertilization capacity of striped bass *Morone saxatilis* spermatozoa following cryopreservation. *Aquaculture* 236, 677–686. doi: 10.1016/j.aquaculture.2004.02.029

He, J., Yu, Y., Qin, X.-W., Zeng, R.-Y., Wang, Y.-Y., Li, Z.-M., et al. (2019). Identification and functional analysis of the Mandarin fish (*Siniperca chuatsi*) hypoxia-inducible factor-1α involved in the immune response. *Fish Shellfish Immunol.* 92, 141–150. doi: 10.1016/j.fsi.2019.04.298

Huang, M., Zhao, Q., Yin, J., Cao, S., Chen, H., and Duan, R. (2022). The toxic effects of chronic atrazine exposure on the intestinal microbiota, metabolism and transcriptome of *Pelophylax nigromaculatus* larvae. *J. Hazard. Mater.* 440, 129817. doi: 10.1016/j.jhazmat.2022.129817

Huyben, D., Vidakovic, A., Sundh, H., Sundell, K., Kiessling, A., and Lundh, T. (2019). Haematological and intestinal health parameters of rainbow trout are influenced by dietary live yeast and increased water temperature. *Fish Shellfish Immunol.* 89, 525–536. doi: 10.1016/j.fsi.2019.04.047

Janda, J. M., and Abbott, S. L. (2006). The genus hafnia: from soup to nuts. *Clin. Microbiol. Rev.* 19, 12–28. doi: 10.1128/CMR.19.1.12-28.2006

Jian, S., Yang, B., Zhao, J., Lv, Z., Li, K., Guan, H., et al. (2020). Technique for raising large-scale seedling of *Gymnocypris eckloni* in Qinghai. *Hebei Fish.* 2020 (03), 24–26 +49. doi: 10.3969/j.issn.1004-6755.2020.03.007

Jin, Y., Wu, S., Zeng, Z., and Fu, Z. (2017). Effects of environmental pollutants on gut microbiota. *Environ. pollut.* 222, 1–9. doi: 10.1016/j.envpol.2016.11.045

Johansson, M. E. V., and Hansson, G. C. (2016). Immunological aspects of intestinal mucus and mucins. *Nat. Rev. Immunol.* 16, 639–649. doi: 10.1038/nri.2016.88

Kim, C.-H., Park, C. J., Kim, E. J., and Nam, Y. K. (2021). Transcriptional modulation patterns of abalone *Haliotis discus hannai* hypoxia inducible factor-1α (HIF-1α) in interdependent crosstalk between hypoxia, infection, and environmental stresses. *Aquacult. Rep.* 19, 100566. doi: 10.1016/j.aqrep.2020.100566

Kokou, F., Sasson, G., Nitzan, T., Doron-Faigenboim, A., Harpaz, S., Cnaani, A., et al. (2018). Host genetic selection for cold tolerance shapes microbiome composition and modulates its response to temperature. *Elife* 7, e36398. doi: 10.7554/eLife.36398

Konturek, P. C., Brzozowski, T., and Konturek, S. J. (2011). Stress and the gut: pathophysiology, clinical consequences, diagnostic approach and treatment options. *J. Physiol. Pharmacol.* 62, 591–599.

Kumar, S., Sahu, N. P., Pal, A. K., Subramanian, S., Priyadarshi, H., and Kumar, V. (2011). High dietary protein combats the stress of *Labeo rohita* fingerlings exposed to heat shock. *Fish Physiol. Biochem.* 37, 1005–1019. doi: 10.1007/s10695-011-9504-1

Lambert, G. P. (2009). Stress-induced gastrointestinal barrier dysfunction and its inflammatory effects. *J. Anim. Sci.* 87, E101–E108. doi: 10.2527/jas.2008-1339

Lemaire, O. N., Méjean, V., and Iobbi-Nivol, C. (2020). The Shewanella genus: ubiquitous organisms sustaining and preserving aquatic ecosystems. *FEMS Microbiol. Rev.* 44, 155–170. doi: 10.1093/femsre/fuz031

Li, J., Duan, Y., Kong, W., Gao, H., Fu, S., Li, H., et al. (2024b). Heat stress affects swimming performance and induces biochemical, structural, and transcriptional changes in the heart of *Gymnocypris eckloni*. *Aquacult. Rep.* 35, 101998. doi: 10.1016/j.aqrep.2024.101998

Li, L., Liu, Z., Quan, J., Lu, J., Zhao, G., and Sun, J. (2022). Dietary nanoselenium supplementation for heat-stressed rainbow trout: effects on organizational structure, lipid changes, and biochemical parameters as well as heat-shock-protein- and selenoprotein-related gene expression. *Fish Physiol. Biochem.* 48, 707–722. doi: 10.1007/s10695-022-01084-2

Li, L., Liu, Z., Quan, J., Sun, J., Lu, J., and Zhao, G. (2023a). Dietary nano-selenium alleviates heat stress-induced intestinal damage through affecting intestinal antioxidant capacity and microbiota in rainbow trout (*Oncorhynchus mykiss*). *Fish Shellfish Immunol.* 133, 108537. doi: 10.1016/j.fsi.2023.108537

Li, X., Shi, C., Yang, B., Li, Q., and Liu, S. (2023b). High temperature aggravates mortalities of the Pacific oyster (*Crassostrea gigas*) infected with *Vibrio*: A perspective from homeostasis of digestive microbiota and immune response. *Aquaculture* 568, 739309. doi: 10.1016/j.aquaculture.2023.739309

Li, H., Zhang, G., Liu, Y., Gao, F., Ye, X., Lin, R., et al. (2024a). Hypoxia-inducible factor 1α inhibits heat stress-induced pig intestinal epithelial cell apoptosis through eif2α/ATF4/CHOP signaling. *Sci. Total Environ.* 924, 171649. doi: 10.1016/j.scitotenv.2024.171649

Li, Z., Zhao, Z., Luo, L., Wang, S., Zhang, R., Guo, K., et al. (2023c). Immune and intestinal microbiota responses to heat stress in Chinese mitten crab (*Eriocheir sinensis*). *Aquaculture* 563, 738965. doi: 10.1016/j.aquaculture.2022.738965

Lin, Y., Miao, L.-H., Liu, B., Xi, B.-W., Pan, L.-K., and Ge, X.-P. (2021). Molecular cloning and functional characterization of the hypoxia-inducible factor-1α in bighead carp (*Aristichthys nobilis*). *Fish Physiol. Biochem.* 47, 351–364. doi: 10.1007/s10695-020-00917-2

Liu, X., Ma, Z., Wang, Y., Jia, H., Wang, Z., and Zhang, L. (2023). Heat stress exposure cause alterations in intestinal microbiota, transcriptome, and metabolome of broilers. *Front. Microbiol.* 14. doi: 10.3389/fmicb.2023.1244004

Liu, Y., Wang, J., Ding, J., Zhang, Y., Hou, C., Shen, W., et al. (2024). Effects of hypoxia stress on oxidative stress, apoptosis and microorganisms in the intestine of large yellow croaker (*Larimichthys crocea*). *Aquaculture* 581, 740444. doi: 10.1016/j.aquaculture.2023.740444

Livak, K. J., and Schmittgen, T. D. (2001). Analysis of relative gene expression data using real-time quantitative PCR and the 2−ΔΔCT method. *Methods* 25, 402–408. doi: 10.1006/meth.2001.1262

Llewellyn, M. S., Boutin, S., Hoseinifar, S. H., and Derome, N. (2014). Teleost microbiomes: the state of the art in their characterization, manipulation and importance in aquaculture and fisheries. *Front. Microbiol.* 5. doi: 10.3389/fmicb.2014.00207

Lu, S., Xian, T., Wang, D., Wang, C., Liu, Y., Liu, H., et al. (2022). Effects of traditional Chinese medicines on biochemical parameters, antioxidant capacity and heat shock protein expression in rainbow trout (*Oncorhynchus mykiss*) under heat stress. *Aquacult. Res.* 53, 6148–6157. doi: 10.1111/are.16088

Luo, Z., Tian, M., Yang, G., Tan, Q., Chen, Y., Li, G., et al. (2022). Hypoxia signaling in human health and diseases: implications and prospects for therapeutics. *Sig Transduct Target Ther.* 7, 1–30. doi: 10.1038/s41392-022-01080-1

Ming, J., Xie, J., Xu, P., Ge, X., Liu, W., and Ye, J. (2012). Effects of emodin and vitamin C on growth performance, biochemical parameters and two HSP70s mRNA expression of Wuchang bream (*Megalobrama amblycephala* Yih) under high temperature stress. *Fish Shellfish Immunol.* 32, 651–661. doi: 10.1016/j.fsi.2012.01.008

Montero, D., Izquierdo, M. S., Tort, L., Robaina, L., and Vergara, J. M. (1999). High stocking density produces crowding stress altering some physiological and biochemical parameters in gilthead seabream, Sparus aurata, juveniles. *Fish Physiol. Biochem.* 20, 53–60. doi: 10.1023/A:1007719928905

Munro, D., and Treberg, J. R. (2017). A radical shift in perspective: mitochondria as regulators of reactive oxygen species. *J. Exp. Biol.* 220, 1170–1180. doi: 10.1242/jeb.132142

Nayak, S. K. (2010). Role of gastrointestinal microbiota in fish. *Aquacult. Res.* 41, 1553–1573. doi: 10.1111/are.2010.41.issue-11

Novelli, B., Socorro, J. A., Caballero, M. J., Otero-Ferrer, F., Segade-Botella, A., and Molina Domínguez, L. (2015). Development of seahorse (*Hippocampus reidi*, Ginsburg 1933): histological and histochemical study. *Fish Physiol. Biochem.* 41, 1233–1251. doi: 10.1007/s10695-015-0082-5

Olsen, R. E., Sundell, K., Mayhew, T. M., Myklebust, R., and Ringø, E. (2005). Acute stress alters intestinal function of rainbow trout, *Oncorhynchus mykiss* (Walbaum). *Aquaculture* 250, 480–495. doi: 10.1016/j.aquaculture.2005.03.014

Orbach, R., and Su, X. (2020). Surfing on membrane waves: microvilli, curved membranes, and immune signaling. *Front. Immunol.* 11. doi: 10.3389/fimmu.2020.02187

Park, D. S., Gu, B.-H., Park, Y. J., Joo, S. S., Lee, S.-S., Kim, S.-H., et al. (2021). Dynamic changes in blood immune cell composition and function in Holstein and Jersey steers in response to heat stress. *Cell Stress Chaperones* 26, 705–720. doi: 10.1007/s12192-021-01216-2

Parra-Medina, R., Quintero-Ronderos, P., and Rodríguez, É.G. (2013).The complement system. In: *Autoimmunity: From Bench to Bedside* (El Rosario University Press). Available online at: https://www.ncbi.nlm.nih.gov/books/NBK459482/ (Accessed May 12, 2024).

Pavelka, M., and Roth, J. (2010). "Small intestine: absorptive cells," in *Functional Ultrastructure: Atlas of Tissue Biology and Pathology*. Eds. M. Pavelka and J. Roth (Springer, Vienna), 224–225. doi: 10.1007/978-3-211-99390-3_116

Pérez-Casanova, J. C., Afonso, L. O. B., Johnson, S. C., Currie, S., and Gamperl, A. K. (2008). The stress and metabolic responses of juvenile Atlantic cod Gadus morhua L. to an acute thermal challenge. *J. Fish Biol.* 72, 899–916. doi: 10.1111/j.1095-8649.2007.01763.x

Polsky, L., and von Keyserlingk, M. A. G. (2017). *Invited review:* Effects of heat stress on dairy cattle welfare. *J. Dairy Sci.* 100, 8645–8657. doi: 10.3168/jds.2017-12651

Przepiura, T., de, C. S., Herrerias, T., Kandalski, P. K., Zaleski, T., MaChado, C., et al. (2019). Metabolic responses in *Antarctic Nototheniidae* brains subjected to thermal stress. *Brain Res.* 1708, 126–137. doi: 10.1016/j.brainres.2018.12.004

Qin, H., Long, Z., Huang, Z., Ma, J., Kong, L., Lin, Y., et al. (2023). A comparison of the physiological responses to heat stress of two sizes of juvenile spotted seabass (*Lateolabrax maculatus*). *Fishes* 8, 340. doi: 10.3390/fishes8070340

Ran, C., Huang, L., Hu, J., Tacon, P., He, S., Li, Z., et al. (2016). Effects of dietary live and heat-inactive baker's yeast on growth, gut health, and disease resistance of Nile tilapia under high rearing density. *Fish Shellfish Immunol.* 56, 263–271. doi: 10.1016/j.fsi.2016.07.001

Reda, R. M., El-Murr, A., Abdel-Basset, N. A., Metwally, M. M. M., and Ibrahim, R. E. (2024). Infection dynamics of Shewanella spp. in Nile tilapia under varied water temperatures: A hematological, biochemical, antioxidant-immune analysis, and histopathological alterations. *Fish Shellfish Immunol.* 149, 109588. doi: 10.1016/j.fsi.2024.109588

Rich, A. F., and Naguib, M. (2024). Shewanella xiamenensis-associated ulcerative dermatitis in koi carp (*Cyprinus rubrofuscus*). *J. Fish Dis.* 47, e13942. doi: 10.1111/jfd.13942

Ricklin, D., Reis, E. S., Mastellos, D. C., Gros, P., and Lambris, J. D. (2016). Complement component C3 - the "Swiss army knife innate immunity host defense. *Immunol. Rev.* 274, 33–58. doi: 10.1111/imr.12500

Ruan, G., Li, S., He, N., Fang, L., and Wang, Q. (2022). Short-term adaptability to non-hyperthermal stress: Antioxidant, immune and gut microbial responses in the red swamp crayfish, *Procambarus clarkii*. *Aquaculture* 560, 738497. doi: 10.1016/j.aquaculture.2022.738497

Sanders, K. M., Koh, S. D., Ro, S., and Ward, S. M. (2012). Regulation of gastrointestinal motility—insights from smooth muscle biology. *Nat. Rev. Gastroenterol. Hepatol.* 9, 633–645. doi: 10.1038/nrgastro.2012.168

Sekirov, I., Russell, S. L., Antunes, L. C. M., and Finlay, B. B. (2010). Gut microbiota in health and disease. *Physiol. Rev.* 90, 859–904. doi: 10.1152/physrev.00045.2009

Sepulveda, J., and Moeller, A. H. (2020). The effects of temperature on animal gut microbiomes. *Front. Microbiol.* 11. doi: 10.3389/fmicb.2020.00384

Slimen, I. B., Najar, T., Ghram, A., Dabbebi, H., Ben Mrad, M., and Abdrabbah, M. (2014). Reactive oxygen species, heat stress and oxidative-induced mitochondrial damage. A review. *Int. J. Hyperther.* 30, 513–523. doi: 10.3109/02656736.2014.971446

Song, Z., Li, K., and Li, K. (2024). Acute effects of the environmental probiotics *Rhodobacter sphaeroides* on intestinal bacteria and transcriptome in shrimp *Penaeus vannamei*. *Fish Shellfish Immunol.* 145, 109316. doi: 10.1016/j.fsi.2023.109316

Sonnenburg, J. L., Chen, C. T. L., and Gordon, J. I. (2006). Genomic and metabolic studies of the impact of probiotics on a model gut symbiont and host. *PloS Biol.* 4, e413. doi: 10.1371/journal.pbio.0040413

Soriano, E. L., Ramírez, D. T., Araujo, D. R., Gómez-Gil, B., Castro, L. I., and Sánchez, C. G. (2018). Effect of temperature and dietary lipid proportion on gut microbiota in yellowtail kingfish *Seriola lalandi* juveniles. *Aquaculture* 497, 269–277. doi: 10.1016/j.aquaculture.2018.07.065

Srivastava, P. (2002). Roles of heat-shock proteins in innate and adaptive immunity. *Nat. Rev. Immunol.* 2, 185–194. doi: 10.1038/nri749

Stewart, H. A., Aboagye, D. L., Ramee, S. W., and Allen, P. J. (2019). Effects of acute thermal stress on acid–base regulation, haematology, ion-osmoregulation and aerobic metabolism in Channel Catfish *(Ictalurus punctatus*). *Aquacult. Res.* 50, 2133–2141. doi: 10.1111/are.14093

Strocchi, S., Reggiani, F., Gobbi, G., Ciarrocchi, A., and Sancisi, V. (2022). The multifaceted role of EGLN family prolyl hydroxylases in cancer: going beyond HIF regulation. *Oncogene* 41, 3665–3679. doi: 10.1038/s41388-022-02378-8

Sundh, H., Kvamme, B. O., Fridell, F., Olsen, R. E., Ellis, T., Taranger, G. L., et al. (2010). Intestinal barrier function of Atlantic salmon (*Salmo salar L.*) post smolts is reduced by common sea cage environments and suggested as a possible physiological welfare indicator. *BMC Physiol.* 10, 22. doi: 10.1186/1472-6793-10-22

Taylor, C. T., and Colgan, S. P. (2017). Regulation of immunity and inflammation by hypoxia in immunological niches. *Nat. Rev. Immunol.* 17, 774–785. doi: 10.1038/nri.2017.103

Treinin, M., Shliar, J., Jiang, H., Powell-Coffman, J. A., Bromberg, Z., and Horowitz, M. (2003). HIF-1 is required for heat acclimation in the nematode Caenorhabditis elegans. *Physiol. Genomics* 14, 17–24. doi: 10.1152/physiolgenomics.00179.2002

Tsai, A. P., Dong, C., Lin, P. B.-C., Messenger, E. J., Casali, B. T., Moutinho, M., et al. (2022). PLCG2 is associated with the inflammatory response and is induced by amyloid plaques in Alzheimer's disease. *Genome Med.* 14, 17. doi: 10.1186/s13073-022-01022-0

Vancamelbeke, M., and Vermeire, S. (2017). The intestinal barrier: a fundamental role in health and disease. *Expert Rev. Gastroenterol. Hepatol.* 11, 821–834. doi: 10.1080/17474124.2017.1343143

Wade, N. M., Clark, T. D., Maynard, B. T., Atherton, S., Wilkinson, R. J., Smullen, R. P., et al. (2019). Effects of an unprecedented summer heatwave on the growth performance, flesh colour and plasma biochemistry of marine cage-farmed Atlantic salmon (*Salmo salar*). *J. Thermal Biol.* 80, 64–74. doi: 10.1016/j.jtherbio.2018.12.021

Wang, J., Fan, H., Xia, S., Shao, J., Tang, T., Chen, L., et al. (2022b). Microbiome, transcriptome, and metabolomic analyses revealed the mechanism of immune response to diarrhea in rabbits fed antibiotic-free diets. *Front. Microbiol.* 13. doi: 10.3389/fmicb.2022.888984

Wang, A. R., Ran, C., Ringø, E., and Zhou, Z. G. (2018). Progress in fish gastrointestinal microbiota research. *Rev. Aquacult.* 10, 626–640. doi: 10.1111/raq.12191

Wang, F., Wang, L., Liu, D., Gao, Q., Nie, M., Zhu, S., et al. (2022a). Chromosome-level assembly of *Gymnocypris eckloni* genome. *Sci. Data* 9, 464. doi: 10.1038/s41597-022-01595-w

Wanghe, K., Feng, C., Tang, Y., Qi, D., Ahmad, S., Nabi, G., et al. (2022). Phylogenetic relationship and taxonomic status of *Gymnocypris eckloni* (*Schizothoracinae*) based on specific locus amplified fragments sequencing. *Front. Ecol. Evol.* 10. doi: 10.3389/fevo.2022.933632

Wei, M., Zheng, T., Lu, S., Qiang, J., Tao, Y.-F., Li, Y., et al. (2024). Ammonia-N stress on tissue structure,enzyme activity andintestinal microbiota of *Macropterus salmoides*. *Acta Hydrobiol. Sin.* 48, 10–22.

Wu, Y., Liu, X., Wang, Q., Xu, Y., and Bao, Z. (2008). Studies on the ultrastructure of spermiogenesis and spermatozoon of tongue fish, *Cynoglossus semilaevis günther*. *Aquacult. Res.* 39, 1467–1474. doi: 10.1111/are.2008.39.issue-14

Wu, Y., and Wu, C. (1992). *The fishes of the Qinghai – Xizang plateau* (Sichuan, China: Science and Technology Press).

Wu, J.-M., Xiao, L., Cheng, X.-K., Cui, L.-X., Wu, N.-H., and Shen, Y.-F. (2003). PKCε Is a unique regulator for hsp90β Gene in heat shock response *. *J. Biol. Chem.* 278, 51143–51149. doi: 10.1074/jbc.M305537200

Wu, Y., You, X., Sun, W., Xiong, G., Shi, L., Qiao, Y., et al. (2021). Insight into acute heat stress on meat qualities of rainbow trout (*Oncorhynchus mykiss*) during short-time transportation. *Aquaculture* 543, 737013. doi: 10.1016/j.aquaculture.2021.737013

Xu, D., Zhou, S., and Sun, L. (2018). RNA-seq based transcriptional analysis reveals dynamic genes expression profiles and immune-associated regulation under heat stress in *Apostichopus japonicus*. *Fish Shellfish Immunol.* 78, 169–176. doi: 10.1016/j.fsi.2018.04.037

Yang, C., Dong, J., Sun, C., Li, W., Tian, Y., Liu, Z., et al. (2022a). Exposure to heat stress causes downregulation of immune response genes and weakens the disease resistance of *Micropterus salmoides*. *Comp. Biochem. Physiol. Part D: Genomics Proteomics* 43, 101011. doi: 10.1016/j.cbd.2022.101011

Yang, L., Fang, J., Peng, X., Cui, H., He, M., Zuo, Z., et al. (2017). Study on the morphology, histology and enzymatic activity of the digestive tract of *Gymnocypris eckloni Herzenstein*. *Fish Physiol. Biochem.* 43, 1175–1185. doi: 10.1007/s10695-017-0363-2

Yang, P.-C., He, S.-H., and Zheng, P.-Y. (2007). Investigation into the signal transduction pathway via which heat stress impairs intestinal epithelial barrier function. *J. Gastroenterol. Hepatol.* 22, 1823–1831. doi: 10.1111/j.1440-1746.2006.04710.x

Yang, S., Zhang, C., Xu, W., Li, D., Feng, Y., Wu, J., et al. (2022b). Heat stress decreases intestinal physiological function and facilitates the proliferation of harmful intestinal microbiota in sturgeons. *Front. Microbiol.* 13. doi: 10.3389/fmicb.2022.755369

Yang, Y., Zhu, X., Huang, Y., Zhang, H., Liu, Y., Xu, N., et al. (2022c). RNA-seq and 16S rRNA analysis revealed the effect of deltamethrin on channel catfish in the early stage of acute exposure. *Front. Immunol.* 13. doi: 10.3389/fimmu.2022.916100

Yu, K., Huang, Z., Xiao, Y., and Wang, D. (2022). Shewanella infection in humans: Epidemiology, clinical features and pathogenicity. *Virulence* 13, 1515–1532. doi: 10.1080/21505594.2022.2117831

Yu, J., Zhong, D., Li, S., Zhang, Z., Mo, H., and Wang, L. (2023). Acute temperature stresses trigger liver transcriptome and microbial community remodeling in largemouth bass (*Micropterus salmoides*). *Aquaculture* 573, 739573. doi: 10.1016/j.aquaculture.2023.739573

Zhang, Y., Li, Z., Kholodkevich, S., Sharov, A., Feng, Y., Ren, N., et al. (2020). Microcystin-LR-induced changes of hepatopancreatic transcriptome, intestinal microbiota, and histopathology of freshwater crayfish (*Procambarus clarkii*). *Sci. Total Environ.* 711, 134549. doi: 10.1016/j.scitotenv.2019.134549

Zhang, C., Wang, S., Hu, L., Fang, H., Chen, G., Ma, X., et al. (2023). Analysis of circRNA expression in peripheral blood of *Holstein cows* in response to heat stress. *Int. J. Mol. Sci.* 24, 10150. doi: 10.3390/ijms241210150

Zhang, X.-D., Zhu, Y.-F., Cai, L.-S., and Wu, T.-X. (2008). Effects of fasting on the meat quality and antioxidant defenses of market-size farmed large yellow croaker (*Pseudosciaena crocea*). *Aquaculture* 280, 136–139. doi: 10.1016/j.aquaculture.2008.05.010

Zhao, J., Zhao, B., Kong, N., Li, F., Liu, J., Wang, L., et al. (2023). Increased abundances of potential pathogenic bacteria and expressions of inflammatory cytokines in the intestine of oyster *Crassostrea gigas* after high temperature stress. *Dev. Comp. Immunol.* 141, 104630. doi: 10.1016/j.dci.2022.104630

Zheng, T., Tao, Y., Lu, S., Qiang, J., and Xu, P. (2022). Integrated Transcriptome and 16S rDNA Analyses Reveal That Transport Stress Induces Oxidative Stress and Immune and Metabolic Disorders in the Intestine of Hybrid Yellow Catfish (*Tachysurus fulvidraco*♀ × *Pseudobagrus vachellii*♂). *Antioxidants* 11, 1737. doi: 10.3390/antiox11091737

Zhou, C., Duan, Y., Li, J., Fu, S., Bai, S., Zhuang, Y., et al. (2024). Decoding the intestinal response to heat stress in *Gymnocypris eckloni*: Insights from a thorough analysis of microbiome and transcriptome. *Aquaculture* 591, 741112. doi: 10.1016/j.aquaculture.2024.741112

Zhou, C., Gao, P., and Wang, J. (2023). Comprehensive analysis of microbiome, metabolome, and transcriptome revealed the mechanisms of intestinal injury in rainbow trout under heat stress. *Int. J. Mol. Sci.* 24, 8569. doi: 10.3390/ijms24108569

Zhou, C., Yang, S., Ka, W., Gao, P., Li, Y., Long, R., et al. (2022). Association of gut microbiota with metabolism in rainbow trout under acute heat stress. *Front. Microbiol.* 13. doi: 10.3389/fmicb.2022.846336

Zhu, T., Li, X., Wu, X., and Yang, D. (2022). Temperature acclimation alters the thermal tolerance and intestinal heat stress response in a tibetan fish *Oxygymnocypris stewarti*. *Front. Microbiol.* 13. doi: 10.3389/fmicb.2022.898145

Zhu, L., Nie, L., Zhu, G., Xiang, L., and Shao, J. (2013). Advances in research of fish immune-relevant genes: a comparative overview of innate and adaptive immunity in teleosts. *Dev. Comp. Immunol.* 39, 39–62. doi: 10.1016/j.dci.2012.04.001

frontiers | Frontiers in Marine Science

TYPE Original Research
PUBLISHED 01 August 2024
DOI 10.3389/fmars.2024.1444929

OPEN ACCESS

EDITED BY
Yiming Li,
Fishery Machinery and Instrument Research Institute, China

REVIEWED BY
Basanta Kumar Das,
Central Inland Fisheries Research Institute (ICAR), India
Maocang Yan,
Zhejiang Mariculture Research Institute, China

*CORRESPONDENCE
Yinghui Dong
dongyinghui118@126.com
Nianjun Xu
xunianjun@nbu.edu.cn

RECEIVED 06 June 2024
ACCEPTED 17 July 2024
PUBLISHED 01 August 2024

CITATION
Sun G, Lv L, Yao H, Lin Z, Xu N and Dong Y (2024) Integrated application of multi-omics and biochemical analysis revealed the physiological response mechanism of ammonia nitrogen tolerance in the razor clam (*Sinonovacula constricta*). *Front. Mar. Sci.* 11:1444929. doi: 10.3389/fmars.2024.1444929

Integrated application of multi-omics and biochemical analysis revealed the physiological response mechanism of ammonia nitrogen tolerance in the razor clam (*Sinonovacula constricta*)

Gaigai Sun[1,2], Liyuan Lv[2,3], Hanhan Yao[3], Zhihua Lin[2,3], Nianjun Xu[1]* and Yinghui Dong[2,4]*

[1]School of Marine Sciences, Ningbo University, Ningbo, China, [2]Ninghai Institute of Mariculture Breeding and Seed Industry, Zhejiang Wanli University, Ninghai, China, [3]Key Laboratory of Aquatic Germplasm Resources of Zhejiang, College of Biological & Environmental Sciences, Zhejiang Wanli University, Ningbo, China, [4]College of Advanced Agricultural Sciences, Zhejiang Wanli University, Ningbo, China

As one of the major limiting environment factors in aquaculture, ammonia nitrogen brings severe threat to the growth and survival of aquatic animals, especially mollusk in benthic zones. However, the molecular mechanism underlying the toxic response and tolerance of mollusks to ammonia nitrogen remain unclear. In this study, transcriptome, metabolome and physiological indicators were combined to investigate the metabolic mechanism of adult razor clam (*Sinonvacula constricta*), which was exposed to ~46mg/L ammonia nitrogen for 1 day (A1) and 10 days (A10). It was observed that compared with A1, the contents of free amino acids, including taurine (Tau), alanine (Ala) and arginine (Arg), the activities of immune-related enzymes acid phosphatase (ACP) and alkaline phosphatase (AKP), and antioxidation-related enzymes superoxide dismutase (SOD) and glutathione peroxidase (GPX) in hepatopancreas, were significantly increased in A10, while the content of malondialdehyde (MDA) was significantly decreased ($P < 0.05$). Furthermore, the contents of glucose and pyruvate in hepatopancreas, foot and hemolymph urea nitrogen (HUN) were significantly changed ($P < 0.05$). Meantime, the comparative transcriptome analysis between A1 and A10 groups revealed the effects of ammonia stress on immune defense, antioxidant system and metabolic pathway. Likewise, metabolomic analysis showed that ammonia exposure interfered with amino acid metabolism, lipid metabolism and carbohydrate metabolism, with metabolism related-genes changed according to RNA-seq analysis. By comparing the metabolites and transcripts profiles of A10 and A1, the expression of some genes involved in detoxification and ammonia excretion was significantly changed. Combined with the changes in metabolites, we speculated

that the convert endogenous ammonia to alanine, alanine-glucose cycle and urea synthesis might be adaptive strategies of the razor clam after ammonia stress. Collectively, the combination of physiological, transcriptome and metabolome will greatly contribute to the progressively understand the toxicity of ammonia exposure and the defense mechanism of razor clam against ammonia toxicity, and provide new sights on the potential molecular mechanisms of ammonia adaptive strategies in benthic mollusk.

KEYWORDS

Sinonovacula constricta, ammonia challenge, multi-omics, alanine-glucose cycle, adaptive strategies

1 Introduction

Over the past decades, ammonia nitrogen, a common pollutant in aquatic ecosystem, has been one of the major limiting factors affecting farmed animals in semi-intensive and intensive farming systems. It is worth noting that un-ionized form (NH_3-N) and ion form (NH_4^+) are two existing forms of ammonia nitrogen in water. Among them, NH_3-N exhibits stronger toxicity due to its ability to diffuse through cell membrane (in this study, the term "ammonia nitrogen" refers to the sum of NH_3-N and NH_4^+) (Cong et al., 2019). Generally, ammonia nitrogen can be kept at a very low concentration in most aquatic ecosystems (< 2mg/L) (Romano and Zeng, 2013). However, ammonia nitrogen in marine sediments can exceed 39mg/L (Romano and Zeng, 2013) and reach as high as 46mg/L (Cui et al., 2022) during semi-intensive and intensive farming processes due to increased anthropogenic activities such as agricultural fertilizers. In aquaculture systems, with the input of a large amount of feed and the excretion of cultured animals, ammonia accumulated over time, seriously affecting the growth and survival of farmed animals (Zhao et al., 2020). So far, the level of ammonia nitrogen in aquaculture has become a common concern and an urgent problem to be solved (Bernasconi and Uglow, 2011).

Many studies have been carried out based on the toxicity of ammonia nitrogen to aquatic animals, and some detoxication metabolic mechanisms of ammonia tolerance and adaptation have been found in fish. Among them, the gulf toadfish (*Opsanus beta*) (Veauvy et al., 2005), Magadi tilapia (*Alcolapia graham* (Ip and Chew, 2010), Atlantic hagfish (*Myxine glutinosa*) (Edwards et al., 2015) and other fish have found that the synthesis of glutamine and urea, the role of Rhesus glycoproteins (Rh protein) play an important role in the detoxification metabolism of ammonia nitrogen. In addition, decapod crustaceans have also evolved related ammonia excretion or metabolic mechanisms to avoid ammonia accumulation in blood. For example, studies on green shore crab (*Carcinus maenas*) (Weihrauch et al., 2002), Chinese mitten-handed crab (*Eriocheir sinensis*) (Hong et al., 2007), Amazon river shrimp (*Macrobrachium amazonicum*) (Pinto et al., 2016) and swimming crab (*Portunus trituberculatus*) (Meng et al., 2021) have shown that ammonia can be actively excreted along an inwardly directed gradient through the coordinated action of several transporters, such as Na^+/K^+-ATPase (NKA), V-type H^+-ATPase (VHA) and K^+-channels. Not only that, the internal ammonia can be converted into free amino acids, especially glutamine, which can participate in a variety of metabolic and synthetic biochemical reactions in the body (Hong et al., 2007). However, the related study on invertebrates, especially bivalves, is still in a primary stage.

The razor clam (*Sinonvacula constricta*), is a marine bivalve with important economic and ecological significance, which is loved by consumers because of its delicious taste and rich nutrition. In 2022, the annual production of razor clam is 847,626 tons (from China Fishery Statical Yearbook, 2023). In the current mixed farming model of aquaculture system, the clams with fish, shrimp, crabs were widely used to improve economic benefits (Sun et al., 2021a). In this farming mode, with a large amount of deposition and decay of surplus food, as well as dead organisms in the sediment, the razor clam, as a benthic bivalve, often lives in mudflats or under 30–40cm of mud in ponds, faces a more severe ammonia nitrogen environment than other aquatic animals. In the previous study, we found that the median lethal concentration of the razor clam was 244.55mg/L for 96h (Lv et al., 2022), while the semi-lethal concentration of other bivalves was relatively low, such as Asiatic hard clam (*Meretrix meretrix*) was 92.37mg/L (Chen et al., 2010), and Venus clam (*Cyclina sinensis*) was 65.79mg/L (Ge et al., 2021). These findings indicated that the razor clam has a strong tolerance to ammonia nitrogen. Moreover, our study also found that synthesis of glutamine was an important ammonia detoxification strategy for the razor clam after ammonia exposure (Zhang et al., 2020a). However, why do razor clams have such a high tolerance for ammonia nitrogen? Is the detoxification mechanism of mollusk different from that of other aquatic animals? These questions have not been definitively answered. In this study, physiological index measurement, transcriptomic and metabolomic were analyzed to study the tolerance and detoxification mechanism of the razor clam to ammonia nitrogen stress.

2 Materials and methods

2.1 Ammonia challenge and sample collection

The razor clam (shell length of 61.34 ± 3.21mm, wet weight 13 ± 1.05g), consisting of 1200 individuals at age of one year, were collected in June 2022 in the Genetic Breeding Research Center of Zhejiang Wanli University, China, and all experimental procedures were approved by the Institutional Animal Care and Use Committee (IACUC) of Zhejiang Wanli University, China. Then, the clams were aerated and acclimated in a 500L recirculating seawater tank with temperature of 23 ± 0.5°C, salinity of 22 ± 0.5, and fed the microalgae (*Chaetoceros muelleri*) twice a day.

After seven days domestication, clams were divided into six tanks (100L, N = 200 for per tank), among which three tanks were treated as ammonia nitrogen stress group (AG) and the other three tanks were treated as control group (CG) without ammonia nitrogen. It is worth noting that ammonium chloride (NH_4Cl, BBI, Sangon, Shanghai, China) was used as raw material to prepare total ammonia nitrogen. According to relevant reports, the concentration of ammonia nitrogen in intensive culture system can reach up to 46mg/L (Cui et al., 2022). For the present study, total concentrations of ammonia nitrogen of 0mg/L (CG) and 46mg/L (AG) were used to understand the adverse effects of high ammonia nitrogen on razor clam in culture environment. Notably, the actual concentrations of CG and AG were 0.13 ± 0.38 and 46 ± 3.17mg/L, respectively. The method for determination of ammonia nitrogen concentration in water was described by Zhang et al. (2020a). The ammonia concentration in the AG was regulated by adding NH_4Cl solution to the seawater. Throughout the experiment, the pH of the water was checked by HACH HQ30d pH meter (Hach, Loveland, CO, United States) and kept at a relatively constant value, that is, when the pH was greater than or less than 8, it was regulated by sodium dihydrogen phosphate (NaH_2PO_4) and 2mg/L sodium bicarbonate ($NaHCO_3$), respectively (Zhang et al., 2020a). All the clams were monitored and the dead individuals were removed in time. The stress lasted for 10 days (240h). Then, the hepatopancreas, foot and hemolymph of 12 clams from each group were collected at 0, 6, 12, 24, 48, 72, 144, and 240h for the determination of physiological indexes (including free amino acids, enzyme activities, malondialdehyde content, glucose and pyruvate levels and changes in hemolymph urea nitrogen). In addition, the hepatopancreas of another six clams in each group at 24 and 240h were frozen at -80°C liquid nitrogen for subsequent transcriptome and metabolome analysis.

2.2 Free amino acids analysis

Hepatopancreas from AG and CG at 0 (C0), 24 (A1) and 240h (A10) were selected for free amino acids (FAAs) content analysis. Before detection, the hepatopancreas tissue was freeze-dried for 24h, and then grinded into powder. Then, 5mL of 0.01mol/L HCl was added to every 0.1g sample for hydrolysis for 30min and centrifuged at 12000g for 2min. The supernatant after centrifugation was added with 8% sulfosalicylic acid and mixed overnight. After overnight, the sample were centrifuged again at 12000g for 2min. The supernatant was collected and diluted with 0.02mol/L HCl. Then the diluted supernatant was filtered by 0.22μm filter membrane and analyzed by L-8900 automatic amino acid analyzer (Hitachi High-Tech Corporation, Japan) (Zhu et al., 2024).

2.3 Physiological parameters of hepatopancreas, foot and hemolymph

Hepatopancreas and foot from each group were collected at 0, 6, 12, 24, 48, 72, 144, and 240h, respectively, and the corresponding tissue extracts suggested by the kit were homogenized in the refrigerator at the ratio of 1:9 by weight (g) to volume (mL). Different mixtures were centrifuged according to the instructions of different kits. Then, the supernatant was taken for enzyme activity and malondialdehyde content in hepatopancreas and glucose and pyruvate content in hepatopancreas and foot. Next, the activity of enzymes (immune-related enzymes acid phosphatase (ACP) and alkaline phosphatase (AKP), and antioxidation-related enzymes superoxide dismutase (SOD) and glutathione peroxidase (GPX)) and the content of MDA, glucose and pyruvate were detected using corresponding kits (Note that in addition to pyruvate assay kits from Sangon Shanghai, China, the rest of the kits were from Nanjing Jiancheng Bioengineering Institute, China) according to the manufacturer's instructions. Likewise, the hemolymph urea nitrogen (HUN) was also determined according to the kit instructions (Nanjing Jiancheng Bioengineering Institute, China).

2.4 Transcriptomic analysis

2.4.1 RNA extraction and transcriptome sequencing

Total RNA was extracted from hepatopancreas of each group by Trizol reagent (Omega, Norcross, GA, United States) according to the instructions of the manufacturer. Then, the concentration and purity of the total RNA was quantified by NanoDrop spectrophotometers (Thermo Scientific, Waltham, MA, United States) and Agilent Bioanalyzer 2100 (Agilent Technologies, Santa Clara, United States). Next, all RNA-seq procedures were performed on Illumina Hiseq 2000 platform as described by the Novogene Company (Beijing, China).

2.4.2 Transcriptome assembly and gene annotation

Clean data were filtered to remove joint sequence and low-quality reads. Meanwhile, Q20, Q30 and GC content of the clean data were all calculated. HISAT2 software was used to compare clean reads with the reference genome of the razor clam (Dong et al., 2020), and the location information of reads on the reference genome was obtained.

Gene expression levels were estimated using RSEM (Li and Dewey, 2011). The featureCounts software (Liao et al., 2014) was used to filter out genes with low read counts before performing gene expression analysis. Genes between AG and CG with an adjusted P value < 0.05 found by DESeq2 were assigned as differentially expressed. In addition, the fold change > 2 and false discovery rate (FDR) of 0.05 were used as key indicators for differentially expressed gene (DEGs) screening.

2.4.3 GO and KEGG analysis of the DEGs

GO and KEGG enrichment analysis were performed by clusterProfiler R package (Yu et al., 2012). The enrichment analysis was based on hypergeometric distribution principle, in which the differential gene sets were the differential genes obtained from significant difference analysis and annotated into Go and KEGG database, with a cutoff q-value of 0.05.

2.4.4 Quantitative real time PCR analysis

To verify the results of RNA-seq, seven DEGs were randomly selected for quantitative real time PCR (qRT-PCR). The specific experimental methods of qRT-PCR, including total RNA extraction, cDNA synthesis, selection of internal reference genes (*ribosomal protein S9*, *RS9*) (Zhao et al., 2018) (Table 1) and data processing were consistent with those previous reported by Sun et al. (2021b).

2.5 Metabolomic analysis

To gain a more effective understanding of the mechanisms of ammonia nitrogen reactions and tolerance, differential metabolites in hepatopancreas tissues of clams (N = 6) from each group were evaluated through non-targeted GC-MS metabolomics techniques. Tissues (100mg) were ground with liquid nitrogen, and the homogenate was resuspended with pre-cooled 80% methanol through the well vortex. The sample were incubated on ice for 5min and centrifuged at 4°C for 15000g for 20min. The supernatant was diluted with LC-MS grade water to a final concentration of 53% methanol. The sample were then transferred to fresh Eppendorf tubes and centrifuged at 15000g, 4°C for 20min. Finally, the supernatant was injected into LC-MS/MS system for analysis (Want et al., 2012). More details were available in Supplementary Material 1.

2.6 Statistical analysis

The enzyme activity and content of MDA in hepatopancreas were evaluated by one-way ANOVA and all data were presented as means ± standard of the means (SE). All statistical analyses were performed in SPSS 22 (International Business Machines (IBM) Corporation, Chicago, United States) and the results were considered significantly different when $P < 0.05$.

3 Results

3.1 Physiological parameters

3.1.1 The change of free amino acids content stressed by ammonia nitrogen

The results of the determination of total free amino acids in hepatopancreas of the razor clam after ammonia nitrogen stress showed that among the 16 amino acids detected, except histidine

TABLE 1 Primers and sequences used in the experiments.

Primer	Sequence (5′-3′)	Product size (bp)	GenBank accession No.
ARG-F	AACCCATAGCCCGT	370	KZS21480.1
ARG-R	ATAGCAGATTACCCGA		
RhB-F	TATGGTGCCCTCTTT	235	NXK44169.1
RhB-R	GCCTTGCTTATTCCT		
ALT-F	GTTCTGCTGTCTGCTT	112	XP_020901578.1
ALT-R	CGGTCATCTTCGTATT		
CA-F	TCTCCATCTTTTATGACCCC	301	TMS22568.1
CA-R	ATGATACCCAGCACCGC		
GPX-F	GACACTCCAATCTCCG	377	MK301158.1
GPX-R	GCTACGCTATATCTCCAC		
VHA-F	ATAGGATACAACAGGCG	453	XP_038127943.1
VHA-R	TGGGATACCACGAAGA		
NHE-F	ACATAGACGATTCCGA	186	XP_016590485.1
NHE-R	AAGCAGCCAATACAGA		
RS9-F	TGAAGTCTGGCGTGTCAAGT	117	NP_001085809.1
RS9-R	CGTCTCAAAAGGGCATTACC		

(His, no significant changes), the other 15 amino acids had significant changes of varying degrees (Table 2). Compared with C0, aspartic acid (Asp), threonine (Thr), serine (Ser), glutamic acid (Glu), glycine (Gly), alanine (Ala), valine (Val), methionine (Met), isoleucine (Ile), leucine (Leu), tyrosine (Tyr), phenylalanine (Phe) and lysine (Lys) were significantly down-regulated in A1 ($P < 0.05$). In A10, Asp, Thr, Ser, Glu, Met, Ile, Leu, Tyr, Phe and Lys were significantly down-regulated ($P < 0.05$), while taurine (Tau), Ala and arginine (Arg) were significantly up-regulated ($P < 0.05$).

3.1.2 Ammonia nitrogen stress increased enzyme activity, MDA and HUN content

The activities of four enzymes including ACP, AKP, SOD, GPX and the content of MDA and HUN at different times after ammonia nitrogen stress were shown in Figure 1. The enzyme activity of two immune-related enzymes (AKP and ACP) showed no significant change at 0~24h, and both showed a significant increase at 48h ($P < 0.05$), and then continued until the end of the experiment (Figure 1A). The activity of SOD increased significantly at 0~48h ($P < 0.05$), and reached the highest level at 72h, and then increased at the later stage (Figure 1B). GPX activity increased significantly at 0~24h ($P < 0.05$), decrease significantly at 48h ($P < 0.05$), and then increased rapidly at 72h until the end of the experiment ($P < 0.05$) (Figure 1B). The content of MDA increased continuously from the beginning to 24h, and decreased significantly at 48h ($P < 0.05$) and continued until the end of the experiment (Figure 1C). The content of HUN increased from the outset to 12h ($P < 0.05$), decreased from 24~48h ($P < 0.05$), and then showed an upward trend at 72h and continued until the end of the experiment (Figure 1D).

TABLE 2 Content of free amino acids in hepatopancreas of *S. constricta*.

FAAs	C0 (mg/g)	A1 (mg/g)	A10 (mg/g)
Tau	5.98 ± 0.15	6.91 ± 1.11	8.22 ± 0.29**
Ala	19.29 ± 3.37	18.72 ± 2.21*	22.81 ± 1.24*
His	0.56 ± 0.03	0.61 ± 0.19	0.50 ± 0.08
Arg	3.17 ± 0.15	2.30 ± 0.39	4.72 ± 0.02**
Leu	2.38 ± 0.19	0.34 ± 0.13**	0.84 ± 0.29**
Tyr	1.61 ± 0.21	0.43 ± 0.05**	0.38 ± 0.15**
Phe	3.08 ± 1.97	0.69 ± 0.06**	0.79 ± 0.31**
Lys	2.60 ± 0.49	1.08 ± 0.11**	1.94 ± 0.19**
Asp	1.33 ± 0.17	0.76 ± 0.04**	0.51 ± 0.06**
Thr	2.35 ± 0.31	0.81 ± 0.18**	1.24 ± 0.22**
Ser	1.54 ± 0.20	0.78 ± 0.22**	1.27 ± 0.11**
Glu	5.59 ± 0.60	4.03 ± 0.58**	3.89 ± 0.13**
Gly	11.58 ± 0.93	8.21 ± 1.28**	5.19 ± 0.56**
Val	1.75 ± 0.12	1.28 ± 0.20**	1.55 ± 0.10
Met	1.60 ± 0.14	0.43 ± 0.12**	0.76 ± 0.07**
Ile	0.99 ± 0.10	0.14 ± 0.03**	0.53 ± 0.12**

Tau, Taurine; Asp, Aspartic acid; Thr, Threonine; Ser, Serine; Glu, Glutamic acid; Gly, Glycine; Ala, Alanine; Val, Valine; Met, Methionine; Ile, Isoleucine; Leu, Leucine; Tyr, Tyrosine; Phe, Phenylalanine; Lys, Lysine; His, Histidine; Arg, Arginine; Asterisk (*) indicated a significant difference between the ammonia-stressed group and control group (*P < 0.05; **P < 0.01).

3.1.3 Ammonia nitrogen stress increased glucose and pyruvate content

The changes of glucose and pyruvate in hepatopancreas and foot at different time after ammonia stress were shown in Figure 2. As the results shows, the glucose in the foot increased significantly at 0~48h ($P < 0.05$), and then decreased at 72h ($P < 0.05$) but was still significantly higher than the initial ammonia stress content (Figure 2A). Likewise, the content of pyruvate in the foot increased significantly at 0~72h ($P < 0.05$), reached the peak at 72h, and then showed a decreasing trend until the end of the experiment (Figure 2B). The glucose content in hepatopancreas increased gradually in the first 12h ($P < 0.05$), and then decreased briefly at 24h ($P < 0.05$) and then stabilized (Figure 2C). The content of pyruvate in hepatopancreas showed significantly high expression at 12h ($P < 0.05$) and 144h ($P < 0.05$), and the expression level in other time periods was generally the same, but still significantly higher than that at the initial stage of the experiment (Figure 2D).

3.2 DEGs analysis

The data quality of each sample in this experiment was summarized in Supplementary Material 2 and the raw data were submitted to NCBI (accession number: PRJNA1083772, https://www.ncbi.nlm.nih.gov/bioproject/PRJNA1083772). A total of 44,339,646 clean reads (93.44% of raw data) were obtained from the reference transcriptome after low quality sequences filtering by pruning the sequencing adapters/poly-N. The G and C bases in clean data accounted for 40.25~42.84%. The percentage of Q30 bases was higher than 94.29% and the radio of mapped reads was all more than 79.15%. A total of 2,777 DEGs were identified between A1 and A10 (adjusted *p*-value ≤ 0.05 and absolute log2 fold change ≥ 1), including 1,283 upregulated genes and 1494 downregulated genes after ammonia nitrogen stress (Figure 3A).

To elucidate the biochemical pathways affected by ammonia nitrogen, DEGs were mapped with KEGG database (Figure 3B). Most DEGs were related to the "lysosome", followed by "phagosome", "starch and sucrose metabolism", "DNA replication", "oxidative phosphorylation", "nucleotide metabolism" and "linoleic acid metabolism". According to the NR annotation, most DEGs were involved in phagocytosis [*hepatocyte growth factor-regulated tyrosine kinase substrate* (*HGS*) and *C-type mannose receptor 2* (*CMR2*)], apoptosis (*caspase recruitment domain* (*CARD*) and *inhibitor of apoptosis-promoting Bax1* (*BI-1*)), immune system (*interleukin-17* (*IL-17*) and *toll-like receptor* 8 (*TLR*8)), oxidative damage (*cytochrome P450* (*CYP450*) and *glutathione peroxidase* (*GPX*)) and molecular chaperones (*heat shock protein beta*-1 (*HSPβ*1), *heat shock protein 70* (*HSP70*), *heat shock protein 90* (*HSP90*)), and so on (Table 3). In addition, the genes involved in ammonia detoxification and ammonia excretion, including *glutamate pyruvate transaminase2* (*GPT2*), *xanthine dehydrogenase* (*XDH*),

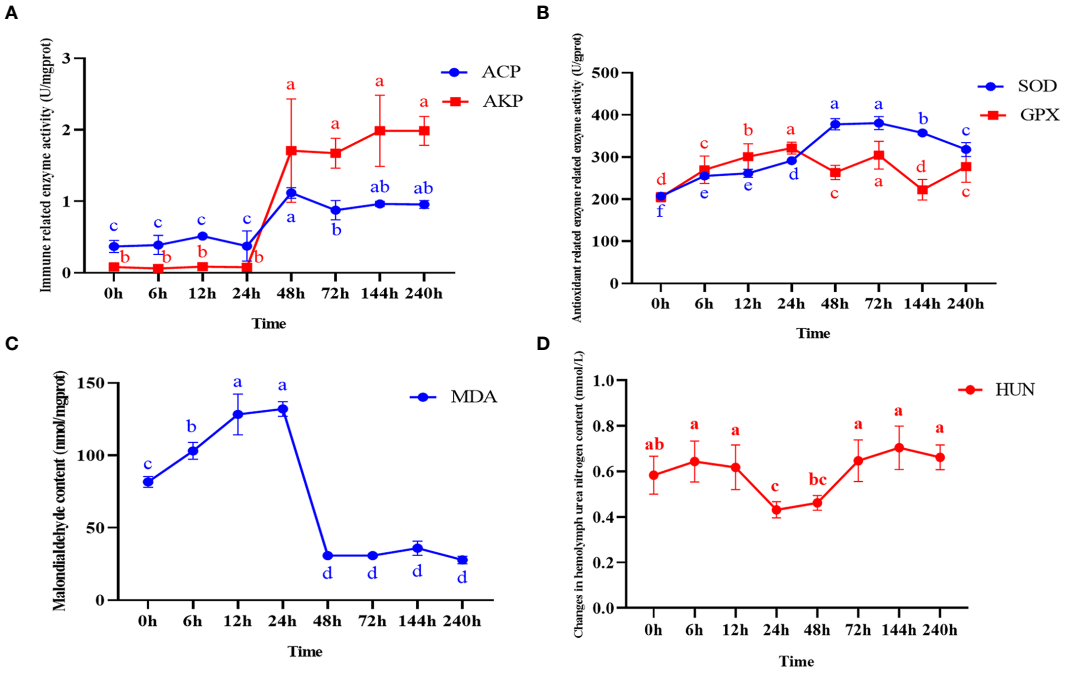

FIGURE 1
Enzyme activity and malondialdehyde content in hepatopancreas and changes in hemolymph urea nitrogen content after ammonia nitrogen stress. **(A)** Change in immune-related enzyme activity. **(B)** Antioxidant related enzyme activity changes. **(C)** Malondialdehyde content changes. **(D)** Changes in hemolymph urea nitrogen content. Values were expressed as mean ± S. **(D)** (N = 6). Data with different letters showed significant difference among tissues using one-way ANOVA ($P < 0.05$).

xanthine oxidase (*XO*), *carbonic anhydrase* (*CA*), *arginase* 1 (*Arg* 1), *ammonium transporter Rh type B* (*Rh-B*), *V-type proton ATPase* (*VHA*) and Na^+/H^+ *exchanger* (*NHE*) were also changed significantly after ammonia exposure (Table 3). In order to further validate the transcriptome data, the expression levels of seven DEGs were detected by qRT-PCR, and the results showed similar expression patterns to those of RNA-seq (Figure 4).

To further understand the biological significance of DEGs, we classified the DEGs in hepatopancreas as GO and categorized them by cellular component, molecular function and biological process (Figure 3C). Of the three GO categories, the molecular functions were the largest group, followed by biology processes and cellular components. These terms in molecular functions mainly include "hydrolase activity, acting on glycosyl bonds", "hydrolase activity, hydrolyzing O-glycosyl compounds", "serine-type peptidase activity", "serine hydrolase activity", "microtubule binding", "tubulin binding", "peptidase activity", "serine-type endopeptidase activity", "peptidase activity, acting on L-amino acid peptides" and "sulfuric ester hydrolase activity".

3.3 Differential metabolite analysis

Untargeted metabolomics technology (LC-MS/MS) was used to investigate the metabolic changes in hepatopancreas of the razor clam, and 1,393 different metabolites were identified. The PCA result showed a significant separation (account for 29.52% of the variation) on PC1 between AG and CG (Figure 5A). The PLS-DA results of AG and CG, with R2Y=0.94 and Q2Y=-0.11, showed that the AG were clearly separated from the CG, also suggesting significant changes of metabolites between these two groups (Figure 5B). According to VIP > 1.0, FC > 1.2 or FC < 0.833 and $P < 0.05$, the differential metabolites were screened. In comparison group A10 and A1, 119 metabolites were significantly different, 61 metabolites were up-regulated and 58 metabolites were down-regulated. In addition, according to the classification coefficient, the model is stable and can be used to fitness and forecast (Figure 5C).

Among these metabolites, the classes involved in "amino acid metabolism (tryptophan metabolism, histidine metabolism, tyrosine metabolism, cysteine and methionine metabolism, alanine, aspartate and glutamate metabolism, arginine biosynthesis and phenylalanine, tyrosine and tryptophan biosynthesis)", "fatty acid metabolism (biosynthesis of unsaturated fatty acids, glycerophospholipid metabolism and alpha-linolenic acid metabolism)" and "carbohydrate metabolism (glyoxylate and dicarboxylate metabolism and citrate cycle)" were overrepresented (Figure 5D). Some amino acids including arginine, proline, histidine, lysine and so on, showed obvious increased, which was a response to ammonia stress. According to the results of transcriptome and metabolome, the related metabolites such as citrulline and ornithine increase significantly in alanine-glucose cycle and urea cycle, and the expression level of related gene (*ARG*, *alanine aminotransferase* (*ALT*), etc.), changes significantly, indicating that ammonia detoxification and metabolism occur in the body of razor clam after ammonia stress (Figure 6).

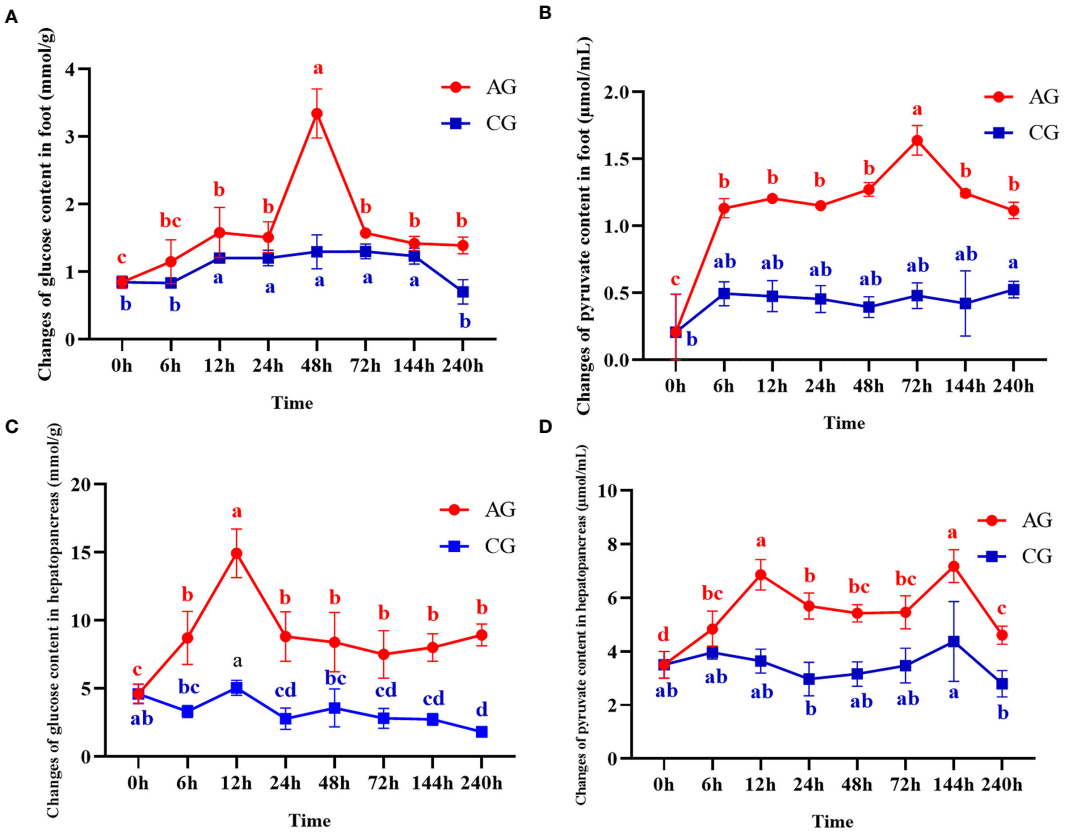

FIGURE 2
Changes of glucose and pyruvate contents after ammonia nitrogen stress. **(A)** Change of glucose content in foot. **(B)** Changes of pyruvate content in foot. **(C)** Change of glucose content in hepatopancreas. **(D)** Changes of pyruvate content in hepatopancreas. Values were expressed as mean ± S. **(D)** (N = 6). Data with different letters showed significant difference among tissues using one-way ANOVA ($P < 0.05$).

4 Discussion

The high concentration of ammonia nitrogen in aquaculture water is a serious threat to the life and safety of aquatic organisms. Here, the studies investigated the toxicity of ammonia to marine aquatic invertebrates, such as Asian clam (*Corbicula fluminea*) (Zhang et al., 2019), Manila clam (*Ruditapes philippinarum*) (Cong et al., 2021), Chinese mitten crab (*Eriocheir sinensis*) (Wang et al., 2021) and Pacific white shrimp (*Litopenaeus vannamei*) (Cui et al., 2022). Among them, in our previous studies, the toxicity and tolerant mechanism to ammonia nitrogen in the razor clam were also discussed (Zhang et al., 2020a; Sun et al., 2021b; Hu et al., 2023), but there was no comprehensive and complete molecular mechanism to explain its high tolerance to ammonia nitrogen. In the current study, a combination of transcriptome, metabolome and physiological indicators were used to explore the molecular response mechanism of the razor clam to ammonia stress. Understanding the toxic mechanism of ammonia to the mollusks represented by razor clam is of great significance for marker-assisted breeding and breeding of ammonia-tolerant variety in the razor clam.

4.1 Ammonia nitrogen stress causes oxidative stress, enhances immune response and affects ion transport

Lysosomes are organelles that receive and degrade macromolecules through endocytosis, phagocytosis and autophagy (Luzio et al., 2007). The phagocytosis of phagosomes plays an important role as an immune barrier against the entry of foreign harmful substances into the body. Exposure to 2.0 mg/L ammonia nitrogen for one week significantly reduced lysosomal integrity (up to 33%) in green-lipped mussel (*Perna viridis*) (Fang et al., 2008). Likewise, studies in *R. philippinarum* have shown that ammonia exposure could significantly reduce the integrity of lysosomes in a dose-dependent manner (Cong et al., 2017). In addition, studies on rockfish (*Sebastes schlegelii*) have also confirmed that ammonia exposure significantly reduces phagocytosis and lysosome activity (Kim et al., 2015). In this study, there were significantly changes in the lysosome and phagosome pathways (most of which were reduced in gene expression), which may further demonstrate the disruption of immune defenses following ammonia stress. Comparative

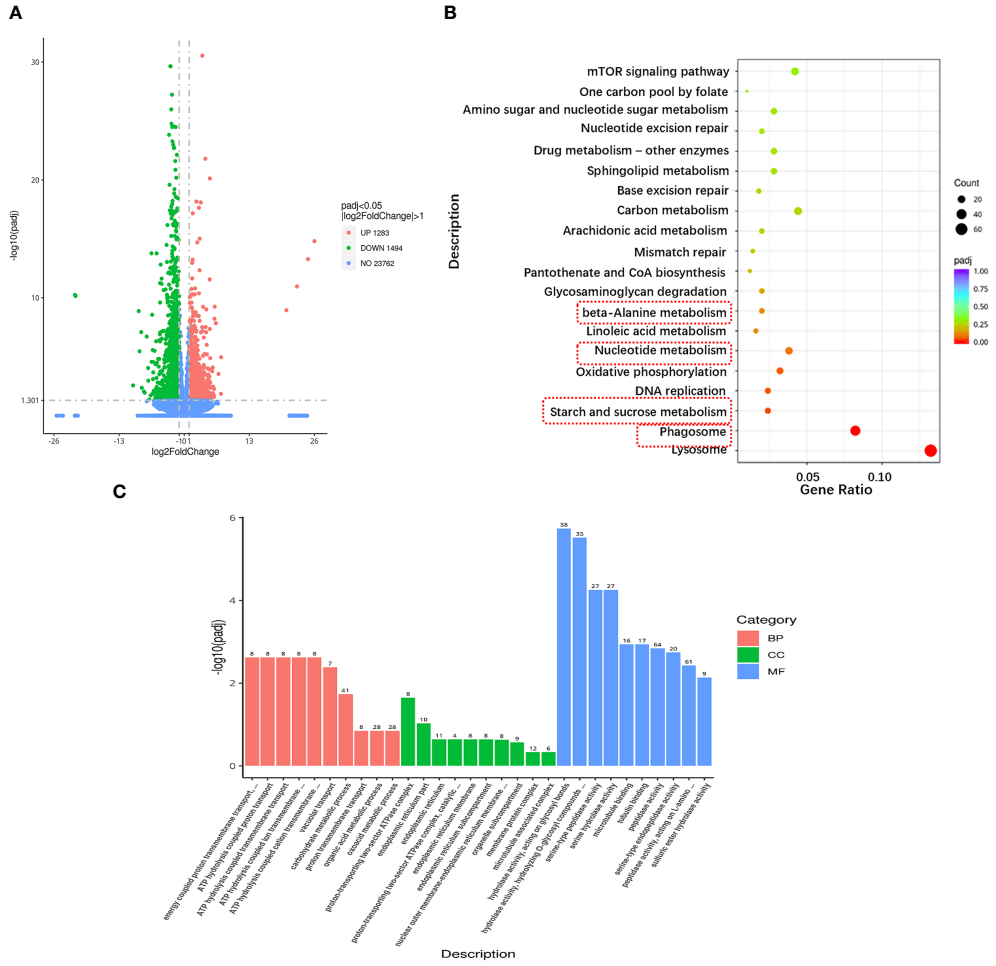

FIGURE 3
Transcriptional changes in hepatopancreas of the razor clam under ammonia nitrogen stress. **(A)** The volcano plot showing gene expression in hepatopancreas of the razor clam after ammonia nitrogen stress. Red and green dots represent significantly upregulated and downregulated genes, grey dots indicate no significant difference. **(B)** KEGG pathway enrichment analysis of the DEGs between A1 and A10. **(C)** GO enrichment analysis of the DEGs between A1 and A10.

transcriptomic analysis showed significant changes in several immune-related genes such as *interleukin-17*, *toll-like receptor 8*, *toll-like receptor tollo* and *AKP*. Similarly, in physiological experiments, the activity of AKP and ACP were also increased significantly in the comparison between A10 and A1. We speculated that the increased expression of immune-related genes is related to the destruction of the immune system of razor clam after prolonged exposure to ammonia, and similar studies have also confirmed this conjecture (Cui et al., 2017; Qi et al., 2017; Zhang et al., 2018).

Oxidative stress was one of the causes of cytotoxicity in aquatic animals caused by environmental stress such as temperature and ammonia (Zhang et al., 2020b). In this study, the activity of SOD increased due to ammonia exposure, while the activity of GPX increased first and then decreased. SOD breaks down superoxide (O_2^-) into oxygen (O_2) and hydrogen peroxide (H_2O_2), and GPX breaks down H_2O_2 into O_2 and H_2O (Meng et al., 2021). With the extension of ammonia stress time, the increase of SOD activity can lead to the increase of H_2O_2, while the decrease of GPX activity can lead to accumulation of H_2O_2. Elevated levels of MDA after a period of ammonia exposure indicate that the accumulation of H_2O_2 levels can cause damage to lipids. Previous studies have shown that *heat shock proteins 70* (*HSP70*) and *HSP90* can play an important role in protecting the body from oxidative stress under environmental stress conditions (Liang et al., 2020). Our study found that ammonia exposure changed the transcription levels of *HSP70* and *HSP90* genes in the razor clam, similarly to the trend of *HSP70* and *HSP90* genes in mud eel (*Takifugu obscurus*) (Hangzo et al., 2017) and Chinese strip-necked turtle (*Mauremys sinensis*) (Liang et al., 2020) when exposed to ammonia nitrogen. In addition, oxidative stress may induce DNA damage (Meng et al., 2021). The expression of two important genes, *proliferating cell nuclear antigen* (*PCNA*) and *growth arrest and DNA damage-inducible protein GADD45 alpha* (*GADD45α*), were significantly increased between A1 and A10. *PCNA* is a homologous trimer protein that can participate in different pathways of DNA repair, including nucleotide and base excision repair, as well as mismatch repair (Scovassi and Prosperi, 2006). *GADD45* family genes can regulate DNA damage in cell under various stress stimuli, and *GADD45α* is a key enzyme in the

TABLE 3 Gene expression change with KEGG pathways after ammonia exposure.

Pathway/Gene	*P* value	Log2FC	Up/Down
Phagocytosis			
Hepatocyte growth factor-regulated tyrosine kinase substrate	7.53E-21	-2.53	down
C-type mannose receptor 2	1.12E-07	1.35	up
Apoptosis			
Caspase recruitment domain	7.61E-04	1.06	up
inhibitor of apoptosis-promoting Bax1	1.22E-11	-1.28	down
Antioxidant system			
Cytochrome P450	8.46E-08	-1.68	down
Glutathione peroxidase	2.46E-08	-2.03	down
Immune system			
Interleukin-17	1.35E-09	4.38	up
Toll-like receptor 8	4.96E-04	2.45	up
Toll-like receptor Tollo	2.94E-05	5.05	up
Molecular chaperones			
Heat shock protein beta-1	4.38E-03	-1.84	down
Heat shock protein 70	5.51E-12	1.24	up
Heat shock protein 90	2.93E-07	1. 30	up
Ammonia detoxification			
Arginase-1	1.55E-03	1.52	up
Lutamate pyruvate transaminase 2	2.2E-16	1.70	up
Xanthine dehydrogenase/oxidase	2.50E-05	1.44	up
Ammonia excretion			
Carbonic anhydrase	3.05E-04	1.27	up
Ammonium transporter Rh type B	2.63E-03	2.64	up
V-type proton ATPase subunit B	1.37E-28	-1.70	down
V-type proton ATPase subunit G 1	5.53E-26	-1.45	down
V-type proton ATPase 16 kDa proteolipid subunit	4.41E-22	-1.26	down
V-type proton ATPase subunit S1	6.83E-21	-1.43	down
V-type proton ATPase catalytic subunit A	2.14E-18	-1.39	down
V-type proton ATPase subunit D	2.34E-16	-1.47	down
Na^+/H^+ exchanger	5.64E-06	-1.27	down

antioxidant defense system, and the direct interaction with other necessary replication factors can coordinate the promotion of nucleotide excision repair of damaged DNA (Siafakas and Richardson, 2009). The significant upregulation of these two genes suggests that ammonia exposure may cause DNA damage and trigger DNA repair mechanisms in the razor clam.

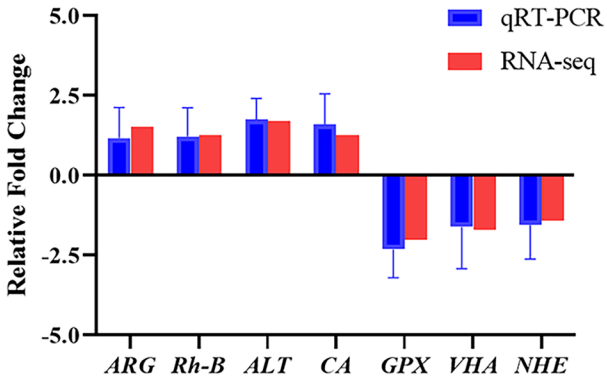

FIGURE 4
Expression of seven DEGs from the transcriptome analysis validated by qRT-PCR. Data were normalized to *RS9* as the reference and presented as a fold to validate the transcriptomic analysis results. ARG, arginase 1; Rh-B, ammonium transporter Rh type B; ALT, alanine aminotransferase; CA, carbonic anhydrase; GPX, glutathione peroxidase; VHA, V-type proton ATPase; NHE, Na^+/H^+ exchanger.

Some fish could excrete part of an ammonia load against high ambient levels. It appears that the giant mudskipper (*Periophthalmodon schlosseri*), is able to survive both high ammonia levels in the water and terrestrial exposure by actively excreting ammonium ions (Ip et al., 2001). And related studies have shown that ammonium ion clearance on the gills of giant mudskipper may be the result of a variety of ion transport genes (*NKA*, *VHA*, *CA* and *NHE*, etc.) (Randall and Tsui, 2002). While the mRNA expression levels of *VHA* and *NHE* were down-regulated in this study. This result seems unexpected, possibly because they mainly play an important role in the process of gill ammonia excretion, and similar results have been reported in crabs, other marine invertebrates and fish (Martin et al., 2011). Our previous results also confirmed that the mRNA expression levels of *VHA* and *NHE* were indeed increased in gills after ammonia nitrogen stress (Lv et al., 2022).

4.2 Correlation between ammonia tolerance and amino acid metabolism

Ammonia in fish is mainly produced by amino acid metabolism, so they can reduce the production of ammonia by reducing amino acid metabolism to prevent the increase of ammonia concentration in the body. Some fish, such as pond loach (*Misgurnus anguillicaudatus*) (Chew et al., 2001; Tsui et al., 2002) and swamp eel (*Monopterus albus*) (Ip et al., 2004), reduce the ammonia content in the body by reducing the amino acid metabolism, which is one of the effective strategies to deal with ammonia nitrogen toxicity, and this strategy does not require the participation of external energy (Chew and Ip, 2014). However, this situation also inhibits the use of amino acids as an energy source by certain aquatic animals. Therefore, some fish (e.g., *P. schlosseri*) will metabolize some amino acids while inhibiting protein hydrolysis and amino acids metabolism to ensure the energy supply of the body (Ip et al., 2001). Certain amino acids (Glutamine, Arg, His, Pro, etc.) can be converted into Glu, and Glu under the

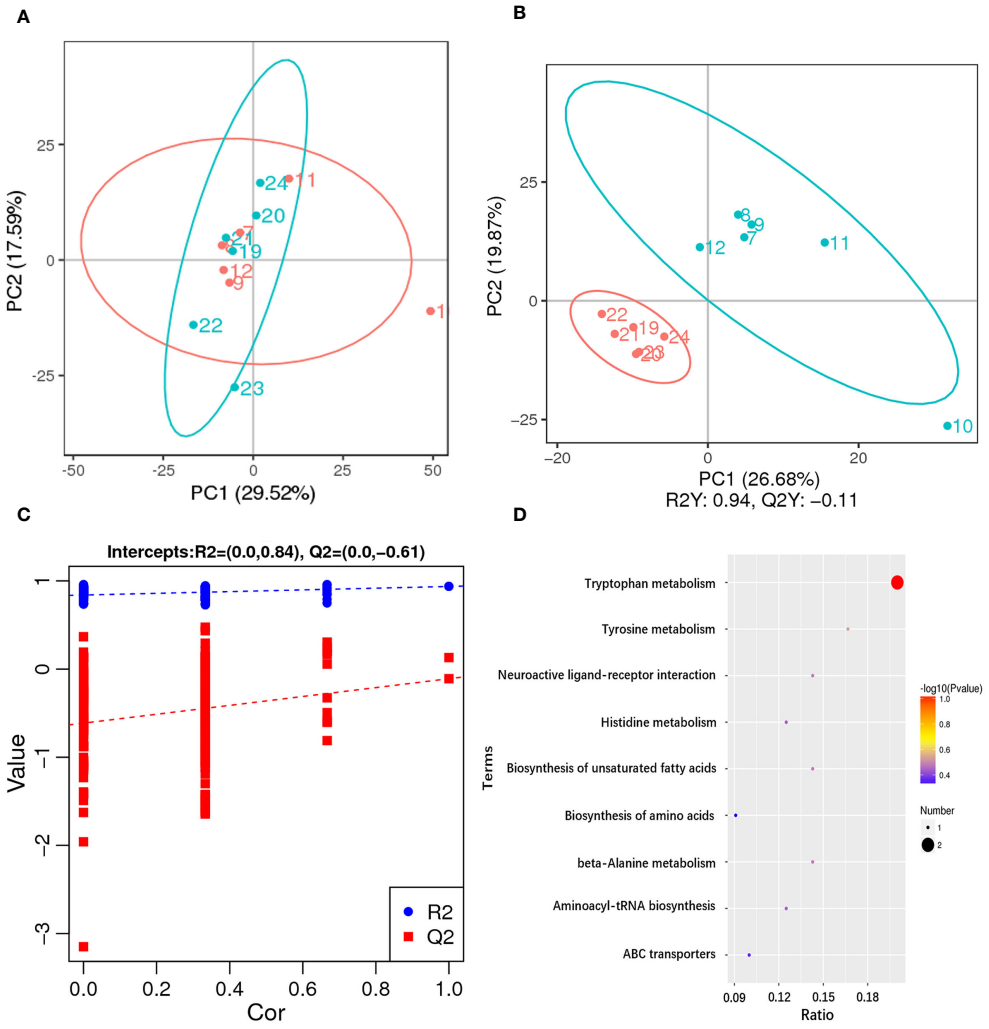

FIGURE 5
Metabolome changes in hepatopancreas of the razor clam after ammonia stress. **(A)** The PCA scores plot for the razor clam in CG (blue) and AG (red). **(B)** PLS-DA score plots for the razor clam in CG (blue) and AG (red). **(C)** PLS-DA permutation test. **(D)** KEGG enrichment analysis of differential metabolites.

action of transamination to produce α-ketoglutaric acid (α-KG), α-KG can be converted to malic acid through the Krebs cycle, malic acid is converted to pyruvate under the action of *malic enzyme*, pyruvate plus Glu under the action of *ALT* to produce Ala without the release of ammonia (Ip et al., 2001). If a continuous supply of pyruvate is available, transamination will continue to produce Ala to reduce internal contamination caused by endogenous ammonia produce in the body. In this study, amino acid metabolism in the transcriptome and metabolome of razor clam at A1 and A10 were significantly changed, and the contents of Arg, Pro, His and Lys in the differential metabolites were significantly up-regulated ($P < 0.05$), which was consistent with the content changes of Arg and Lys in the free amino acid content determination experiment. In addition, the content of Ala occupies the highest proportion in the determination of free amino acids, and it is also significantly up-regulated in A10 vs A1 ($P < 0.05$). What's more, the content of pyruvate in hepatopancreas increased significantly after ammonia nitrogen stress. In conclusion, it can be speculated that the razor clam may reduce the ammonia concentration in the body by converting endogenous ammonia to Ala through partial amino acid metabolism.

In vertebrates, when adverse conditions (limited water availability, anaerobic metabolism, etc.) increase ammonia production or impair excretion/detoxification, alanine is produced in their extrahepatic tissues and is consumed within the liver as an NH_4^+ carrier as part of alanine-glucose cycle (also referred to as the Cahill cycle, Felig et al., 1970; Felig, 1973). In this cycle, glucose in the extrahepatic tissues is glycolyzed to produce pyruvate, which is then transaminated by *ALT* to form alanine. The newly synthesized alanine enters the liver with the blood for deamination, and the free ammonia is excreted through the urea cycle. The pyruvate in liver cells is converted to glucose by gluconeogenesis, and then transported to muscle by blood circulation, and then decomposed to produce pyruvate (Felig et al., 1970; Felig, 1973). In the present study, transcriptome results showed that the expression of genes related to glycogen metabolism (e.g., *hexokinase*, *enolase 4*, *phosphoglucomutase* and *trehalase*) was significantly upregulated

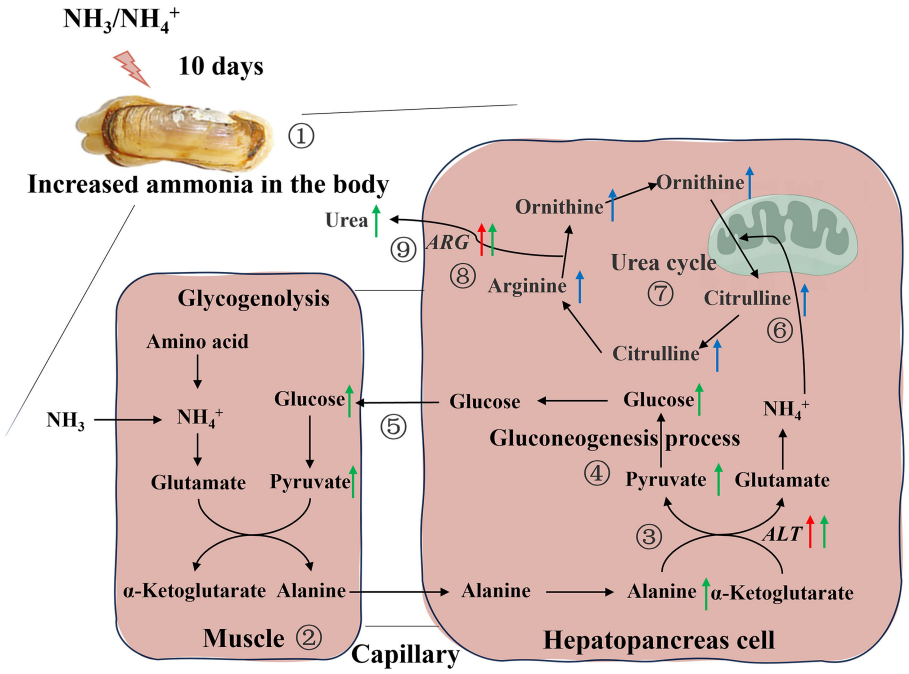

FIGURE 6
Schematic overview of the alteration in physiological parameters, transcriptome and metabolome in hepatopancreas of the razor clam after ammonia stress. Red, blue and green arrows represent changes in genes, metabolites, and physiological parameters, respectively. 1. The razor clam was exposed to ~46mg/L ammonia nitrogen environment for 10days, and the increase of stress time leads to an increase ammonia in the body; 2. In muscle cell, glucose was produced by glycolysis to pyruvate, and further to alanine; 3. Alanine enters the hepatopancreas through the hemolymph and was catalyzed by *alanine aminotransferase* (*ALT*) to produce pyruvate and glutamate; 4. Pyruvate was converted to glucose during gluconeogenesis process, which was reused by tissues and muscles; 5. The glucose from the hepatopancreas re-enters in the muscle cells and notably that four pathways, 2, 3, 4 and 5, constitute the alanine-glucose cycle; 6, 7, 8. The ammonia produced by glutamate metabolism in the alanine-glucose cycle enters the urea cycle and activates this cycle (the content of arginine and citrulline were significantly changed, and the mRNA expression of *arginase* (*ARG*) and hemolymph urea nitrogen were increased).

in the comparison of A1 and A10 ($P < 0.05$). Interestingly, the expression levels of *ALT* and *ARG* genes were also significantly up-regulated in A1 and A10 ($P < 0.05$, this was confirmed by subsequent qRT-PCR results). Combined with the differential metabolites of A1 and A10, it was found that arginine, ornithine, citrulline and other metabolites related to urea cycle increased. Based on the above findings, it can be inferred that the body of razor clam may also reduce the accumulation of ammonia through the alanine-glucose cycle and urea cycle. To verify this hypothesis, the content of glucose, pyruvate in hepatopancreas and foot and HUN were measures after ammonia nitrogen stress. The results showed that the contents of glucose, pyruvate and HUN in different tissues increased significantly after ammonia nitrogen stress ($P < 0.05$). Similar results were found in mangrove crab (*Helice formosensis*), which may use a combination of urea cycle and ammonia detoxification to maintain nitrogen homeostasis in the presence of adverse factors (Allen et al., 2021). In addition, one study in Asian seabass (*Lates calcariffer*) also found a reciprocal relation between the muscle and liver of the fish to remove excess ammonia (Jahanbani et al., 2023). Based on our previous experimental results (including the functional verification of *glutamate dehydrogenase*, *glutamine synthetase* and *glutaminase* after ammonia nitrogen stress) (Zhang et al., 2020a; Sun et al., 2021a, Sun et al., 2021b; Lv et al., 2022), we hypothesized that the alanine-glucose cycle and synthesis of glutamine in the muscles and hepatopancreas of the razor clam manages and detoxify the increased ammonia by activating a number of enzymes and the urea cycle.

In conclusion, this study investigated the toxicity of hepatopancreas to ammonia and the tolerance mechanism of ammonia in the razor clam under ~46mg/L ammonia nitrogen stress for 1 and 10 days by means of physiological indicators, transcriptome and metabolome methods. The results showed that exposure to ammonia nitrogen could significantly reduce phagocytosis and lysosomal activity of razor clam, induce oxidative stress and activate innate immune response. Faced with the challenge of ammonia stress, the razor clam takes active measures to deal with and resist the toxic reaction caused by the increase of ammonia nitrogen stress time. According to our experimental results, the convert endogenous ammonia to alanine, the enhancement of alanine-glucose cycle and urea synthesis may be the possible mechanisms for the tolerance of razor clam to ammonia nitrogen. These results provide a new perspective for understanding the tolerance mechanism of ammonia nitrogen in benthic bivalves.

Data availability statement

The datasets presented in this study can be found in online repositories. The names of the repository/repositories and accession number(s) can be found in the article/Supplementary Material.

Ethics statement

The animal study was approved by Institutional Animal Care and Use Committee (IACUC) of Zhejiang Wanli University, China. The study was conducted in accordance with the local legislation and institutional requirements.

Author contributions

GS: Data curation, Validation, Writing – original draft. LL: Funding acquisition, Writing – review & editing. HY: Funding acquisition, Writing – review & editing. ZL: Funding acquisition, Writing – review & editing. NX: Methodology, Writing – review & editing. YD: Methodology, Visualization, Writing – review & editing.

Funding

The author(s) declare financial support was received for the research, authorship, and/or publication of this article. This work was supported by National Natural Science Foundation of China (32202918), Key Scientific and Technological Grant of Zhejiang for Breeding New Agricultural Varieties (2021C02069–7), Ningbo Major Project of Science and Technology (2021Z114) and National Marine Genetic Resource Center Program.

Conflict of interest

The authors declare that the research was conducted in the absence of any commercial or financial relationships that could be construed as a potential conflict of interest.

Publisher's note

All claims expressed in this article are solely those of the authors and do not necessarily represent those of their affiliated organizations, or those of the publisher, the editors and the reviewers. Any product that may be evaluated in this article, or claim that may be made by its manufacturer, is not guaranteed or endorsed by the publisher.

Supplementary material

The Supplementary Material for this article can be found online at: https://www.frontiersin.org/articles/10.3389/fmars.2024.1444929/full#supplementary-material

References

Allen, G. J. P., Wang, M. C., Tseng, Y. C., and Weihrauch, D. (2021). Effects of emersion on acid-base regulation, osmoregulation, and nitrogen physiology in the semi-terrestrial mangrove crab, *Helice formosensis*. *J. Comp. Physiol. B.* 191, 455–468. doi: 10.1007/s00360-021-01354-0

Bernasconi, C., and Uglow, R. J. (2011). Purineolytic capacity response of *Nephrops norvegicus* to prolonged emersion: an ammonia detoxification process. *Aquat. Biol.* 11, 263–270. doi: 10.3354/ab00320

Chen, J., Huang, H., Xu, H., He, H., and Fan, W. (2010). Ammonia effects the survival and the energy budget of clam *Meretrix meretrix*. *Mar. Sci.* 34, 40–46. doi: 10.3724/SP.J.1077.2010.01263

Chew, S. F., and Ip, Y. K. (2014). Excretory nitrogen metabolism and defence against ammonia toxicity in air-breathing fishes. *J. Fish Biol.* 84, 603–638. doi: 10.1111/jfb.12279

Chew, S. F., Jin, Y., and Ip, Y. K. (2001). The loach *Misgurnus anguillicaudatus* reduces amino acid catabolism and accumulates alanine and glutamine during aerial exposure. *Physiol. Biochem. Zoology.* 74, 226–237. doi: 10.1086/319663

Cong, M., Li, Y., Xu, H., Lv, J., Wu, H., and Zhao, Y. (2021). Ammonia nitrogen exposure caused structural damages to gill mitochondria of clam *Ruditapes philippinarum*. *Ecotoxicology Environ. Safety.* 222, 112528. doi: 10.1016/j.ecoenv.2021.112528

Cong, M., Wu, H., Cao, T., Ji, C., and Lv, J. (2019). Effects of ammonia nitrogen on gill mitochondria in clam *Ruditapes philippinarum*. *Environ. Toxicoloogy Pharmacol.* 65, 46–52. doi: 10.1016/j.etap.2018.12.003

Cong, M., Wu, H., Yang, H., Zhao, J., and Lv, J. (2017). Gill damage and neurotoxicity of ammonia nitrogen on the clam *Ruditapes philippinarum*. *Ecotoxicology.* 26, 459–469. doi: 10.1007/s10646-017-1777-4

Cui, Y., Ren, X., Li, J., Zhai, Q., Feng, Y., Xu, Y., et al. (2017). Effects of ammonia-N stress on metabolic and immune function via the neuroendocrine system in *Litopenaeus vannamei*. *Fish Shellfish Immunol.* 64, 270–275. doi: 10.1016/j.fsi.2017.03.028

Cui, Y., Zhao, N., Wang, C., Long, J., Chen, Y., Deng, Z., et al. (2022). Acute ammonia stress-induced oxidative and heat shock responses modulated by transcription factors in *Litopenaeus vannamei*. *Fish Shellfish Immunol.* 128, 181–187. doi: 10.1016/j.fsi.2022.07.060

Dong, Y., Zeng, Q., Ren, J., Yao, H., Lv, L., He, L., et al. (2020). The chromosome-level genome assembly and comprehensive transcriptomes of the razor clam (*Sinonovacula constricta*). *Front. Genet.* 11. doi: 10.3389/fgene.2020.00664

Edwards, S. L., Arnold, J., Blair, S. D., Pray, M., Bradley, R., Erikson, O., et al. (2015). Ammonia excretion in the Atlantic hagfish (*Myxine glutinosa*) and responses of an Rhc glycoprotein. *Am. J. Physiology-Regulatory Integr. Comp. Physiol.* 308, R769–R778. doi: 10.1152/ajpregu.00355.2014

Fang, J. K., Wu, R. S., Chan, A. K., Yip, C. K., and Shin, P. K. (2008). Influences of ammonia-nitrogen and dissolved oxygen on lysosomal integrity in green-lipped mussel *Perna viridis*: laboratory evaluation and field validation in Victoria harbour, Hongkong. *Mar. pollut. Bulletin.* 56, 2052–2058. doi: 10.1016/j.marpolbul.2008.08.003

Felig, P. (1973). The glucose-alanine cycle. *Metabolism* 22, 179–207. doi: 10.1016/0026-0495(73)90269-2

Felig, P., Pozefsky, T., Marliss, E., and Cahill, G. F. Jr. (1970). Alanine: key role in gluconeogenesis. *Science.* 167, 1003–1004. doi: 10.1126/science.167.3920.1003

Ge, H., Liang, X., Liu, J., Cui, Z., Guo, L., Li, L., et al. (2021). Effects of acute ammonia exposure on antioxidant and detoxification metabolism in clam *Cyclina sinensis*. *Ecotoxicology Environ. Safety.* 15, 211:111895. doi: 10.1016/j.ecoenv.2021.111895

Hangzo, H., Banerjee, B., Saha, S., and Saha, N. (2017). Ammonia stress under high environmental ammonia induces Hsp70 and Hsp90 in the mud eel, *Monopterus cuchia*. *Fish Physiol. Biochem.* 43, 77–88. doi: 10.1007/s10695-016-0269-4

Hong, M., Chen, L., Sun, X., Gu, S., Zhang, L., and Chen, Y. J. (2007). Metabolic and immune responses in Chinese mitten-handed crab (*Eriocheir sinensis*) juveniles exposed to elevated ambient ammonia. *Comp. Biochem. Physiol. Part C: Toxicol. Pharmacol.* 145, 363–369. doi: 10.1016/j.cbpc.2007.01.003

Hu, C., Dai, W., Zhu, X., Yao, H., Lin, Z., Dong, Y., et al. (2023). Expression and functional analysis of *AMT1* gene responding to high ammonia stress in razor clam (*Sinonovacula constricta*). *Anim. (Basel).* 13, 1638. doi: 10.3390/ani13101638

Ip, Y. K., and Chew, S. F. (2010). Ammonia production, excretion, toxicity, and defense in fish: a review. *Front. Physiol.* 1. doi: 10.3389/fphy.2010.00134

Ip, Y. K., Lim, C. B., Chew, S. F., Wilson, J. M., and Randall, D. J. (2001). Partial amino acid catabolism leading to the formation of alanine in *Periophthalmodon schlosseri* (mudskipper): a strategy that facilitates the use of amino acids as the energy source during locomotory activity on land. *J. Exp. Biol.* 204, 1615–1624. doi: 10.1242/jeb.204.9.1615

Ip, Y. K., Tay, A. S., Lee, K. H., and Chew, S. F. (2004). Strategies for surviving high concentrations of environmental ammonia in the swamp eel *Monopterus albus*. *Physiol. Biochem. Zoology.* 77, 390–405. doi: 10.1086/383510

Jahanbani, A., Shahriari, A., and Mohammadian, T. (2023). Ureagenesis of Asian seabass (*Lates calcarifer*) under ammonia stress and overcrowding. *Aquaculture.* 576, 739810. doi: 10.1016/j.aquaculture.2023.739810

Kim, S. H., Kim, J. H., Park, M. A., Hwang, S. D., and Kang, J. C. (2015). The toxic effects of ammonia exposure on antioxidant and immune responses in rockfish, *Sebastes schlegelii* during thermal stress. *Environ. Toxicol. Pharmacol.* 40, 954–959. doi: 10.1016/j.etap.2015.10.006

Li, B., and Dewey, C. N. (2011). RSEM: accurate transcript quantification from RNA-Seq data with or without a reference genome. *BMC Bioinf.* 12, 323. doi: 10.1186/1471-2105-12-323

Liang, L., Huang, Z., Li, N., Wang, D., Ding, L., Shi, H., et al. (2020). Effects of ammonia exposure on antioxidant function, immune response and NF-κB pathway in Chinese strip-necked turtle (*Mauremys sinensis*). *Aquat. Toxicology.* 229, 105621. doi: 10.1016/j.aquatox.2020.105621

Liao, Y., Smyth, G. K., and Shi, W. (2014). featureCounts: an efficient general purpose program for assigning sequence reads to genomic features. *Bioinformatics.* 230, 923–930. doi: 10.1093/bioinformatics/btt656

Luzio, J. P., Pryor, P. R., and Bright, N. A. (2007). Lysosomes: fusion and function. *Nat. Rev. Mol. Cell Biol.* 8, 622–632. doi: 10.1038/nrm2217.v

Lv, L., Ren, J., Zhang, H., Sun, C., Dong, Y., and Lin, Z. (2022). Transcriptomic analysis of gill and hepatopancreas in razor clam (*Sinonovacula constricta*) exposed to acute ammonia. *Front. Mar. Science.* 9. doi: 10.3389/fmars.2022.832494

Martin, M., Fehsenfeld, S., Sourial, M. M., and Weihrauch, D. (2011). Effects of high environmental ammonia on branchial ammonia excretion rates and tissue Rh-protein mRNA expression levels in seawater acclimated Dungeness crab *Metacarcinus magister*. *Comp. Biochem. Physiol. Part A: Mol. Integr. Physiol.* 160, 267–277. doi: 10.1016/j.cbpa.2011.06.012

Meng, X., Jayasundara, N., Zhang, J., Ren, X., Gao, B., Li, J., et al. (2021). Integrated physiological, transcriptome and metabolome analyses of the hepatopancreas of the female swimming crab *Portunus trituberculatus* under ammonia exposure. *Ecotoxicology Environ. Safety.* 228, 113026. doi: 10.1016/j.ecoenv.2021.113026

Pinto, M. R., Lucena, M. N., Faleiros, R. O., Almeida, E. A., McNamara, J. C., and Leone, F. A. (2016). Effects of ammonia stress in the Amazon river shrimp *Macrobrachium amazonicum* (Decapoda, Palaemonidae). *Aquat. Toxicology.* 170, 13–23. doi: 10.1016/j.aquatox.2015.10.021

Qi, X. Z., Xue, M. Y., Yang, S. B., Zha, J. W., Wang, G. X., and Ling, F. (2017). Ammonia exposure alters the expression of immune-related and antioxidant enzymes-related genes and the gut microbial community of crucian carp (*Carassius auratus*). *Fish Shellfish Immunol.* 70, 485–492. doi: 10.1016/j.fsi.2017.09.043

Randall, D. J., and Tsui, T. K. (2002). Ammonia toxicity in fish. *Mar. pollut. Bulletin.* 45, 17–23. doi: 10.1016/S0025-326X(02)00227-8

Romano, N., and Zeng, C. (2013). Toxic effects of ammonia, nitrite, and nitrate to decapod crustaceans: a review on factors influencing their toxicity, physiological consequences, and coping mechanisms. *Rev. Fisheries Sci. Aquaculture.* 21, 1–21. doi: 10.1080/10641262.2012.753404

Scovassi, A. I., and Prosperi, E. (2006). Analysis of proliferating cell nuclear antigen (PCNA) associated with DNA. *Methods Mol. Biol.* 314, 457–475. doi: 10.1385/1-59259-973-7:457

Siafakas, A. R., and Richardson, D. R. (2009). Growth arrest and DNA damage-45 alpha (GADD45α). *Int. J. Biochem. Cell Biol.* 41, 986–989. doi: 10.1016/j.biocel.2008.06.018

Sun, G., Dong, Y., Sun, C., Yao, H., and Lin, Z. (2021b). Vital role of *glutamate dehydrogenase* gene in ammonia detoxification and the association between its SNPs and ammonia tolerance in *Sinonovacula constricta*. *Front. Physiol.* 12. doi: 10.3389/fphys.2021.664804

Sun, G., Sun, C., He, J., Yao, H., Dai, W., Lin, Z., et al. (2021a). Characterizing the role of *glutamine synthetase* gene on ammonia nitrogen detoxification metabolism of the razor clam *Sinonovacula constricta*. *Front. Mar. Science.* 8. doi: 10.3389/fmars.2021.793118

The ministry of agriculture and fishery of the People's Republic of China (2023). *Chinese fishery statistical yearbook 2023* (Beijing: China Agriculture Press).

Tsui, T. K., Randall, D. J., Chew, S. F., Jin, Y., Wilson, J. M., and Ip, Y. K. (2002). Accumulation of ammonia in the body and NH_3 volatilization from alkaline regions of the body surface during ammonia loading and exposure to air in the weather loach. *Misgurnus anguillicaudatus. J. Exp. Biol.* 205, 651–659. doi: 10.1242/jeb.205.5.651

Veauvy, C. M., McDonald, M. D., Van Audekerke, J., Vanhoutte, G., Van Camp, N., van der Linden, A., et al. (2005). Ammonia affects brain nitrogen metabolism but not hydration status in the gulf toadfish (*Opsanus beta*). *Aquat. Toxicol.* 74, 32–46. doi: 10.1016/j.aquatox.2005.05.003

Wang, T., Yang, C., Zhang, T., Liang, H., Ma, Y., Wu, Z., et al. (2021). Immune defense, detoxification, and metabolic changes in juvenile *Eriocheir sinensis* exposed to acute ammonia. *Aquat. Toxicology.* 240, 105989. doi: 10.1016/j.aquatox.2021.105989

Want, E. J., Masson, P., Michopoulos, F., Wilson, I. D., Theodoridis, G., Plumb, R. S., et al. (2012). Global metabolic profiling of animal and human tissues via UPLC-MS. *Nat. Protoc.* 8, 17–32. doi: 10.1038/nprot.2012.135

Weihrauch, D., Ziegler, A., Siebers, D., and Towle, D. W. J. (2002). Active ammonia excretion across the gills of the green shore crab *Carcinus maenas*: participation of Na^+/K^+- ATPase, V-type H^+-ATPase and functional microtubules. *J. Exp. Biol.* 205, 2765–2775. doi: 10.1242/jeb.205.18.2765

Yu, G., Wang, L. G., and Han, Y. (2012). clusterProfiler: an R package for comparing biological themes among gene clusters. *Omics.* 16, 284–287. doi: 10.1089/omi.2011.0118

Zhang, M., Li, M., Wang, R., and Qian, Y. (2018). Effects of acute ammonia toxicity on oxidative stress, immune response and apoptosis of juvenile yellow catfish *Pelteobagrus fulvidraco* and the mitigation of exogenous taurine. *Fish Shellfish Immunol.* 79, 313–320. doi: 10.1016/j.fsi.2018.05.036

Zhang, H., Sun, G., Lin, Z., Yao, H., and Dong, Y. (2020a). The razor clam *Sinonovacula constricta* uses the strategy of conversion of toxic ammonia to glutamine in response to high environmental ammonia exposure. *Mol. Biol. Rep.* 47, 9579–9593. doi: 10.1007/s11033-02006018-w

Zhang, T., Yan, Z., Zheng, X., Fan, J., Wang, S., Wei, Y., et al. (2019). Transcriptome analysis of response mechanism to ammonia stress in Asian clam (*Corbicula fluminea*). *Aquat. Toxicology.* 214, 105235. doi: 10.1016/j.aquatox.2019.105235

Zhang, T., Yan, Z., Zheng, X., Wang, S., Fan, J., and Liu, Z. (2020b). Effects of acute ammonia toxicity on oxidative stress, DNA damage and apoptosis in digestive gland and gill of Asian clam (*Corbicula fluminea*). *Fish Shellfish Immunol.* 99, 514–525. doi: 10.1016/j.fsi.2020.02.046

Zhao, X., Fu, J., Jiang, L., Zhang, W., Shao, Y., Jin, C., et al. (2018). Transcriptome-based identification of the optimal reference genes as internal controls for quantitative RT-PCR in razor clam (*Sinonovacula constricta*). *Genes Genomics* 40, 603–613. doi: 10.1007/s13258-018-0661-9

Zhao, M., Yao, D., Li, S., Zhang, Y., and Aweya, J. J. (2020). Effects of ammonia on shrimp physiology and immunity: a review. *Rev. Aquaculture.* 12, 2194–2211. doi: 10.1111/raq.12429

Zhu, J., Xu, H., Zou, Z., Yao, H., Lin, Z., and Dong, Y. (2024). Effects of medium- and long-term high-salinity environments on free amino acid content and related genes of. *Sinonovacula constricta. Front. Mar. Sci.* 11. doi: 10.3389/fmars.2024.1368952

frontiers | Frontiers in Marine Science

TYPE Original Research
PUBLISHED 08 August 2024
DOI 10.3389/fmars.2024.1453516

OPEN ACCESS

EDITED BY
Yiming Li,
Fishery Machinery and Instrument Research Institute, China

REVIEWED BY
Xiaochen Yuan,
Anhui Agricultural University, China
Shan He,
Huazhong Agricultural University, China

*CORRESPONDENCE
Zheng-Yong Wen
zhengyong_wen@126.com
Qiong Shi
shiqiong@szu.edu.cn;
shiqiong@genomics.cn

†These authors have contributed equally to this work

RECEIVED 23 June 2024
ACCEPTED 23 July 2024
PUBLISHED 08 August 2024

CITATION
Zhou B, Wei X-Y, Wen Z-Y, Wang B, Zhao Y-Y, Zeng W-H, He Y, Prathomya P, Lv Y-Y, Li Y-P, Wang J, Li R, Li X-G, Zhou J, Zhang S-Y, Fan J-D and Shi Q (2024) Molecular characterization of *fad6* gene and its transcriptional changes in response to different initial diets and nutritional status in yellow catfish (*Pelteobagrus fulvidraco*). *Front. Mar. Sci.* 11:1453516. doi: 10.3389/fmars.2024.1453516

Molecular characterization of *fad6* gene and its transcriptional changes in response to different initial diets and nutritional status in yellow catfish (*Pelteobagrus fulvidraco*)

Bo Zhou[1†], Xiu-Ying Wei[2,3†], Zheng-Yong Wen[2,3,4,5*], Bin Wang[1], Yu-Ying Zhao[2,3], Wan-Hong Zeng[2,4], Yu He[2,4], Panita Prathomya[6], Yun-Yun Lv[2,3,5], Yan-Ping Li[2,3,5], Jun Wang[2,3], Rui Li[2,3], Xu-Guang Li[7], Jun Zhou[7], Shi-Yong Zhang[7], Jun-De Fan[8] and Qiong Shi[2,3,5,9*]

[1]Fisheries Research Institute, Sichuan Academy of Agricultural Sciences, Yibin, China, [2]Key Laboratory of Sichuan Province for Fishes Conservation and Utilization in the Upper Reaches of the Yangtze River, Neijiang Normal University, Neijiang, China, [3]College of Life Science, Neijiang Normal University, Neijiang, China, [4]School of Animal Science, Yangtze University, Jingzhou, China, [5]Shenzhen Key Lab of Marine Genomics, Guangdong Provincial Key Lab of Molecular Breeding in Marine Economic Animals, BGI Academy of Marine Sciences, BGI Marine, Shenzhen, China, [6]Department of Animal and Aquatic Sciences, Faculty of Agriculture, Chiang Mai University, Chiang Mai, Thailand, [7]National Genetic Breeding Center of Channel Catfsh, Freshwater Fisheries Research Institute of Jiangsu Province, Nanjing, China, [8]Yueyang Yumeikang Biotechnology Co., Ltd., Yueyang, China, [9]Laboratory of Aquatic Genomics, College of Life Sciences and Oceanography, Shenzhen University, Shenzhen, China

Fatty acid desaturases (FADs) are rate-limiting enzymes for the biosynthesis of highly unsaturated fatty acids (HUFAs). As a new member of the FAD family, Fad6 and its roles remain unclear in various teleost fishes. In this study, we identified a *fad6* gene from yellow catfish (yc*fad6*) and determined its spatiotemporal expression patterns and responses to different initial diets and nutritional status in yellow catfish. Our results showed that the open reading frame (ORF) of yc*fad6* was 1,080 bp in length, encoding a protein of 359 amino acids. Multiple protein sequences alignment proved that *fad6* is highly conserved among diverse vertebrates. Meanwhile, phylogenetic analysis revealed that Southern catfish and yellow catfish were clustered into one branch, supporting evolutionary consistence between the *fad6* gene and fish morphology. Moreover, comparisons of genomic synteny and gene structure revealed functional and evolutionary conservation of the *fad6* gene in various teleost fishes. Tissue distribution analysis by quantitative RT-PCR demonstrated that the yc*fad6* gene was extensively expressed in examined tissues, with higher transcription levels in the heart and liver. Meanwhile, yc*fad6* gene was widely expressed in various developmental stages, indicating Fad6 may play important roles in HUFA biosynthesis at early developmental stages in yellow catfish. Functional experiments verified that the transcription of yc*fad6* decreased significantly with the extension of feeding time (with egg yolk or *Artemia nauplii*) at the early developmental stages, indicating that a diet rich in HUFA can remarkably inhibit the transcription of yc*fad6* in yellow catfish. In addition, yc*fad6*

transcription was significantly reduced after a short-term (24-h) or long-term food deprivation (1-week) and then continued to decrease during refeeding, suggesting that nutritional states can affect the transcription of yc*fad6*, which further regulates the metabolism of HUFAs. Anyway, these fundamental findings provide basic references for further investigating evolutionary and physiological functions of the *fad6* gene in yellow catfish as well as in other teleost fishes.

KEYWORDS

yellow catfish, *fad6*, HUFA biosynthesis, gene expression, nutritional regulation

Introduction

Highly unsaturated fatty acids (HUFAs) are essential for promotion of normal growth and development in various organisms, and play important roles in maintaining the structure and function of cell membranes, energy metabolism signal transduction, and other physiological activities (Awada et al., 2013; Muhlhausler and Ailhaud, 2013; Nayak et al., 2017). Representative HUFAs, such as docosahexaenoic acid (DHA, 22:6n-3), eicosapentaenoic acid (EPA, 20:5n-3), and arachidonic acid (ARA, 20:4n-6), are critical fatty acids with important roles in fatty acids metabolism, maintaining cell membrane integrity and fluidity, eicosanoid synthesis, inflammation, and cell division signaling and regulation (Kuah et al., 2016; Lopes-Marques et al., 2018). HUFAs are mainly obtained from diets, and fish meat is the primary source of HUFAs consumption for human (Li et al., 2019a, 2020; Xie et al., 2021). Indeed, fishes usually have the capacity to biosynthesize HUFAs through a series of desaturation and elongation reactions from several C_{18} PUFA precursors, such as α-linolenic acid (ALA, 18:3n-3) and linoleic acid (LA, 18:2n-6) (Monroig et al., 2011; Zou et al., 2019). These reactions are mainly regulated by two rate-limiting enzymes, namely elongases of very long chain fatty acids (Elovls) and fatty acid desaturases (Fads) (Zeng et al., 2023). The former can prolong the carbon chain of fatty acids, while the latter can introduce an unsaturated double bond between two specific carbon atoms (Li et al., 2010; Wen et al., 2020).

Fatty acid desaturases (FADs) have been widely reported in plants and animals, and they play important roles in maintaining the structure and function of biofilms (Xie et al., 2021; Halim et al., 2022). In general, two different Fad-like desaturases have been identified in mammals, including FAD1 (Δ5 desaturase) and FAD2 (Δ6 desaturase) (Guillou et al., 2010). Differently, *fad1* gene is only found in cartilaginous fish and early evolutionary fish (such as sea chubs), but *fad2* gene is widely identified in almost all teleost fishes (Castro et al., 2016; Dong et al., 2018; Lopes-Marques et al., 2018). Interestingly, teleost usually contain variable number of *fad2* gene in various species, such as one copy in zebrafish (*Danio rerio*) (Blahova et al., 2022), two copies in rabbitfish (*Siganus canaliculatus*) (Li et al., 2010; Dong et al., 2018; Li et al., 2019b), three copies in Nile tilapia (*Oreochromis niloticus*) (Castro et al., 2016; Chen et al., 2018; Dong et al., 2018; Jangprai and Boonanuntanasarn, 2018) or even four copies in Atlantic salmon (*Salmo salar*) (Hastings et al., 2004; Monroig et al., 2010). However, some species such as the pufferfish (*Takifugu rubripes*) and spotted green pufferfish (*Tetraodon nigroviridis*) do not have any *fad* genes (Castro et al., 2016; Dong et al., 2018). The various copies of *fad2* gene in different fish species may be caused by the whole-genome duplication events occurred in teleost (Li et al., 2020; Wen et al., 2020). Recently, a new member of the *fad* gene family (*fad6*) has been identified and it is shown to be widespread in vertebrates. The teleost *fad6* gene was firstly cloned and characterized in golden pompano (*Trachinotus ovatus*), and functional experiments demonstrated that this Fad6 desaturase owns capacity of Δ8/Δ5/Δ4 enzyme activities and thus participates in endogenous synthesis of HUFAs (Zhu et al., 2018). However, the exact roles of Fad6 are still rarely unknown in teleost, and therefore more studies are required to resolve these issues.

Yellow catfish (*Pseudobagrus fulvidraco*), belonging to the order Siluriformes and the family Bagridae, is a benthic omnivorous fish that commonly found in freshwater (Wei et al., 2023). Due to its high nutritional value and good taste, yellow catfish has been widely cultured in Asian countries, especially in China (Liu et al., 2019). Thus far, numerous studies have focused on various aspects such as breeding habits, developmental biology, lipid metabolism, and toxicology in yellow catfish (Yang et al., 2010; Liu et al., 2019; Fang et al., 2020). Meanwhile, several live prey species enriched with HUFAs (such as cladoceran) or artificial feeds containing HUFAs (such as egg yolk) are commonly used as initial diets in cultivation of yellow catfish industry (Wei et al., 2014; Zhou et al., 2016). Regarding HUFAs biosynthesis, *fad2* and *elovl5* genes were cloned and their transcriptional regulation by leptin system was determined (Song et al., 2015). Additionally, a teleost-specific fatty acid elongase (*elovl8*) gene was identified in yellow catfish, and its potential roles in HUFAs biosynthesis and fatty acids metabolism were investigated (Zeng et al., 2023). However, the structural and functional characteristics of the *fad6* gene involved in HUFAs biosynthesis are still unknown in yellow catfish. In the present study, the *fad6* gene was identified in yellow catfish

(yc*fad6*), and then its molecular and evolutionary properities were characterized. Meanwhile, the spatio-temporal expression patterns of the yc*fad6* gene were also examined. Furthermore, the regulatory effects of different nutritional status on the yc*fad6* transcription were also explored. Our findings will not only offer basic data for further investigations on the physiological functions of Fad6 in teleost, but also provide novel insights into the regulatory mechanism for HUFAs synthesis in various vertebrates.

Materials and methods

Fish sampling and feeding trails

The yellow catfish (body weight = 32.6 ± 3.1g) used in this study were obtained from Neijiang Fish Farm (Neijiang, China) and were transported to net cages (1 m × 1 m × 1 m) erected in a 16-m^2 micro-flowing water fish pond in the College of Life Sciences at Neijiang Normal University (Neijiang, China). Fishes were kept in the cages under natural light and dark conditions (12 L/12 D) with a constant flow of filtered water at 24-26°C. Fishes were fed with commercial feeds (3-4% of body weight) at 19:00 every day. Fishes were acclimated to these conditions for 2 weeks before the formal experiments, showing a normal feeding pattern during this acclimation period.

After acclimation, five fishes were randomly selected for tissue distribution studies. These fishes were anesthetized on ice before decapitation, and 12 tissue samples including adipose, barbel, brain, gill, gonad, heart, intestine, kidney, liver, muscle, spleen, and stomach, were collected and immediately frozen in liquid nitrogen until use.

For the short-term food deprivation experiment, fishes were divided into five tanks (10 fishes per tank) and these fishes were fed simultaneously at 18:30, then five fishes were separately selected from each tank for sampling livers at 18:30 (0 h), 21:30 (3 h), 00:30 (6 h), 06:30 (12 h), and 18:30 (24 h) after feeding. For the long-term food deprivation experiment, fishes were assigned to three experimental tanks (marked with A, B, and C groups; 10 fishes per tank; A group was fed but B and C groups were fasted) for one week. Subsequently, five fishes were randomly selected from the B group and their livers were sampled at 18:30. Meanwhile, fishes in both A and C groups were fed at 18:30, and they were allowed to feeding for half an hour before sampling their livers at 19:00. All samples were immediately frozen in liquid nitrogen and then stored at -80°C until use.

Meanwhile, fertilized eggs of yellow catfish used in this study were obtained by artificial breeding in our laboratory at Neijiang Normal University. During incubation, the development status of embryos was observed under a microscope, and five embryos or larvae were respectively sampled at each time point including 0, 3, 6, 12, 24, 36, 48, 72, and 96 h after fertilization at the early developmental stages. Similarly, samples were frozen in liquid nitrogen and then stored at -80°C until use.

Diets with different contents of HUFAs, including *A. nauplii* or egg yolk, were separately used as larval feeds to investigate the potential effects of various diets on transcription of *fad6* in yellow catfish. The nutritional content of these diets can be observed in a previous study (Zhou et al., 2016). Meanwhile, approximately 200 larvae were randomly selected and then fed with different diets on day 4 after hatching (three parallel experiments were designed for each group). During the experiment, 25% water changes were carried out daily, the oxygenation pump was kept continuously oxygenated and the dissolved oxygen in the water was maintained above 6 mg/L. Fishes were fed at 8:00, 12:00, 16:00, and 20:00 to ensure sufficient diet supplements in the experimental tanks. The experiment was lasted for three days, and five offsprings from each tank were collected at 24, 48, and 72 h after feeding. Finally, samples were immediately frozen in liquid nitrogen and stored at -80°C.

Total RNA extraction and cDNA template preparation

About 50~100 mg liver tissues were selected for total RNA isolation with a commercial RNA extraction kit (Tiangen, Beijing, China). After validation by agarose gel electrophoresis, the RNA concentration was measured by an Agilent 2100 bioanalyzer (Musen, Shanghai, China), and then the RNA was reversely transcribed to cDNA by using the Revert Aid First Stand cDNA Synthesis Kit (Thermo Fisher Scientific, Waltham, USA) for subsequent work.

Identification of *fad6* gene in yellow catfish

Protein-similarity blast was conducted to identify the *fad6* gene from the yellow catfish genome in NCBI database using several known fish Fad6 protein sequences as queries. Then, we designed two pairs of primers (Supplementary Table 1) with the Primer Premier 5.0 software to amplify the ORF regions of yc*fad6*.

Basic cycling conditions of the PCRs were set as follows: a denaturing stage at 94°C for 30 s, gene-specific annealing at 55°C for 30 s, and an elongation stage at 72°C for 60 s, a total of 34 cycles. Subsequently, target fragments were obtained and purified for Sanger sequencing. Finally, PCR products were cloned into the pMD-19T vector (TaKaRa, Dalian, China) and then sequenced at Sangon Co. Ltd. (Guangzhou, China) to ensure accuracy of the potential *fad6* gene in yellow catfish.

Sequence comparison and evolutionary analysis of the *fad6* gene

The sequence of yc*fad6* was validated by BLAST (http://www.ncbi.nlm.nih.gov/BLAST) in the NCBI database. After validation, the Primer 5.0 software was applied to predict corresponding protein sequence. Multiple sequences alignment was conducted in MEGA11 using the MegAlign model, and the alignment results were annotated using GeneDoc 2.7 (Wei et al., 2023). Meanwhile, comparative analyses of genomic synteny and

gene structure were performed to determine the evolution pattern of *fad6* genes in teleost.

Additionally, a phylogenetic tree was constructed on the basis of the protein sequences of various teleost to investigate the evolutionary history of the *fad6* gene family. All Fad6 protein sequences used for the phylogeny construction were downloaded from the NCBI database. Details of the selected Fad6 family proteins are shown in Supplementary Table 2. The phylogeny was established with the neighbor joining (NJ) method to explore the evolutionary relationship among *fad6* gene family in vertebrates.

Quantitative real-time PCR

Total RNA was extracted from fish tissues and first-strand cDNA was synthesized in the same way as described above (in subsection 2.2). Subsequently, the mRNA level of yc*fad6* was detected by qRT-PCR on a Light Cycler Real-Time System (Roche Life Science, Indianapolis, IN, USA), and the final volume of this reaction system was maintained at 20 μL. Meanwhile, the relative expression level of mRNA was normalized with *β-actin* (Supplementary Table 1) after assessing the stability of five reference genes (*β-actin*, *GAPDH*, *EF1α*, *Tubα 1* and *18S*). Finally, the relative transcription level of *fad6* was calculated using the Pfaffl method (Yang et al., 2018; Wen et al., 2019). Sequences of the specific primers used for qRT-PCRs are provided in Supplementary Table 1.

Statistical analysis

All data are expressed as mean ± SEM (standard errors of the mean). Statistical analysis was performed with SPSS 22.0 (IBM, Armonk, NY, USA) and GraphPad Prism 7.0 (GraphPad Prism Software Inc., San Diego, CA, USA). Significant differences were calculated using the one-way analysis of variance (ANOVA) followed by Tukey's and Duncan's multiple range tests, after confirming data normality and homogeneity of variances. The difference among groups was considered as significant when $P < 0.05$.

Results

Molecular characterization of the *fad6* gene in yellow catfish

In this study, we identified the *fad6* gene from yellow catfish for the first time. The ORF of yc*fad6* was 1,080 bp, predicted to encode a protein of 359 amino acids. Multiple sequences alignment showed that protein sequences of Fad6s were unconservative in the N-terminal but were highly conserved in the core FADS-like domains including three highly conserved histidine signature motifs (HXXH, HXXXHH, HXXHH; see more details in Figure 1).

Phylogenetic analysis

In this study, a phylogenetic tree inferred by the neighbor-joining method was constructed with a series of protein sequences of vertebrate *fad6* genes, showing high bootstrap values (Figure 2). The tree was divided into two groups, including teleost and the other vertebrates. The topology also displayed that yellow catfish (*P. fulvidraco*) was clustered with channel catfish (*I. Punctatus*), striped catfish (*P. hypophthalmus*), North African catfish (*C. gariepinus*), and Southern catfish (*S. meridionalis*), and it showed the closest relationship with the Southern catfish. All clades with high scores and the tetrapods were used as the outgroup (Figure 2).

FIGURE 1
Multiple sequences alignment of Fad6 among yellow catfish and other representative teleost. Three highly conserved histidine regions (HXXH, HXXXH, HXXHH) are highlighted within black boxes. Eight conserved histidine residues are marked in red type. Membrane-FADS-like domains are underlined.

10.3389/fmars.2024.1453516

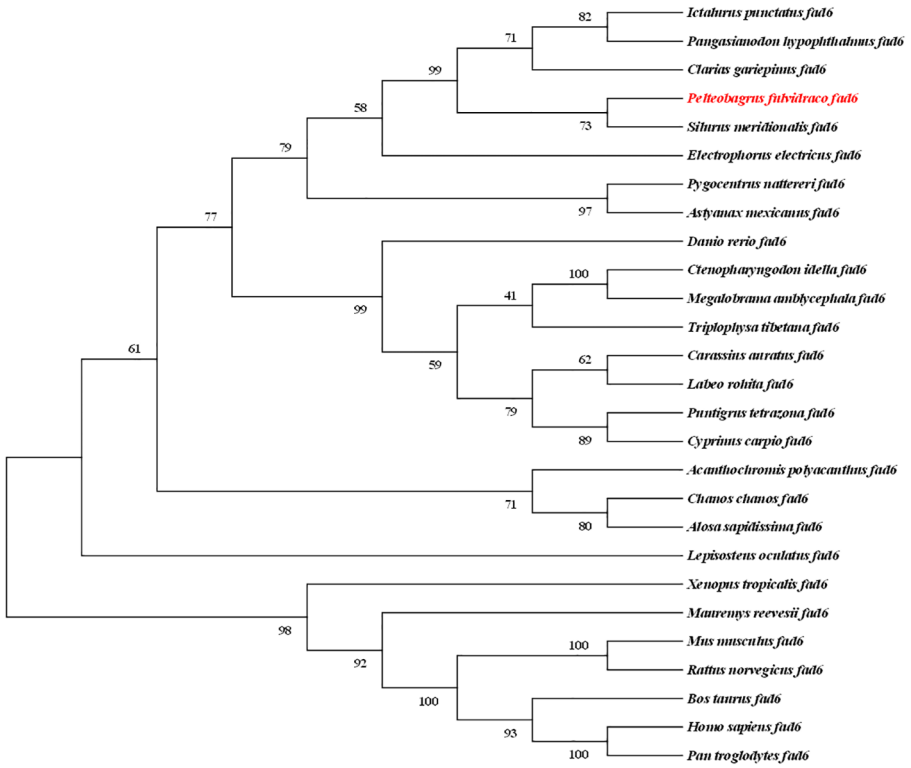

FIGURE 2
Phylogeny reveals the evolutionary history of *fad6* gene family in vertebrates. Numbers on the branches represent the reliability of this tree. Tetrapod *fad6* genes were set as the outgroup. The aimed species investigated in the present study is highlighted in red type.

Genetic synteny and gene structure comparison

Comparative genomics was conducted to investigate the genomic characteristics of the *fad6* gene in eight representative fish species. Our results revealed a highly conserved gene cluster *mrp138-fdxr-hid1b-ush1gb-fad6-trim16-tvp23b-exoc7-plaub*, which was identified in almost all the selected representative fish genomes (Figure 3). Meanwhile, a gene structure comparison of the *fad6* gene in eight fishes was also conducted. It appears that *fad6* genes in *L. rohita*, *P. tetrazona*, *C. idella*, *D. rerio*, *M. amblycephala*, *C. gariepinus* and *P. hypophthalmus* had similar gene structures, containing six exons and five introns. However, the *P. fulvidraco fad6* contained seven exons and six introns, although it shared a

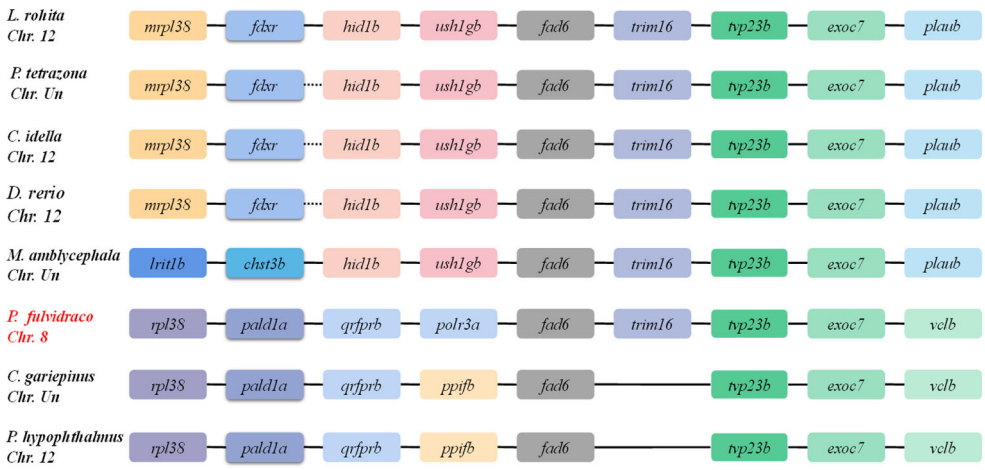

FIGURE 3
Genetic synteny of *fad6* in representative fish genomes. These colorful blocks represent different genes. The solid lines represent intergenic regions. The target yellow catfish is highlighted in red.

conserved coding sequence (CDS) with the other seven fish *fad6* genes (Figure 4).

Tissue distribution pattern of *fad6* in yellow catfish

Transcription of the yc*fad6* gene in 12 tissues of yellow catfish was measured and analyzed by qRT-PCR. Our results showed that yc*fad6* was widely transcribed in various tissues including adipose, barbel, brain, gill, gonad, heart, intestine, kidney, liver, muscle, spleen, and stomach (Figure 5). The highest transcription level was present in the heart, which is followed by the liver, adipose, brain, gill, gonad, intestine, kidney, and muscle, while the least transcription levels were detected in the beard, spleen and stomach (Figure 5).

Expression pattern of *fad6* gene at early developmental stages in yellow catfish

qRT-PCR was performed to detect the transcription of yc*fad6* at different developmental stages, and the results demonstrated that the yc*fad6* gene was transcribed at all examined stages (Figure 6). As observed in Figure 6, the transcription level of *fad6* gene was significantly decreased at 0, 3 and 6 h after fertilization, and then dramatically increased at 12, 24, 36, 48, and 72 h after fertilization, and finally further elevated to the highest expression level at 96 h after fertilization (Figure 6).

Effects of different initial diets on the transcription of *fad6* gene in yellow catfish

Transcriptional changes of the yellow catfish larvae *fad6* gene in response to different initial diets (with different concentrations of HUFAs) were determined (Figure 7). Our results showed that the transcription level of the yc*fad6* gene was significantly decreased at 2 and 3 d after invariably feeding with egg yolk (Figure 7A). Similarly, the transcription level of the yc*fad6* gene was also obviously decreased at 2 and 3 d after feeding with *A. nauplii* as the initial feed (Figure 7B).

Effects of fasting and refeeding on the *fad6* transcription in yellow catfish

Hepatic *fad6* gene transcription levels were measured after a short-term (24-h) or long-term fasting (1-week) and

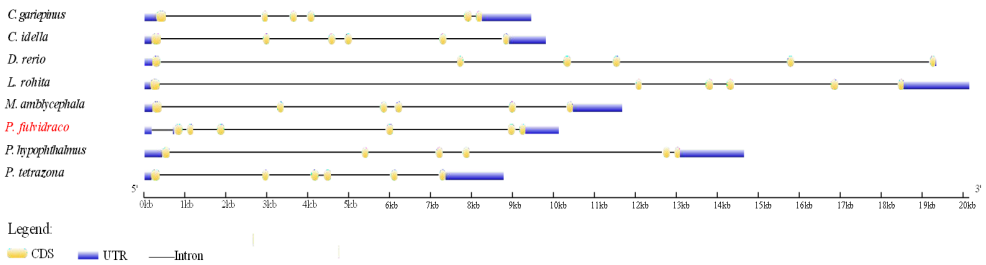

FIGURE 4
Comparison of the *fad6* gene structure in eight representative teleost fishes. The colorful blocks and solid lines represent the exons and introns, respectively. UTR (untranslated region) and CDS (coding sequence) are represented by blue and yellow blocks, respectively. The aimed species investigated in the present study is highlighted in red type.

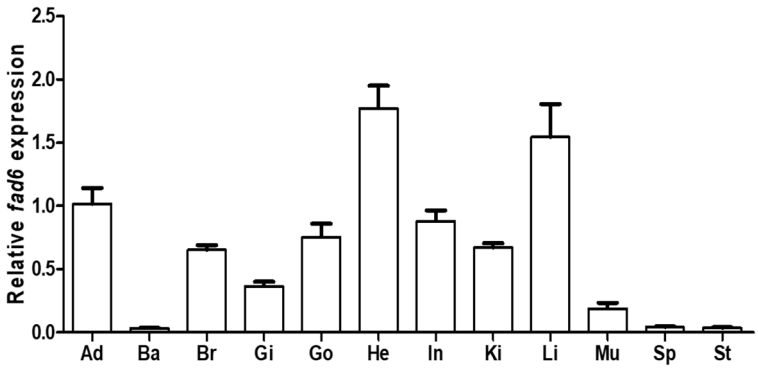

FIGURE 5
Tissue distribution of the yc*fad6* gene in yellow catfish. Examined tissues include adipose (Ad), barbel (Ba), brain (Br), gill (Gi), gonad (Go), heart (He), intestine (In), kidney (Ki), liver (Li), muscle (Mu), spleen (Sp), and stomach (St). *β-actin* was selected as the internal reference gene. Data are expressed as mean ± standard error (n = 5).

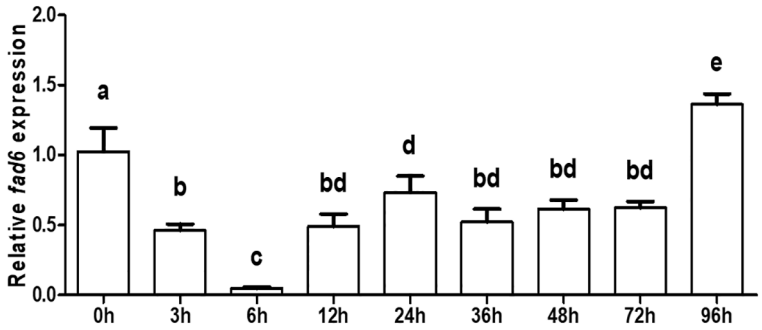

FIGURE 6
Gene expression pattern of the yc*fad6* gene at the early developmental stages. *β-actin* was selected as the internal reference gene. Data are expressed as mean ± standard error (n = 5). Different lowercase letters above the bars mean significant difference among groups.

refeeding to investigate the effects of various nutritional status on the HUFA biosynthesis in yellow catfish. For the short-term fasting experiment, *fad6* transcription levels were found to be significantly elevated at 3 h after fasting and then returned to the control levels at 6, 12, and 24 h after food deprivation (Figure 8A). For the long-term experiment, *fad6* transcription levels were significantly decreased in fishes from the 1-week fasting group in comparison with those in the control group (Figure 8B). However, refeeding had no dramatical effect on the transcription of hepatic *fad6* in yellow catfish (Figure 8B).

Discussion

Fatty acid desaturases play important roles in regulating the synthesis of unsaturated fatty acids in vertebrates (Wu et al., 2018). Thus far, lots of studies have focused on the regulatory roles of Fads in HUFAs biosynthesis both in mammals and teleost. However, as a new member identified recently in the Fads family, Fad6 and its roles of are still largely unknown. In this study, the *fad6* gene of yellow catfish was identified and characterized for the first time, and its ORF was validated to be 1,080 bp in length, encoding a protein of 359 amino acids. The length of ycFad6 is shorter than that in golden pompano (*T. ovatus*) (Zhu et al., 2018), suggesting that the *fad6* gene may be species-specific among various fish species. Multiple sequence alignment revealed that the ycFad6 contained three highly conserved histidine motifs (HXXH, HXXXHH, HXXHH) and a FADS-like domain, which were similar to other Fad6 proteins from diverse fish species. Our findings are consistent with the report of golden pompano (Zhu et al., 2018), indicating that these conserved motifs and domains may be essential for iron ligand binding and enzyme activity (Lin et al., 2018; Soo et al., 2020).

Previous studies have shown that gene copy number was varied for *fad2* in teleost, such as two copies in rabbitfish (Li et al., 2010; Dong et al., 2018; Li et al., 2019b), three copies in Nile tilapia (Castro et al., 2016; Chen et al., 2018; Dong et al., 2018; Jangprai and Boonanuntanasarn, 2018) and four copies in Atlantic salmon (Hastings et al., 2004; Monroig et al., 2010). Differently, our comparative analyses of genomic synteny and gene structure revealed that the desaturase gene obtained in this study is the *fad6* gene and there is only one single copy of this gene in various vertebrate genomes. Meanwhile, a highly conserved gene cluster *mrp138-fdxr-hid1b-ush1gb-fad6-trim16-tvp23b-exoc7-plaub* was identified in all the selected representative fish genomes, indicating that the physiological functions of Fad6 should be conserved in teleost. Additionally, gene structure comparison revealed that the *fad6* gene in teleost commonly

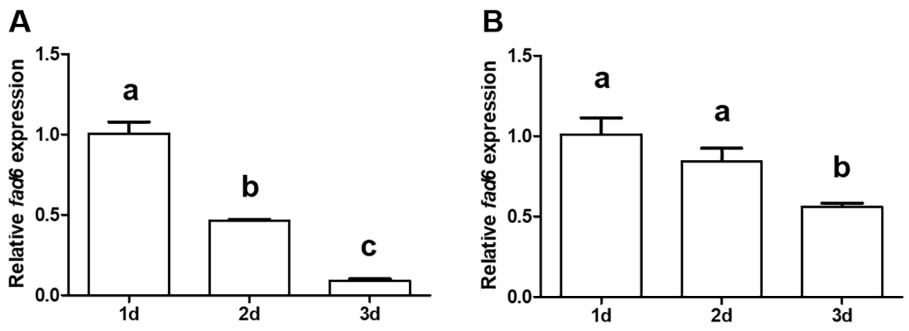

FIGURE 7
Effect of dietary egg yolk **(A)** or *A. nauplii* **(B)** on the transcription of yc*fad6* in yellow catfish larvae. *β-actin* was selected as the internal reference gene. Data are expressed as mean ± standard error (n = 5). Different lowercase letters above the bars mean significant difference among groups.

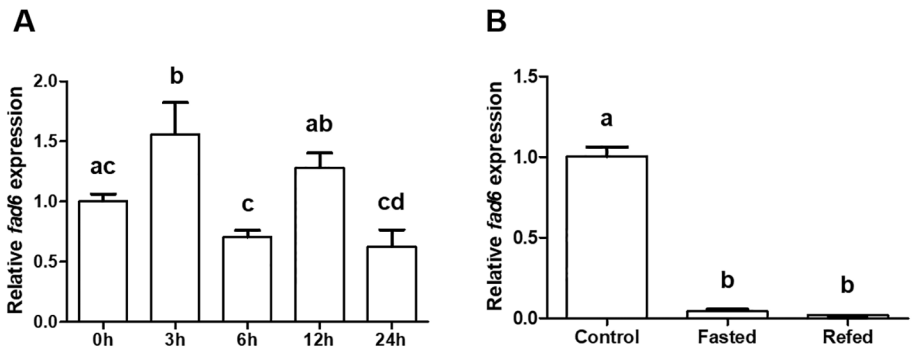

FIGURE 8
Effects of 24-h fasting **(A)** or 1-week fasting and refeeding **(B)** on yc*fad6* transcription in yellow catfish. *β-actin* was selected as the internal reference gene. Data are expressed as mean ± standard error (n = 5). Different lowercase letters above the bars mean significant difference among groups.

contains six exons and five introns, which further supported its conservation and potentially similar functions in various teleost. The phylogenetic analysis showed that the evolutionary history of *fad6* was in line with the putative species evolution. Further results showed that *fad6* gene in yellow catfish (*P. fulvidraco*) was clustered with that in Southern catfish (*S. meridionalis*), suggesting their close relationship; indeed, both catfish species belong to the same order Siluriformes (Wei et al., 2023).

Tissue distribution assays showed that the *fad6* gene was transcribed in all the examined tissues, with the highest transcription levels in the heart and liver, which is different from the pattern in golden pompano (Zhu et al., 2018). It seems that the tissue distribution pattern of *fad6* is species-specific and the gene may play different roles in diverse teleost. Notably, the yc*fad6* was highly transcribed in the liver, which is the primary organ for endogenous HUFAs biosynthesis (Wen et al., 2020; Zeng et al., 2023), implying that ycFad6 may play an important role in the endogenous HUFAs biosynthesis (Xu et al., 2020; Blahova et al., 2022).

The transcription patterns of yc*fad6* at different developmental stages were detected by qRT-PCR. These results showed that the transcription of yc*fad6* was significantly decreased at 0-6 h, and then dramatically increased at 12-72 h, suggesting that endogenous HUFAs biosynthesis was inhibited at the early stages of embryonic development (0-6 h), and the HUFAs biosynthesis process was initiated to meet the demand of HUFAs requirement from 12 h after fertilization. Similar phenomenon was observed in zebrafish, since its *fad* mRNA levels were very low until 9 h after fertilization (Leonard et al., 2002; Monroig et al., 2009), suggesting that the HUFAs biosynthesis process may be also restricted during the early embryogenesis of zebrafish. Additionally, the increased tendency of yc*fad6* expression was observed at 12 h after fertilization in our current study, which is in line with those findings at the early development stages of zebrafish embryos (Monroig et al., 2009). This implies that HUFAs biosynthesis is required for early embryonic development, although the precise patterns may be different among various species.

Notably, sufficient dietary HUFAs supplement is crucial for healthy growth and development to fishes (Morais et al., 2015). Thus far, several live prey species enriched with HUFAs (such as *Limnodrilus hoffmeisteri*, *rotifers*, *A. nauplii*, and cladoceran) or artificial feeds containing HUFAs (such as egg yolk, artificial compound feeds) are commonly used as initial diets in fish farming (Wei et al., 2014; Zhou et al., 2016). A previous study investigated the effects of different initial diets on the growth performance and survival rate of yellow catfish larvae, and found that adequate palatable diet is an important factor to affect the growth and survive of yellow catfish larvae (Yang et al., 2010). In our present study, we observed that the transcription level of yc*fad6* was gradually decreased in 1-3 d after feeding with egg yolk or *A. nauplii*, respectively. This phenomenon indicates that the initial diets with high concentrations of HUFAs can significantly inhibit the transcription of yc*fad6* in yellow catfish. Indeed, HUFAs-rich diets supplement is usually required for the normal growth and development of fish larvae, as well as for quality improvement of the offspring.

Nutritional status can also affect the HUFAs biosynthesis in teleost, and a recent study revealed that food deprivation can induce down-regulation of Δ4*fad* in the liver of senegalese sole (*Solea senegalensis*) (Morais et al., 2015). In our present study, we found that *fad6* transcription in yellow catfish was significantly increased at 3 h after feeding and then decreased to the control levels, suggesting that food intake may promote the HUFAs biosynthesis but a short-term of fasting may inhibit such process. Consistently, hepatic *fad6* was determined to be significantly downregulated after one week of fasting but without significantly changes after refeeding in yellow catfish, indicating that a long-term food deprivation can also restrict the process of HUFAs biosynthesis, although rescue of food supplement cannot return the HUFAs biosynthesis after this long-term food deprivation.

In summary, the *fad6* gene was identified and characterized in yellow catfish, and its molecular and biological characteristics were determined. Meanwhile, spatio-temporal expression patterns of this gene were also detected. In addition, transcriptional changes of the yc*fad6* gene in response to different initial diets and nutritional status were also investigated. Our findings not only offer basic data for further studies on physiological functions of the *fad6* gene in teleost, but also provide novel insights into the regulatory mechanism for HUFAs synthesis in various vertebrates.

Data availability statement

The original contributions presented in the study are included in the article/Supplementary Material. Further inquiries can be directed to the corresponding authors.

Ethics statement

The animal study was approved by Animal Care and Use Committee of Neijiang Normal University. The study was conducted in accordance with the local legislation and institutional requirements.

Author contributions

BZ: Formal analysis, Investigation, Writing – original draft. X-YW: Formal analysis, Investigation, Writing – original draft. Z-YW: Conceptualization, Funding acquisition, Project administration, Supervision, Writing – review & editing. BW: Formal analysis, Investigation, Writing – original draft. Y-YZ: Formal analysis, Investigation, Writing – original draft. W-HZ: Investigation, Software, Writing – original draft. YH: Investigation, Writing – original draft. PP: Investigation, Writing – original draft. Y-PL: Software, Writing – original draft. Y-YL: Investigation, Writing – original draft. JW: Funding acquisition, Investigation, Writing – original draft. RL: Investigation, Writing – original draft. X-GL: Investigation, Writing – original draft. JZ: Investigation, Writing – original draft. S-YZ: Funding acquisition, Investigation, Software, Writing – original draft. J-DF: Investigation, Writing – original draft. QS: Conceptualization, Supervision, Writing – review & editing.

Funding

The author(s) declare that financial support was received for the research, authorship, and/or publication of this article. This work was financially supported by the Natural Science Fund of Sichuan Province of China (No. 2023NSFSC1221), the Project of Sichuan Provincial Department of Science and Technology (No. 2022ZYZFSC22004; No. 2023YFN0048), the Research Fund from Key Laboratory of Sichuan Province for Fishes Conservation and Utilization in the Upper Reaches of the Yangtze River (No. NJTCSC23-3), the Important New Varieties Selection Project of Jiangsu Province (No. PZCZ201742), Provincial science and technology innovative program for carbon peak and carbon neutrality of Jiangsu of China (No. BE2022422), and the Cooperation Fund from Sichuan University (No. 2022H013).

Conflict of interest

Author J-DF was employed by the company Yueyang Yumeikang Biotechnology Co., Ltd.

The remaining authors declare that the research was conducted in the absence of any commercial or financial relationships that could be construed as a potential conflict of interest.

The handling editor YL declared a past co-authorship with the authors JW, ZYW, YL.

Publisher's note

Supplementary material

The Supplementary Material for this article can be found online at: https://www.frontiersin.org/articles/10.3389/fmars.2024.1453516/full#supplementary-material

References

Awada, M., Meynier, A., Soulage, C. O., Hadji, L., Géloën, A., Viau, M., et al. (2013). *n-3* PUFA added to high-fat diets affect differently adiposity and inflammation when carried by phospholipids or triacylglycerols in mice. *Nutr. Metab.* 10, 1–14. doi: 10.1186/1743-7075-10-23

Blahova, Z., Franek, R., Let, M., Blaha, M., Psenicka, M., and Mraz, J. (2022). Partial *fads2* Gene Knockout Diverts LC-PUFA Biosynthesis via an Alternative Delta 8 Pathway with an Impact on the Reproduction of Female Zebrafish (*Danio rerio*). *Genes* 13, 700. doi: 10.3390/genes13040700

Castro, L. F., Tocher, D. R., and Monroig, O. (2016). Long-chain polyunsaturated fatty acid biosynthesis in chordates: Insights into the evolution of Fads and Elovl gene repertoire. *Prog. Lipid. Res.* 62, 25–40. doi: 10.1016/j.plipres.2016.01.001

Chen, C. Y., Guan, W. T., Xie, Q. M., Chen, G. L., He, X. L., Zhang, H. L., et al. (2018). *n-3* essential fatty acids in Nile tilapia, *Oreochromis niloticus*: Bioconverting LNA to DHA is relatively efficient and the LC-PUFA biosynthetic pathway is substrate limited in juvenile fish. *Aquaculture* 495, 513–522. doi: 10.1016/j.aquaculture.2018.06.023

Dong, Y. W., Zhao, J. H., Chen, J. L., Wang, S. Q., Liu, Y., Zhang, Q. H., et al. (2018). Cloning and characterization of Delta 6/Delta 5 fatty acyl desaturase (*Fad*) gene promoter in the marine teleost *Siganus canaliculatus*. *Gene* 647, 174–180. doi: 10.1016/j.gene.2018.01.031

Fang, D. A., Yang, X. J., Zhou, Y. F., Xu, D. P., Yang, Y., and Qin, C. (2020). Discovery of the indicator role of period 2 in yellow catfish (*Pelteobagrus fulvidraco*) food intake during early life development stages. *Chronobiol. Int.* 37, 629–640. doi: 10.1080/07420528.2020.1752706

Guillou, H., Zadravec, D., Martin, P. G., and Jacobsson, A. (2010). The key roles of elongases and desaturases in mammalian fatty acid metabolism: Insights from transgenic mice. *Prog. Lipid. Res.* 49, 186–199. doi: 10.1016/j.plipres.2009.12.002

Halim, N., Ali, M. S. M., Leow, A. T. C., and Rahman, R. (2022). Membrane fatty acid desaturase: biosynthesis, mechanism, and architecture. *Appl. Microbiol. Biotechnol.* 106, 5957–5972. doi: 10.1007/s00253-022-12142-3

Hastings, N., Agaba, M. K., Tocher, D. R., Zheng, X., Dickson, C. A., Dick, J. R., et al. (2004). Molecular cloning and functional characterization of fatty acyl desaturase and elongase cDNAs involved in the production of eicosapentaenoic and docosahexaenoic acids from alpha-linolenic acid in Atlantic salmon (*Salmo salar*). *Mar. Biotechnol.* 6, 463–474. doi: 10.1007/s10126-004-3002-8

Jangprai, A., and Boonanuntanasarn, S. (2018). Ubiquitous promoters direct the expression of fatty acid Delta-6 desaturase from Nile tilapia (*Oreochromis niloticus*) in *Saccharomyces cerevisiae*. *J. Mol. Microbiol. Biotechnol.* 28, 281–292. doi: 10.1159/000499568

Kuah, M. K., Jaya-Ram, A., and Shu-Chien, A. C. (2016). A fatty acyl desaturase (*fads2*) with dual Δ6 and Δ5 activities from the freshwater carnivorous striped snakehead *Channa striata*. *Comp. Biochem. Physiol. A. Mol. Integr. Physiol.* 201, 146–155. doi: 10.1016/j.cbpa.2016.07.007

Leonard, A. E., Kelder, B., Bobik, E. G., Chuang, L. T., Lewis, C. J., Kopchick, J. J., et al. (2002). Identification and expression of mammalian long-chain PUFA elongation enzymes. *Lipids* 37, 733–740. doi: 10.1007/s11745-002-0955-6

Li, Y., Monroig, O., Zhang, L., Wang, S., Zheng, X., Dick, J. R., et al. (2010). Vertebrate fatty acyl desaturase with Δ4 activity. *Proc. Natl. Acad. Sci. U. S. A.* 107, 16840–16845. doi: 10.1073/pnas.1008429107

Li, Y., Wen, Z. Y., You, C. H., Xie, Z. Y., Tocher, D. R., Zhang, Y. L., et al. (2020). Genome wide identification and functional characterization of two LC-PUFA biosynthesis elongase (*elovl8*) genes in rabbitfish (*Siganus canaliculatus*). *Aquaculture* 522, 735127. doi: 10.1016/j.aquaculture.2020.735127

Li, Y. Y., Yin, Z. Y., Dong, Y. W., Wang, S. Q., Monroig, O., Tocher, D. R., et al. (2019b). Ppar is involved in the transcriptional regulation of liver LC-PUFA biosynthesis by targeting the 65 fatty acyl desaturase gene in the marine teleost *siganus canaliculatus*. *Mar. Biotechnol.* 21, 19–29. doi: 10.1007/s10126-018-9854-0

Li, Y., Zhao, J., Dong, Y., Yin, Z., Li, Y., Liu, Y., et al. (2019a). Sp1 is involved in vertebrate LC-PUFA biosynthesis by upregulating the expression of liver desaturase and elongase genes. *Int. J. Mol. Sci.* 20, 5066. doi: 10.3390/ijms20205066

Lin, Z., Huang, Y., Zou, W., Rong, H., Hao, M., and Wen, X. (2018). Cloning, tissue distribution, functional characterization and nutritional regulation of a fatty acyl Elovl5 elongase in chu's croaker *Nibea coibor*. *Gene* 659, 11–21. doi: 10.1016/j.gene.2018.03.046

Liu, Q. N., Yang, T. T., Wang, C., Jiang, S. H., Zhang, D. Z., Tang, B. P., et al. (2019). A non-mammalian Toll-like receptor 26 (*TLR26*)gene mediates innate immune responses in yellow catfish *Pelteobagrus fulvidraco*. *Fish. Shellfish. Immunol.* 95, 491–497. doi: 10.1016/j.fsi.2019.11.005

Lopes-Marques, M., Kabeya, N., Qian, Y., Ruivo, R., Santos, M. M., Venkatesh, B., et al. (2018). Retention of fatty acyl desaturase 1 (*fads1*) in Elopomorpha and Cyclostomata provides novel insights into the evolution of long-chain polyunsaturated fatty acid biosynthesis in vertebrates. *BMC Evol. Biol.* 18, 157. doi: 10.1186/s12862-018-1271-5

Monroig, O., Li, Y., and Tocher, D. R. (2011). Delta-8 desaturation activity varies among fatty acyl desaturases of teleost fish: high activity in delta-6 desaturases of marine species. *Comp. Biochem. Physiol. B. Biochem. Mol. Biol.* 159, 206–213. doi: 10.1016/j.cbpb.2011.04.007

Monroig, O., Rotllant, J., Sánchez, E., Cerdá-Reverter, J. M., and Tocher, D. R. (2009). Expression of long-chain polyunsaturated fatty acid (LC-PUFA) biosynthesis genes during zebrafish *Danio rerio* early embryogenesis. *Biochim. Biophys. Acta* 1791, 1093–1101. doi: 10.1016/j.bbalip.2009.07.002

Monroig, O., Zheng, X., Morais, S., Leaver, M. J., Taggart, J. B., and Tocher, D. R. (2010). Multiple genes for functional 6 fatty acyl desaturases (*Fad*) in Atlantic salmon (*Salmo salar L.*): gene and cDNA characterization, functional expression, tissue distribution and nutritional regulation. *Biochim. Biophys. Acta* 1801, 1072–1081. doi: 10.1016/j.bbalip.2010.04.007

Morais, S., Mourente, G., Martínez, A., Gras, N., and Tocher, D. R. (2015). Docosahexaenoic acid biosynthesis via fatty acyl elongase and Δ4-desaturase and its modulation by dietary lipid level and fatty acid composition in a marine vertebrate. *Biochim. Biophys. Acta* 1851, 588–597. doi: 10.1016/j.bbalip.2015.01.014

Muhlhausler, B. S., and Ailhaud, G. P. (2013). Omega-6 polyunsaturated fatty acids and the early origins of obesity. *Curr. Opin. Endocrinol. Diabetes. Obes.* 20, 56–61. doi: 10.1097/MED.0b013e32835c1ba7

Nayak, M., Saha, A., Pradhan, A., Samanta, M., and Giri, S. S. (2017). Dietary fish oil replacement by linseed oil: Effect on growth, nutrient utilization, tissue fatty acid composition and desaturase gene expression in silver barb (*Puntius gonionotus*) fingerlings. *Comp. Biochem. Physiol. B. Biochem. Mol. Biol.* 205, 1–12. doi: 10.1016/j.cbpb.2016.11.009

Song, Y. F., Luo, Z., Pan, Y. X., Zhang, L. H., Chen, Q. L., and Zheng, J. L. (2015). Three unsaturated fatty acid biosynthesis-related genes in yellow catfish *Pelteobagrus fulvidraco*: Molecular characterization, tissue expression and transcriptional regulation by leptin. *Gene* 563, 1–9. doi: 10.1016/j.gene.2014.12.014

Soo, H. J., Sam, K. K., Chong, J., Lau, N. S., Ting, S. Y., Kuah, M. K., et al. (2020). Functional characterisation of fatty acyl desaturase, Fads2, and elongase, Elovl5, in the Boddart's goggle-eyed goby *Boleophthalmus boddarti* (Gobiidae) suggests an incapacity for long-chain polyunsaturated fatty acid biosynthesis. *J. Fish. Biol.* 97, 83–99. doi: 10.1111/jfb.14328

Wei, X. Y., Wang, J., Guo, S. T., Lv, Y. Y., Li, Y. P., Qin, C. J., et al. (2023). Molecular characterization of a teleost-specific toll-like receptor 22 (*tlr22*) gene from yellow catfish (*Pelteobagrus fulvidraco*) and its transcriptional change in response to poly I:C and *Aeromonas hydrophila* stimuli. *Fish. Shellfish. Immunol.* 134, 108579. doi: 10.1016/j.fsi.2023.108579

Wei, G. L., Xu, G. C., Gu, R. B., Du, F. K., and Xu, P. (2014). Effects of dietary high unsaturated fatty acids on FAD gene expression in different tissues of Japanese grenadier anchovy (*Coilia nasus*). *Jiangsu. Agric. Sci.* 42, 233–236.

Wen, Z. Y., Li, Y., Bian, C., Shi, Q., and Li, Y. Y. (2020). Genome-wide identification of a novel *elovl4* gene and its transcription in response to nutritional and osmotic regulations in rabbitfish (*Siganus canaliculatus*). *Aquaculture* 529, 735666. doi: 10.1016/j.aquaculture.2020.735666

Wen, Z. Y., Wang, J., Bian, C., Zhang, X., Li, J., Peng, Y., et al. (2019). Molecular cloning of two *kcnk3* genes from the Northern snakehead (*Channa argus*) for quantification of their transcriptions in response to fasting and refeeding. *Gen. Comp. Endocrinol.* 281, 49–57. doi: 10.1016/j.ygcen.2019.05.016

Wu, D. L., Huang, Y. H., Liu, Z. Q., Yu, P., Gu, P. H., Fan, B., et al. (2018). Molecular cloning, tissue expression and regulation of nutrition and temperature on Δ6 fatty acyl desaturase-like gene in the red claw crayfish (*Cherax quadricarinatus*). *Comp. Biochem. Physiol. B. Biochem. Mol. Biol.* 225, 58–66. doi: 10.1016/j.cbpb.2018.07.003

Xie, D., Chen, C., Dong, Y., You, C., Wang, S., Monroig, Ó., et al. (2021). Regulation of long-chain polyunsaturated fatty acid biosynthesis in teleost fish. *Prog. Lipid. Res.* 82, 101095. doi: 10.1016/j.plipres.2021.101095

Xu, H., Ferosekhan, S., Turkmen, S., Afonso, J. M., Zamorano, M. J., and Izquierdo, M. (2020). Influence of Parental Fatty Acid Desaturase 2 (*fads2*) Expression and Diet on Gilthead Seabream (*Sparus aurata*) Offspring *fads2* Expression during Ontogenesis. *Animals* 10, 2191. doi: 10.3390/ani10112191

Yang, S., Wen, Z. Y., Zou, Y. C., Qin, C. J., Wang, J., Yuan, D. Y., et al. (2018). Molecular cloning, tissue distribution, and effect of fasting and refeeding on the expression of neuropeptide Y in *Channa argus*. *Gen. Comp. Endocrinol.* 259, 147–153. doi: 10.1016/j.ygcen.2017.11.017

Yang, R. B., Xie, C. X., Fan, Q. X., Gao, C., and Fang, L. B. (2010). Effects of feeding frequency and bait type on the growth and survival of *Pelteobagrus fulvidraco* pups and juveniles. *Chin. J. Appl. Environ.* 302, 112–123.

Zeng, W. H., Wei, X. Y., Qin, W., Shi, Q., Guo, S. T., Prathomya, P., et al. (2023). Molecular characterization, spatiotemporal expression patterns of fatty acid elongase (*elovl8*) gene, and its transcription changes in response to different diet stimuli in yellow catfish (*Pelteobagrus fulvidraco*). *Front. Mar. Sci.* 10, 1270776. doi: 10.3389/fmars.2023.1270776

Zhou, X., Zhan, Z. J., Ji, Y. P., Yu, Q. W., Shang, G. L., Xu, H. H., et al. (2016). Effects of bait types on growth and survival of *Pelteobagrus fulvidraco* pups and young fish at different stages of life. *Jiangsu. Agric. Sci.* 44, 324–327.

Zhu, K. C., Song, L., Guo, H. Y., Guo, L., Zhang, N., Liu, B. S., et al. (2018). Identification of fatty acid desaturase 6 in golden pompano *trachinotus ovatus* (Linnaeus 1758) and its regulation by the PPARαb transcription factor. *Int. J. Mol. Sci.* 20, 23. doi: 10.3390/ijms20010023

Zou, W., Lin, Z., Huang, Y., Limbu, S. M., and Wen, X. (2019). Molecular cloning and functional characterization of elongase (*elovl5*) and fatty acyl desaturase (*fads2*) in sciaenid, *Nibea diacanthus* (Lacepède 1802). *Gene* 695, 1–11. doi: 10.1016/j.gene.2019.01.033

frontiers | Frontiers in Marine Science

TYPE Original Research
PUBLISHED 09 August 2024
DOI 10.3389/fmars.2024.1443710

OPEN ACCESS

EDITED BY
Yi-Feng Li,
Shanghai Ocean University, China

REVIEWED BY
Carlo C. Lazado,
Norwegian Institute of Food, Fisheries and Aquaculture Research (Nofima), Norway
Lluis Tort,
Autonomous University of Barcelona, Spain

*CORRESPONDENCE
Jorge M. O. Fernandes
jorge.m.fernandes@nord.no

†PRESENT ADDRESS
Jorge M. O. Fernandes,
Institute of Marine Sciences (ICM-CSIC), Barcelona, Spain

RECEIVED 04 June 2024
ACCEPTED 22 July 2024
PUBLISHED 09 August 2024

CITATION
Lopes TdS, Costas B, Ramos-Pinto L, Reynolds P, Imsland AKD, Aragão C and Fernandes JMO (2024) Lumpfish physiological response to chronic stress. *Front. Mar. Sci.* 11:1443710. doi: 10.3389/fmars.2024.1443710

Lumpfish physiological response to chronic stress

Tiago da Santa Lopes[1,2,3], Benjamin Costas[3,4], Lourenço Ramos-Pinto[3], Patrick Reynolds[1], Albert K. D. Imsland[5,6], Cláudia Aragão[7,8] and Jorge M. O. Fernandes[2*†]

[1]R&D Small Scale Department, Gildeskål Forskningsstasjon AS, Inndyr, Norway, [2]Faculty of Biosciences and Aquaculture, Nord University, Bodø, Norway, [3]A2S Aquatic Animal Health Group, Interdisciplinary Centre of Marine and Environmental Research (CIIMAR), Matosinhos, Portugal, [4]Instituto de Ciências Biomédicas Abel Salazar (ICBAS-UP), Universidade do Porto, Porto, Portugal, [5]Department of Biological Sciences, University of Bergen, Bergen, Norway, [6]Aquaculture Research, Akvaplan-niva Iceland Office, Kópavogur, Iceland, [7]Centro de Ciências do Mar (CCMAR/CIMAR LA), Faro, Portugal, [8]Aquaculture Research Group, Universidade do Algarve, Faro, Portugal

In this study, we explored the effects of chronic stress on lumpfish (*Cyclopterus lumpus*) physiological, immune response, health, and plasma free amino acids. 3 groups of lumpfish were exposed to 1-minute air exposure. 1 group was exposed to stress once per week, a second group exposed 2 times per week, and a third group exposed 4 times per week. The present study revealed significant alterations in immunity and increased nutritional demands, particularly the branched chain amino acids and lysine. Cortisol levels fluctuated, with significantly higher levels halfway through the experiment on the groups that were stressed more often. Though, by the end of the experiment, there were no significant differences in cortisol levels between groups. Regardless of stress exposure, cataract developed in virtually all sampled fish, pointing toward a potential dietary imbalance. A transient immunomodulation of stress was visible. While in early stages stress had an immune enhancing effect, as seen by the increase in plasma nitric oxide and peroxidase in the group most frequently exposed to stress, these differences were not apparent by the end of the experiment. Additionally, the worst health condition was found in this group. Our results underscore the complex interplay between stress, immunity and nutrition, highlighting the need for tailored dietary strategies and improved rearing practices.

KEYWORDS

cleaner fish, lumpfish, salmon farming, stress, health, welfare, amino acids

1 Introduction

Lumpfish, naturally occurring along the Norwegian shores, have been documented grazing on sea lice[1]. For this particular trait, lumpfish have garnered attention from the salmon farming industry (Imsland et al., 2018). The deployment of these fish in salmon farms has surged in response to escalating ectoparasitic infestations impacting salmonid

aquaculture (Fiskeridirektoratet, 2021; Imsland et al., 2021). While the effectiveness of this species as delousing agents remains a subject of debate, one aspect is indisputable: the welfare of deployed lumpfish is concerning (Stien et al., 2020).

Beyond the economic benefits, the welfare of aquaculture animals has important ethical considerations. Our society is based on principles of justice and solidarity, and it is our responsibility to uphold these values not only in relation to humanity but also in regard to our environment. This responsibility extends to the animals and the finite natural resources our civilization relies upon (Charter of Fundamental Rights of the European Union, 2012; The European Green Deal, 2019). Consequently, sustainability and welfare have emerged as vital considerations, sparking extensive research and dialogue (Bovenkerk and Meijboom, 2013; Brown, 2015). As we delve in this paper on the physiological and immunological facets of lumpfish, it is imperative to underscore the ethical dimension of animal welfare.

Indeed, while production of lumpfish has surged during the past decade, the welfare standards did not follow suit (Garcia de Leaniz et al., 2022; Reynolds et al., 2022). This has culminated in disconcerting reports from the Norwegian Food Safety Authority regarding elevated mortality rates, disease outbreaks and unknown fate of a large portion of deployed lumpfish (Mattilsynet, 2020; Stien et al., 2020). It is crucial to deepen our understanding on the species physiology and requirements, as a cornerstone for improvement of welfare standards.

Stress is an inherent aspect of a teleost's life in aquaculture. Common stressors encompass netting and transferring, transport, daily operations involving handling, sorting, crowding, disease outbreaks, social stress and aggression, among others, all of which can elicit a stress response (Sneddon et al., 2016; Afonso, 2020). Briefly, the nervous system regulates the immediate response, by altering hormonal activity (Reid et al., 1998). Endocrine alterations help prepare the organism for immunological challenges like infection and wound repair, essential for survival. This neural-endocrine-immune conversation involves two main stress axes, the brain-sympatho-chromaffin axis (BSC) and the hypothalamus-pituitary-interrenal axis (HPI) (Wendelaar Bonga, 1997; Tort, 2011). These axes play pivotal roles in the teleost stress response, which can be manifest along three stages. The BSC axis is instantly activated upon stress perception, resulting in the release of catecholamine hormones such as epinephrine and norepinephrine. The HPI axis, on the other hand, exhibits a slight latency, being prompted minutes after, resulting in the release of cortisol by the interrenal cells in the head-kidney. Both catecholamines and cortisol release orchestrate the fallout of the stress response, mediating energy mobilization and modulating immunity. The metabolic changes following the action of the stress hormones are part of the second stage in the stress response. The third stage ensues when the organism is unable to successfully cope and overcome stress, leaving lasting maladaptations such as alterations in behavior and immune suppression (Barton and Iwama, 1991; Wendelaar Bonga, 1997; Schreck and Tort, 2016).

The intertwining of teleost stress and immune responses is well documented (Tort, 2011; Urbinati et al., 2020). This link emerges from a crosstalk between the neuroendocrine and immune systems, being expressed through a network of nerves, hormones, cytokines, and neuropeptides (Tort et al., 2003; Verburg-Van Kemenade et al., 2009; Yada and Tort, 2016). Most immune cells express receptors for neuropeptides, neurotransmitters, and hormones that, upon binding, alter transcription and cell activity. On an initial stage, perception of stress can induce the release of pro-inflammatory cytokines, namely interleukin-1β, interleukin-6, interleukin-12, tumor necrosis factor-α (Mosser and Edwards, 2008; Tort, 2011; Verburg-van Kemenade et al., 2011; Khansari et al., 2017). Mounting evidence supports the role of pro-inflammatory cytokines as early molecular initiators of the host inflammatory response through interaction with peripheral nerve terminals (Molfino et al., 2009). These findings highlight the intricate interplay between neuronal, endocrine, and immune systems.

Although most stressors cannot be eliminated, they can however, be mitigated. Increasing our understanding on the lumpfish stress physiology and its interconnectedness with health, nutrient requirements and the immune response opens the door for various stress-mitigating strategies (Ashley, 2007; Andersen et al., 2016; Sneddon et al., 2016; Martos-Sitcha et al., 2020). In fact, stress mitigating dietary strategies have been a major area of research in aquaculture (Kaushik and Seiliez, 2010; Herrera et al., 2019; Ciji and Akhtar, 2021). While improving aquaculture standards and welfare measures is key, nutrition is arguably one of the most important aspects for ensuring good health. Missing nutrient needs leads to disorders, and in many cases, a total disruption of fish health. Amino acids (AAs), for instance, have received particular attention (Costas et al., 2011a; Azeredo et al., 2017). In addition to being the building blocks of proteins, some AAs play functional roles in several physiological processes including growth, immune functions and energy metabolism. Some are also necessary for the synthesis of non-protein molecules like neurotransmitters and hormones (Li et al., 2009; Andersen et al., 2016; Ahmad et al., 2021). Certain AAs are only available through diet, deemed essential amino acids (EAA), as the organism cannot produce them, and as such their requirements must be known (Li et al., 2009). Stress modulates the need for certain nutrients, including AAs (Aragão et al., 2008) which means that if a diet does not take this into consideration, there is a risk of falling short on the nutritional demands, leading to potential disorders (Li et al., 2007; Yoneda et al., 2009; Ramos-Pinto, 2020). A practical and accurate way of assessing the potential increased needs in certain AAs levels in a diet for a particular fish, is by analyzing the free AAs in plasma (Aragão et al., 2008; Costas et al., 2011a). In this study, we research the nexus between chronic stress, health and immune functions with a focus on the effects in plasma free AAs.

2 Material and methods

2.1 Fish and tanks

Artic Seafood Group (Mørkvedbukta, Bodø, Norway) supplied 408 lumpfish juveniles with a mean weight of 58.5 ± 1.9

g which were transferred to Mørkvedbukta research station (Nord University, Mørkvedbukta, Norway). Upon arrival, fish health was assessed for all individuals, following a well described system tailored for visual health inspection of lumpfish (Reynolds et al., 2022). Lumpfish remained undisturbed for three weeks in indoor 1000 L flowthrough seawater tanks at an initial stocking density of 2.84 g L^{-1}. During this acclimation period and throughout the study, fish were fed 2% body weight with a commercial diet (Skretting's Clean Assist, 1.8 mm pellet size, Skretting, Stavanger, Norway) using feeding automats. Six meals were given throughout the day, following a 12h light-dark photoperiod. The daily routine consisted of checking feed levels in the automats, water temperature (7.6 ± 0.3°C), salinity (34.3 ± 0.3 ‰) and dissolved oxygen (7.8 ± 0.2 mg L^{-1}). In addition, fish behavior, such as feeding and hovering, was observed daily in each tank.

2.2 Study design and experimental layout

Four triplicate groups of lumpfish with an initial mean (± SD) weight of 89.8 ± 4.5 g (n = 34; N = 408) were established from the original population (groups 0C, 1S, 2S and 4S). Group numbers represent the number of times the groups were subject to stress per week, with letter "C" indicating control group and "S" stress group. This means that group 4S was exposed 4 times per week to the selected stressor, while group 0C was the control group, remaining undisturbed until sampling. The groups were distributed randomly across tanks. The stress exposure was scheduled randomly, occurring at different days of the week, at different times throughout the day, to avoid predictability. Disturbance of the fish was kept at absolute minimum, validated by the cortisol levels in the control group throughout the experiment. Netting the fish was followed with a chronometer to ensure consistency between tanks and was completed under 30 seconds. The air exposure was also timed with a chronometer and lasted exactly 1 minute. Air exposure was chosen as a stressor for its practical implication in aquaculture and it has been validated as stressor for lumpfish according to the procedures described by Lopes et al. (2023). This chronic stress experiment lasted for 10 weeks. On the day preceding sampling, lumpfish were fasted to minimize effects on biomarkers prompted by feeding (Arends et al., 1999). Sampling occurred always 1 h after stress exposure. Samplings were conducted on the 2^{nd}, 6^{th} and 10^{th} week and the health assessments were recorded in each sampling point.

2.3 Health and growth

Lumpfish health was evaluated every two weeks. Sampled fish were visually inspected following the Lumpfish Health Scoring System guidelines (LHSS) (Reynolds et al., 2022) and the health score registered. Cataracts were scored for size and opacity using a portable slit lamp (Heine, Gilching, Germany). Cataract incidence was calculated as $\frac{n^{o} \text{ of fish with cataract}}{n^{o} \text{ of fish sampled}} * 100$. Length and weight were measured and the specific growth rate (SGR) calculated[37].

2.4 Blood and liver sampling and tissue preparation

For sampling, 3 individuals from each tank were swiftly removed and euthanized with 1600 mg L^{-1} metacaine (tricaine methanesulphonate, Sigma Aldrich Co, St. Louis, Missouri, USA) (Skår et al., 2017).

Blood was drawn from the caudal vein in less than 3 min onto a heparinized vacutainer (BD, Plymouth, UK), and centrifuged at 2000 × g for 5 min at 4 °C. The resulting plasma was transferred to 1.8 ml cryotubes, snap-frozen in liquid nitrogen and stored at −80°C.

Liver biopsies (approximately 1 cm^3) were promptly taken consistently from the same area of the liver, the inferior part of the right lobe, using a scalpel, with each sample being divided into two aliquots and snap-frozen in liquid nitrogen. Biopsies were stored into two separate 1.8 ml cryotubes designated for oxidative stress and metabolite assays. For preparation of liver samples for metabolite analyses, frozen liver was finely minced in a 50 ml Falcon tube. A high-performance dispersing instrument (SilentCrusher M, Heidolph Instruments, Schwabach, Germany) was employed for mechanical disruption, in 7.5 vol. ice-cold 6% (w/v) perchloric acid. The homogenate was neutralized with an equal volume of 1 M $KHCO_3$, then centrifuged at 13,000 × g for 30 min at 4°C. Samples for oxidative stress analysis were prepared in a similar manner but using a different buffer: 1:10 volume K phosphate buffer (KPB) (0.1 M K_2HPO_4, 0.1 M KH_2PO_4, pH 7.4, Sigma Aldrich Co). To measure lipid peroxidation (LPO), 200 µL homogenate aliquots were retrieved. To each lipid peroxidation aliquot, 4 µL of 4% 3,5-di-tert-4-butylhydroxytoluene (BHT, in methanol, Sigma Aldrich Co.) were added before centrifugation to inhibit lipid peroxidation. The remaining homogenates were then centrifuged at 10,000 × g for 20 min at 4°C and the supernatants stored in separate aliquots at −80°C until use for oxidative stress assays.

2.5 Stress and metabolic biomarkers in plasma and liver

Plasma cortisol levels were quantified utilizing a commercial ELISA kit (IBL International GMBH, Hamburg-Nord, Germany) that had been previously validated and adapted for lumpfish (da Santa Lopes et al., 2023). The procedure involved the extraction of cortisol in plasma using diethyl ether at a 1:20 proportion. Following extraction, phosphate buffer infused with 1 g L^{-1} gelatine (pH 7.6) was added in a 2:1 proportion, thoroughly mixed and added to the microtiter plates, where kit recommendations ensued. For the quantification of plasma glucose, lactate and triglycerides, alongside hepatic lactate and triglycerides we used Spinreact kits (Spinreact) adapted to 96-well micro-plates (Costas et al., 2011a). Following the protocol outlined by Costas et al (Costas et al., 2014), plasma total proteins were assessed in 1:50 (v/v) diluted samples using Pierce™ BCA Protein Assay Kit (Thermo Fisher Scientific; USA). The resulting microplates of each parameter were read with the use of Synergy HT Microplate Reader (BioTek Instruments, Winooski, VT USA).

2.6 Plasma immune parameters

Lysozyme was measured using a turbidimetric test following the adaptation by Costas et al. (2011a) (Costas et al., 2011a) from the assay described by Ellis (1990) (Ellis, 1990a). To determine the amount of lysozyme present in the samples, a standard curve was established, where lyophilized hen egg white lysozyme (Sigma Aldrich Co.) was successively diluted in sodium phosphate buffer (0.05 M, pH 6.2).

Total peroxidase activity was quantified following Quade and Roth's colorimetric procedure (Quade and Roth, 1997), where one unit of peroxidase activity is defined by the quantity of peroxidase required to produce an absorbance change of 1 OD.

The protease levels in plasma were measured according to the methods described by Ellis (Ellis, 1990b) and Machado et al (MaChado et al., 2020). The principle behind the method is to evaluate the degradation of azocasein when incubated with plasma, using a trypsin solution (5 mg ml^{-1} in 0.5% $NaHCO_3$, pH 8.3) instead of plasma as positive control.

Plasma bactericidal activity was investigated by determining the overall capacity of plasma in eliminating selected bacteria, following Machado et al.'s adaptations (MaChado et al., 2015) of the protocol described by Graham et al. (Graham and Secombes, 1988) which has been standardized and validated for several fish species (Azeredo et al., 2019; Reis et al., 2021; Magalhães et al., 2023). For this assay, 20 µL of each plasma sample were added to U-shaped 96-well plate. Then, 20 µL *Vibrio anguillarum* (1 x 10^6 cfu ml^{-1}) were added in each well, and left incubating at 25°C for 2.5 h. Subsequently, 25 µL of 3- (4, 5-dimethyl-2-yl)-2,5-diphenyl tetrazolium bromide (1 mg mL^{-1}; Sigma Aldrich Co) was added and incubated for an additional 10 min at the same temperature for formazan formation. After centrifugation at 2000 × g for 10 min, the precipitate was dissolved in 200 µL of dimethyl sulfoxide (Sigma Aldrich Co.). Absorbance of the dissolved formazan was measured at 560 nm. Bactericidal activity was expressed as a percentage, determined from the difference in surviving bacteria relative to the positive control (100%).

Total plasma nitrite and nitrate were assessed as proxy for nitric oxide (NO) production using a colorimetric kit (Roche Diagnostics GmbH, Mannheim, Germany), as these compounds are a product of NO degradation. A sodium nitrite standard curve was developed to allow calculation of total nitrite in the samples.

2.7 Hepatic oxidative stress

Hepatic enzymatic activity was studied to understand the extent of oxidative damage in liver. Homogenized liver samples were used to assess lipid peroxidation (LPO), superoxide dismutase (SOD) and catalase (CAT) activities in addition to total protein concentration. The methodology delineated by Claiborne (1985) (Claiborne, 1985) and adapted by Peixoto et al. (Peixoto et al., 2021) was used to determine CAT. This was done by measuring the decrement in H_2O_2 concentration. The observed data is translated into enzyme activity expressed as enzyme units per milligram of total protein (U mg^{-1} protein). To determine SOD, we used the protocol illustrated by Lima et al. (Lima et al., 2007) and modified by Almeida et al (Almeida et al., 2010). Enzymatic activity is calculated based on the amount of enzyme necessary to inhibit 50% of cytochrome c reduction rate, instigated by the presence of superoxide radicals. Lipid peroxidation was measured using thiobarbituric acid-reactive substances (TBARSs) (Bird and Draper, 1984; Aloísio Torres et al., 2002). The total protein concentration of liver samples was determined following the protocol adapted by Costas et al. (Costas et al., 2014) employing the Pierce™ BCA Protein Assay Kit (Thermo Fisher Scientific, USA).

2.8 Plasma free amino acids

The free amino acid profile from plasma samples was determined by ultra-high-performance liquid chromatography (UPLC) on a Waters Reversed-Phase Amino Acid Analysis System, using norvaline as an internal standard. All samples were deproteinized by centrifugal ultrafiltration (10 kDa cut-off, 2500 × g, 20 min, 4°C). After deproteinization, samples were pre-column derivatised with Waters AccQ Fluor Reagent (6-aminoquinolyl-N-hydroxysuccinimidyl carbamate) using the AccQ Tag method (Waters, USA). Amino acids were identified by retention times of standard mixtures and pure standards (Sigma-Aldrich). Instrument control, data acquisition and processing were achieved using Waters Empower software.

2.9 Statistical analysis

The ensuing results are expressed as mean ± standard error. All data were subject to statistical analysis by testing for homogeneity and normality of variances using Levene's and Kolmogrov-Smirnov tests, respectively. To address skewed data on plasma cortisol, plasma and liver lactate and liver triglycerides, the data of these parameters was transformed logarithmically. Identification and comparison of significant differences on all parameters within each timepoint was performed by one-way ANOVA (p value< 0.05), followed by Tukey HSD *post hoc* test (Zar, 1984). Statistical analyses were carried out using IBM SPSS v25.0 0 (IBM Corp., Armonk, New York, USA).

3 Results

3.1 Cortisol

Analysis of cortisol in lumpfish plasma revealed significant differences at 2 and 6 weeks of the chronic stress experiment (Figure 1). At two weeks, mean cortisol levels were highest on group 1s (17.12 ± 4.62 ng ml^{-1}), being significantly higher than control group 0c (7.73 ± 1.50 ng ml^{-1}). Cortisol levels at 6 weeks

10.3389/fmars.2024.1443710

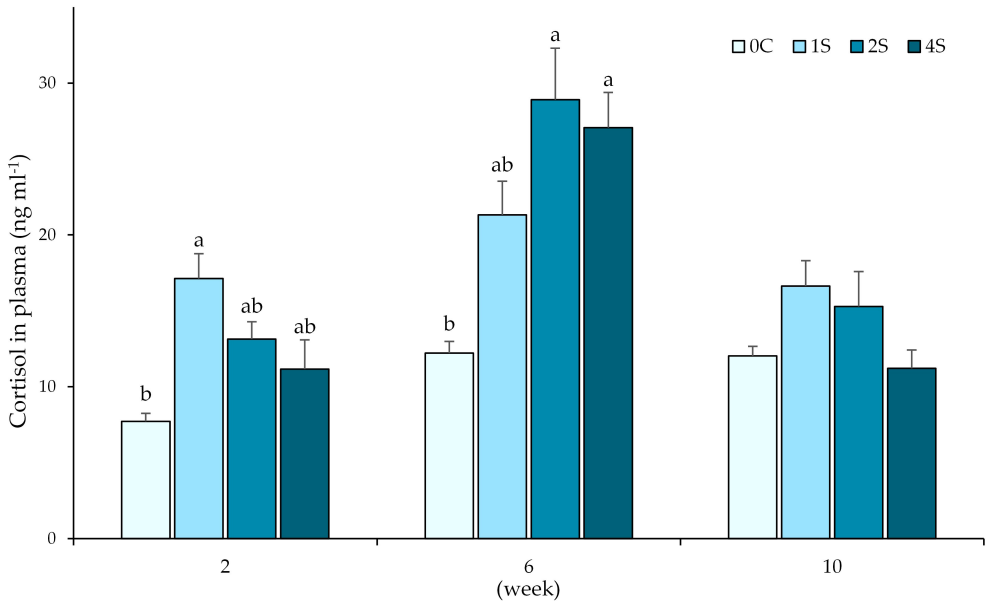

FIGURE 1
Plot of cortisol levels (ng ml $^{-1}$) in plasma (expressed as average ± SE) in undisturbed lumpfish (0c) and in lumpfish exposed to air for 1 minute (1s; 2s and 4s) on 2nd, 6th and 10th week samplings. Letters represent significant differences between groups within the same timepoint (ANOVA, Tukey, $p < 0.05$).

were significantly increased for groups 2s (28.90 ± 9.59 ng ml^{-1}) and 4s (27.07 ± 6.53 ng ml^{-1}), when compared to the control group 0c (12.22 ± 2.16 ng ml^{-1}). By the end of the experiment, no significant differences were observed between groups.

3.2 Glucose

Glucose analysis revealed significant differences at week 2, where group 2s had higher glucose levels than control group and group 1s (Supplementary Figure 1). No significant differences were observed in the following sampling points.

3.3 Lactate

Plasma levels of lactate were not altered by the exposure to air (Supplementary Figure 2), with no significant differences found in any timepoint.

3.4 Triglycerides

Significant differences were found in triglyceride levels in both plasma and liver samples (Figure 2). In the 6th week sampling, groups 2s (2.70 ± 0.21 mM) and 4s (2.68 ± 0.14 mM) had lower triglyceride levels than control group 0c (3.35 ± 0.13 mM). In addition, liver samples from groups 2s (4.42 ± 0.81 mM) and 4s (3.39 ± 0.20 mM) at the 10th week sampling, had also the lowest levels, with a significant decrease when compared with control group 0c (6.84 ± 0.61 mM).

3.5 Plasma immune parameters

Immune parameters revealed significant differences between groups (Figure 3). Peroxidase activity was highest in group 1s at 6th week sampling point (9.4 ± 1.0 units ml^{-1}), being significantly higher than peroxidase levels found in control group (4.5 ± 0.8 units ml^{-1}).

Significant differences were also found in protease activity both in 2nd and 10th week. On 2nd week, group 0c (2.0 ± 0.1%) and 1s (2.0 ± 0.1%) had lower protease activity when compared to groups 2s (2.4 ± 0.1%) and 4s (2.3 ± 0.1%). By week 10, group 1s had significantly higher protease activity (2.3 ± 0.1%) than group 2s (1.9 ± 0.1%).

Lysozyme levels were significantly lower in group 2s (36.8 ± 2.6 µg ml^{-1}) than in control group 0c (48.0 ± 3.0 µg ml^{-1}) at the 2nd week sampling, with no more significant differences found thereafter.

Bactericidal activity was highest in groups 2s (43.5 ± 2.7%) and 4s (45.7 ± 2.5%) when compared to group 0c (26.1 ± 4.1%) and 1s (21.5 ± 3.5%) during week 6.

All the other groups had significantly lower levels of nitric oxide than control group (0.12 ± 0.01 µM) in week 2. However, in week 6, group 2s (0.08 ± 0.004 µM) had highest levels of nitric oxide, being significantly higher than control group (0.03 ± 0.01 µM).

3.6 Plasma free amino acids

Plasma free AA analyses revealed significant differences on week 6, in all 3 branched-chain amino acids (BCAAs: isoleucine, leucine and valine), and lysine (Figure 4). Group 4s had significantly lower levels of the 4 AAs when compared to control group. Isoleucine and valine levels were also statistically lower in group

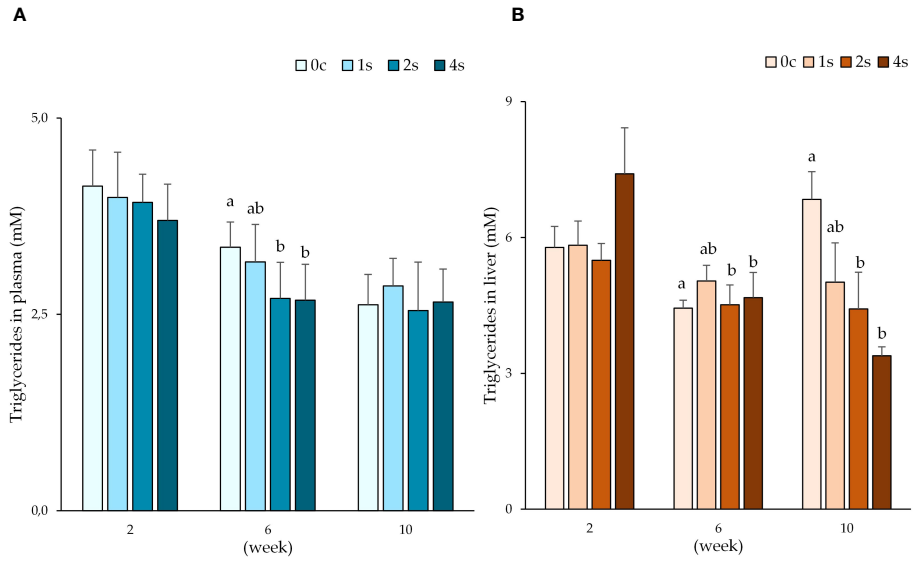

FIGURE 2
Plot of triglyceride levels (mM) in plasma **(A)** and liver **(B)** expressed as average ± SE in undisturbed lumpfish (0c) and in lumpfish exposed to air for 1 minute (1s; 2s and 4s) on 2nd, 6th and 10th week samplings. Letters represent significant differences for the same tissue between different groups within the same timepoint (ANOVA, Tukey, p< 0.05).

2s than group 0c. No differences were found between group 1s and control group in this timepoint. There were no significant differences in the remaining AA (Supplementary Table 1) between groups neither in the 6th nor at the 10th week.

3.7 Health and growth

No mortalities occurred during the whole trial period. Lumpfish started with an overall mean weight of 89.8 ± 0.6 g. There were no significant differences in growth between any group, however by end of the study, the control group "0c" had the highest group average weight (226.1 ± 13.8 g), with the highest specific growth rate (SGR) of 1.3%, followed by 1s with a final mean weight of 211.0 ± 11.6 (SGR 1.2%). Group 2s had a final mean weight of 197.8 ± 10.8 g by the end of the experiment (SGR 1.1%), with group 4s having the lowest mean weight at the end sampling, with 184.5 ± 8.2 g (SGR 1.1%). The health score was measured following the LHSS, revealing an increase in health deterioration in all groups, with 100% of fish in group 4s entering concerning area (health score > 2) by week 6 (Figure 5). Cataract incidence was below 25% for all groups on the day of transfer, however, it quickly rose up to virtually 100% by week 6 (Figure 6). At the last sampling point, cataract incidence was 100% for all stressed groups, and 92.0 ± 8.3% for the control group. There were no significant differences both in health score and cataract incidence between the different groups.

4 Discussion

The negative impacts of chronic stress on teleost health are undeniable, having been extensively demonstrated (Pickering and Pottinger, 1989; Barton and Iwama, 1991; Mommsen et al., 1999). In aquaculture rearing, fish frequently encounter prolonged or repeated stress, typically leading to immune suppression (Fast et al., 2008). The immunosuppressive effects of stress lead to impaired disease resistance, opening the door for opportunistic pathogens, and other health complications (Saeij et al., 2003). Lumpfish are no exception, even though lacking the evident reactive fight-or-flight response characteristic of many teleosts such as salmon (Hale, 2000). Several studies have confirmed the stress response of lumpfish to a variety of stress exposures, such as crowding, temperature, behavioral cues, and air exposure (Jørgensen et al., 2017; da Santa Lopes et al., 2023; Espmark et al., 2019; Noble et al., 2019; Staven et al., 2019; Remen et al., 2022). However, there is a lack of research connecting the lumpfish chronic stress exposure to immunity, overall health, and specific nutritional requirements. In this study, cortisol served as reliable indicator of HPI activation, with cortisol levels in the control group (0c) being kept under 15 ng ml^{-1} throughout the study. In comparison, the highest cortisol levels were found in groups stressed twice a week (2s) and 4 times per week (4s), in week 6. This coincided with a higher bactericidal activity also found at this time point. In addition, the proxy analysis of NO revealed its highest levels in all stressed groups, being significantly higher than control, in group 2s. Moreover, peroxidase activity also trended higher in stressed groups, with lowest levels on the undisturbed fish. In fact, peroxidase activity was statistically higher in the group stressed only once a week. The immune analysis of samples taken at week 6 hints at a potential immune-enhancing effect on stressed groups, as seen by the increased NO, bactericidal and peroxidase activities. This is not unheard of, with several studies depicting this occasionally paradoxical effect of stress on immunity (Tort, 2011). Acute stress can boost immunity by

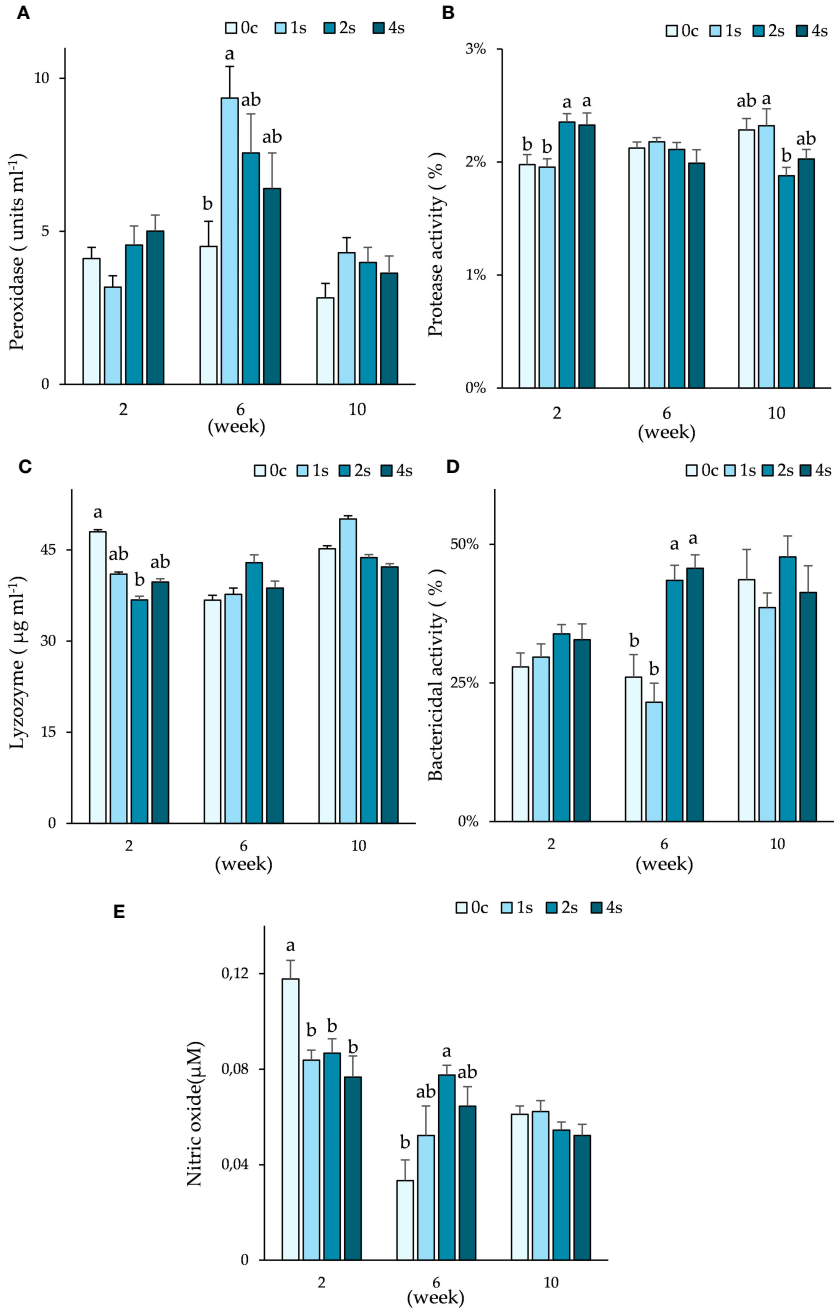

FIGURE 3
Plots of immune parameters: peroxidase **(A)**; protease activity **(B)**; lysozyme **(C)**; bactericidal activity **(D)** and nitric oxide **(E)** in plasma. Expressed as average ± SE in undisturbed lumpfish (0c) and in lumpfish exposed to air for 1 minute (1s; 2s and 4s) on weeks 2, 6 and 10. Letters represent significant differences between different groups within the same timepoint (ANOVA, Tukey, p< 0.05).

preparing the organism for immediate challenges. Cortisol released during a short-term stress adjusts leukocyte activity and cytokine levels, resulting in increased immunoprotection (Castillo et al., 2009; Yada and Tort, 2016; Khansari et al., 2017). Increased immunity can be beneficial, with an animal being more prepared to deal with immune challenge, but it can also be physiologically demanding. Under immune challenge, energy and resource allocations are diverted from certain physiological processes such as reproduction, and growth (Sadoul and Vijayan, 2016; Schreck and Tort, 2016; Yada and Tort, 2016). However, without a significant challenge, the energy budget might be sufficient to accommodate the increased energy demands of an immune enhancement caused by a mild stress. Accordingly, we have not seen any significant differences in weight between the different stress groups. Moreover, innate immune cell populations such as neutrophil and activated macrophages are mobilized, increasing in immune activation sites in response to acute stress, even without an initial immune challenge (Wojtaszek et al., 2002; Tort, 2011). Neutrophils are prime effectors of peroxidase activity, while macrophages are key NO releasers, and their increased numbers

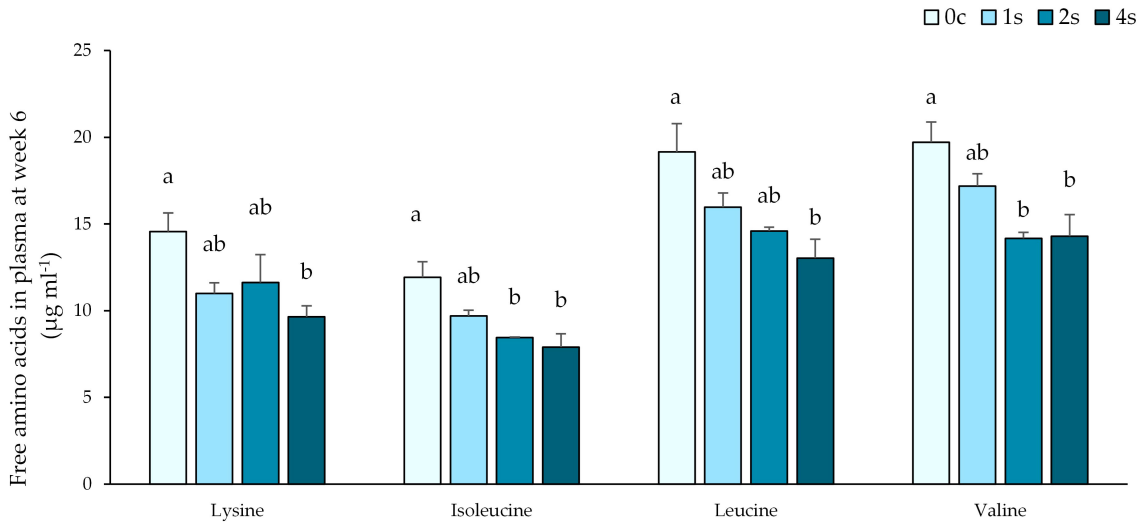

FIGURE 4
Plasma free amino acid levels of 4 essential AAs (Lysine; Isoleucine; Leucine and Valine) expressed as average ± SE in undisturbed lumpfish (0c) and in lumpfish exposed to air for 1 minute (1s; 2s and 4s) on sampling at week 6. Letters represent significant differences between different groups within the same timepoint (ANOVA, Tukey, p< 0.05).

prepare the organism for a potential challenge, effectively enhancing immunoprotection. Despite not looking directly to leukocyte population dynamics in this study, we did find the highest levels in peroxidase activity and nitric oxide in stressed groups. Nonetheless, prolonged stressed exposure can bring the immune enhancing effects to a halt, leading to subsequent immunosuppression (Mommsen et al., 1999; Dhabhar, 2008; Yada and Tort, 2016). Indeed, in our findings, the immune enhancing effects faded, with immune analysis at the end sampling showing no significant differences between undisturbed and stressed fish in any parameter. Stress shifts how fish use their energy and resources, prioritizing immediate survival over, reproduction, growth, and even immune functions. In fact, in our study, despite not being statistically significant, we saw a trend for lower growth in the more frequently stressed group 4s, while scoring the worst health, which was mostly explained by worsened skin erosion. Fin erosion is one of the first conditions seen in chronically stressed fish, where skin barrier defenses and maintenance erode, giving an opportunity for pathogens to flourish (Latremouille, 2003; Ellis et al., 2008). Adequate nutrition is paramount to maintain the epithelial structure and integrity of this important defensive barrier, and in fact, lysine deficiency has been attributed as potential cause of fin erosion (Lall, 2010; Hardy, 2012).

The influence of stress on teleost nutritional requirements has been explored in several aquaculture species. Often, stress exposure

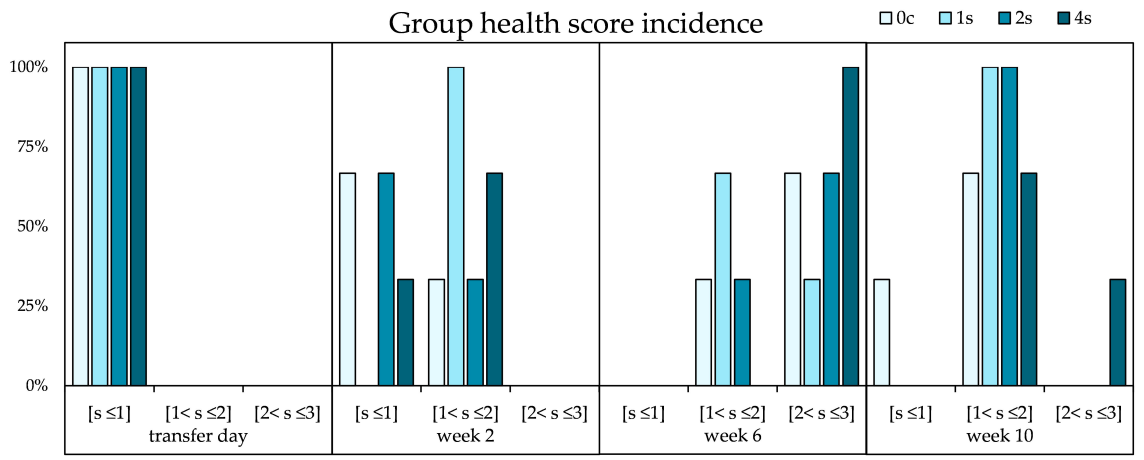

FIGURE 5
Percentage of incidence of group health scores throughout the experiment for undisturbed lumpfish (0c) and lumpfish groups exposed to stress (1s; 2s and 4s). "s" means score; [s< 1] is the category of scores below; [1< s ≤2] is for scores above 1 and below or equal to 2; and [2< s ≤3] is for the scores above 2 and below or equal to 3. Chi square analysis revealed no significant differences. The results are presented as a percentage.

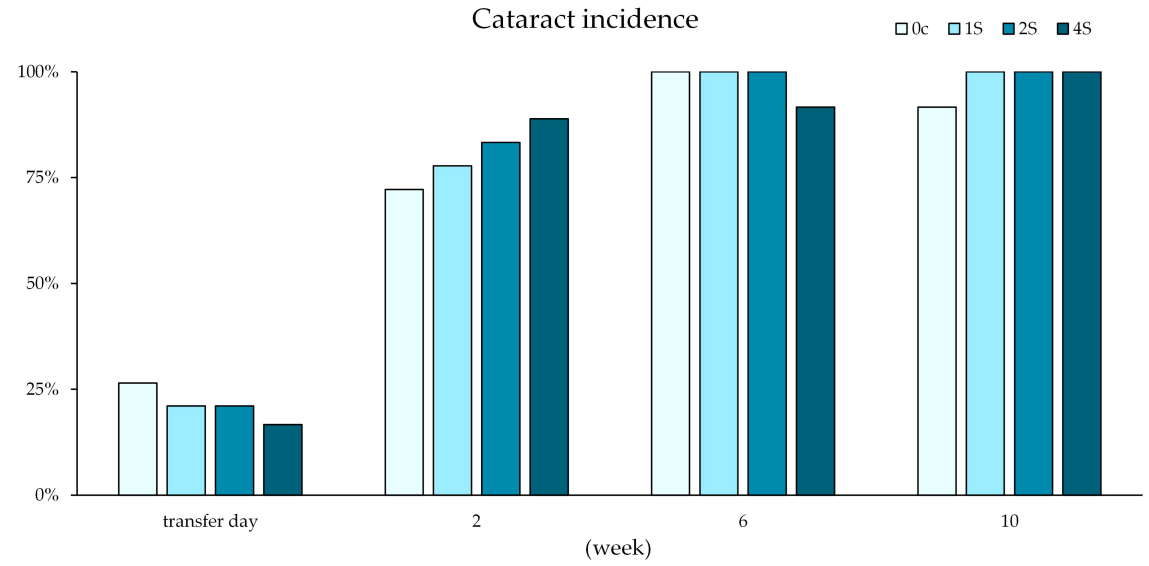

FIGURE 6
Plot of cataract incidence on undisturbed lumpfish (0c) and lumpfish exposed to stress (1s; 2s and 4s). Cataract incidence expressed as %.

triggers an elevation of nutritional needs, to fuel the stress response, causing an energy, nutrient and oxygen reallocation mediated by catecholamines and cortisol. As seen in this study, stressed groups 4s and 2s displayed modulation of hepatic energy mobilization, with lowered triglyceride levels by the end of the experiment. Modulation of energy substrate preference was also seen in a previous study of our group, on acute stress exposure with lumpfish (da Santa Lopes et al., 2023). Cortisol also modulates the AA metabolism (Aragão et al., 2008). Indeed, Costas et al. (2011a) demonstrated that exposing Senegalese sole (*Solea senegalensis*) to stress led to a modulation in AAs requirements (Costas et al., 2011a). Moreover, chronically stressed Senegalese sole dropped plasma free EAA concentrations, which according to authors can be due to either increased energetic demands or synthesis of important compounds needed to cope with stress (Costas et al., 2008). This corresponds to findings from the present study, where free plasma BCAAs and lysine levels were significantly lower in the most chronically stressed group, when compared to undisturbed fish. AAs such as BCAAs are ubiquitous, being used as building blocks of proteins, utilized as energy substrate and as signaling molecules (Van Waarde, 1988; Neinast et al., 2019; Ahmad et al., 2021). BCAAs integrate the AA chain composing virtually all proteins, including proteins relevant in the immune and antioxidant defense system. Oxidative stress is one of the outcomes of a stressed organism (Lushchak and Bagnyukova, 2007; Aschbacher et al., 2013; Sánchez-Muros et al., 2013). It increases nutritional demands, as the organism ups production of antioxidant defenses such as glutathione (GSH), superoxide dismutase and catalase to clear the reactive oxygen species (Iwasa et al., 2013; Espinosa-Diez et al., 2015). BCAA can be a key precursor of glutamate, which is necessary for GSH synthesis (Wu et al., 2004). In fact, dietary BCAA supplementation has proved effective in increasing expression of proteins involved in antioxidant defenses (Ichikawa et al., 2012; Iwasa et al., 2013). In addition, leucine is a potent activator of the mTOR pathway, which controls protein synthesis and cellular growth. Stress, through glucocorticoid action, has been shown to modulate mTOR activity, affecting protein synthesis and other metabolic processes (Valenzuela et al., 2018). Oxidative stress has been shown to alter mTOR in rats, being associated to retinal pathologies (Wang et al., 2022), a fact that should be better understood in fish.

Cataracts are a concerning disorder in cultured lumpfish (Imsland et al., 2021). Being an indicator of malnutrition and/or sub-optimal rearing conditions, cataracts can undermine the welfare of aquaculture species (Bjerkås et al., 2006; Peuhkuri et al., 2009). Lumpfish are deployed with the ultimate goal of preying on sea lice attached to salmons. If the eye health is undermined, this objective is most certainly unmet. In addition to this performance impairment from the eye of the farmer, there is also the welfare aspect, as lumpfish with poor eye health are also more likely to be ill adjusted for adequately feeding (Jonassen et al., 2017). It is reasonable to think that lumpfish, given the cataract severity and cohabiting with many considerably larger predatory teleosts such as salmon, will be less capable of adequately finding food. Naturally, as malnutrition progresses, the health of such fish will only erode.

In an epidemiological study of wild and farmed lumpfish, cataract incidence was significantly lower in wild mature lumpfish (Jonassen et al., 2017). The authors could not explain the cataract prevalence with an unbalance in histidine levels, as it has been previously reported in the salmonid aquaculture (Waagbø et al., 2010). The authors of the study suggested the cataract prevalence in lumpfish to be potentially related to disturbance in nutrient metabolism and malnutrition, via an AA imbalance, worsened by sub-optimal rearing. In addition, among the various AAs found

with a significant positive correlation with cataract score, was lysine. In the present study, we could not observe significant differences in cataract prevalence between undisturbed and stressed fish, underpinning this urgent need for improved commercial diets and optimized rearing procedures. However, we did find an increase in BCAAs and lysine requirement on the group 4s. Lysine is both a precursor of polyamine synthesis and plays a pivotal role in collagen fiber integrity. Polyamines play an important role in cell growth and differentiation, while also providing stability for lens' proteins such as crystallin and regulating osmotic stress (Wallace et al., 2003; Bloemendal et al., 2004; Mischiati et al., 2020; Munley et al., 2021; Han et al., 2022). Moreover, lysine is crucial for collagen synthesis which is of utmost importance for the structural integrity of the eye (Lythgoe, 1975; Bunce et al., 1990). Oxidative stress, which increases with stress, is highly correlated to caractogenesis, as the lens proteins and lipids suffer from the accumulation of reactive oxygen species (Varma et al., 1984; Berthoud and Beyer, 2009; Deering et al., 2023). An imbalance in dietary lysine can, thus, cripple the ability of the organism in, not only maintaining adequate antioxidant balance, but also, in tissue healing and maintenance, through impaired collagen and polyamine production.

Chronic stress will cause a sustained elevated release of cortisol until habituation or desensitization (Vijayan and Leatherland, 1990; Sopinka et al., 2016). In the early stages, the increase in cortisol will potentially result in enhanced immune functions, preparing the organism for challenge, as seen in this study, where bactericidal capacity was enhanced. With time, the sustained elevated cortisol levels will start having deleterious effects on the overall health of the fish (Opinion et al., 2023). The high energy and resource expenditure of maintaining an organism on this state of alertness will start to take its toll. The impact of the shift of resources from other biological functions to fuel the stress response will become increasingly noticeable (Schreck and Tort, 2016). Growth becomes impaired and immune functions suppressed as resources such as specific EAAs lack. If diet does not account for the increase expenditure, the building blocks will become scarce or insufficient (Winberg et al., 2016). As such, the oxidant–antioxidant balance will be disrupted, unleashing the cellular damage caused by high ROS levels (Sopinka et al., 2016). Disease resistance will be hampered, as immune suppression unfolds. Signs of health worsening will emerge, such as fin erosion and deteriorating eye health, exacerbated by sub-optimal nutrition. With the defenses lowered, opportunistic pathogens may carpe diem, exploiting this weakness (Pickering and Pottinger, 1989; Dhabhar, 2008; Yada and Tort, 2016). Thus, the absence of tailored aquafeeds for lumpfish that consider potentially elevated nutritional requirements, together with the lack of optimized rearing standards, results in a concerning puzzle that is the welfare status of lumpfish. If lumpfish are to be used as biological delousers in Atlantic salmon farming, there should be a focus on welfare improvement and stress mitigation research. To this end, it is important to consider dietary strategies that embrace increased nutritional demands together with improved aquacultures practices (Ashley, 2007; Costas, 2011; Costas et al., 2011b; Segner et al., 2012; Andersen et al., 2016; Sneddon et al., 2016; MaChado et al., 2018; Martos-Sitcha et al., 2020).

5 Conclusion

Lumpfish have been on the spotlight for their grim health and welfare situation. While they are assisting salmon farmers with their quest for mitigating the sea lice impacts, lumpfish welfare must be assured.

In this study, we shed light on the intricate modulatory effects of chronic stress on health, immunity, and potential nutritional requirements. The higher levels of cortisol in group 4s during the 6th week sampling subsided by the end of the experiment. Moreover, the immune-modulatory effects of cortisol were visible, with changes in plasma nitric oxide, bactericidal activity and peroxidase levels on stressed groups. Moreover, and although not significantly, the trend for lower growth and worse health score was seen in the most frequently stressed group. The cataract prevalence was high, nearly 100% among all groups, regardless of stress, pointing toward causes not just exclusive to stress experienced by lumpfish. There were clear modulatory effects of chronic stress on plasma free BCAAs and lysine levels, suggesting increased nutritional demands in lumpfish under chronic stressful conditions, which should be explored in future stress-immunonutrition research endeavors.

Data availability statement

The raw data supporting the conclusions of this article will be made available by the authors, without undue reservation.

Ethics statement

The animal study was approved by Norwegian Food Safety Authority (NFSA) under the application FOTS ID 26739. The study was conducted in accordance with the local legislation and institutional requirements.

Author contributions

TL: Conceptualization, Data curation, Formal Analysis, Funding acquisition, Investigation, Methodology, Project administration, Resources, Validation, Visualization, Writing – original draft, Writing – review & editing. BC: Conceptualization, Formal Analysis, Funding acquisition, Methodology, Resources, Supervision, Writing – review & editing. LR: Formal Analysis, Investigation, Methodology, Writing – review & editing. PR: Conceptualization, Funding acquisition, Investigation, Methodology, Project administration, Resources, Supervision, Writing – review & editing. AI: Conceptualization, Funding acquisition, Project administration, Resources, Supervision, Writing – review & editing. CA: Formal Analysis, Investigation, Methodology, Resources, Writing – review & editing. JF: Conceptualization, Funding acquisition, Investigation, Project administration, Resources, Supervision, Writing – review & editing.

Funding

The author(s) declare financial support was received for the research, authorship, and/or publication of this article. This study was financed by the Research Council of Norway, project number 317607; by the Gildeskål Forskningsstasjon AS; by Nord University, by Skretting AS; Lerøy Seafood Group, the Norwegian Seafood Research Fund (VEIEN, 901798) and the Icelandic Research Council (Rannís, 186971-0611). Gildeskål Forskningsstasjon AS, Skretting AS, and Lerøy Seafood Group were not involved in the study design, collection, analysis, interpretation of data, the writing of this article, or the decision to submit it for publication. The work presented in this paper was supported by national funds through the Foundation for Science and Technology (FCT, Portugal) within the scope of UIDB/04423/2020, UIDP/04423/2020, UIDB/04326/2020, UIDP/04326/2020, LA/P/0101/2020 and DL57/2016/CP1361/CT0033). JMOF acknowledges the grant 'Severo Ochoa Centre of Excellence' accreditation (CEX2019-000928-S) funded by AEI 10.13039/501100011033.

Acknowledgments

The authors thank the support and assistance provided by Mørkvedbukta Research Station's staff and by CIIMAR's A2S team.

Conflict of interest

Authors TL and PR were employed by company Gildeskål Forskningsstasjon AS.

The remaining authors declare that the research was conducted in the absence of any commercial or financial relationships that could be construed as a potential conflict of interest.

Publisher's note

Supplementary material

The Supplementary Material for this article can be found online at: https://www.frontiersin.org/articles/10.3389/fmars.2024.1443710/full#supplementary-material

References

Afonso, L. O. B. (2020). Identifying and managing maladaptive physiological responses to aquaculture stressors. *Fish Physiol.* 38, 163–191. doi: 10.1016/bs.fp.2020.10.002

Ahmad, I., Ahmed, I., Fatma, S., and Peres, H. (2021). Role of branched-chain amino acids on growth, physiology and metabolism of different fish species: A review. *Aquaculture Nutr.* 27, 1270–1289. doi: 10.1111/anu.13267

Almeida, J. R., Oliveira, C., Gravato, C., and Guilhermino, L. (2010). Linking behavioural alterations with biomarkers responses in the European seabass *Dicentrarchus labrax* L. exposed to the organophosphate pesticide fenitrothion. *Ecotoxicology (London England)* 19, 1369–1381. doi: 10.1007/s10646-010-0523-y

Aloísio Torres, M., Pires Testa, C., Gáspari, C., Beatriz Masutti, M., Maria Neves Panitz, C., Curi-Pedrosa, R., et al. (2002). Oxidative stress in the mussel *Mytella guyanensis* from polluted mangroves on Santa Catarina Island, Brazil. *Mar. pollut. Bull.* 44, 923–932. doi: 10.1016/S0025-326X(02)00142-X

Andersen, S. M., Waagbø, R., and Espe, M. (2016). Functional amino acids in fish nutrition, health and welfare. *Front. Bioscience (Elite Edition)* 8, 143–169. doi: 10.2741/757

Aragão, C., Corte-Real, J., Costas, B., Dinis, M. T., and Conceição, L. E. C. (2008). Stress response and changes in amino acid requirements in Senegalese sole (*Solea Senegalensis* Kaup 1858). *Amino Acids* 34, 143–148. doi: 10.1007/s00726-007-0495-2

Arends, R. J., Mancera, J. M., Muñoz, J. L., Wendelaar Bonga, S. E., and Flik, G. (1999). The stress response of the gilthead sea bream (*Sparus aurata* L.) to air exposure and confinement. *J. Endocrinol.* 163, 149–157. doi: 10.1677/joe.0.1630149

Aschbacher, K., O'donovan, A., Wolkowitz, O. M., Dhabhar, F. S., Su, Y., and Epel, E. (2013). Good stress, bad stress and oxidative stress: insights from anticipatory cortisol reactivity. *Psychoneuroendocrinology* 38, 1698–1708. doi: 10.1016/j.psyneuen.2013.02.004

Ashley, P. J. (2007). Fish welfare: Current issues in aquaculture. *Appl. Anim. Behav. Sci.* 104, 199–235. doi: 10.1016/j.applanim.2006.09.001

(2012). *Charter of Fundamental Rights of the European Union*. Available online at: https://eur-lex.europa.eu/legal-content/EN/TXT/?uri=celex%3AC2012%2F326%2F02.

(2019). *The European Green Deal*. Available online at: https://eur-lex.europa.eu/legal-content/EN/TXT/?uri=COM%3A2019%3A640%3AFIN.

Azeredo, R., MaChado, M., Martos-Sitcha, J. A., Martínez-Rodríguez, G., Moura, J., Peres, H., et al. (2019). Dietary Tryptophan Induces Opposite Health-Related Responses in the Senegalese Sole (*Solea Senegalensis*) Reared at Low or High Stocking Densities with Implications in Disease Resistance. *Front. Physiol.* 10. doi: 10.3389/FPHYS.2019.00508/BIBTEX

Azeredo, R., Serra, C. R., Oliva-Teles, A., and Costas, B. (2017). Amino acids as modulators of the European seabass, *Dicentrarchus labrax*, innate immune response: An in *vitro* approach. *Sci. Rep.* 7, 18009. doi: 10.1038/s41598-017-18345-3

Barton, B. A., and Iwama, G. K. (1991). Physiological changes in fish from stress in aquaculture with emphasis on the response and effects of corticosteroids. *Annu. Rev. Fish Dis.* 1, 3–26. doi: 10.1016/0959-8030(91)90019-G

Berthoud, V. M., and Beyer, E. C. (2009). Oxidative stress, lens gap junctions, and cataracts. *Antioxidants Redox Signaling* 11, 339. doi: 10.1089/ars.2008.2119

Bird, R. P., and Draper, H. H. (1984). Comparative studies on different methods of malonaldehyde determination. *Methods Enzymology* 105, 299–305. doi: 10.1016/S0076-6879(84)05038-2

Bjerkås, E., Breck, O., and Waagbø, R. (2006). The role of nutrition in cataract formation in farmed fish. *CAB Reviews: Perspect. Agriculture Veterinary Science Nutr. Natural Resour.* 1, 16–16. doi: 10.1079/PAVSNNR20061033

Bloemendal, H., De Jong, W., Jaenicke, R., Lubsen, N. H., Slingsby, C., and Tardieu, A. (2004). Ageing and vision: Structure, stability and function of lens crystallins. *Prog. Biophysics Mol. Biol.* 86, 407–485. doi: 10.1016/j.pbiomolbio.2003.11.012

Bovenkerk, B., and Meijboom, F. L. B. (2013). Fish welfare in aquaculture: explicating the chain of interactions between science and ethics. *J. Agric. Environ. Ethics* 26, 41–61. doi: 10.1007/S10806-012-9395-X/FIGURES/1

Brown, C. (2015). "Fish intelligence, sentience and ethics," in *Animal Cognition*, vol. 18. (New York, US: Springer Verlag), 1–17. doi: 10.1007/s10071-014-0761-0

Bunce, G. E., Kinoshita, J., and Horwitz, J. (1990). Nutritional factors in cataract. *Annu. Rev. Nutr.* 10, 233–254. doi: 10.1146/annurev.nu.10.070190.001313

Castillo, J., Teles, M., Mackenzie, S., and Tort, L. (2009). Stress-related hormones modulate cytokine expression in the head kidney of gilthead seabream (*Sparus aurata*). *Fish Shellfish Immunol.* 27, 493–499. doi: 10.1016/j.fsi.2009.06.021

Ciji, A., and Akhtar, M. S. (2021). Stress management in aquaculture: a review of dietary interventions. *Rev. Aquaculture* 13, 2190–2247. doi: 10.1111/raq.12565

Claiborne, A. (1985). "Catalase activity," in *Handbook Methods for Oxygen Radical Research*. Ed. R. A. Greenwald (Boca Raton, US: CRC Press), 283–284. doi: 10.1201/9781351072922

Costas, B. (2011). *Stress mitigation in sole (Solea Senegalensis) through improved nitrogen nutrition: amino acid utilization, disease resistance and immune status* (Porto, Portugal: University of Porto).

Costas, B., Aragão, C., Mancera, J. M., Dinis, M. T., Conceição, L. E. C., and Refojos, B. C. (2008). High stocking density induces crowding stress and affects amino acid metabolism in Senegalese sole *Solea Senegalensis* (Kaup 1858) juveniles. *Aquaculture Res.* 39, 1–9. doi: 10.1111/j.1365-2109.2007.01845.x

Costas, B., Conceição, L. E. C., Aragão, C., Martos, J. A., Ruiz-Jarabo, I., Mancera, J. M., et al. (2011a). Physiological responses of Senegalese sole (*Solea Senegalensis* Kaup 1858) after stress challenge: Effects on non-specific immune parameters, plasma free amino acids and energy metabolism. *Aquaculture* 316, 68–76. doi: 10.1016/j.aquaculture.2011.03.011

Costas, B., Conceição, L. E. C., Dias, J., Novoa, B., Figueras, A., and Afonso, A. (2011b). Dietary arginine and repeated handling increase disease resistance and modulate innate immune mechanisms of Senegalese sole (*Solea Senegalensis* Kaup 1858). *Fish Shellfish Immunol.* 31, 838–847. doi: 10.1016/j.fsi.2011.07.024

Costas, B., Simões, I., Castro-Cunha, M., and Afonso, A. (2014). Non-specific immune responses of *Senegalese sole*, *Solea Senegalensis* (Kaup), head-kidney leucocytes against Tenacibaculum maritimum. *J. Fish Dis.* 37, 765–769. doi: 10.1111/jfd.12171

da Santa Lopes, T., Costas, B., Ramos-Pinto, L., Reynolds, P., Imsland, A. K. D., and Fernandes, J. M. O. (2023). Exploring the effects of acute stress exposure on lumpfish plasma and liver biomarkers. *Animals* 13, 3623. doi: 10.3390/ani13233623

Deering, M. J., Paradis, H., Ahmad, R., Al-Mehiawi, A. S., and Gendron, R. L. (2023). The role of dietary vitamin A in mechanisms of cataract development in the teleost lumpfish (*Cyclopterus lumpus* L). *J. Fish Dis.* 47, 1–15. doi: 10.1111/JFD.13899

Dhabhar, F. S. (2008). Enhancing versus Suppressive Effects of Stress on Immune Function: Implications for Immunoprotection versus Immunopathology. *Allergy Asthma Clin. Immunology* 4, 2. doi: 10.1186/1710-1492-4-1-2

Ellis, A. E. (1990a). "Lysozyme assays," in *Techniques in Fish Immunology*. Eds. J. S. Stolen, T. C. Fletcher, D. P. Anderson, B. S. Roberson and W. B. van Muiswinkel (SOS Publications, Fair Haven), 101–103.

Ellis, A. E. (1990b). Serum Antiproteases in Fish. In: J.S. Stolen, T.C. Fletcher, D.P. Anderson, B.S. Roberson and W.B. van Muiswinkel editors. *Techniques in Fish Immunology. 1st ed*. (Fair Haven, MA, USA: SOS Publications) pp. 95–99. Available at: https://cir.nii.ac.jp/crid/1573950399902395392.bib?lang=en.

Ellis, T., Oidtmann, B., St-Hilaire, S., Turnbull, J. F., North, B. P., Macintyre, C. M., et al. (2008). "Fin erosion in farmed fish," in *Fish Welfare* (Oxford, UK: Blackwell Publishing Ltd), 121–149. doi: 10.1002/9780470697610.ch9

Espinosa-Diez, C., Miguel, V., Mennerich, D., Kietzmann, T., Sánchez-Pérez, P., Cadenas, S., et al. (2015). Antioxidant responses and cellular adjustments to oxidative stress. *Redox Biol.* 6, 183–197. doi: 10.1016/j.redox.2015.07.008

Espmark, Å. M., Noble, C., Kolarevic, J., Marit Berge, G., Hansen Aas, G., Tuene, S., et al. (2019). *Welfare in cleaner fish – operational welfare indicators (OWI) - RENSVEL*. Nofima Rapport, 12/2019. Available online at: www.nofima.no.

Fast, M. D., Hosoya, S., Johnson, S. C., and Afonso, L. O. B. (2008). Cortisol response and immune-related effects of Atlantic salmon (*Salmo salar* Linnaeus) subjected to short- and long-term stress. *Fish Shellfish Immunol.* 24, 194–204. doi: 10.1016/j.fsi.2007.10.009

Fiskeridirektoratet (2021). *Aquaculture statistics: Use of cleanerfish 1998-2021* (Oslo, Norway: Norwegian Directorate of Fisheries). Available at: https://www.fiskeridir.no/English/Aquaculture/Statistics/Cleanerfish-Lumpfish-and-Wrasse.

Garcia de Leaniz, C., Gutierrez Rabadan, C., Barrento, S. I., Stringwell, R., Howes, P. N., Whittaker, B. A., et al. (2022). Addressing the welfare needs of farmed lumpfish: Knowledge gaps, challenges and solutions. *Reviews in Aquaculture*, vol. 14, 139–155. doi: 10.1111/raq.12589

Graham, S., and Secombes, C. J. (1988). The production of a macrophage-activating factor from rainbow trout *Salmo gairdneri* leucocytes. *Immunology* 65, 293.

Hale, M. E. (2000). Startle responses of fish without Mauthner neurons: escape behavior of the lumpfish (*Cyclopterus lumpus*). *Biol. Bull.* 199, 180–182. doi: 10.2307/1542886

Han, W., Li, H., and Chen, B. (2022). Research progress and potential applications of spermidine in ocular diseases. *Pharmaceutics* 14, 1500. doi: 10.3390/pharmaceutics14071500

Hardy, R. W. (2012). "The nutritional pathology of teleosts," in *Fish Pathology* (New Jersey, US: Wiley-Blackwell), 402–424. doi: 10.1002/9781118222942.ch10

Herrera, M., Mancera, J. M., and Costas, B. (2019). The use of dietary additives in fish stress mitigation: Comparative endocrine and physiological responses. *Front. Endocrinol.* 10. doi: 10.3389/FENDO.2019.00447/BIBTEX

Ichikawa, K., Okabayashi, T., Shima, Y., Iiyama, T., Takezaki, Y., Munekage, M., et al. (2012). Branched-chain amino acid-enriched nutrients stimulate antioxidant DNA repair in a rat model of liver injury induced by carbon tetrachloride. *Mol. Biol. Rep.* 39, 10803–10810. doi: 10.1007/s11033-012-1974-4

Imsland, A. K. D., Hanssen, A., Nytrø, A. V., Reynolds, P., Jonassen, T. M., Hangstad, T. A., et al. (2018).). It works! Lumpfish can significantly lower sea lice infestation in large-scale salmon farming. *Biol. Open* 7, bio036301. doi: 10.1242/bio.036301

Imsland, A. K. D., Reynolds, P., Hangstad, T. A., Kapari, L., Maduna, S. N., Hagen, S. B., et al. (2021). Quantification of grazing efficacy, growth and health score of different lumpfish (*Cyclopterus lumpus* L.) families: Possible size and gender effects. *Aquaculture* 530, 735925. doi: 10.1016/j.aquaculture.2020.735925

Iwasa, M., Kobayashi, Y., Mifuji-Moroka, R., Hara, N., Miyachi, H., Sugimoto, R., et al. (2013). Branched-chain amino acid supplementation reduces oxidative stress and prolongs survival in rats with advanced liver cirrhosis. *PLoS One* 8, e70309. doi: 10.1371/journal.pone.0070309

Jonassen, T., Hamadi, M., Remø, S. C., and Waagbø, R. (2017). An epidemiological study of cataracts in wild and farmed lumpfish (*Cyclopterus lumpus* L.) and the relation to nutrition. *J. Fish Dis.* 40, 1903–1914. doi: 10.1111/jfd.12664

Jørgensen, E. H., Haatuft, A., Puvanendran, V., and Mortensen, A. (2017). Effects of reduced water exchange rate and oxygen saturation on growth and stress indicators of juvenile lumpfish (*Cyclopterus lumpus* L.) in aquaculture. *Aquaculture* 474, 26–33. doi: 10.1016/j.aquaculture.2017.03.019

Kaushik, S. J., and Seiliez, I. (2010). Protein and amino acid nutrition and metabolism in fish: current knowledge and future needs. *Aquaculture Res.* 41, 322–332. doi: 10.1111/are.2010.41.issue-3

Khansari, A. R., Carles Balasch, J., Reyes-López, F. E., and Tort, L. (2017). Stressing the inflammatory network: Immuno-endocrine responses to allostatic load in fish NANOAu-Effects of gold nanoparticles to aquatic organisms View project. *Article J. Mar. Sci. Technol.* 8, 401.

Lall, S. P. (2010). "Disorders of nutrition and metabolism," in *Fish diseases and disorders*, vol. 2. (Oxfordshire, UK: CABI), 202–237. doi: 10.1079/9781845935535.0202

Latremouille, D. N. (2003). Fin erosion in aquaculture and natural environments. *Rev. Fisheries Sci.* 11, 315–335. doi: 10.1080/10641260390255745

Li, P., Mai, K., Trushenski, J., and Wu, G. (2009). New developments in fish amino acid nutrition: towards functional and environmentally oriented aquafeeds. *Amino Acids* 37, 43–53. doi: 10.1007/s00726-008-0171-1

Li, P., Yin, Y.-L., Li, D., Woo Kim, S., and Wu, G. (2007). Amino acids and immune function. *Br. J. Nutr.* 98, 237–252. doi: 10.1017/S000711450769936X

Lima, I., Moreira, S. M., Osten, J. R., Soares, A. M. V. M., and Guilhermino, L. (2007). Biochemical responses of the marine mussel *Mytilus galloprovincialis* to petrochemical environmental contamination along the North-western coast of Portugal. *Chemosphere* 66, 1230–1242. doi: 10.1016/j.chemosphere.2006.07.057

Lushchak, V. I., and Bagnyukova, T. V. (2007). Hypoxia induces oxidative stress in tissues of a goby, the rotan *Perccottus glenii*. *Comp. Biochem. Physiol. Part B: Biochem. Mol. Biol.* 148, 390–397. doi: 10.1016/j.cbpb.2007.07.007

Lythgoe, J. N. (1975). The structure and function of iridescent corneas in teleost fishes. *Proc. R. Soc. London. Ser. B. Biol. Sci.* 188, 437–457. doi: 10.1098/rspb.1975.0030

MaChado, M., Arenas, F., Svendsen, J. C., Azeredo, R., Pfeifer, L. J., Wilson, J. M., et al. (2020). Effects of water acidification on Senegalese sole *Solea Senegalensis* health status and metabolic rate: implications for immune responses and energy use. *Front. Physiol.* 11. doi: 10.3389/FPHYS.2020.00026/BIBTEX

MaChado, M., Azeredo, R., Díaz-Rosales, P., Afonso, A., Peres, H., Oliva-Teles, A., et al. (2015). Dietary tryptophan and methionine as modulators of European seabass (*Dicentrarchus labrax*) immune status and inflammatory response. *Fish Shellfish Immunol.* 42, 353–362. doi: 10.1016/j.fsi.2014.11.024

MaChado, M., Azeredo, R., Fontinha, F., Fernández-Boo, S., Conceição, L. E. C., Dias, J., et al. (2018). Dietary methionine improves the european seabass (*Dicentrarchus labrax*) immune status, inflammatory response, and disease resistance. *Front. Immunol.* 9. doi: 10.3389/fimmu.2018.02672

Magalhães, R., Martins, N., Fontinha, F., Olsen, R. E., Serra, C. R., Peres, H., et al. (2023). Dietary ARA, DHA, and carbohydrate ratios affect the immune status of gilthead sea bream juveniles upon bacterial challenge. *Animals* 13, 1770. doi: 10.3390/ani13111770

Martos-Sitcha, J. A., Mancera, J. M., Prunet, P., and Magnoni, L. J. (2020). Editorial: welfare and stressors in fish: challenges facing aquaculture. *Front. Physiol.* 11. doi: 10.3389/fphys.2020.00162

Mattilsynet (2020). *Nasjonal tilsynskampanje 2018/2019 Velferd Hos Rensefisk* (Oslo, Norway: The Norwegian Food Safety Authority's National Inspection Projects). Available at: https://www.mattilsynet.no/fisk_og_akvakultur/akvakultur/rensefisk/mattilsynet_sluttrapport_rensefiskkampanje_2018:2019.37769/binary/Mattilsynetsluttrapportrensefiskkampanje2018-2019.

Mischiati, C., Feriotto, G., Tabolacci, C., Domenici, F., Melino, S., Borromeo, I., et al. (2020). Polyamine oxidase is involved in spermidine reduction of transglutaminase type 2-catalyzed βH-crystallins polymerization in calcium-induced experimental cataract. *Int. J. Mol. Sci.* 21, 5427. doi: 10.3390/ijms21155427

Molfino, A., Rossi-Fanelli, F., and Laviano, A. (2009). The interaction between pro-inflammatory cytokines and the nervous system. *Nat. Rev. Cancer* 9, 224–224. doi: 10.1038/nrc2507-c1

Mommsen, T. P., Vijayan, M. M., and Moon, T. W. (1999). Cortisol in teleosts: Dynamics, mechanisms of action, and metabolic regulation. *Rev. Fish Biol. Fisheries* 9, 211–268. doi: 10.1023/A:1008924418720/METRICS

Mosser, D. M., and Edwards, J. P. (2008). Exploring the full spectrum of macrophage activation. *Nat. Rev. Immunol.* 8, 958–969. doi: 10.1038/nri2448

Munley, K. M., Liu, D., and Galvez, F. (2021). Increased polyamine levels and maintenance of γ-aminobutyric acid (Gaba) homeostasis in the gills is indicative of osmotic plasticity in killifish. *Comp. Biochem. Physiol. Part A: Mol. Integr. Physiol.* 257, 110969. doi: 10.1016/j.cbpa.2021.110969

Neinast, M., Murashige, D., and Arany, Z. (2019). Branched chain amino acids. *Annu. Rev. Physiol.* 81, 139. doi: 10.1146/annurev-physiol-020518-114455

Noble, C., Iversen, M. H., Lein, I., Kolarevic, J., Johansen, L.-H., Berge, G. M., et al. (2019). *Rensvel OWI fact sheet series: An introduction to Operational and Laboratory-based Welfare Indicators for lumpfish (Cyclopterus lumpus L.)* (Tromsø, Norway: Nofima). Available at: https://www.fhf.no/prosjekter/prosjektbasen/901136/.

Opinion, A. G. R., Vanhomwegen, M., De Boeck, G., and Aerts, J. (2023). Long-term stress induced cortisol downregulation, growth reduction and cardiac remodeling in Atlantic salmon. *J. Exp. Biol.* 226, jeb246504. doi: 10.1242/jeb.246504

Peixoto, D., Pinto, W., Gonçalves, A. T., MaChado, M., Reis, B., Silva, J., et al. (2021). Microalgal biomasses have potential as ingredients in microdiets for Senegalese sole (*Solea Senegalensis*) post-larvae. *J. Appl. Phycology* 33, 2241–2250. doi: 10.1007/s10811-021-02431-1

Peuhkuri, N., Bjerkås, E., Brännäs, E., Piironen, J., Primmer, C., and Taskinen, J. (2009). *Looking fish in the eye- cataract as a problem in fish farming*. Available online at: http://norden.diva-portal.org/smash/get/diva2:700809/FULLTEXT01.pdf.

Pickering, A. D., and Pottinger, T. G. (1989). Stress responses and disease resistance in salmonid fish: Effects of chronic elevation of plasma cortisol. *Fish Physiol. Biochem.* 7, 253–258. doi: 10.1007/BF00004714

Quade, M. J., and Roth, J. A. (1997). A rapid, direct assay to measure degranulation of bovine neutrophil primary granules. *Veterinary Immunol. Immunopathology* 58, 239–248. doi: 10.1016/S0165-2427(97)00048-2

Ramos-Pinto, L. (2020). *Amino acids as key mediators of immune status and nutritional condition in fish* Vol. 93 (Porto, Portugal: University of Porto). University of Porto.

Reid, S. G., Bernier, N. J., and Perry, S. F. (1998). The adrenergic stress response in fish: Control of catecholamine storage and release. *Comp. Biochem. Physiol. - C Pharmacol. Toxicol. Endocrinol.* 120, 1–27. doi: 10.1016/S0742-8413(98)00037-1

Reis, B., Ramos-Pinto, L., Martos-Sitcha, J. A., MaChado, M., Azeredo, R., Fernández-Boo, S., et al. (2021). Health status in gilthead seabream (*Sparus aurata*) juveniles fed diets devoid of fishmeal and supplemented with Phaeodactylum tricornutum. *J. Appl. Phycology* 33, 979–996. doi: 10.1007/S10811-021-02377-4/METRICS

Remen, M., Nes, A. M., Hangstad, T. A., Geraudie, P., Reynolds, P., Urskog, T. C., et al. (2022). Temperature and size-dependency of lumpfish (*Cyclopterus lumpus*) oxygen requirement and tolerance. *Aquaculture* 548, 737576. doi: 10.1016/j.aquaculture.2021.737576

Reynolds, P., Imsland, A. K. D., and Boissonnot, L. (2022). Causes of mortality and loss of lumpfish *Cyclopterus lumpus*. *Fishes* 7, 328. doi: 10.3390/fishes7060328

Sadoul, B., and Vijayan, M. M. (2016). Stress and growth. *Fish Physiol.* 35, 167–205. doi: 10.1016/B978-0-12-802728-8.00005-9

Saeij, J. P. J., Verburg-Van Kemenade, L. B. M., Van Muiswinkel, W. B., and Wiegertjes, G. F. (2003). Daily handling stress reduces resistance of carp to *Trypanoplasma borreli: In vitro* modulatory effects of cortisol on leukocyte function and apoptosis. *Dev. Comp. Immunol.* 27, 233–245. doi: 10.1016/S0145-305X(02)00093-9

Sánchez-Muros, M. J., Villacreces, S., Miranda-de la Lama, G., de Haro, C., and García-Barroso, F. (2013). Effects of chemical and handling exposure on fatty acids, oxidative stress and morphological welfare indicators in gilt-head sea bream (*Sparus aurata*). *Fish Physiol. Biochem.* 39, 581–591. doi: 10.1007/S10695-012-9721-2/METRICS

Schreck, C. B., and Tort, L. (2016). The concept of stress in fish. *Fish Physiol.* 35, 1–34. doi: 10.1016/B978-0-12-802728-8.00001-1

Segner, H., Sundh, H., Buchmann, K., Douxfils, J., Snuttan Sundell, K., Mathieu, C., et al. (2012). Health of farmed fish: its relation to fish welfare and its utility as welfare indicator. *Fish Physiol. Biochem.* 38, 85–105. doi: 10.1007/s10695-011-9517-9

Skår, M. W., Haugland, G. T., Powell, M. D., Wergeland, H. I., and Samuelsen, O. B. (2017). Development of anaesthetic protocols for lumpfish (*Cyclopterus lumpus* L.): Effect of anaesthetic concentrations, sea water temperature and body weight. *PloS One* 12, e0179344. doi: 10.1371/journal.pone.0179344

Sneddon, L. U., Wolfenden, D. C. C., and Thomson, J. S. (2016). Stress management and welfare. *Fish Physiol.* 35, 463–539. doi: 10.1016/B978-0-12-802728-8.00012-6

Sopinka, N. M., Donaldson, M. R., O'Connor, C. M., Suski, C. D., and Cooke, S. J. (2016). Stress indicators in fish. *Fish Physiol.* 35, 405–462. doi: 10.1016/B978-0-12-802728-8.00011-4

Staven, F. R., Nordeide, J. T., Imsland, A. K., Andersen, P., Iversen, N. S., and Kristensen, T. (2019). Is habituation measurable in lumpfish *Cyclopterus lumpus* when used as cleaner fish in atlantic salmon *Salmo salar* aquaculture? *Front. Veterinary Sci.* 6. doi: 10.3389/FVETS.2019.00227/BIBTEX

Stien, L. H., Størkersen, K. V., and Gåsnes, S. K. (2020). Analyse av dødelighetsdata fra spørreundersøkelse om velferd hos rensefisk. *Rapport fra havforskningen*, 2020-6. Havforskningsinstituttet, Trondheim, Norway. Available at: https://www.hi.no/hi/nettrapporter/rapport-fra-havforskningen-2020-6.

Tort, L. (2011). Stress and immune modulation in fish. *Dev. Comp. Immunol.* 35, 1366–1375. doi: 10.1016/j.dci.2011.07.002

Tort, L., Balasch, J. C., and Mackenzie, S. (2003). Fish immune system. A crossroads between innate and adaptive responses. *Inmunología* 22, 277–286.

Urbinati, E. C., Zanuzzo, F. S., and Biller, J. D. (2020). Stress and immune system in fish. *Biol. Physiol. Freshw. Neotropical Fish*, 93–114. doi: 10.1016/B978-0-12-815872-2.00005-1

Valenzuela, C. A., Zuloaga, R., Mercado, L., Einarsdottir, I. E., Björnsson, B. T., Valdés, J. A., et al. (2018). Chronic stress inhibits growth and induces proteolytic mechanisms through two different nonoverlapping pathways in the skeletal muscle of a teleost fish. *Am. J. Physiol. - Regul. Integr. Comp. Physiol.* 314, R102–R113. doi: 10.1152/AJPREGU.00009.2017/ASSET/IMAGES/LARGE/ZH60121793710008.JPEG

Van Waarde, A. (1988). Biochemistry of non-protein nitrogenous compounds in fish including the use of amino acids for anaerobic energy production. *Comp. Biochem. Physiol. Part B: Comp. Biochem.* 91, 207–228. doi: 10.1016/0305-0491(88)90136-8

Varma, S. D., Chand, D., Sharma, Y. R., Kuck, J. F., and Richards, R. D. (1984). Oxidative stress on lens and cataract formation: role of light and oxygen. *Curr. Eye Res.* 3, 35–58. doi: 10.3109/02713688408997186

Verburg-van Kemenade, B. M. L., Ribeiro, C. M. S., and Chadzinska, M. (2011). Neuroendocrine–immune interaction in fish: Differential regulation of phagocyte activity by neuroendocrine factors. *Gen. Comp. Endocrinol.* 172, 31–38. doi: 10.1016/j.ygcen.2011.01.004

Verburg-Van Kemenade, B. M. L., Stolte, E. H., Metz, J. R., and Chadzinska, M. (2009). Chapter 7 neuroendocrine–immune interactions in teleost fish. *Fish Physiol.* 28, 313–364. doi: 10.1016/S1546-5098(09)28007-1

Vijayan, M. M., and Leatherland, J. F. (1990). High stocking density affects cortisol secretion and tissue distribution in brook charr, *Salvelinus fontinalis*. *J. Endocrinol.* 124, 311–318. doi: 10.1677/joe.0.1240311

Waagbøø, R., Tröße, C., Koppe, W., Fontanillas, R., and Breck, O. (2010). Dietary histidine supplementation prevents cataract development in adult Atlantic salmon, *Salmo salar* L., in seawater. *Br. J. Nutr.* 104, 1460–1470. doi: 10.1017/S0007114510002485

Wallace, H. M., Fraser, A. V., and Hughes, A. (2003). A perspective of polyamine metabolism. *Biochem. J.* 376, 1. doi: 10.1042/bj20031327

Wang, Y., Fung, N. S. K., Lam, W. C., and Lo, A. C. Y. (2022). mTOR signalling pathway: A potential therapeutic target for ocular neurodegenerative diseases. *Antioxidants* 11, 1304. doi: 10.3390/antiox11071304

Wendelaar Bonga, S. E. (1997). The stress response in fish. *Physiol. Rev.* 77, 591–625. doi: 10.1152/physrev.1997.77.3.591

Winberg, S., Höglund, E., and Øverli, Ø. (2016). Variation in the neuroendocrine stress response. *Fish Physiol.* 35, 35–74. doi: 10.1016/B978-0-12-802728-8.00002-3

Wojtaszek, J., Dziewulska-Szwajkowska, D., Lozińska-Gabska, M., Adamowicz, A., and Dugaj, A. (2002). Hematological effects of high dose of cortisol on the carp (*Cyprinus carpio* L.): cortisol effect on the carp blood. *Gen. Comp. Endocrinol.* 125, 176–183. doi: 10.1006/gcen.2001.7725

Wu, G., Fang, Y. Z., Yang, S., Lupton, J. R., and Turner, N. D. (2004). Glutathione metabolism and its implications for health. *J. Nutr.* 134, 489–492. doi: 10.1093/jn/134.3.489

Yada, T., and Tort, L. (2016). Stress and disease resistance: immune system and immunoendocrine interactions. *Fish Physiol.* 35, 365–403. doi: 10.1016/B978-0-12-802728-8.00010-2

Yoneda, J., Andou, A., and Takehana, K. (2009). Regulatory roles of amino acids in immune response. *Curr. Rheumatol. Rev.* 5, 252–258. doi: 10.2174/157339709790192567

Zar, J. H. (1984). *Biostatistical analysis. 2nd ed* (New Jersey, USA: Prentice-Hall).

frontiers | Frontiers in Marine Science

TYPE Original Research
PUBLISHED 23 August 2024
DOI 10.3389/fmars.2024.1462589

OPEN ACCESS

EDITED BY
Yiming Li,
Fishery Machinery and Instrument Research Institute, China

REVIEWED BY
Zhi Liao,
Zhejiang Ocean University, China
Yongbo Bao,
Zhejiang Wanli University, China

*CORRESPONDENCE
Chuangye Yang
yangcy@gdou.edu.cn

RECEIVED 10 July 2024
ACCEPTED 07 August 2024
PUBLISHED 23 August 2024

CITATION
Li F, Liu J, Gao Z, Yang C, Sun L, Liao Y and Deng Y (2024) Transcriptomic analyses of *Pinctada fucata martensii* responses under stress of titanium dioxide nanoparticles. *Front. Mar. Sci.* 11:1462589. doi: 10.3389/fmars.2024.1462589

Transcriptomic analyses of *Pinctada fucata martensii* responses under stress of titanium dioxide nanoparticles

Fengfeng Li[1], Jiaen Liu[1], Zixin Gao[1], Chuangye Yang[1]*, Liwei Sun[2], Yongshan Liao[3,4] and Yuewen Deng[1,3,4,5]

[1]Fisheries College, Guangdong Ocean University, Zhanjiang, China, [2]Southern Marine Science and Engineering Guangdong Laboratory (Guangzhou), Guangzhou, China, [3]Pearl Research Institute, Guangdong Ocean University, Zhanjiang, China, [4]Pearl Breeding and Processing Engineering Technology Research Centre of Guangdong Province, Zhanjiang, China, [5]Guangdong Provincial Key Laboratory of Aquatic Animal Disease Control and Healthy Culture, Zhanjiang, China

Titanium dioxide nanoparticles (TiO_2-NPs) released into the environment is becoming more prevalent due to their increased usage, marine TiO_2-NPs contamination is escalating concerns in coastal areas. To understand the potential impact of TiO_2-NPs on transcript changes in pearl oyster (*Pinctada fucata martensii*), transcriptome analysis on the gill tissues of pearl oysters was conducted after 14-day TiO_2-NPs exposure and 7-day brief recovery. A total of 911 differentially expressed genes (DEGs) were identified between the control group (TC) and the experimental group (TE) exposed to 14-day TiO_2-NPs. Gene ontology (GO) analyses of the DEGs demonstrated their substantial enrichments in functions related to "hydrolase activity", "oxidoreductase activity", and "DNA integration". The Kyoto Encyclopedia of Genes and Genomes (KEGG) pathways analyses of the DEGs indicated enrichment in several pathways, including "ubiquitin-mediated protein hydrolysis", "ECM-receptor interactions", "NOD-like receptor signaling pathway", "Toll-like receptor", and "FOXO signaling pathway". This suggests that exposure to TiO_2-NPs intensifies oxidative stress and apoptosis in pearls oysters, leading to negative effects such as disrupted protein homeostasis, decreased biomineralization activity, reduced neuronal excitability, weakened immune response, and reduced cellular metabolism. Transcriptome analysis identified 844 DEGs between the TE and recovery group (TR), which underwent a 7-day brief recovery period. GO analyses of the DEGs demonstrated their substantial enrichments in functions related to "DNA integration", "obsolete oxidation-reduction process", and "proteolysis". KEGG pathways analyses of the DEGs indicated enrichment in several pathways, including "lysine degradation", "glycine, serine, and threonine metabolism", and "NOD-like receptor signaling pathway". The findings indicated that although pearl oysters showed only slight relief after 7 days of brief recovery, they

continued to experience negative effects from TiO_2-NP exposure. Our findings shed light on the complex responses of pearl oysters to TiO_2-NPs stress and offer valuable theoretical insights into the toxicological impact of TiO_2-NPs on pearl oysters.

KEYWORDS

TiO_2-NPs, *Pinctada fucata martensii*, transcriptomics, protein homeostasis, oxidative stress

1 Introduction

Titanium dioxide nanoparticles (TiO_2-NPs) demonstrate remarkable UV-absorbing properties, outstanding chemical stability, high opacity, and excellent resistance to fading. These unique characteristics make TiO_2-NPs an essential component in numerous consumer goods, including sunblocks, cosmetics, pharmaceuticals, coatings, fabrics, polymers, paper, and wood treatments (Aitken et al., 2006). TiO_2-NPs can enter environments via production, transportation, usage, and disposal stages, thereby posing risks to diverse aquatic organisms and their ecosystem (Shi et al., 2016; Carbuloni et al., 2020). High-concentration TiO_2-NPs have been detected in coastal waters, with even greater accumulations observed in sediments (Garner and Keller, 2014). Based on model computations, the TiO_2-NP concentration in surface waters and wastewater varies from dozens to several hundred micrograms per liter (Sun et al., 2016). Concentrations have been recorded to be 900 μg/L in the surface water near French Mediterranean beaches (Labille et al., 2020). The titanium dioxide levels were found exceeding the 1.85 ± 0.55 ng/g detection limit by analyzing the bivalve shellfish from northern China coastal cities, indicating notable accumulation (Li and Gao, 2014). Increased levels of TiO_2-NPs pose significant threats to various marine organisms, leading to increased concerns about the ecological and physiological impact of TiO_2-NPs. A growing body of evidence has demonstrated that TiO_2-NPs can lead to various adverse effects, including reduced fertilization success (Gallo et al., 2016), decreased metabolism (Johari et al., 2013; Muller et al., 2014), delayed embryonic development (Libralato et al., 2013), impaired immune response (Ringwood et al., 2009; Rocha et al., 2014), intestinal microbiome disorders (Chen et al., 2022b; Duan et al., 2023; Li et al., 2024a), and DNA damage (Hu et al., 2017).

RNA sequencing (RNA-seq) is used to identify gene expression patterns under environmental stress. This method is crucial for examining the overall functional arrangement of genes and investigating the control mechanisms of biological metabolic pathways. In recent years, transcriptomics technology has been extensively employed in toxicological studies of aquatic organisms exposed to pollutants. By examining changes in gene expression under toxic stress, this technology can reveal the intrinsic toxicity of pollutants in aquatic organisms at the transcriptional level, facilitating the prediction and prevention of pollutant toxicity in aquatic organisms and the environments (Sharon et al., 2013; Liu et al., 2020). Banni et al. (2016) examined the impact of TiO_2-NPs and 2,3,7, 8-tetrachlorodibenzo-p-dioxins on genes related to the digestive glands of *Mytilus galloprovincialis* using a combination of transcriptomics and immunohistochemistry. Zhou et al. (2024) used transcriptomic methods to discover that TiO_2-NP exposure triggers lipid metabolism disorders, immune defense disruption, and oxidative stresses in *Acipenser schrenckii*. These findings underscore the effectiveness of transcriptomics in providing a comprehensive analysis of the impact of TiO_2-NPs on aquatic organisms.

Pinctada fucata martensii, native to southern China, Southeast Asia, Australia, India, and Japan (Yang et al., 2019, 2023), are filter-feeding mollusks renowned for their high economic values, contributing near 90% of the world's marine pearl production (He et al., 2020; Wu et al., 2022). Raft and pile cultures are the primary cultural approaches of offshore pearl oysters (Yang et al., 2017). Nevertheless, escalating nearshore marine pollution has recently placed pearl oysters under significant threat. TiO_2-NPs are prone to condensation and deposition on the surface of sediments. The gills of marine bivalves are the primary organs exposed to waterborne pollutants and serve as major detoxification organs in these species, rendering gene expression in this organ highly prone to alterations (Brandts et al., 2018). This study used RNA-Seq analysis of gill tissue to identify the potential genes and pathways affected by TiO_2-NPs in pearl oysters after 14-day exposure and 7-day brief recovery, providing a theoretical basis of TiO_2-NPs' effects on pearl oysters.

2 Materials and methods

2.1 Exposure of pearl oysters to TiO_2-NPs

The anatase form of TiO_2-NPs, approximately 5–10 nm in size, was obtained from Shanghai McLean Biochemical Technology (Shanghai, China). TiO_2-NPs were initially added to filtered seawater and homogenized for 20 min using an LC-JY92-TTN

ultrasonic homogenizer (65 W; Lichen Bonsi Instrument Technology, China) to prepare 1 g/L nanoparticle suspension. The suspension was subsequently diluted with seawater to a final TiO_2-NPs concentration of 5 mg/L.

The pearl oysters with intact and uniform-sized shells (shell width with 26.81 ± 2.53 mm) were selected from a fast-growing, black-selective line of pearl oysters (Deng et al., 2013), sourced from Liusha Bay, China. The pearl oysters were cleaned to remove biofoulings and cultured in cylindrical barrels (300 L) for 7 days. Then the pearl oysters were exposed to 5 mg/L TiO_2-NPs for 14 days (treatment phase) and subsequently cultured in TiO_2-NP-free seawater for 7 days (recovery phase). Pearl oysters were fed unicellular algae (morning: 20,000 cells/mL *Chlorella*; evening: 10,000 cells/mL *Platymonas subcordiformis*) during the study period. The experiment comprised three parallel groups, each consisting of 30 pearl oysters. The water in the barrels was daily refreshed, and TiO_2-NPs suspension was added to each barrel maintain a constant TiO_2-NPs concentration of 5mg/L. On days 0, 14, and 21, we randomly selected 2 pearl oysters from each parallel group, designated the control (TC), experimental (TE), and recovery (TR). Gill tissues were clipped and frozen in liquid nitrogen and then stored at −80°C for subsequent analyses. No dead pearl oysters were found during the exposure and recovery periods.

2.2 RNA extraction and library construction

RNA extraction and purification from the gill tissue were conducted utilizing TRIzol (Invitrogen, CA, USA) following instructions from the manufacturer. The purity and quantity of total RNA was evaluated utilizing a NanoDrop ND-1000 (NanoDrop, Wilmington, DE, USA). Oligo(dT) magnetic beads (Dynabeads Oligo, No. 25-61005, Thermo Fisher, USA) were utilized in two consecutive purification steps to specifically capture mRNA containing PolyA tails. NEBNext® Magnesium RNA Fragmentation technology (product number E6150S, USA) was used to fragment the captured mRNA at a high temperature of 94°C for 5 to 7 min. Subsequently, the DNA-RNA complex double strands into pure DNA double strands. Simultaneously, a dUTP solution (product number R0133, Thermo Fisher, California, USA) was added to smooth the ends of the double-stranded DNA. Subsequently, A bases were added to each end to and used magnetic beads for fragment size screening and purification. The UDG enzyme (NEB, product number m0280, Massachusetts, USA) was then used to digest the double-stranded DNA, followed by PCR amplification. Thus, a library was constructed with a 300 bp ± 50 bp fragment size. In accordance with the standard process provided by LC Bio-Technology Co., Ltd. (Hangzhou, China), Illumina Novaseq™ 6000 was utilized for dual-end PE150 sequencing.

2.3 Bioinformatics analyses of RNA-seq

Cutadapt ver. 1.9 was utilized to discard adapter sequences, polyA sequences, polyG sequences, and other low-quality reads. FastQC ver. 0.11.9 was used to verify the GC content and Q20/30 content of the quality-controlled reads. HISAT2 ver. 2.0.4 was utilized to align the reads to the reference genome (Zheng et al., 2023). StringTie ver. 2.1.6 was employed for gene transcription or assembly using FPKM quantification. The reads were assembled with StringTie ver. 1.3.4d, using default parameters. The gffcompare ver. 0.9.8 was selected for comprehensive transcriptomic reconstruction. The R package EdgeR was then utilized to examine the difference between sample genes, defining significant difference as twice difference ratio > or < 0.5 times and p value < 0.05 (Robinson et al., 2010). Finally, Kyoto Encyclopedia of Genes and Genomes (KEGG) and gene ontology (GO) gene enrichments analyses were performed utilizing DAVID software. Raw transcriptome sequences data have been deposited at Genome Sequence Archive (GSA) under accession CRA017826.

2.4 Gene expression validation

Eight DEGs were randomly selected for qRT-PCR experiments to determine whether the results of RNA-seq data were reliable. β-Actin was used as the internal reference gene. Primers were designed using Primer Premier 5.0 software as shown in Supplementary Table 1. The total mixture of 10 μL of each sample was reacted by the following procedure: denaturation at 95°C for 5 min, followed by 40 amplification cycles (95°C for 10 s, 60°C for 15 s for annealing, and 72°C for 15 s for extension). Expression levels of different genes were analyzed using the $2^{-\Delta\Delta CT}$ method (Livak and Schmittgen, 2001).

3 Results

3.1 Transcriptome sequencing

Illumina sequencing generated a significant number of raw reads (758,415,850), which were processed to yield 737,017,614 high-quality clean reads following quality control (QC). The GC contents of these reads ranged from 38.5% to 40%, with Q30 and Q20 quality scores ranging from 96.93% to 97.52% and 99.97% to 99.98%, respectively, as detailed in Table 1. Subsequently, a substantial proportion of the genes (61.95%–67.44%) were aligned successfully with the reference genome. This alignment rate highlights the suitability and reliability of sequencing data for follow-up analytical procedures.

3.2 Detection of differentially expressed genes at different experimental periods

Further differential expression analyses revealed 911 DEGs between the TC and the TE, with 390 downregulated and 521 upregulated in the TC in comparison to the TE (Figure 1). Among these, Cytochrome P450 4A25 (PIN0130055), toll-like receptor 13 (PIN0061698), DNA damage-inducible protein GADD45 gamma

10.3389/fmars.2024.1462589

TABLE 1 Summary of sequencing quality and annotation results.

Sample	Raw Data	Valid Data	Valid Ratio (reads)	Q20%	Q30%	GC content%	Mapped reads
TC1	32386114	31605872	97.59	99.97	97.12	39.50	20590581 (65.15%)
TC2	40495812	39388364	97.27	99.98	97.31	39.50	26443594 (67.14%)
TC3	41246484	40113990	97.25	99.97	97.27	39.50	26235833 (65.40%)
TC4	36327138	35354150	97.32	99.97	97.22	39.50	21902326 (61.95%)
TC5	38432986	37181954	96.74	99.98	97.52	39.50	24313435 (65.39%)
TC6	38887062	37821322	97.26	99.97	97.23	39.50	24316076 (64.29%)
TE1	38779560	37672548	97.15	99.97	97.24	38.50	23417337 (62.16%)
TE2	43661260	42422590	97.16	99.97	97.23	39.50	26907831 (63.43%)
TE3	36839476	35906184	97.47	99.97	97.38	39.50	22550883 (62.81%)
TE4	45824350	44640396	97.42	99.97	97.15	40.00	28952056 (64.86%)
TE5	45630492	44422588	97.35	99.97	97.14	39.00	29365397 (66.10%)
TE6	40980192	39882088	97.32	99.97	97.14	39.50	25996906 (65.18%)
TR1	43830504	42419362	96.78	99.98	97.30	39.50	27699419 (65.30%)
TR2	43413570	42196960	97.20	99.97	96.93	39.50	27080947 (64.18%)
TR3	47130618	45804880	97.19	99.97	97.19	39.00	30198648 (65.93%)
TR4	52324586	50979916	97.43	99.97	97.14	39.50	33672004 (66.05%)
TR5	46114218	44446490	96.38	99.98	97.32	39.50	29762848 (66.96%)
TR6	46111428	44757960	97.06	99.98	97.36	39.50	30185390 (67.44%)

(PIN0103192), and several other genes expression exhibited significant upregulation, as illustrated in Figure 2. Conversely, pyridoxal 5'-phosphate synthase subunit SNZERR (PIN0051258), gamma-glutamyltranspeptidase 1-like isoform X1 (PIN0020608), DNA damage-inducible protein GADD45 gamma (PIN0103192), ATP-binding cassette sub-family B member 6 (PIN0010578), and other genes expression exhibited significant downregulation. Furthermore, we identified 844 DEGs between the TE and the TR, including 517 downregulated and 327 upregulated in TE in comparison to the TR (Figure 1). Similarly, gamma-glutamyltranspeptidase 1-like isoform X1 (PIN0020608), ATP-binding cassette (ABC) sub-family B member 6 (PIN0010578), and several other genes expression exhibited significant upregulation after a short recovery. Conversely, genes, such as toll-like receptor 3 (PIN0120448) and heat shock 70 kDa protein 12B (PIN0060012), were substantially downregulated (Figure 3). These significantly altered genes are sensitive to TiO_2 NP-induced stress and may play an important role in physiological processes.

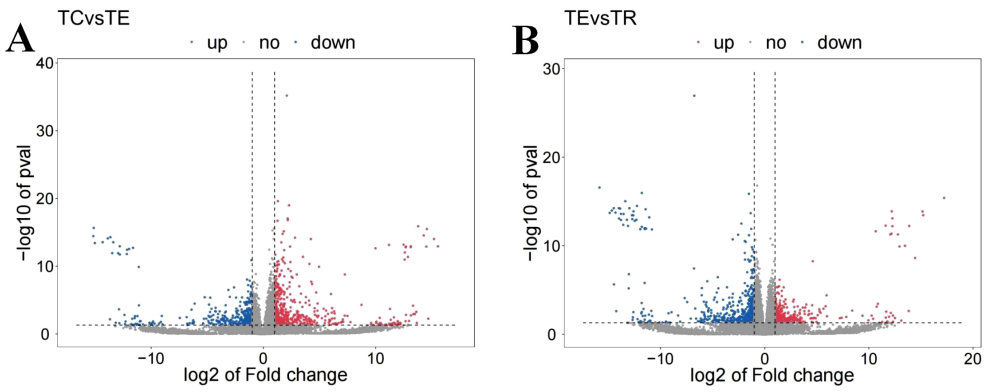

FIGURE 1
(A) Differential gene expression analyses between TC and TE. **(B)** Differential gene expression analyses between TE and TR. Red indicates the upregulated gene expression level, blue indicates the downregulated gene expression level, and grey indicated insignificant differential expression.

10.3389/fmars.2024.1462589

FIGURE 2
A heatmap showing the differential gene expression analyses between TC and TE.

3.3 GO analyses

GO enrichments analyses of the DEGs annotated 3373 and 2577 DEGs across molecular functions, cellular components, and biological process in the TC and TE groups and TE and TR groups, respectively. We selected the 30 entries with the highest enrichment levels for bar charts plotting (Figure 4A). Among them, the most annotated DEGs in the TC and TE groups were “metal ion binding”, “DNA binding”, “ATP binding”, “deoxyribonucleotide biosynthetic process”, “DNA recombination”, “mitotic spindle assembly”, “RNA-dependent DNA biosynthetic process”, “DNA integration”, and “nucleus”. In the TE and TR groups, the most annotated DEGs were “biological process”, “proteolysis”, “zinc ion binding”, “metal ion binding”, “obsolete oxidation-reduction process”, “DNA integration”, “DNA binding”, and “integral component of membrane” (Figure 4B).

3.4 KEGG enrichments analyses

KEGG enrichments analyses demonstrated the enrichments of a total of 369 DEGs in 129 signaling pathways in the TC and TE groups (Figure 5A). Notably, these pathways included significant enrichment in “vitamin B6 metabolism”, “glycine, serine, and threonine metabolism”, “biosynthesis of unsaturated fatty acids”, “ubiquitin-mediated protein hydrolysis”. Furthermore, the “ABC transporter”, and “ECM-receptor interactions”, “NOD-like receptor signaling pathway”, “Toll-like receptor”, “neuroactive ligand-

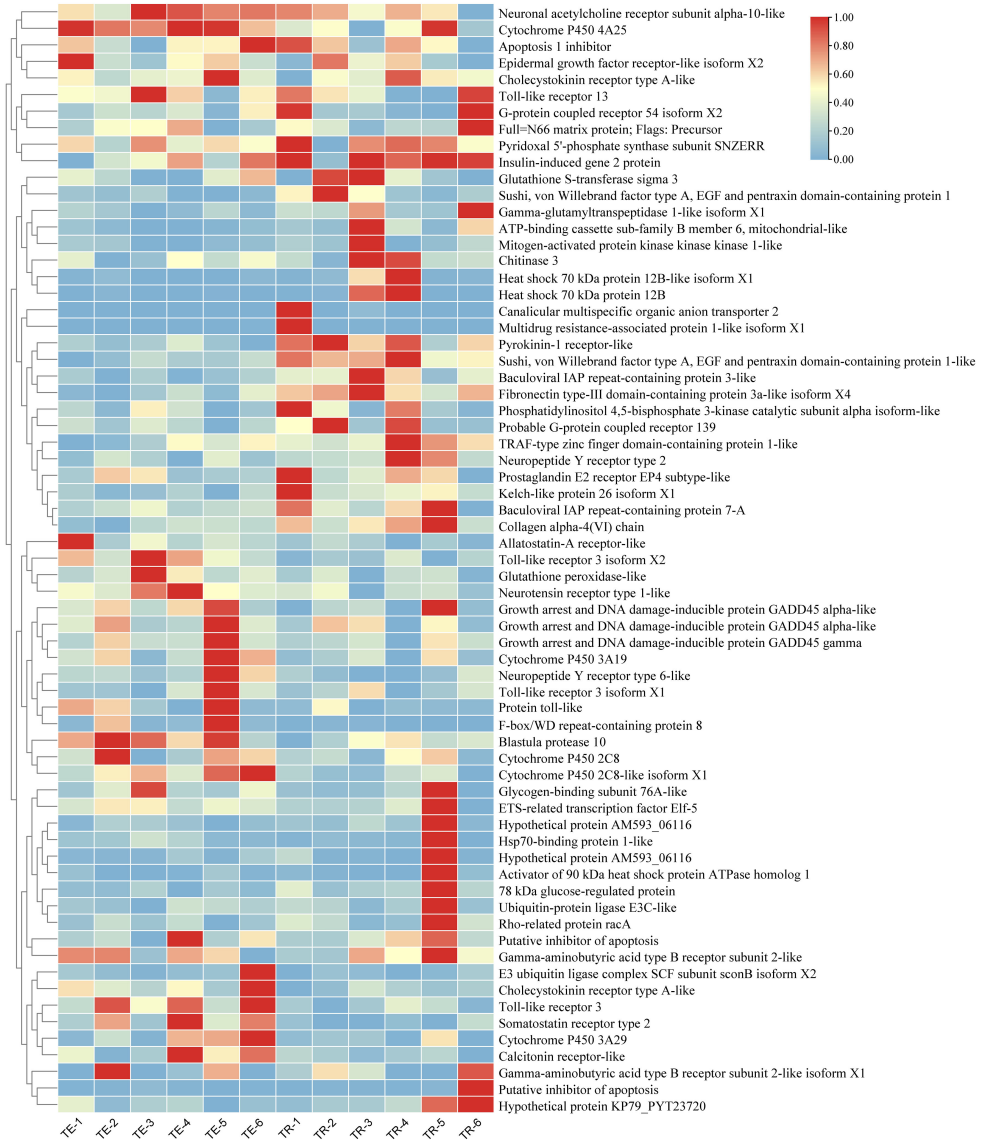

FIGURE 3
A heatmap showing the differential gene expression analyses between TE and TR.

receptor interaction signaling pathway", "lysosomal pathway", "phagosomal pathway", "FOXO signaling pathway", and "glutathione metabolite" were also identified to be associated with pearl oysters' responses to TiO_2-NPs exposure. Conversely, a total of 284 DEGs in the TE and TR groups were enriched in 102 signaling pathways (Figure 5B). Notably, significant enrichment was observed in "lysine degradation", "glycine, serine, and threonine metabolism", "NOD-like receptor signaling pathway", and other pathways.

3.5 qRT-PCR validation

To assess the accuracy of the RNA-seq results, 8 DEGs were randomly selected for qRT-PCR in each of the TC vs TE and TE vs TR groups. qRT-PCR selective gene expression trends were consistent with DEG analyses, suggesting that the transcriptome data were reliable (Figure 6).

4 Discussion

The survival of aquatic organisms is significantly affected by salinity, oxygen content, temperature, and pollutants in the water (Valavanidis et al., 2006). In particular, environmental chemicals pose various toxic threats to aquatic organisms, such as DNA damage, oxidative stress, inflammation, apoptosis, and cell death (Lim et al., 2022; Wang et al., 2023). To withstand complex and variable living environments, intertidal bivalves have developed highly intricate adaptive mechanisms (Falfushynska et al., 2020). Considerable research interest has recently been focused on the potential impacts of TiO_2-NPs on marine bivalves (Abdel-Latif

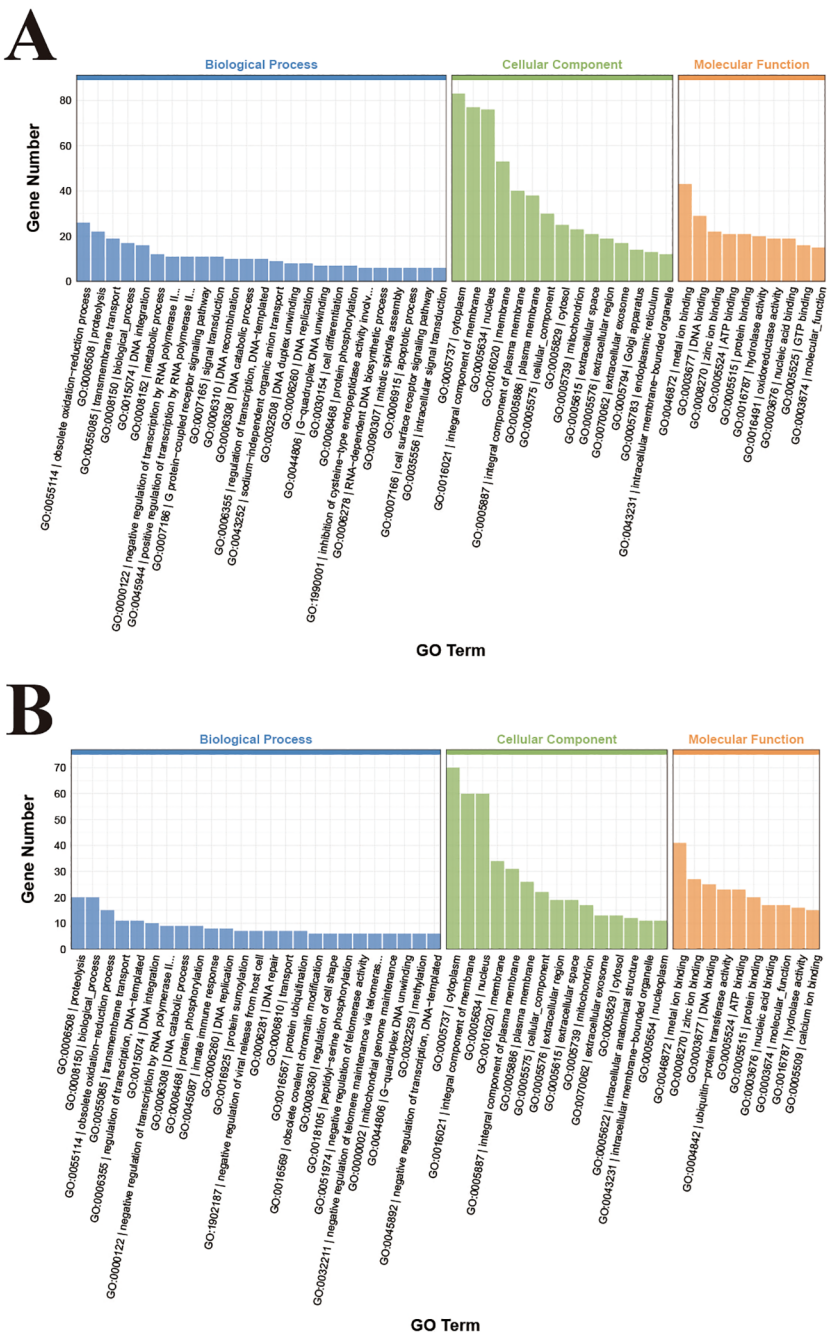

FIGURE 4
GO terms enrichment analysis of DEGs in TC and TE **(A)**, TE and TR **(B)**.

et al., 2020; Li et al., 2021). This study revealed the molecular response mechanisms of pearl oysters after exposure to TiO_2-NPs, providing crucial insights into evaluating the potential toxic impacts of TiO_2-NPs on these organisms.

4.1 TiO_2-NPs cause of oxidative stress

TiO_2-NPs function as prooxidants that can enter cell membrane, inducing mitochondrial damage (Barmo et al., 2013). It triggers excessive cellular production of reactive oxygen species (ROS), leading to compromised membrane permeability (Girardello et al., 2016). Under such conditions, living beings may experience oxidative stress due to excessive ROS production when the cellular antioxidant defense system becomes overwhelmed (Ray et al., 2012). To mitigate the harmful impacts of ROS, numerous animals can employ antioxidant defensing mechanisms, including non-enzymatic components (such as carotenoids and glutathione) and enzymatic components (such as glutathione peroxidase and superoxide dismutase) (Yang et al., 2017). We detected the

10.3389/fmars.2024.1462589

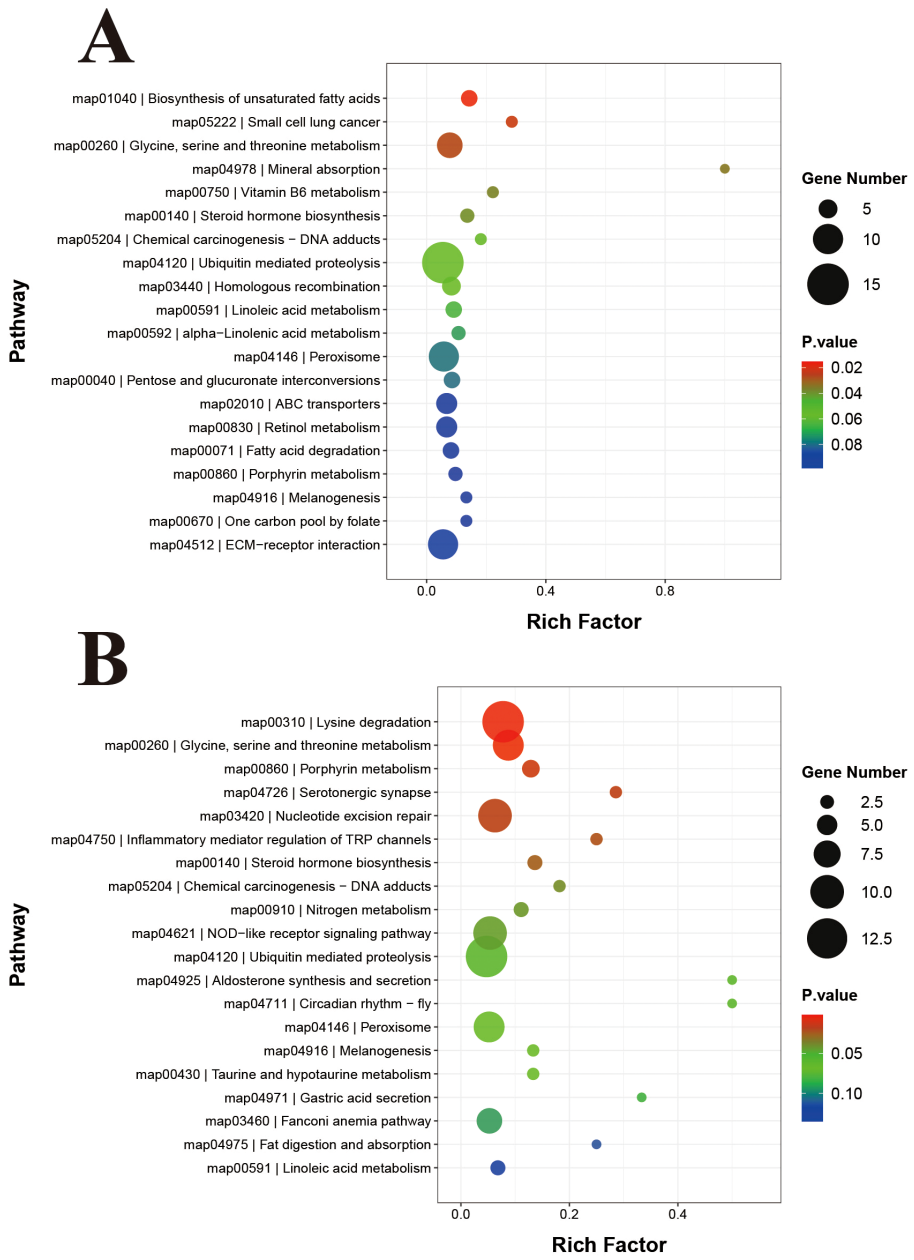

FIGURE 5
KEGG pathway enrichment analysis of DEGs in TC and TE **(A)**, TE and TR **(B)**.

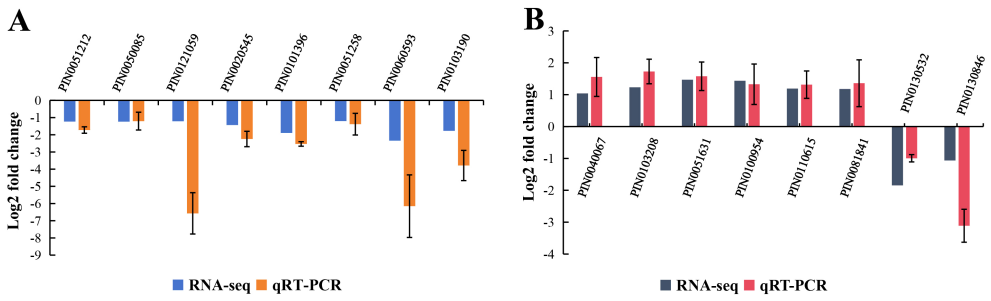

FIGURE 6
Validation of RNA-seq data by qRT-PCR in TC and TE groups **(A)**, TE and TR groups **(B)**.

substantial enrichment of the DEGs in the glutathione metabolism pathway under TiO_2-NP stress. Genes encoding glutathione peroxidase-like (PIN0101396), gamma-glutamyltranspeptidase 1-like isoform X1 (PIN0020608), glutathione S-transferase sigma 3 (PIN0052777), microsomal glutathione S-transferase 2 (PIN0060908), and aminopeptidase N (PIN0020097) were substantially downregulated. According to these results, pearl oysters experience oxidative stress under TiO_2-NP stress, being consistent with our prior finding (Li et al., 2024b).

Here, we observed notable enrichment of vitamin B6 metabolism in the KEGG pathway enrichment. Specifically, we found that the pyridoxal 5'-phosphate synthase subunit SNZERR (PIN0051258), which is involved in vitamin B6 metabolism, was downregulated in response to oxidative stress. Pyridoxal-5'-phosphate (PLP) acts as the physiologically active coenzyme of vitamin B6, potentially playing pivotal roles in antioxidation (Schneider et al., 2000). PLP can directly scavenge free radicals for lipid peroxidation inhibition. Alternatively, PLP acts indirectly as a coenzyme of the glutathione antioxidant defense system (Liu et al., 2013). Studies have indicated that deficiencies in vitamin B6 can weaken antioxidant defensing mechanisms and increase oxidative stresses (Danielyan and Chailyan, 2020). This study demonstrated that TiO_2-NPs exposure induced downregulation of pyridoxal 5'-phosphate synthase subunit SNZERR (PIN0051258), which is involved in vitamin B6 metabolism, thereby affecting vitamin B6 synthesis and increasing oxidative stress in pearl oysters.

Aquatic species depend on the multi-xenobiotic resistance (MXR) mechanism as a key defensing mechanism against environmental toxins, minimizing intracellular accumulation of toxins and potential damage (Kurelec, 1995), which is mediated by the ABC transporter (Kingtong et al., 2007). The relationship between ABC transporters and nanoparticles has gained increasing attention (Yin et al., 2023). Kingtong et al. (2007) demonstrated the significant roles of ABC transporters in the detoxification metabolic mechanism of *Saccostrea forskali* after exposure to tributyltin. Research on mussel gill cells has demonstrated the upregulation of Abcb1 by silver NPs, aiding in silver NPs detoxification (Katsumiti et al., 2015). Bhagat et al. (2022) reported that polystyrene and metal oxide nanoparticles disrupt ABC transporters' functionality in zebrafish embryos, resulting in increased aluminum and cerium ion toxicity. Similarly, Georgantzopoulou et al. (2016) found that the MXR system could be inhibited by silver nanoparticles in *Daphnia magna* larvae, leading to increased calcineurin accumulation. After TiO_2-NPs exposure, significant downregulation was observed in genes linked to the ABC transporters pathway, including ABC sub-family B member 6, mitochondrial-like (PIN0010578), multidrug resistance-associated protein 1-like isoform X1 (PIN0080856), and canalicular multispecific organic anion transporter 2 (PIN0080857). This indicates that TiO_2-NPs inhibit the activity of ABC transporter protein activity, thereby worsening oxidative stress and particle accumulation in pearl oysters. After a brief 7-day recovery period, genes associated with ABC transporters and glutathione metabolism pathways exhibited significant upregulation, indicating an increase in oxidative stress in pearl oysters.

Cytochrome P450, a class of monooxygenase, is crucial for the syntheses and metabolisms of various hormones, such as glucocorticoids and mineralocorticoids, which are essential for stress response (Urlacher and Girhard, 2012). Increased P450 production in aquatic organisms typically indicates they are experiencing stress (Ibrahim et al., 2021). For instance, elevated transcription of the cytochrome P450 gene was observed in the kidney, gill, and liver tissues of Nile tilapia following exposure to *Aeromonas hydrophila* (Hal and El-Barbary, 2020). An upregulation was observed in genes such as cytochrome P450 4A25 (PIN0130055), cytochrome P450 2C8 (PIN0120270), cytochrome P450 3A19 (PIN0100308), cytochrome P450 2C8-like isoform X1 (PIN0140634), and cytochrome P450 3A29 (PIN0100307) following 14-day TiO_2-NPs exposure, indicating that TiO_2-NPs exposure induces oxidative stress in pearl oysters. After a brief recovery period, the related cytochrome P450 gene expression was downregulated compared with that of the TE group, which also indicates that brief recovery can alleviate stress in pearl oysters.

4.2 TiO_2-NPs changes in immune activities

Exposure to TiO_2-NPs can adversely affect bivalves' immune system (Wei et al., 2023). Bivalves primarily depend on innate immunity due to their lack acquired immune system (Jiang et al., 2017). Microbial recognition by innate immunity is mediated by pattern recognition receptors, which bind to pathogen-associated molecular patterns, the conserved microbial molecules. Toll-like receptors detect microorganisms in extracellular cellular lumens and phagosomes, whereas the Nod-like family of receptors recognize intracellular pathogens, triggering transcriptional responses and activating inflammatory vesicles (Chamaillard et al., 2003; Inohara et al., 2005). Innate immune receptors interact with specific microbial ligands to generate signaling pathways triggering host transcriptional response linked to inflammation. Research has demonstrated that bacterial lysis in phagosomes is crucial for acquired and innate immune response development (Herskovits et al., 2007). Phagosome maturation involves regulatory interactions with other membrane organelles, such as regenerating endosomes, late endosomes, and lysosomes. Furthermore, the lysosomes-phagosomes fusion can release toxic compounds that effectively kill and fragment major bacteria (Luzio et al., 2007). Lysosomes play pivotal roles in various physiological functions, such as immune responses, energy metabolism, cell survival, cell membrane repair, and cellular homeostasis, most of which rely on lysosomes' protease activities (Martínez-Fábregas et al., 2018). We detected substantial upregulation of the toll-like receptor 13 (PIN0061698), toll-like receptor 3 isoform X2 (PIN0061696), and toll-like receptor 3 isoform X1 (PIN0061693) genes after exposure to TiO_2-NPs. Furthermore, the expression of some genes in the NOD-like receptor signaling pathway, lysosome pathway, and phagosome pathway was substantially upregulated, indicating that TiO_2-NPs exposure activates the immune system of pearl oysters and improves their immune ability to resist the invasion of TiO_2-NPs, being consistent with our prior finding (Li

et al., 2024a, b). We observed substantial downregulation of the toll-like receptor 3 (PIN0120448) and protein toll-like (PIN0071163) genes after a brief recovery period. In addition, the NOD-like receptor signaling, lysosome, and phagosome pathways remained substantially upregulated compared with the TE group, indicating that brief recovery may alleviate immune stress in pearl oysters.

4.3 TiO_2-NPs induces apoptosis

Apoptosis is critical for the immune response of mollusks (Zhang et al., 2022). The FOXO signaling pathway is associated with apoptosis, DNA repair, and several cellular pathways (Chen et al., 2022a). In aquaculture, there is increasing research interest in investigating the changes in the FOXO pathway caused by environmental stress. For instance, studies have demonstrated that acute hypoxia induces changes in the FOXO signaling pathway in *Hypophthalmichthys nobilis* (Chen et al., 2021) and *Oncorhynchus mykiss* (Wu et al., 2023). Additionally, Ma et al. (2023) revealed that high-temperature stress mitigates cellular apoptosis by regulating the expressions of FOXO target genes related to apoptosis, thereby mediating liver injury in *Brachymystax lenok tsinlingensis*. After exposure to TiO_2-NPs, the expressions of genes related to the FoxO signaling pathway were substantially downregulated, including epidermal growth factor receptor-like isoform X2 (PIN0140090), growth arrest and DNA damage-inducible protein GADD45 gamma (PIN0103192), growth arrest and DNA damage-inducible protein GADD45 alpha-like (PIN0103191, PIN0103190), growth arrest and DNA-damage-inducible protein GADD45 gamma (PIN0103188), and phosphatidylinositol 4,5-bisphosphate 3-kinase catalytic subunit alpha isoform-like (PIN0101618). This indicates that exposure to TiO_2-NPs inhibits the FOXO pathway and induces apoptosis. Gadd45 α is known to be activated in response to DNA damage (Salvador et al., 2013). Martin-Folgar et al. (2022) discovered that exposure of *Danio rerio* to plastic particles at a concentration of 0.1 ppm resulted in upregulation of GADD450 expression, whereas exposures to 0.5 and 3 ppm led to downregulation of GADD450 gene expression. Consistent with observations of Martin-Folgar et al. (2022), we also observed a significant downregulation of Gadd45 expression in pearl oysters after 14 days of TiO_2-NPs exposure, which indicates that TiO_2-NPs may have impacted the DNA repair mechanism of pearl oysters by affecting the overall repair capacity of DNA, potentially leading to apoptosis.

Inhibitors of apoptosis proteins (IAP) protect aquatic organisms from the detrimental impacts of atmospheric exposure, thereby extending their survival time (Zhou et al., 2021). A significant upregulation of IAPs in oysters exposed to high temperatures, air, and low salinity has been demonstrated previously (Zhang et al., 2012). Under hypoxia in pearl oysters (Yang et al., 2023) and manila clams (Nie et al., 2020), the expressions of IAPs were substantially upregulated to activate their apoptotic systems in response to survival conditions. Nevertheless, baculovirus IAP repeat sequence protein 3-like (PIN0060593), baculovirus IAP repeat sequence protein 7-A (PIN0060592), and putative apoptosis inhibitory factors (PIN0070159, PIN0070593) were found to be downregulated under the conditions of TiO_2-NPs exposure, leading to apoptosis and affecting cell viability and proliferation.

4.4 Energy supply and energy expenditure

Bivalves are particularly vulnerable to nanoparticle toxicity in aquatic environments because of their filter-feeding strategy and sessile lifestyle. Nanoparticles, which are often agglomerated, are trapped in their gills and can enter the digestive system through endocytosis, leading to harmful effects (Gornati et al., 2016; Li et al., 2021). Nanomicroplastics have been demonstrated to disrupt the digestive system of shellfish, impairing nutrient absorption and consequently affecting shellfish health (Cole et al., 2020; Cappello et al., 2021). Furthermore, *Mytilus edulis* could absorb 100 nm microplastic particles, which affect the filtration activity of these organisms, produce pseudofaeces, and consume energy (Wegner et al., 2012).

Gluconeogenesis and glycolysis are critical metabolic pathways involved in carbohydrate synthesis and catabolism (Jitrapakdee, 2012). Studies have demonstrated that shellfish maintain energy balance under stress conditions by boosting glycolysis (Sun et al., 2021; Hu et al., 2022). During pathogen infections, the host requires increased energy to fight and survive the infection. However, relying solely on sugar metabolism is insufficient to support the higher energy requirements of the host due to its limited carbohydrate content. Proteins and lipids serve as crucial alternative energy sources to meet the increased energy demands of the host. Lipids contribute significantly to animal adaptation to adverse environments, in addition to supporting normal growth and development by providing energy (Chen et al., 2013; Liu et al., 2016). Studies have demonstrated that zebrafish experience increased glucose consumption and energy supply deficits after exposure to NPs (Chen et al., 2020). In *Crassostrea gigas* larvae, stimulation by OsHV-1 infection resulted in large-scale mortality, likely attributed to reduced oyster feeding activity and significant disruption of lipid metabolism within the organisms (Young et al., 2017). After exposure to TiO_2-NPs, KEGG secondary pathways analysis revealed significant enrichment in pathways related to carbohydrate metabolism. Specifically, the expression of most related genes within the glycolytic pathways, pentose and glucuronate interconversion pathway, citrate cycle pathway, and nucleotide and amino sugars metabolism pathway was substantially downregulated. Furthermore, key genes associated with energy metabolisms, such as glycogen-binding subunit 76A-like (PIN0121059), 78 kDa glucose-regulated protein (PIN0111091), and insulin-induced gene 2 protein (PIN0010512) were substantially downregulated. This indicates a reduction in sugar and carbohydrate supply to the organism from pearl oysters exposed to TiO_2-NPs. Most genes in the KEGG secondary pathways associated with amino acid metabolism, such as methionine and cysteine metabolism pathways, threonine, serine, and glycine metabolism pathways, lysine degradation pathway, and arginine and proline metabolism pathways, were substantially downregulated. Conversely, most genes involved in pathways

associated with lipid metabolism, such as steroid hormone biosynthesis, unsaturated fatty acids biosynthesis, linoleic acid metabolism, and fatty acid degradation pathways, were substantially upregulated. This indicates that under TiO_2-NPs stress, lipid metabolism becomes the primary energy supply for pearl oysters. We speculate that sugars, carbohydrates, and proteins may primarily supply energy during the pre-exposure phase of TiO_2-NPs, and then switch to lipids during the post-exposure phase of the exposure. However, further studies are required to confirm this hypothesis. After a brief recovery period, secondary pathways related to glycan biosynthesis and metabolism, lipid metabolism, amino acid metabolism, and nucleotide metabolism exhibited significant upregulation, revealing the restored energy supply in pearl oysters after alleviating the stress induced by TiO_2-NPs.

Under TiO_2-NPs stress, the downregulated DEGs substantially enriched the GO terms associated with "mitotic spindle assembly", "deoxyribonucleotide biosynthetic process", "RNA-dependent DNA biosynthetic process", "DNA recombination", and "DNA integration". Extended exposure to TiO_2-NPs may cause cellular injury, potentially disrupting metabolic activities within cells. This suppression of cellular processes is hypothesized to be a strategic response to conserve energy under TiO_2-NPs-induced stress.

4.5 TiO_2-NPs disrupt protein homeostasis

Ensuring protein equilibrium is essential for maintaining physiological function, as it involves a dynamic balance between synthesis and degradation. The accumulation of damaged or misfolded proteins within cells can be toxic and disrupt normal cellular processes (Sherman and Goldberg, 2001). The HSP70 family members are crucial for maintaining protein homeostasis by facilitating newly produced and denatured peptides' folding into native conformation as well as the refolding of proteins forming aggregates within cells (Fu et al., 2014; Artigaud et al., 2015). Overexpression of HSP70 genes is often pivotal for enhancing resistance to various stresses, a common phenomenon observed among aquatic organisms exposed to pollutants (Ivanina et al., 2009). For instance, the proliferation of the HSP70 gene family and the overexpression of the HSP70 gene are believed to significantly contribute to the capability of oysters' high-temperature withstanding (Ivanina et al., 2009). Distinct amplification of HSP70 was identified in bivalve shellfish, such as the *Crassostrea hongkongensis* (Brandts et al., 2018). Conversely, HSP70 downregulation has been reported in *Mytilus galloprovincialis* after exposure to heat stress and cadmium (Izagirre et al., 2014). Transcript levels of hsp70 in the gill tissues of *Mytilus galloprovincialis* were observed to decrease after simultaneous exposure to nanoplastics and carbamazepine (Brandts et al., 2018). In our experiments, we observed substantial downregulation of the heat shock 70 kDa protein 12B (PIN0060012), heat shock 70 kDa protein 12B-like isoform X4 (PIN0131632), and HSP70-binding protein 1-like (PIN0050777) genes. However, inactivating these gene transcripts does not necessarily indicate low HSP70 protein levels. High HSP70 level has been demonstrated to cause transcription factors inactivation through a negative feedback mechanism (Pinsino et al., 2017). HSP70 proteins aid in the lysosomal degradation of aggregated proteins, using either molecular chaperone-assisted autophagy or the ubiquitin-proteasome system (Rokutan, 2000). Based on reports, animals can regulate misfolded peptides breakdown through the ubiquitin-proteasome mechanism (Hampton, 2002). Ubiquitin genes activation is stimulated to break down unrepairable proteins in a heat-sensitive abalone lineage (Chen et al., 2019). Whiteleg shrimp (*Penaeus vannamei*) responds to stress by upregulating ubiquitin gene expression after a short-term microplastic exposure (Han et al., 2021). After exposure to TiO_2-NPs, substantial decreased expression of 13 genes, such as ubiquitin-protein ligase E3C-like (PIN0100476) and apoptosis 1 inhibitor (PIN0060591) was observed, indicating that the downregulation of genes involved in the ubiquitin-mediated protein hydrolysis pathway could affect the ability of pearl oyster to remove misfolded proteins, thereby resulting in cytotoxicity. Heat shock 70 kDa protein 12B (PIN0060012) and heat shock 70 kDa protein 12B-like isoform X1 (PIN0081248) remained downregulated following a short-term recovery period of 7 days. In addition, although seven genes in the ubiquitin-mediated proteolysis pathway were upregulated, six genes remained downregulated, indicating that the short-term recovery period was insufficient to restore pearl oysters to normal levels. These findings reveal that TiO_2-NPs can significantly affect protein homeostasis in pearl oysters.

4.6 TiO_2- NPs disrupt neuronal excitability

In invertebrates, neurons play crucial roles in receiving and processing environmental information. Furthermore, neurons positively regulate synaptic structural plasticity and function, enhancing adaptive capacity under stressful conditions (Konstantinos et al., 2012). In *Limulus polyphemus*, neurons contribute to osmotic stress tolerance and adaptation through several processes, such as depolarization of membrane potentials, modulation of burst frequencies, and alteration of spiking patterns (David and Sidney, 1981). However, prolonged stress can lead to irreversible neuronal damage (Samokhvalov et al., 2008). For instance, TiO_2-NP stress downregulates related genes in pearl oyster neurons, leading to decreased neuronal excitability and inhibited neuronal activity (Yang et al., 2023). Furthermore, Guan et al. (2018) discovered that high-concentration TiO_2-NPs induced substantial neurotoxic effects on *Tegillarca granosa*. In addition, NPs are potentially neurotoxic for mammals and teleosts (Sheng et al., 2016; Ze et al., 2016). Neurofunctions are directly linked to the signaling pathway of neuroactive ligand-receptor interactions (Duan et al., 2016). Neuronal function is affected by neuroactive ligands that bind to intracellular receptors, which in turn can bind with transcription factors and regulate gene expressions (Xu et al., 2012). Disruption of genes associated with neuroactive ligand-receptor interaction results in compromised memory functions (Papassotiropoulos and de Quervain, 2015). Wei et al. (2020) reported that silica nanoparticles cause developmental neurotoxicity in zebrafish embryos by disrupting the signaling pathway of neuroactive ligand-receptor interactions. Similarly, Gainey and Greenberg (2003) observed that neurotransmitters that are both excitatory, such as acetylcholine, and inhibitory, such as gamma-aminobutyric acid, are important for

mollusks' neural signal transduction. Previous studies have highlighted the vital roles of neurotransmitter receptors in responding to changes in neurotransmitters (Mao et al., 2017). Consequently, the downregulation of genes encoding these receptors demonstrates that TiO_2-NPs exposure may disrupt various physiological processes regulated by neurotransmitters (Guan et al., 2018). Here, we identified a total of 23 DEGs significantly associated with pathways related to "neuroactive ligand-receptor interaction." Following 14-day TiO_2-NPs exposure, there was an indication of inhibited neuronal activity, marked by substantial downregulation of various neuron-related genes, such as activator of 90 kDa heat shock protein ATPase homolog 1 (PIN0090777), gastrin/cholecystokinin type B receptor-like (PIN2170002), ETS-related transcription factor Elf-5 (PIN0050085), prostaglandin E2 receptor EP4 subtype-like (PIN0100254), cholecystokinin receptor type A-like (PIN0071117), neuronal acetylcholine receptor subunit alpha-10-like (PIN0051212), hypothetical protein KP79_PYT23720 (PIN0110990), pyrokinin-1 receptor-like (PIN0101895), G-protein coupled receptor 54 isoform X2 (PIN0010507), neuropeptide Y receptor type 2 (PIN0030378), probable G-protein coupled receptor 139 (PIN0070411), gamma-aminobutyric acid type B receptor subunit 2-like (PIN0020047), and gamma-aminobutyric acid type B receptor subunit 2-like isoform X1 (PIN0051226). These genes are known to play crucial roles in regulating nervous system processes, such as synaptic transmission, strength, and maturation. After 7 days of recovery, a total of 10 DEGs were significantly associated with pathways related to "neuroactive ligand-receptor interaction," indicating that the transient recovery period restored neuronal activity. Furthermore, seven neuronal genes, including somatostatin receptor type 2 (PIN0101576), allatostatin-A receptor-like (PIN0111909), calcitonin receptor-like (PIN0010366), blastula protease-10 (PIN0091326), cholecystokinin receptor type A-like (PIN0080212), neuropeptide Y receptor type 6-like (PIN0120125), and neurotensin receptor type 1-like (PIN0090157), remained significantly downregulated. This indicates that even after 7 days of recovery, the neuronal activity of pearl oysters could not return to normal levels.

4.7 Impact of TiO_2-NPs on biomineralization activity

Biomineralization is a biological process by which organisms control and promote mineral substances precipitation, such as pearls and shells, through biological mechanisms (Yang et al., 2021). Increased phenanthrene levels, seawater acidification, temperature changes, hypoxia, and pollution can impact the expressions of genes related to shell and pearl formation in economic pearl oysters (Jafari et al., 2023; Yang et al., 2023). Du et al. (2017) discovered that chitin plays a pivotal role as the primary organic matrix in the formation of nacre in the shell of *Pinctada fucata martensii*. The researchers also hypothesized that genes encoding chitinase could have had substantial effects on the biomineralization process (Du et al., 2017). After exposure to TiO_2-NPs, the expression levels of chitinase 1 (PIN0102750), chitinase 3 (PIN0101472), and chitinase-3-like protein 1 (PIN0140499) were substantially downregulated. Studies have demonstrated that proteins containing VWA domains, particularly collagen-related VWA-containing proteins (VWAP), are critical for the organic matrix of nacre and are essential for the formation of nacreous shells in *Pinctada fucata martensii* (Du et al., 2017). A protein discovered in the shell of Pteria sterna, referred to as N66, has been isolated and investigated, indicating that it exhibits activity similar to carbonic anhydrase and can generate crystalline forms of calcium carbonate under laboratory conditions (Rivera-Perez et al., 2019). The shell matrix serves as a complex system that facilitates interactions between proteins and minerals, proteins and proteins, as well as the epithelium and minerals (Marin et al., 2012), being critical for the biomineralization process (Sedanza et al., 2022). Here, the expressions of von Willebrand factor type A (PIN0110615), Full=N66 matrix protein (PIN0020545), and larval shell matrix protein 3 (PIN0090029) genes associated with pearl oyster biomineralization were substantially downregulated in the TE group compared with the TC group following exposure to TiO_2-NPs. This indicates that TiO_2-NPs negatively affected the biomineralization capacity of pearl oysters. This finding is consistent with our previous study, which demonstrated that TiO_2-NP stress damages pearl oyster microstructure (Li et al., 2024a). Moreover, research has indicated that the kelch-like gene plays a role in the prismatic shell layer formation in pearl oysters (Yang et al., 2022). Shell formation involves a co-expression network of extracellular matrix (ECM)-related proteins (Du et al., 2017). The ECM comprises structural and functional macromolecules, such as fibers (e.g., collagen, fibronectin) (Mariman and Wang, 2010). After 7 days of recovery, the biomineralization-related genes kelch-like protein 26 isoform X1 (PIN0081045), von Willebrand factor type A (PIN0110615, PIN0053245), fibronectin type-III domain-containing protein 3a-like isoform X4 (PIN0081841), and collagen alpha-4(VI) chain (PIN0111490) were observed upregulated, indicating that a short recovery period restored some biomineralization capacity of pearl oysters, being consistent with our prior finding (Li et al., 2024b).

5 Conclusion

In this study, transcriptomic analysis was conducted to assess the effects of TiO_2-NPs stress on gene expression in pearl oyster. A total of 911 and 844 DEGs were identified in the TC vs TE groups and the TE vs TR groups, respectively. These findings indicate that exposure to TiO_2-NPs conditions disrupts protein homeostasis, reduces biomineralization, decreases neuronal excitability, promotes apoptosis, inhibits immune responses, and induces oxidative stress. These findings help to provided a significant reference to evaluate the threat of TiO_2-NPs to pearl oysters in the general ecological environment. Nevertheless, future studies are required for a better assessment of these issues, such as whether a longer recovery period can restore their normal levels, the potential interaction of TiO_2-NPs with variable environments (such as water temperature, salinity, and the presence of other pollutants), more comprehensive understanding of the systemic effects of TiO_2-NPs, and how TiO_2-NPs affect pearl oysters populations and their role in the ecosystem.

Data availability statement

The raw sequence data reported in this paper have been deposited in the Genome Sequence Archive in National Genomics Data Center, China National Center for Bioinformation/Beijing Institute of Genomics, Chinese Academy of Sciences (GSA: CRA017826) that are publicly accessible at https://ngdc.cncb.ac.cn/gsa.

Ethics statement

The manuscript presents research on animals that do not require ethical approval for their study.

Author contributions

FL: Data curation, Formal analysis, Investigation, Methodology, Writing – original draft, Writing – review & editing. JL: Data curation, Methodology, Writing – original draft. ZG: Data curation, Writing – original draft. CY: Conceptualization, Writing – original draft, Writing – review & editing. LS: Data curation, Writing – original draft. YL: Conceptualization, Writing – original draft. YD: Funding acquisition, Writing – review & editing.

Funding

The author(s) declare financial support was received for the research, authorship, and/or publication of this article. This work was supported by the Science and Technology Program of Guangdong Province (Grant No. 2023A1515011769), National Natural Science Foundation of China (Grant No. 32102817), Department of Education of Guangdong Province (Grant No. 2020ZDZX1045 and 2021KCXTD026), the Earmarked Fund for CARS-49, Special Fund for Guangdong Province's Science and Technology Innovation Strategy (Grant No. pdjh2024a191), the Program for Scientific Research Start-Up Funds of Guangdong Ocean University (060302022304).

Acknowledgments

We are very grateful to Marine Pearl Science and Technology Backyard in Leizhou of Guangdong for collecting samples. The authors would like to thank TopEdit (www.topeditsci.com) for its linguistic assistance during the preparation of this manuscript. Transcriptomic analysis was assisted by Biotree Biotech Co.,Ltd. (Shanghai, China).

Conflict of interest

The authors declare that the research was conducted in the absence of any commercial or financial relationships that could be construed as a potential conflict of interest.

The reviewer [YB] declared a past co-authorship with the author [YD] to the handling editor.

Publisher's note

Supplementary material

The Supplementary Material for this article can be found online at: https://www.frontiersin.org/articles/10.3389/fmars.2024.1462589/full#supplementary-material

References

Abdel-Latif, H. M. R., Dawood, M. A. O., Menanteau-Ledouble, S., and El-Matbouli, M. (2020). Environmental transformation of n-TiO_2 in the aquatic systems and their ecotoxicity in bivalve mollusks: A systematic review. *Ecotox Environ. Safe* 200, 110776. doi: 10.1016/j.ecoenv.2020.110776

Aitken, R. J., Chaudhry, M. Q., Boxall, A. B. A., and Hull, M. (2006). Manufacture and use of nanomaterials: current status in the UK and global trends. *Occup. Med-Oxford* 56, 300–306. doi: 10.1093/occmed/kql051

Artigaud, S., Richard, J., Thorne, M. A. S., Lavaud, R., Flye-Sainte-Marie, J., Jean, F., et al. (2015). Deciphering the molecular adaptation of the king scallop (*Pecten maximus*) to heat stress using transcriptomics and proteomics. *Bmc. Genomics* 16, 998. doi: 10.1186/s12864-015-2132-x

Banni, M., Sforzini, S., Balbi, T., Corsi, I., Viarengo, A., and Canesi, L. (2016). Combined effects of n-TiO_2 and 2,3,7,8-TCDD in *Mytilus galloprovincialis* digestive gland: A transcriptomic and immunohistochemical study. *Environ. Res.* 145, 135–144. doi: 10.1016/j.envres.2015.12.003

Barmo, C., Ciacci, C., Canonico, B., Fabbri, R., Cortese, K., Balbi, T., et al. (2013). *In vivo* effects of n-TiO_2 on digestive gland and immune function of the marine bivalve *Mytilus galloprovincialis*. *Aquat. Toxicol.* 132, 9–18. doi: 10.1016/j.aquatox.2013.01.014

Bhagat, J., Zang, L. Q., Kaneco, S., Nishimura, N., and Shimada, Y. (2022). Combined exposure to nanoplastics and metal oxide nanoparticles inhibits efflux pumps and causes oxidative stress in zebrafish embryos. *Sci. Total. Environ.* 835, 155436. doi: 10.1016/j.scitotenv.2022.155436

Brandts, I., Teles, M., Gonçalves, A. P., Barreto, A., Franco-Martinez, L., Tvarijonaviciute, A., et al (2018). Effects of nanoplastics on Mytilus galloprovincialis after individual and combined exposure with carbamazepine. *Sci. Total. Environ.* 643, 775–784. doi: 10.1016/j.scitotenv.2018.06.257

Cappello, T., De Marco, G., Conti, G. O., Giannetto, A., Ferrante, M., Mauceri, A., et al. (2021). Time-dependent metabolic disorders induced by short-term exposure to polystyrene microplastics in the Mediterranean mussel *Mytilus galloprovincialis*. *Ecotoxicol. Environ. Saf.* 209, 111780. doi: 10.1016/j.ecoenv.2020.111780

Carbuloni, C. F., Savoia, J. E., Santos, J. S. P., Pereira, C. A. A., Marques, R. G., Ribeiro, V. A. S., et al. (2020). Degradation of metformin in water by TiO_2-ZrO_2 photocatalysis. *J. Environ.* 262, 110347. doi: 10.1016/j.jenvman.2020.110347

Chamaillard, M., Girardin, S. E., Viala, J., and Philpott, D. J. (2003). Nods, Nalps and Naip: intracellular regulators of bacterial-induced inflammation. *Cell Microbiol.* 5, 581–592. doi: 10.1046/j.1462-5822.2003.00304.x

Chen, G., Pang, M. X., Yu, X. M., Wang, J. R., and Tong, J. O. (2021). Transcriptome sequencing provides insights into the mechanism of hypoxia adaption in bighead carp (*Hypophthalmichthys nobilis*). *Comp. Biochem. Phys. D.* 40, 100891. doi: 10.1016/j.cbd.2021.100891

Chen, J. Y., Qiu, J. Y., Yang, C. Y., Liao, Y. S., He, M. X., Mkuye, R., et al. (2022a). Integrated transcriptomic and metabolomic analysis sheds new light on adaptation of Pinctada fucata martensii to short-term hypoxic stress. *Mar. pollut. Bull.* 187, 114534. doi: 10.1016/j.marpolbul.2022.114534

Chen, N., Huang, Z. K., Lu, C. K., Shen, Y. W., Luo, X., Ke, C. H., et al. (2019). Different transcriptomic responses to thermal stress in heat-tolerant and heat-sensitive pacific abalones indicated by cardiac performance. *Front. Physiol.* 9. doi: 10.3389/fphys.2018.01895

Chen, P. B., Huang, J., Rao, L. Y., Zhu, W. G., Yu, Y. H., Xiao, F. S., et al. (2022b). Environmental effects of nanoparticles on the ecological succession of gut microbiota across zebrafish development. *Sci. Total. Environ.* 806, 150963. doi: 10.1016/j.scitotenv.2021.150963

Chen, Q. L., Gong, Y., Luo, Z., Zheng, J. L., and Zhu, Q. L. (2013). Differential effect of waterborne cadmium exposure on lipid metabolism in liver and muscle of yellow catfish *Pelteobagrus fulvidraco*. *Aquat. Toxicol.* 142, 380–386. doi: 10.1016/j.aquatox.2013.09.011

Chen, Q. Q., Lackmann, C., Wang, W. Y., Seiler, T. B., Hollert, H., and Shi, H. H. (2020). Microplastics lead to hyperactive swimming behaviour in adult zebrafish. *Aquat. Toxicol.*, 224, 105521. doi: 10.1016/j.aquatox.2020.105521

Cole, M., Liddle, C., Consolandi, G., Drago, C., Hird, C., Lindeque, P. K., et al. (2020). Microplastics, microfibres and nanoplastics cause variable sub-lethal responses in mussels (*Mytilus* spp.). *Mar. pollut. Bull.* 160, 111552. doi: 10.1016/j.marpolbul.2020.111552

Danielyan, K. E., and Chailyan, S. G. (2020). Chapter 16 - New properties of vitamin B6 or pyridoxine in experimental oxidative stress in the brain. *Mol. Nutr. Food. Res.* 301, 322. doi: 10.1016/B978-0-12-811907-5.00017-8

David, J. P., and Sidney, K. P. (1981). Adaptation and tolerance of invertebrate nervous systems to osmotic stress. *J. Exp. Zool.* 215, 237–245. doi: 10.1002/jez.1402150303

Deng, Y. W., Fu, S., Lu, Y. Z., Du, X. D., Wang, Q. H., Huang, H. L., et al. (2013). Fertilization, hatching, survival, and growth of third-generation colored pearl oyster (*Pinctada martensii*) stocks. *J. Appl. Aquac.* 25, 113–120. doi: 10.1080/10454438.2013.788311

Du, X. D., Fan, G. Y., Jiao, Y., Zhang, H., Guo, X. M., Huang, R. L., et al. (2017). The pearl oyster *Pinctada fucata martensii* genome and multi-omic analyses provide insights into biomineralization. *Gigascience* 6, 100240. doi: 10.5524/100240

Duan, Y. F., Yang, Y. K., Zhang, Z., Xing, Y. F., and Li, H. (2023). Toxicity of titanium dioxide nanoparticles on the histology, liver physiological and metabolism, and intestinal microbiota of grouper. *Mar. pollut. Bull.* 187, 114600. doi: 10.1016/j.marpolbul.2023.114600

Duan, J. C., Yu, Y., Li, Y., Li, Y. B., Liu, H. C., Jing, L., et al. (2016). Low-dose exposure of silica nanoparticles induces cardiac dysfunction via neutrophil-mediated inflammation and cardiac contraction in zebrafish embryos. *Nanotoxicology* 10, 575–585. doi: 10.3109/17435390.2015.1102981

Falfushynska, H., Piontkivska, H., and Sokolova, I. M. (2020). Effects of intermittent hypoxia on cell survival and inflammatory responses in the intertidal marine bivalves *Mytilus edulis* and *Crassostrea gigas*. *J. Exp. Biol.* 223, 217026. doi: 10.1242/jeb.217026

Fu, X., Sun, Y., Wang, J., Xing, Q., Zou, J., Li, R., et al. (2014). Sequencing-based gene network analysis provides a core set of gene resource for understanding thermal adaptation in Zhikong scallop *Chlamys farreri*. *Mol. Ecol. Resour.* 14, 184–189. doi: 10.1111/1755-0998.12169

Gainey, L. F., and Greenberg, M. J. (2003). Nitric oxide mediates seasonal muscle potentiation in clam gills. *J. Exp. Biol.* 206, 3507–3520. doi: 10.1242/jeb.00573

Gallo, A., Boni, R., Buttino, I., and Tosti, E. (2016). Spermiotoxicity of nickel nanoparticles in the marine invertebrate *Ciona intestinalis* (ascidians). *Nanotoxicology* 10, 1096–1104. doi: 10.1080/17435390.2016.1177743

Garner, K. L., and Keller, A. A. (2014). Emerging patterns for engineered nanomaterials in the environment: a review of fate and toxicity studies. *J. Nanopart. Res.* 16, 2503. doi: 10.1007/s11051-014-2503-2

Georgantzopoulou, A., Cambier, S., Serchi, T., Kruszewski, M., Balachandran, Y. L., Grysan, P., et al. (2016). Inhibition of multixenobiotic resistance transporters (MXR) by silver nanoparticles and ions *in vitro* and in Daphnia magna. *Sci. Total. Environ.* 569, 681–689. doi: 10.1016/j.scitotenv.2016.06.157

Girardello, F., Leite, C. C., Branco, C. S., Roesch-Ely, M., Fernandes, A. N., Salvador, M., et al. (2016). Antioxidant defences and haemocyte internalization in *Limnoperna fortunei* exposed to TiO_2 nanoparticles. *Aquat. Toxicol.* 176, 190–196. doi: 10.1016/j.aquatox.2016.04.024

Gornati, R., Longo, A., Rossi, F., Maisano, M., Sabatino, G., Mauceri, A., et al. (2016). Effects of titanium dioxide nanoparticle exposure in *Mytilus galloprovincialis* gills and digestive gland. *Nanotoxicology* 10, 807–817. doi: 10.3109/17435390.2015.1132348

Guan, X. F., Shi, W., Zha, S. J., Rong, J. H., Su, W. H., and Liu, G. X. (2018). Neurotoxic impact of acute TiO_2 nanoparticle exposure on a benthic marine bivalve mollusk, *Tegillarca granosa*. *Aquat. Toxicol.* 200, 241–246. doi: 10.1016/j.aquatox.2018.05.011

Hal, A. M., and El-Barbary, M. I. (2020). Gene expression and histopathological changes of Nile tilapia (*Oreochromis niloticus*) infected with *Aeromonas hydrophila* and *Pseudomonas fluorescens*. *Aquaculture* 526, 735392. doi: 10.1016/j.aquaculture.2020.735392

Hampton, R. Y. (2002). ER-associated degradation in protein quality control and cellular regulation. *Curr. Opin. Cell Biol.* 14, 476–482. doi: 10.1016/S0955-0674(02)00358-7

Han, J. E., Choi, S. K., Jeon, H. J., Park, J. K., Han, S. H., Jeong, J., et al. (2021). Transcriptional response in the whiteleg shrimp (*Penaeus vannamei*) to short-term microplastic exposure. *Aquac* 20, 100713. doi: 10.1016/j.aqrep.2021.100713

He, C. Z., Hao, R. J., Deng, Y. W., Yang, C. Y., and Du, X. D. (2020). Response of pearl oyster *Pinctada fucata martensii* to allograft-induced stress from lipid metabolism. *Fish. Shellfish. Immunol.* 98, 1001–1007. doi: 10.1016/j.fsi.2019.11.028

Herskovits, A. A., Auerbuch, V., and Portnoy, D. A. (2007). Bacterial Ligands generated in a phagosome are targets of the cytosolic innate immune system. *PLoS. Pathog.* 3, e51. doi: 10.1371/journal.ppat.0030051

Hu, Z., Feng, J., Song, H., Zhou, C., Yang, M. J., Shi, P., et al. (2022). Metabolic response of *Mercenaria mercenaria* under heat and hypoxia stress by widely targeted metabolomic approach. *Sci. Total. Environ.* 809, 151172. doi: 10.1016/j.scitotenv.2021.151172

Hu, M. H., Lin, D. H., Shang, Y. Y., Hu, Y., Lu, W. Q., and Huang, X. Z. (2017). CO_2-induced pH reduction increases physiological toxicity of nano-TiO_2 in the mussel *Mytilus coruscus*. *Sci. Rep.* 2017, 40015. doi: 10.1038/srep40015

Ibrahim, D., Neamat-Allah, A. N. F., Ibrahim, S. M., Eissa, H. M., Fawzey, M. M., Mostafa, D. I. A., et al. (2021). Dual effect of selenium loaded chitosan nanoparticles on growth, antioxidant, immune related genes expression, transcriptomics modulation of caspase 1, cytochrome P450 and heat shock protein and *Aeromonas hydrophila* resistance of Nile Tilapia (*Oreochromis niloticus*). *Fish. Shellfish. Immunol.* 110, 91–99. doi: 10.1016/j.fsi.2021.01.003

Inohara, N., Chamaillard, M., McDonald, C., and Nuñez, G. (2005). NOD-LRR proteins: Role in host-microbial interactions and inflammatory disease. *Annu. Rev. Biochem.* 75, 355–383. doi: 10.1146/annurev.biochem.74.082803.133347

Ivanina, A. V., Taylor, C., and Sokolova, I. M. (2009). Effects of elevated temperature and cadmium exposure on stress protein response in eastern oysters *Crassostrea virginica* (Gmelin). *Aquat. Toxicol.* 91, 245–254. doi: 10.1016/j.aquatox.2008.11.016

Izagirre, U., Errasti, A., Bilbao, E., Múgica, M., and Marigómez, I. (2014). Combined effects of thermal stress and Cd on lysosomal biomarkers and transcription of genes encoding lysosomal enzymes and HSP70 in mussels, *Mytilus galloprovincialis*. *Aquat. Toxicol.* 149, 145–156. doi: 10.1016/j.aquatox.2014.01.013

Jafari, F., Naeemi, A. S., Sohani, M. M., and Noorinezhad, M. (2023). Effect of elevated temperature, sea water acidification, and phenanthrene on the expression of genes involved in the shell and pearl formation of economic pearl oyster (*Pinctada radiata*). *Mar. pollut. Bull.* 196, 115603. doi: 10.1016/j.marpolbul.2023.115603

Jiang, Y. S., Tang, X. X., Zhou, B., Sun, T. L., Chen, H. M., Zhao, X. Y., et al. (2017). The ROS-mediated pathway coupled with the MAPK-p38 signalling pathway and antioxidant system plays roles in the responses of *Mytilus edulis* haemocytes induced by BDE-47. *Aquat. Toxicol.* 187, 55–63. doi: 10.1016/j.aquatox.2017.03.011

Jitrapakdee, S. (2012). Transcription factors and coactivators controlling nutrient and hormonal regulation of hepatic gluconeogenesis. *Int. J. Biochem. Cell. Biol.* 44, 33–45. doi: 10.1016/j.biocel.2011.10.001

Johari, S. A., Kalbassi, M. R., Soltani, M., and Yu, I. J. (2013). Toxicity comparison of colloidal silver nanoparticles in various life stages of rainbow trout (*Oncorhynchus mykiss*). *Iran. J. Fish. Sci.* 12, 76–7V. doi: 10.1071/MF12106

Katsumiti, A., Gilliland, D., Arostegui, I., and Cajaraville, M. P. (2015). Mechanisms of toxicity of ag nanoparticles in comparison to bulk and ionic ag on mussel hemocytes and gill cells. *Plos. One* 10, e129039. doi: 10.1371/journal.pone.0129039

Kingtong, S., Chitramvong, Y., and Janvilisri, T. (2007). ATP-binding cassette multidrug transporters in Indian-rock oyster *Saccostrea forskali* and their role in the export of an environmental organic pollutant tributyltin. *Aquat. Toxicol.* 85, 124–132. doi: 10.1016/j.aquatox.2007.08.006

Konstantinos, K., Camilla, N., and Roger, P. (2012). Neuronal responses to physiological stress. *Front. Genet.* 3. doi: 10.3389/fgene.2012.00222

Kurelec, B. (1995). Inhibition of multixenobiotic resistance mechanism in aquatic organisms: ecotoxic consequences. *Sci. Total. Environ.* 171, 197–204. doi: 10.1016/0048-9697(95)04689-4

Labille, J., Slomberg, D., Catalano, R., Robert, S., Apers-Tremelo, M. L., Boudenne, J. L., et al. (2020). Assessing UV filter inputs into beach waters during recreational activity: A field study of three French Mediterranean beaches from consumer survey to water analysis. *Sci. Total. Environ.* 706, 136010. doi: 10.1016/j.scitotenv.2019.136010

Li, P. M., and Gao, X. L. (2014). Trace elements in major marketed marine bivalves from six northern coastal cities of China: Concentrations and risk assessment for human health. *Ecotox. Environ. Safe.* 109, 1–9. doi: 10.1016/j.ecoenv.2014.07.023

Li, Z. Q., Hu, M. H., Song, H. T., Lin, D. H., and Wang, Y. J. (2021). Toxic effects of nano-TiO_2 in bivalves-A synthesis of meta-analysis and bibliometric analysis. *J. Environ. Sci-China.* 104, 188–203. doi: 10.1016/j.jes.2020.11.013

Li, F. F., Lin, Y. J., Yang, C. Y., Yan, Y. L., Hao, R. J., Mkuye, R., et al. (2024a). Effects of titanium dioxide nanoparticle exposure on the gut microbiota of pearl oyster (*Pinctada fucata martensii*). *Comp. Biochem. Phys. C.* 280, 109906. doi: 10.1016/J.CBPC.2024.109906

Li, F. F., Xie, Y. F., Yang, C. Y., Ye, Q. X., Wang, F. Y., Liao, Y. S., et al. (2024b). The physiological responses to titanium dioxide nanoparticles exposure in pearl oysters

(*Pinctada fucata martensii*). *Mar. Environ. Res.* 195, 106345. doi: 10.1016/j.marenvres.2024.106345

Libralato, G., Minetto, D., Totaro, S., Micetic, I., Pigozzo, A., Sabbioni, E., et al. (2013). Embryotoxicity of TiO_2 nanoparticles to Mytilus galloprovincialis (Lmk). *Mar. Environ. Res.* 92, 71–78. doi: 10.1016/j.marenvres.2013.08.015

Lim, S., Kang, H., Kwon, B., Lee, J. P., Lee, J., and Choi, K. (2022). Zebrafish (*Danio rerio*) as a model organism for screening nephrotoxic chemicals and related mechanisms. *Ecotoxicol. Environ. Saf.* 242, 113842. doi: 10.1016/j.ecoenv.2022.113842

Liu, Z. Q., Li, Y. M., Perez, E., Jiang, Q. C., Chen, Q., Jiao, Y., et al. (2020). Polystyrene nanoplastic induces oxidative stress, immune defense, and glycometabolism change in *Daphnia pulex*: Application of transcriptome profiling in risk assessment of nanoplastics. *J. Hazard. Mater.* 402, 123778. doi: 10.1016/j.jhazmat.2020.123778

Liu, Z. Q., Lv, W. W., Huang, Y. H., Fan, B., Li, Y. M., and Zhao, Y. L. (2016). Effects of cadmium on lipid metabolism in female estuarine crab, *Chiromantes dehaani*. *Comp. Biochem. Physiol. C. Toxicol. Pharmacol.* 188, 9–16. doi: 10.1016/j.cbpc.2016.06.002

Liu, H. H., Shih, T. S., Huang, H. R., Huang, S. C., Lee, L. H., and Huang, Y. C. (2013). Plasma homocysteine is associated with increased oxidative stress and antioxidant enzyme activity in welders. *Sci. World J.* 2013, 1–8. doi: 10.1155/2013/370487

Livak, K. J., and Schmittgen, T. D. (2001). Analysis of relative gene expression data using real-time quantitative PCR and the $2^{-\Delta\Delta CT}$ method. *Methods* 25, 402–408. doi: 10.1006/meth.2001.1262

Luzio, J. P., Pryor, P. R., and Bright, N. A. (2007). Lysosomes: fusion and function. *Nat. Rev. Mol. Cell. Biol.* 8, 622–632. doi: 10.1038/nrm2217

Ma, F., Zhao, L., Ma, R. L., Wang, J., and Du, L. Q. (2023). FoxO signaling and mitochondria-related apoptosis pathways mediate tsinling lenok trout (*Brachymystax lenok tsinlingensis*) liver injury under high temperature stress. *Int. J. Biol. Macromol.* 251, 126404. doi: 10.1016/j.ijbiomac.2023.126404

Mao, L. M., Wang, H. H., and Wang, J. Q. (2017). Antagonism of muscarinic acetylcholine receptors alters synaptic ERK phosphorylation in the rat forebrain. *Neurochem. Res.* 42, 1202–1210. doi: 10.1007/s11064-016-2157-9

Mariman, E. C. M., and Wang, P. (2010). Adipocyte extracellular matrix composition, dynamics and role in obesity. *Cell. Mol. Life. Sci.* 67, 1277–1292. doi: 10.1007/s00018-010-0263-4

Marin, F., Le Roy, N., and Marie, B. J. (2012). The formation and mineralization of mollusk shell. *Front. Biosci.* 4, 1099–1125. doi: 10.2741/s321

Martínez-Fábregas, J., Prescott, A., van Kasteren, S., Pedrioli, D. L., McLean, I., Moles, A., et al. (2018). Lysosomal protease deficiency or substrate overload induces an oxidative-stress mediated STAT3-dependent pathway of lysosomal homeostasis.Nat. *Commun* 9, 5343. doi: 10.1038/s41467-018-07741-6

Martin-Folgar, R., Torres-Ruiz, M., de Alba, M., Cañas-Portilla, A. I., González, M. C., and Morales, M. (2022). Molecular effects of polystyrene nanoplastics toxicity in zebrafish embryos (*Danio rerio*). *Chemosphere* 312, 137077. doi: 10.1016/J.chemosphere.2022.137077

Muller, E. B., Hanna, S. K., Lenihan, H. S., Miller, R., and Nisbet, R. M. (2014). Impact of engineered zinc oxide nanoparticles on the energy budgets of *Mytilus galloprovincialis*. *J. Sea. Res.* 94, 29–36. doi: 10.1016/j.seares.2013.12.013

Nie, H. T., Wang, H. M., Jiang, K. Y., and Yan, X. W. (2020). Transcriptome analysis reveals differential immune related genes expression in *Ruditapes philippinarum* under hypoxia stress: potential HIF and NF-κB crosstalk in immune responses in clam. *BMC Genom* 21, 318. doi: 10.1186/s12864-020-6734-6

Papassotiropoulos, A., and de Quervain, D. J. F. (2015). Failed drug discovery in psychiatry: time for human genome-guided solutions. *Trends. Cogn. Sci.* 19, 183–187. doi: 10.1016/j.tics.2015.02.002

Pinsino, A., Bergami, E., Della Torre, C., Vannuccini, M. L., Addis, P., Secci, M., et al. (2017). Amino-modified polystyrene nanoparticles affect signalling pathways of the sea urchin (*Paracentrotus lividus*) embryos. *Nanotoxicology* 11, 201–209. doi: 10.1080/17435390.2017.1279360

Ray, P. D., Huang, B. W., and Tsuji, Y. (2012). Reactive oxygen species (ROS) homeostasis and redox regulation in cellular signaling. *Cell. Signal* 24, 981–990. doi: 10.1016/j.cellsig.2012.01.008

Ringwood, A. H., Levi-Polyachenko, N., and Carroll, D. L. (2009). Fullerene exposures with oysters: embryonic, adult, and cellular responses. *Environ. Sci. Technol.* 43, 7136–7141. doi: 10.1021/es900621j

Rivera-Perez, C., de Areyano, J. J. O. R., and Hernandez-Saavedra, N. Y. (2019). Purification and functional analysis of the shell matrix protein N66 from the shell of the pearl oyster *Pteria sterna*. *Comp. Biochem. Phys. B* 235, 19–29. doi: 10.1016/j.cbpb.2019.05.007

Robinson, M. D., McCarthy, D. J., and Smyth, G. K. (2010). edgeR: a Bioconductor package for differential expression analysis of digital gene expression data. *Bioinformatics* 26, 139–140. doi: 10.1093/bioinformatics/btp616

Rocha, T. L., Gomes, T., Cardoso, C., Letendre, J., Pinheiro, J. P., Sousa, V. S., et al. (2014). Immunocytotoxicity, cytogenotoxicity and genotoxicity of cadmium-based quantum dots in the marine mussel *Mytilus galloprovincialis*. *Mar. Environ. Res.* 101, 29–37. doi: 10.1016/j.marenvres.2014.07.009

Rokutan, K. (2000). Role of heat shock proteins in gastric mucosal protection. *J. Gastroenterol. Hepatol.* 15, D12–D19. doi: 10.1046/j.1440-1746.2000.02144.x

Salvador, J. M., Brown-Clay, J. D., and Fornace, A. J. (2013). Gadd45 in stress signaling, cell cycle control, and apoptosis. *Adv. Exp. Med. Biol.* 793, 1–19. doi: 10.1007/978-1-4614-8289-5_1

Samokhvalov, V., Scott, B. A., and Crowder, C. M. (2008). Autophagy protects against hypoxic injury in *C-elegans*. *Autophagy* 4, 1034–1041. doi: 10.4161/auto.6994

Schneider, G., Kack, H., and Lindqvist, Y. (2000). The manifold of vitamin B6 dependent enzymes. *Structure* 8, 1–6. doi: 10.1016/S0969-2126(00)00085-X

Sedanza, M. G., Yoshida, A., Kim, H. J., Yamaguchi, K., Osatomi, K., and Satuito, C. G. (2022). Identification and characterization of the larval settlement pheromone protein components in adult shells of *crassostrea gigas*: A novel function of shell matrix proteins. *Int. J. Mol. Sci.* 23, 9816. doi: 10.3390/ijms23179816

Sharon, D., Tilgner, H., Grubert, F., and Snyder, M. (2013). A single-molecule long-read survey of the human transcriptome. *Nat. Biotech.* 31, 1009. doi: 10.1038/nbt.2705

Sheng, L., Wang, L., Su, M. Y., Zhao, X. Y., Hu, R. P., Yu, X. H., et al. (2016). Mechanism of TiO_2 nanoparticle-induced neurotoxicity in zebrafish (*Danio rerio*). *Environ. Toxicol.* 31, 163–175. doi: 10.1002/tox.22031

Sherman, M. Y., and Goldberg, A. L. (2001). Cellular defenses against unfolded proteins: a cell biologist thinks about neurodegenerative diseases. *Neuron* 29, 15–32. doi: 10.1016/s0896-6273(01)00177-5

Shi, X. ,. M., Li, Z. X., Chen, W., Qiang, L. W., Xia, J. C., Chen, M., et al. (2016). Fate of TiO_2 nanoparticles entering sewage treatment plants and bioaccumulation in fish in the receiving streams. *Nanoimpact* 3-4, 96–103. doi: 10.1016/j.impact.2016.09.002

Sun, T. Y., Bornhöft, N. A., Hungerbühler, K., and Nowack, B. (2016). Dynamic probabilistic modeling of environmental emissions of engineered nanomaterials. *Environ. Sci. Technol.* 50, 4701–4711. doi: 10.1021/acs.est.5b05828

Sun, X. J., Tu, K., Li, L., Biao, W., Wu, L., Liu, Z. H., et al. (2021). Integrated transcriptome and metabolome analysis reveals molecular responses of the clams to acute hypoxia. *Mar. Environ. Res.* 168, 105317. doi: 10.1016/j.marenvres.2021.105317

Urlacher, V. B., and Girhard, M. (2012). Cytochrome P450 monooxygenases: an update on perspectives for synthetic application. *Trends. Biotechnol.* 30, 26–36. doi: 10.1016/j.tibtech.2011.06.012

Valavanidis, A., Vlahogianni, T., Dassenakis, M., and Scoullos, M. (2006). Molecular biomarkers of oxidative stress in aquatic organisms in relation to toxic environmental pollutants. *Ecotoxicol. Environ. Saf.* 64, 178–189. doi: 10.1016/j.ecoenv.2005.03.013

Wang, K., Che, W. A., Duan, M. M., Wang, C. J., Li, X. W., and He, L. (2023). Effects of broflanilide on oxidative stress and expression of apoptotic genes in zebrafish (*Danio rerio*) gill. *B. Environ. Contam. Tox.* 110, 91–91. doi: 10.1007/s00128-023-03733-5

Wegner, A., Besseling, E., Foekema, E. M., Kamermans, P., and Koelmans, A. A. (2012). Effects of nanopolystyrene on the feeding behavior of the blue mussel (*Mytilus edulis* L.). *Environ. Toxicol. Chem.* 31, 2490–2497. doi: 10.1002/etc.1984

Wei, J. L., Liu, J. H., Liang, S., Sun, M. Q., and Duan, J. C. (2020). Low-dose exposure of silica nanoparticles induces neurotoxicity via neuroactive ligand-receptor interaction signaling pathway in zebrafish embryos. *Int. J. Nanomed.* 15, 4407–4415. doi: 10.2147/IJN.S254480

Wei, S. S., Sun, B. Y., Liu, C. H., Sokolova, I., Waiho, K., Fang, J. K. H., et al. (2023). Nano-TiO_2 aggravates the adverse effect of pentachlorophenol on antioxidant and immune response in anti-predatory mussels. *Sci. Total. Environ.* 893, 164836. doi: 10.1016/j.scitotenv.2023.164836

Wu, S. J., Huang, J. Q., Li, Y. J., and Pan, Y. C. (2023). Dynamic and systemic regulatory mechanisms in rainbow trout (*Oncorhynchus mykiss*) in response to acute hypoxia and reoxygenation stress. *Aquaculture* 572, 739540. doi: 10.1016/j.aquaculture.2023.739540

Wu, H. L., Yang, C. Y., Hao, R. J., Liao, Y. S., Wang, Q. H., and Deng, Y. W. (2022). Lipidomic insights into the immune response and pearl formation in transplanted pearl oyster *Pinctada fucata martensii*. *Front. Immunol.* 13. doi: 10.3389/fimmu.2022.1018423

Xu, L. M., Li, J. R., Huang, Y., Zhao, M., Tang, X., and Wei, L. P. (2012). AutismKB: an evidence-based knowledgebase of autism genetics. *Nucleic. Acids Res.* 40, 1016–1022. doi: 10.1093/nar/gkr1145

Yang, C. Y., Hao, R. J., Deng, Y. W., Liao, Y. S., Wang, Q. H., Sun, R. J., et al. (2017). Effects of protein sources on growth, immunity and antioxidant capacity of juvenile pearl oyster *Pinctada fucata martensii*. *Fish. Shellfish. Immunol.* 67, 411–418. doi: 10.1016/j.fsi.2017.06.037

Yang, C. Y., Wu, H. L., Chen, J. Y., Liao, Y. S., Mkuye, R., Deng, Y. W., et al. (2023). Integrated transcriptomic and metabolomic analysis reveals the response of pearl oyster (*Pinctada fucata martensii*) to long-term hypoxia. *Mar. Environ. Res.* 191, 106133. doi: 10.1016/j.marenvres.2023.106133

Yang, C. Y., Yang, J. M., Hao, R. J., Du, X. D., and Deng, Y. W. (2019). Molecular characterization of OSR1 in *Pinctada fucata martensii* and association of allelic variants with growth traits. *Aquaculture* 516, 734617. doi: 10.1016/j.aquaculture.2019.734617

Yang, C. Y., Zeng, Y. T., Liao, Y. S., Deng, Y. W., Du, X. D., and Wang, Q. H. (2021). Integrated GC-MS- and LC-MS-Based Untargeted Metabolomics Studies of the Effect of Vitamin D3 on Pearl Production Traits in Pearl Oyster *Pinctada fucata martensii*. *Front. Mol. Biosci.* 8. doi: 10.3389/fmolb.2021.614404

Yang, C. Y., Zhang, C. S., Huang., J., Hao, R. J., Shi, S. L., Huang, R. L., et al. (2022). Sequence and SNP analysis of Kelch▪like gene from pearloyster *Pinctada fucata martensii*. *J. Dalian Ocean Univ.* 37, 146. doi: 10.16535/j.cnki.dlhyxb.2021-146

Yin, J., Hu, J., Deng, X. D., Zheng, Y., and Tian, J. J. (2023). ABC transporter-mediated MXR mechanism in fish embryos and its potential role in the efflux of nanoparticles. *Ecotoxicol. Environ. Saf.* 263, 115397. doi: 10.1016/j.ecoenv.2023.115397

Young, T., Kesarcodi-Watson, A., Alfaro, A. C., Merien, F., Nguyen, T. V., Mae, H., et al. (2017). Differential expression of novel metabolic and immunological biomarkers in oysters challenged with a virulent strain of OsHV-1. *Dev. Comp. Immunol.* 73, 229–245. doi: 10.1016/j.dci.2017.03.025

Ze, X., Su, M. Y., Zhao, X. Y., Jiang, H., Hong, J., Yu, X. H., et al. (2016). TiO_2 nanoparticle-induced neurotoxicity may be involved in dysfunction of glutamate metabolism and its receptor expression in mice. *Environ. Toxicol.* 31, 655–662. doi: 10.1002/tox.22077

Zhang, X. K., Fan, C., Zhang, X. Z., Li, Q. Z., Li, Y. C., Ma, P. Z., et al. (2022). Transcriptome Analysis of *Crassostrea sikamea* (♀) × *Crassostrea gigas* (♂) Hybrids Under and After Thermal Stress. *J. Ocean Univ. China* 21, 213–224. doi: 10.1007/s11802-022-4829-1

Zhang, G. F., Fang, X. D., Guo, X. M., Li, L., Luo, R. B., Xu, F., et al. (2012). The oyster genome reveals stress adaptation and complexity of shell formation. *Nature* 490, 49–54. doi: 10.1038/nature11413

Zheng, Z., Hao, R. J., Yang, C. Y., Jiao, Y., Wang, Q. H., Huang, R. L., et al. (2023). Genome-wide association study analysis to resolve the key regulatory mechanism of biomineralization in *Pinctada fucata martensii*. *Mol. Ecol. Resour.* 23, 680–693. doi: 10.1111/1755-0998.13743

Zhou, Z., Liu, T., Kong, J., Zeng, S., and Zhu, J. Q. (2024). Toxicity and transcriptome sequencing analyses of *Acipenser schrenckii* under titanium dioxide nanoparticles stress. *Aquacult. Rep.* 36, 102091. doi: 10.1016/J.AQREP.2024.102091

Zhou, C., Song, H., Feng, J., Hu, Z., Yu, Z. L., Yang, M. J., et al. (2021). RNA-Seq analysis and WGCNA reveal dynamic molecular responses to air exposure in the hard clam. *Mercenaria mercenaria. Genomics* 113, 2847–2859. doi: 10.1016/j.ygeno.2021.06.025

Frontiers in Marine Science

Explores ocean-based solutions for emerging global challenges

The third most-cited marine and freshwater biology journal, advancing our understanding of marine systems and addressing global challenges including overfishing, pollution, and climate change.

Discover the latest Research Topics

See more →

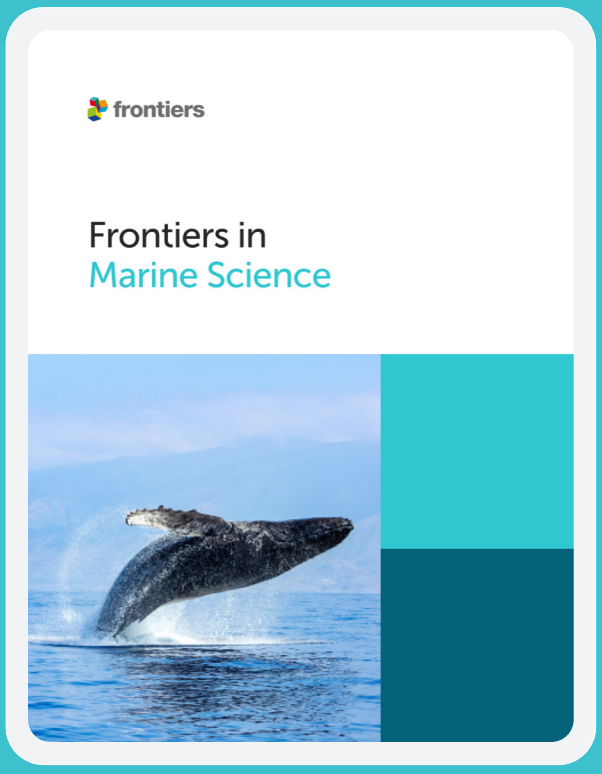

Frontiers

Avenue du Tribunal-Fédéral 34
1005 Lausanne, Switzerland
frontiersin.org

Contact us

+41 (0)21 510 17 00
frontiersin.org/about/contact